

UC Irvine

UC Irvine Electronic Theses and Dissertations

Title

Assigning the Absolute Configuration of Amines and Synthesis of Allium and Alkaloid Natural Products

Permalink

<https://escholarship.org/uc/item/8sz166dm>

Author

Burtea, Alexander

Publication Date

2019

Peer reviewed|Thesis/dissertation

UNIVERSITY OF CALIFORNIA,
IRVINE

Assigning the Absolute Configuration of Amines and Synthesis of Allium and Alkaloid Natural
Products

DISSERTATION

submitted in partial satisfaction of the requirements
for the degree of

DOCTOR OF PHILOSOPHY

in Chemistry

by

Alexander Burtea

Dissertation Committee:
Professor Scott D. Rychnovsky, Chair
Professor Larry E. Overman
Professor Sergey V. Pronin

DEDICATION

To my family

TABLE OF CONTENTS

LIST OF TABLES.....	viii
LIST OF FIGURES.....	ix
LIST OF SCHEMES.....	x
LIST OF GRAPHS.....	xiii
LIST OF ABBREVIATIONS.....	xiv
ACKNOWLEDGEMENTS.....	xvii
CIRRICULUM VITAE.....	xx
ABSTRACT OF THE DISSERTATION.....	xxiii
Chapter 1. Assigning the Absolute Configuration of Amines Using the Competing Enantioselective Conversion (CEC) Method.....	1
1.1 Abstract	1
1.1 Introduction	2
1.1.1 The Competing Enantioselective Conversion Method	3
1.2 Previous Work.....	4
1.2.1 CEC of Alcohols	4
1.2.2 CEC of Primary Amines	5
1.2.3 Inspiration from Bode's Work	6
1.3 Results	8
1.3.1 Synthesis of the Pseudo-enantiomeric Acyl Transfer Reagents	8
1.3.2 Selectivity and ESI-MS Quantification Validation.....	9
1.3.3 Optimization of the CEC Reaction for Cyclic Amines.....	10
1.3.4 Synthesis of Chiral Piperidines.....	13
1.3.5 Substrate Scope Investigation	14
1.3.6 Triple-Quadruple Mass Spectrometer as a Mode of Detection	16
1.3.7 Substrate Scope Expansion.....	17
1.3.8 Unsuccessful Substrates.....	20
1.3.9 Future Work	21
1.4 Conclusions	22
1.5 Experimental Section	22

1.5.1	General Experimental	22
1.5.2	Chemicals.....	23
1.5.3	General Procedure #1: CEC General Reaction Procedure.....	24
1.5.4	General procedure #2: Sulfinimide formation	25
1.5.5	General procedure #3: Grignard addition and ring closure	26
1.5.6	General procedure #4: Chiral auxiliary cleavage.....	26
1.5.7	ESI-MS product ratio measurement verification:	27
1.5.8	Compound Characterization:	27
1.6	References	37
Chapter 2.	Progress Towards the Synthesis of the Western Fragment of Phainanoid F	40
2.1	Abstract	40
2.2	Introduction	41
2.2.1	Phyllanthus hainanensis and Phainanoids A-F	41
2.3	Previous Work.....	43
2.3.1	Guangbin Dong's Successful Intramolecular Alkenylation Approach.....	43
2.3.2	Triflate Fragmentation Spirocyclization Approach	43
2.3.3	Wolff Ring Contraction Approach.....	45
2.4	Results	46
2.4.1	Revising the Wolff Ring Expansion Route.....	46
2.4.2	Benzoin Condensation to Form the Desired Enone	49
2.4.3	[2+2] Cycloaddition Using Carvone	51
2.5	Conclusions	54
2.6	Experimental Section	54
2.6.1	General Experimental:	54
2.6.2	Compound Characterization:	55
2.7	References	67
Chapter 3.	Synthesis of Kujounins A ₁ and A ₂ Using a Biosynthesis Inspired Approach	69
3.1	Abstract	69
3.2	Introduction	70
3.2.1	Allium Species	70
3.2.2	Isolation of Kujounins A ₁ and A ₂ and Proposed Biosynthesis	70
3.3	Synthesis of Kujounins A ₁ and A ₂	73

3.3.1	Initial Approach	73
3.3.2	Revised Approach to the Synthesis of Kujounins A ₁ and A ₂	75
3.3.3	Summary of the Synthesis of Kujounin A ₂ and Future Directions	86
3.4	Conclusions	87
3.5	Experimental Section	88
3.5.1	General Experimental Details	88
3.5.2	Chemicals.....	89
3.5.3	Compound Characterization	89
3.5.4	DP4+ Analysis of triacetate intermediates 3-68-Major and 3-68-Minor.....	97
3.6	References	109
Chapter 4.	Total Synthesis of the Proposed Structure of (–)-Himeradine A.....	113
4.1	Abstract	113
4.2	Introduction	114
4.2.1	Lycopodium Alkaloids.....	114
4.2.2	Biosynthetic Proposal	115
4.2.3	Isolation and Background of (–)-Himeradine A	116
4.3	Previous Work.....	117
4.3.1	Carter’s Synthesis of the Quinolizidine Fragment of (–)-Himeradine A.....	117
4.3.2	Shair’s Total Synthesis of the Proposed Structure of (–)-Himeradine A.....	118
4.3.3	Rychnovsky’s Total Synthesis of (+)-Fastigiatine.....	120
4.3.4	Rychnovsky’s Initial Studies Towards (–)-Himeradine A.....	123
4.4	Results	128
4.4.1	Asymmetric Synthesis of Piperidine 4-71 via Glorius Hydrogenation	128
4.4.2	Nickel Catalyzed Cross-electrophile Coupling to Form Pyridine 4-98	130
4.4.3	Attempts at Minisci Chemistry to Synthesize Pyridine 4-98	132
4.4.4	Attempts at Picoline Lithiation to Synthesize Pyridine 4-108	133
4.4.5	Pyridine N-Oxide Approach Towards Forming Pyridine 4-108	134
4.4.6	Resolution of Piperidine 4-71 with DBTA	135
4.4.7	Sulfamidate Approach Towards the Synthesis of Elaborated Piperidine 4-65	137
4.4.8	Model System Used to Validate Late-Stage Quinolizidine Formation	142
4.4.9	Successful Route for the Synthesis of the Proposed Structure of (–)-Himeradine A 143	
4.4.10	Comparison of (–)-Himeradine A Spectral Data	146

4.4.11	Full Synthetic Route and Future Work	148
4.5	Conclusions	149
4.6	Experimental Section	150
4.6.1	General Experimental Details	150
4.6.2	Compound Characterization:	151
4.6.3	Data for 4-114 Crystal Structure	157
4.7	References	193
Appendix A	CEC analysis spectra.....	196
Appendix B	NMR Spectra	214

LIST OF TABLES

Table 1-1. Optimization of reaction concentrations for the CEC reaction.....	11
Table 1-2. Optimization of solvent for the CEC reaction.	12
Table 1-3. Optimization of temperature and time for the CEC reaction.....	13
Table 1-4. CEC substrate scope evaluation of amines.	15
Table 1-5. Investigation of the selectivity difference between acyl transfer reagents 1-30 and 1-31 and bromo acyl transfer reagents 1-74 and 1-75	18
Table 1-6. Substrate scope investigation of the amine CEC reaction.	19
Table 1-7. Medicinally relevant amines in which the stereochemistry was successfully assigned by the CEC.....	20
Table 2-1. Optimization of the Robinson annulation.....	50
Table 2-2. Failed attempts at coupling alkyne 2-80 and bromide 2-81	53
Table 3-1. Alkylation of acetonide protected <i>L</i> -ascorbic acid.	74
Table 3-2. Optimization of the Tsuji-Trost alkylation of <i>L</i> -ascorbic acid.	79
Table 3-3. Tricyclic core formation and sulfur installation.	81
Table 3-4. Unsuccessful solvent screen optimization for installation of the sulfur moiety.	84
Table 4-1. Nickel catalyzed cross-electrophile coupling optimization.	131
Table 4-2. Optimization of the salt resolution of piperidine 4-71	136
Table 4-3. Comparison how the ¹³ C ppm shifts at each carbon of (–)-himeradine A (4-17).....	193

LIST OF FIGURES

Figure 1-1. General procedure for a CEC reaction.	3
Figure 1-2. Energy diagram displaying two separate resolutions.	4
Figure 1-3. Process for assigning the absolute configuration of secondary alcohols and select examples that were successfully assigned.	5
Figure 1-4. Preliminary mnemonic for assigning the absolute configuration of amines using acyl transfer reagents 1-30 and 1-31	16
Figure 1-5. Substrates unsuccessfully assigned by the CEC method.	21
Figure 2-1. Structure of phainanoids A-F.	41
Figure 2-2. Structures of Cyclosporin and Azathioprine.	42
Figure 3-1. Structures of the natural products isolated by the Matsuda group.	71
Figure 4-1. The <i>Lycopodium</i> structural classes.	114
Figure 4-2. Structure of himeradine A and related <i>Lycopodium</i> alkaloids.	116
Figure 4-3. <i>Lycopodium</i> alkaloids envisioned to be synthesized by common intermediate 4-57	123
Figure 4-4. Carbon numbering of himeradine A (a) and carbon shift deviations from the isolated natural product (b).	148

LIST OF SCHEMES

Scheme 1-1. Processes for assigning the absolute configuration of primary amines.....	6
Scheme 1-2. Bode's catalytic kinetic resolution of cyclic amines.	6
Scheme 1-3. Bode's kinetic resolution of cyclic amines with various acyl groups.	7
Scheme 1-4. Proposed process for determining the absolute configuration of amines using the CEC method.....	8
Scheme 1-5. Synthesis of the pseudo-enantiomeric acyl transfer reagents.....	9
Scheme 1-6. Kinetic resolution using acyl transfer reagents 1-30 and 1-31 (a) and synthesis of amides 1-38 and 1-39	9
Scheme 1-7. Synthesis of chiral cyclic amines using Ellman's auxiliary.	14
Scheme 1-8. Bode and Kozlowski's proposed transition state for the kinetic resolution of cyclic amines.	21
Scheme 1-9. Example of a general CEC reaction with the corresponding ESI-MS spectra.	25
Scheme 2-1. The Dong group's approach to the western portion of the phainanoids.....	43
Scheme 2-2. Retrosynthesis of the triflate fragmentation approach.....	44
Scheme 2-3. Cyclobutane formation and attempted elimination (a). Attempted triflate fragmentation (b).	44
Scheme 2-4. Attempted elimination in the absence of the ester group.	45
Scheme 2-5. Retrosynthesis of fragment 2-14 utilizing a Wolff ring contraction.	45
Scheme 2-6. Forward synthesis towards fragment 2-14	46
Scheme 2-7. Mechanism for the Nazarov cyclization.....	46
Scheme 2-8. Revised retrosynthesis using the Wieland-Miescher ketone.	47
Scheme 2-9. Synthesis of key intermediate 2-44 for the Nazarov cyclization.....	47
Scheme 2-10. Attempted nazarov cyclization of diol 2-44 (a) and mechanism for the formation of each product (b).	48
Scheme 2-11. Selectivity for the deprotonation of <i>trans</i> - and <i>cis</i> -decalins.....	48
Scheme 2-12. Revised retrosynthesis utilizing a benzoin condensation to form key tricycle.	49
Scheme 2-13. Formation of trione 2-70	49
Scheme 2-14. Attempted synthesis of the western fragment of the phainanoids using a benzoin condensation.	51
Scheme 2-15. Retrosynthesis of the [2+2] route towards the synthesis of the western fragment of the phainanoids.	51
Scheme 2-16. Alkylation of L-carvone (a) and bromination of 3-coumaranone (b).....	52
Scheme 2-17. Attempted ketalization of alkyne 2-80	53
Scheme 2-18. Sonagashira cross-coupling to form desired benzofuran 2-88	54
Scheme 3-1. Proposed biosynthesis of the kujounins by the Matsuda group.	71
Scheme 3-2. Proposed biosynthesis of the kujounins by the Rychnovsky group.	72
Scheme 3-3. Initial retrosynthesis of kujounin A ₂	73
Scheme 3-4. Formation of the core of the kujounins A ₁ and A ₂	74
Scheme 3-5. Palladium catalyzed alkylation of ascorbic acid by the Moreno-Manas group.....	75
Scheme 3-6. Palladium catalyzed alkylation of L-ascorbic acid.....	76

Scheme 3-7. Attempted synthesis of enantiopure allylic carbonate 3-47 .	77
Scheme 3-8. Synthesis of allylic carbonate 3-53 by enzymatic resolution.	78
Scheme 3-9. Proposed mechanism of carbonate racemization for a terminal olefin (a) and multi-substituted olefin (b).	80
Scheme 3-10. Failed attempts at forming kujounin A ₂ from various anomeric sulfur derivatives.	82
Scheme 3-11. Sulfur installation toward the synthesis of kujounin A ₂ .	83
Scheme 3-12. Irreproducible end game for the synthesis of kujounin A ₂ .	85
Scheme 3-13. Optimized end game for the synthesis of kujounin A ₂ .	86
Scheme 3-14. Full forward synthesis of kujounin A ₂ .	87
Scheme 4-1. Biosynthetic proposal based on radiolabeling studies.	115
Scheme 4-2. MacLean's proposed biosynthesis of the pentacyclic core of fastigiatine and himeradine A.	117
Scheme 4-3. Carter's synthesis of the quinolizidine fragment of (–)-himeradine A.	118
Scheme 4-4. Shair's synthesis of their key lactam intermediate towards (–)-himeradine A.	119
Scheme 4-5. Shair's synthesis of their key piperidine intermediate 4-43 .	119
Scheme 4-6. Shair's endgame for the synthesis of the proposed structure of (–)-himeradine A.	120
Scheme 4-7. Rychnovsky's synthesis of (+)-fastigiatine.	121
Scheme 4-8. Rychnovsky's second-generation synthesis of (+)-fastigiatine.	122
Scheme 4-9. Initial retrosynthetic analysis towards the synthesis of (–)-himeradine A.	124
Scheme 4-10. Synthetic route to access functionalize piperidine 4-66 .	125
Scheme 4-11. Rationale for the diastereoselectivity of alkylation of 2-substituted <i>N</i> -Boc piperidines (a) and <i>cis</i> -2,4-substituted <i>N</i> -Boc piperidines (b).	126
Scheme 4-12. Attempted resolution of piperidine 4-66 using Ellman's auxiliary.	126
Scheme 4-13. Unexpected resolution using a Hartwig amination.	127
Scheme 4-14. Resolution using an Overman rearrangement.	127
Scheme 4-15. End-game validation for the synthesis of (–)-himeradine A.	128
Scheme 4-16. Mechanism of hydrogenation of pyridines containing a chiral auxiliary.	129
Scheme 4-17. Asymmetric synthesis of piperidine 4-71 using a Glorius hydrogenation.	129
Scheme 4-18. Synthesis of Grignard reagent 4-97 .	130
Scheme 4-19. Attempted alkylation of heterocycles using MacMillan's spin-center-shift photoredox Minisci reaction.	132
Scheme 4-20. Attempted Minisci reaction into bromopicoline 4-68 .	133
Scheme 4-21. Attempted lithiation of bromopicoline 4-68 .	134
Scheme 4-22. Three step sequence to accessing N-oxide 4-111 .	135
Scheme 4-23. Large scale production of racemic piperidine 4-71 .	135
Scheme 4-24. Optimized resolution of piperidine 4-71 with a crystal structure and functional group protections.	137
Scheme 4-25. Retrosynthesis to synthesize fully elaborated piperidine 4-65 using a sulfamidate.	138
Scheme 4-26. Alkylation of piperidine 4-72 with a sulfamidate.	138
Scheme 4-27. Attempted formation of sulfamidate 4-123 using a key Tsuji-Trost amination.	139

Scheme 4-28. Attempts at oxidizing sulfamidite 4-122 to sulfamidate 4-123 (a) and attempts at directly transforming amino alcohol 4-121 into sulfamidate 4-123 using sulfuryl reagents (b).	140
Scheme 4-29. Attempted one-step synthesis of sulfamidate 4-131	140
Scheme 4-30. Novel approach toward the formation of sulfamidate 4-123	141
Scheme 4-31. Attempted synthesis of sulfamidate 4-123 from L-homoserine.	142
Scheme 4-32. Model system to examine the late stage quinolizidine formation.	143
Scheme 4-33. Successful sequence for the synthesis of fully elaborated piperidine 4-65	143
Scheme 4-34. Suzuki cross-coupling, conjugate addition, and silyl deprotection.	145
Scheme 4-35. Testing the tosylation and oxidation using the undesired diastereomer.	145
Scheme 4-36. Tosylation and oxidation using the diastereomer.	146
Scheme 4-37. Final trans-annular Mannich reaction to afford himeradine A.	146
Scheme 4-38. Rychnovsky's complete synthetic sequence for the synthesis of the proposed structure of (-)-himeradine A.	149

LIST OF GRAPHS

Graph 1-1. The theoretically expected percent of 1-38 relative to total ion count of 1-38 and 1-39 versus the experimental percentages.....	10
Graph 1-2. The theoretically expected percent of 1-38 relative to total ion count of 1-38 and 1-39 versus the experimental percentages.....	17
Graph 4-1. Carbon shift differences between the isolated natural product and the synthetic himeradine A.....	147

LIST OF ABBREVIATIONS

Å	Angstroms
Ac	Acetate
AIBN	2,2'-Azobis(2-methylpropionitrile)
aq.	Aqueous
Atm	Atmosphere
ax	Axial
Boc	tert-Butyloxycarbonyl
Bn	Benzyl
Bu	Butyl
Bz	Benzoate
°C	Degree Celsius
CSA	Camphorsulfonic acid
d	day(s)
δ	Chemical shift
DBU	1,8-Diazabicycloundec-7-ene
DCM	Dichloromethane
DIBAL-H	Diisobutylaluminium hydride
DIPEA	N,N-Diisopropylethylamine
DMP	Dess-Martin periodinane
DMSO	Dimethyl sulfoxide
DMAP	4-Dimethylaminopyridine
DMPU	1,3-Dimethyl-tetrahydropyrimidinone
dppf	1,1'-bis(diphenylphosphino)ferrocene
dr	diastereomeric ratio
ee	enantiomeric excess
eq	equatorial
Et	Ethyl

g gram
h Hour(s)
HF Hydrofluoric acid
HFIP hexafluoro isopropanol
HMPA Hexamethylphosphoramide
HMDS 1,1,1,3,3,3-Hexamethyldisilazane
HRESIMS High-resolution electrospray ionization mass spectrometry
HPLC High pressure liquid chromatography
Hz Hertz
IR Infrared spectrometry
J Coupling constant
L liter
LD Lethal dose
LDA Lithium diisopropylamide
 μ micro
m-CPBA 3-Chloroperoxybenzoic acid
m milli
M Molar
Me methyl
MHz Megahertz
min Minute(s)
MOM Methoxymethyl
MPLC Medium pressure liquid chromatography
MS Molecular sieves
NMP N-Methyl-2-pyrrolidone
NMR Nuclear Magnetic Resonance
NOE Nuclear Overhauser Effect
Ph Phenyl

PMB p-Methoxybenzyl ether
Pr propyl
PPTS Pyridinium p-toluenesulfonate
PTSA p-Toluenesulfonic acid
Py Pyridine
rt Room Temperature
rxn Reaction
SAR Structure Activity Relationship
sec secondary
t tert
TASF Tris(dimethylamino)sulfonium difluorotrimethylsilicate
TBAF Tetra-n-butylammonium fluoride
TBDPS *tert*-Butyldiphenylsilyl
TBS *tert*-Butydimethylsilyl
TES Triethylsilyl
TIPS Triisopropylsilyl
Tf Trifluoromethanesulfonate
TFA Trifluoroacetic acid
THF Tetrahydrofuran
THPO Tetrahydropyranone
TLC Thin-layer chromatography
TMEDA Tetrahmethylethylenediamine
TMS Trimethylsilyl
Ts Tosyl

ACKNOWLEDGEMENTS

First and foremost, I want to thank Professor Scott Rychnovsky for accepting me into his group and guiding me through graduate school. I have learned more than I can ever imagine and am very grateful for the freedom you gave me in your lab. You allowed me to try all the crazy ideas I had and were always extremely supportive. I could not have asked for a better advisor. Thank you. I want to thank Professor Larry Overman and Professor Sergey Pronin for giving me advise about chemistry and being on my thesis committee.

Jacob, Michael, and Yuriy, you guys were the best mentors I could ask. Even though you guys played jokes on me and teased me my first two years, you guys always had my back. It was extremely fun having you guys in lab with me. I will never forget all of the crazy nights at Eureka. Thank you for being great friends!

Chuck, Valdes, Leah, and Sunshine, you guys were awesome to have in lab. I hope I did not annoy all of you too much with clapping, yelling, and loud music. I hope that Chuck and Sunshine can continue the clapping through the labs as a tradition! Also, Chuck needs to stop being so quiet. Greg, Sarah, Eric, Justin, Alex Wagner, Renzo, Richard, you guys were a pleasure to have in the lab. I want to thank each and every one of you for your guidance and help through graduate school. Nick, Tyler, and Spencer, thanks for basically being part of the Rychnovsky lab. I enjoyed having you guys right next door. It was great talking chemistry and going out to Eureka after work! Vanderwal and Pronin labs, you guys were awesome colleagues and I could not imagine a better group of people to work with.

I want to thank God for giving me the strength to get through school and keep me on the right path. It has been a tough journey, but well worth it. I also want to thank my family for all

their support. The Sarega, Ursan, Bratiloveanu, Burtea, Waldrop, Larson, Meiloaica, Davila, Toca, and Dunagan family have always been there for me and have shown me so much love. Thank you!

All the cousins and friends, we are such a tight nit group and I could not imagine a better group of people to always hang out with. Andrew, David, Brati, Lucian, Cat, Dita, Harvey, AJ, Caius, Stevo, Adrian, Tim, Johnny, David B., Monica, Carole, Natacha, Anna, Susan, Naomi, and Becky, you guys are the best! RRR for life!

Sherrie and Brian, thank you for the constant support over the last five years. Both of you showed me so much love from the start. Thank you for being amazing parents in law. Mia Nuti, thank you for taking care of me as a child and loving me. I appreciate you and all the sacrifices you made for me. I love you. Kim and Lila, thank you for loving me and my family so much. We are beyond appreciative for housing us for so many years. Not many people are kind enough to open their home like you guys have. I am so honored to call you my aunt and uncle.

Vik, Andrea, Anna, and Lisa, I love you guys to the moon and back. I am so thankful to have such amazing family members and siblings that are so supportive. We have always been there for each other, through the highs and lows. You guys are the best! Little Everly, you have brought so much joy into all of our lives. We all love you more than you will ever know.

Mica and Ticu, I don't know if there could be better people in this world. I have learned so much from both of you and cannot imagine where I would be if I did not have your influences in my life. Thank you for taking care of me, providing for me, spoiling me, teaching me, and loving me. I will never forget what you told me Ticu: "Rădăcinile cartei sunt amara, dar roadele ei sint dulci." I took it to heart and pursued school like you always told me. I love you Mica and Ticu. I will always miss you Ticu.

Mom and Dad, I want to thank you for everything you have done for me. You both have always been extremely supportive and willing to do anything for me. I would not be the person I am today without your guidance and love. I am so grateful to have the best parents in the world. I cannot wait to finally be able to spoil you guys!

Last but not least, I want to thank my beautiful wife Lindsay. She has been with me from the beginning of graduate school. All the late nights in lab and weekends spent away from her were tough, but she stuck it out with me and always loved me unconditionally. I could not have done this without you Lindsay and I cannot wait to enjoy the rest of my life with you!

CURRICULUM VITAE

Alexander Burtea

Education

Ph.D. University of California, Irvine

Organic Chemistry

*Advisor: Prof. Scott D. Rychnovsky***Irvine, CA**

Aug 2014 - present

B.S. California State University, Fullerton

Biochemistry (summa cum laude)

*Advisor: Prof. Nicholas T. Salzameda***Fullerton, CA**

Aug 2009 - June 2013

Experience

University of California, Irvine*Graduate Research Assistant**Advisor: Prof. Scott D. Rychnovsky***Irvine, CA**

Aug 2014 - Present

Total Synthesis of the Proposed Structure of (–)-Himeradine A

- Currently developing a synthetic route to (–)-himeradine A which intercepts a common bromo-enone intermediate that has been used to synthesize various *Lycopodium* alkaloids in our lab.

Synthesis of Kujounin A₁ and A₂

- Designed and developed an expedient six step synthesis of kujounin A₁ and A₂. The synthesis utilizes a key Tsuji-Trost alkylation of L-ascorbic acid, which provides the carbon core of both natural products. Our lab is currently waiting on bioactivity results from the National Cancer Institute.

Determining the Absolute Configuration of Cyclic Amines Using the Competing Enantioselective Conversion Method

- Designed and developed a simple and effective method to assign the absolute configuration of amines using pseudo-enantiomeric acyl transfer reagents. The method was optimized to be analyzed by tandem quadrupole mass spectrometry, which permits the use of micrograms of material and requires no work-up.

Second-Generation Synthesis of (+)-Fastigiatine Inspired by Conformational Studies

- Assisted in the completion of a second-generation synthesis of (+)-fastigiatine, which addressed two problematic steps in the original synthesis from our lab.

University of California, Irvine*Teaching Assistant*

General and Organic Chemistry Lectures and Labs

- Assist students with proper laboratory techniques such as chromatography, volumetric analysis, and calorimetry.

- Regularly grade lab reports, including written instructions on proper scientific writings and formalisms.

Irvine, CA

Aug 2014 - Present

Exova*Wet Chemist*

- Using current Good Manufacturing Practices (cGMP), various tests were conducted for quality assurance of active pharmaceutical ingredients, common laboratory chemicals, and food additives using United States Pharmacopeia (USP), European Pharmacopeia (Ph. Eur.), Japanese Pharmacopeia (JP), and Food Chemical Codex (FCC) protocols.

Santa Fe Springs, CA

July 2013 - July 2014

- Prepared Certificate of Analysis (COA) for each subject that was tested.
- Collaborated with the Food and Drug Administration (FDA) upon unannounced inspections.

California State University, Fullerton

Undergraduate Research Assistant

Advisor: Prof. Nicholas T. Salzameda

Discovery and Optimization of Small Molecule Inhibitors for the Botulinum Neurotoxin Type A

- Synthesized hundreds of small molecules using solid phase synthesis.
- Screened each compound via a high-throughput Fluorescence Resonance Energy Transfer (FRET) assay.
- Calculated IC₅₀ values for compounds of interest and used computational docking studies (Molsoft) to guide the structure-activity relationship (SAR) study.

Fullerton, CA

Aug 2009 - June 2013

California State University, Fullerton

Howard Hughes Medical Institute Research Scholar

Advisor: Prof. Maria Linder

- Presented my research to various high schools in order to promote STEM research programs.
- Organized and hosted departmental seminars of prominent chemistry faculty.

Fullerton, CA

Aug 2011 - June 2013

Publications

1. King, R. P.; Wagner, A. J.; **Burtea, A.**; King, S. M. "Asymmetric Synthesis of an Enantioenriched Alcohol and Determination of Absolute Configuration: A Discovery-Based Undergraduate Laboratory Experiment." *Manuscript in preparation*.
2. **Burtea, A.**; Rychnovsky, S. D. "Biosynthesis-inspired Approach to Kujounin A₂ Using a Stereoselective Tsuji-Trost Alkylation." *Org. Lett.* **2018**, *20*, 5849–5852.
3. DeForest, J.C.; Suryan, G.; Samame, R.A.; **Burtea, A.**; Rychnovsky, S. D. "Second-Generation Synthesis of (+)-Fastigiatine Inspired by Conformational Studies." *J. Org. Chem.* **2018**, *83*, 8914–8925.
4. **Burtea, A.**; Rychnovsky, S. D. "Determination of the Absolute Configuration of Cyclic Amines with Bode's Chiral Hydroxamic Esters Using the Competing Enantioselective Conversion Method." *Org. Lett.* **2017**, *19*, 4195–4198.
5. **Burtea, A.**; Salzameda, N. T. "Discovery and SAR study of a sulfonamide hydroxamic acid inhibitor for the botulinum neurotoxin serotype A light chain." *Med. Chem. Commun.* **2014**, *5*, 706–710.

Presentations

1. **Burtea, A.**; Rychnovsky, S. D. "Assigning the absolute configuration of amines using the competing enantioselective conversion method." Moving Molecules from the Academic Lab to the Clinic, Irvine, CA. May 25, 2017.
2. **Burtea, A.**; Rychnovsky, S. D. "Assigning the absolute configuration of amines using the competing enantioselective conversion method." American Chemical Society 253rd national meeting, San Francisco, CA. April 2-6, 2017.
3. **Burtea, A.**; Salzameda, N. T. "Discovery and development of a small molecule inhibitor for the botulinum neurotoxin Type A." CSU Program for Education and Research in Biotechnology 25th Annual CSU Biotechnology Symposium, Anaheim, CA. January 3-5, 2013.
4. **Burtea, A.**; Salzameda, N. T. "Discovery and development of a small molecule inhibitor for the botulinum neurotoxin Type A." American Chemical Society 243rd national meeting, San Diego, CA. March 25-29, 2012.
5. **Burtea, A.**; Fawaz A.; Salzameda, N. T. "Discovery and Optimization of Small Molecule Inhibitors for the Botulinum Neurotoxin type E Protease." CSU Program for Education and Research in Biotechnology 24th Annual CSU Biotechnology Symposium, Santa Clara, CA. January 5-7, 2012.

6. **Burtea, A.**; Fawaz, A.; Salzameda, N. T. "Discovery and development of small molecule inhibitors for the botulinum neurotoxin E protease." American Chemical Society 241st national meeting, Anaheim, CA. March 27-31, 2011.

Skills

- Thorough understanding of synthetic organic lab techniques, which include air-free reactions, handling pyrophoric reagents, normal and reverse-phase chromatography (Teledyne ISCO and Biotage Isolera).
- Understanding of instrumental protocol necessary for operation of High Performance Liquid Chromatography (HPLC), Mass-Spectrometry, and Liquid Chromatography-Mass Spectrometry (LCMS).
- Experienced in acquisition and interpretation of 1-D and 2-D nuclear magnetic resonance (NMR) experiments.

Honors and Awards

- | | |
|--|------------------------------|
| ○ Howard Hughes Medical Institute Full Scholarship Program | Sept 2011 - June 2013 |
| ○ American Institute of Chemists Foundation Award, CSUF | May 2013 |
| ○ Glenn Nagel Undergraduate research Award, CSUPERB | Jan 2013 |
| ○ Dean's List, CSUF | Sep 2009 - June 2013 |
| ○ Associated Student Inc. Research Grant, CSUF | Mar 2011 |

ABSTRACT OF THE DISSERTATION

Assigning the Absolute Configuration of Amines Using the Competing Enantioselective Conversion (CEC) Method

Progress Towards the Synthesis of the Western Fragment of Phainanoid F

Synthesis of Kujounins A₁ and A₂ Using a Biosynthesis Inspired Approach

Total Synthesis of the Proposed Structure of (-)-Himeradine A

By

Alexander Burtea

Doctor of Philosophy in Chemistry

University of California, Irvine, 2019

Professor Scott D. Rychnovsky, Chair

The first chapter of this thesis focuses on the development of the competing enantioselective conversion method (CEC) for the assignment of the absolute configuration of amines. This method utilizes Bode's hydroxamic esters as the source of chirality. The optimization and control studies for this method are discussed in detail. Many examples, including complex drugs and natural products, are examined and a preliminary mnemonic was developed.

The second chapter focuses on the efforts toward the synthesis of the western fragment of phainanoid F. Background is given on the previous failed routes in our laboratory and how they led to the new synthetic route. Three different approaches toward the fragment are discussed, one

which failed, and the other two that are not yet complete. If efforts are placed in these approaches, it seems likely that one will afford the western fragment in due time.

The third chapter will provide details on the synthesis of kujounins A₁ and A₂ in our laboratory. Kujounin A₂ was synthesized in 7 steps from L-ascorbic acid based on a biomimetic approach. A new biosynthetic pathway is presented that seems likely to produce the kujounins. A key Tsuji-Trost reaction followed by an ozonolysis afforded the core of the natural product in just two steps. The sensitive disulfide moiety was more difficult to install but was accomplished in a few steps. Biological activity studies are pending.

The last chapter discusses the total synthesis of the proposed structure of (–)-himeradine A. An overview of background and previous work accomplished on himeradine A in our lab is provided. The total synthesis was completed in just 17 longest linear steps and only 10 of those steps required column chromatography. This synthesis features a key tartaric acid salt resolution of a piperidine, a B-alkyl Suzuki of two complex fragments, a photoredox conjugate addition, and a transannular Mannich reaction that forms 5 bonds in 1 step. The spectral data was consistent with Shair's synthetic sample and had some discrepancies with the isolated natural product. Epimers of himeradine A will be synthesized in our laboratory in due time.

Chapter 1. Assigning the Absolute Configuration of Amines Using the Competing Enantioselective Conversion (CEC) Method

1.1 Abstract

The development of the Competing Enantioselective Conversion (CEC) method for assigning the absolute configuration of cyclic amines is described herein. This method utilizes two pseudo-enantiomeric acyl transfer reagents based on Bode's chiral hydroxamic acids. The analysis is operationally simple, only requires micrograms of material, and can be completed in six hours. The method was successful in assigning the absolute configuration of many chiral amines, including two drugs and two natural products.

1.1 Introduction

Determining the absolute configuration of an enantioenriched stereocenter is an essential step in the discovery of natural and synthetic molecules.¹ Due to the lack of practical methods, this is often the most difficult aspect of the chemical characterization process. Current methods to assign absolute stereochemistry include circular dichroism (CD), Mosher's method, and X-ray crystallographic analysis. However, these methods can be difficult to perform, time-intensive, and may lead to incorrect assignment.²

Circular Dichroism relies on comparing the experimental and theoretical differential absorption spectra generated by subjecting a chiral molecule to both left and right circularly polarized infrared light. Substantial computer power is required to generate the theoretical spectra and experimental spectra often contain instrument or solvent artifacts which complicate the analysis.³ Mosher's method utilizes a chiral derivatizing agent, α -methoxy- α -trifluoromethylphenylacetic acid (MTPA), or its corresponding acid chloride. In two separate reactions, a secondary alcohol or amine of unknown absolute configuration can be reacted with (*R*)- and (*S*)-MTPA to form two diastereomeric MTPA esters or amides. Each product is then analyzed by ¹H or ¹⁹F NMR, and comparison of the chemical shift difference between the two diastereomers formed allows for elucidation of absolute configuration.⁴ While routinely used, this method requires a significant amount of material to carry out both reactions, as well as four to six hours of active effort over a one to two day period.⁵

X-ray crystallography can be used to assign the absolute configuration of crystalline substrates through the analysis of a molecule's diffraction pattern. While considered to be the most accurate method, many small organic molecules are not crystalline, and a crystal of a certain size, quality, and shape is necessary to get meaningful data.⁶ Unfortunately, even with the current

methods available, many molecules have been misassigned or tentatively assigned, and later reassigned through total synthesis.⁷ Therefore, there remains a need for a practical, robust, and rapid method for the assignment of the absolute configuration of stereocenters.

1.1.1 The Competing Enantioselective Conversion Method

Over the past nine years the Rychnovsky lab has been developing the competing enantioselective conversion (CEC) method towards assigning the absolute stereochemistry of various functional groups. The basis of this method is founded upon classical kinetic resolution principals. However, instead of derivatizing a racemic starting material to obtain enantioenriched product, enantioenriched starting material is used. For instance, if an enantioenriched starting material (A) is reacted in two separate reactions, one with an (*R*)-resolving reagent and the other with an (*S*)-resolving reagent, they would produce the same product (B) (Figure 1-1). However, the rates of these reactions would differ. One resolving reagent would be the “matched” case, while the other would be the “mismatched.” The “matched” case would lead to a fast reaction and therefore high conversion. Thus, by measuring the conversion of these separate reactions, one can use an empirically derived mnemonic developed through testing a number of substrates with known configuration and assign the configuration.

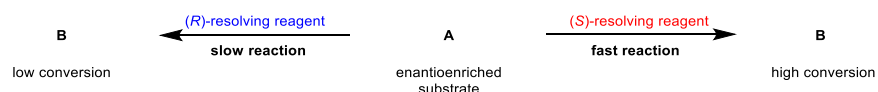


Figure 1-1. General procedure for a CEC reaction.

The theory behind the difference in the two reaction rates can be explained by figure 1-2. If starting material A is reacted with (*S*)-resolving agent to produce product B, there will be an activation energy of ΔG_S^\ddagger . Similarly, the reaction with (*R*)-resolving agent will result in activation energy ΔG_R^\ddagger . One of these, in this case ΔG_S^\ddagger , will be lower in energy which will allow for a faster

reaction with the “matched” resolving reagent. The other will be higher in energy and thus a slower reaction. The $\Delta\Delta G^\ddagger$ is the difference in energy between the two diastereomeric transition states which ultimately leads to the difference in rates of the reactions.

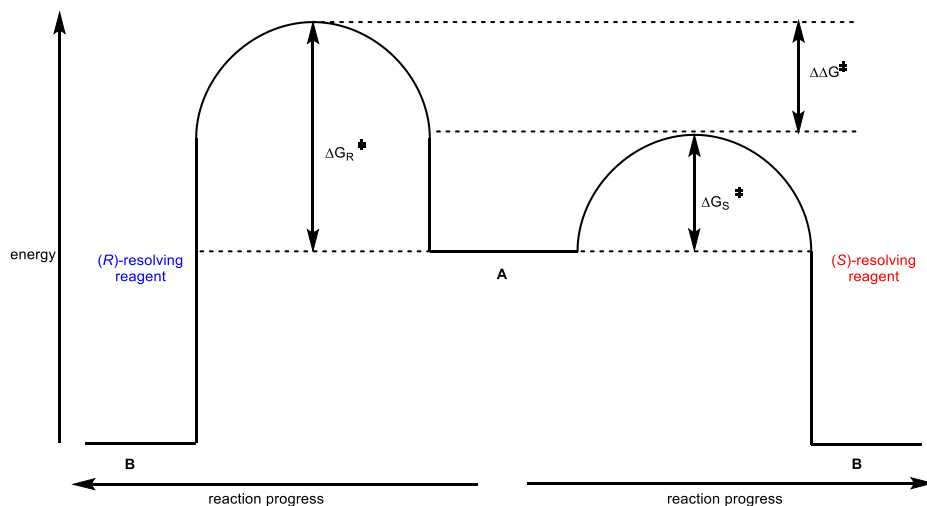


Figure 1-2. Energy diagram displaying two separate resolutions.

1.2 Previous Work

1.2.1 CEC of Alcohols

Currently, there are two separate approaches to the CEC method. The first approach uses two parallel reactions, each containing a single enantiopure substrate (1-1), and one of the two enantiomers of a kinetic resolution reagent, in this case homobenzotetramisole (HBTM) (Figure 1-3). The substrate preferentially reacts with either (*R*)-HBTM or (*S*)-HBTM, and measuring the amount of product formed in each reaction by ^1H NMR or TLC displays which reagent reacted faster. Using a mnemonic, the absolute configuration of the substrate can be extrapolated based on which reagent reacted faster with the substrate. This approach was successfully used to assign the configuration of many chiral alcohols including the select examples shown below.⁸ The same

catalytic system was also used in assigning the absolute configuration of lactams and oxazolidinones.⁹

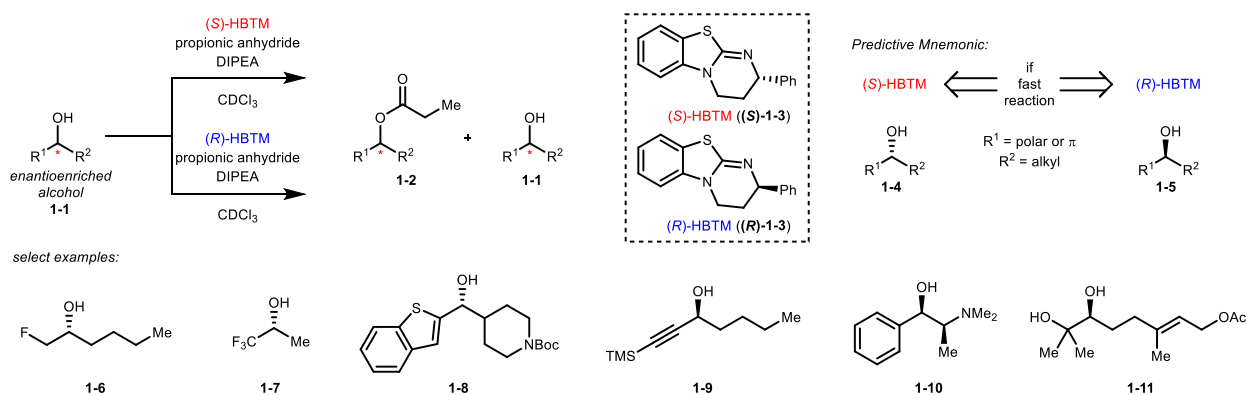
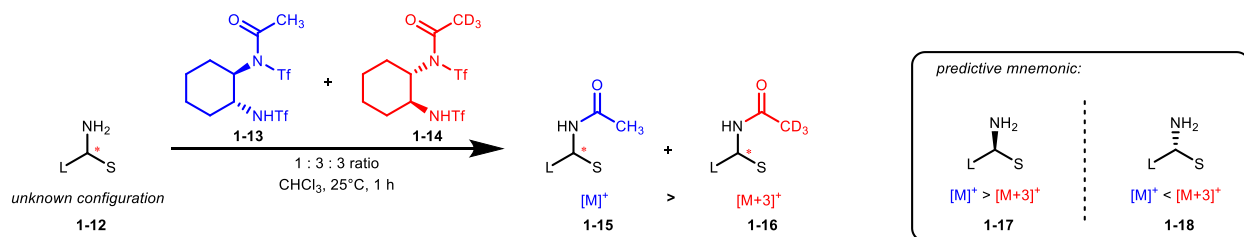


Figure 1-3. Process for assigning the absolute configuration of secondary alcohols and select examples that were successfully assigned.

1.2.2 CEC of Primary Amines

The CEC method was further expanded to primary amines in 2012. However, this method was conducted in a slightly different manner. This approach of the CEC method allowed the absolute configuration of a stereocenter to be determined through only a single reaction (Scheme 1-1). Rather than analyzing multiple reactions through ^1H NMR, each reaction was evaluated by measuring the amount of each product formed using electrospray ionization mass spectrometry (ESI-MS). This approach reveals which reagent reacts preferentially, allowing extrapolation of the absolute configuration via a predictive mnemonic. Previous work in the Rychnovsky laboratory used this method to assign the configuration of primary amines using Mioskowski's enantioselective acylating agents.¹⁰ This method utilized an acetyl group on one enantiomer of the kinetic resolution reagent (**1-13**) and acetyl- d_3 (**1-14**) on the other. However, this system lacked selectivity for secondary amines and had issues with loss of deuterium atoms over time, thus complicating the analysis and making it necessary to develop a more consistent method.

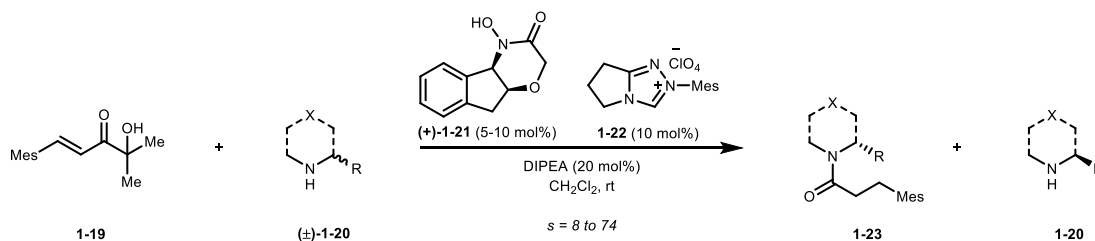
Scheme 1-1. Processes for assigning the absolute configuration of primary amines.



1.2.3 Inspiration from Bode's Work

In 2011, Bode and co-workers published a novel method for the kinetic resolution of cyclic secondary amines.¹¹ Their initial report involved the use of catalytic amounts of NHC **1-22** alongside hydroxamic acid (+)-**1-21** as a cocatalyst (Scheme 1-2). The mechanism for this reaction is as follows: deprotonated NHC **1-22** adds into α' -hydroxyenone **1-19**, which induces a retro-benzoin reaction. The resulting Breslow intermediate is protonated twice to afford the active acylazolium specie which chemoselectively acylates hydroxamic acid (+)-**1-21** in the presence of the amine. The acylated hydroxamic acid can then enantioselectively transfer the acyl group to the amine. They were able to successfully apply this chemistry to a variety of piperidines, morpholines, piperazines, and even a few azepanes with selectivity values that ranged from 8 to 74.

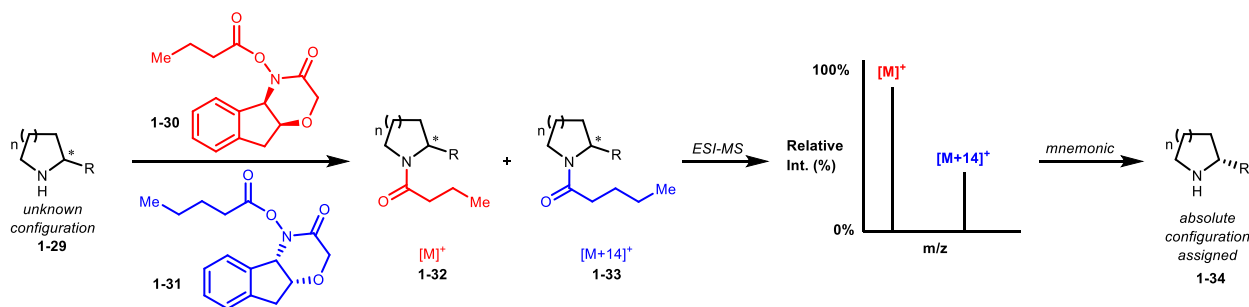
Scheme 1-2. Bode's catalytic kinetic resolution of cyclic amines.



In the same report, they examined the effects of using different acyl groups on the resolution of amines (Scheme 1-3). In order to simplify the analysis, they synthesized four different hydroxamic esters (**1-25** – **1-28**) and used them in stoichiometric amounts. They were able to

in the mass spectrum. By analyzing the relative ratio of products formed via ESI-MS, the preferentially reacting acyl transfer reagent can be determined, and the stereochemistry of the amine elucidated using a mnemonic.

Scheme 1-4. Proposed process for determining the absolute configuration of amines using the CEC method.

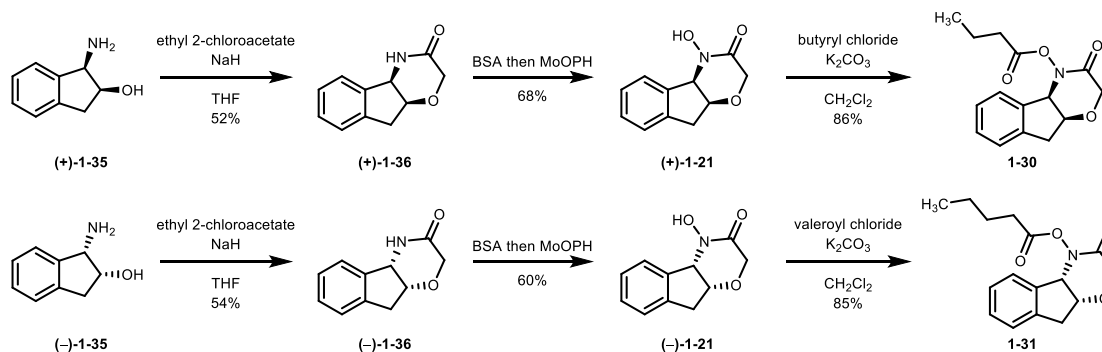


1.3 Results

1.3.1 Synthesis of the Pseudo-enantiomeric Acyl Transfer Reagents

With a feasible proposed CEC method in hand, the first task was to prepare the two pseudo-enantiomers. Each acyl transfer reagent was synthesized from the respective enantiomer of the commercially available amino-indanol **1-35** (Scheme 1-5). Treatment of **1-35** with ethyl chloroacetate afforded morpholinone **1-36**, which, when treated with *N,O*-Bis(trimethylsilyl)acetamide (BSA) followed by oxodiperoxymolybdenum(pyridine)(hexamethylphosphoric triamide) (MoOPH), afforded hydroxamic acid **1-21**. Acylation with either butyryl or valeryl chloride provided the two pseudo-enantiomeric acyl transfer reagents **1-30** and **1-31**, respectively. This route was performed on multi-gram scale and efficiently allows for access to each pseudo-enantiomeric acyl transfer reagent.

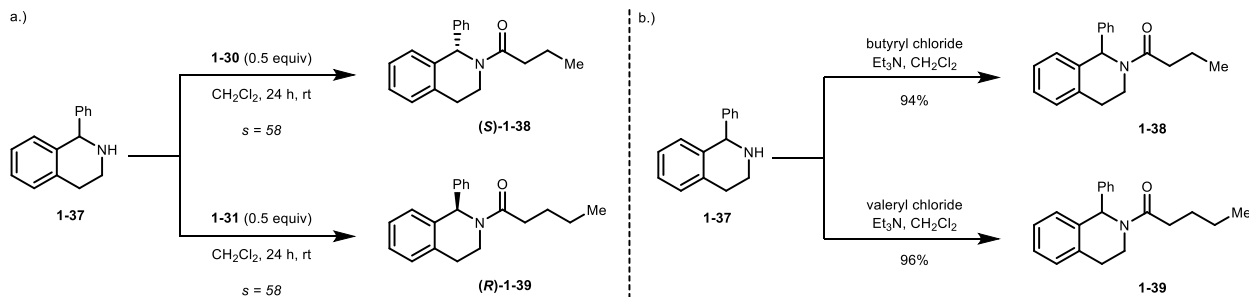
Scheme 1-5. Synthesis of the pseudo-enantiomeric acyl transfer reagents



1.3.2 Selectivity and ESI-MS Quantification Validation

With each pseudo-enantiomeric acyl transfer reagent synthesized, we needed to validate that there was no selectivity difference between them. Bode previously demonstrated that the selectivity value between a three- and five-carbon acyl group on the hydroxamic acid (**1-21**) had no difference in selectivity (Scheme 1-3). However, we wanted to assure that the same was true for a four- and five-carbon acyl group. Thus, we accomplished this by conducting kinetic resolutions of racemic amine **1-37** with each acyl transfer reagent separately (Scheme 1-6, a). To no surprise, the selectivity value of each resolution was identical.

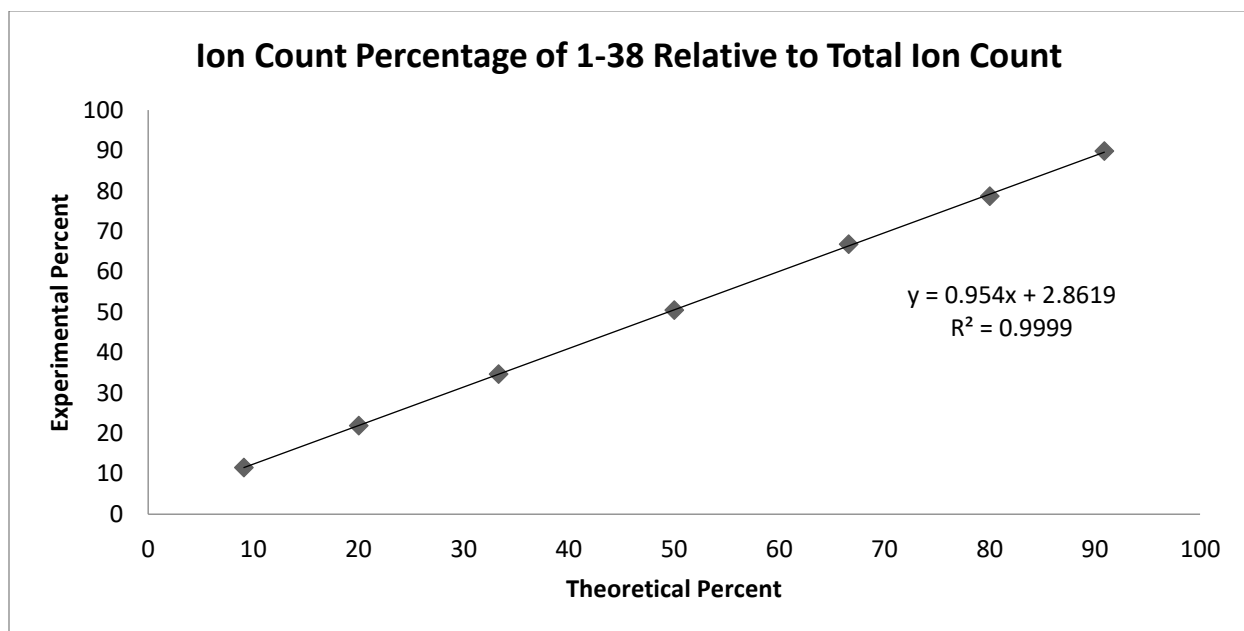
Scheme 1-6. Kinetic resolution using acyl transfer reagents **1-30** and **1-31** (a) and synthesis of amides **1-38** and **1-39**.



The last control experiment that was necessary before testing the CEC reaction was ensuring that there was no difference between the ionization of the two amides formed from the CEC reaction by ESI-MS. In order to do so, amides **1-38** and **1-39** were synthesized by acylating amine **1-37** with either butyryl or valeryl chloride (Scheme 1-6, b). Seven solutions were prepared

containing the following mixtures of **1-38:1-39**: 10:1, 4:1, 2:1, 1:1, 1:2, 1:4, and 1:10. Each mixture was analyzed by ESI-MS and the ion count of the $[M+H]^+$ and $[M+Na]^+$ was summed to get the total ion count for **1-38** and **1-39**. A validation curve was generated by plotting the theoretical percent ion count of **1-38** in seven different ratios of **1-38** to **1-39** versus the experimental percent ion count of **1-38** (Graph 1-1).

Graph 1-1. The theoretically expected percent of **1-38** relative to total ion count of **1-38** and **1-39** versus the experimental percentages.



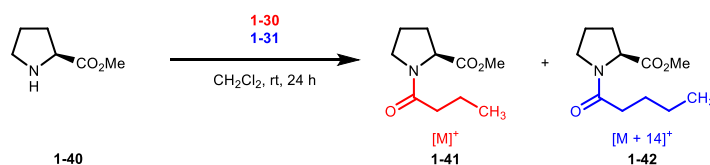
The resulting plot shows a linear trend, as one would expect, with an R^2 value near 1. This gave us confidence that the ESI-MS was a viable instrument for providing accurate ratios of amides formed in the CEC reaction. After verifying that the pseudo-enantiomeric acyl transfer reagents presented no difference in selectivity and that the ESI-MS was a suitable instrument for analysis of the amides formed in the reaction, we turned to optimizing the CEC reaction for cyclic amines.

1.3.3 Optimization of the CEC Reaction for Cyclic Amines

Though Bode stated that five-membered cyclic amines showed poor selectivity in the kinetic resolutions, we found that L-proline methyl ester (**1-40**) gave suitable selectivity for our

CEC reaction. Thus, L-proline methyl ester was chosen as the model substrate for optimization due to ease of access and structural simplicity. Concentration of the amine and acyl transfer reagents were first optimized and the ratio of amine to acyl transfer reagents was tested (Table 1-1, entries 1-3). It was found that increasing the amount of acyl transfer reagents in solution led to lower product ratios but higher conversion. When the reaction concentrations were decreased, this led to increased product ratios and decreased percent conversions, as expected (entries 4-6).

Table 1-1. Optimization of reaction concentrations for the CEC reaction.



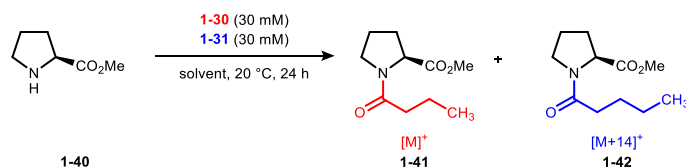
entry	[amine] (mM)	[1] (mM)	[2] (mM)	$[M]^+$:	$[M+14]^+$	σ^a	% conv
1	2	20	20	20	:	80	1	30
2	4	40	40	22	:	78	1	49
3	8	80	80	23	:	77	1	72
4	10	100	100	24	:	76	2	82
5	10	50	50	21	:	79	1	71
6	10	30	30	21	:	79	1	62

^a Standard deviation calculated based on three trials

After screening various reaction concentrations, an extensive solvent screen was performed (Table 1-2). An amine concentration of 4 mM and a concentration of 40 mM for each **1-30** and **1-31** was chosen because the conversion was low enough to allow for further optimization and high enough to see product in the ESI-MS. Chlorinated solvents and polar solvents were shown to be compatible with this method (entries 1-7). Phenyl containing solvents seemed to drastically increase the percent conversion while still maintaining a high product ratio (entries 8-10). Etheral solvents increased product ratios (entries 11-14) and linear chain etheral solvents also significantly increased the percent conversion (entries 12 and 14). Interestingly, the highest ratios were observed when using branched alcoholic solvent (entries 16-17). There was a direct

correlation of increasing ratio when going from a primary to secondary to tertiary alcoholic solvent. Due to high selectivity and conversion, *tert*-amyl alcohol was chosen as the optimal solvent.

Table 1-2. Optimization of solvent for the CEC reaction.



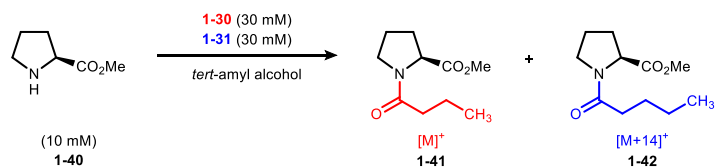
entry	solvent	[M] ⁺	:	[M+14] ⁺	σ ^a	% conv
1	CH ₂ Cl ₂	22	:	78	1	49
2	CHCl ₃	15	:	85	2	49
3	MeCN	22	:	78	1	55
4	DMSO	19	:	81	1	53
5	DMF	19	:	81	2	52
6	EtOAc	16	:	84	0	62
7	acetone	22	:	78	1	41
8	benzene	19	:	81	0	77
9	toluene	16	:	84	0	76
10	trifluorotoluene	21	:	79	0	78
11	THF	14	:	86	0	58
12	Et ₂ O	13	:	87	0	75
13	1,4-dioxane	16	:	84	1	59
14	Bu ₂ O	19	:	81	1	86
15	MeOH	23	:	77	2	52
16	<i>i</i> -PrOH	11	:	89	0	81
17	<i>tert</i> -amyl alcohol	9	:	91	0	77

^a Standard deviation calculated based on three trials.

After an exhaustive solvent screen, attention was pointed toward minimizing the reaction time (Table 1-3). Thus, temperatures of 20, 40, and 60 °C for 1, 3, and 6 hours were tested. As expected, when the temperature was increased, the product ratio decreased and the percent conversion increased. The reproducibility of the ratios was also more consistent when allowing longer reaction times and higher temperatures. This is due to the fact that higher conversion leads to higher ion count on the ESI-MS, which generally leads to more consistent data. Table 1-3, entry

9 was chosen as the optimized reaction conditions, because it maintained a high ratio while driving the reaction to near completion.

Table 1-3. Optimization of temperature and time for the CEC reaction.



entry	time (h)	temp (°C)	[M] ⁺	:	[M+14] ⁺	σ ^a	% conv
1	1	20	4	:	96	3	7
2	3	20	8	:	92	2	22
3	6	20	7	:	93	1	37
4	1	40	9	:	91	2	16
5	3	40	8	:	92	1	43
6	6	40	9	:	91	2	68
7	1	60	12	:	88	1	52
8	3	60	11	:	89	0	89
9	6	60	13	:	87	0	98

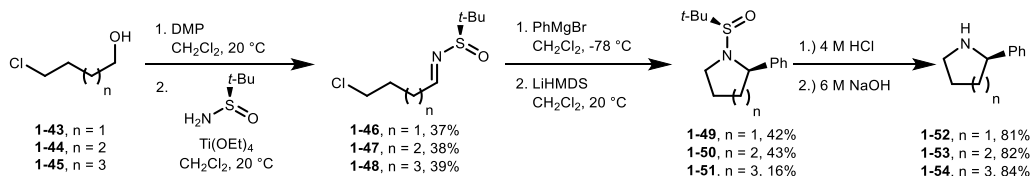
^a Standard deviation calculated based on three trials.

1.3.4 Synthesis of Chiral Piperidines

With an optimized CEC reaction in hand, we turned our attention to synthesizing chiral amines in order to investigate the substrate scope of the reaction. This was accomplished in a literature precedented five-step sequence using Ellman's auxiliary as the chiral source (Scheme 1-7). DMP oxidation followed by condensation of Ellman's auxiliary using chloroalcohol **1-43**, **1-44**, or **1-45** afforded the resulting sulfinimides. The low yields of this two-step sequence were attributed to the volatility of the resulting aldehyde. Regardless, phenyl magnesium bromide was added into each sulfinimide followed by base treatment with LiHMDS to complete the cyclization. In the case of **1-51**, the cyclization proved difficult due to the formation of a 7-membered ring. Acid cleavage of the chiral auxiliary followed by a basic workup provided pyrrolidine **1-52**, piperidine **1-53**, and azepane **1-54**. This sequence was also attempted with other Grignard reagents,

such as methyl and vinyl magnesium bromide, however, the resulting free amines proved difficult to isolate due to the volatile nature of each compound.

Scheme 1-7. Synthesis of chiral cyclic amines using Ellman's auxiliary.



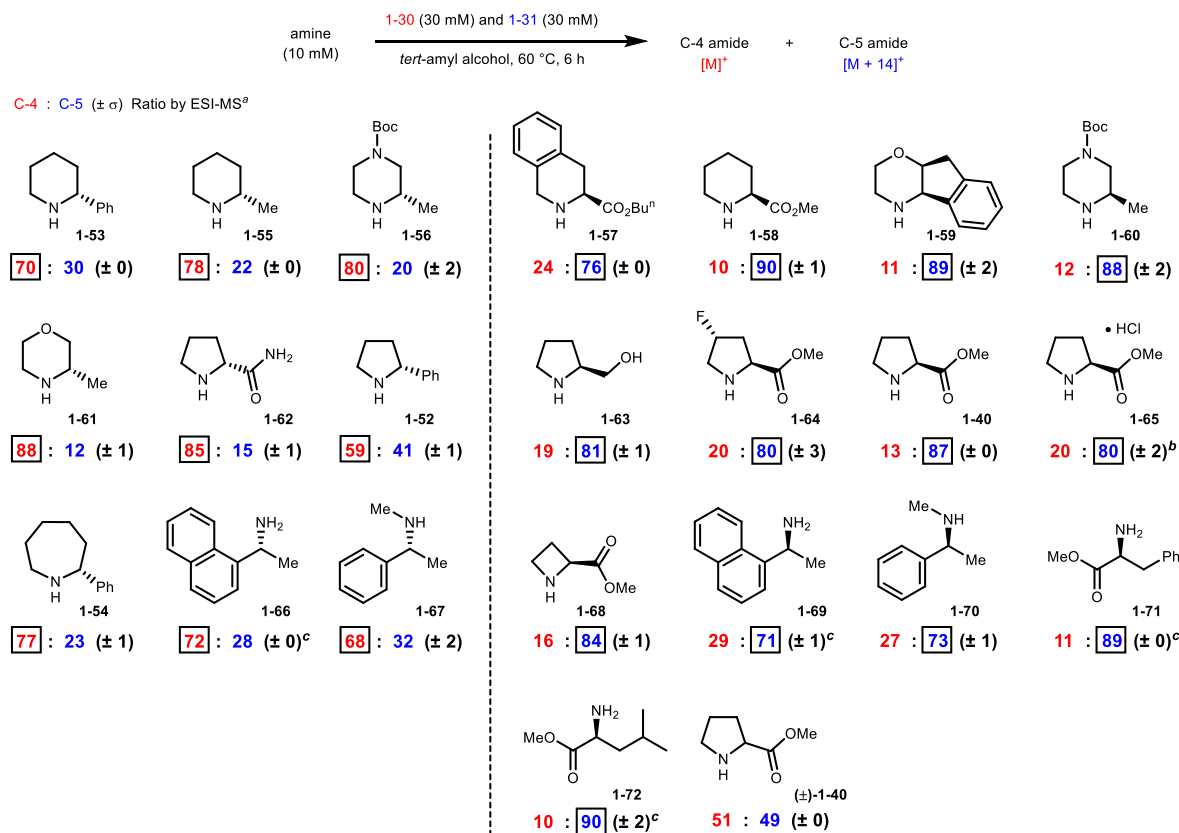
1.3.5 Substrate Scope Investigation

The results of the CEC reaction with a variety of amines are presented in Table 1-4. The reactions were run in small vials with 100 μ L of solvent; each evaluation used only 1.0 μ mol of substrate (e.g. 0.16 mg of amine **1-53**). This illustrates one of the major advantages of using ESI-MS as the source of analysis of the CEC reactions. As another control experiment, racemic proline methyl ester ((\pm)-**1-40**) was run under these conditions and gave nearly a 50:50 ratio of C4 to C5 acylation. We conclude that the difference in acylation rate between the four- and five-carbon acyl transfer reagents is negligible. Again, this conclusion is consistent with Bode's observation that three- and five-carbon acyl groups lead to the same enantioselectivity.

Six-membered ring structures **1-53** – **1-61** showed reasonable selectivity regardless of the adjacent substituent's identity or the presence of other heteroatoms in the ring. The five-membered ring examples **1-62** – **1-65** showed larger variations in their selectivity but were sufficient enough to assign configuration in each case. The hydrochloride salt (**1-65**) was used directly in the reaction by adding triethylamine to liberate the free amine *in situ*. The seven-membered ring azepane (**1-54**) resulted in selectivity similar to the corresponding piperidine **1-53** and azetidine **1-68** had similar selectivity to L-proline methyl ester **1-40**. Finally, a few non-cyclic secondary amine (**1-67** and **1-70**) and some primary amines were examined. The primary amines were much more

reactive which allowed us to run the reactions at room temperature for 1 hour. These non-cyclic amines showed selectivity when a π -system was present next to the stereocenter.

Table 1-4. CEC substrate scope evaluation of amines.



^a Calculated based on three trials. ^b Reaction was run with 1 μ L of triethylamine. ^c Reaction was run at 20 $^\circ$ C for 1 hour.

From inspecting the results in table 1-4, it is apparent that a trend exists. In all cases presented for the cyclic amines, if the amine is drawn in the orientation shown above (R group to the right) and the R group is pointed backwards, formation of the C4 amide was dominant. Conversely, if the R group was pointed forwards, the C5 amide was the major product. For the non-cyclic amines, if the π -system is drawn to the left and the amine is pointed backwards then the C4-amide was dominant. These trends allowed us to form a preliminary mnemonic for assigning the absolute configuration of amines using acyl transfer reagents **1-30** and **1-31** (Figure 1-4). This

mnemonic seems to be robust for cyclic amines and should be used with caution when trying to assign non-cyclic amines because the mnemonic is based on only few substrates.



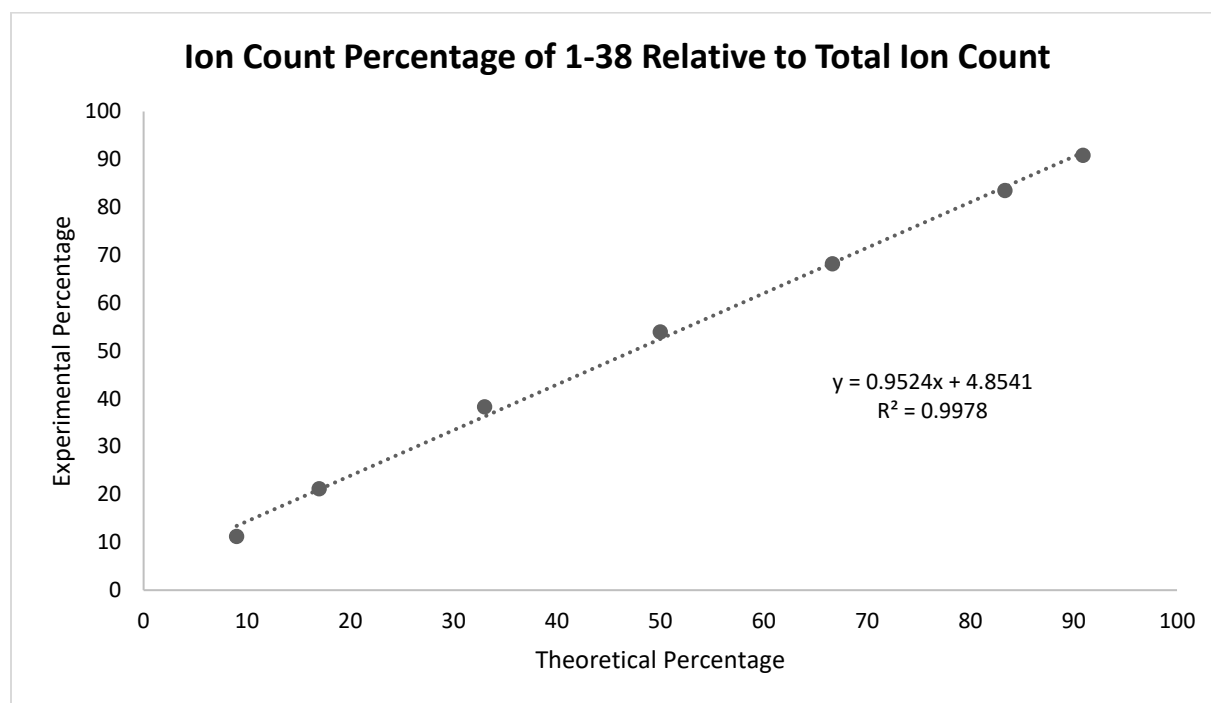
Figure 1-4. Preliminary mnemonic for assigning the absolute configuration of amines using acyl transfer reagents **1-30** and **1-31**.

1.3.6 Triple-Quadruple Mass Spectrometer as a Mode of Detection

Upon investigating the substrate scope of this CEC reaction, we realized that some substrates, once acylated, contained the same m/z as either the resulting hydroxamic acid (**1-21**) or one of the acyl transfer reagents (**1-30** or **1-31**). Due to this limitation by ESI-MS, we investigated the use of a triple quadrupole mass spectrometer (QqQ MS). Not only is a QqQ MS more sensitive than an ESI-MS, but it also allows for separation of compounds present in a complex mixture through a column followed by the quadrupoles. The QqQ MS only searches for desired compound masses and if two substances contain the same mass, they can be differentiated via retention time.

We first wanted to validate the quantification capability of the QqQ MS as we did previously for the ESI-MS (Graph 1-2). We did so in the same manner by preparing seven solutions containing the following mixtures of **1-38**:**1-39**: 10:1, 4:1, 2:1, 1:1, 1:2, 1:4, and 1:10. Each mixture was analyzed by QqQ MS and the ion counts of **1-38** and **1-39** were obtained. A validation curve was generated by plotting the theoretical percent ion count of **1-38** in seven different ratios of **1-38** to **1-39** versus the experimental percent ion count of **1-38** (Graph 1-2). Just like before, the resulting plot showed a linear trend with an R^2 value near 1. This gave us confidence that the QqQ MS was a viable instrument for providing accurate ratios of amides formed in the CEC reaction.

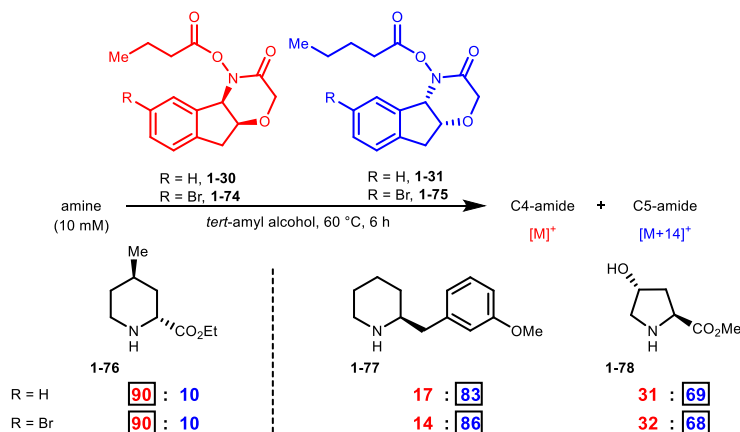
Graph 1-2. The theoretically expected percent of **1-38** relative to total ion count of **1-38** and **1-39** versus the experimental percentages.



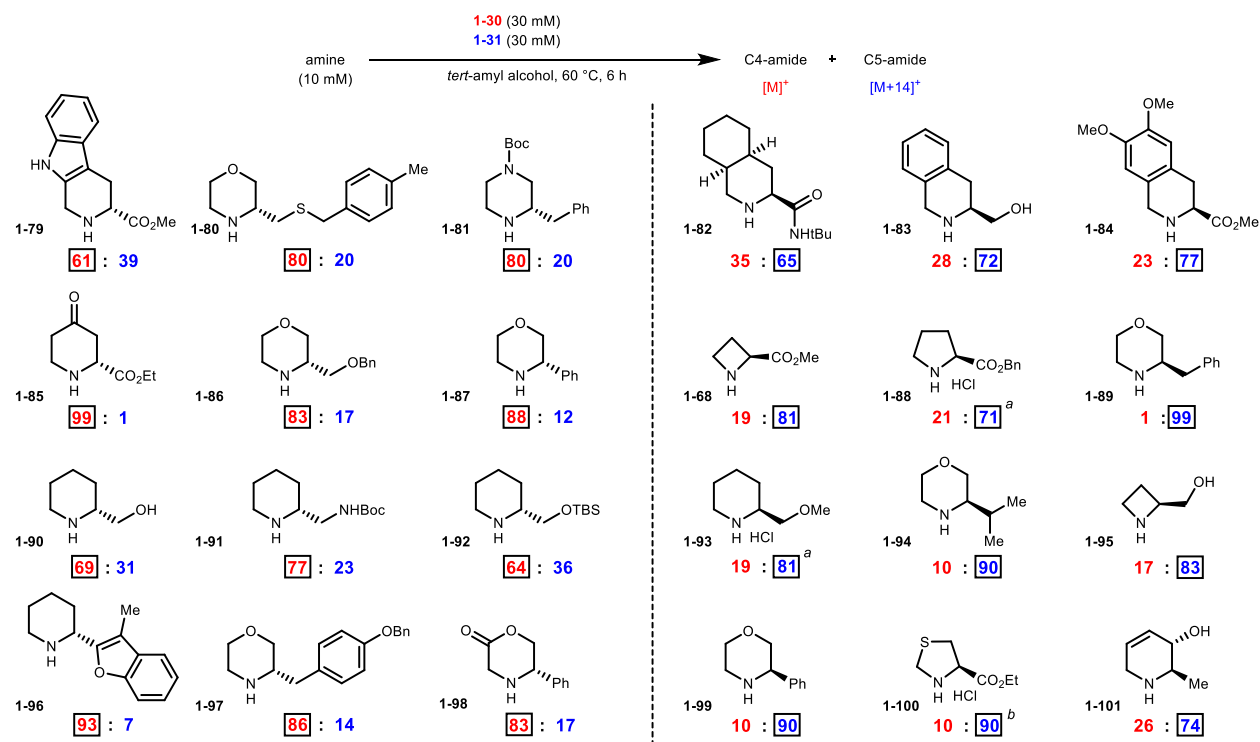
1.3.7 Substrate Scope Expansion

At this point in the project, I was joined by Charles Dooley III and Christina Mitilian in an effort to further expand the scope of this CEC reaction. We began by exploring a new set of acyl transfer reagents that were reported by Bode to have superior selectivity in the resolution of amines. Each brominated hydroxamic acid was purchased from Sigma-Aldrich and acylated to provide **1-74** and **1-75** (Table 1-5). Unfortunately, when using our CEC conditions, we observed no major selectivity difference on substrates **1-76**, **1-77**, and **1-78**. These results convinced us that the brominated acyl transfer reagents can be used for the CEC reactions, but provided no substantial benefit. With grams of the non-brominated acyl transfer reagents in hand, we proceeded to investigate the scope of this method with **1-30** and **1-31**.

Table 1-5. Investigation of the selectivity difference between acyl transfer reagents **1-30** and **1-31** and bromo acyl transfer reagents **1-74** and **1-75**.



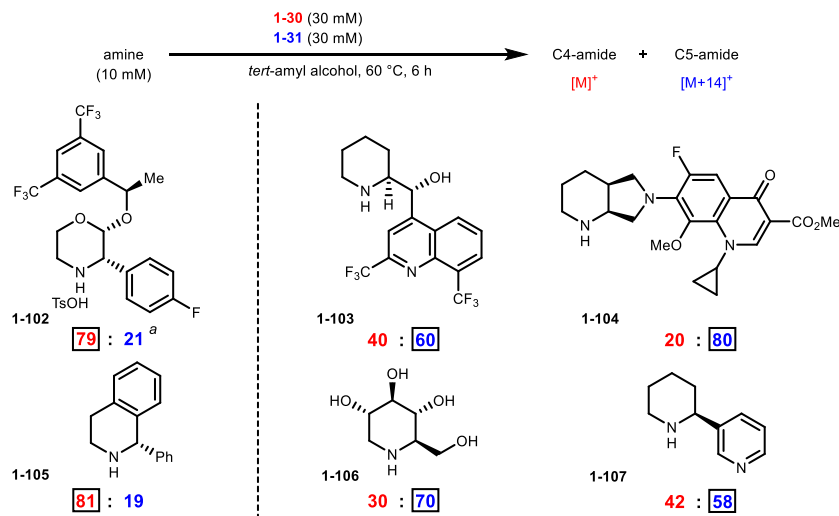
A variety of new substrates were examined with the CEC method using the QqQ MS as a mode of product detection (Table 1-6). Many of the substrates were purchased while all the morpholines were donated by the Salzameda group. Substrate **1-101** was donated by the Vanderwal group and **1-96** was donated by Bo Qu at Boehringer Ingelheim. All morpholines and piperazine **1-81** were successfully assigned with good selectivity. Substrate **1-79** showcased the ability to chemoselectively react with the more reactive secondary amine over the indole nitrogen. Azetidines **1-68** and **1-95** demonstrated that 4-membered rings are suitable for this method. Benzofuran **1-96** illustrated that some bulky groups are tolerated at that position, however other large aryl groups were unsuccessful. In the case of thiol **1-100**, the reaction was run for 48 hours due to lack of reactivity presumably due to the sulfur pulling electron density from the amine. This large substrate table demonstrates the versatility and generality of this CEC method.

Table 1-6. Substrate scope investigation of the amine CEC reaction.

^a Reaction was run with 1 μL of triethylamine. ^b Reaction was run at for 48 hours.

With a large number of amines examined by the CEC reaction, we turned to investigate medically relevant amines (Table 1-7). Amines **1-102** and **1-105** are precursors to Aprepitant (Emend) and Solifenacin (Vesicare), respectively, and were successfully assigned by the CEC method with good selectivity. Mefloquine (**1-103**), sold under the brand name Lariam, was also assigned, albeit in low selectivity. Interestingly, Bode reports the kinetic resolution of Mefloquine in much higher selectivity.¹² The methyl ester derivative of Moxifloxacin (**1-104**), which is an antibiotic used to treat a number of bacterial infections, was successfully assigned. Moxifloxacin is on the World Health Organization's List of Essential Medicines. Finally, the two natural products, 1-deoxynojirimycin **1-106** (α -glucosidase inhibitor) and anabasine **1-107** (insecticide), were successful substrates in this CEC method. Ritalin, used to treat ADHD, was also examined but did not show the expected selectivity.

Table 1-7. Medicinally relevant amines in which the stereochemistry was successfully assigned by the CEC.



^a Reaction was run with 1 μ L of triethylamine.

1.3.8 Unsuccessful Substrates

This newly developed CEC method is quite general in terms of substrates, but there are some limitations. Figure 1-5 displays examples that were unsuccessful using our CEC analysis. If the substrate is too sterically hindered (**1-108** and **1-109**) the acyl transfer reagents will not react. In the case of pyrrolidine **1-110** we observed reactivity, but the reaction was not selective. It is not apparent as to why this particular pyrrolidine was not selective, however we generally observe pyrrolidines to be less selective than 6-membered rings. Substrates **1-111** and **1-112** were not reactive with our system due to the highly electron-withdrawing “CF₃” groups. Another class of amines that were unreactive with our acyl transfer reagents were aniline based amines (**1-113** and **1-114**). Having the aryl group directly attached to the amine decreases its nucleophilicity enough to cease acylation. Lastly, *cis*-2,4-disubstituted piperidines (**1-115**) proved to be unselective.

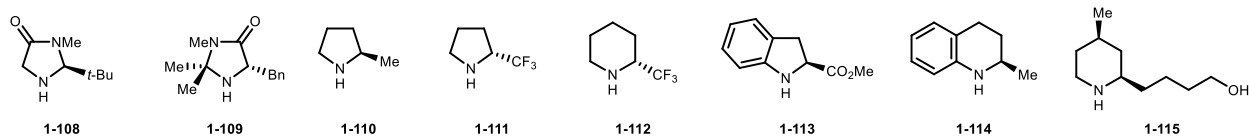
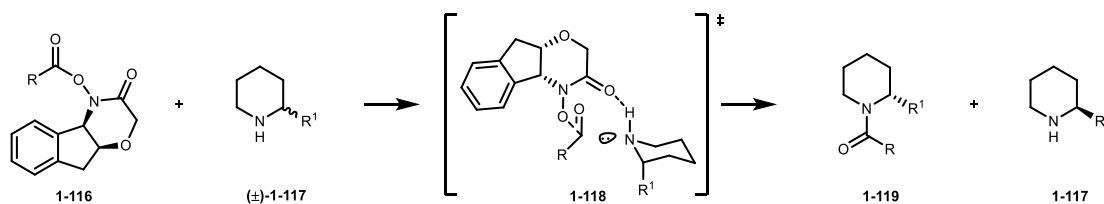


Figure 1-5. Substrates unsuccessfully assigned by the CEC method.

The lack of selectivity for *cis*-2,4-disubstituted piperidines can be rationalized by Bode and Kozlowski's proposed transition state for the reaction (Scheme 1-8).¹³ The Kozlowski group was able to perform DFT calculations that revealed a concerted seven-membered transition state (**1-118**) to be the lowest energy.¹⁴ They found that this pathway was 11 kcal/mol lower in energy than the next lowest pathway. Through DFT calculations they were also able to identify a model for the diastereomeric transition state. To their surprise, the calculations suggested that the nitrogen α -substituent must adopt an axial conformation while the N-H hydrogen bonds with the carbonyl of the hydroxamic ester. According to this model, *cis*-2,4-disubstituted piperidines would need to force both substituents in the axial position, which is very high in energy, to obtain selectivity. Bode also observed this trend with *cis*-2,4-disubstituted piperidines.

Scheme 1-8. Bode and Kozlowski's proposed transition state for the kinetic resolution of cyclic amines.



1.3.9 Future Work

The stereochemistry of many amines has been successfully assigned by this CEC method. However, this method falls short with some very important substrate classes. Aniline-based cyclic amines (tetrahydroquinolines and dihydroindoles) were unreactive with the current acyl transfer

reagents. Therefore, further studies are necessary to ensure that this class of amines may also be compatible with this method.

One possible solution to this issue would be examining various Lewis acids as additives in the reaction. This may enhance the electrophilicity of the acyl transfer reagents enough to induce reactivity while still maintaining selectivity. Another idea would be altering the structure of the acyl transfer reagents to make it more reactive. This could potentially be accomplished by adding a trifluoromethyl group to the aryl ring of the acyl transfer reagents, which can be done by a cross-coupling of the bromo-hydroxamic acids (**1-74** and **1-75**) and a trifluoromethyl group.

1.4 Conclusions

In summary, a new CEC method has been developed for assigning the absolute configuration of cyclic amines, which showed good results with four-, five-, six-, and seven-membered rings. The method is based on the chiral hydroxamic acids developed by Bode's group. Easily accessible pseudo-enantiomeric reagents **1-30** and **1-31** were reacted with the amines and the product ratios were analyzed by either ESI-MS or QqQ MS. The method requires only micrograms of material and can be completed in one day. The method is sensitive, and preliminary results suggest that it can be used with acyclic amines. The configuration of many medicinally relevant and complex compounds were successfully assigned using this method which suggests that this procedure should be useful in medicinal chemistry and natural products chemistry. We will continue to develop the scope of the method in due time.

1.5 Experimental Section

1.5.1 General Experimental

All CEC reactions were carried out under air. CDCl₃ was dried using Na₂SO₄ before use.

All volumetric glassware and NMR tubes were oven-dried prior to use. ^1H NMR and ^{13}C NMR spectra were recorded at 500 MHz and 125 MHz at 298.0 K unless stated otherwise. Chemical shifts (δ) were referenced to either TMS or the residual solvent peak. The ^1H NMR spectra data are presented as follows: chemical shift, multiplicity (s = singlet, d = doublet, t = triplet, q = quartet, m = multiplet, dd = doublet of doublets, ddd = doublet of doublet of doublets, dddd = doublet of doublet of doublet of doublets, dt = doublet of triplets, dq = doublet of quartets, ddq = doublet of doublet of quartets, app. = apparant), coupling constant(s) in hertz (Hz), and integration. High-resolution mass spectrometry was performed using GC-CI-TOF.

Unless otherwise stated, synthetic reactions were carried out in flame- or oven-dried glassware under an atmosphere of argon. All commercially available reagents were used as received unless stated otherwise. Solvents were purchased as ACS grade or better and as HPLC-grade and passed through a solvent purification system equipped with activated alumina columns prior to use. Thin layer chromatography (TLC) was carried out using glass plates coated with a 250 μm layer of 60 Å silica gel. TLC plates were visualized with a UV lamp at 254 nm, or by staining with *p*-anisaldehyde, potassium permanganate, phosphomolybdic acid, or vanillin. Liquid chromatography was performed using forced flow (flash chromatography) with an automated purification system on prepacked silica gel (SiO_2) columns unless otherwise stated. Infrared (IR) spectroscopy was performed on a Varian 640-IR on potassium bromide salt plates. Optical rotations were taken on a JASCO P-1010 polarimeter using a glass 50 mm cell with a D-line at 589 nm. Electrospray ionization mass spectrometry (ESI-MS) was analyzed on a Waters LCT Classic spectrometer in positive mode with flow injection.

1.5.2 Chemicals

All purchased chemicals were used without further purification unless otherwise noted.

CDCl₃ was purchased from Cambridge Isotope Laboratories. Propionic anhydride was purchased from Sigma-Aldrich. The following chemicals were purchased from Combi-Blocks: (2*S*)-2-methylpiperidine (**1-55**), (3*S*)-3-methylmorpholine (**1-61**), (2*R*)-pyrrolidine-2-carboxamide (**1-62**), and methyl (2*S*)-piperidine-2-carboxylate (**1-58**). The following chemicals were bought from Oakwood Chemical: tert-butyl (3*S*)-3-methylpiperazine-1-carboxylate (**1-56**), tert-butyl (3*R*)-3-methyl piperazine-1-carboxylate (**1-60**), (1*S*)-1-(naphthalen-1-yl)ethan-1-amine (**1-69**), and (1*R*)-1-(naphthalen-1-yl)ethan-1-amine (**1-66**). The following chemicals were purchased from Sigma-Aldrich: methyl (2*S*)-pyrrolidine-2-carboxylate (**1-40**), methyl (2*S*)-pyrrolidine-2-carboxylate hydrochloride (**1-65**), methyl [(1*R*)-1-phenylethyl]amine (**1-67**), methyl [(1*S*)-1-phenylethyl]amine (**1-70**) methyl (2*S*)-2-amino-4-methylpentanoate (**1-72**), methyl (2*S*)-2-amino-3-phenylpropanoate (**1-71**). [(2*S*)-pyrrolidin-2-yl]methanol (**1-63**) was purchased from Synthonix.

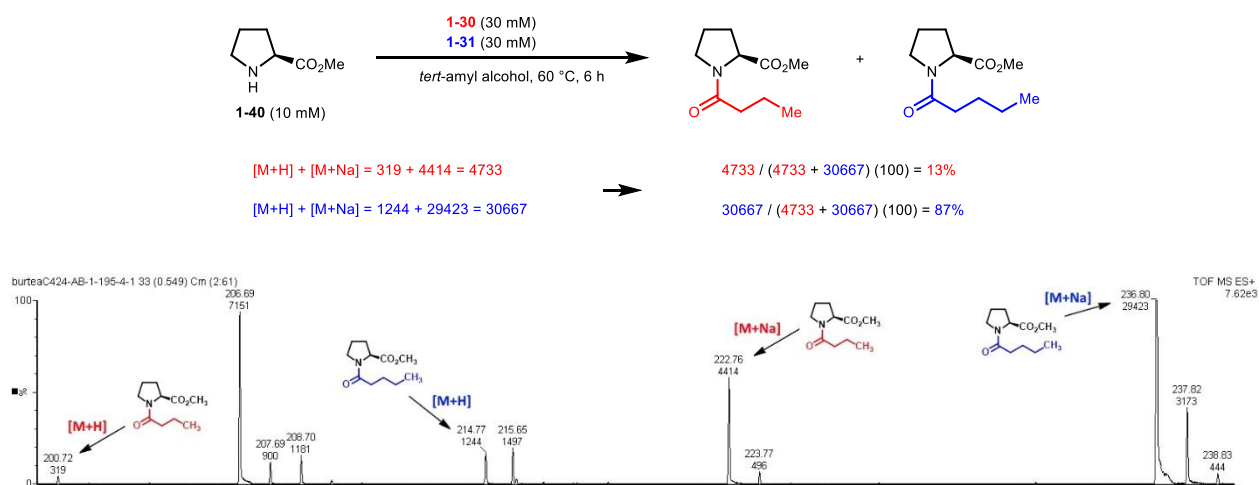
1.5.3 General Procedure #1: CEC General Reaction Procedure

The respective amine was weighed into a volumetric flask and diluted to volume with the *tert*-amyl alcohol to make a 10 mM stock amine solution (serial dilution was performed with suitable initial solvent if substrate was insoluble in *tert*-amyl alcohol). Each acyl transfer reagent (**1-30** and **1-31**) was weighed into separate volumetric flasks and diluted to volume with CH₂Cl₂ to make stock volumetric solutions. The appropriate amount of each acyl transfer reagent solution was added to a single separate volumetric flask in order to make a 60 mM one to one molar equivalent solution of each acyl transfer reagent and diluted to volume with CH₂Cl₂. To an amber mass spectrometer sample vial was added 50 uL of the 60 mM one to one acyl transfer reagent stock solution. The vial was concentrated *in vacuo* before 100 uL of the 10 mM amine solution was added. The vial was sealed with an aluminum cap and shaken lightly to mix the contents. The mixture was allowed to stand for the designated amount of time, at the designated temperature,

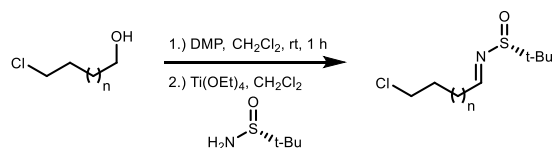
after which the cap was removed and 100 equivalents of propionic anhydride was added. The mixture was allowed to stand for 15 minutes after which 700 μL of gas chromatography grade methanol was added. The solution was mixed and 75 μL were transferred to a separate amber mass spectrometry vial containing 325 μL of methanol. The contents of the vial were mixed and the sample was analyzed by ESI-MS. In each case, the ion counts of the corresponding protonated and sodiated peaks were analyzed unless otherwise noted (due to peak overlap with other compounds in the mixture).

The following is an example CEC reaction with the corresponding ESI-MS spectra. The peaks corresponding to the $[\text{M}+\text{H}]$ and $[\text{M}+\text{Na}]$ for each amide is shown. The ion count (second number above each peak) is summed for each amide product and the ratio is calculated.

Scheme 1-9. Example of a general CEC reaction with the corresponding ESI-MS spectra.



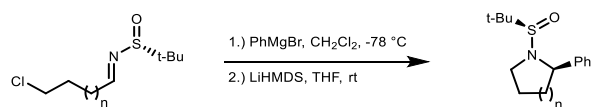
1.5.4 General procedure #2: Sulfinamide formation



To a solution of the corresponding alcohol in CH_2Cl_2 was added Dess-Martin Periodinane (DMP). After stirring for 1 hour, the reaction was quenched with an aqueous mixture of saturated

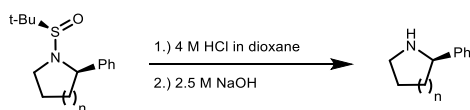
Na₂S₂O₃ and NaHCO₃ and then extracted with CH₂Cl₂ (3x). The organic layer was dried (Na₂SO₄), filtered, and concentrated under reduced pressure in an ice bath. To this crude mixture was added CH₂Cl₂, Ti(OEt)₄, and (*R*)-2-methylpropane-2-sulfinamide and the reaction was allowed to stir for 16 hours. The reaction was then quenched with saturated NaCl and filtered through celite. The resulting mixture was extracted with EtOAc (3x), dried (Na₂SO₄), filtered, and concentrated under reduced pressure. The resulting crude mixture was purified by column chromatography (silica gel, 1:1 Hex:EtOAc).

1.5.5 General procedure #3: Grignard addition and ring closure



A solution of the sulfinimide in CH₂Cl₂ was cooled to -78 °C for 10 minutes. The Grignard reagent was added dropwise while the solution was stirring rigorously. The reaction progress was monitored by TLC and saturated aqueous NH₄Cl was added upon reaction completion. The mixture was extracted with CH₂Cl₂ (3x), dried (Na₂SO₄), filtered, and concentrated under reduced pressure. Crude NMR was taken for diastereomeric ratio determination. The crude mixture was dissolved in THF before lithium bis(trimethylsilyl)amide was added dropwise. The reaction progress was monitored by TLC and saturated aqueous NH₄Cl was added upon reaction completion. The mixture was extracted with CH₂Cl₂ (3x), dried (Na₂SO₄), filtered, and concentrated under reduced pressure. The resulting crude mixture was purified by column chromatography (silica gel, 1:1 Hex:EtOAc).

1.5.6 General procedure #4: Chiral auxiliary cleavage

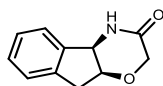


To a solution of cyclized product in MeOH was added 4 M HCl in dioxane. After stirring for 30 minutes, the solution was concentrated and water was added. The solution was extracted with EtOAc (2x). The aqueous layer was then basified with 2.5 M NaOH to pH 13. The solution was extracted with EtOAc (3x) and the organic layer was washed with brine. The organic layer was dried (Na₂SO₄), filtered, and concentrated under reduced pressure. No purification was necessary for the isolated product.

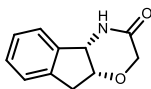
1.5.7 ESI-MS product ratio measurement verification:

To a 2 mL volumetric flask was added amide **1-38** (30.9 mg) and diluted to volume with methanol to make a 55.3 mM solution. From this solution, 18.1 μ L was transferred to a 10 mL volumetric flask and diluted to volume with methanol to make a 0.100 mM solution of **1-38**. To a separate 2 mL volumetric flask was added amide **1-39** (40.4 mg) and diluted to volume with methanol to make a 68.9 mM solution. From this solution, 14.5 μ L was transferred to a 10 mL volumetric flask and diluted to volume with methanol to make a 0.100 mM solution of **1-39**. From each 0.100 mM solution, the appropriate amount was added to a mass spectrometry vial and diluted with methanol to 200 μ L to afford the following mixtures of **1-38:1-39** = 10:1, 4:1, 2:1, 1:1, 1:2, 1:4, and 1:10. Each mixture was analyzed by ESI-MS and the ion count of [M+H]⁺ and [M+Na]⁺ was summed to obtain the total ion count for **1-38** and **1-39**.

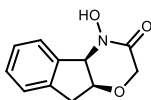
1.5.8 Compound Characterization:



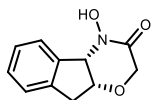
(4aR,9aS)-4,4a,9,9a-tetrahydroindeno[2,1-b][1,4]oxazin-3(2H)-one ((+)-1-36): Compound was synthesized using the known procedure and spectral data were consistent with those previously reported for this compound.¹⁵



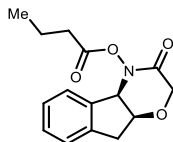
(4aS,9aR)-4,4a,9,9a-tetrahydroindeno[2,1-b][1,4]oxazin-3(2H)-one ((-)-1-36): Compound was synthesized using known procedure and spectral data were consistent with those previously reported for this compound.¹⁵



(4aR,9aS)-4-hydroxy-4,4a,9,9a-tetrahydroindeno[2,1-b][1,4]oxazin-3(2H)-one ((+)-1-21): Compound was synthesized using the known procedure and spectral data were consistent with those previously reported for this compound.¹¹



(4aS,9aR)-4-hydroxy-4,4a,9,9a-tetrahydroindeno[2,1-b][1,4]oxazin-3(2H)-one ((-)-1-21): Compound was synthesized using the known procedure and spectral data were consistent with those previously reported for this compound.¹¹



(4aR,9aS)-3-oxo-2,3,9,9a-tetrahydroindeno[2,1-b][1,4]oxazin-4(4aH)-yl butyrate (1-30): To a flask containing hydroxamic acid (+)-1-21 (50 mg, 0.24 mmol) was added CH₂Cl₂ (2.4 mL) and K₂CO₃ (33 mg, 0.24 mmol). The reaction mixture was stirred for 10 min before butyryl chloride (25 μ L, 0.24 mmol) was added in one portion and allowed to stir overnight. The solution was filtered, concentrated *in vacuo*, and purified via column chromatography (silica gel, 1:1 Hex:EtOAc) to yield **1-30** as a light orange oil (58 mg, 86%).

TLC $R_f = 0.53$ (silica gel, 50:50 Hex:EtOAc)

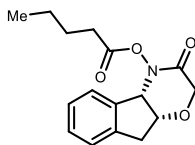
Optical Rotation $[\alpha]_D^{22} = -37.5$ ($c = 1.00$, CHCl_3)

^1H NMR (500 MHz, CDCl_3) δ 7.54 (d, $J = 7.2$ Hz, 1H), 7.35 – 7.26 (m, 3H), 5.03 (d, $J = 4.4$ Hz, 1H), 4.76 (t, $J = 4.3$ Hz, 1H), 4.32 (q, $J = 16.3$ Hz, 2H), 3.21 (app dd, $J = 16.9, 5.0$ Hz, 1H), 3.12 (app d, $J = 16.9$ Hz, 1H), 2.65 – 2.53 (m, 2H), 1.88–1.77 (m, 2H), 1.06 (t, $J = 7.5$ Hz, 3H).

^{13}C NMR (125 MHz, CDCl_3) δ 170.3, 162.7, 139.7, 138.6, 129.0, 127.5, 125.4, 124.9, 78.5, 67.5, 67.4, 37.4, 33.6, 18.4, 13.6.

IR (FT-IR) 2967, 1790, 1696, 1328, 1115 cm^{-1} .

HRMS (ESI-TOF) m/z calcd for $\text{C}_{15}\text{H}_{17}\text{NO}_4$ ($\text{M} + \text{Na}$) $^+$: 298.1055, found 298.1058.



(4aS,9aR)-3-oxo-2,3,9,9a-tetrahydroindeno[2,1-b][1,4]oxazin-4(4aH)-yl pentanoate (1-31):

To a flask containing hydroxamic acid (–)-**1-21** (50 mg, 0.24 mmol) was added CH_2Cl_2 (2.4 mL) and K_2CO_3 (33 mg, 0.24 mmol). The reaction mixture was stirred for 10 min before valeryl chloride (29 μL , 0.24 mmol) was added in one portion and allowed to stir overnight. The solution was filtered, concentrated *in vacuo*, and purified via column chromatography (silica gel, 1:1 Hex:EtOAc) to yield **1-31** as a clear oil (60 mg, 85%).

TLC $R_f = 0.58$ (silica gel, 50:50 Hex:EtOAc)

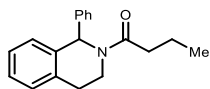
Optical Rotation $[\alpha]_D^{23} = +42.8$ ($c = 1.00$, CHCl_3)

^1H NMR (500 MHz, CDCl_3) δ 7.54 (d, $J = 7.2$ Hz, 1H), 7.34 – 7.27 (m, 3H), 5.03 (d, $J = 4.4$ Hz, 1H), 4.77 (t, $J = 4.3$ Hz, 1H), 4.33 (q, $J = 16.3$ Hz, 2H), 3.22 (app dd, $J = 16.9, 4.9$ Hz, 1H), 3.13 (app d, $J = 16.8$ Hz, 1H), 2.67 – 2.56 (m, 2H), 1.80 – 1.74 (m, 2H), 1.50–1.42 (m, 2H), 0.96 (t, $J = 7.4$ Hz, 3H).

^{13}C NMR (125 MHz, CDCl_3) δ 170.6, 162.8, 139.7, 138.6, 129.1, 127.6, 125.5, 125.0, 78.6, 67.5, 67.5, 37.5, 31.6, 26.9, 22.3, 13.8.

IR (FT-IR) 2959, 1789, 1696, 1328, 1115 cm^{-1} .

HRMS (ESI-TOF) m/z calcd for $\text{C}_{16}\text{H}_{19}\text{NO}_4$ ($\text{M} + \text{Na}$) $^+$: 312.1212, found 312.1221.



1-(1-phenyl-3,4-dihydroisoquinolin-2(1H)-yl)butan-1-one (1-38): To a solution of 1-phenyl-1,2,3,4-tetrahydroisoquinoline (50 mg, 0.24 mmol) in CH_2Cl_2 (0.45 mL) was added Et_3N (50 μL , 0.36 mmol). Butyryl chloride (27 μL , 0.26 mmol) was then added and allowed to stir for one hour. The reaction mixture was then concentrated *in vacuo* and purified via column chromatography (silica gel, 1:1 Hex:EtOAc) to yield **1-38** as a clear oil (63 mg, 94%) isolated as a 8:2 mixture of rotamers.

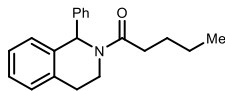
TLC R_f = 0.64 (silica gel, 50:50 Hex:EtOAc)

^1H NMR (500 MHz, CDCl_3) δ 7.34 – 7.15 (m, 9.10H), 7.10 (d, J = 7.3 Hz, 0.89H), 6.98 (s, 0.80H), 4.32 – 4.22 (m, 0.28H), 3.84 – 3.73 (m, 0.90H), 3.52 – 3.38 (m, 0.90H), 3.38 – 3.29 (m, 0.31H), 2.99 (ddd, J = 16.6, 11.1, 5.8 Hz, 0.94H), 2.94 – 2.88 (m, 0.23H), 2.88 – 2.79 (m, 0.87H), 2.77 – 2.65 (m, 0.28H), 2.56 (dd, J = 15.1, 7.5 Hz, 0.29H), 2.49 (dd, J = 15.1, 7.5 Hz, 0.27H), 2.38 (ddq, J = 22.8, 15.2, 7.6 Hz, 1.79H), 1.77 – 1.65 (m, 2.21H), 0.97 (q, J = 7.6 Hz, 3.26H).

^{13}C NMR (125 MHz, CDCl_3) δ 171.6, 142.8, 135.6, 134.5, 129.1, 128.8, 128.3, 128.1, 127.8, 127.6, 127.4, 127.3, 127.1, 126.4, 126.3, 59.9, 55.1, 39.8, 38.1, 35.8, 35.7, 29.2, 27.8, 18.9, 18.8, 14.1.

IR (FT-IR) 2961, 2874, 1640, 1450, 1428 cm^{-1} .

HRMS (ESI-TOF) m/z calcd for $\text{C}_{19}\text{H}_{21}\text{NO}$ ($\text{M} + \text{Na}$) $^+$: 302.1521, found 302.1513.



1-(1-phenyl-3,4-dihydroisoquinolin-2(1H)-yl)pentan-1-one (1-39): To a solution of 1-phenyl-1,2,3,4-tetrahydroisoquinoline (51 mg, 0.24 mmol) in CH₂Cl₂ (0.45 mL) was added Et₃N (50 μL, 0.36 mmol). Valeryl chloride (32 μL, 0.26 mmol) was then added and allowed to stir for one hour. The reaction mixture was then concentrated *in vacuo* and purified via column chromatography (silica gel, 1:1 Hex:EtOAc) to yield **1-39** as a clear oil (69 mg, 96%) isolated as a 8:2 mixture of rotamers.

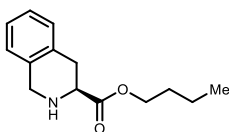
TLC R_f = 0.67 (silica gel, 50:50 Hex:EtOAc)

¹H NMR (500 MHz, CDCl₃) δ 7.34 – 7.14 (m, 9.51H), 7.10 (d, *J* = 7.4 Hz, 0.84H), 6.98 (s, 0.80H), 6.04 (s, 0.23H), 4.32 – 4.23 (m, 0.27H), 3.85 – 3.72 (m, 0.92H), 3.52 – 3.41 (m, 0.93H), 3.39 – 3.29 (m, 0.27H), 3.05 – 2.95 (m, 1.01H), 2.94 – 2.89 (m, 0.20H), 2.84 (dt, *J* = 16.1, 3.4 Hz, 0.92H), 2.71 (dd, *J* = 10.7, 5.4 Hz, 0.28H), 2.58 (dd, *J* = 15.0, 7.5 Hz, 0.28H), 2.51 (dd, *J* = 15.2, 7.6 Hz, 0.26H), 2.47 – 2.34 (m, 1.84H), 1.76 – 1.60 (m, 2.32H), 1.44 – 1.31 (m, 2.28H), 1.00 – 0.85 (m, 3.45H).

¹³C NMR (125 MHz, CDCl₃) δ 171.8, 142.8, 135.5, 134.5, 129.0, 128.7, 128.7, 128.7, 128.3, 128.0, 127.7, 127.6, 127.3, 127.2, 127.0, 126.4, 126.2, 59.9, 55.0, 39.8, 38.1, 33.5, 33.4, 29.2, 27.8, 27.6, 27.4, 22.7, 14.0.

IR (FT-IR) 2956, 2871, 1641, 1450, 1429 cm⁻¹.

HRMS (ESI-TOF) *m/z* calcd for C₂₀H₂₃NO (M + Na)⁺ : 316.1677, found 316.1679.



butyl (3S)-1,2,3,4-tetrahydroisoquinoline-3-carboxylate (1-57): To a solution of (3S)-1,2,3,4-tetrahydroisoquinoline-3-carboxylic acid (300 mg, 1.69 mmol) in *n*-butanol (2.10 mL) was added thionyl chloride (0.720 mL, 3.72 mmol). The reaction was heated to 120 °C for 16 hours before it was concentrated *in vacuo* and saturated aqueous NaHCO₃ was added (3 mL). The solution was extracted with CH₂Cl₂ (3 x 6 mL), dried (Na₂SO₄), filtered, concentrated *in vacuo*, and purified by flash column chromatography (EtOAc/Hex) on silica to yield **1-57** as a clear oil (331 mg, 84%).

TLC R_f = 0.38 (silica gel, 60:40 Hex:EtOAc)

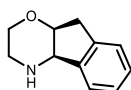
Optical Rotation [α]_D²² = -100 (*c* = 1.05, CH₂Cl₂)

¹H NMR (500 MHz, CDCl₃) δ 7.13 – 7.07 (m, 3H), 7.01 – 6.99 (m, 1H), 4.19 – 4.14 (m, 2H), 4.11 – 4.01 (m, 2H), 3.69 (dd, *J* = 10.2, 4.6 Hz, 1H), 3.05 (dd, *J* = 16.1, 4.6 Hz, 1H), 2.92 (dd, *J* = 16.3, 10.2 Hz, 1H), 2.26 (s, 1H), 1.64 (dt, *J* = 14.8, 6.7 Hz, 2H), 1.38 (dq, *J* = 14.9, 7.4 Hz, 2H), 0.93 (t, *J* = 7.5 Hz, 3H).

¹³C NMR (125 MHz, CDCl₃) δ 173.1, 134.8, 133.1, 129.1, 126.2, 126.0, 126.0, 64.8, 55.9, 47.3, 31.6, 30.6, 19.0, 13.7.

IR (FT-IR) 2960, 1735, 1188, 910, 733 cm⁻¹.

HRMS (ESI-TOF) *m/z* calcd for C₁₄H₁₉NO₂ (M + Na)⁺ : 256.1313, found 256.1325.



(4aR,9aS)-2H,3H,4H,4aH,9H,9aH-indeno[2,1-b][1,4]oxazine (1-59): To a solution of (+)-**1-36** (100 mg, 0.529 mmol) in THF (5.6 mL) at 0 °C was added LiAlH₄ (69.4 mg, 1.83 mmol). The reaction was allowed to stir for 24 hours at room temperature before saturated aqueous NaHCO₃ (2 mL) was added dropwise. The mixture was filtered through celite, extracted with CH₂Cl₂ (3 x 6 mL), dried (Na₂SO₄), filtered, concentrated *in vacuo*, and purified by flash column chromatography (EtOAc/Hex) on silica to yield **1-59** as a colorless oil (39.0 mg, 42%).

TLC $R_f = 0.24$ (silica gel, EtOAc)

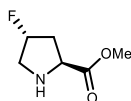
Optical Rotation $[\alpha]_D^{22} = +48.0$ ($c = 1.00$, CHCl_3)

$^1\text{H NMR}$ (500 MHz, CDCl_3) δ 7.43 (d, $J = 6.8$ Hz, 1H), 7.34 – 7.28 (m, 3H), 4.37 (t, $J = 3.6$ Hz, 1H), 4.30 (d, $J = 3.6$ Hz, 1H), 3.74 (dd, $J = 8.9, 2.3$ Hz, 1H), 3.65 (td, $J = 11.1, 2.2$ Hz, 1H), 3.04 (dd, $J = 16.3, 4.2$ Hz, 1H), 2.99 – 2.89 (m, 2H), 2.73 (d, $J = 13.0$ Hz, 1H), 2.37 (s, 1H).

$^{13}\text{C NMR}$ (125 MHz, CDCl_3) δ 141.7, 141.6, 127.5, 126.7, 125.6, 123.5, 77.7, 66.4, 60.6, 40.6, 37.8.

IR (FT-IR) 2907, 2249, 1083, 909, 748 cm^{-1} .

HRMS (ESI-TOF) m/z calcd for $\text{C}_{11}\text{H}_{13}\text{NO}$ ($\text{M} + \text{H}$) $^+$: 176.1075, found 176.1073.



methyl (2S,4R)-4-fluoropyrrolidine-2-carboxylate (1-64): To a solution of 1-tert-butyl 2-methyl (2S,4R)-4-fluoropyrrolidine-1,2-dicarboxylate (66.0 mg, 0.267 mmol) in CH_2Cl_2 (1.0 mL) was added TFA (1.0 mL). The reaction was allowed to stir for 3 hours at room temperature before the solution was concentrated *in vacuo*. The resulting salt was free based by stirring with excess K_2CO_3 in CH_2Cl_2 (1 mL) for 1 hour before filtering the mixture and concentrating *in vacuo* to yield **1-64** as a clear oil (24.0 mg, 61%).

TLC $R_f = 0.28$ (silica gel, EtOAc)

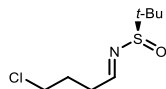
Optical Rotation $[\alpha]_D^{22} = -12.1$ ($c = 0.10$, CH_2Cl_2)

$^1\text{H NMR}$ (500 MHz, CDCl_3) δ 5.24 (dt, $J = 54.1, 4.0$ Hz, 1H), 4.06 (t, $J = 8.0$ Hz, 1H), 3.74 (s, 3H), 3.32 – 3.22 (m, 2H), 2.44 (ddd, $J = 22.7, 14.7, 7.8$ Hz, 1H), 2.31 (s, 1H), 2.07 (dddd, $J = 37.0, 14.6, 8.1, 4.7$ Hz, 1H).

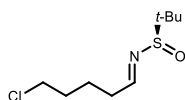
$^{13}\text{C NMR}$ (125 MHz, CDCl_3) δ 174.8, 95.3, 93.9, 58.6, 53.8, 53.6, 52.5, 37.8, 37.6.

IR (FT-IR) 3053, 2985, 1733, 1265, 738 cm^{-1} .

HRMS (ESI-TOF) m/z calcd for $C_6H_{10}FNO_2$ ($M + H$)⁺ : 148.0774, found 148.0769.



(S)-N-[(1E)-4-chlorobutylidene]-2-methylpropane-2-sulfinamide (1-46): Following General Procedure #2, the reaction of 4-chlorobutan-1-ol, 85% (1.11 mL, 9.21 mmol) in CH_2Cl_2 (61.0 mL) with Dess-Martin Periodinane (5.08 g, 12.0 mmol), followed by $Ti(OEt)_4$ (2.12 mL, 10.3 mmol) and (*R*)-2-methylpropane-2-sulfinamide (1.12 g, 9.21 mmol) afforded **1-46** (0.715 g, 37%) as a yellow oil. Spectral data were consistent with those previously reported for this compound.¹⁶



(S)-N-[(1E)-5-chloropentylidene]-2-methylpropane-2-sulfinamide (1-47): Following General Procedure #2, the reaction of 5-chloropentan-1-ol (2.97 mL, 24.5 mmol) in CH_2Cl_2 (163 mL) with Dess-Martin Periodinane (13.5 g, 31.8 mmol), followed by $Ti(OEt)_4$ (5.64 mL, 26.9 mmol) and (*R*)-2-methylpropane-2-sulfinamide (2.97 g, 24.5 mmol) afforded **1-47** (2.09 g, 38%) as a yellow oil. $R_f = 0.70$ (1:1 Hex:EtOAc)

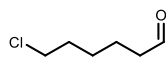
Optical Rotation $[\alpha]_D^{22} = -192.5$ ($c = 1.00$, CH_2Cl_2)

¹H NMR (500 MHz, $CDCl_3$) δ 8.00 (t, $J = 4.5$ Hz, 1H), 3.49 (t, $J = 6.3$ Hz, 2H), 2.49 (td, $J = 7.0$, 4.5 Hz, 2H), 1.86 – 1.67 (m, 4H), 1.11 (s, 9H).

¹³C NMR (125 MHz, $CDCl_3$) δ 168.7, 56.5, 44.4, 35.2, 31.9, 22.6, 22.3.

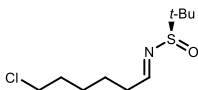
IR (FT-IR) 3053, 1624, 1265, 1075, 739 cm^{-1} .

HRMS (ESI-TOF) m/z calcd for $C_9H_{18}NOSCl$ ($M + Na$)⁺: 246.0695, found 246.0695.

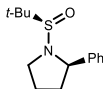


6-chlorohexanal (1-118): To a flask at -78 °C with CH_2Cl_2 (32 mL) was added oxalyl chloride (0.940 mL, 11.0 mmol). A solution of dimethyl sulfoxide (1.04 mL, 14.6 mmol) in 6.0 mL CH_2Cl_2

was added dropwise and the solution was allowed to stir for 30 minutes at $-78\text{ }^{\circ}\text{C}$. A solution of 6-chlorohexan-1-ol, 95% (1.03 mL, 7.32 mmol) in CH_2Cl_2 (11.0 mL) was then added dropwise and allowed to stir for 30 minutes. Triethylamine was then added dropwise and allowed to stir for 2 hours at $-78\text{ }^{\circ}\text{C}$, which was then warmed to room temperature and allowed to stir for an additional 2 hours. The solution was then quenched with a saturated aqueous NH_4Cl solution (10 mL), extracted with 30 mL CH_2Cl_2 (3x), dried (Na_2SO_4), concentrated *in vacuo*, and purified by flash column chromatography (EtOAc/Hex) on silica to yield **1-118** as a yellow oil (722 mg, 73%). Spectral data were consistent with those previously reported for this compound.¹⁷

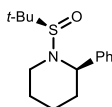


(S)-N-[(1E)-6-chlorohexylidene]-2-methylpropane-2-sulfonamide (1-48): To a flask containing 6-chlorohexanal (**1-118**) (722 mg, 5.36 mmol) and CH_2Cl_2 (11.0 mL) was added (*R*)-2-methylpropane-2-sulfonamide (2.97 g, 24.5 mmol) and CuSO_4 (1.89 g, 11.8 mmol). The reaction was allowed to stir for 24 hours, after which the reaction mixture was filtered through celite. The resulting solution was concentrated *in vacuo* and purified by flash column chromatography (EtOAc/Hex) on silica to afford **1-48** (676 mg, 53%) as a yellow oil. Spectral data were consistent with those previously reported for this compound.¹⁸

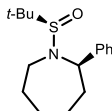


(2R)-1-[(R)-2-methylpropane-2-sulfinyl]-2-phenylpyrrolidine (1-49): Following General Procedure #3, the reaction of **1-46** (0.250 g, 1.19 mmol) in CH_2Cl_2 (6.00 mL) with a 1 M solution of phenylmagnesium bromide in THF (2.38 mL, 2.38 mmol), followed by a 1 M solution of lithium bis(trimethylsilyl)amide in THF (1.19 mL, 1.19 mmol) with THF (6.0 mL) afforded **1-49** (126 mg,

42%) as a yellow oil. Spectral data were consistent with those previously reported for this compound.¹⁹



(2R)-1-[(R)-2-methylpropane-2-sulfinyl]-2-phenylpiperidine (1-50): Following General Procedure #3, the reaction of **1-47** (0.311 g, 1.39 mmol) in CH₂Cl₂ (7.0 mL) with a 1 M solution of phenylmagnesium bromide in THF (2.78 mL, 2.78 mmol), followed by a 1 M solution of lithium bis(trimethylsilyl)amide in THF (1.39 mL, 1.39 mmol) with THF (7.0 mL) afforded **1-50** (159 mg, 43%) as a yellow oil. Spectral data were consistent with those previously reported for this compound.²⁰



(2S)-1-[(R)-2-methylpropane-2-sulfinyl]-2-phenylazepane (1-51): To a flask containing sulfinamide **1-48** (441 mg, 1.85 mmol) in CH₂Cl₂ (9.25 mL) at -78 °C was added a 0.630 M phenyl magnesium bromide solution in THF (5.00 mL, 3.15 mmol). The solution was allowed to stir for 2 hours at -78 °C before it was warmed to room temperature and stirred for 3 hours. The solution was then quenched with a saturated aqueous NH₄Cl solution (8 mL), extracted with CH₂Cl₂ (3 x 25 mL), dried (Na₂SO₄), and concentrated *in vacuo*. The resulting oil was placed in microwave vial. The vial was then charged with NaI (262 mg, 1.75 mmol) and DMF (1.60 mL). A 0.910 M solution of KHMDS in THF (0.570 mL, 0.520 mmol) was then added and the vial was sealed. The solution was placed in a microwave reactor for 1 hour at 130 °C. The solution was then quenched with a saturated aqueous NH₄Cl solution (10 mL), extracted with CH₂Cl₂ (3 x 8 mL), dried (Na₂SO₄), concentrated *in vacuo*, and purified by flash column chromatography (EtOAc/Hex) on

silica to afforded **1-51** (83.0 mg, 16%) as a white solid. Spectral data were consistent with those previously reported for this compound.²¹



(2R)-2-phenylpyrrolidine (1-52): Following General Procedure #4, the reaction of **1-49** (104 mg, 0.414 mmol) in MeOH (3.10 mL) with 4 M HCl in dioxane (0.610 mL) afforded **1-52** (49.0 mg, 81%) as a yellow oil. Spectral data were consistent with those previously reported for this compound.¹⁹



(2R)-2-phenylpiperidine (1-53): Following General Procedure #4, the reaction of **1-50** (127 mg, 0.479 mmol) in MeOH (3.10 mL) with 4 M HCl in dioxane (0.610 mL) afforded **1-53** (63.0 mg, 82%) as a yellow oil. Spectral data were consistent with those previously reported for this compound.²²



(2S)-2-phenylazepane (1-54): Following General Procedure #4, the reaction of **1-51** (51 mg, 0.18 mmol) in MeOH (0.90 mL) with 4 M HCl in dioxane (0.18 mL) afforded **1-54** (27 mg, 84%) as a yellow oil. Spectral data were consistent with those previously reported for this compound.²³

1.6 References

1. (a) Seco, J. M.; Quiñoá, E.; Riguera, R., The Assignment of Absolute Configuration by Nmr. *Chem. Rev.* **2004**, *104*, 17–118; (b) Wenzel, T. J.; Chisholm, C. D., Assignment of Absolute Configuration Using Chiral Reagents and Nmr Spectroscopy. *Chirality* **2011**, *23*, 190–214.
2. Boyd, D. R.; Sharma, N. D.; Barr, S. A.; Carroll, J. G.; Mackerracher, D.; Malone, J. F., Synthesis and Absolute Stereochemistry Assignment of Enantiopure Dihydrofuro- and Dihydropyrano-Quinoline Alkaloids. *J. Chem. Soc., Perkin Trans. 1* **2000**, 3397–3405.
3. Freedman, T. B.; Cao, X.; Dukor, R. K.; Nafie, L. A., Absolute Configuration Determination of Chiral Molecules in the Solution State Using Vibrational Circular Dichroism. *Chirality* **2003**, *15*, 743–758.

4. Dale, J. A.; Dull, D. L.; Mosher, H. S., .Alpha.-Methoxy-.Alpha.-Trifluoromethylphenylacetic Acid, a Versatile Reagent for the Determination of Enantiomeric Composition of Alcohols and Amines. *J. Org. Chem.* **1969**, *34*, 2543–2549.
5. Hoye, T. R.; Jeffrey, C. S.; Shao, F., Mosher Ester Analysis for the Determination of Absolute Configuration of Stereogenic (Chiral) Carbinol Carbons. *Nat. Protoc.* **2007**, *2*, 2451–2458.
6. Flack, H. D.; Bernardinelli, G., The Use of X-Ray Crystallography to Determine Absolute Configuration. *Chirality* **2008**, *20*, 681–690.
7. Nicolaou, K. C.; Snyder, S. A., Chasing Molecules That Were Never There: Misassigned Natural Products and the Role of Chemical Synthesis in Modern Structure Elucidation. *Angew. Chem. Int. Ed.* **2005**, *44*, 1012–1044.
8. (a) Burns, A. S.; Wagner, A. J.; Fulton, J. L.; Young, K.; Zakarian, A.; Rychnovsky, S. D., Determination of the Absolute Configuration of β -Chiral Primary Alcohols Using the Competing Enantioselective Conversion Method. *Org. Lett.* **2017**, *19*, 2953–2956; (b) Wagner, A. J.; David, J. G.; Rychnovsky, S. D., Determination of Absolute Configuration Using Kinetic Resolution Catalysts. *Org. Lett.* **2011**, *13*, 4470–4473; (c) Wagner, A. J.; Miller, S. M.; King, R. P.; Rychnovsky, S. D., Nanomole-Scale Assignment and One-Use Kits for Determining the Absolute Configuration of Secondary Alcohols. *J. Org. Chem.* **2016**, *81*, 6253–6265; (d) Wagner, A. J.; Rychnovsky, S. D., Kinetic Analysis of the HBTM-Catalyzed Esterification of an Enantiopure Secondary Alcohol. *Org. Lett.* **2013**, *15*, 5504–5507; (e) Wagner, A. J.; Rychnovsky, S. D., Determination of Absolute Configuration of Secondary Alcohols Using Thin-Layer Chromatography. *J. Org. Chem.* **2013**, *78*, 4594–4598.
9. Perry, M. A.; Trinidad, J. V.; Rychnovsky, S. D., Absolute Configuration of Lactams and Oxazolidinones Using Kinetic Resolution Catalysts. *Org. Lett.* **2013**, *15*, 472–475.
10. (a) Miller, S. M.; Samame, R. A.; Rychnovsky, S. D., Nanomole-Scale Assignment of Configuration for Primary Amines Using a Kinetic Resolution Strategy. *J. Am. Chem. Soc.* **2012**, *134*, 20318–20321; (b) Arseniyadis, S.; Valleix, A.; Wagner, A.; Mioskowski, C., Kinetic Resolution of Amines: A Highly Enantioselective and Chemoselective Acetylating Agent with a Unique Solvent-Induced Reversal of Stereoselectivity. *Angew. Chem. Int. Ed.* **2004**, *43*, 3314–3317.
11. Binanzer, M.; Hsieh, S.-Y.; Bode, J. W., Catalytic Kinetic Resolution of Cyclic Secondary Amines. *J. Am. Chem. Soc.* **2011**, *133*, 19698–19701.
12. Kreituss, I.; Chen, K.-Y.; Eitel, S. H.; Adam, J.-M.; Wuitschik, G.; Fettes, A.; Bode, J. W., A Robust, Recyclable Resin for Decagram Scale Resolution of (\pm)-Mefloquine and Other Chiral *N*-Heterocycles. *Angew. Chem. Int. Ed.* **2016**, *55*, 1553–1556.
13. Wanner, B.; Kreituss, I.; Gutierrez, O.; Kozlowski, M. C.; Bode, J. W., Catalytic Kinetic Resolution of Disubstituted Piperidines by Enantioselective Acylation: Synthetic Utility and Mechanistic Insights. *J. Am. Chem. Soc.* **2015**, *137*, 11491–11497.
14. Allen, S. E.; Hsieh, S.-Y.; Gutierrez, O.; Bode, J. W.; Kozlowski, M. C., Concerted Amidation of Activated Esters: Reaction Path and Origins of Selectivity in the Kinetic Resolution of Cyclic Amines Via *N*-Heterocyclic Carbenes and Hydroxamic Acid Cocatalyzed Acyl Transfer. *J. Am. Chem. Soc.* **2014**, *136*, 11783–11791.
15. Vora, H. U. L., S. P.; Reynolds, N. T.; Kerr, M. S.; Read de Alaniz, J., Preparation of Chiral and Achiral Triazolium Salts: Carbene Precursors with Demonstrated Synthetic Utility. *Org. Synth.* **2010**, *87*, 350–361.

16. Reddy, L. R.; Prashad, M., Asymmetric Synthesis of 2-Substituted Pyrrolidines by Addition of Grignard Reagents to Γ -Chlorinated *N*-*tert*-Butanesulfinyl Imine. *Chem. Commun.* **2010**, *46*, 222–224.
17. JoséAurell, M.; Ceita, L.; Mestres, R.; Tortajada, A., Dienediolates of Unsaturated Carboxylic Acids in Synthesis. Aldehydes and Ketones from Alkyl Halides, by Ozonolysis of β,Γ -Unsaturated α -Alkyl Carboxylic Acids. The Role of a Tertiary Amine in the Cleavage of Ozonides. *Tetrahedron* **1997**, *53*, 10883–10898.
18. Senter, T. J.; Schulte, M. L.; Konkol, L. C.; Wadzinski, T. E.; Lindsley, C. W., A General, Enantioselective Synthesis of 1-Azabicyclo[*m.n.0*]Alkane Ring Systems. *Tetrahedron Lett.* **2013**, *54*, 1645–1648.
19. Leemans, E.; Mangelinckx, S.; De Kimpe, N., Asymmetric Synthesis of 2-Arylpyrrolidines Starting from Γ -Chloro *N*-(*tert*-Butanesulfinyl)Ketimines. *Chem. Commun.* **2010**, *46*, 3122–3124.
20. Rajender Reddy, L.; Das, S. G.; Liu, Y.; Prashad, M., A Facile Asymmetric Synthesis of Either Enantiomer of 2-Substituted Pyrrolidines. *J. Org. Chem.* **2010**, *75*, 2236–2246.
21. Pablo, Ó.; Guijarro, D.; Yus, M., Synthesis of Nitrogenated Heterocycles by Asymmetric Transfer Hydrogenation of *N*-(*tert*-Butylsulfinyl)Haloimines. *J. Org. Chem.* **2013**, *78*, 9181–9189.
22. Martins, J. E. D.; Contreras Redondo, M. A.; Wills, M., Applications of *N'*-Alkylated Derivatives of TsDPEN in the Asymmetric Transfer Hydrogenation of C=O and C=N Bonds. *Tetrahedron: Asymmetry* **2010**, *21*, 2258–2264.
23. Zhang, Y.; Kong, D.; Wang, R.; Hou, G., Synthesis of Chiral Cyclic Amines Via Ir-Catalyzed Enantioselective Hydrogenation of Cyclic Imines. *Org. Biomol. Chem.* **2017**, *15*, 3006–3012.

Chapter 2. Progress Towards the Synthesis of the Western Fragment of Phainanoid F

2.1 Abstract

Phainanoids A-F are potent immunosuppressive triterpenoid compounds that were isolated from *Phyllanthus hainnensis*. Due to their unique cyclobutane moiety and impressive biological activity, our lab pursued the synthesis of the western fragment. Herein, we describe the progress towards the synthesis of the western portion of the phainanoids. Two separate synthetic routes were studied. The first route utilizes an enantioselective Robinson annulation to forge the decalin core of the fragment, followed by a key benzoin condensation. The second route consists of a key Sonagashira cross-coupling to assemble all the necessary carbon atoms of the fragment. Both routes remain unfinished, but provide promise towards the successful synthesis of the western fragment of the phainanoids.

2.2 Introduction

2.2.1 *Phyllanthus hainanensis* and Phainanoids A-F

For many years, natural products and their derivatives have been used as sources of medicinal therapeutics. Natural products are of great interest because of their vast diversity in nature and bioactive properties.¹ *Phyllanthus* is a plant genus that is well-known and has produced a wide variety of bioactive molecules.² Many of the *Phyllanthus* species have been used as folk medicines to treat hepatitis B, kidney and urinary bladder disturbances, intestinal infections, and diabetes.³

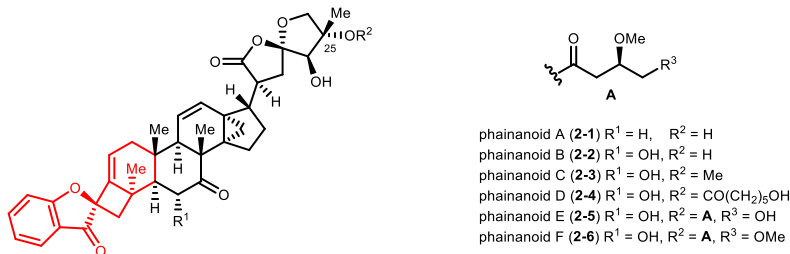


Figure 2-1. Structure of phainanoids A-F.

In 2015, the Yue group reported the isolation and characterization of six new potent immunosuppressive compounds, phainanoids A-F from the *Phyllanthus hainanensis* Merr. plant, a shrub native to the Hainan island of China (Figure 2-1).⁴ Immunosuppressive agents are drugs that inhibit biological activity of the immune system. They are used to treat autoimmune diseases and to prevent the rejection of organ transplants. Current immunosuppressive drugs, such as cyclosporine A (CsA) (2-7) and rapamycin (2-8), are effective but also cause serious adverse effects, such as lipodystrophy, hyperglycemia, liver toxicity, and increased susceptibility to infection (Figure 2-2).⁵ Therefore, development of new immunosuppressive therapeutics is necessary.

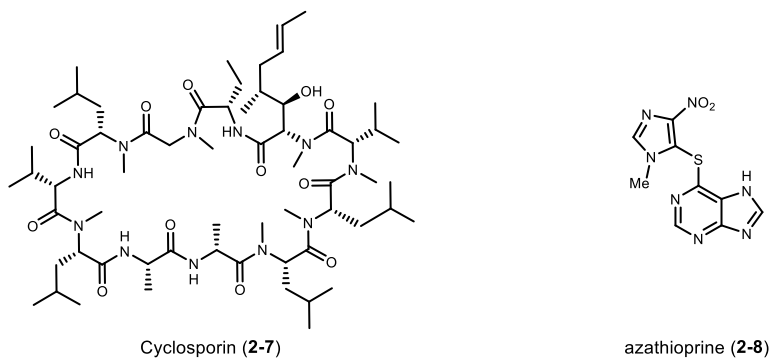


Figure 2-2. Structures of Cyclosporin and Azathioprine.

The phainanoid compounds (**2-1** – **2-6**) demonstrated remarkably potent activity when tested with *in vitro* immunosuppressive assays. When tested against the ConA-induced proliferation of T lymphocytes, the IC_{50} values ranged from 2.04 ± 0.01 to 192.8 ± 0.01 nM while CsA had an IC_{50} of 14.2 ± 0.01 nM. Against LPS-induced proliferation of B lymphocytes, the IC_{50} values ranged from $<1.60 \pm 0.01$ to 249.5 ± 0.01 nM while CsA was 352.9 ± 0.01 nM. These results proved phainanoid C, D, and F to be more potent than CsA against the ConA-induced proliferation of T lymphocytes, and phainanoids A-F to be more potent than CsA against LPS-induced proliferation of B lymphocytes, with phainanoid F (**2-6**) being the most potent in each case.

The Yue group concluded that the 4,5-spirocyclic ether and/or the 5,5-spirolactone were crucial for immunosuppressive activities because no other 13,30-cyclodammarane triterpenoids have been reported to contain this type of bioactivity. Through their Structure-Activity Relationship (SAR) study they showed that the R_1 hydroxyl group is not vital for bioactivity (**2-1** and **2-2** had no obvious change in IC_{50}) and methylation or acylation of the C-25 hydroxyl is crucial (**2-3** – **2-6** showed improved bioactivity).

These compounds exhibit a new and highly modified triterpenoid structural motif not found in other natural products of this family. Other 13,30-cyclodammarane-containing triterpenoids

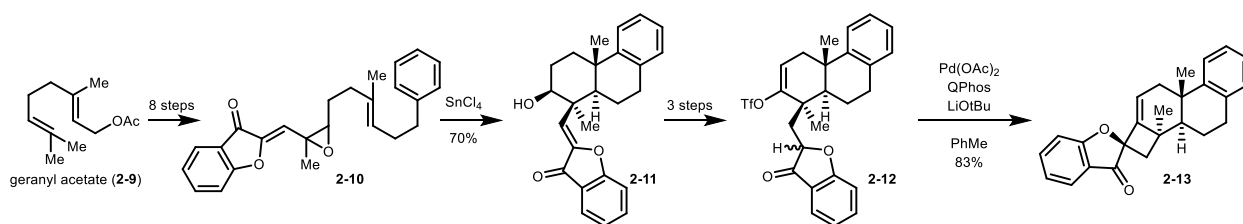
have been reported (e.g. dichapetalins), but the 3*H*-spiro[benzofuran-2,1'-cyclobutan]-3-one and 1,6-dioxaspiro[4.4] nonan-2-one motifs are unique to the phainanoid family.

2.3 Previous Work

2.3.1 Guangbin Dong's Successful Intramolecular Alkenylation Approach

In 2017, the Guangbin Dong group successfully utilized a key palladium-catalyzed intramolecular alkenylation approach to form the western portion of the phainanoids (Scheme 2-1).⁶ They start the synthesis with geranyl acetate (**2-9**) and take 8 steps to make epoxide **2-10**. They perform a vinyl oxirane-mediated polyene cyclization to construct most of the carbon framework. Alcohol **2-11** was further derivatized into vinyl triflate **2-12** in three steps. The key intramolecular alkenylation afforded the desired spirocycle (**2-13**) in 83% yield and as a single diastereomer. Computational studies suggested that the major diastereomer arises from stabilization from a favorable coordinative interaction between the carbonyl π -bond electrons and the palladium.

Scheme 2-1. The Dong group's approach to the western portion of the phainanoids.

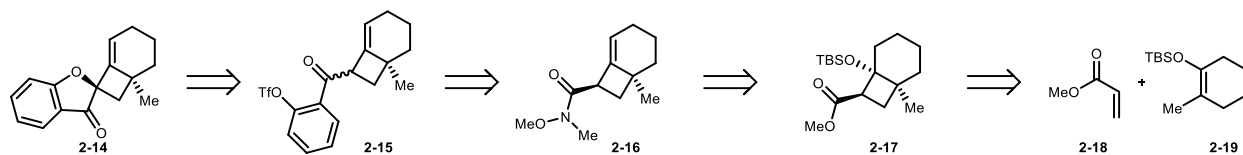


2.3.2 Triflate Fragmentation Spirocyclization Approach

Dr. Jacob DeForest from the Rychnovsky group pioneered initial approaches toward the synthesis of the western fragment of the phainanoids.⁷ The first approach was based on a triflate fragmentation to form the spirocycle (Scheme 2-2). The aryl triflate (**2-15**) would arise from an aryl addition into Weinreb amide **2-16** which would come from an elimination of TBS alcohol **2-**

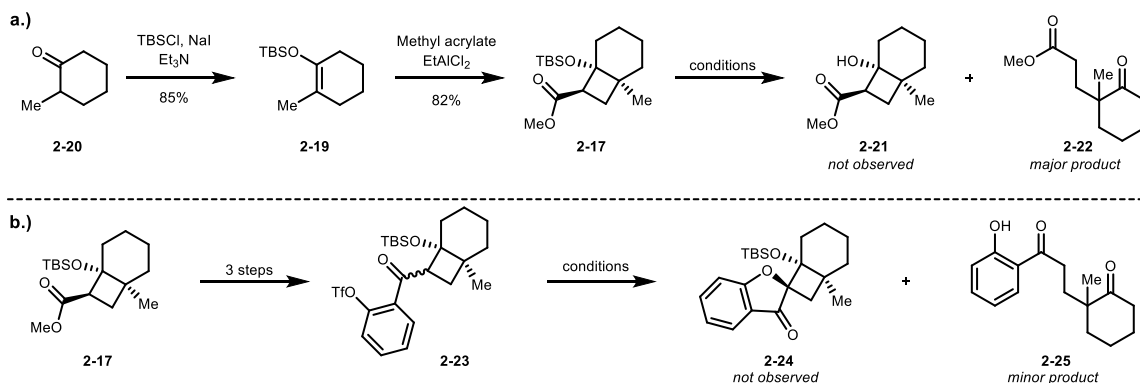
17 The cyclobutane would be installed via a [2+2] cycloaddition with methyl acrylate (**2-18**) and enoxysilane **2-19**.

Scheme 2-2. Retrosynthesis of the triflate fragmentation approach.



Cyclobutane **2-17** was smoothly formed by trapping as the enoxysilane (**2-19**) followed by a [2+2] cycloaddition with methyl acrylate (Scheme 2-3, a). Unfortunately, upon deprotection of the TBS group, the retro-aldol product (**2-22**) was observed as the major product. To try and circumvent this issue, ester **2-17** was converted to aryl triflate **2-23** in three steps and subjected to various triflate fragmentation conditions, although it was met with no success (Scheme 2-3, b). The respective retro-aldol product (**2-25**) was observed as the minor product.

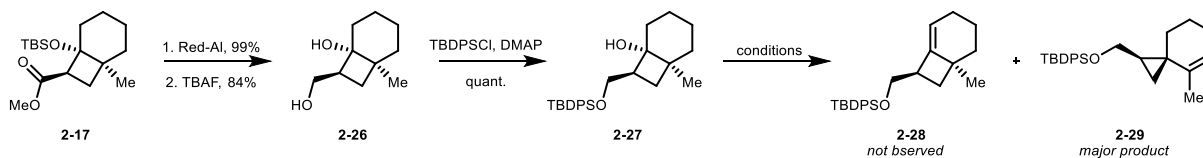
Scheme 2-3. Cyclobutane formation and attempted elimination (a). Attempted triflate fragmentation (b).



Efforts were then focused on mitigating the retro-aldol reaction by removing the ester group (Scheme 2-4). Ester **2-17** was reduced using Red-Al followed by TBAF deprotection of the TBS group to yield diol **2-26**. The primary alcohol was protected as the TBDPS alcohol and subjected to various dehydration conditions. Unfortunately, the desired product (**2-28**) was not

observed, instead vinyl cyclopropane **2-29** was the major product. This product is thought to form through a cyclobutyl-cyclopropylcarbinyl cation rearrangement. Due to the inability to circumvent the retro-aldol and vinyl cyclopropane formation, our lab ultimately abandoned this route.

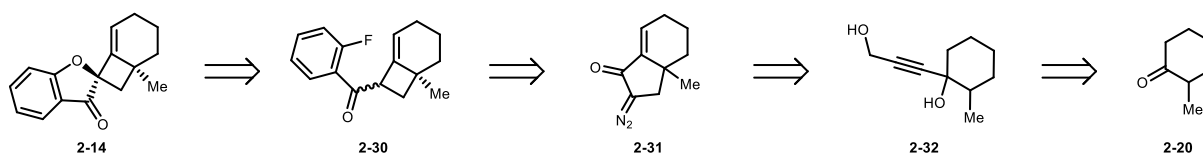
Scheme 2-4. Attempted elimination in the absence of the ester group.



2.3.3 Wolff Ring Contraction Approach

The next approach avoided a [2+2] cycloaddition and instead utilized a Wolff ring contraction to install the cyclobutane. Our group envisioned forming fragment **2-14** from an α -hydroxylation and a S_NAr reaction of aryl fluoride **2-30** (Scheme 2-5). The cyclobutane would arise from a photochemical Wolff ring contraction of diazo intermediate **2-31**, which would come from an acid mediated Nazarov cyclization of **2-32**. The respective diol would ultimately be formed from nucleophilic addition into ketone **2-20**.

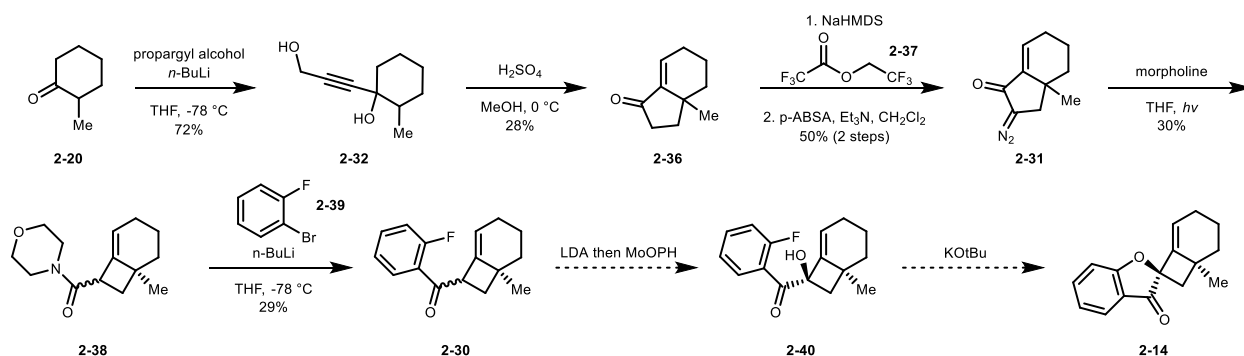
Scheme 2-5. Retrosynthesis of fragment **2-14** utilizing a Wolff ring contraction.



The forward synthesis began with formation of the dianion of propargyl alcohol and its addition into ketone **2-20** to form diol **2-32** (Scheme 2-6). The diol was further treated with sulfuric acid to induce the Nazarov cyclization to afford enone **2-36**, albeit in low yield. This low yield was attributed to the volatility of the product. The mechanism begins with a Meyer-Schuster/Rupe rearrangement to form pentadienyl cation **2-33** which undergoes an electrocyclization to form

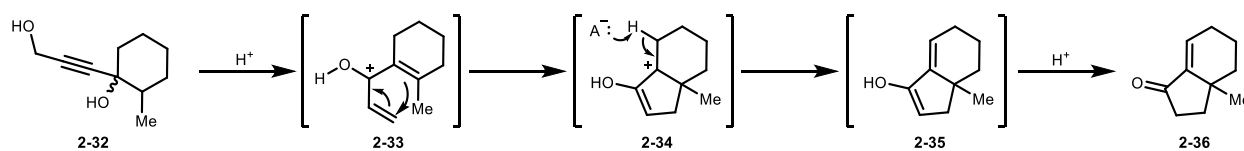
oxyallyl cation **2-34** (Scheme 2-7). This goes through an elimination to form diene **2-35**, which tautomerizes to yield enone **2-36**.

Scheme 2-6. Forward synthesis towards fragment **2-14**.



Deprotonation of **2-36** and treatment with reagent **2-37** followed by diazo transfer with *p*-ABSA produced diazo compound **2-31** (Scheme 2-6). The Wolff ring contraction and subsequent aryl addition were successful, although low yields were observed. Due to obligations with other projects, Dr. Jacob DeForest was unable to continue the sequence.

Scheme 2-7. Mechanism for the Nazarov cyclization.



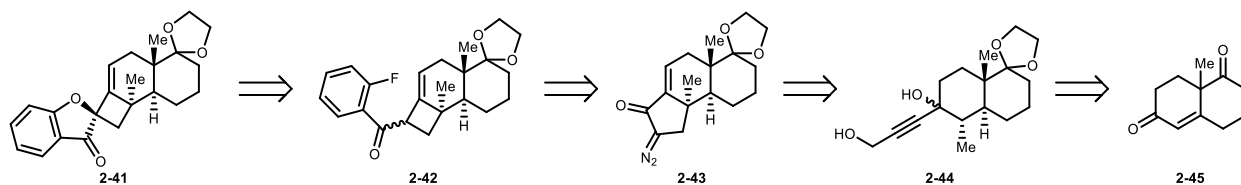
2.4 Results

2.4.1 Revising the Wolff Ring Expansion Route

Upon Dr. Jacob DeForest's departure from the project, we decided to go back and revise the current Wolff ring contraction route. We wanted to use the same disconnections but utilize the Wieland-Miescher ketone (**2-45**) as our starting material (Scheme 2-8). This approach had three clear advantages. It would add an extra 6-membered ring, which maps on to the phainoid scaffolds, and would mitigate the volatility issue with intermediate **2-36**. The last advantage would

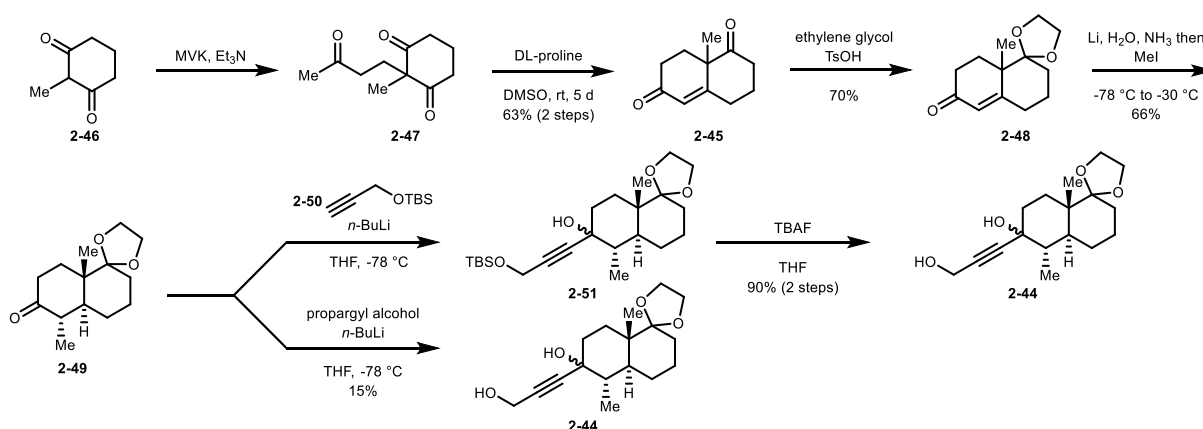
be the capability of rendering this synthesis asymmetric, since the enantiopure form of **2-45** is known.⁸

Scheme 2-8. Revised retrosynthesis using the Wieland-Miescher ketone.



We began the synthesis of the Wieland-Miescher ketone (**2-45**) utilizing 2-methyl-1,3-cyclohexanedione (**2-46**) and methyl vinyl ketone in a Robinson annulation (Scheme 3-9). Protection of the ketone in the presence of the enone was accomplished using ethylene glycol with TsOH. Diastereoselective birch reduction/alkylation afforded *trans*-decalin **2-49** in 66% yield as a single diastereomer. Addition of dianionic propargyl alcohol to the respective ketone gave 15% yield of diol **2-44** as a mixture of diastereomers. The low yield was attributed to the poor solubility of the dianion. Using TBS protected propargyl alcohol (**2-50**) as the nucleophile followed by TBAF deprotection yielded the same diol in 90% yield over two steps.

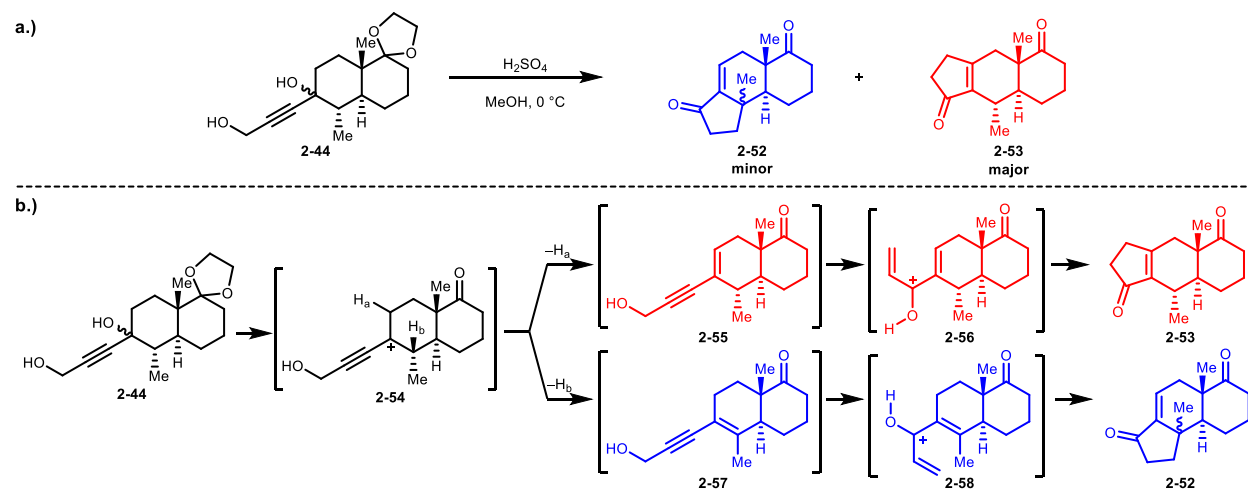
Scheme 2-9. Synthesis of key intermediate **2-44** for the Nazarov cyclization.



With diol **2-44** in hand, we attempted the Meyer-Schuster/Rupe rearrangement followed by the Nazarov cyclization. To our surprise, the major product we observed was enone **2-53**

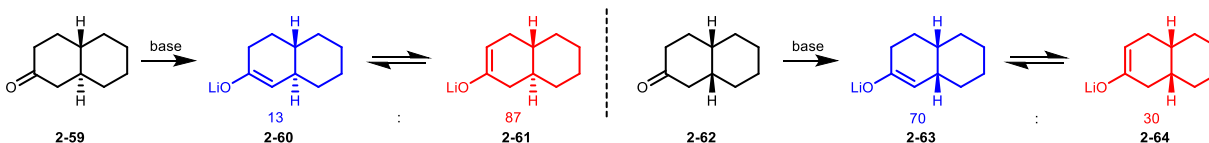
(Scheme 2-10, a). The mechanism for the formation of each product is shown in Scheme 2-10, b. Cation intermediate **2-54** can either be deprotonated at H_a or H_b. Deprotonation of H_a forms the undesired tricyclic product, while deprotonation of H_b yields desired product.

Scheme 2-10. Attempted nazarov cyclization of diol **2-44** (a) and mechanism for the formation of each product (b).



These results were shocking because a simpler system (**2-32**) gave mainly the desired product. After searching the literature, it came to our attention that the House group conducted studies on the deprotonation of *trans*- and *cis*-decalins. They found that if *trans*-decalin **2-59** is treated with base, it will form enolates **2-60** and **2-61** in a 13:87 ratio, respectively. If using *cis*-decalin, the selectivity is flipped. This result can be rationalized by the difference in torsional strain in each enolate. Unfortunately, even after many attempts of overcoming this undesired reactivity, we were ultimately unsuccessful. This forced us to take a different approach towards forming the desired enone (**2-52**).

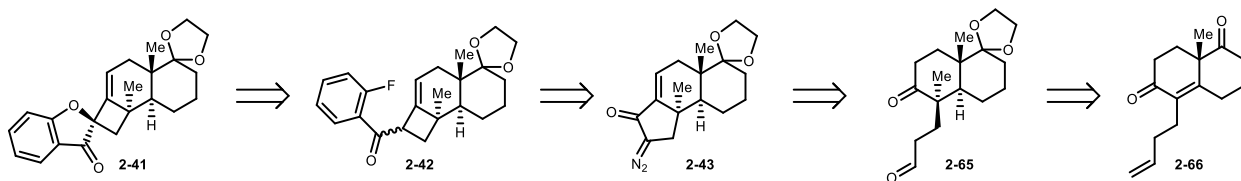
Scheme 2-11. Selectivity for the deprotonation of *trans*- and *cis*-decalins.



2.4.2 Benzoin Condensation to Form the Desired Enone

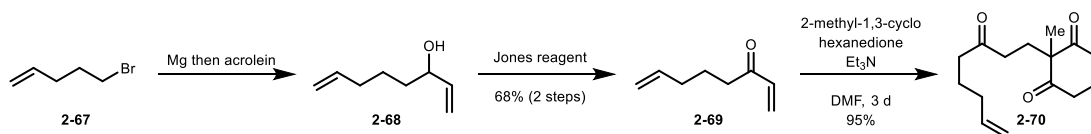
Since the Nazarov cyclization was not a viable route to the desired tricycle (**2-52**), we decided to use a key intramolecular benzoin condensation of **2-65** (Scheme 2-12). This intermediate would arise from Wieland-Miescher ketone derivative **2-66** in a few steps. The remainder of the steps would remain the same, utilizing a Wolff ring contraction.

Scheme 2-12. Revised retrosynthesis utilizing a benzoin condensation to form key tricycle.



The forward sequence began with Grignard formation using alkyl bromide **2-67** in the presence of magnesium metal followed by quenching with acrolein (Scheme 2-13). The resulting allylic alcohol (**2-68**) was directly exposed to Jones reagent to provide enone **2-69** in 68% yield over two steps. Michael addition with 2-methyl-1,3-cyclohexanedione proceeded smoothly to form trione **2-70** in 95% yield.

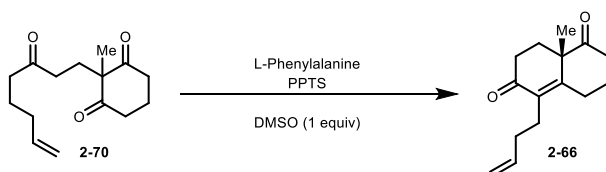
Scheme 2-13. Formation of trione **2-70**.



With trione **2-70** in hand, we sought to render this synthesis asymmetric by utilizing an amino acid catalyst for an enantioselective aldol cyclization. Though proline is known to give moderate enantioselectivity for the formation of the Wieland-Miescher ketone, it gave **2-66** in poor *ee*. Luckily, we found a report by the Shibasaki group in which they use L-phenylalanine to catalyze the aldol condensation to form various Wieland-Miescher and Hajos-Parrish ketones in high *ee*. Thus, we attempted the reported conditions using PPTS and L-phenylalanine, which

yielded 59% of product **2-66** in 74% *ee* (Table 2-1, entry 1). Doubling the reaction time to 10 days had no major effect on the reaction (entry 2). Decreasing the temperature by ten degrees increased the enantioselectivity of the reaction, but decreased the yield (entry 3). Switching the solvent from DMSO to DMF decreased the yield (entry 4). Finally, starting the temperature of the reaction at 30 °C and increasing it gradually over ten days to 70 °C gave a much higher yield and an 82% *ee* of **2-66** (entry 5).

Table 2-1. Optimization of the Robinson annulation.



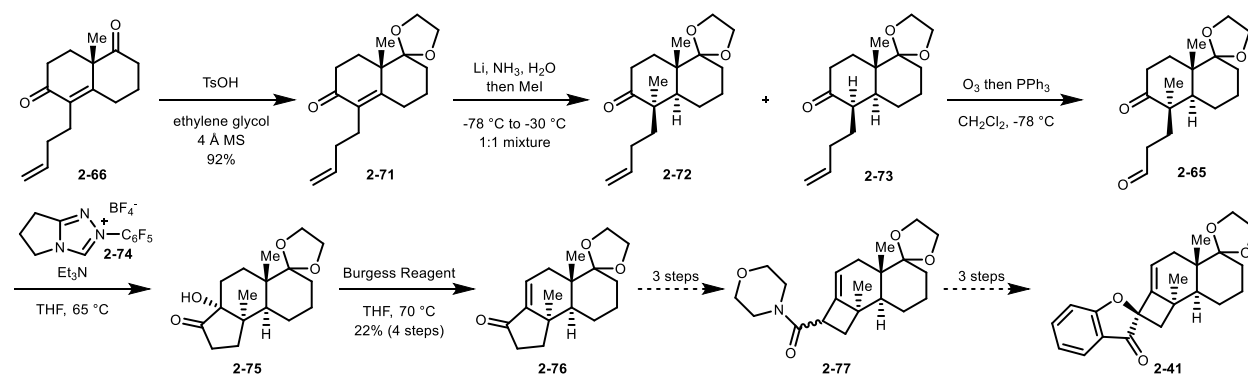
entry	temp (°C)	time (d)	PPTS (mol%)	L-phe (mol%)	yield (%)	<i>ee</i> (%)
1	50	5	50	30	59	74
2	50	10	50	30	54	75
3	40	5	100	100	50	83
4 ^a	40	5	100	100	39	82
5	30 to 70	10	50	30	73	82

^a DMF was used instead of DMSO.

Content with the optimization of the Robinson annulation, we ventured forward in the synthesis. Protection of enone **2-66** with ethylene glycol smoothly provided ketal **2-71** in high yield (Scheme 2-14). Subsequent Birch reduction followed by quenching with methyl iodide afforded the desired ketone **2-72**, albeit as an inseparable 1:1 mixture with ketone **2-73**. Unfortunately, after many attempts at optimizing the reduction/alkylation sequence, the desired product was always obtained as a 1:1 mixture with the undesired ketone. Consequently, the mixture was taken forward to ozonolysis, which yielded product that was still not separable from the respective by-product. This mixture was carried forward to the NHC catalyzed benzoin

condensation followed by a dehydration using Burgess reagent, at which point the by-product was separable. The four-step sequence gave a 22% yield of enone **2-76** overall. Due to the lack of material at the forefront and an inseparable by-product from the Birch reduction, the remaining six steps of this sequence were never completed. Instead, the route was revised again.

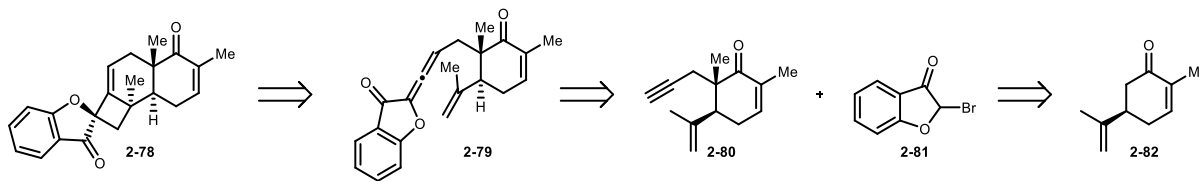
Scheme 2-14. Attempted synthesis of the western fragment of the phainanoids using a benzoin condensation.



2.4.3 [2+2] Cycloaddition Using Carvone

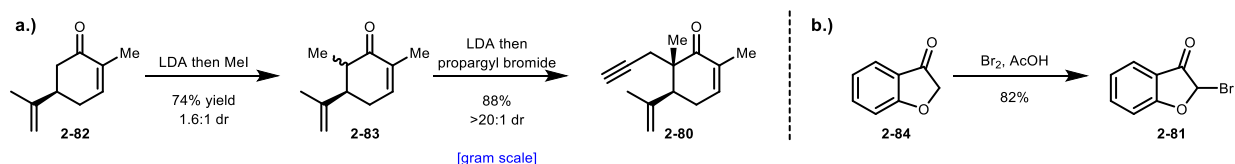
The final route attempted was vastly different from the previous ones since it bypassed any Wolff ring contraction and Nazarov cyclization. We envisioned making fragment **2-78** through a [2+2] cycloaddition using allene **2-79** (Scheme 2-15). This allene would arise from coupling of alkyne **2-80** and bromocoumaranone **2-81**, which ultimately originates from L-carvone (**2-82**). This route had the advantage of a low step count and the ability to use a cheap “chiral pool” molecule.

Scheme 2-15. Retrosynthesis of the [2+2] route towards the synthesis of the western fragment of the phainanoids.



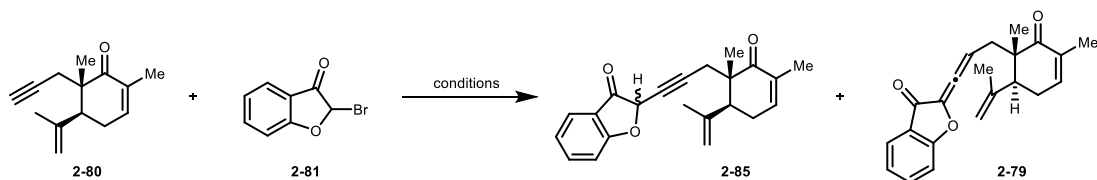
Initial experimentation began with the alkylation of L-carvone (Scheme 2-16, a). Deprotonation of **2-82** with LDA followed by a methyl iodide quench provided **2-83** in 74% yield as a 1.6:1 mixture of diastereomers. The diastereomeric mixture was subjected to the same basic conditions, but quenched with propargyl bromide to form alkyne **2-80** in 88% yield as a single diastereomer. This sequence proved to be robust on gram scale and a viable route to alkyne **2-80**. To form the desired coupling partner, 3-coumaranone (**2-84**) was brominated using bromine with acetic acid (Scheme 2-16, b).

Scheme 2-16. Alkylation of L-carvone (a) and bromination of 3-coumaranone (b).



With both coupling partners in hand, we turned our attention to a potential nucleophilic displacement to form the desired C-C bond (Table 2-2). Initially we used sodium hydride to deprotonate the terminal alkyne, but this led to decomposition of the material (entry 1). Using stronger bases, such as *n*-BuLi and KHMDS, also resulted in decomposition of the material (entries 2 and 3). We presumed this could be due to either γ -deprotonation to form the extended enolate or the alkyne adding into another molecule of **2-80**. We decided to use a weaker base (DBU) in the presence of silver nitrate, but this generated the same result (entry 4).

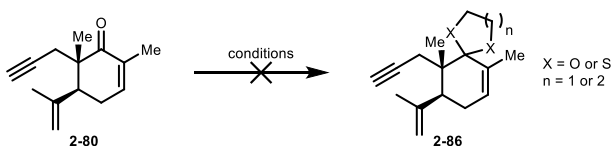
Table 2-2. Failed attempts at coupling alkyne **2-80** and bromide **2-81**.



entry	conditions	result
1	NaH, DMF, rt	decomposition
2	<i>n</i> -BuLi, THF, -78 °C	decomposition
3	KHMDS, THF, -78 °C	decomposition
4	AgNO ₃ , DBU, CH ₂ Cl ₂ , rt	decomposition

To try and circumvent potential side reactivity, we aimed to protect the electrophilic carbonyl (Scheme 2-17). This protection would eliminate any possibility of 1,2- or 1,4-addition into the enone. At this point, Charles J. Dooley III joined the project and attempted to protect the enone (**2-80**). Unfortunately, after screening many conditions he was never able to form the desired ketal.

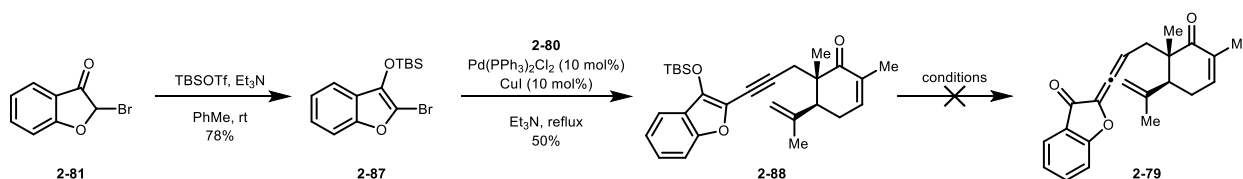
Scheme 2-17. Attempted ketalization of alkyne **2-80**.



We quickly realized that direct nucleophilic displacement was difficult, which led us to employ palladium cross-coupling chemistry to forge the desired bond. Enoxysilane **2-87** was formed in 78% yield by treating ketone **2-81** with TBSOTf in the presence of base (Scheme 2-18). The Sonagashira cross-coupling smoothly provided benzofuran **2-87** in 50% yield. Finally, we attempted to deprotect the enoxysilane to form the desired allene (**2-79**), however this was met with no success. We mainly observed decomposition or a complex mixture of products. Currently,

the project stands at this step and has yet to be accomplished. Future studies on this deprotection and allene formation would allow for investigation of the final [2+2] cycloaddition. Unfortunately, obligations with other projects did not allow us to further pursue this route.

Scheme 2-18. Sonagashira cross-coupling to form desired benzofuran **2-88**.



2.5 Conclusions

The chemistry described in this chapter provides a foundation for the potential synthesis of the western fragment of the phainanoids. An initial route using the Wieland-Miescher ketone proved unsuccessful due to a non-regioselective Nazarov cyclization (Scheme 2-10). This issue was addressed by using a benzoin condensation to forge the desired cyclopentanone, although this route was plagued with formation of an inseparable side product from the Birch reduction. The third route provided in this chapter is the most ideal in terms of step count, but may be the toughest sequence to complete. Ultimately, the second route has pitfalls, but seems the most viable for the completion of the desired fragment.

2.6 Experimental Section

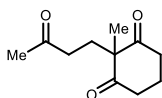
2.6.1 General Experimental:

All glassware and NMR tubes were oven-dried prior to use. ^1H NMR and ^{13}C NMR spectra were recorded at 500 MHz and 125 MHz at 298.0 K unless stated otherwise. Chemical shifts (δ) were referenced to either TMS or the residual solvent peak. The ^1H NMR spectra data are presented as follows: chemical shift, multiplicity (s = singlet, d = doublet, t = triplet, q = quartet, m =

multiplet, dd = doublet of doublets, ddd = doublet of doublet of doublets, dt = doublet of triplets, app. = apparant), coupling constant(s) in hertz (Hz), and integration. High-resolution mass spectrometry was performed using GC-CI-TOF.

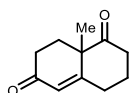
Unless otherwise stated, synthetic reactions were carried out in flame- or oven-dried glassware under an atmosphere of argon. All commercially available reagents were used as received unless stated otherwise. Solvents were purchased as ACS grade or better and as HPLC-grade and passed through a solvent purification system equipped with activated alumina columns prior to use. Thin layer chromatography (TLC) was carried out using glass plates coated with a 250 μm layer of 60 Å silica gel. TLC plates were visualized with a UV lamp at 254 nm, or by staining with *p*-anisaldehyde, potassium permanganate, phosphomolybdic acid, or vanillin. Liquid chromatography was performed using forced flow (flash chromatography) with an automated purification system on prepacked silica gel (SiO_2) columns unless otherwise stated. Infrared (IR) spectroscopy was performed on a Varian 640-IR on potassium bromide salt plates. Optical rotations were taken on a JASCO P-1010 polarimeter using a glass 50 mm cell with a D-line at 589 nm. Electrospray ionization mass spectrometry (ESI-MS) was analyzed on a Waters LCT Classic spectrometer in positive mode with flow injection.

2.6.2 Compound Characterization:

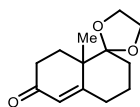


2-methyl-2-(3-oxobutyl)cyclohexane-1,3-dione (2-47): To a flask containing 2-methyl-1,3-cyclohexanedione (**2-46**) (10.1 g, 80.0 mmol) was added methyl vinyl ketone (8.59 mL, 92.7 mmol) followed by triethylamine (0.12 mL, 0.800 mmol). The heterogenous mixture was allowed to stir overnight before adding activated charcoal (3.00 g) and stirring at 45 °C for 30 min. The

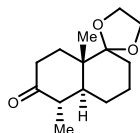
resulting black mixture was filtered through a pad of silica with EtOAc (300 mL) and concentrated to yield trione **2-47** (15.7 g) in quantitative yield as a crude yellow oil which was directly used in the next step without purification. Spectral data were consistent with those previously reported for this compound.⁹



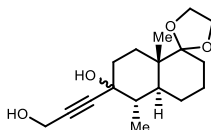
8a-methyl-3,4,8,8a-tetrahydronaphthalene-1,6(2*H*,7*H*)-dione (2-45): To a flask containing crude trione **2-47** (15.7 g, 80.0 mmol) was added DMSO (74.5 mL) followed by *DL*-proline (0.43 g, 3.70 mmol). The mixture was allowed to stir for 5 days before the DMSO was distilled off. The crude mixture was purified by flash column chromatography (EtOAc/Hex) on silica to yield enone **2-45** (9.00 g, 63% over 2 steps) as a yellow oil. Spectral data were consistent with those previously reported for this compound.⁹



8a-methyl-3,4,8,8a-tetrahydro-2*H*-spiro[naphthalene-1,2'-[1,3]dioxolan]-6(7*H*)-one (2-48): To a flame-dried flask containing enone **2-45** (8.80 g, 49.4 mmol), ethylene glycol (120 mL), and 4 Å mol sieves was added TsOH (9.40 g, 49.4 mmol) in one portion. The solution was allowed to stir for one hour before filtering the reaction into a solution of saturated aqueous NaHCO₃ with ice. The aqueous solution was extracted with EtOAc (4 x 200 mL) and the organic layer was washed with brine (300 mL). The organic layer was dried (Na₂SO₄), concentrated *in vacuo*, and purified via column chromatography (EtOAc/Hex) on silica gel to afford ketal **2-48** (7.70 g, 70%) as a clear oil. Spectral data were consistent with those previously reported for this compound.¹⁰



(±)-(4a*S*,5*S*,8a*S*)-5,8a-dimethylhexahydro-2*H*-spiro[naphthalene-1,2'-[1,3]dioxolan]-6(5*H*)-one (2-49): A flame-dried flask equipped with a glass dewar condenser was cooled to $-78\text{ }^{\circ}\text{C}$ and charged with NH_3 (32 mL) and lithium wire (47.0 mg, 6.75 mmol). Once the solution turned a deep blue color, a solution of enone **2-48** (300 mg, 1.35 mmol) in THF (0.70 mL) was added dropwise and the reaction was warmed to $-30\text{ }^{\circ}\text{C}$ and allowed to stir for 4 h. Water (24.3 μL , 1.35 mmol) was then added dropwise and allowed to stir for an additional hour before the addition of MeI (0.42 mL, 6.75 mmol) in one portion. The mixture was allowed to stir overnight while the temperature warmed to $23\text{ }^{\circ}\text{C}$ and the NH_3 evaporated. Saturated aqueous NH_4Cl (50 mL) was added and extracted with CH_2Cl_2 (3 x 50 mL), dried (Na_2SO_4), concentrated *in vacuo*, and purified via column chromatography (EtOAc/Hex) on silica gel to afford ketone **2-49** (211 mg, 66%) as a clear oil. Spectral data were consistent with those previously reported for this compound.¹¹



(±)-(4a*S*,5*S*,8a*S*)-6-(3-hydroxyprop-1-yn-1-yl)-5,8a-dimethyloctahydro-2*H*-spiro[naphthalene-1,2'-[1,3]dioxolan]-6-ol (2-44): A flame-dried flask was charged with alkyne **2-50** (161 mg, 0.940 mmol) and THF (2.0 mL). The solution was cooled to $-78\text{ }^{\circ}\text{C}$ before the dropwise addition of *n*-BuLi (2.32 M in THF, 0.390 mL, 0.900 mmol). The reaction was allowed to stir for 1 h before the dropwise addition of ketone **2-49** (107 mg, 0.450 mmol) in THF (0.5 mL). After stirring for another 2 h at $-78\text{ }^{\circ}\text{C}$ the flask was taken out of the dry-ice/acetone bath and was allowed to warm to room temperature before the addition of saturated aqueous NH_4Cl (5 mL). The mixture was extracted with CH_2Cl_2 (3 x 10 mL), dried (Na_2SO_4), and concentrated *in vacuo*. The crude mixture was directly dissolved in THF (1 mL) and TBAF (1 M in THF, 0.900 mL, 0.900 mmol) was added. The solution was stirred at room temperature overnight before water (5 mL)

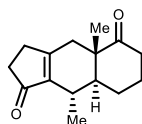
was added and extracted with EtOAc (3 x 5 mL), dried (Na₂SO₄), concentrated *in vacuo*, and purified via column chromatography (EtOAc/Hex) on silica gel to afford a 1:1.5 mixture of diastereomers of diol **2-44** (119 mg, 90% over 2 steps) as a yellow oil.

TLC R_f = 0.22 (silica gel, 50:50 Hex:EtOAc)

¹H NMR (500 MHz, CDCl₃, mixture of diastereomers) δ 4.30 (s, 2H, minor diastereomer), 4.26 (s, 2H, major diastereomer), 3.96 – 3.88 (m, 3H, mixture of diastereomers), 3.87 – 3.79 (m, 1H, mixture of diastereomers), 1.95 – 1.88 (m, 2H, mixture of diastereomers), 1.87 – 1.72 (m, 2H, mixture of diastereomers), 1.71 – 1.61 (m, 4H, mixture of diastereomers), 1.60 – 1.41 (m, 4H, mixture of diastereomers), 1.05 (d, *J* = 6.6 Hz, 6H, minor diastereomer), 0.99 (d, *J* = 3.7 Hz, 6H, major diastereomer).

¹³C NMR (125 MHz, CDCl₃, mixture of diastereomers) δ 113.0, 112.8, 90.5, 86.8, 84.4, 81.3, 73.4, 70.4, 65.2, 65.2, 65.1, 65.0, 51.0, 51.0, 44.2, 42.4, 42.3, 41.3, 41.0, 39.8, 36.2, 35.2, 30.1, 30.0, 27.8, 24.7, 23.5, 23.4, 22.9, 22.9, 14.8, 14.1, 14.1, 13.1.

HRMS (ESI-TOF) *m/z* calcd for C₁₅H₂₀O₂Na (M + Na)⁺ :, found



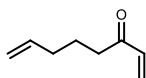
(±)-(4a*S*,8a*S*,9*S*)-4a,9-dimethyl-3,4,4a,6,7,8,8a,9-octahydro-1*H*-cyclopenta[*b*]naphthalene-1,5(2*H*)-dione (2-53): Diol **2-44** (18 mg, 0.061 mmol) was dissolved in MeOH (0.5 mL) and treated with concentrated H₂SO₄ (0.5 mL) dropwise at room temperature. The solution was allowed to stir for 2 h before extracting with CH₂Cl₂ (3 mL). The organic layer was washed with saturated aqueous NaHCO₃ (3 x 5 mL), dried (Na₂SO₄), concentrated *in vacuo*, and purified via column chromatography (EtOAc/Hex) on silica to afford **2-53** (9.0 mg, 63%) as a clear oil.

TLC R_f = 0.80 (silica gel, 50:50 Hex:EtOAc)

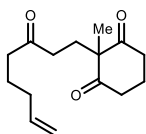
¹H NMR (500 MHz, CDCl₃) δ 2.72 – 2.51 (m, 3H), 2.44 – 2.22 (m, 6H), 2.11 (ddd, J = 12.4, 5.9, 3.0 Hz, 1H), 2.06 – 1.99 (m, 1H), 1.65 – 1.46 (m, 2H), 1.36 (ddd, J = 11.8, 9.9, 3.3 Hz, 1H), 1.25 (d, J = 6.8 Hz, 3H), 1.00 (s, 3H).

¹³C NMR (125 MHz, CDCl₃) δ 215.0, 208.5, 171.7, 139.7, 49.9, 48.2, 37.8, 37.2, 35.2, 30.8, 30.0, 25.8, 24.3, 17.4, 16.0.

HRMS (ESI-TOF) *m/z* calcd for C₁₅H₂₀O₂Na (M + Na)⁺ : 255.1361, found 255.1352.



octa-1,7-dien-3-one (2-69): To a flask containing magnesium turnings (936 mg, 39.0 mmol) in Et₂O (20.0 mL) was added 5-bromopent-1-ene (3.58 mL, 30.0 mmol) in Et₂O (20.0 mL) dropwise over one hour. The solution was cooled to -10 °C and acrolein (2.80 mL, 42.0 mmol) was added dropwise over 30 minutes. After stirring for an additional 30 minutes, the reaction was quenched with a saturated aqueous NH₄Cl solution (50 mL), filtered through celite, extracted with Et₂O (3 x 30 mL), dried (Na₂SO₄), concentrated *in vacuo* and dissolved in acetone (20 mL). The solution was cooled to 0 °C and Jones reagent was added dropwise until a brown-yellow color remained. The reaction was then quenched with isopropanol (1 mL) and brine (30 mL) was added. The mixture was extracted with Et₂O (3 x 30 mL), dried (Na₂SO₄), concentrated *in vacuo*, and purified via column chromatography (CH₂Cl₂) on silica to afford **2-69** (2.53 g, 68%) as a clear oil. Spectral data were consistent with those previously reported for this compound.¹²



2-methyl-2-(3-oxooct-7-en-1-yl)cyclohexane-1,3-dione (2-70): To a flask containing 2-methyl-1,3-cyclohexanedione (772 mg, 6.12 mmol) was added DMF (1.00 mL), enone **2-69** (913 mg, 7.35 mmol), and triethylamine (17.0 μL, 0.120 mmol). The reaction mixture was stirred for 72 hours

before charcoal (3.00 g) was added and the resulting mixture was stirred at 45 °C for 30 minutes. The solution was filtered through silica gel with EtOAc (4 x 30 mL), concentrated *in vacuo*, and purified by flash column chromatography (EtOAc/Hex) on silica to yield **2-70** (637 mg, 95%) as a yellow oil.

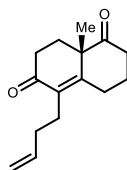
TLC R_f = 0.44 (silica gel, 60:40 Hex:EtOAc)

¹H NMR (500 MHz, CDCl₃) δ 5.71 (ddt, J = 17.0, 10.2, 6.7 Hz, 1H), 5.00 – 4.90 (m, 2H), 2.75 – 2.64 (m, 2H), 2.59 (ddd, J = 16.1, 7.4, 5.2 Hz, 2H), 2.33 (t, J = 7.5 Hz, 2H), 2.30 – 2.24 (m, 2H), 2.06 – 1.95 (m, 5H), 1.92 – 1.81 (m, 1H), 1.64 – 1.55 (m, 2H), 1.19 (s, 3H).

¹³C NMR (125 MHz, CDCl₃) 210.1, 209.7, 138.0, 115.3, 64.4, 42.0, 37.8, 37.5, 33.1, 29.8, 22.7, 19.9, 17.7.

IR (FT-IR) 2939, 1736, 1710, 1669, 1242 cm⁻¹.

HRMS (ESI-TOF) m/z calcd for C₁₅H₂₂O₃Na (M + Na)⁺ : 273.1467, found 273.1474.



(8aS)-5-(but-3-en-1-yl)-8a-methyl-1,2,3,4,6,7,8,8a-octahydronaphthalene-1,6-dione (2-66):

To a flask containing trione **2-70** (8.20 g, 32.8 mmol) was added DMSO (2.33 mL, 32.8 mmol), *L*-phenylalanine (1.62 g, 9.83 mmol), and pyridinium *p*-toluenesulfonate (4.12 g, 16.4 mmol). The reaction mixture was stirred at 30 °C for 3 days, 40 °C for 4 days, 50 °C for 3 days, and 70 °C for 1 day before a solution of saturated aqueous NaHCO₃ (15 mL) was added. The resulting solution was extracted with EtOAc (3 x 20 mL), washed with brine (30 mL), dried (Na₂SO₄), concentrated *in vacuo*, and purified by flash column chromatography (EtOAc/Hex) on silica to yield **2-66** (5.52 g, 73%, 82% *ee*) as a yellow oil. Enantiomeric excess (*ee*) was determined using chiral HPLC on

an Agilent Series 1100 HPLC instrument using a Chiralpack AS-H column with a guard column with a flow rate of 1 mL/min of 10% isopropanol in *n*-hexane monitored at 254 nm wavelength.

TLC $R_f = 0.59$ (silica gel, 60:40 Hex:EtOAc)

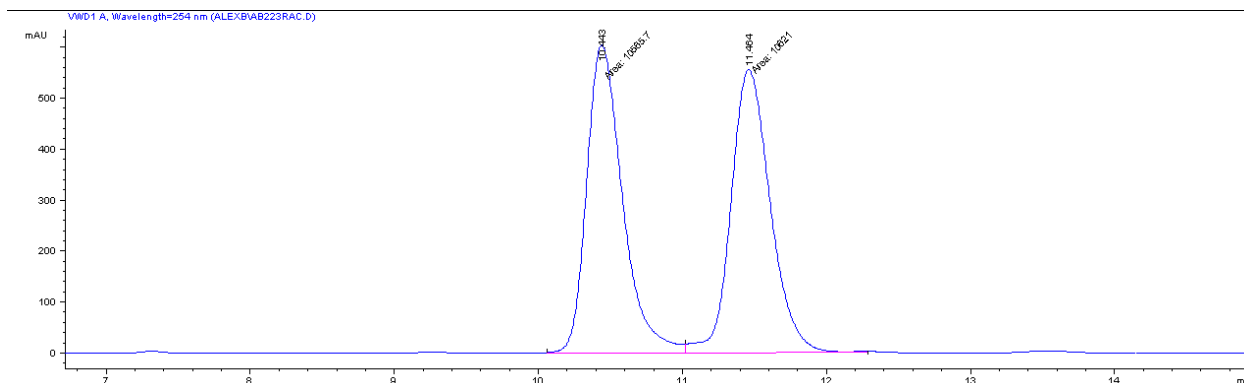
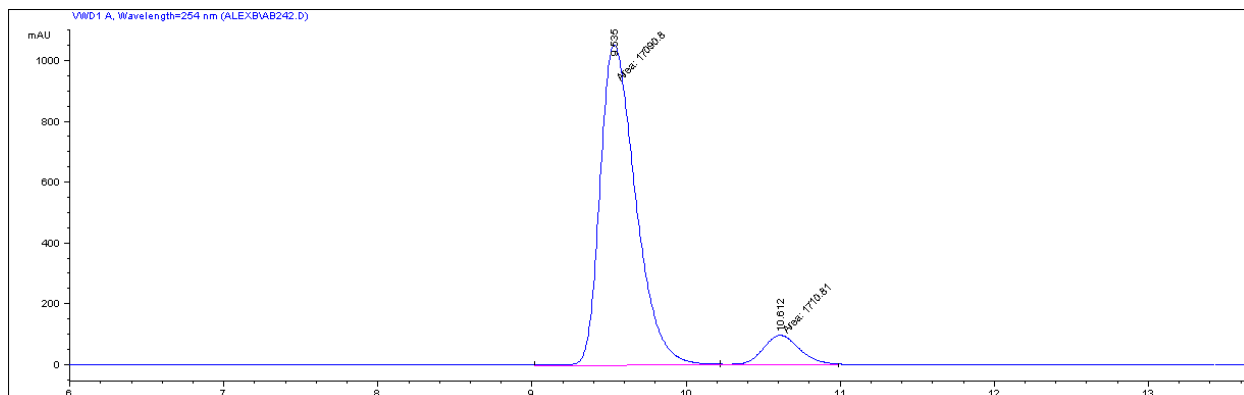
Optical Rotation $[\alpha]^{22}_D = +110.4$ ($c = 1.00$, CH_2Cl_2)

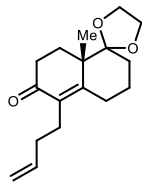
^1H NMR (500 MHz, CDCl_3) δ 5.74 (ddt, $J = 17.0, 10.1, 6.8$ Hz, 1H), 5.02 – 4.85 (m, 2H), 2.85 (dt, $J = 15.3, 3.9$ Hz, 1H), 2.65 (ddd, $J = 15.6, 11.3, 6.3$ Hz, 1H), 2.51 – 2.34 (m, 6H), 2.16 – 1.95 (m, 5H), 1.74 – 1.62 (m, 1H), 1.39 (s, 3H).

^{13}C NMR (125 MHz, CDCl_3) δ 212.1, 197.4, 159.1, 138.0, 134.6, 115.1, 51.0, 37.3, 33.6, 29.6, 27.0, 25.0, 23.7, 22.3.

IR (FT-IR) 3053, 2986, 1706, 1264, 703 cm^{-1} .

HRMS (ESI-TOF) m/z calcd for $\text{C}_{15}\text{H}_{21}\text{O}_2$ ($\text{M} + \text{H}$) $^+$: 233.1542, found 233.1542.





(8'aS)-5'-(but-3-en-1-yl)-8'a-methyl-3',4',6',7',8',8'a-hexahydro-2'H-spiro[1,3-dioxolane-2,1'-naphthalene]-6'-one (2-71): To a flask containing enone **2-66** (51 mg, 0.22 mmol) was added ethylene glycol (0.50 mL), *p*-toluenesulfonic acid monohydrate (42 mg, 0.22 mmol), and 4 Å mol sieves. The reaction was stirred overnight before a solution of saturated aqueous NaHCO₃ (2 mL) was added. The resulting solution was extracted with EtOAc (3 x 5 mL), washed with brine (7 mL), dried (Na₂SO₄), concentrated *in vacuo*, and purified by flash column chromatography (EtOAc/Hex) on silica to yield **2-71** (56 mg, 92%) as a yellow oil.

TLC R_f = 0.62 (silica gel, 60:40 Hex:EtOAc)

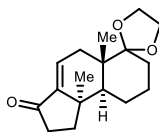
Optical Rotation [α]²²_D = +69.6 (*c* = 1.00, CH₂Cl₂)

¹H NMR (500 MHz, CDCl₃) δ 5.76 (ddt, *J* = 17.0, 10.1, 6.8 Hz, 1H), 4.91 (ddd, *J* = 13.6, 11.1, 1.3 Hz, 2H), 4.01 – 3.83 (m, 4H), 2.74 – 2.61 (m, 1H), 2.52 – 2.09 (m, 6H), 1.98 (dd, *J* = 15.0, 7.2 Hz, 2H), 1.86 (td, *J* = 13.5, 4.5 Hz, 1H), 1.79 (dtd, *J* = 15.2, 5.0, 2.3 Hz, 1H), 1.70 – 1.53 (m, 3H), 1.32 (s, 3H).

¹³C NMR (125 MHz, CDCl₃) δ 198.4, 160.8, 138.4, 134.2, 114.6, 112.8, 65.4, 65.2, 45.4, 34.0, 33.7, 29.9, 26.6, 26.6, 25.1, 21.8, 21.3.

IR (FT-IR) 3054, 1660, 1422, 1265, 704 cm⁻¹.

HRMS (ESI-TOF) *m/z* calcd for C₁₇H₂₄O₃Na (M + Na)⁺ : 299.1623, found 299.1634.



(5aS,9aS,9bR)-5a,9b-dimethyl-1,2,3,5,5a,7,8,9,9a,9b-decahydrospiro[cyclopenta[a]

naphthalene-6,2'-[1,3]dioxolane]-3-one (2-76): To a flask containing condensed ammonia (8.00 mL) at $-78\text{ }^{\circ}\text{C}$ was added lithium wire (12.5 mg, 1.81 mmol) and the solution was allowed to stir until the lithium was dissolved and a dark blue color persisted. Enone **2-71** (100 mg, 0.363 mmol) in THF (0.20 mL) was added to the solution. The reaction was warmed to $-30\text{ }^{\circ}\text{C}$ and allowed to stir for 3 hours before water (6.50 μL , 0.363 mmol) was added and stirred for an additional 1.5 hours. Methyl iodide (113 μL , 1.81 mmol) was then added in one portion and the reaction was allowed to stir for 1 hour at $-30\text{ }^{\circ}\text{C}$ before warming to room temperature overnight. The resulting solution was quenched with saturated aqueous NH_4Cl (2 mL), extracted with CH_2Cl_2 (3 x 7 mL), dried (Na_2SO_4), concentrated *in vacuo*, and purified by flash column chromatography (EtOAc/Hex) on silica. This reaction produced an inseparable mixture of **2-72** and **2-73**, which forced the mixture to be taken on through the next three steps.

The mixture was added to a flask containing CH_2Cl_2 (5.0 mL) at $78\text{ }^{\circ}\text{C}$ before ozone was bubble through the solution until a blue color appeared and then it was allowed to stir for 15 minutes. Oxygen was then bubbled through the solution until the color disappeared. Triphenylphosphine (100 mg, 0.380 mmol) was added and the solution was allowed to stir overnight before it was concentrated and purified by flash column chromatography (EtOAc/Hex) on silica to provide impure **2-65**.

The mixture was placed in a flask containing THF (0.70 mL), triethylamine (5.78 μL , 0.0410 mmol), and NHC **2-74** (15.0 mg, 0.0410 mmol). The reaction was heated to $66\text{ }^{\circ}\text{C}$ for 24 hours before it was quenched with saturated aqueous NH_4Cl (1 mL), extracted with CH_2Cl_2 (3 x 5 mL), dried (Na_2SO_4), concentrated *in vacuo*, and purified by flash column chromatography (EtOAc/Hex) on silica to provide impure **2-75**.

The mixture was placed in a flask containing THF (0.7 mL). The flask was then charged with Burgess reagent (61.0 mg, 0.250 mmol) and heated to reflux for 1.5 hours before water (1 mL) was added. The mixture was extracted with EtOAc (3 x 5 mL), dried (Na₂SO₄), concentrated *in vacuo*, and purified by flash column chromatography (EtOAc/Hex) on silica to yield **2-76** (22.0 mg, 22% over 4 steps) as a clear oil.

TLC R_f = 0.65 (silica gel, 60:40 Hex:EtOAc)

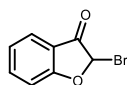
Optical Rotation [α]²²_D = -134.0 (*c* = 0.20, CH₂Cl₂)

¹H NMR (500 MHz, CDCl₃) δ 6.61 (dd, *J* = 7.9, 2.7 Hz, 1H), 4.08 – 3.84 (m, 4H), 2.41 (ddd, *J* = 19.5, 10.9, 8.8 Hz, 1H), 2.29 – 2.17 (m, 2H), 2.09 (dd, *J* = 16.5, 8.0 Hz, 1H), 1.93 (dd, *J* = 12.9, 3.2 Hz, 1H), 1.79 (dd, *J* = 20.8, 11.8 Hz, 2H), 1.73 – 1.47 (m, 5H), 1.40 (ddd, *J* = 25.7, 12.9, 3.8 Hz, 1H), 1.09 (s, 3H), 0.91 (s, 3H).

¹³C NMR (125 MHz, CDCl₃) δ 207.1, 146.7, 130.2, 112.6, 65.3, 65.0, 47.7, 44.3, 42.9, 35.3, 30.8, 30.5, 29.3, 27.7, 23.2, 21.3, 15.1.

IR (FT-IR) 3053, 2985, 1712, 1265, 739 cm⁻¹.

HRMS (ESI-TOF) *m/z* calcd for C₁₇H₂₄O₃Na (*M* + Na)⁺ : 299.1623, found 299.1628.

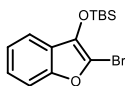


2-bromobenzofuran-3(2H)-one (2-81): Benzofuran-3(2H)-one (**2-84**) (200 mg, 1.49 mmol) was dissolved in Et₂O (3 mL) and cooled to 0 °C. To this solution was added Br₂ (73.0 μL, 1.42 mmol) dropwise, followed by AcOH (85.0 μL, 1.49 mmol). After 5 min of stirring, the reaction was quenched by the addition of saturated aqueous Na₂S₂O₃ (3 mL). The resulting solution was extracted with Et₂O (3 x 3 mL), dried (MgSO₄), concentrated *in vacuo*, and purified by flash column chromatography (EtOAc/Hex) on silica to yield bromide **2-81** (260 mg, 82%) as a white solid.

TLC $R_f = 0.32$ (silica gel, 90:10 Hex:EtOAc)

^1H NMR (500 MHz, CDCl_3) δ 7.77 (d, $J = 7.7$ Hz, 1H), 7.69 (t, $J = 7.8$ Hz, 1H), 7.22 (t, $J = 7.5$ Hz, 1H), 7.17 (d, $J = 8.4$ Hz, 1H), 6.50 (d, $J = 1.8$ Hz, 1H).

^{13}C NMR (125 MHz, CDCl_3) δ 194.6, 170.4, 138.9, 125.7, 124.1, 118.0, 114.1, 75.8.

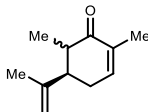


((2-bromobenzofuran-3-yl)oxy)(tert-butyl)dimethylsilane (2-87): To a flame-dried flask was added bromide **2-81** (100 mg, 0.469 mmol), triethylamine (80.0 μL , 0.563 mmol), toluene (5.0 mL), and finally TBSOTf (120 μL , 0.516 mmol). The reaction was stirred for 1 h before the toluene layer was removed and concentrated. The crude material was purified via flash column chromatography (10% EtOAc in hex) on basic alumina to provide enoxysilane **2-87** (120 mg, 78%) as a yellow oil.

TLC $R_f = 0.91$ (silica gel, 90:10 Hex:EtOAc)

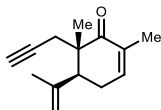
^1H NMR (600 MHz, CDCl_3) δ 7.48 – 7.45 (m, 1H), 7.38 – 7.35 (m, 1H), 7.27 – 7.19 (m, 2H), 1.09 (s, 9H), 0.27 (s, 6H).

^{13}C NMR (150 MHz, CDCl_3) δ 153.6, 136.7, 124.6, 124.5, 122.9, 118.1, 115.2, 111.5, 25.8, 18.3, -3.8.



(5R)-2,6-dimethyl-5-(prop-1-en-2-yl)cyclohex-2-en-1-one (2-83): To a flame-dried flask containing diisopropylamine (5.85 mL, 41.6 mmol) in THF (38 mL) at -10 $^\circ\text{C}$ was added *n*-BuLi (2.32 M in hexane, 17.9 mL, 41.5 mmol) dropwise. This solution was stirred for 30 min before the dropwise addition of *R*-(-)-carvone (**2-82**) (4.80 g, 31.9 mmol) in THF (45.0 mL). After stirring for 2 h, MeI (10.0 mL, 160 mmol) was added as quickly as possible and the solution was allowed

to stir from $-10\text{ }^{\circ}\text{C}$ to room temperature overnight. The mixture was then acidified with 3 M HCl (20 mL) extracted with Et_2O (3 x 60 mL), dried (MgSO_4), concentrated *in vacuo*, and purified by flash column chromatography (EtOAc/Hex) on silica to yield enone **2-83** (3.86 g, 74%) in a 1.6:1 mixture of diastereomers as a yellow oil. Spectral data were consistent with those previously reported for this compound.¹³



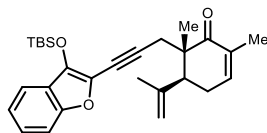
(5S,6S)-2,6-dimethyl-5-(prop-1-en-2-yl)-6-(prop-2-yn-1-yl)cyclohex-2-en-1-one (2-80): To a flame-dried flask containing diisopropylamine (1.11 mL, 7.92 mmol) in THF (7.3 mL) at $-10\text{ }^{\circ}\text{C}$ was added *n*-BuLi (2.32 M in hexane, 3.42 mL, 7.92 mmol) dropwise. This solution was stirred for 30 min before the dropwise addition of enone **2-83** as a mixture of diastereomers (1.00 g, 6.09 mmol) in THF (8.60 mL). After stirring for 2 h, propargyl bromide (2.31 mL, 30.4 mmol) was added as quickly as possible and the solution was allowed to stir from $-10\text{ }^{\circ}\text{C}$ to room temperature overnight. The mixture was then acidified with 3 M HCl (5 mL), extracted with Et_2O (3 x 30 mL), dried (MgSO_4), concentrated *in vacuo*, and purified by flash column chromatography (EtOAc/Hex) on silica to yield a single diastereomer of alkyne **2-80** (1.08 g, 88%) as a clear oil.

TLC $R_f = 0.42$ (silica gel, 90:10 Hex:EtOAc)

Optical Rotation $[\alpha]_D^{21} = -18.6$ ($c = 1.87$, CHCl_3)

$^1\text{H NMR}$ (600 MHz, CDCl_3) δ 6.64 (s, 1H), 4.89 (d, $J = 21.1$ Hz, 2H), 3.07 (dd, $J = 8.4, 5.8$ Hz, 1H), 2.70 (dd, $J = 16.6, 1.9$ Hz, 1H), 2.47 – 2.34 (m, 2H), 2.11 (dd, $J = 16.4, 2.2$ Hz, 1H), 1.96 (s, 1H), 1.76 (s, 3H), 1.75 (s, 3H), 1.01 (s, 3H).

$^{13}\text{C NMR}$ (150 MHz, CDCl_3) δ 202.0, 144.8, 143.2, 134.0, 114.9, 81.7, 70.9, 48.6, 47.2, 28.6, 26.5, 23.3, 18.9, 16.4.



(5S,6S)-6-(3-(3-((tert-butyl dimethylsilyl)oxy)benzofuran-2-yl)prop-2-yn-1-yl)-2,6-dimethyl-5-(prop-1-en-2-yl)cyclohex-2-en-1-one (2-88): A flame-dried flask equipped with a reflux condenser was charged with enoxysilane **2-87** (230 mg, 0.712 mmol), Pd(PPh₃)₂Cl₂ (42.0 mg, 0.0593 mmol), CuI (11.3 mg, 0.0593 mmol), Et₃N (6.0 mL), and finally alkyne **2-80** (120 mg, 0.593 mmol). The atmosphere of the flask was evacuated by vacuum and filled with argon (3x) before refluxing for 3 h. The mixture was then cooled to room temperature and saturated aqueous NH₄Cl (5 mL) was added. The mixture was extracted with EtOAc (3 x 10 mL), washed with brine (10 mL), dried (Na₂SO₄), filtered, concentrated *in vacuo*, and purified by flash column chromatography (EtOAc/Hex) on silica to yield benzofuran **2-88** (133 mg, 50%) as a yellow oil.

TLC R_f = 0.63 (silica gel, 90:10 Hex:EtOAc)

Optical Rotation [α]²²_D = -71.3 (*c* = 1.17, CHCl₃)

¹H NMR (500 MHz, CDCl₃) δ 7.46 (d, *J* = 7.8 Hz, 1H), 7.33 – 7.25 (m, 2H), 7.19 (t, *J* = 7.6 Hz, 1H), 6.69 – 6.64 (m, 1H), 4.96 (s, 2H), 3.18 (t, *J* = 6.8 Hz, 1H), 3.09 (d, *J* = 16.8 Hz, 1H), 2.55 – 2.44 (m, 3H), 1.81 (s, 6H), 1.14 (s, 3H), 1.07 (s, 9H), 0.26 (s, 3H), 0.25 (s, 3H).

¹³C NMR (125 MHz, CDCl₃) δ 201.7, 152.7, 144.9, 143.1, 141.6, 134.1, 126.8, 125.6, 124.1, 122.5, 118.8, 115.2, 111.5, 98.3, 73.0, 48.8, 47.7, 28.7, 28.3, 25.8, 23.3, 19.2, 18.3, 16.5, -4.0, -4.1.

HRMS (ESI-TOF) *m/z* calcd for C₂₈H₃₆O₃SiNa (M + Na)⁺ : 471.2332, found 471.2349.

2.7 References

1. Michael, J. P., Indolizidine and Quinolizidine Alkaloids. *Nat. Prod. Rep.* **2008**, *25*, 139–165.

2. (a) Ren, Y.; Lantvit, D. D.; Deng, Y.; Kanagasabai, R.; Gallucci, J. C.; Ninh, T. N.; Chai, H.-B.; Soejarto, D. D.; Fuchs, J. R.; Yalowich, J. C.; Yu, J.; Swanson, S. M.; Kinghorn, A. D., Potent Cytotoxic Arylnaphthalene Lignan Lactones from *Phyllanthus Poilanei*. *J. Nat. Prod.* **2014**, *77*, 1494–1504; (b) Zhao, J.-Q.; Wang, Y.-M.; He, H.-P.; Li, S.-H.; Li, X.-N.; Yang, C.-R.; Wang, D.; Zhu, H.-T.; Xu, M.; Zhang, Y.-J., Two New Highly Oxygenated and Rearranged Limonoids from *Phyllanthus Cochinchinensis*. *Org. Lett.* **2013**, *15*, 2414–2417; (c) Youkwan, J.; Srisomphot, P.; Sutthivaiyakit, S., Bioactive Constituents of the Leaves of *Phyllanthus polyphyllus* Var. *Siamensis*. *J. Nat. Prod.* **2005**, *68*, 1006–1009.
3. Calixto, J. B.; Santos, A. R. S.; Filho, V. C.; Yunes, R. A., A Review of the Plants of the Genus *Phyllanthus*: Their Chemistry, Pharmacology, and Therapeutic Potential. *Med. Res. Rev.* **1998**, *18*, 225–258.
4. Fan, Y.-Y.; Zhang, H.; Zhou, Y.; Liu, H.-B.; Tang, W.; Zhou, B.; Zuo, J.-P.; Yue, J.-M., Phainanoids a–F, a New Class of Potent Immunosuppressive Triterpenoids with an Unprecedented Carbon Skeleton from *Phyllanthus Hainanensis*. *J. Am. Chem. Soc.* **2015**, *137*, 138–141.
5. Kahan, B. D., Individuality: The Barrier to Optimal Immunosuppression. *Nat. Rev. Immunol.* **2003**, *3*, 831–838.
6. Xie, J.; Wang, J.; Dong, G., Synthetic Study of Phainanoids. Highly Diastereoselective Construction of the 4,5-Spirocyclic Via Palladium-Catalyzed Intramolecular Alkenylation. *Org. Lett.* **2017**, *19*, 3017–3020.
7. DeForest, J. C. Progress Towards the Total Synthesis of (-)-Batrachotoxin a, Computationally Inspired Second-Generation Synthesis of (+)-Fastigiatine, Progress Towards the Total Synthesis of (-)-Himeradine a and Strategies Towards the 4,5-Spirocyclic Fragment of Phainanoid F. Ph. D. Dissertation, University of California, Irvine, Irvine, CA, 2017.
8. Bui, T.; Barbas, C. F., A Proline-Catalyzed Asymmetric Robinson Annulation Reaction. *Tetrahedron Lett.* **2000**, *41*, 6951–6954.
9. Bradshaw, B.; Etxebarria-Jardí, G.; Bonjoch, J.; Vióquez, S. F.; Guillena, G.; Nájera, C.; Hughes, D., Synthesis of (*S*)-8a-Methyl-3,4,8,8a-Tetrahydro-1,6-(2*h*,7*h*)-Naphthalenedione Via *N*-Tosyl-(*S*_a)-Binam-L-Prolinamide Organocatalysis *Org. Synth.* **2011**, *88*, 330–341.
10. Hatzellis, K.; Pagona, G.; Spyros, A.; Demetzos, C.; Katerinopoulos, H. E., Correction of the Structure of a New Sesquiterpene from *Cistus Creticus* Ssp. *Creticus*. *J. Nat. Prod.* **2004**, *67*, 1996–2001.
11. Burns, D. J.; Mommer, S.; O'Brien, P.; Taylor, R. J. K.; Whitwood, A. C.; Hachisu, S., Stereocontrolled Synthesis of the AB Rings of Samaderine C. *Org. Lett.* **2013**, *15*, 394–397.
12. Qian, M.; Covey, D. F., The Efficient and Enantiospecific Total Synthesis of Cyclopenta[*b*]Phenanthrenes Structurally-Related to Neurosteroids. *Adv. Synth. Catal.* **2010**, *352*, 2057–2061.
13. Gesson, J.-P.; Jacquesy, J.-C.; Renoux, B., A New Chiral Route toward Terpenoids. Annulation of Carvone to trans- and cis-Fused Bicyclic Synthons. *Tetrahedron* **1989**, *45*, 5853–5866.

Chapter 3. Synthesis of Kujounins A₁ and A₂ Using a Biosynthesis Inspired Approach

3.1 Abstract

A new biosynthesis was proposed for the kujounins A₁ and A₂ beginning from L-ascorbic acid (vitamin C), which in turn inspired a synthetic approach to kujounin A₂. The tricyclic ring system was assembled in two steps using a stereoselective Tsuji–Trost reaction followed by ozonolysis. The chemically labile disulfide was introduced in several more steps. These results will make kujounin and its analogues available for further evaluation.

3.2 Introduction

3.2.1 *Allium* Species

Allium species are plants that are commonly consumed as foods (onions and garlic) and have been used as traditional folk medicine in Europe, Asia, and America for centuries. Throughout history, *Allium sativum* L. has been used to treat leprosy, heart disease, cancer, animal bites, gangrene, and even the plague. In fact, *Allium sativum*, *Allium cepa*, and *Allium schoenoprasum* have been designated as anticancer foods by the National Cancer Institute of the United States. More recently, sulfur compounds from allium have been found to show many pharmaceutical activities, including antibacterial activity,¹ inhibition of macrophage activation,² and inhibition of inflammation by blocking nuclear factor kappa B (NF- κ B) activation.³ Due to the vast medicinal properties of *Allium* species, they have been a subject of synthetic interest to chemists.

3.2.2 Isolation of Kujounins A₁ and A₂ and Proposed Biosynthesis

In 2018, the Matsuda group isolated rare multicyclic disulfide natural products from *Allium fitsulosum* ‘Kujou,’ which is a Welsh onion from the southern area of Kyoto, Japan.⁴ The structures of the three natural products isolated are shown below (Figure 3-1). The structures of kujounin A₁ (**3-1**) and allium sulfoxide A₁ (**3-3**) were unambiguously assigned by X-ray crystallography and the structure of kujounin A₂ (**3-2**) was assigned by 1-D and 2-D NMR. These natural products, specifically the kujounins, are considered rare due to their multicyclic scaffold. Not many exocyclic disulfide containing natural products contain more than one ring system.

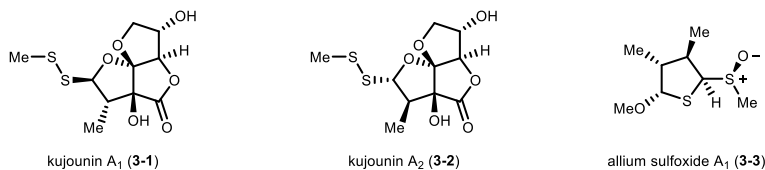
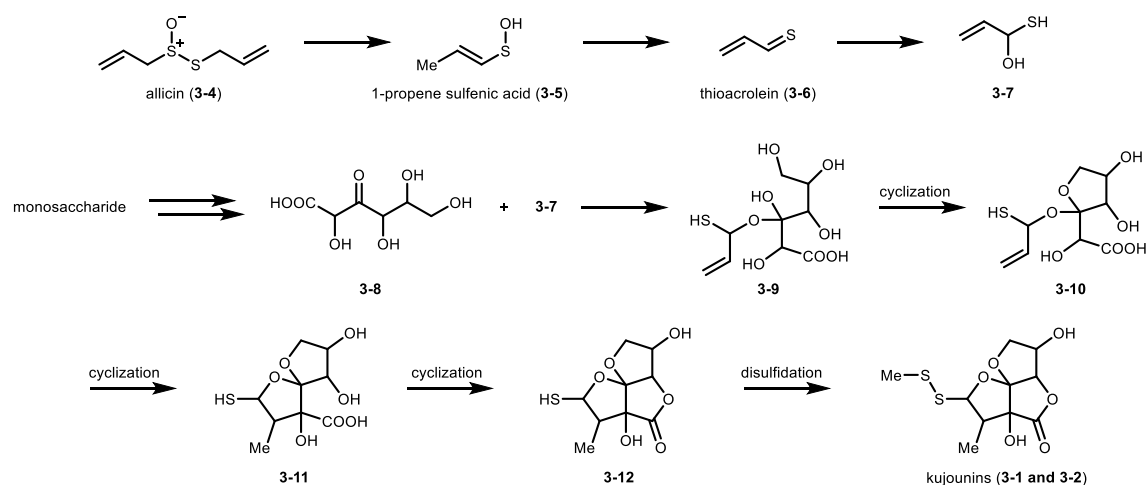


Figure 3-1. Structures of the natural products isolated by the Matsuda group.

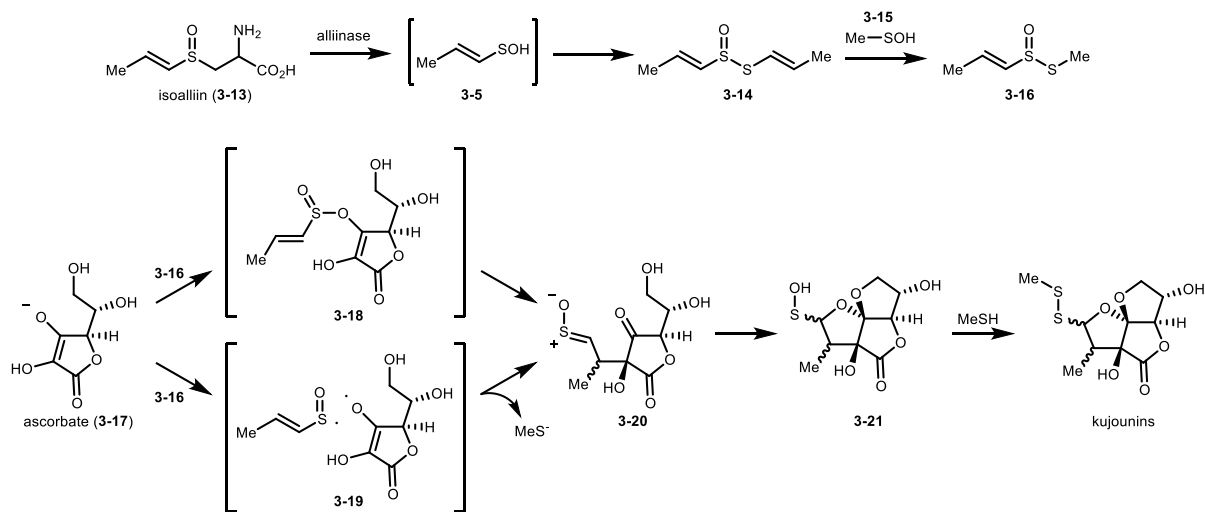
The Matsuda group proposed a biosynthesis of both natural products starting from alliin (3-4), which is a known compound in *Allium* species, and a non-specified monosaccharide (Scheme 3-1). Alliin is reported to form thioacrolein (3-6) from 1-propene sulfenic acid (3-5), which they presume forms unstable intermediate 3-7 through a hydration. This intermediate is further proposed to attack ketone 3-8, which would come from a monosaccharide. Intermediate 3-9 cyclizes on the hemiketal followed by another cyclization of the α -hydroxy carboxylic acid onto the olefin to form 3-11. The authors state that this type of radical based cyclization has never been reported in biological systems, but similar types of cyclizations can be performed using Bu_3SnH . The third cyclization forms lactone 3-12 and a final disulfidation would afford the kujounin natural products.

Scheme 3-1. Proposed biosynthesis of the kujounins by the Matsuda group.



After careful review of this proposed biosynthesis, it seemed too complex and unprecedented. Our lab envisioned a completely different biosynthetic route which utilized L-ascorbic acid (**3-17**) as the main source of carbons and oxygenation (Scheme 3-2). L-ascorbic acid maps on quite well to the kujounins framework and even contains the correct configuration for the lactone and secondary alcohol. The remainder of the molecule would arise from isoalliin (**3-13**) which is a stable precursor to many reactive sulfur compounds in allium species. The enzyme alliinase is responsible for generating unstable sulfenic acid **3-5** which can react with itself to make thiosulfinate **3-14**. Isoalliin is responsible for forming lacrimatory factor propanethial *S*-oxide via intermediate **3-5** by the aid of lacrimatory factor synthase.⁵ The methylthio fragment is presumed to stem from methiin following a similar pathway, which upon exchange of the sulfinic acid fragments would generate 1-propenyl methyl thiosulfinate **3-16**.⁶

Scheme 3-2. Proposed biosynthesis of the kujounins by the Rychnovsky group.



All of the necessary atoms for the formation of the kujounins are contained in ascorbate (**3-17**) and thiosulfinate **3-16**. Upon combining the two, the key C–C bond can be formed by a one- or two-electron process. The two-electron pathway would utilize intermediate **3-18** which can undergo a facile [3,3] sigmatropic rearrangement to forge the desired C–C bond. The other

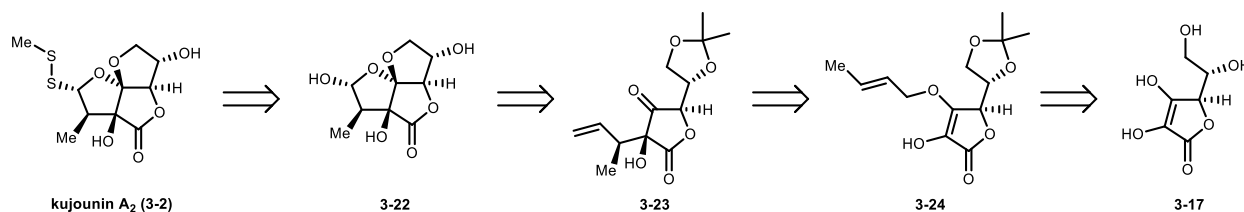
pathway would involve the radical pair **3-19**, which would combine to form the same C–C bond. Both routes lead to the formation of *S*-oxide **3-20** and methanethiolate. Stepwise cyclization of **3-20** to **3-21** followed by disulfide formation with residual methanethiol leads to kujounin A₁ and A₂.

3.3 Synthesis of Kujounins A₁ and A₂

3.3.1 Initial Approach

Inspired by our proposed biosynthesis of Kujounins A₁ and A₂, we pursued their syntheses from L-ascorbic acid. We envisioned a late stage disulfide installation from lactol **3-22**, which would be obtained from ozonolysis of alkene **3-23**. This alkene would arise from a key Claisen rearrangement of **3-24**, which would come from a well precedented alkylation of commercially available L-ascorbic acid (**3-17**) with *trans*-crotyl bromide (Scheme 3-3).

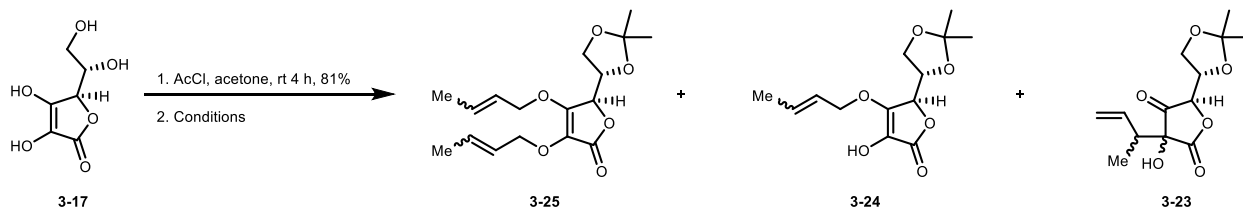
Scheme 3-3. Initial retrosynthesis of kujounin A₂.



We began the synthesis by protecting L-ascorbic acid (**3-17**) using catalytic acetyl chloride in acetone to form the corresponding acetonide in 81% yield (Table 3-1). Chemoselective alkylation of the acetonide was reported by various groups, including the direct 2-*O*-alkylation using *trans*-crotyl bromide by the Wimalasena group.⁷ They reported forming **3-24** in a 72% yield with a 7:3 ratio of *O* vs. *C* alkylation. However, in our hands, we obtained *ca.* 58% as a mixture of *O* (**3-24**) and *C* alkylation (**3-23**) as well as double *O* alkylation (**3-25**), which was separable by chromatography (Table 3-1, entry 1). The stereochemical analysis was further complicated due

to the fact that technical grade *trans*-crotyl bromide contains a significant amount of *cis* isomer. Cesium carbonate (entry 2) and phase-transfer catalysis (entry 3) were also attempted but resulted in mixtures of products.⁸ Lastly, we turned to Mitsunobu conditions (entry 4), but this also provided a complex mixture of products.⁹

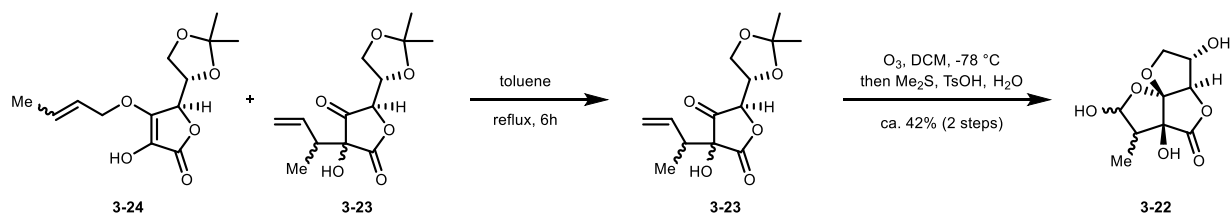
Table 3-1. Alkylation of acetonide protected *L*-ascorbic acid.



entry	conditions	result
1	<i>trans</i> -crotyl bromide, K ₂ CO ₃ , DMSO/THF	mixture
2	<i>trans</i> -crotyl bromide, Cs ₂ CO ₃ , acetone	mixture
3	<i>trans</i> -crotyl bromide, TBAI, KOH, H ₂ O/EtOAc	mixture
4	<i>trans</i> -crotyl alcohol, PPh ₃ , DEAD, THF	mixture

Since optimization of the alkylation was met with no success, we decided to directly subject the mixture of alkylated products to Claisen conditions in order to provide **3-23** (Scheme 3-4).^{7b} The rearrangement occurred, although, as expected a mixture of diastereomers was produced. Thus, the reaction mixture was taken on crude to oxidative cleavage using ozone followed by treatment with dimethyl sulfide, *p*-toluenesulfonic acid, and water in order to form the aldehyde and deprotect the acetonide all in one-pot. To no surprise, the reaction afforded **3-22** as a mixture of diastereomers in *ca.* 42% yield over two steps. This transformation was a major success for the synthesis since we were able to form the core of both natural products in only four steps from *L*-ascorbic acid.

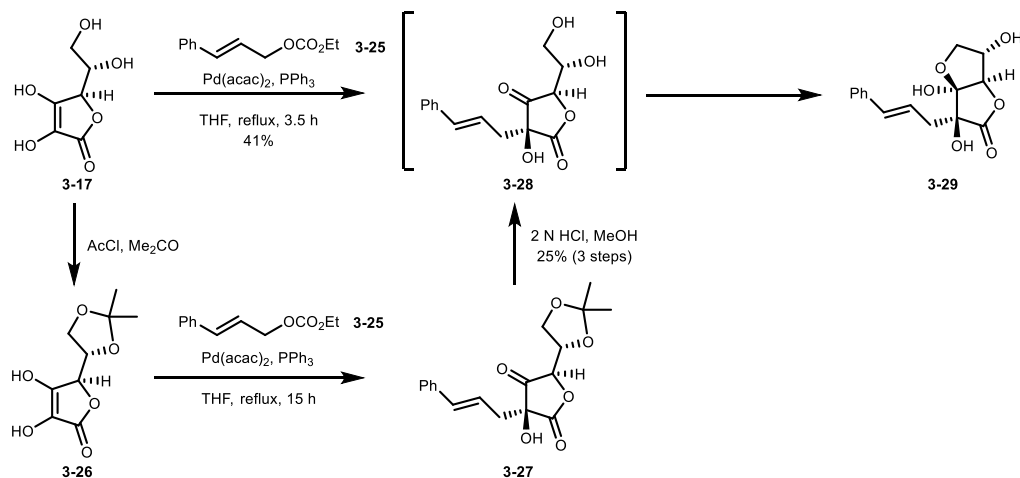
Scheme 3-4. Formation of the core of the kujounins A₁ and A₂.



3.3.2 Revised Approach to the Synthesis of Kujounins A_1 and A_2

Though we were able to make the core of the kujounins, none of the diastereomers were separable by silica gel chromatography, which made this route undesirable and difficult to proceed with. Thus, we turned to the literature to find alternative selective methods of alkylating ascorbic acid. In 1990, the Moreno-Manas group published a palladium catalyzed selective C-alkylation of ascorbic acid.¹⁰ They illustrated that L-ascorbic acid can be chemo- and diastereoselectively alkylated with allyl carbonates using palladium catalysis.¹¹ Specifically, they were able to alkylate L-ascorbic acid with carbonate **3-25** to afford triol **3-29** (no open-form (**3-28**) was detected by NMR) as a single diastereomer in 41% yield (**Scheme 3-5**). They also performed the same chemistry using acetonide **3-26** followed by deprotection, to afford the same product **3-29** but in much lower yield. This illustrated the benefit of using unprotected L-ascorbic acid as the nucleophile, which decreases the step count and overall efficiency.

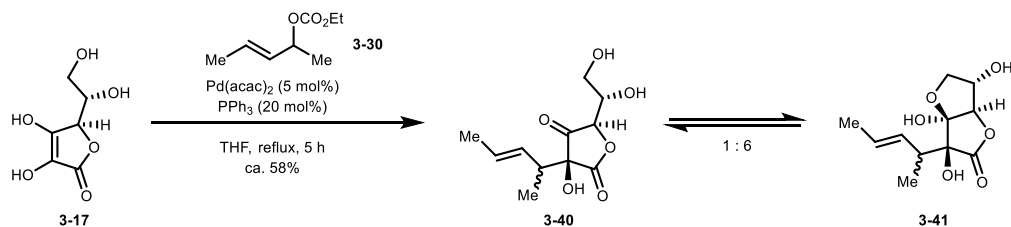
Scheme 3-5. Palladium catalyzed alkylation of ascorbic acid by the Moreno-Manas group.



Inspired by this work, we turned our attention to palladium catalyzed alkylation of L-ascorbic acid. This method sparked our interest because it had three clear advantages over the Claisen approach. We would be able to by-pass any acetonide protection of the diol while also being able to control the diastereoselectivity of both the tertiary alcohol and the methyl group. The methyl stereocenter would be controlled by using an enantiopure allylic carbonate.

We began with a test reaction using racemic allylic carbonate **3-30**, which proceeded to form the carbon-carbon bond in ca. 58% yield (**Scheme 3-6**). Product **3-40** was isolated only as a mixture of diastereomers at the methyl stereocenter and not the tertiary alcohol, presumably because the electrophile approached from the less hindered face of L-ascorbic acid. Contrary to the literature, we did observe a 1:6 ratio of opened (**3-40**) to closed (**3-41**) product by NMR analysis.

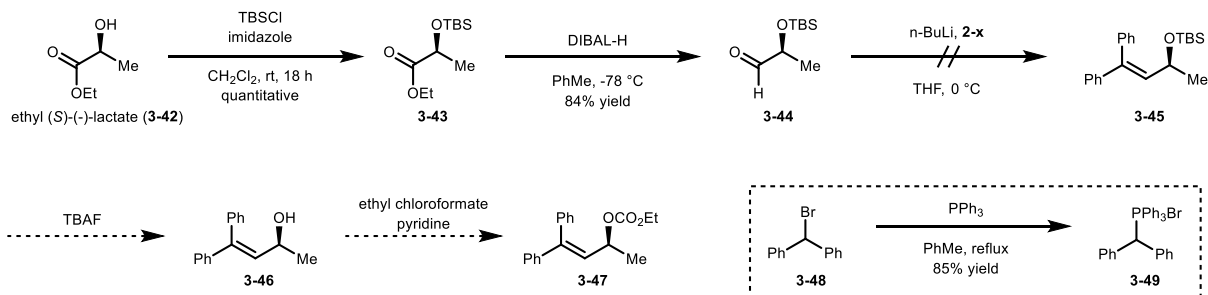
Scheme 3-6. Palladium catalyzed alkylation of L-ascorbic acid.



With this result in hand we turned to performing the reaction with an enantiopure allylic carbonate in order to set the methyl stereocenter of **3-41**. We sought to target allylic carbonate **3-47** in order to provide regioselectivity during the alkylation step by having two bulky phenyl groups (Scheme 3-7). The synthesis began with a TBS protection of enantiopure ethyl (*S*)-(-)-lactate (**3-42**), which proceeded in quantitative yield to provide ester **3-43**.¹² Reduction of ethyl ester **3-43** with DIBAL-H gave aldehyde **3-44** in 84% yield which was directly subjected to Wittig condition. Phosponium salt **3-49** was made by refluxing **3-48** with PPh₃ which was deprotonated and allowed to react with aldehyde **3-44**, but unfortunately the reaction did not proceed.¹³ Instead

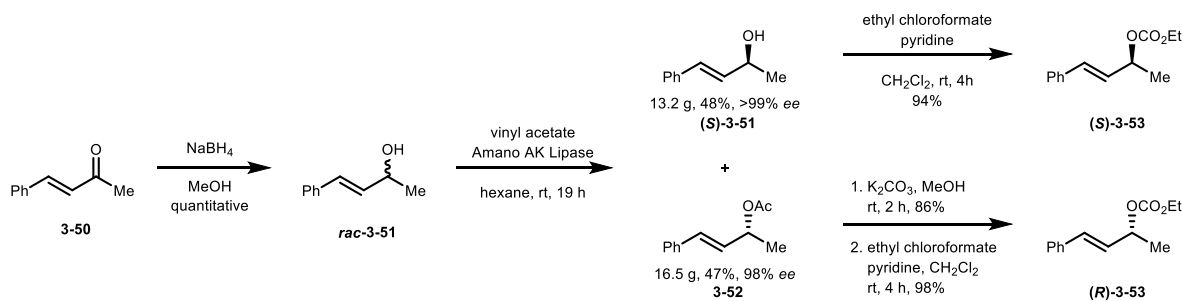
most of the phosphonium salt was recovered as well as the aldehyde, presumably due to the steric bulk of the diphenyl moiety.

Scheme 3-7. Attempted synthesis of enantiopure allylic carbonate **3-47**.

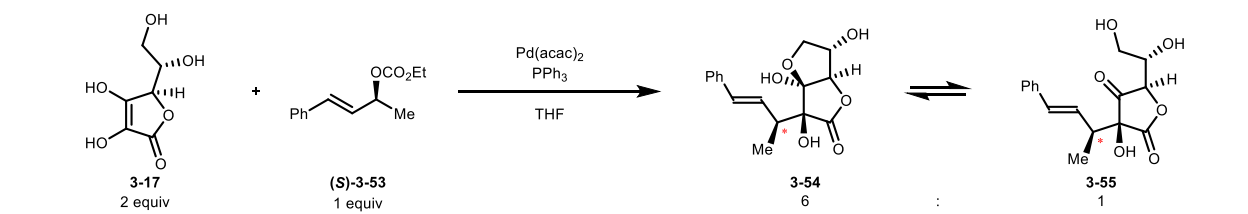


Upon reevaluation of the desired allylic carbonate, we realized that the diphenyl moiety was unnecessary to obtain good regioselectivity. Having one phenyl group is preceded to provide the desired regio-isomer, which is driven by conjugation.¹⁴ With this in mind, we sought to synthesize the known allylic carbonate (*S*)-**3-53** (Scheme 3-8). We turned to an enzymatic resolution strategy because it would allow quick access to both enantiomers of the allylic carbonate.¹⁵ Reduction of benzylideneacetone (**3-50**) with NaBH₄ in MeOH gave racemic allylic alcohol **3-51** in quantitative yield on a 30 gram scale with no purification necessary. Resolution of *rac*-**3-51** with Amano AK Lipase provided allylic alcohol (*S*)-**3-51** in 48% yield and >99% *ee* and allylic acetate **3-52** in 47% yield and 98% *ee*. Allylic alcohol (*S*)-**3-51** was directly transformed to allylic carbonate (*S*)-**3-53** with ethyl chloroformate while allylic acetate **3-52** was first deprotected with K₂CO₃ in MeOH and then derivatized to allylic carbonate (*R*)-**3-53** in excellent yields.

Scheme 3-8. Synthesis of allylic carbonate **3-53** by enzymatic resolution.



With each carbonate in hand, we sought to optimize the Tsuji-Trost alkylation for diastereoselectivity and high yield (Table 3-2). Initially, we used racemic carbonate **3-53** at room temperature for 24 hours in order to gauge the diastereoselectivity at the methyl stereocenter (entry 1). These conditions provided **3-54** in 86% yield and a 63:37 dr, which indicated some diastereoselective control from the substrate. Next, we used enantiopure carbonate (**S**)-**3-53** at 70 °C and room temperature, which provided similar yields and dr (entries 2 and 3). Upon cooling the reaction from 0 °C to room temperature or simply using DMSO as the solvent, the dr of the reaction was improved to 90:10 (entry 4 and 5). Keeping the reaction at 0 °C yielded a single diastereomer but dropped the yield to 40%, presumably due to poor solubility of ascorbic acid at low temperature in THF (entry 6). Lastly, we examined enantiomeric carbonate (**R**)-**3-53** and found that the dr was 54:46, which still favored the methyl beta, indicating strong substrate control over diastereoselectivity (entry 7). Alkene **3-54** is crystalline and diastereomerically pure samples were available by recrystallization, which is why entry 4 was used as the optimal conditions for the synthesis.

Table 3-2. Optimization of the Tsuji-Trost alkylation of L-ascorbic acid.


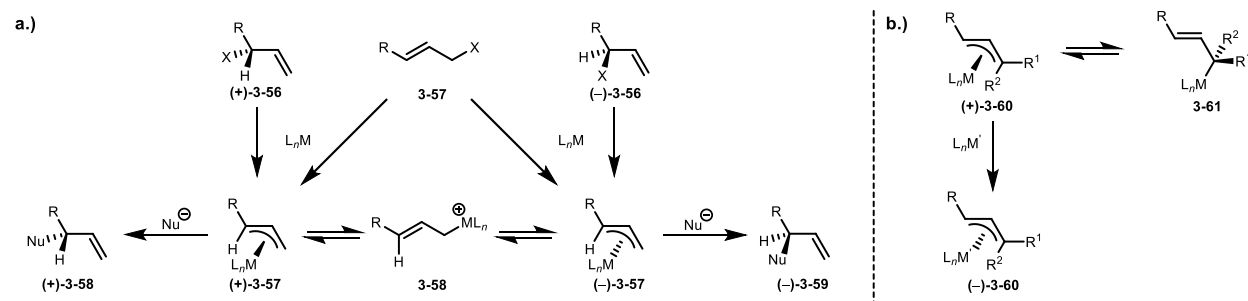
entry	temp (°C)	time (h)	Pd(acac) ₂ (mol%)	PPh ₃ (mol%)	yield (%)	Me _β : Me _α ^a
1 ^b	23 °C	24	3	12	86	63 : 37
2	70 °C	5	5	20	85	77 : 23
3	23 °C	24	3	25	86	82 : 18
4	0 °C to 23 °C	24	3	12	91	90 : 10
5 ^c	23 °C	24	3	12	86	90 : 10
6	0 °C	24	3	12	40	99 : 1
7 ^d	23 °C	24	5	20	88	54 : 46

^a All ratios were obtained by subsequent ozonolysis of crude material and analyzing the lactol proton shifts by NMR. ^b Racemic carbonate (**3-53**) was used. ^c DMSO was used as the solvent. ^d Carbonate (**R**)-**3-53** was used.

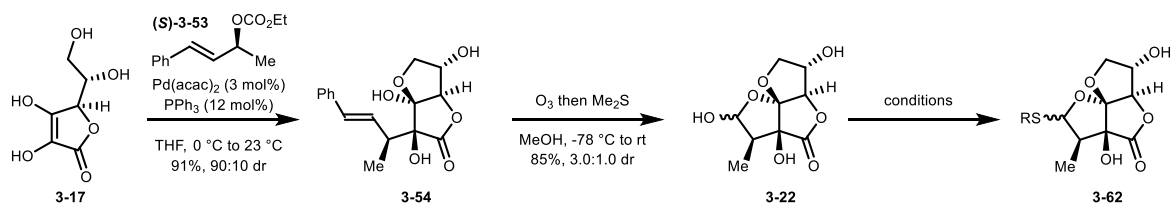
Initially, we were shocked by the diastereoselectivity of the reaction because Tsuji-Trost alkylations are known to retain stereochemistry of the carbonate when a soft nucleophile is used and invert it when a hard nucleophile is used. Although, in our case we observed scrambling of stereochemistry which provided mixtures of beta and alpha epimers at the methyl stereocenter. Upon further investigation in the literature, it is known that allylic carbonates can racemize using palladium catalysis.¹⁶ For a terminal olefin, starting with either carbonate (+)-**3-56**, (-)-**3-56**, or **3-57** would form either (+)-**3-57** or (-)-**3-57** when treated with palladium(0) (Scheme 3-9, a). Each η^3 -complex can equilibrate with η^1 -complex (**3-58**), which contains no stereocenter, and in turn scrambles the stereochemistry. In our case, having a multi-substituted olefin would provide η^3 -complex (+)-**3-60** which is in equilibrium with η^1 -complex **3-61** but stereochemistry is preserved (Scheme 3-9, b). However, η^3 -complex (+)-**3-60** can be intercepted by another palladium (0)

species ($L_nM^?$) and invert the stereochemistry. This is seemingly the effect we observe in the case of the Tsuji-Trost alkylation in table 3-2.

Scheme 3-9. Proposed mechanism of carbonate racemization for a terminal olefin (**a**) and multi-substituted olefin (**b**).



After developing robust conditions for production of diastereomerically pure **3-54**, we formed tricyclic lactol **3-22** via a facile ozonolysis in 85% yield and a 3:1 dr at the lactol stereocenter. We then turned our attention to installing sulfur at the anomeric position (Table 3-3). First attempts were based off the work of the Davis lab where they were able to convert pyranoses and furanoses into glycosyl thiols using Lawesson's reagent.¹⁷ They propose that Lawesson's reagent reacts with the aldehyde of the open form of a lactol to provide the anomeric sulfide. This approach was attractive to us because they showcased that the reaction was suitable to free hydroxyls and acetates. Unfortunately, reactions at various temperatures and time points using Lawesson's reagent never afforded product, instead complex mixtures were obtained (entries 1-4). Phosphorus pentasulfide was also examined as a sulfur source since it is known to be superior to Lawesson's reagent in various cases, although it was ultimately met with no success (entries 5 and 6).¹⁸ These results might suggest that our substrate only existed as the closed lactol isomer or that the anomeric thiol was intrinsically unstable.

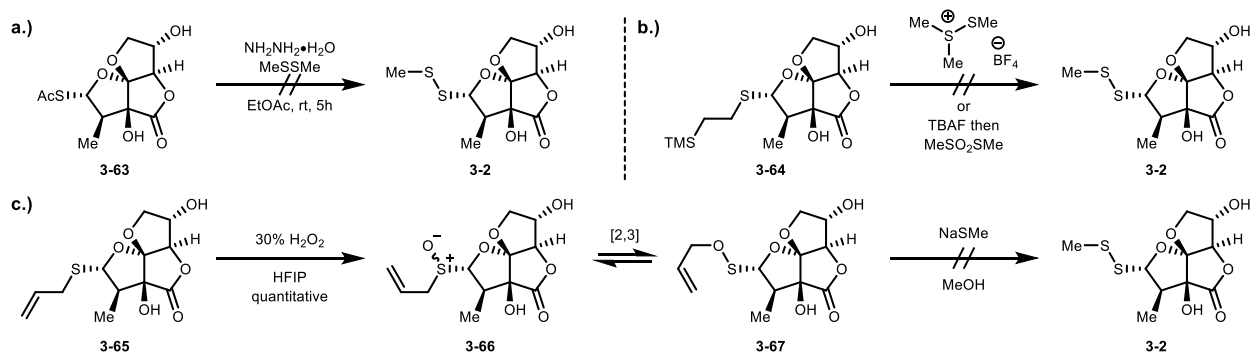
Table 3-3. Tricyclic core formation and sulfur installation.

entry	conditions	R	yield (%), dr
1	Lawesson's reagent, dioxane, 110 °C, 2 days	H	0
2	Lawesson's reagent, dioxane, 80 °C, 24 hours	H	0
3	Lawesson's reagent, dioxane, 100 °C, 3 hours	H	0
4	Lawesson's reagent, dioxane, rt, 24 hours	H	0
5	P ₄ S ₁₀ , pyridine, 110 °C, 4 hours	H	0
6	P ₄ S ₁₀ , HMDO, MeCN, 90 °C, ON	H	0
7	DMC, Na ₂ S ₂ O ₃ ·5H ₂ O, Et ₃ N, H ₂ O/MeCN, 0 °C	NaO ₃ S-	0
8	TMSOTf, (TMS) ₂ S, CH ₂ Cl ₂ , 50 °C, ON	H	0
9	Re ₂ O ₇ , AcSH, CH ₂ Cl ₂ , rt, ON	Ac	0
10	BF ₃ ·OEt ₂ , AcSH, CH ₂ Cl ₂ , 0 °C to rt, ON	Ac	trace
11	AcSH, dioxane, 100 °C, ON	Ac	trace
12	amberlyst 15, AcSH, dioxane, 100 °C, ON	Ac	10, >20:1
13	allyl mercaptan, HCl in dioxane, rt, 3 h	allyl	73, 1:1.2
14	TMSCH ₂ CH ₂ SH, HCl in dioxane, rt, 3h	TMSCH ₂ CH ₂ -	40, >20:1

Our efforts turned to direct activation of the lactol alcohol to effect the desired transformation. Triol **3-22** was treated with 2-chloro-1,3-dimethylimidazolium chloride (DMC) to activate the lactol followed by sodium thiosulfate pentahydrate (Na₂S₂O₃·5H₂O) to attempt formation of the Bunte salt, but no product was formed (entry 7).¹⁹ The use of Lewis acids failed to install a sulfur atom, with the exception of BF₃·OEt₂ which produced trace amounts (entries 8-10).²⁰ Treating **3-22** with thioacetic acid at 100 °C also formed trace amounts of product and the addition of amberlyst 15 resin seemed to slightly improve the yield to 10% as a single diastereomer

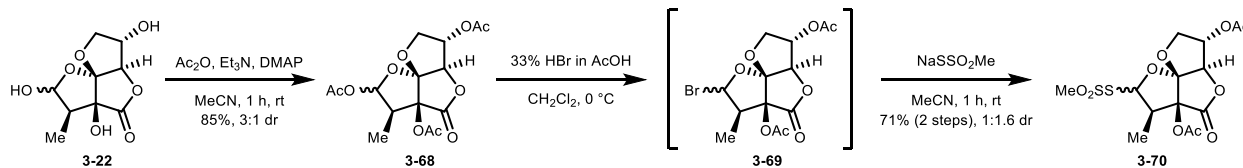
(entries 11 and 12). Using allyl mercaptan as the nucleophile and HCl as the activator produced product in 73% yield and a 1:1.2 dr (entry 13). Similarly, using 2-(trimethylsilyl)ethanethiol with HCl afforded product in 40% yield as a single diastereomer (entry 14).

Scheme 3-10. Failed attempts at forming kujounin A₂ from various anomeric sulfur derivatives.

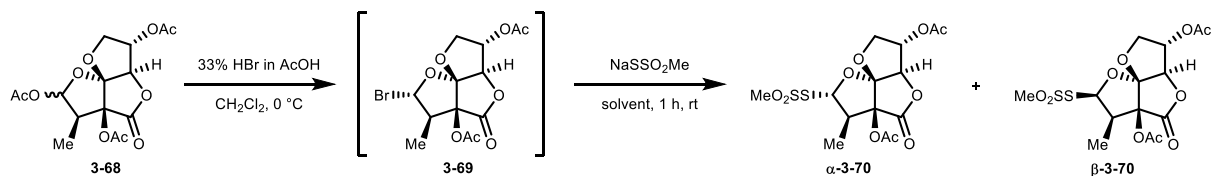


We attempted to elaborate each product with a sulfur incorporated from Table 3-3 into kujounin A₂, although all attempts were unsuccessful (Scheme 3-10). First, anomeric acetate **3-63** was treated with hydrazine hydrate and dimethyl disulfide in hopes of a one-pot deprotection and disulfide formation (Scheme 3-10, a).²¹ Trimethylsilyl ether **3-64** was charged with dimethyl(methylthio) sulfonium tetrafluoroborate (DMTSE), which instantly consumed the starting material yet produced no product (Scheme 3-10, b).²² Using TBAF as the fluoride source and an electrophilic source of methyl sulfide was also not productive. Allyl sulfide **3-65** was oxidized to the corresponding sulfoxide in quantitative yield as a mixture of diastereomers (Scheme 3-10, c). Since allyl sulfoxides are known to undergo Mislow-Evans [2,3] rearrangements, we attempted to trap sulfenate ester **3-67** with NaSMe as the thiophile in order to afford the natural product.²³ Unfortunately, these reaction conditions led to decomposition.

Scheme 3-11. Sulfur installation toward the synthesis of kujounin A₂.



Ultimately, we resorted to robust carbohydrate chemistry to install the sulfur moiety. Triol **3-22** was acylated using acetic anhydride in the presence of base and DMAP to afford triacetate **3-68** in 85% yield and 3:1 dr (Scheme 3-11). The two diastereomers were separated and computational modeling of NMR chemical shifts using the DP4+ method suggested the major isomer as the α -acetate and the minor being the β -acetate.²⁴ The diastereomeric mixture of acetate **3-68** was treated with 33% HBr in acetic acid to provide anomeric bromide **3-69** as one major diastereomer, which NOE studies showed the α -bromide. This sensitive bromide was not purified but rather directly exposed to sodium methylthiosulfonate to yield 71% of product **3-70** in a 1:1.6 dr, presumably favoring the undesired β -diastereomer.²⁵ Favoring the β -isomer was no surprise, as one would expect an S_N2 mechanism to yield this diastereomer. The desired α -isomer presumably arises from competing S_N1 reactivity. In an effort to increase diastereoselectivity, we conducted a solvent screen which is shown in Table 3-4. Changing to a polar protic solvent drastically decreased the yield but increased the dr for the desired isomer (entries 1-4). Polar aprotic solvents tended to have higher yields than the polar protic solvents but mainly favored the β -isomer and in the case of THF, dioxane, and EtOAc significant amounts of starting bromide was recovered (entries 5-10). Addition of NaI to the reaction diminished the yield and using toluene as the solvent with TBAB gave modest yield with the undesired epimer being the major product (entries 11 and 12).

Table 3-4. Unsuccessful solvent screen optimization for installation of the sulfur moiety.

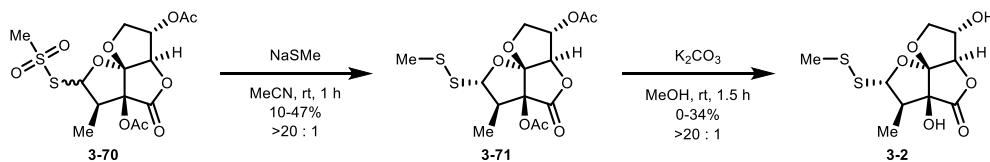
entry	solvent	3-69 recovered (%) ^a	yield (%) ^a	dr (α : β) ^a
1	MeOH	0	7	9.7 : 1
2	EtOH	0	2	3.0 : 1
3	<i>i</i> PrOH	0	4	1 : 2.0
4	<i>tert</i> -amyl alcohol	5	16	1 : 1.1
5	DMF	14	27	1 : 1.7
6	DMSO	0	14	1.3 : 1
7	THF	28	21	1 : 3.0
8	dioxane	18	25	1.4 : 1
9	EtOAc	50	11	1 : 6.2
10	acetone	0	53	1 : 3.1
11 ^b	acetone	0	3	1 : >95
12 ^c	toluene	5	36	1 : 6.6

^a Based on NMR analysis using 5,6-dibromobenzo[d][1,3]dioxole as the standard over 2 steps. ^b Sodium iodide was added to the reaction. ^c Tetra-*n*-butylammonium bromide was added to the reaction.

The optimization was met with no success, thus the original conditions were used to push the synthesis forward. Thiosulfonate **3-70** was treated with sodium thiomethoxide to afford disulfide **3-71** as essentially a single diastereomer, although the reaction was not reliable and yields varied drastically (Scheme 3-13). We hypothesized that the acidic protons of the thiosulfonate methyl may have caused problems under basic conditions. The final step was also problematic because the natural product was base labile. Using basic conditions to cleave the acetates did provide the natural product, but leaving the reaction too long under these conditions seemed to

cause decomposition. The spectroscopic properties of synthetic kujounin A₂ were consistent with those originally reported for the natural product.⁴

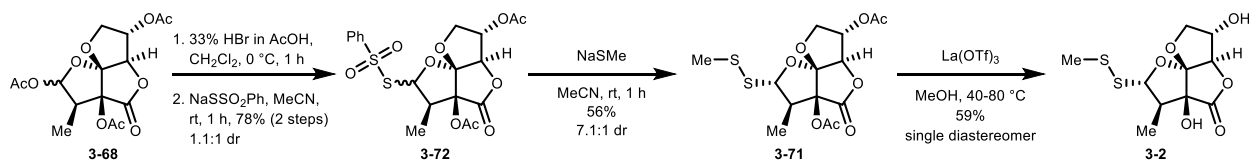
Scheme 3-12. Irreproducible end game for the synthesis of kujounin A₂.



With the natural product in hand we were able to assign structures for the α - and β -isomers because the α -isomers of **3-2**, **3-71**, and **3-70** all contained distinctive 10 Hz coupling constants at the anomeric proton whereas the β -isomers showed 6.7 Hz. With the structures of each diastereomer assigned, we were left with the last task of optimizing the last two steps of the sequence. Based on our hypothesis of the acidity of the thiosulfonate methyl protons causing decomposition under basic conditions, we decided to avoid this by using sodium phenylthiosulfonate as our sulfur nucleophile (Scheme 3-14).²⁶ To our delight, this increased the yield to 78% of **3-72** and the dr improved to 1.1:1 favoring the desired α -isomer. The subsequent reaction was also improved. Using **3-72** as the respective electrophile gave a 56% yield in a 7.1:1 dr favoring the desired α -isomer and improved the reliability of the reaction. Furthermore, switching from basic conditions to Lewis acid-catalyzed deprotection of the acetates provided much higher yield of the natural product as a single diastereomer.²⁷ It is worth mentioning that hydrolysis of the secondary acetate was much faster than the tertiary and unreacted tertiary acetate was recovered in 30% yield with a 2.5:1 dr favoring the α -isomer. This reaction was not optimized due to lack of time, but longer reaction times could presumably increase the yield. Obtaining a single diastereomer from a 7.1:1 mixture of **3-71** was surprising yet advantageous for us. We

believe cleavage of the tertiary acetate is diastereoselective, with the less sterically congested α -isomer hydrolyzing more quickly.

Scheme 3-13. Optimized end game for the synthesis of kujounin A₂.

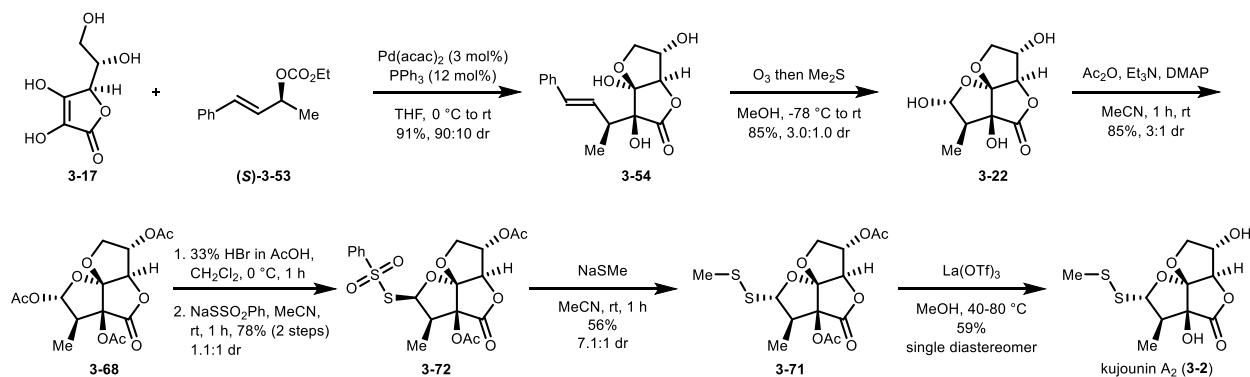


3.3.3 Summary of the Synthesis of Kujounin A₂ and Future Directions

The complete synthesis of kujounin A₂ is summarized below in Scheme 3-15. This sequence is short and effective. It utilizes a key Tsuji-Trost alkylation to devise the majority of the carbon framework and set two stereocenters. It is worth noting that this alkylation was ineffective in providing synthetically useful selectivity for the α -methyl isomer of **3-54** (Table 3-2, entry 7), which impeded our stereoselective synthesis of kujounin A₁ (**3-1**). Even so, we were able to carry mixtures of multiple diastereomers through the seven-step sequence and successfully synthesize kujounin A₁, albeit as an inseparable mixture of diastereomers. Kujounin A₂ was sent to the National Cancer Institute (NCI) for biological activity examination and we await the results.

With both natural products in hand, we decided to examine experimentally our proposed biosynthesis of the kujounins (Scheme 3-2). An onion was blended in water with excess L-ascorbic acid and allowed to stand overnight. The crude mixture was filtered and extracted with ethyl acetate. The organic material was examined by TLC and a spot matched the R_f of kujounin A₂, although further analysis by carbon NMR revealed that no natural product was present.

Scheme 3-14. Full forward synthesis of kujounin A₂.



The complete sequence affords the natural product in a short number of steps, but further investigation can shorten the sequence and expel the need for protecting group manipulations. This can potentially be accomplished by finding an appropriate activator of the lactol. Another matter that merits examination is the stereoselectivity of the Tsuji-Trost alkylation. Using appropriate chiral ligands with a racemic allylic carbonate may be able to overcome the undesired substrate control. If the biological data is promising, a structure-activity-relationship (SAR) should be conducted. Using different thiols with electrophile **3-72** would afford a variety of disulfides.

3.4 Conclusions

In summary, a robust route has been developed for the synthesis of kujounin A₂. It utilizes L-ascorbic acid (**3-17**) as the starting material, which provides the source of chirality, all of the oxygenation, and the majority of the carbon framework. A key Tsuji-Trost alkylation sets two stereocenters and forms a main carbon-carbon bond. Ozonolysis affords the core structure of the natural product. Unfortunately, direct functionalization of the lactol was unsuccessful, but using acetate activation and protection proved viable. Further manipulations yielded kujounin A₂ in only seven steps. This is the first total synthesis of the kujounins and biological activity studies are pending.

3.5 Experimental Section

3.5.1 General Experimental Details

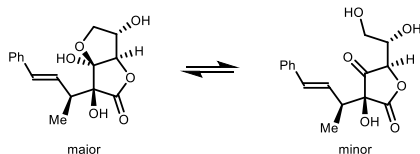
CDCl_3 was dried using Na_2SO_4 before use. ^1H NMR and ^{13}C NMR spectra were recorded at 500 MHz and 125 MHz at 298.0 K unless stated otherwise. Chemical shifts (δ) were referenced to either TMS or the residual solvent peak. The ^1H NMR spectra data are presented as follows: chemical shift, multiplicity (s = singlet, d = doublet, t = triplet, q = quartet, m = multiplet, dd = doublet of doublets, ddd = doublet of doublet of doublets, dddd = doublet of doublet of doublet of doublets, dt = doublet of triplets, dq = doublet of quartets, ddq = doublet of doublet of quartets, app. = apparent), coupling constant(s) in hertz (Hz), and integration. High-resolution mass spectrometry was performed using ESI-TOF.

Unless otherwise stated, synthetic reactions were carried out in flame- or oven-dried glassware under an atmosphere of argon. All commercially available reagents were used as received unless stated otherwise. Solvents were purchased as ACS grade or better and as HPLC-grade and passed through a solvent purification system equipped with activated alumina columns prior to use. Thin layer chromatography (TLC) was carried out using glass plates coated with a 250 μm layer of 60 \AA silica gel. TLC plates were visualized with a UV lamp at 254 nm, or by staining with *p*-anisaldehyde, potassium permanganate, phosphomolybdic acid, or vanillin. Liquid chromatography was performed using forced flow (flash chromatography) with an automated purification system on prepacked silica gel (SiO_2) columns unless otherwise stated. Infrared (IR) spectroscopy was performed on potassium bromide salt plates. Optical rotations were taken using a glass 50 mm cell with a sodium D-line at 589 nm. Electrospray ionization mass spectrometry (ESI-MS) was analyzed in positive mode with flow injection.

3.5.2 Chemicals

All purchased chemicals were used without further purification unless otherwise noted. CDCl₃ was purchased from Cambridge Isotope Laboratories. Pd(acac)₂ was purchased from Combi-Blocks. The following chemicals were purchased from Sigma Aldrich: PPh₃, Me₂S, NaSSO₂Ph (technical grade, 85%), HBr in acetic acid (33% (w/w)), and NaSMe. (*S,E*)-ethyl (4-phenylbut-3-en-2-yl) carbonate ((*S*)-**3-53**) was prepared by the method of Kazmaier.^{16a-c}

3.5.3 Compound Characterization



(3*S*,3*aS*,6*S*,6*aR*)-3,3*a*,6-trihydroxy-3-((*S,E*)-4-phenylbut-3-en-2-yl)tetrahydrofuro[3,2-*b*]furan-2(3*H*)-one (3-54) and (3*S*,5*R*)-5-((*S*)-1,2-dihydroxyethyl)-3-hydroxy-3-((*S,E*)-4-phenylbut-3-en-2-yl)furan-2,4(3*H*,5*H*)-dione (3-55): To a solution of Pd(acac)₂ (21.0 mg, 0.0681 mmol) in THF (20 mL) was added PPh₃ (71.0 mg, 0.272 mmol). The reaction was allowed to stir for ten min before L-ascorbic acid (**3-17**) (786 mg, 4.54 mmol) was added in one portion followed by (*S,E*)-ethyl (4-phenylbut-3-en-2-yl) carbonate ((*S*)-**3-53**) (500 mg, 2.27 mmol) in THF (3.0 mL). The flask was evacuated and refilled with argon three times. The reaction mixture was cooled to 0 °C with a large ice bath and allowed to stir for 24 h from 0 °C to room temperature as the ice bath melted. The resulting yellow mixture was filtered through a short plug of silica with EtOAc (150 mL). The solution was concentrated *in vacuo* and purified by flash column chromatography (EtOAc/Hex) on silica to yield a 6:1 mixture of **3-54** to **3-55** as a white solid (632 mg, 91%). A sample was recrystallized to analytical purity for characterization.

TLC R_f = 0.47 (silica gel, 15:85 Hex:EtOAc)

Melting Point 78 °C – 80 °C

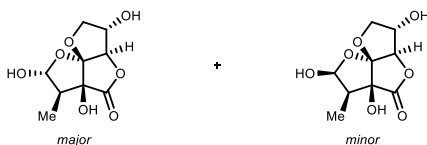
Optical Rotation $[\alpha]_D^{22} = -20.4$ ($c = 1.08$, MeOH)

$^1\text{H NMR}$ (600 MHz, CD_3OD , mixture of isomers) δ 7.40 – 7.36 (m, 2H, major and minor isomers), 7.28 (t, $J = 7.7$ Hz, 2H, major and minor isomers), 7.22 – 7.17 (m, 1H, major and minor isomer), 6.52 (d, $J = 15.6$ Hz, 1H, minor isomer), 6.46 – 6.38 (m, 2H, major isomer), 6.11 (dd, $J = 15.8, 8.8$ Hz, 1H, minor isomer), 4.58 (s, 1H, minor isomer), 4.44 (s, 1H, major isomer), 4.38 (dd, $J = 5.8, 3.6$ Hz, 1H, major isomer), 4.19 (dd, $J = 9.8, 5.8$ Hz, 1H, major isomer), 4.12 – 4.09 (m, 1H, minor isomer), 4.04 (dd, $J = 9.8, 3.6$ Hz, 1H, major isomer), 3.62 (d, $J = 7.1$ Hz, 2H, minor isomer), 2.90 – 2.81 (m, 1H, major and minor isomers), 1.31 (d, $J = 6.9$ Hz, 3H, major isomer), 1.26 (d, $J = 6.8$ Hz, 3H, minor isomer).

$^{13}\text{C NMR}$ (150 MHz, CD_3OD , major isomer) δ 178.1, 138.6, 133.1, 130.5, 129.5, 128.3, 127.3, 109.0, 89.1, 81.6, 75.9, 75.3, 44.1, 15.1. (150 MHz, CD_3OD , minor isomer) δ 209.4, 175.6, 138.0, 134.9, 129.6, 128.8, 127.5, 127.4, 84.4, 77.3, 71.6, 62.6, 45.7, 13.6.

IR (FT-IR) 3458, 2874, 1767, 1323 cm^{-1} .

HRMS (ESI-TOF) m/z calcd for $\text{C}_{16}\text{H}_{18}\text{O}_6\text{Na}$ ($\text{M} + \text{Na}$) $^+$: 329.1001, found 329.1006.



(3S,3aR,5aS,6R,7R,8aR)-3,5a,7-trihydroxy-6-methyltetrahydro-2H-difuro[3,2-b:2',3'-c]furan-5(5aH)-one (major) and (3S,3aR,5aS,6R,7S,8aR)-3,5a,7-trihydroxy-6-methyltetrahydro-2H-difuro[3,2-b:2',3'-c]furan-5(5aH)-one (minor) (3-22): A flask containing alkene **3-54** (and ketone **3-55**) (3.25 g, 10.6 mmol) and MeOH (109 mL) at -78 °C was treated with ozone until the solution turned purple/blue in color. The reaction was then purged with oxygen until the color disappeared. The flask was removed from the cooling bath and dimethyl sulfide (1.20 mL, 16.3 mmol) was added. The solution was allowed to stir for 2 h before

concentrated *in vacuo*, and the residue was purified by flash column chromatography (EtOAc/Hex) on silica to yield **3-22** as a foamy solid in a 1:3 mixture of diastereomers. (2.14 g, 85%):

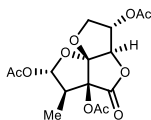
TLC R_f = 0.21 (silica gel, 15:85 Hex:EtOAc)

^1H NMR (500 MHz, CD_3OD , mixture of diastereomers) δ 5.34 (d, J = 4.7 Hz, 1H, minor isomer), 5.28 (d, J = 5.1 Hz, 1H, major isomer), 4.64 (d, J = 2.4 Hz, 1H, major isomer), 4.55 (d, J = 1.6 Hz, 1H, minor isomer), 4.28 (td, J = 4.7, 2.5 Hz, 1H, major isomer), 4.25 – 4.22 (m, 1H, minor isomer), 4.10 – 4.04 (m, 1H, major and minor isomer), 3.99 (dd, J = 9.8, 4.3 Hz, 1H, major and minor isomer), 2.42 (qd, J = 7.0, 4.7 Hz, 1H, minor isomer), 2.23 (qd, J = 7.2, 5.1 Hz, 1H, major isomer), 1.12 (d, J = 7.1 Hz, 3H, minor isomer), 1.08 (d, J = 7.1 Hz, 3H, major isomer).

^{13}C NMR (125 MHz, CD_3OD , major diastereomer) δ 176.5, 116.2, 105.4, 91.6, 80.4, 75.2, 74.9, 47.4, 9.3. (125 MHz, CD_3OD , minor diastereomer) δ 175.8, 118.8, 103.0, 91.2, 79.7, 75.2, 75.1, 44.9, 7.3.

IR (FT-IR) 3339, 2951, 1778, 1645 cm^{-1}

HRMS (ESI-TOF) m/z calcd for $\text{C}_9\text{H}_{12}\text{O}_7\text{Na}$ ($\text{M} + \text{Na}$) $^+$: 255.0481, found 255.0480.



(3S,3aR,5aS,6R,7S,8aR)-6-methyl-5-oxotetrahydro-2H-difuro[3,2-b:2',3'-c]furan-

3,5a,7(5H)-triyyl triacetate (3-68 major): To a flask containing a mixture of diastereomers of lactol **3-22** (300 mg, 1.29 mmol) dissolved in MeCN (4.3 mL) was added Ac_2O (0.61 mL, 6.46 mmol), Et_3N (0.90 mL, 6.46 mmol), and DMAP (26 mg, 0.065 mmol). After stirring for 1 h at room temperature, the dark brown reaction mixture was concentrated *in vacuo*, and the residue was purified by flash column chromatography (EtOAc/Hex) on silica to yield **3-68 major** as a clear oil (295 mg, 64%):

TLC $R_f = 0.57$ (silica gel, 55:45 Hex:EtOAc).

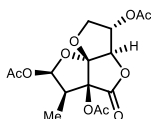
Optical Rotation $[\alpha]_D^{24} = -38.3$ ($c = 1.00$, CHCl_3).

$^1\text{H NMR}$ (600 MHz, CDCl_3) δ 6.06 (d, $J = 2.6$ Hz, 1H), 5.43 (td, $J = 6.8, 3.7$ Hz, 1H), 4.88 (d, $J = 3.8$ Hz, 1H), 4.39 (dd, $J = 9.8, 7.2$ Hz, 1H), 3.95 (dd, $J = 9.7, 6.6$ Hz, 1H), 2.63 (qd, $J = 7.3, 2.6$ Hz, 1H), 2.13 (s, 3H), 2.06 (s, 3H), 2.04 (s, 3H), 1.21 (d, $J = 7.4$ Hz, 3H).

$^{13}\text{C NMR}$ (150 MHz, CDCl_3) δ 171.1, 169.9, 169.5, 169.2, 114.7, 100.0, 89.9, 81.0, 76.1, 73.7, 46.2, 20.9, 20.5, 19.9, 11.3.

IR (FT-IR) 2974, 1798, 1746, 1369 cm^{-1} .

HRMS (ESI-TOF) m/z calcd for $\text{C}_{15}\text{H}_{18}\text{O}_{10}\text{Na}$ ($\text{M} + \text{Na}$) $^+$: 381.0798, found 381.0797.



(3S,3aR,5aS,6R,7R,8aR)-6-methyl-5-oxotetrahydro-2H-difuro[3,2-b:2',3'-c]furan-

3,5a,7(5H)-triyyl triacetate (3-68 minor): From the same reaction mixture generating **3-68 major**, **3-68 minor** was isolated by chromatography as a yellow oil (98 mg, 21%):

TLC $R_f = 0.46$ (silica gel, 55:45 Hex:EtOAc).

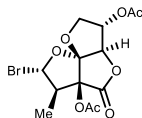
Optical Rotation $[\alpha]_D^{24} = +26.1$ ($c = 1.00$, CHCl_3).

$^1\text{H NMR}$ (600 MHz, CDCl_3) δ 6.27 (d, $J = 4.7$ Hz, 1H), 5.37 (ddd, $J = 6.6, 5.6, 3.1$ Hz, 1H), 4.87 (d, $J = 2.9$ Hz, 1H), 4.40 (dd, $J = 10.0, 6.6$ Hz, 1H), 4.03 (dd, $J = 9.9, 5.5$ Hz, 1H), 2.64 (qd, $J = 7.0, 4.8$ Hz, 1H), 2.21 (s, 3H), 2.13 (s, 3H), 2.10 (s, 3H), 1.21 (d, $J = 7.0$ Hz, 3H).

$^{13}\text{C NMR}$ (150 MHz, CDCl_3) δ 170.0, 170.0, 169.8, 169.6, 117.4, 98.3, 88.9, 80.3, 76.2, 73.8, 45.6, 21.2, 20.7, 20.2, 7.2.

IR (FT-IR) 2976, 1798, 1746, 1372 cm^{-1} .

HRMS (ESI-TOF) m/z calcd for $\text{C}_{15}\text{H}_{18}\text{O}_{10}\text{Na}$ ($\text{M} + \text{Na}$) $^+$: 381.0798, found 381.0786.



(3S,3aR,5aS,6R,7S,8aR)-7-bromo-6-methyl-5-oxotetrahydro-2H-difuro[3,2-b:2',3'-c]furan-3,5a(5H)-diyl diacetate (3-69): To a flask containing a mixture of acetates **3-68 major** and **3-68 minor** (247 mg, 0.689 mmol) was added CH₂Cl₂ (7.0 mL) and the mixture was cooled to 0 °C. A solution of HBr in acetic acid (33% w/w) (0.20 mL) was added dropwise, and the solution was allowed to stir for 1 h at 0 °C before the acid was quenched with saturated aqueous NaHCO₃ (5.0 mL). The mixture was extracted with CH₂Cl₂ (3x 5 mL), dried (Na₂SO₄), filtered, concentrated *in vacuo* to yield crude **3-69** as a yellow oil in quantitative yield. The resulting oil was used in the next step as a crude product without purification. NMR data is tabulated for the major diastereomer below.

¹H NMR (600 MHz, CDCl₃) δ 6.42 (d, J = 4.7 Hz, 1H), 5.38 (ddd, J = 6.8, 6.1, 3.3 Hz, 1H), 4.89 (d, J = 3.3 Hz, 1H), 4.48 (dd, J = 9.8, 6.9 Hz, 1H), 4.07 (dd, J = 9.9, 6.0 Hz, 1H), 2.72 (qd, J = 6.7, 4.7 Hz, 1H), 2.23 (s, 3H), 2.10 (s, 3H), 1.35 (d, J = 6.7 Hz, 3H).

¹³C NMR (150 MHz, CDCl₃) δ 169.9, 169.8, 169.2, 118.5, 91.1, 88.7, 80.2, 75.9, 74.1, 48.6, 20.7, 20.2, 10.8.



(3S,3aR,5aS,6R,7R,8aR)-6-methyl-5-oxo-7-((phenylsulfonyl)thio)tetrahydro-2H-difuro[3,2-b:2',3'-c]furan-3,5a(5H)-diyl diacetate (major) and (3S,3aR,5aS,6R,7S,8aR)-6-methyl-5-oxo-7-((phenylsulfonyl)thio)tetrahydro-2H-difuro[3,2-b:2',3'-c]furan-3,5a(5H)-diyl diacetate (minor) (3-72): To a flask containing crude bromide **3-69** was added MeCN (7.0 mL), followed by NaSSO₂Ph (technical grade, 85%) (239 mg, 1.03 mmol). The heterogenous mixture was

allowed to stir for 1 h before saturated aqueous NH_4Cl (6 mL) was added. The mixture was extracted with CH_2Cl_2 (3 x 10 mL), dried (Na_2SO_4), filtered, concentrated *in vacuo*, and purified by flash column chromatography (EtOAc/Hex) on silica to yield **3-72** as a yellow oil in a 1:1.1 mixture of diastereomers (255 mg, 78% over 2 steps).

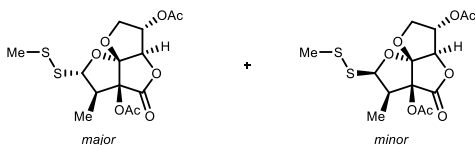
TLC: $R_f = 0.61$ (silica gel, 50:50 Hex:EtOAc)

$^1\text{H NMR}$ (600 MHz, CDCl_3 , mixture of diastereomers) δ 7.98 – 7.86 (m, 2H, major and minor isomer), 7.64 – 7.50 (m, 3H, major and minor isomer), 6.15 (d, $J = 6.5$ Hz, 1H, major isomer), 5.66 (d, $J = 9.9$ Hz, 1H, minor isomer), 5.25 (td, $J = 5.9, 3.0$ Hz, 1H, minor isomer), 5.22 (td, $J = 6.4, 3.2$ Hz, 1H, major isomer), 4.77 (d, $J = 3.3$ Hz, 1H, major isomer), 4.64 (d, $J = 2.9$ Hz, 1H, minor isomer), 4.30 (dd, $J = 10.0, 6.3$ Hz, 1H, major isomer), 4.16 (dd, $J = 9.8, 6.7$ Hz, 1H, major isomer), 3.85 (dd, $J = 10.0, 5.4$ Hz, 1H, minor isomer), 3.55 (dd, $J = 9.8, 6.2$ Hz, 1H, minor isomer), 2.94 (q, $J = 6.9$ Hz, 1H, major isomer), 2.49 (dq, $J = 9.7, 6.9$ Hz, 1H, minor isomer), 2.17 (s, 3H, minor isomer), 2.11 (s, 3H, major isomer), 2.06 (s, 3H, major isomer), 2.01 (s, 3H, minor isomer), 1.21 (d, $J = 7.0$ Hz, 3H, minor isomer), 1.18 (d, $J = 7.0$ Hz, 3H, major isomer).

$^{13}\text{C NMR}$ (150 MHz, CDCl_3 , major diastereomer) δ 169.8, 169.1, 168.8, 145.7, 133.7, 129.0, 127.2, 116.9, 95.0, 88.2, 80.6, 75.7, 72.8, 46.8, 20.6, 20.1, 8.9. (150 MHz, CDCl_3 , minor diastereomer) δ 169.7, 169.2, 168.9, 145.5, 134.1, 129.3, 127.2, 115.9, 92.7, 87.7, 80.6, 75.7, 73.0, 46.8, 20.6, 20.0, 9.0.

IR (FT-IR) 2359, 1798, 1748, 1227 cm^{-1} .

HRMS (ESI-TOF) m/z calcd for $\text{C}_{19}\text{H}_{20}\text{O}_{10}\text{S}_2\text{Na}$ ($\text{M} + \text{Na}$) $^+$: 495.0396, found 495.0381.



(3S,3aR,5aS,6R,7S,8aR)-6-methyl-7-(methyldisulfaneyl)-5-oxotetrahydro-2H-difuro[3,2-b:2',3'-c]furan-3,5a(5H)-diyl diacetate (major) and (3S,3aR,5aS,6R,7R,8aR)-6-methyl-7-(methyldisulfaneyl)-5-oxotetrahydro-2H-difuro[3,2-b:2',3'-c]furan-3,5a(5H)-diyl diacetate (minor) (3-71): To a flask containing thiosulfonate **3-72** (83 mg, 0.176 mmol) as a mixture of diastereomer was added MeCN (1.8 mL) followed by NaSMe (25 mg, 0.351 mmol). The heterogenous mixture was allowed to stir for 1 h before saturated aqueous NH₄Cl (4 mL) was added. The mixture was extracted with CH₂Cl₂ (3 x 5 mL), dried (Na₂SO₄), filtered, concentrated *in vacuo*, and purified by flash column chromatography (EtOAc/Hex) on silica to yield **3-71** as a clear oil as a 1:7.1 mixture of diastereomers (37 mg, 56%).

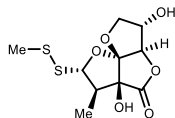
TLC: $R_f = 0.59$ (silica gel, 60:40 Hex:EtOAc)

¹H NMR (500 MHz, CDCl₃, mixture of diastereomers) δ 5.55 (d, $J = 6.7$ Hz, 1H, minor isomer), 5.35 – 5.31 (m, 1H, major and minor isomers), 5.11 (d, $J = 10.0$ Hz, 1H, major isomer), 4.88 (d, $J = 2.1$ Hz, 1H, major isomer), 4.86 (d, $J = 3.0$ Hz, 1H, minor isomer), 4.41 (dd, $J = 9.9, 6.6$ Hz, 1H, minor isomer), 4.33 (dd, $J = 10.4, 5.4$ Hz, 1H, major isomer), 4.08 (dd, $J = 10.4, 3.7$ Hz, 1H, major isomer), 4.01 (dd, $J = 9.9, 5.7$ Hz, 1H, minor isomer), 2.84 – 2.78 (m, 1H, major and minor isomers), 2.50 (s, 3H, minor isomer), 2.47 (s, 3H, major isomer), 2.21 (s, 3H, minor isomer), 2.19 (s, 3H, major isomer), 2.10 (s, 3H, minor isomer), 2.09 (s, 3H, major isomer), 1.27 (d, $J = 7.2$ Hz, 3H, minor isomer), 1.19 (d, $J = 6.9$ Hz, 3H, major isomer).

¹³C NMR (125 MHz, CDCl₃, major diastereomer) δ 169.9, 169.2, 169.0, 116.5, 93.7, 87.4, 81.4, 75.7, 73.6, 45.7, 24.7, 20.8, 20.2, 8.1. (125 MHz, CDCl₃, minor diastereomer) δ 170.0, 169.6, 169.5, 116.8, 99.7, 88.8, 81.1, 76.1, 73.3, 46.7, 23.9, 20.8, 20.3, 8.9.

IR (FT-IR) 2924, 2357, 1798, 1746 cm⁻¹.

HRMS (ESI-TOF) m/z calcd for C₁₄H₁₈O₈S₂Na (M + Na)⁺ : 401.0341, found 401.0330.



Kujounin A₂ (3-2): To a flask containing diacetate **3-71** (37 mg, 0.0978 mmol) was added MeOH (2.0 mL) followed by La(OTf)₃ (344 mg, 0.567 mmol). The reaction was allowed to stir at 40 °C for 24 h, 45 °C for 24 h, 50 °C for 24 h, followed by 80 °C for 3 h before the mixture was concentrated. Brine (5 mL) was added and the mixture was extracted with EtOAc (3 x 5 mL), dried (Na₂SO₄), filtered, concentrated *in vacuo*, and purified by flash column chromatography (EtOAc/Hex) on silica to yield **3-2** as a clear oil (17 mg, 59%).

TLC R_f = 0.36 (silica gel, 40:60 Hex:EtOAc)

Optical Rotation [α]²³_D = -86.5 (*c* = 0.40, MeOH)

¹H NMR (600 MHz, CDCl₃) δ 5.19 (d, *J* = 9.8 Hz, 1H), 4.84 (s, 1H), 4.47 (s, 1H), 4.27 (dd, *J* = 10.3, 1.6 Hz, 1H), 4.12 (dd, *J* = 10.4, 4.3 Hz, 1H), 2.77 (dq, *J* = 9.8, 6.8 Hz, 1H), 2.50 (s, 3H), 1.19 (d, *J* = 6.9 Hz, 3H).

¹³C NMR (150 MHz, CDCl₃) δ 172.5, 117.3, 95.5, 87.8, 78.6, 75.5, 73.9, 46.3, 24.9, 7.9. (The isolation paper contains a discrepancy in the ¹³C tabulation table, reporting a carbon peak at 75.0, although the spectra for isolated kujounin A₂ shows the carbon peak at 75.4)

IR (FT-IR) 3435, 2924, 1788, 1192 cm⁻¹.

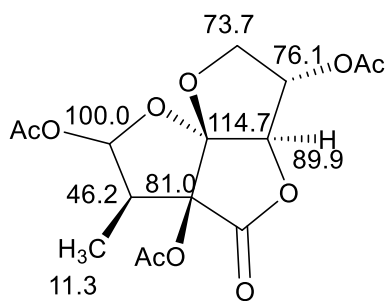
HRMS (ESI-TOF) *m/z* calcd for C₁₀H₁₄O₆S₂Na (M + Na)⁺ : 317.0129, found 317.0131.

3.5.4 DP4+ Analysis of triacetate intermediates 3-68-Major and 3-68-Minor

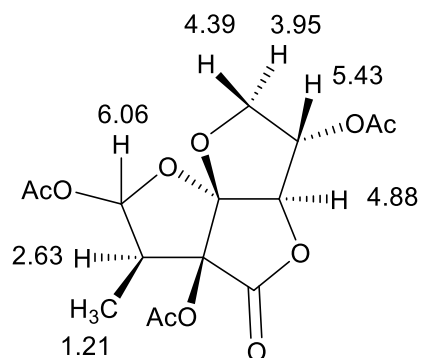
Experimental chemical shifts for the 3-68-major and 3-68-minor isomers:

3-68 (major isomer)

^{13}C shifts:

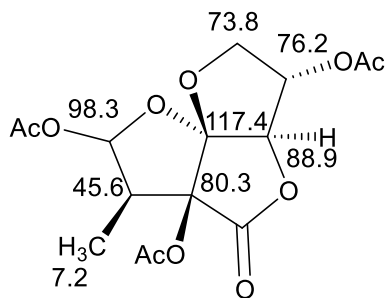


^1H shifts:

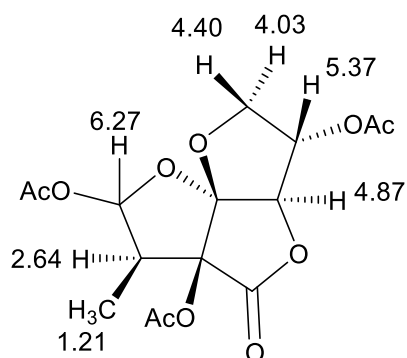


3-68 (minor isomer)

^{13}C shifts:



^1H shifts:



Computation methods and DP4+ analysis follows the method developed by Sarotti: Grimblat, N.; Zanardi, M. M.; Sarotti, A. M. Beyond DP4: an Improved Probability for the Stereochemical Assignment of Isomeric Compounds Using Quantum Chemical Calculations of NMR Shifts. *J. Org. Chem.* **2015**, *80*, 12526–12534.

Boltzmann averages for the calculated alpha anomeric acetate conformers of **3-68**:

Calculate Boltzmann Weighted Shielding Tensors for one isomer

Compounds **26 alpha** (kujounin paper 2018)
 geometry B3LYP/6-31+g(d,p)
 NMR-GIAO rmpw1pw91/6-31+g(d,p)
 minimum energy -1334.4808

Conformer Names	M0001	M0005	M0014
Energy (NMR level, H)	-1334.4808	-1334.4801	-1334.4807
Energy (Kcal/mol)	0.00	0.41	0.07
Boltzmann factor	1.0000	0.4990	0.8924
Boltzmann Scaling	0.418	0.209	0.373

Nuclei Label	Isotropic Shielding Tensors			nuclei	ST: weighted
5C	80.1754	77.0641	83.186	C	80.65
16C	92.4827	95.4686	96.1605	C	94.48
4C	104.7954	106.7448	106.5932	C	105.87
11C	112.4188	112.7159	112.2873	C	112.43
3C	117.3935	117.6618	117.036	C	117.32
2C	122.468	120.3041	124.4436	C	122.75
14C	144.8127	146.5957	146.3266	C	145.75
21C	181.9099	186.6932	186.662	C	184.68
17H	25.6074	25.0066	25.2477	H	25.348
8H	26.0427	26.471	26.2143	H	26.196
9H	26.3194	26.6927	26.5049	H	26.467
1H	26.809	27.1705	26.9266	H	26.928
7H	27.5985	27.4006	27.7427	H	27.611
15H	28.9352	28.951	29.1551	H	29.021
22H	30.5272	30.2481	30.2772	H	30.376
23H	30.1308	30.3158	30.2716	H	30.222
24H	30.2327	30.5093	30.5057	H	30.392
MeH average				H	30.330

Boltzmann averages for the calculated beta anomeric acetate conformers of **3-68**:

Calculate Boltzmann Weighted Shielding Tensors for one isomer

Compounds **26 beta** (kujounin paper 2018)
 geometry B3LYP/6-31+g(d,p)
 NMR-GIAO rmpw1pw91/6-31+g(d,p)
 minimum energy -1334.4832

Conformer Names	M0004	M0009	M0016
Energy (NMR level, H)	-1334.4821	-1334.4832	-1334.482
Energy (Kcal/mol)	0.72	0.00	0.75
Boltzmann factor	0.2949	1.0000	0.2819
Boltzmann Scaling	0.187	0.634	0.179

Nuclei Label	Isotropic Shielding Tensors			nuclei	ST: weighted
5C	74.713	79.5626	75.1145	C	77.86
15C	98.2491	97.7065	98.187	C	97.89
4C	105.4652	106.2304	106.3547	C	106.11
10C	112.9997	111.9927	113.0909	C	112.38
3C	117.4982	117.0617	118.2938	C	117.36
2C	118.8753	124.2864	121.2076	C	122.72
13C	147.284	146.7234	147.5458	C	146.98
18C	186.8319	186.6459	187.0953	C	186.76
36H	25.0855	25.1224	25.1293	H	25.117
35H	26.4763	26.2067	26.407	H	26.293
8H(?)	26.7303	26.5327	27.0156	H	26.656
1H	27.0466	26.9017	27.0081	H	26.948
7H	27.3721	27.7386	27.2728	H	27.587
14H	28.8346	28.9409	28.8677	H	28.908
19H	30.0906	30.1183	30.0975	H	30.109
20H	30.3437	30.3164	30.3515	H	30.328
21H	30.5773	30.5678	30.6069	H	30.577
18C-MeH average				H	30.338

DP4+ Analysis used the published excel spreadsheet by Sarotti. The results for the **3-68** major isomer are shown below. Isomer 1 is the alpha triacetate **3-68**, and isomer 2 is the beta triacetate **3-68**. The **3-68** major isomer has the alpha anomeric acetate configuration with high probability using this analysis.

	A	B	C	D	E	F	G	H
1	Functional		Solvent?		Basis Set		Type of Data	
2	mPW1PW91		PCM		6-31+G(d,p)		Shielding Tensors	
3								
12			DP4+	99.98%	0.02%	-	-	-
14	Nuclei	sp2?	Experimental	Isomer 1	Isomer 2	Isomer 3	Isomer 4	Isomer 5
15	C		114.7	80.6	77.9			
16	C		100	94.5	97.9			
17	C		89.9	105.9	106.1			
18	C		81	112.4	112.4			
19	C		76.1	117.3	117.4			
20	C		73.7	122.8	122.7			
21	C		46.2	145.7	147.0			
22	C		11.3	184.7	186.8			
23								
24	H		6.06	25.3	25.1			
25	H		5.43	26.2	26.3			
26	H		4.88	26.47	26.66			
27	H		4.39	26.93	26.95			
28	H		3.95	27.61	27.59			
29	H		2.63	29.02	28.91			
30	H		1.21	30.33	30.34			
31								

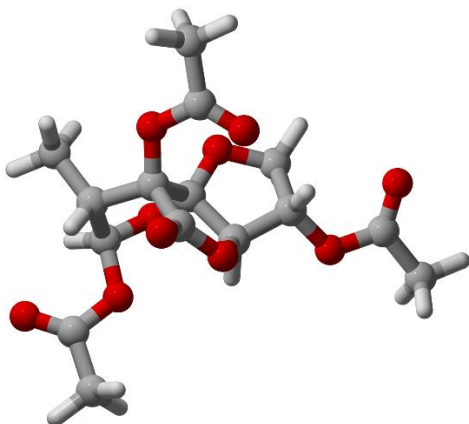
DP4+ Analysis using the published excel spreadsheet. The results for the **3-68** minor isomer are shown below. Isomer 1 is the alpha triacetate **3-68**, and isomer 2 is the beta triacetate **3-68**. The **3-68** minor isomer has the beta anomeric acetate configuration with high probability using this analysis.

	A	B	C	D	E	F	G	H
1	Functional		Solvent?		Basis Set		Type of Data	
2	mPW1PW91		PCM		6-31+G(d,p)		Shielding Tensors	
3								
12			DP4+	0.02%	99.98%	-	-	-
14	Nuclei	sp2?	Experimental	Isomer 1	Isomer 2	Isomer 3	Isomer 4	Isomer 5
15	C		117.4	80.6	77.9			
16	C		98.3	94.5	97.9			
17	C		88.9	105.9	106.1			
18	C		80.3	112.4	112.4			
19	C		76.2	117.3	117.4			
20	C		73.8	122.8	122.7			
21	C		45.6	145.7	147.0			
22	C		7.2	184.7	186.8			
23								
24	H		6.27	25.3	25.1			
25	H		5.37	26.2	26.3			
26	H		4.87	26.47	26.66			
27	H		4.4	26.93	26.95			
28	H		4.03	27.61	27.59			
29	H		2.64	29.02	28.91			
30	H		1.21	30.33	30.34			
31								

All geometries were optimized using B3LYP/6-31g(d) and included full frequency analysis. The NMR GIAO isotropic shielding tensors were calculated at the prior geometry using restricted mpw1pw91/6-31+g(d,p) with the cpcm solvation model for chloroform.

Calculated alpha triacetate conformers of 3-68:

M0001: E(RmPW1PW91) = -1334.48076100



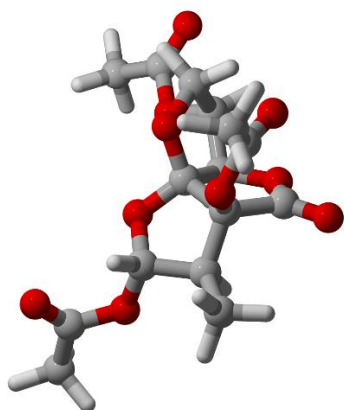
43

A2_triacetate_alpha_cs_NMR_M0001_step1

H	2.9268422	1.1191337	-1.4243580
C	2.1914902	0.3214257	-1.3306850
C	2.2032322	-0.3535243	0.0537150
C	0.7376982	-0.7400003	0.2467400
C	-0.0400568	0.1862007	-0.7221410
O	0.8832612	0.9091737	-1.4603810
H	2.3525832	-0.4237673	-2.1207890
H	2.5318592	0.3402687	0.8269720
H	0.5749482	-1.7910053	0.0047690
O	0.2324022	-0.5090353	1.5680570
C	-0.9729078	1.0342927	0.1875940
C	-0.6855488	0.4923267	1.6094520
O	-1.2300708	0.8418817	2.6203700
C	-2.4090018	0.6971457	-0.2879690
H	-3.0698548	0.5445657	0.5683640
C	-2.1762468	-0.6234893	-1.0390210
H	-2.8989488	-0.8205873	-1.8298460
O	-0.8998398	-0.5497643	-1.5971330
O	3.0024702	-1.5491113	0.0953050
O	-0.7824728	2.4437897	0.1046570
C	-3.0193378	1.7486457	-1.2233810
H	-2.3981648	1.9035457	-2.1114140
H	-3.1329398	2.7076177	-0.7144530
H	-4.0088288	1.4064957	-1.5439310
C	0.3510312	2.9846297	0.6244080
O	1.2061082	2.3333237	1.1804600

C	0.3696052	4.4757637	0.4160820
H	0.3459482	4.7010147	-0.6550950
H	1.2722062	4.8914277	0.8643300
H	-0.5173518	4.9294737	0.8695000
C	4.3489102	-1.3641403	0.0618310
C	5.0737062	-2.6768713	0.2289600
H	6.1443292	-2.5194303	0.0957740
H	4.7066892	-3.4106033	-0.4953660
H	4.8821282	-3.0803283	1.2291410
O	4.8663322	-0.2790203	-0.0796420
O	-2.1791918	-1.7491503	-0.1199900
C	-3.4006448	-2.2522883	0.2057550
C	-3.2678298	-3.4176533	1.1535030
H	-2.6465678	-4.2000653	0.7057760
H	-4.2579378	-3.8122423	1.3834410
H	-2.7722378	-3.0929833	2.0745500
O	-4.4377998	-1.7970833	-0.2239100

M0005: E(RmPW1PW91) = -1334.48010496



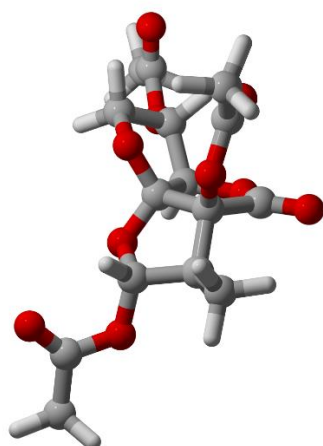
43

A2_triacetate_alpha_cs_NMR_M0005_step1

H	-2.5993262	-1.8941220	-0.6230014
C	-2.4504472	-0.8221880	-0.7817344
C	-2.6542002	-0.0542470	0.5257186
C	-1.2516552	-0.0301780	1.1288576
C	-0.2967042	-0.2279420	-0.0823824
O	-1.0871602	-0.5791500	-1.1783594
H	-3.1015742	-0.4736670	-1.5842434
H	-3.3955402	-0.5173080	1.1787206
H	-1.0507462	0.8925530	1.6757976
O	-1.0476932	-1.1520460	2.0098096
C	0.6876588	-1.3204190	0.4115586
C	0.0209578	-1.9260730	1.6512736
O	0.4017158	-2.8570020	2.3045896
C	1.9342968	-0.4956050	0.7986586

H	1.7450218	-0.0626650	1.7899566
C	1.8553848	0.6773880	-0.1838214
H	2.3613908	0.5046610	-1.1367654
O	0.4700568	0.9112660	-0.4092884
O	-2.9976522	1.3272820	0.2947366
O	1.0646568	-2.2610340	-0.5843544
C	3.2578158	-1.2541920	0.8324556
H	3.5087878	-1.6618810	-0.1501234
H	3.2006738	-2.0827850	1.5445846
H	4.0622758	-0.5819830	1.1481826
C	0.1865828	-3.2526540	-0.9143224
O	-0.8770842	-3.4140340	-0.3634604
C	0.7433958	-4.0945810	-2.0316324
H	0.8428598	-3.4850010	-2.9360454
H	0.0712248	-4.9314170	-2.2223364
H	1.7396408	-4.4635010	-1.7692394
C	-4.2985132	1.5707970	-0.0211504
C	-4.5302082	3.0476280	-0.2233914
H	-5.5756052	3.2181420	-0.4818954
H	-3.8807872	3.4228580	-1.0209984
H	-4.2770692	3.5969490	0.6893006
O	-5.1316382	0.6983780	-0.1178604
O	2.4124158	1.8273760	0.4347996
C	2.9470958	2.7898730	-0.3859224
C	3.4114498	3.9663190	0.4348766
H	2.5510548	4.4390200	0.9207336
H	3.9103128	4.6871080	-0.2134674
H	4.0914088	3.6344270	1.2257376
O	3.0254688	2.6836500	-1.5845514

M0014: E(RmPW1PW91) = -1334.48065361



43

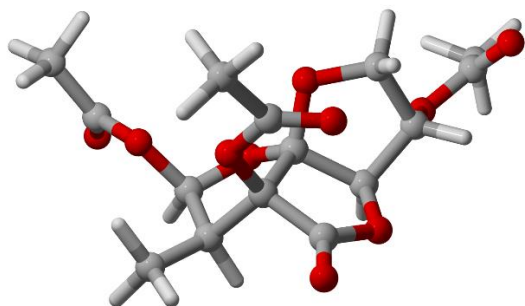
A2_triacetate_alpha_cs_NMR_M0014_step1

H	2.5962942	-0.0917764	-2.0837208
C	1.9504802	-0.6006874	-1.3695008

C	2.4497292	-0.4908824	0.0824862
C	1.1476642	-0.5283844	0.8836042
C	0.0566792	-0.1160784	-0.1294458
O	0.6755802	0.0601896	-1.3724988
H	1.8394382	-1.6553084	-1.6567328
H	2.9773992	0.4499946	0.2427522
H	0.9657492	-1.5229084	1.2948442
O	1.1046192	0.4141056	1.9684052
C	-0.5482978	1.1925956	0.4454992
C	0.2697292	1.4631646	1.7216502
O	0.1363432	2.3893006	2.4730872
C	-2.0085458	0.8090086	0.7871252
H	-2.0117708	0.3903416	1.8011152
C	-2.2426488	-0.3827734	-0.1454158
H	-2.5581508	-0.1080614	-1.1560988
O	-0.9901018	-1.0651304	-0.1826068
O	3.2756432	-1.5940334	0.4907842
O	-0.5570548	2.2846276	-0.4662838
C	-3.0357328	1.9344966	0.7089592
H	-3.1010248	2.3506326	-0.2997318
H	-2.7663258	2.7411956	1.3968602
H	-4.0214038	1.5526746	0.9944942
C	0.6315132	2.8930126	-0.7398378
O	1.6746642	2.5789106	-0.2140828
C	0.4459732	3.9826166	-1.7613448
H	-0.3403958	4.6733686	-1.4423838
H	0.1337822	3.5406916	-2.7136368
H	1.3865162	4.5176506	-1.8938398
C	4.5370112	-1.6130914	-0.0178828
C	5.3329332	-2.7519724	0.5701972
H	4.7895992	-3.6953514	0.4586862
H	5.4811952	-2.5843774	1.6425062
H	6.3005772	-2.8132934	0.0715182
O	4.9385172	-0.8077574	-0.8270138
O	-3.1979978	-1.2517214	0.4282292
C	-3.9218898	-2.0485524	-0.4261968
C	-4.8302608	-2.9559314	0.3634672
H	-5.4554868	-3.5292374	-0.3214418
H	-5.4545178	-2.3696514	1.0450802
H	-4.2294108	-3.6371484	0.9755052
O	-3.8266148	-2.0044664	-1.6271588

Calculated beta triacetate conformers of 26:

M0004: SCF E(RmPW1PW91) = -1334.48207267



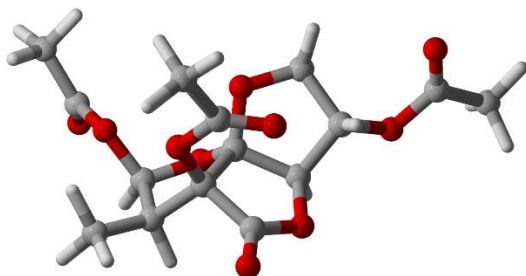
43

A2_triacetate_beta_cs_NMR_M0004_step1

H	2.0148433	-1.5682616	1.4708387
C	2.0970023	-0.5308516	1.1359427
C	2.7626803	-0.4645226	-0.2414423
C	1.5782443	-0.4733246	-1.2069283
C	0.3619863	-0.0242756	-0.3528283
O	0.7772033	0.0274074	0.9768157
H	2.6232153	0.0595204	1.8871037
H	1.7477703	0.1833654	-2.0617663
O	1.2917583	-1.7982186	-1.6894143
C	-0.7316097	-1.0771556	-0.6836243
C	0.0130223	-2.1972446	-1.4222313
O	-0.4432937	-3.2344556	-1.8160683
C	-1.6763527	-0.2980426	-1.6325193
H	-1.2128427	-0.3175196	-2.6280093
C	-1.4972577	1.1422854	-1.1337733
O	-0.1420307	1.2392484	-0.7569923
O	-1.4880007	-1.5276346	0.4313057
C	-3.1019287	-0.8299966	-1.7424953
H	-3.6161947	-0.7791806	-0.7818193
H	-3.0855957	-1.8711456	-2.0784363
H	-3.6673067	-0.2418576	-2.4736213
C	-0.9220717	-2.4253086	1.2837127
O	0.1811313	-2.8958776	1.1242697
C	-1.8635287	-2.7407516	2.4160217
H	-2.0626967	-1.8323596	2.9939647
H	-1.4153947	-3.4992936	3.0580997
H	-2.8198487	-3.0990586	2.0224027
C	4.6514583	0.9296934	0.1212787
C	5.2542953	2.2729944	-0.2067043
H	6.2123703	2.3743764	0.3037857

H	4.5765413	3.0755594	0.1012057
H	5.3984133	2.3647514	-1.2883953
O	5.1588773	0.0668954	0.8017107
O	3.4295003	0.7957384	-0.4617023
H	3.4596743	-1.2861836	-0.4129393
H	-1.6902007	1.9160454	-1.8757653
O	-2.3461687	1.3643004	-0.0032083
C	-2.7331337	2.6551054	0.2385217
C	-3.5107207	2.7331354	1.5281667
H	-4.3344547	2.0125434	1.5211577
H	-3.8952347	3.7447934	1.6610347
H	-2.8551037	2.4731214	2.3662797
O	-2.4790147	3.5816394	-0.4929353

M0009: E(RmPW1PW91) = -1334.48322492



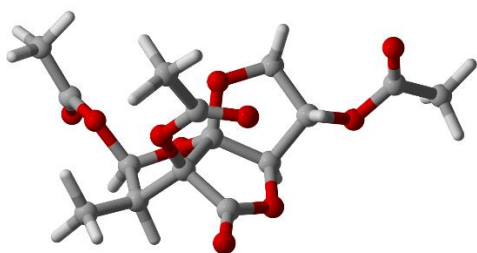
43

A2_triacetate_beta_cs_NMR_M0009_step1

H	-2.0763740	-0.7354650	1.9612900
C	-1.7296910	-0.9839090	0.9591840
C	-2.4704080	-0.2094320	-0.1455070
C	-1.4011330	-0.0780610	-1.2303510
C	-0.0637900	-0.2685570	-0.4822700
O	-0.3571850	-0.5726760	0.8486940
H	-1.8214360	-2.0660580	0.7933960
H	-1.5398090	-0.8278490	-2.0114450
O	-1.3629970	1.2140400	-1.8584760
C	0.6957130	1.0694130	-0.6734860
C	-0.2792400	1.9485230	-1.4786110
O	-0.0927680	3.0789600	-1.8359400
C	1.9283210	0.6777090	-1.5334250
H	1.6150520	0.7325710	-2.5834250
C	2.0568520	-0.8203800	-1.2316480
O	0.7278250	-1.2754930	-1.1035980
O	1.1393060	1.6824140	0.5296680
C	3.1735830	1.5395100	-1.3473990

H	3.5489850	1.4783280	-0.3250120
H	2.9401730	2.5837900	-1.5750220
H	3.9630250	1.2080570	-2.0308400
C	0.2011420	2.2634740	1.3264330
O	-0.9749460	2.3095530	1.0446250
C	0.8364270	2.8268000	2.5693590
H	1.2755510	2.0140970	3.1574300
H	0.0799040	3.3445520	3.1592920
H	1.6433580	3.5161660	2.3024400
C	-4.6929640	-0.9977320	0.1082380
C	-5.8345950	-1.6662580	-0.6168930
H	-6.6654210	-1.8142130	0.0734750
H	-5.5130590	-2.6259800	-1.0330040
H	-6.1587420	-1.0387130	-1.4541600
O	-4.7206680	-0.5730700	1.2412000
O	-3.5945070	-0.9204300	-0.6901150
H	-2.7860870	0.7718060	0.2104040
H	2.5323770	-1.4163450	-2.0094630
O	2.7719060	-0.9895980	-0.0040410
C	3.3681170	-2.2045980	0.2026650
C	3.9561780	-2.2673570	1.5896130
H	4.6239680	-1.4168830	1.7592540
H	4.5001460	-3.2042800	1.7129920
H	3.1515700	-2.2042790	2.3301530
O	3.4063430	-3.0821490	-0.6256720

M0016: E(RmPW1PW91) = -1334.48203009



43

A2_triacetate_beta_cs_NMR_M0016_step1

H	-1.6609809	-1.8765361	-1.8235476
C	-1.8364439	-0.8099471	-1.6599606
C	-2.7684949	-0.5909161	-0.4724716
C	-1.7990819	-0.4796381	0.7089194
C	-0.4497719	-0.0606711	0.0655294
O	-0.5922999	-0.1676501	-1.3188166
H	-2.2139239	-0.3429451	-2.5719026
H	-2.1430279	0.2274969	1.4643014

O	-1.5845949	-1.7548981	1.3408334
C	0.5812001	-1.0215071	0.7152514
C	-0.2675889	-2.1122271	1.3820304
O	0.1281401	-3.0923131	1.9496324
C	1.2720451	-0.1120981	1.7612124
H	0.6008891	-0.0617271	2.6292794
C	1.1682761	1.2653859	1.0914404
O	-0.0702799	1.2605529	0.4163654
O	1.5751571	-1.5238121	-0.1673746
C	2.6522551	-0.5610681	2.2310084
H	3.3642031	-0.5745371	1.4046184
H	2.5903191	-1.5663511	2.6585004
H	3.0262991	0.1188079	3.0042544
C	1.2432871	-2.5215551	-1.0316806
O	0.1510871	-3.0403481	-1.0716836
C	2.4230071	-2.8782191	-1.8976896
H	2.7165521	-2.0106991	-2.4977156
H	2.1540941	-3.7087691	-2.5506556
H	3.2787991	-3.1537171	-1.2734776
C	-4.5091459	0.9265079	0.1194934
C	-5.1143049	2.2657859	-0.2208896
H	-5.9663969	2.4545929	0.4326294
H	-5.4365609	2.2779829	-1.2672656
H	-4.3666609	3.0565609	-0.1009296
O	-4.9017619	0.1614369	0.9703364
O	-3.4316409	0.6727979	-0.6751236
H	-3.5050129	-1.3815991	-0.3212536
H	1.1689171	2.1127759	1.7758864
O	2.2423761	1.4247729	0.1592744
C	2.6324461	2.7060819	-0.1240216
C	3.6763381	2.7046979	-1.2122996
H	4.4955511	2.0261599	-0.9550146
H	4.0549221	3.7172459	-1.3551686
H	3.2306951	2.3417689	-2.1448646
O	2.1911171	3.6823379	0.4330104

3.6 References

1. Cavallito, C. J.; Bailey, J. H., Allicin, the Antibacterial Principle of *Allium sativum*. I. Isolation, Physical Properties and Antibacterial Action. *J. Am. Chem. Soc.* **1944**, *66*, 1950–1951.
2. El-Aasr, M.; Fujiwara, Y.; Takeya, M.; Ikeda, T.; Tsukamoto, S.; Ono, M.; Nakano, D.; Okawa, M.; Kinjo, J.; Yoshimitsu, H.; Nohara, T., Onionin a from *Allium Cepa* Inhibits Macrophage Activation. *J. Nat. Prod.* **2010**, *73*, 1306–1308.
3. Keiss, H.-P.; Dirsch, V. M.; Hartung, T.; Haffner, T.; Trueman, L.; Auger, J.; Kahane, R. m.; Vollmar, A. M., Garlic (*Allium Sativum* L.) Modulates Cytokine Expression in Lipopolysaccharide-Activated Human Blood Thereby Inhibiting Nf-Kb Activity. *J. Nutr.* **2003**, *133*, 2171–2175.

4. Fukaya, M.; Nakamura, S.; Nakagawa, R.; Nakashima, S.; Yamashita, M.; Matsuda, H., Rare Sulfur-Containing Compounds, Kujounins A₁ and A₂ and Allium Sulfoxide A₁, from *Allium Fistulosum* 'Kujou'. *Org. Lett.* **2018**, *20*, 28–31.
5. (a) Imai, S.; Tsuge, N.; Tomotake, M.; Nagatome, Y.; Sawada, H.; Nagata, T.; Kumagai, H., An Onion Enzyme That Makes the Eyes Water. *Nature* **2002**, *419*, 685; (b) Thomson, S. J.; Rippon, P.; Butts, C.; Olsen, S.; Shaw, M.; Joyce, N. I.; Eady, C. C., Inhibition of Platelet Activation by Lachrymatory Factor Synthase (LFS)-Silenced (Tearless) Onion Juice. *J. Agric. Food. Chem.* **2013**, *61*, 10574–10581.
6. (a) Block, E.; Dane, A. J.; Thomas, S.; Cody, R. B., Applications of Direct Analysis in Real Time Mass Spectrometry (DART-MS) in Allium Chemistry. 2-Propenesulfenic and 2-Propenesulfinic Acids, Diallyl Trisulfane S-Oxide, and Other Reactive Sulfur Compounds from Crushed Garlic and Other Alliums. *J. Agric. Food. Chem.* **2010**, *58*, 4617–4625; (b) Lawson, L. D.; Hughes, B. G., Characterization of the Formation of Allicin and Other Thiosulfinates from Garlic. *Planta Med.* **1992**, *58*, 345–350.
7. (a) Wimalasena, K.; Mahindaratne, M. P. D., Chemistry of L-Ascorbic Acid: Regioselective and Stereocontrolled 2-C- and 3-C-Allylation Via Thermal Claisen Rearrangement. *J. Org. Chem.* **1994**, *59*, 3427–3432; (b) Olabisi, A. O.; Mahindaratne, M. P. D.; Wimalasena, K., A Convenient Entry to C2- and C3-Substituted Gulono- Γ -Lactone Derivatives from L-Ascorbic Acid. *J. Org. Chem.* **2005**, *70*, 6782–6789; (c) Olabisi, A. O.; Wimalasena, K., Rational Approach to Selective and Direct 2-O-Alkylation of 5,6-O-Isopropylidene-L-Ascorbic Acid. *J. Org. Chem.* **2004**, *69*, 7026–7032.
8. Thopate, S. R., Chemoselective 3-O-Alkylation of L-Ascorbic Acid under Phase Transfer Catalysis. *Afr. J. Pure. Appl. Chem.* **2012**, *6*, 50–54.
9. Tahir, H.; Hindsgaul, O., Regio- and Chemoselective Alkylation of L-Ascorbic Acid under Mitsunobu Conditions. *J. Org. Chem.* **2000**, *65*, 911–913.
10. Morena-Manas, M.; Pleixats, R.; Villarroya, M., C-Allylation of L-Ascorbic Acid under Palladium(0) Catalysis. *J. Org. Chem.* **1990**, *55*, 4925–4928.
11. (a) Tsuji, J.; Takahashi, H.; Morikawa, M., Organic Syntheses by Means of Noble Metal Compounds XVII. Reaction of Π -Allylpalladium Chloride with Nucleophiles. *Tetrahedron Lett.* **1965**, *6*, 4387–4388; (b) Trost, B. M.; Fullerton, T. J., New Synthetic Reactions. Allylic Alkylation. *J. Am. Chem. Soc.* **1973**, *95*, 292–294; (c) Trost, B. M.; Crawley, M. L., Asymmetric Transition-Metal-Catalyzed Allylic Alkylations: Applications in Total Synthesis. *Chem. Rev.* **2003**, *103*, 2921–2944; (d) Lu, Z.; Ma, S., Metal-Catalyzed Enantioselective Allylation in Asymmetric Synthesis. *Angew. Chem. Int. Ed.* **2007**, *47*, 258–297.
12. Schrof, R.; Altmann, K.-H., Studies Toward the Total Synthesis of the Marine Macrolide Salarin C. *Org. Lett.* **2018**, *20*, 7679–7683.
13. Park, B. S.; Lee, S. W.; Kim, I. T.; Tae, J. S.; Lee, S. H., Synthesis and Photoluminescent Properties of New Ceramidine Derivatives. *Heteroat. Chem.* **2012**, *23*, 66–73.
14. Savoia, D.; Alvaro, G.; Di Fabio, R.; Fiorelli, C.; Gualandi, A.; Monari, M.; Piccinelli, F., Highly Diastereoselective Synthesis of 2,6-di[1-(2-Alkylaziridin-1-yl)alkyl]pyridines, Useful Ligands in Palladium-Catalyzed Asymmetric Allylic Alkylation. *Adv. Synth. Catal.* **2006**, *348*, 1883–1893.
15. Burgess, K.; Jennings, L. D., Enantioselective Esterifications of Unsaturated Alcohols Mediated by a Lipase Prepared from *Pseudomonas* Sp. *J. Am. Chem. Soc.* **1991**, *113*, 6129–6139.
16. (a) Kazmaier, U.; Zumpe, F. L., Chelated Enolates of Amino Acid Esters—Efficient Nucleophiles in Palladium-Catalyzed Allylic Substitutions. *Angew. Chem. Int. Ed.* **1999**, *38*,

- 1468–1470; (b) Kazmaier, U.; Zumpe, F. L., Palladium-Catalyzed Allylic Alkylations without Isomerization—Dream or Reality? *Angew. Chem. Int. Ed.* **2000**, *39*, 802–804; (c) Kazmaier, U.; Zumpe, F. L., Chelated Enolates of Amino Acid Esters – New and Efficient Nucleophiles for Isomerization-Free, Stereoselective Palladium-Catalyzed Allylic Substitutions. *Eur. J. Org. Chem.* **2001**, *2001*, 4067–4076; (d) Trost, B. M.; Verhoeven, T. R., Allylic Substitutions with Retention of Stereochemistry. *J. Org. Chem.* **1976**, *41*, 3215–3216; (e) Trost, B. M.; Verhoeven, T. R., New Synthetic Reactions. Catalytic vs. Stoichiometric Allylic Alkylation. Stereocontrolled Approach to Steroid Side Chain. *J. Am. Chem. Soc.* **1976**, *98*, 630–632.
17. Bernardes, G. J. L.; Gamblin, D. P.; Davis, B. G., The Direct Formation of Glycosyl Thiols from Reducing Sugars Allows One-Pot Protein Glycoconjugation. *Angew. Chem. Int. Ed.* **2006**, *45*, 4007–4011.
18. (a) Curphey, T. J., Thionation with the Reagent Combination of Phosphorus Pentasulfide and Hexamethyldisiloxane. *J. Org. Chem.* **2002**, *67*, 6461–6473; (b) Ozturk, T.; Ertas, E.; Mert, O., A Berzelius Reagent, Phosphorus Decasulfide (P₄S₁₀), in Organic Syntheses. *Chem. Rev.* **2010**, *110*, 3419–3478; (c) Polshettiwar, V.; Kaushik, M. P., Recent Advances in Thionating Reagents for the Synthesis of Organosulfur Compounds. *J. Sulfur Chem.* **2006**, *27*, 353–386.
19. Meguro, Y.; Noguchi, M.; Li, G.; Shoda, S.-i., Glycosyl Bunte Salts: A Class of Intermediates for Sugar Chemistry. *Org. Lett.* **2018**, *20*, 76–79.
20. Sittiwong, W.; Richardson, M. W.; Schiaffo, C. E.; Fisher, T. J.; Dussault, P. H., Re₂O₇-Catalyzed Reaction of Hemiacetals and Aldehydes with O-, S-, and C-Nucleophiles. *Beilstein J. Org. Chem.* **2013**, *9*, 1526–1532.
21. Morais, G. R.; Springett, B. R.; Pauze, M.; Schröder, L.; Northrop, M.; Falconer, R. A., Novel Strategies for the Synthesis of Unsymmetrical Glycosyl Disulfides. *Org. Biomol. Chem.* **2016**, *14*, 2749–2754.
22. (a) Mahadevan, A.; Li, C.; Fuchs, P. L., Silver Fluoroborate Promoted Sulfur Alkylation of β-Silyl Ethyl Sulfides. Selective Synthesis of β-Thioglycosides. *Synth. Commun.* **1994**, *24*, 3099–3107; (b) Chambert, S.; Désiré, J.; Décout, J.-L., The 2-(trimethylsilyl)ethyl Sulfur Group in Synthesis. *Synthesis* **2002**, *16*, 2319–2334; (c) Gerland, B.; Désiré, J.; Lepoivre, M.; Décout, J.-L., Direct Preparation of Nucleoside Vinyl Disulfides from 2-(trimethylsilyl)ethyl Sulfides, an Access to Vinylthiols. *Org. Lett.* **2007**, *9*, 3021–3023.
23. (a) Evans, D. A.; Bryan, C. A.; Sims, C. L., Complementarity of (4 + 2) Cycloaddition Reactions and [2,3] Sigmatropic Rearrangements in Synthesis. New Synthesis of Functionalized Hasubanan Derivatives. *J. Am. Chem. Soc.* **1972**, *94*, 2891–2892; (b) Evans, D. A.; Andrews, G. C.; Sims, C. L., Reversible 1,3 Transposition of Sulfoxide and Alcohol Functions. Potential Synthetic Utility. *J. Am. Chem. Soc.* **1971**, *93*, 4956–4957.
24. Grimblat, N.; Zanardi, M. M.; Sarotti, A. M., Beyond Dp4: An Improved Probability for the Stereochemical Assignment of Isomeric Compounds Using Quantum Chemical Calculations of NMR Shifts. *J. Org. Chem.* **2015**, *80*, 12526–12534.
25. (a) Berglund, P.; DeSantis, G.; Stabile, M. R.; Shang, X.; Gold, M.; Bott, R. R.; Graycar, T. P.; Lau, T. H.; Mitchinson, C.; Jones, J. B., Chemical Modification of Cysteine Mutants of Subtilisin Bacillus Lentus Can Create Better Catalysts Than the Wild-Type Enzyme. *J. Am. Chem. Soc.* **1997**, *119*, 5265–5266; (b) Davis, B. G.; Maughan, M. A. T.; Green, M. P.; Ullman, A.; Jones, J. B., Glycomethanethiosulfonates: Powerful Reagents for Protein Glycosylation. *Tetrahedron: Asymmetry* **2000**, *11*, 245–262; (c) Matsumoto, K.; Davis, B. G.; Jones, J. B., Chemically Modified “Polar Patch” Mutants of Subtilisin in Peptide Synthesis with Remarkably Broad Substrate Acceptance: Designing Combinatorial Biocatalysts. *Chem.: Eur. J.* **2002**, *8*, 4129–4137.

26. Goddard-Borger, E. D.; Stick, R. V., The Synthesis of Various 1,6-Disulfide-Bridged D-Hexopyranoses*. *Aust. J. Chem.* **2005**, *58*, 188–198.
27. DeLorbe, J. E.; Horne, D.; Jove, R.; Mennen, S. M.; Nam, S.; Zhang, F.-L.; Overman, L. E., General Approach for Preparing Epidithiodioxopiperazines from Trioxopiperazine Precursors: Enantioselective Total Syntheses of (+)- and (–)-Gliocladine C, (+)-Leptosin D, (+)-T988c, (+)-Bionectin a, and (+)-Gliocladin A. *J. Am. Chem. Soc.* **2013**, *135*, 4117–4128.

Chapter 4. Total Synthesis of the Proposed Structure of (–)-Himeradine A

4.1 Abstract

The total synthesis of the proposed structure of (–)-himeradine A is described herein. The key features of this route include a dibenzoyl-tartaric acid resolution of a piperidine, diastereoselective N-Boc mediated piperidine allylation, B-alkyl Suzuki cross-coupling, photoredox mediated conjugate addition, and transannular Mannich cyclization. The synthesis was completed in 17 steps in the longest linear sequence and is the shortest to date. The spectral data of our synthetic sample had some discrepancies from that of the isolated natural product, but matched Shair's synthetic sample.

4.2 Introduction

4.2.1 *Lycopodium* Alkaloids

Lycopodium alkaloids were first discovered in 1881 by the isolation of lycopodine from *Lycopodium complanatum* by Bödecker.¹ Since then, there have been over 250 different *Lycopodium* alkaloids isolated and characterized from *Lycopodium* club moss. This class of alkaloids have attracted synthetic chemists due to their complex polycyclic framework and promising bioactivities.²

The *Lycopodium* alkaloids are known to be categorized in one of the four structural classes shown below (Figure 4-1).² The four classes consist of the lycopodine class (**4-1**), lycodine class (**4-2**), fawcettimine class (**4-3**), and miscellaneous class (**4-4**). The numbering for each atom of the structures shown below is based on that of Conroy's original biogenetic proposal.³ The lycopodine class is characterized as generally having a quinolizidine (rings A and C) and containing 4 fused rings. The lycodine class is similar to that of the lycopodines, except the N- β -C1 bond is cleaved and a pyridine or pyridone is formed with C5. The fawcettimine class also contains four fused ring system and is simply a skeletal rearrangement of the lycopodine class. Shifting the C4-C13 bond to form a C4-C12 bond would lead to the fawcettimine class. The last class of *Lycopodiums* are classified as miscellaneous if they do not resemble the previous three classes.

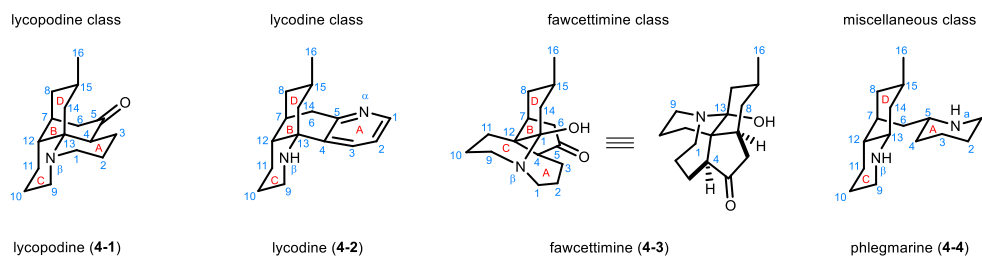
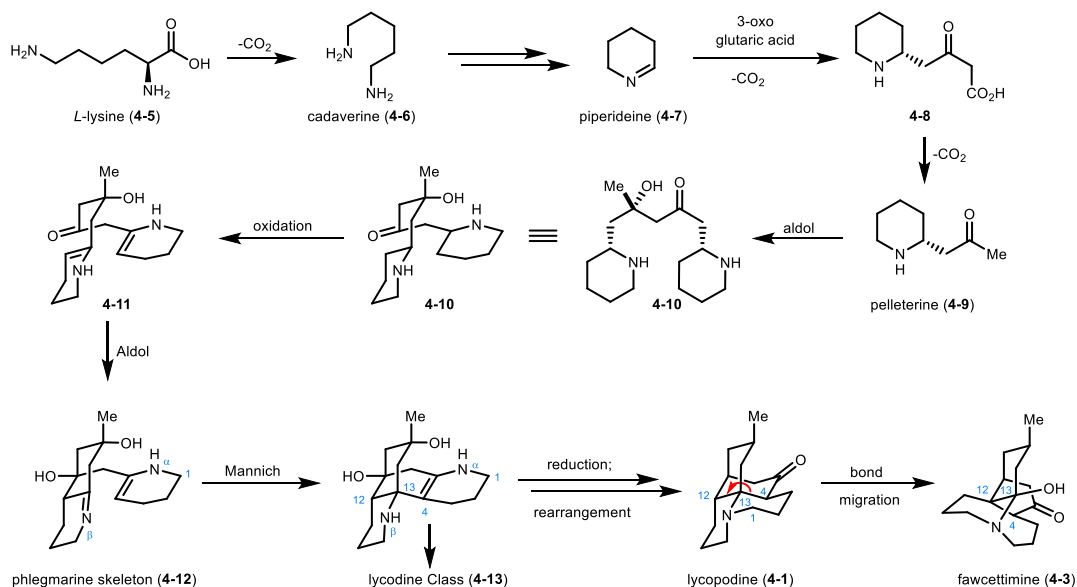


Figure 4-1. The *Lycopodium* structural classes.

4.2.2 Biosynthetic Proposal

The original biosynthetic proposal for the *Lycopodium* alkaloids was presented by Conroy in 1960, but has since then been revised due to ^{13}C and ^{14}C radiolabeling studies.⁴ The biosynthesis is now believed to begin with a decarboxylation of L-lysine (**4-5**) to form cadaverine (**4-6**), which can oxidatively cyclize to provide piperidine (**4-7**) (Scheme 4-1). Subsequent Mannich addition with 3-oxo glutaric acid followed by two successive decarboxylations forms pelleterine (**4-9**). This intermediate can self-dimerize via an aldol reaction to form ketone **4-10**, which can be oxidized to enamine **4-11**. Another aldol reaction allows access to the phlegmarine skeleton, which can undergo a trans-annular Mannich addition to forge the C4-C13 bond, which is found in the lycodine subfamily. Further reductions and rearrangements can lead to the lycopodines (**4-1**). Lastly, a bond migration from the C4-C13 bond to form the C4-C12 bond followed by an oxidation affords fawcettimine (**4-3**).

Scheme 4-1. Biosynthetic proposal based on radiolabeling studies.



4.2.3 Isolation and Background of (-)-Himeradine A

In 2003, the Kobayashi group reported the isolation of a novel C₂₇N₃-type alkaloid from the club moss *Lycopodium chinense*, which was named himeradine A (**4-17**) (Figure 4-2).⁵ It is part of the lycodine subfamily of alkaloids, but contains a C14-C3 linkage similar to that of fastigiatine (**4-16**)⁶, lyconadin D (**4-14**), and E (**4-15**).⁷ Himeradine A is arguably the most complex *Lycopodium* alkaloid that has been discovered to date due to its caged pentacyclic core, seven rings, ten stereocenters, one quaternary center, and a quinolizidine subunit. The Kobayashi group reported that himeradine A exhibited cytotoxicity against murine lymphoma L1210 cells, with an IC₅₀ of 10 µg/mL *in vitro*.

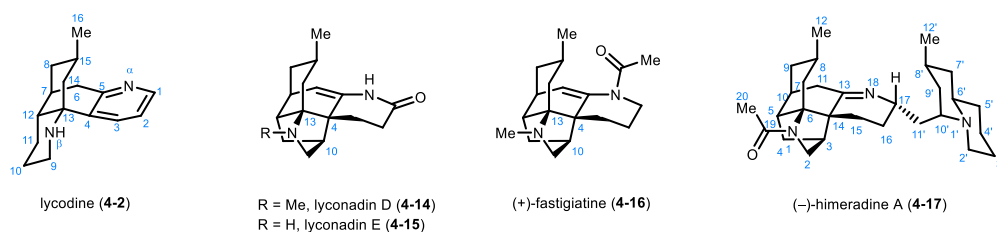


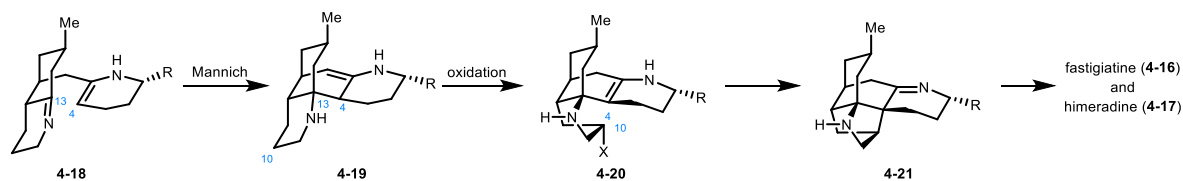
Figure 4-2. Structure of himeradine A and related *Lycopodium* alkaloids.

The structure of (-)-himeradine A was primarily assigned through 1-D and 2-D NMR analysis. The authors also used IR and FABMS/MS to help elucidate the structure. Relative configuration of the pentacyclic core and the quinolizidine subunit were deduced from NOESY correlations. However, determining the relative configuration of the complete structure deemed difficult due to the large distances between the pentacyclic core and the isolated quinolizidine subunit. In particular, the stereochemistry at C17 and C10' was much harder to deduce. They assigned the stereochemistry at those carbons by the NOESY correlations between H17/H10', H11'/H8', H11'/H6', and H11'/H2'. However, the C17 epimer of the proposed structure would

also have these NOESY correlations. The absolute stereochemistry of the molecule was assigned based on analogy to the structure of fastigiatine.

The biosynthesis of the pentacyclic core of both fastigiatine (**4-16**) and himeradine A (**4-17**) was proposed by MacLean and coworkers (Scheme 4-2).^{6b} They believe intermediate **4-18** can undergo a transannular Mannich reaction to form the C4-C13 bond, which can subsequently be oxidized at the C10 position to afford intermediate **4-20**. Finally, enamine **4-20** can close down to forge the C4-C10 bond and provide the pentacyclic core of both fastigiatine and himeradine.

Scheme 4-2. MacLean's proposed biosynthesis of the pentacyclic core of fastigiatine and himeradine A.



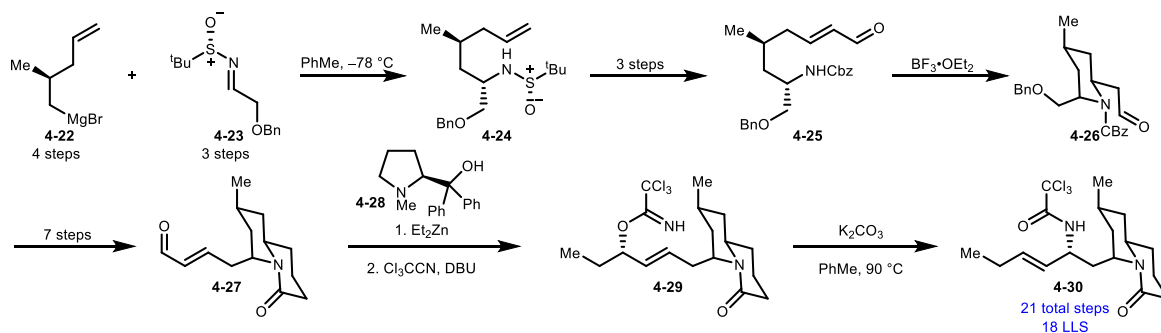
4.3 Previous Work

4.3.1 Carter's Synthesis of the Quinolizidine Fragment of (-)-Himeradine A

In the literature there are many reports of total syntheses and efforts towards various *Lycopodium* alkaloids. Interestingly, (-)-himeradine A (**4-17**) is only reported twice in the literature in the context of synthetic efforts, presumably due to its structural complexity. Carter was the first to report a synthesis of the quinolizidine portion of (-)-himeradine A (**4-17**) in 2011.⁸ He began the synthesis with a Grignard addition of organomagnesium species **4-22** into Ellman imine **4-23** (Scheme 4-3). Chiral Grignard reagent **4-22** was formed in 4 steps from commercial material using Evan's auxiliary and Ellman imine **4-23** was made in a 3-step procedure. The resulting alkene (**4-24**) was converted to enal **4-25** in 3 steps, which was subjected to a key diastereoselective Lewis acid mediated intramolecular heteroatom Michael addition to afford piperidine **4-26**. In another 7 steps they were able to form another enal (**4-27**) into which they

diastereoselectively added an ethyl substituent with diethyl zinc. The last two steps consisted of forming trichloroimidate **4-29** and performing an Overman rearrangement to furnish quinolizidine **4-30**.

Scheme 4-3. Carter's synthesis of the quinolizidine fragment of (–)-himeradine A.



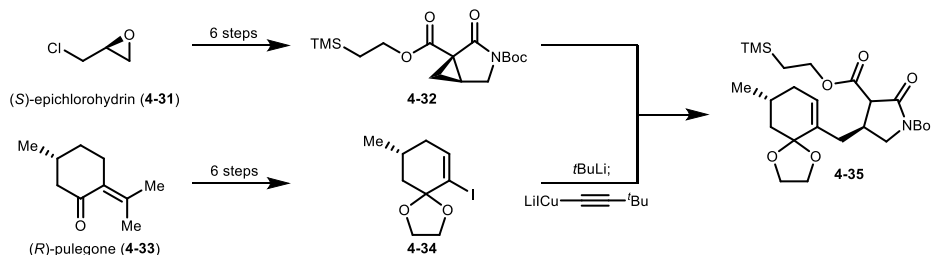
Carter's synthesis involves a nice approach to the quinolizidine portion of himeradine A with an impressive key diastereoselective heteroatom Michael addition step to form the piperidine core, but there are some drawbacks to this route. The longest linear sequence for this synthesis is 18 steps with a total step count of 21, which involves the use of two chiral auxiliaries (formation of **4-22** and **4-23**) and a chiral catalyst for the formation of allylic trichloroimidate **4-29**. Perhaps the main drawback of this route is the viability of converting quinolizidine **4-30** into himeradine A. It seems that this fragment would require many manipulations to convert into himeradine A, including a trichloroacetamide deprotection, lactam reduction, and manipulation of the olefin.

4.3.2 Shair's Total Synthesis of the Proposed Structure of (–)-Himeradine A

In 2014, the Shair group reported a unified approach towards the synthesis of seven membered *Lycopodium* alkaloids.⁹ They successfully synthesized six alkaloids, one of which was the first and only synthesis of the proposed structure of (–)-himeradine A. The sequence involved the coupling of two fragments and a key biomimetic transannular Mannich reaction. The first fragment (**4-35**) was made in 13 total steps (Scheme 4-4). They obtain chirality from (*S*)-epichlorohydrin (**4-31**) and (*R*)-pulegone (**4-33**) to make lactam **4-32** and vinyl iodide **4-34**,

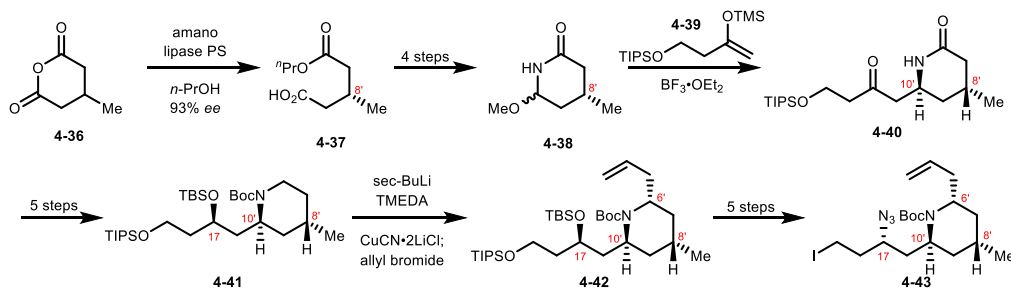
respectively. The two fragments are coupled by a lithium-halogen exchange with *tert*-butyllithium and vinyl iodide **4-34** followed by a transmetalation to the cuprate and finally regioselective opening of cyclopropane **4-32** to yield alkene **4-35**.

Scheme 4-4. Shair's synthesis of their key lactam intermediate towards (–)-himeradine A.



The synthesis of the quinolizidine fragment (**4-43**) was accomplished in 17 steps beginning with an enzymatic resolution of 3-methylglutaric anhydride **4-36** to set the C8' methyl stereocenter (Scheme 4-5). The resulting carboxylic acid **4-37** was further functionalized in 4 steps to furnish lactam **4-38**, which was subjected to a diastereoselective Lewis acid mediated *N*-acyliminium Mannich reaction with enoxysilane **4-39** to set the C10' stereocenter. A Subsequent set of 5 steps provided TBS alcohol **4-41**, which involved a chelate control 1,3-*syn* reduction to set the stereochemistry at C17. The last stereocenter of this fragment (C6') was set via a *N*-Boc directed lithiation to afford alkene **4-42**. Another 5 steps accomplished the synthesis of piperidine **4-43**.

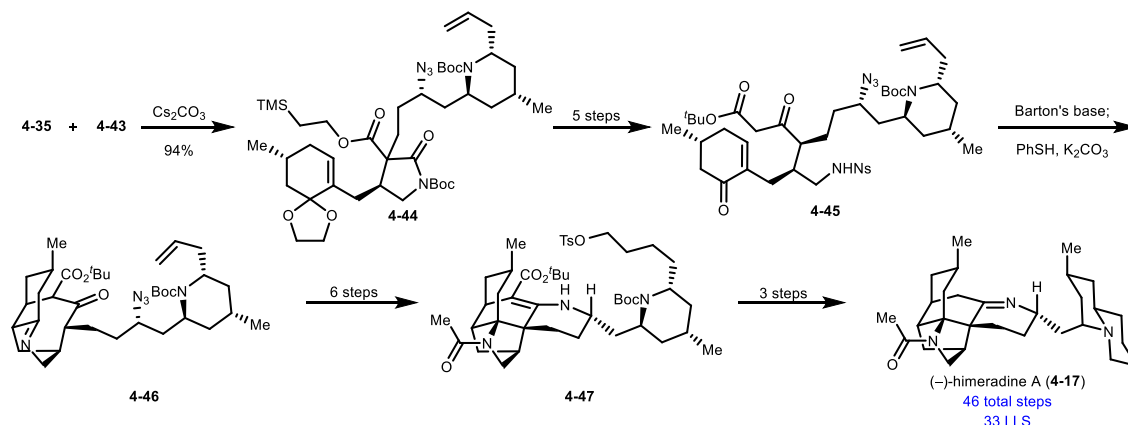
Scheme 4-5. Shair's synthesis of their key piperidine intermediate **4-43**.



Shair was able to connect these fragments via a facile alkylation reaction between iodide **4-43** and 1,3-dicarbonyl **4-35** (Scheme 4-6). Another 5 steps afforded enone **4-45** which was

subjected to basic conditions in order to perform the key *7-endo-trig* intramolecular cyclize followed by a condensation to form imine **4-46**. Nine additional steps afforded the proposed structure of (–)-himeradine A (**4-17**). There were a few discrepancies between the spectroscopic data from Shair’s synthetic sample compared to the isolated natural product by the Kobayashi group. These discrepancies will be discussed later in the chapter. Shair’s synthetic route is effective in making the proposed structure of himeradine A, but is quite lengthy. The entire synthesis contains 33 steps in the longest linear sequence and 46 total steps.

Scheme 4-6. Shair’s endgame for the synthesis of the proposed structure of (–)-himeradine A.

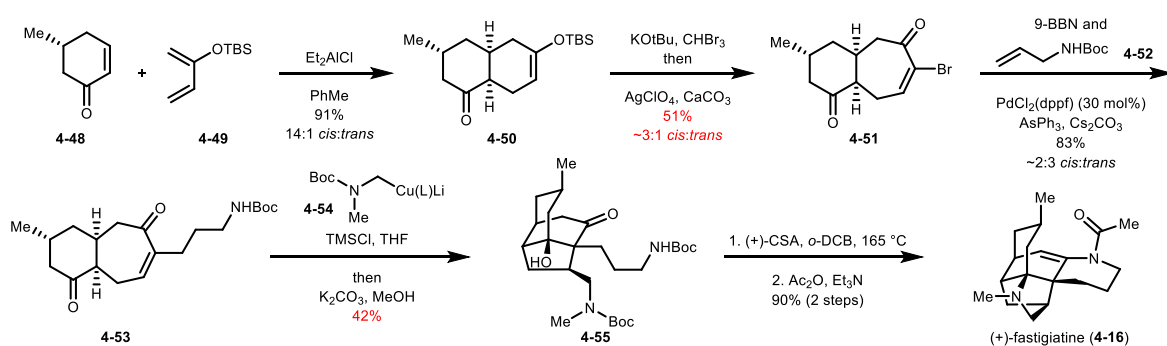


4.3.3 Rychnovsky’s Total Synthesis of (+)-Fastigiatine

Ventures toward the synthesis of the *lycopodium* alkaloids in the Rychnovsky lab began with the 6-step total synthesis of (+)-fastigiatine in 2016.¹⁰ The synthesis begins with a Diels-Alder reaction between enone **4-48**, which was derived from (*R*)-pulegone, and diene **4-49** to provide decalin **4-50** (Scheme 4-7). Dibromocarbene mediated ring expansion further provided bromoenone **4-51**, although this step proved to be troublesome. The yields for this reaction were difficult to consistently reproduce and it afforded a 3:1 mixture of *cis* to *trans* isomers, which complicated the analysis. Despite the inconsistent results, bromoenone **4-51** can be smoothly coupled with allyl carbamate **4-52** via a hydroboration/B-alkyl Suzuki reaction. The mixture of

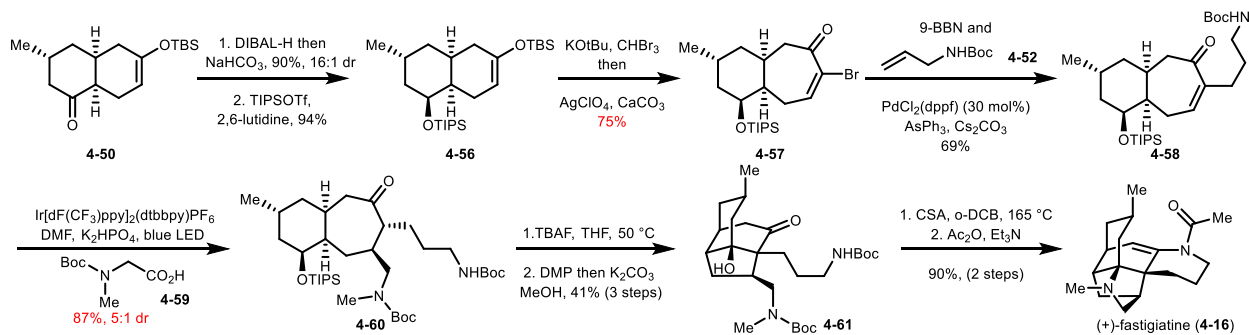
cis- and *trans*-Enone **4-53** was further functionalized by a conjugate addition with cuprate **4-54** followed by basic conditions to form the transannular aldol product. Unfortunately, this transformation produces essentially a 1:1 diastereomeric mixture of products. The last step of the synthesis was an acid catalyzed key biomimetic transannular Mannich to provide the core framework of the molecule, followed by acylation to afford (+)-fastigiatine (**4-16**). This sequence is the shortest synthesis of (+)-fastigiatine to date.

Scheme 4-7. Rychnovsky's synthesis of (+)-fastigiatine.



This concise biomimetic synthesis sparked further interest in our lab towards other lycopodium alkaloids. Although, we were aware that the two problematic steps in the synthesis would hinder the viability of completing synthesis of the other alkaloids. Thus, a second-generation route to (+)-fastigiatine (**4-16**) was completed with the aid of computational modeling. Initial efforts were placed towards improvement of the diastereoselectivity of the conjugate addition. It was envisioned that potential reduction of ketone **4-50** would allow us to place a large protecting group on the resulting alcohol to block the undesired face of the conjugate addition. Computational experimentation predicted that β -stereochemistry at the alcohol with a TIPS protecting group would block the bottom face of the enone. The revised sequence was then tried in order to test the computational results.¹¹

Scheme 4-8. Rychnovsky's second-generation synthesis of (+)-fastigiatine.



After some optimization, it was found that DIBAL-H reduced ketone **4-50** in a 16:1 dr favoring the β -alcohol which could be protected with TIPSOTf in great yield (Scheme 4-8). The subsequent ring expansion was performed under the same conditions as before, but the yield was much higher. We presumed this was due to the inability to form an enolate under the basic conditions. The next hydroboration/B-alkyl Suzuki step proceeded in good yield. The last problematic step was simplified by using MacMillan's photoredox catalysis. This allowed us to bypass the formation of cuprate **4-54**, which was quite laborious to make. We were pleased to see that the conjugate addition gave a 5:1 dr of the desired diastereomer as the computational analysis predicted. Further manipulations provided the natural product in good yields.

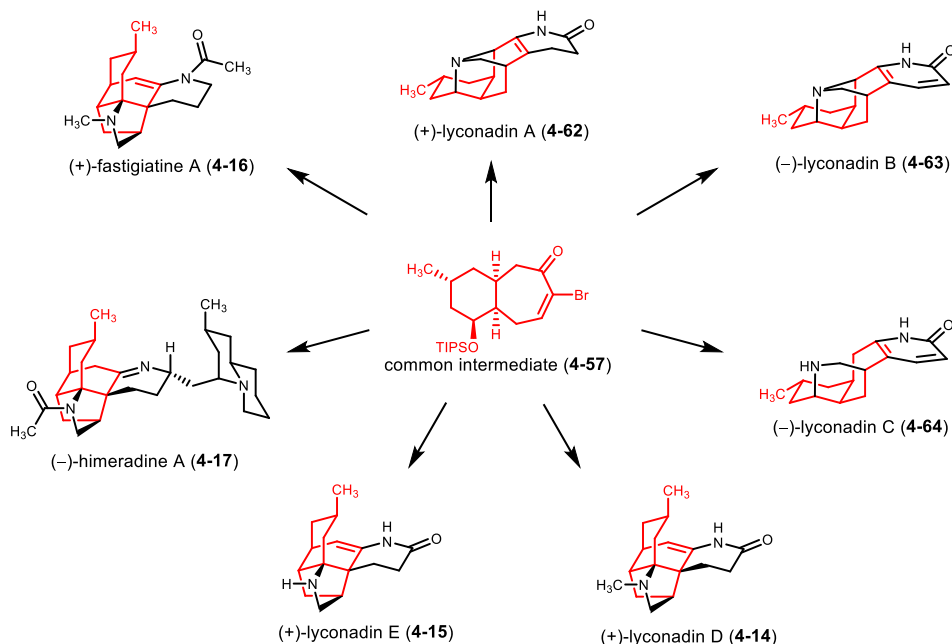


Figure 4-3. *Lycopodium* alkaloids envisioned to be synthesized by common intermediate **4-57**.

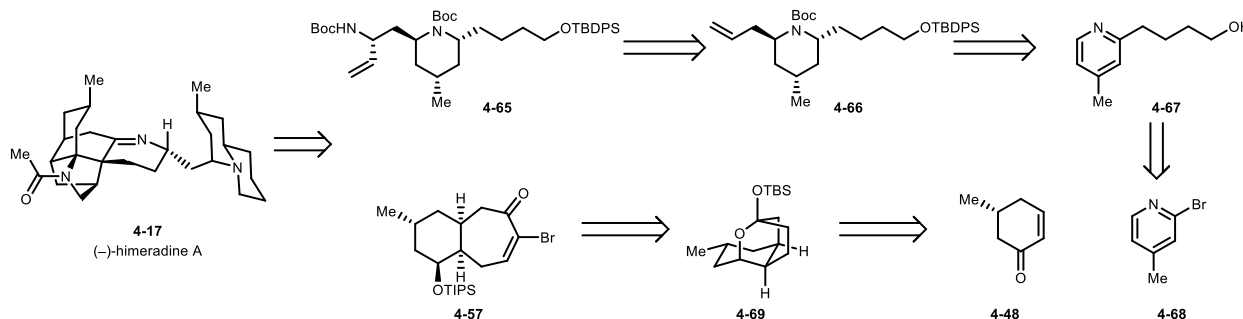
This second-generation synthesis proved to be a much more viable route to access many of the *Lycopodium* alkaloids. This route adds three steps, but has three distinct advantages. The ring expansion of decalin **4-56** works in a more reliable and higher yield, we were able to bypass formation of exotic cuprate **4-54**, and the conjugate addition step provided much higher diastereoselectivity. With the improved synthetic route in hand, our group envisioned applying common intermediate **4-57** towards the synthesis of various *lycopodium* alkaloids (Figure 4-3).

4.3.4 Rychnovsky's Initial Studies Towards (-)-Himeradine A

After the successful first- and second-generation syntheses of fastigiatine in our lab, we began studies toward the synthesis of (-)-himeradine A (**4-17**) which was pioneered by Dr. Jacob C. DeForest.¹² We initially envisioned a similar end-game to that of (+)-fastigiatine (**4-16**), where fragments **4-65** and **4-57** would be coupled and eventually heated in the presence of acid to affect the transannular Mannich cyclization (Scheme 4-9). Bromoenone **4-57** would be synthesized the same as it was in the second-generation synthesis of fastigiatine, starting with chiral enone **4-48**.

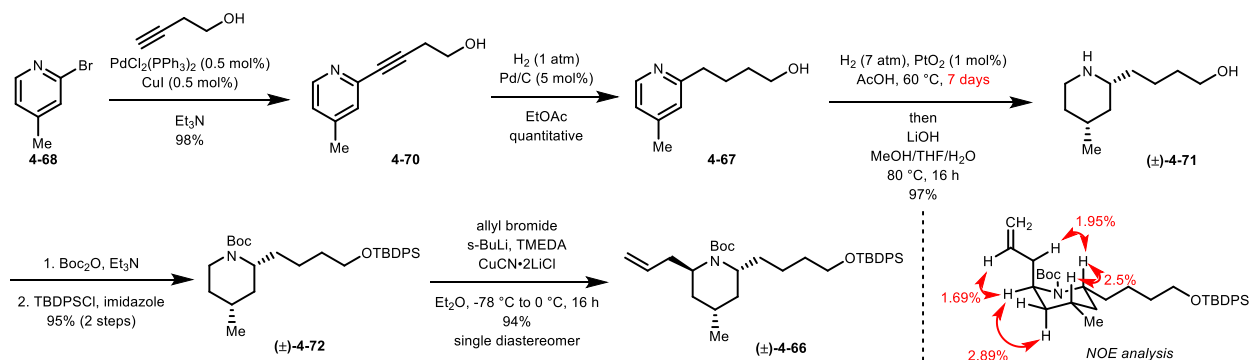
Fragment **4-65** was thought to arise from manipulation of the olefin in intermediate **4-66**, which would in turn be made from a hydrogenation followed by allylation of pyridine **4-67**. Commercially available bromopicoline **4-68** would ultimately serve as the starting material for the construction of the quinolizidine unit.

Scheme 4-9. Initial retrosynthetic analysis towards the synthesis of (–)-himeradine A.



The first step in the sequence was a robust Sonagashira cross-coupling between homopropargyl alcohol and bromopicoline **4-68** (Scheme 4-10). This step was performed on multi-gram scale with low catalyst loadings at room temperature and provided great yields. The next task was making racemic piperidine **4-71**, which was accomplished in a three-step sequence in which alkyne **4-70** was first reduced to alkane **4-67**, followed by a subsequent hydrogenation of the pyridine ring and finally a hydrolysis. This successfully afforded piperidine **4-71** in a great overall yield, but was quite a cumbersome sequence. It required two separate hydrogenation reactions, one of which required 7 days, and a final hydrolysis due to esterification of the free alcohol with acetic acid under these reaction conditions. Unfortunately, any attempt at a global hydrogenation resulted in a complex mixture of products.

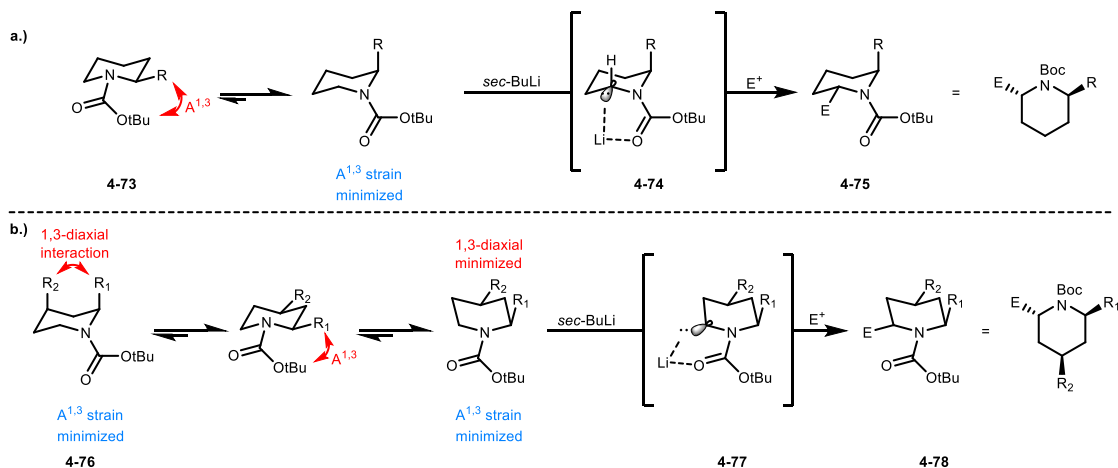
Scheme 4-10. Synthetic route to access functionalize piperidine **4-66**.



Amino alcohol **4-71** was chemoselectively protected using Boc_2O followed by TBDPSCl to provide carbamate **4-72**. The next step in the sequence involved a diastereoselective *N*-Boc directed alkylation, which proceeded in great yield and as a single diastereomer. The relative stereochemistry was confirmed by NOE analysis. The rationale for the diastereoselectivity is well understood for 2-substituted *N*-Boc piperidines.¹³ In order to avoid $A^{1,3}$ strain between the *tert*-butyl of the Boc group and the substituent at the 2-position, the piperidine (**4-73**) adopts a conformation which places the R group axial (Scheme 4-11, a). The carbonyl of the Boc group directs the organolithium to the α -position to deprotonate the equatorial hydrogen, which ultimately yields the *trans*-piperidine (**4-75**).

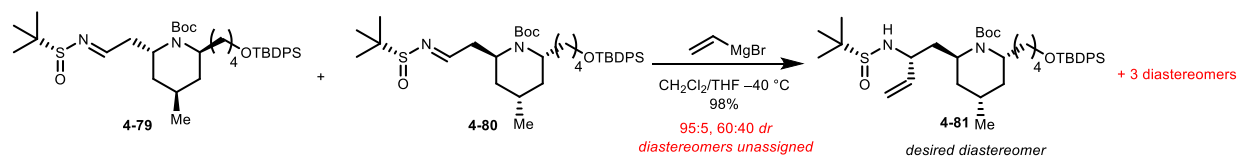
A similar rationale can be invoked for *cis*-2,4-substituted *N*-Boc piperidines (Scheme 4-11, b). Although, in this case if the piperidine undergoes a complete chair flip to avoid $A^{1,3}$ strain as previously explained, it induces an unfavorable 1,3-diaxial interaction between the two substituents (**4-76**). To avoid both of these interactions, the piperidine may adopt a boat conformation which would place all the groups equatorial. The carbonyl of the Boc group can direct the lithiation, which places the newly installed electrophile in the axial position (**4-78**).

Scheme 4-11. Rationale for the diastereoselectivity of alkylation of 2-substituted *N*-Boc piperidines (**a**) and *cis*-2,4-substituted *N*-Boc piperidines (**b**).



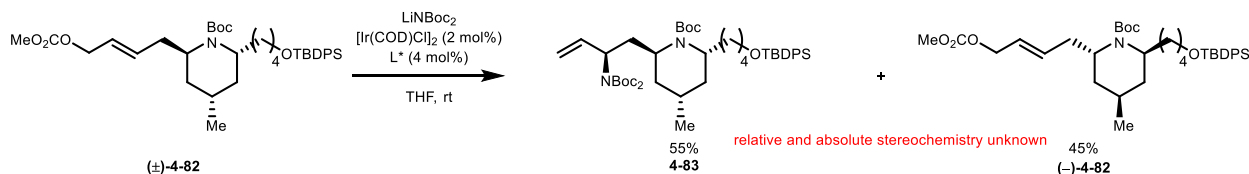
With a scalable route to piperidine (\pm)-**4-66** the next task was to resolve the piperidine and form dicarbamate **4-65**. The first attempt involved the use of Ellman's auxiliary (Scheme 4-12).¹⁴ Racemic olefin **4-66** was converted into the corresponding aldehyde via ozonolysis followed by condensation of Ellman's auxiliary to form diastereomers **4-79** and **4-80**. Addition of vinyl magnesium bromide provided a mixture of 4 diastereomers that were separable, although the stereochemistry of each structure remained ambiguous.

Scheme 4-12. Attempted resolution of piperidine **4-66** using Ellman's auxiliary.



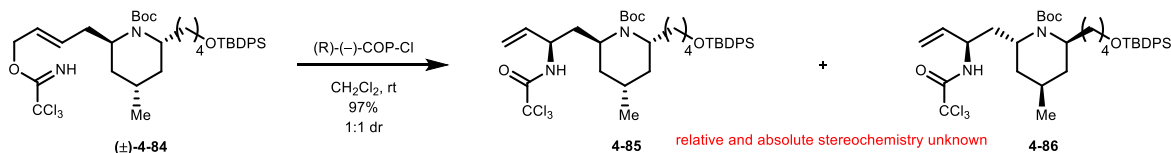
The second attempt at resolving the piperidine involved a Hartwig amination (Scheme 4-13).¹⁵ Racemic carbonate **4-82** was subjected to iridium with a chiral ligand and afforded enantioenriched starting material ($-$)-**4-82** along with bis-Boc allyl amine **4-83**. Unfortunately, the absolute and relative stereochemistry of the recovered starting material and the product were very difficult to assign.

Scheme 4-13. Unexpected resolution using a Hartwig amination.



The last attempt at resolving the piperidine involved an Overman rearrangement (Scheme 4-14). The reaction afforded **4-85** and **4-86** in a 1:1 dr which were separable by chromatography. This transformation was convenient since it was mild and high yielding, but the same issue persisted. The relative and absolute configuration of either diastereomer deemed difficult to assign. Unfortunately, all three attempts at a resolution proved to not be viable for completing the synthesis of himeradine A.

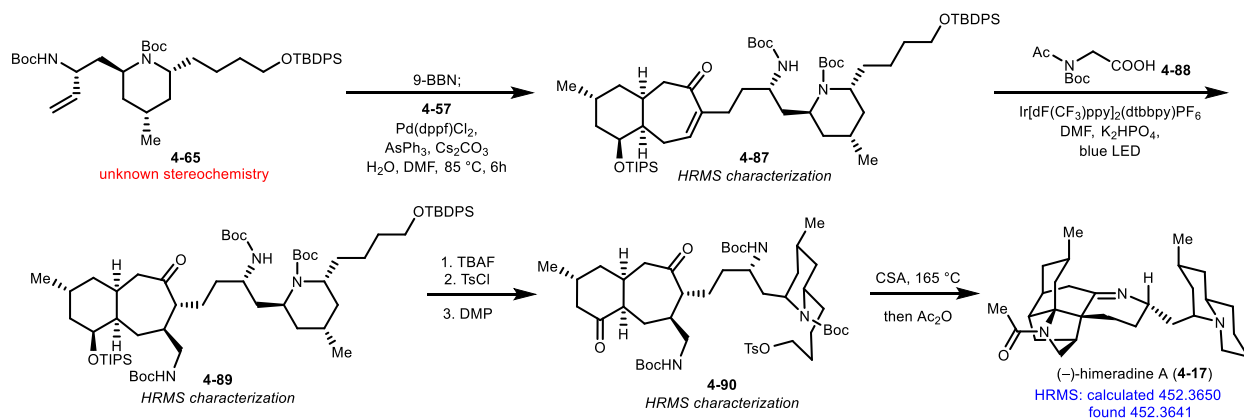
Scheme 4-14. Resolution using an Overman rearrangement.



The unknown stereochemistry of elaborated piperidine **4-65** caused a major set-back in the project. However, to confirm the validity of the end-game sequence, the last few steps of the synthesis was performed with little material from the major diastereomer of the Ellman resolution (Scheme 4-12). Some diastereomer of **4-65** was hydroborated with 9-BBN and directly subjected to Suzuki cross-coupling conditions with bromoenone **4-57** (Scheme 4-15). Enone **4-87** was verified by HRMS before directly subjecting to MacMillan's conditions for photoredox conjugate additions. This reaction seemed to afford tri-carbamate **4-89** by HRMS. The remaining material was taken forward through another 4 steps to presumably make some diastereomer of himeradine A. The HRMS revealed that the compound matched the m/z of himeradine A. The tremendous

efforts of Dr. Jacob C. DeForest paved the way for a successful synthesis of the proposed structure of (–)-himeradine A.

Scheme 4-15. End-game validation for the synthesis of (–)-himeradine A.



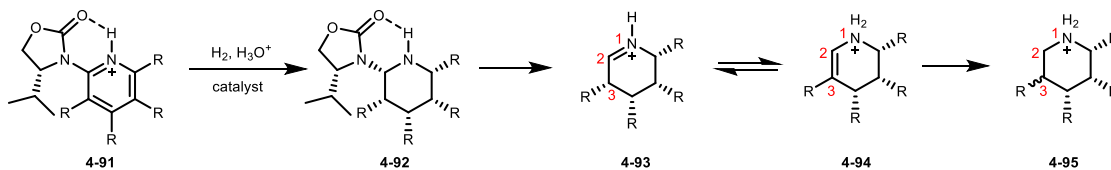
4.4 Results

4.4.1 Asymmetric Synthesis of Piperidine **4-71** via Glorius Hydrogenation

With a promising route in hand, the focus of the project shifted toward accessing piperidine **4-71** in an enantioselective fashion. This would permit us to avoid any late stage resolution since assigning stereochemistry proved difficult at that point. After searching the literature, it seemed that the most promising way to synthesize piperidine **4-71** was through an asymmetric hydrogenation. The Glorius group originally reported a versatile enantioselective *syn*-hydrogenation of pyridines containing Evans' auxiliary at the 2-position in 2004.¹⁶ Their rationale for the selectivity is shown below (Scheme 4-16). Under acidic conditions, the pyridine would be protonated and can hydrogen bond with the carbonyl of the chiral auxiliary to establish a “locked” conformation (**4-91**). This conformation would serve to block one face of the pyridine, which would only allow the hydrogens to approach from the opposite face to produce all *syn* stereochemistry (**4-92**). The resulting aminal would be cleaved under the acidic conditions to form

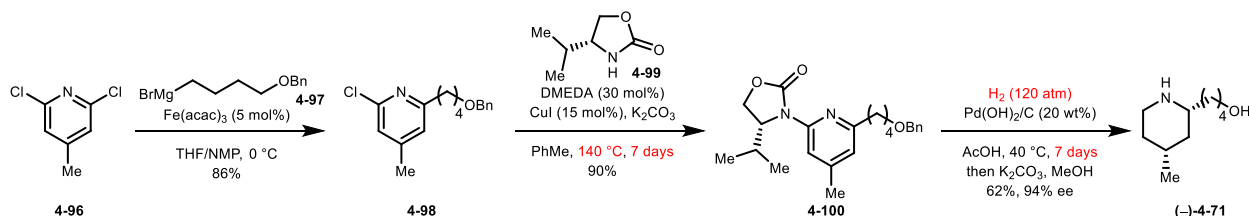
iminium **4-93**, which can tautomerize to enamine **4-94** to eliminate the stereochemistry at position 3. A final reduction would afford chiral piperidine **4-95** and the recoverable auxiliary.

Scheme 4-16. Mechanism of hydrogenation of pyridines containing a chiral auxiliary.



Since our desired piperidine had substituents at the 4- and 6-position of the ring, we were inspired to investigate this route. We began the synthesis using a Kumada coupling between dichloropyridine **4-96** and Grignard reagent **4-97** to afford mono-coupled product in great yield (Scheme 4-17). A subsequent Cu(I) catalyzed cross-coupling using Evans' auxiliary (**4-99**) worked in great yield, although it required one week to go to completion. With pyridine **4-98** in hand, we attempted the asymmetric hydrogenation. The reaction was performed at extremely high pressure (120 atm) for 7 days to produce piperidine (–)-**4-71** in 64% yield and 94% *ee*.

Scheme 4-17. Asymmetric synthesis of piperidine **4-71** using a Glorius hydrogenation.

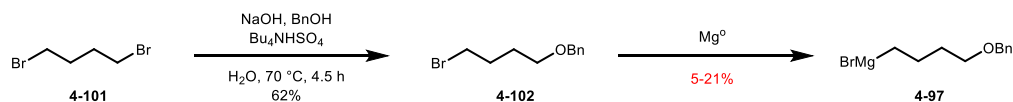


This sequence proved to be successful in construction of enantioenriched piperidine (–)-**4-71**, but each step had major drawbacks. The first step proceeded in great yield and mild conditions, yet formation of Grignard reagent **4-97** proved inefficient. The titer of the Grignard was always much lower than what was expected. The second step was high yielding, but required forcing conditions and long reaction times. The hydrogenation provided great enantioselectivity, but also

required forcing conditions and long reaction times. Under these conditions the free alcohol was also acylated with the acetic acid, thus a subsequent hydrolysis step was required.

With the intention of producing enantiopure piperidine (–)-**4-71** on large scale, we knew the crucial problem was the production of Grignard **4-97**. Thus, efforts were placed towards the production of Grignard **4-97** on scale. Alkyl bromide **4-102** was easily produced in one step from dibromide **4-101** using benzyl alcohol and a phase transfer catalyst under basic conditions (Scheme 4-18). These conditions allowed for the production of more than 60 grams of alkyl bromide **4-102**. Unfortunately, after weeks of screening conditions for the formation of Grignard **4-97**, the best result was a 21% titer. Many combinations of different activators (I_2 , DIBAL-H, $BrCH_2CH_2Br$, etc.), temperatures, solvents, reaction times, and concentrations were tested but none proved effective.

Scheme 4-18. Synthesis of Grignard reagent **4-97**.

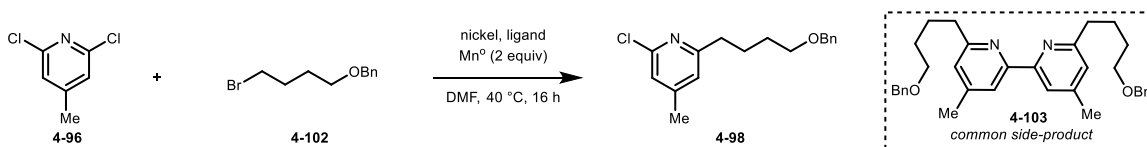


4.4.2 Nickel Catalyzed Cross-electrophile Coupling to Form Pyridine 4-98

With many grams of bromide **4-102** in hand and a failed attempt at an efficient Grignard formation, we knew we had to bypass the Kumada coupling. We turned to some of Weix's chemistry, in which he is able to use alkyl bromides and chloropyridines in cross-electrophile coupling reactions catalyzed by nickel.¹⁷ The reaction was first examined with the optimized conditions from the literature using $NiBr_2 \cdot 3H_2O$ (5 mol%) as the nickel source, BPhen (5 mol%) as the ligand, Mn^0 (2 equiv) as the reductant, and DMF as the solvent (Table 4-1, entry 1). Unfortunately, these conditions yielded no desired product. Simply replacing the $NiBr_2 \cdot 3H_2O$ with $NiCl_2(\text{glyme})$ provided the desired product in 11% yield (entry 2). A ligand screen revealed that

using 4,7-dimethoxy-1,10-phenanthroline with 5 mol% of AIBN in place of BPhen increased the yield to 22%, which was further improved by increasing the loading of the nickel and ligand to 15 mol% (entries 3 and 4). The AIBN is presumed to aid in the initiation of forming the alkyl radical from bromide **4-102**. Further screening found that the much cheaper dtbbpy ligand was also suitable for this transformation in comparable yields to 4,7-dimethoxy-1,10-phenanthroline (entry 5). Lastly, preforming the nickel complex with dtbbpy ligand and using 30 mol% increased the yield to 48% (entry 6). Upon optimization of this reaction, we found that the common side-product observed if the reaction was left stirring too long was the bis coupling of chloropyridine **4-103**.

Table 4-1. Nickel catalyzed cross-electrophile coupling optimization.



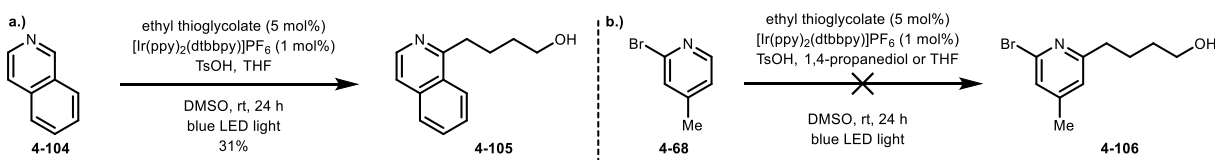
entry	nickel	ligand	additive	NMR yield (%)
1	NiBr ₂ •3H ₂ O (5 mol%)	BPhen (5 mol%)	none	0%
2	NiCl ₂ (glyme) (5 mol%)	BPhen (5 mol%)	none	11%
3	NiCl ₂ (glyme) (5 mol%)	4,7-dimethoxy-1,10-phenanthroline (5 mol%)	AIBN (5 mol%)	22%
4	NiCl ₂ (glyme) (15 mol%)	4,7-dimethoxy-1,10-phenanthroline (15 mol%)	AIBN (5 mol%)	40%
5	NiCl ₂ (glyme) (15 mol%)	dtbbpy (15 mol%)	AIBN (5 mol%)	42%
6	Ni(dtbbpy)Br ₂ (30 mol%)	-	AIBN (5 mol%)	48%

An exhaustive list of conditions was also screened where the temperature, concentration, reaction time, reductant, solvent, and additive (NaI, TFA, AIBN, and TMSCl) were varied. Unfortunately, the best results obtained were using a preformed nickel catalyst at 30 mol% catalyst loading to only yield 48% of product (entry 6). The inefficiency of this reaction ultimately led us to abandon this transformation.

4.4.3 Attempts at Minisci Chemistry to Synthesize Pyridine 4-98

In 2015, the MacMillan group reported the alkylation of heteroarenes using ethers or alcohols as the alkylating agents.¹⁸ They were able to use a photocatalyst combined with a thiol organocatalyst to effectively alkylate heteroarenes. They proposed a mechanism that utilized a spin-center-shift elimination of water to effect the transformation. This approach was very attractive to us because it could potentially allow us to use THF as our alkylating agent and 4 carbon unit in the desired piperidine. We began by examining an exact substrate they tested in the literature (Scheme 4-19, a). To no surprise, the desired product was formed, albeit in much lower yield than was reported. Unfortunately, using the same conditions on bromopicoline **4-68** did not yield any desired product (Scheme 4-19, b). Both THF and 1,4-propanediol were tested as the alkylating agents but neither worked.

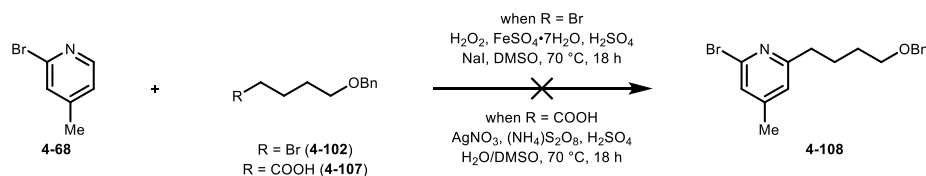
Scheme 4-19. Attempted alkylation of heterocycles using MacMillan's spin-center-shift photoredox Minisci reaction.



With many grams of alkyl bromide **4-102** left, an iron mediated Minisci reaction was examined on bromopicoline **4-68** (Scheme 4-20). Iron sulfate in the presence of hydrogen peroxide, acid, and an alkyl halide is preceded to form the alkyl radical and add into

heteroarenes. These conditions did not afford any desired product. Switching the alkyl bromide with carboxylic acid **4-107** allowed us to use original Minisci conditions to attempt the transformation.¹⁹ Unfortunately, using sulfuric acid, silver nitrate, and ammonium persulfate in combination with bromopicoline **4-68** and carboxylic acid **4-107** did not form product. These conditions were also examined on 2-chloro-4-picoline, but the same outcome was observed. It was predicted that the halogen at the 2-position was preventing the transformation from occurring. To the best of our knowledge, no Minisci reaction is known with a 2-halo-picoline.

Scheme 4-20. Attempted Minisci reaction into bromopicoline **4-68**.

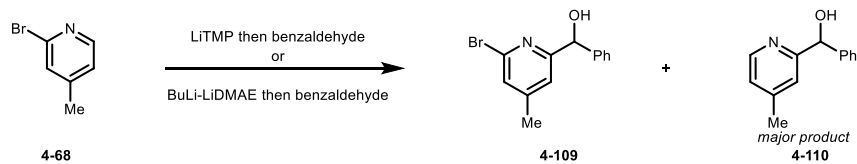


4.4.4 Attempts at Picoline Lithiation to Synthesize Pyridine **4-108**

We decided that Minisci chemistry would be ideal for the desired transformation, but unlikely to be successful. Thus, instead of adding into an electrophilic pyridine we decided to switch polarity and make the pyridine nucleophilic. The pyridine ring system is usually most acidic at the 2- and 4-positions, which can be deprotonated using strong bases. Picolines can also be deprotonated at the methyl position selectively. Bromopyridine **4-68** was subjected to LiTMP and trapped with benzaldehyde to investigate the position of deprotonation (Scheme 4-21). Unfortunately, the major product observed was benzyl alcohol **4-110**. This presumably arises by lithium halogen exchange followed by addition into benzaldehyde. Dimethylaminoethanol was previously reported to form a complex with 2 equivalents of *n*-BuLi to direct lithiation at the 6-position of a pyridine ring containing a halide at the 2-position.²⁰ These conditions were also examined but provided the same result of as using LiTMP. In retrospect, we should have expected

that deprotonation of an arene containing a bromide would mainly result in lithium-halogen exchange.

Scheme 4-21. Attempted lithiation of bromopicoline **4-68**.

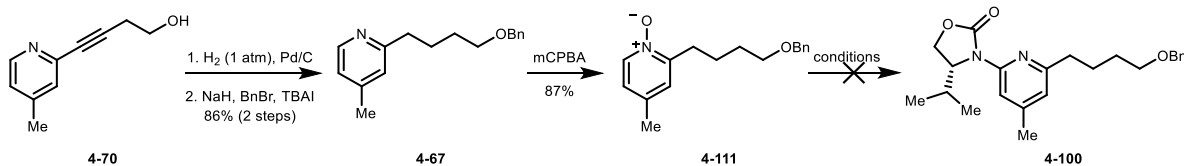


4.4.5 Pyridine *N*-Oxide Approach Towards Forming Pyridine **4-108**

After having no success with efficient Grignard formation, Minisci chemistry, and directed lithiation, we decided to examine potential manipulation of easily accessible alkyne **4-70**. Alkyne **4-70** can be made on multi-gram scale in excellent yield via a Sonagashira cross-coupling (Scheme 4-10). Hydrogenation of the alkyne to the alkane was easily achieved in quantitative yield by using an atmosphere of hydrogen and catalytic Pd/C (Scheme 4-22). The resulting alcohol was protected as the benzyl ether (**4-67**) before forming the *N*-oxide (**4-111**) with *m*CPBA as the oxidant. This three-step sequence was efficient and easily performed on large scale.

The objective of forming the *N*-oxide was to give the ability of a regioselective functionalization at the 6-position. The activation of *N*-oxides is well known by many reagents. Most commonly, POCl₃, SOCl₂, and oxalyl chloride are used, but these reagents all afford the resulting 6-chloropyridine. There are few reports where different activating groups coupled with an appropriate external nucleophile can afford 6-substituted piperidines. In 2010, it was reported that PyBrop can activate pyridine *N*-oxide's and an appropriate nucleophile can substitute alpha to the nitrogen of the pyridine.²¹ They demonstrated a variety of nucleophiles including anilines, amines, amides, sulfonamides, and phenols. Unfortunately, these conditions using Evans auxiliary as the nucleophile did not afford pyridine **4-100** (Scheme 4-22). It was also attempted with oxalyl chloride as the activator, but this was also unsuccessful.

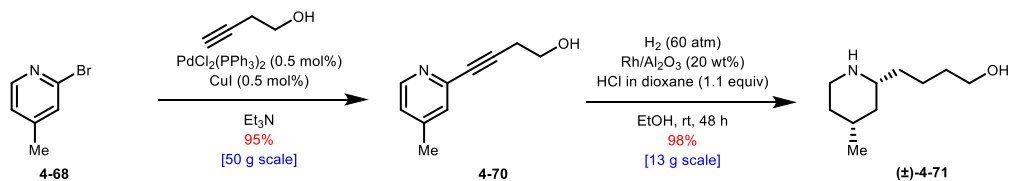
Scheme 4-22. Three step sequence to accessing N-oxide **4-111**.



4.4.6 Resolution of Piperidine **4-71 with DBTA**

After many attempts at developing a robust route to enantiopure piperidine **4-71**, nothing proved to be successful. The Glorius hydrogenation did afford enantiopure **4-71**, but was obviously not a scalable sequence. We knew that the Sonagashira reaction, to access alkyne **4-70**, was robust, scalable, and contained all the carbons necessary to make piperidine **4-71**. With this in mind, we decided to attempt a resolution of racemic **4-71**. The Sonagashira reaction was performed on a 50-gram scale to afford alkyne **4-70** in 95% yield (Scheme 4-23). After some optimization, it was discovered that a global hydrogenation using rhodium on alumina with HCl in dioxane under 60 atmospheres of hydrogen gas efficiently afforded racemic piperidine **4-71** as a single diastereomer. This two-step sequence was performed without any column chromatography.

Scheme 4-23. Large scale production of racemic piperidine **4-71**.



With large amounts of racemic piperidine **4-71** in hand, we investigated a resolution using various chiral acids (Table 4-2). Initially, we tested six different chiral acids (0.5 equiv) with 30 volumes of *i*PrOH as the solvent (entries 1-6). Dibenzoyl-*L*-tartaric acid was the only chiral acid to crystallize when mixed with piperidine **4-71** and it provided a 41% yield and 23% *ee* (entry 6). Switching solvents from *i*PrOH to ethanol improved the *ee* to 40% but dropped the yield slightly (entry 7). Using MeOH as the solvent drastically dropped the yield to 10% but improved the *ee* to

-97% (entry 8). Switching to dibenzoyl-D-tartaric acid and increasing the amount of chiral acid used to 1 equivalent increased the yield to 41% and afforded a 95% *ee* (entry 9). Altering the concentration of the resolution had no beneficial effect on the yield or *ee* (entries 10 and 11).

Table 4-2. Optimization of the salt resolution of piperidine **4-71**.



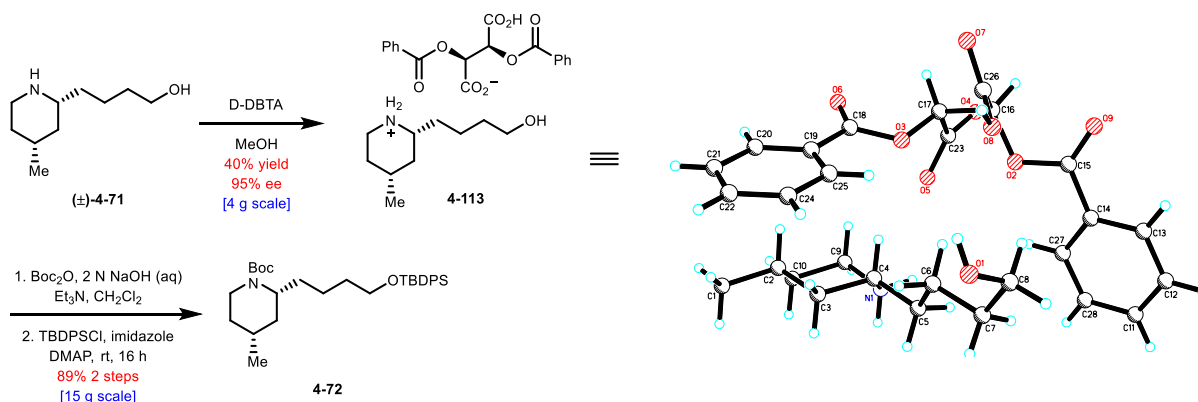
entry	chiral acid	acid (equiv)	solvent	volumes	yield (%) ^a	ee (%) ^{a,b}
1	L-malic acid	0.5	<i>i</i> PrOH	30	N/A	N/A
2	(1 <i>R</i>)-10-camphorsulfonic acid	0.5	<i>i</i> PrOH	30	N/A	N/A
3	(1 <i>R</i> ,3 <i>S</i>)-camphoric acid	0.5	<i>i</i> PrOH	30	N/A	N/A
4	(<i>R</i>)- mandelic acid	0.5	<i>i</i> PrOH	30	N/A	N/A
5	D-tartaric acid	0.5	<i>i</i> PrOH	30	N/A	N/A
6	Dibenzoyl-L-tartaric acid	0.5	<i>i</i> PrOH	30	41	23
7	Dibenzoyl-L-tartaric acid	0.5	EtOH	30	32	40
8	Dibenzoyl-L-tartaric acid	0.5	MeOH	30	10	-97
9	Dibenzoyl-D-tartaric acid	1	MeOH	30	41	95
10	Dibenzoyl-D-tartaric acid	1	MeOH	20	41	89
11	Dibenzoyl-D-tartaric acid	1	MeOH	40	36	95

^a N/A indicates no solid was formed. ^b *ee* was determined by HPLC analysis of the tosylated piperidine.

The optimal conditions for the resolution of piperidine **4-71** were found to be entry 9 of Table 4-2. This procedure was performed on gram scale and was reproducible (Scheme 4-24). The chiral salt was crystallized and X-ray analysis confirmed the relative and absolute stereochemistry of the piperidine (**4-71**). The salt was directly free based and Boc protected in the same pot using biphasic conditions. The crude oil from this reaction mixture was then directly subjected to

TBDPSCI, DMAP, and imidazole to protect the primary alcohol and form **4-72**. Only a single column chromatography step was performed throughout all five steps.

Scheme 4-24. Optimized resolution of piperidine **4-71** with a crystal structure and functional group protections.

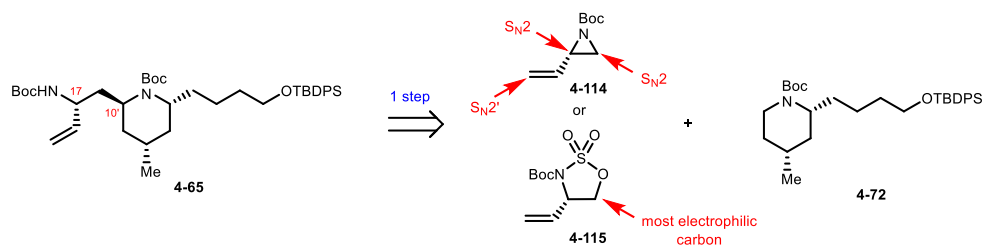


4.4.7 Sulfamidate Approach Towards the Synthesis of Elaborated Piperidine **4-65**

With a robust sequence to synthesize enantioenriched piperidine **4-72**, all efforts were turned to elaboration of the western portion to afford the fully elaborated piperidine (**4-65**). After examining what was previously attempted in our laboratory (Ellman's auxiliary, Hartwig amination, and Overman rearrangement), we made an effort to possibly shorten the sequence. We envisioned a diastereoselective *N*-Boc directed lithiation of **4-72** to set the C10' stereochemistry and coupling with an appropriate electrophile that bears the C17 stereochemistry (Scheme 4-25). This would allow us to transform piperidine **4-72** into fully elaborated piperidine **4-65** in 1 step and be confident in the C17 stereochemistry. The two electrophiles in mind were aziridine **4-114** or sulfamidate **4-115**. Vinyl aziridines are known to be electrophilic at the least hindered and more hindered side, depending on the reaction conditions, via an S_N2 reaction. Unfortunately, they are also known to open via and S_N2' reaction at the olefin, especially with cuprates, Grignards, and lithiates.^{21b} This led us to investigating sulfamidates as possible electrophiles in this reaction. Sulfamidates are well known to be much more electrophilic at the carbon directly bonded to the

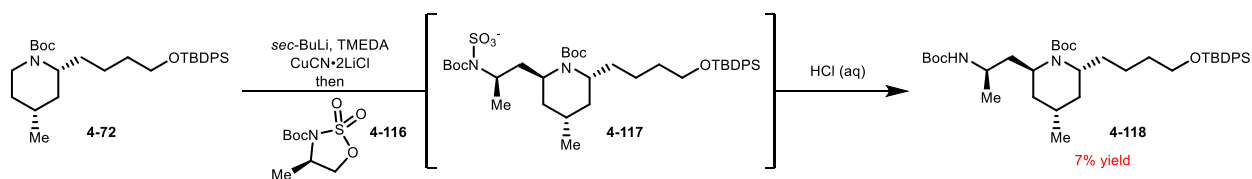
oxygen, presumably due to the electronegativity difference between the oxygen and nitrogen in the molecule.

Scheme 4-25. Retrosynthesis to synthesize fully elaborated piperidine **4-65** using a sulfamidate.



To the best of our knowledge, there are no examples of using aziridines or sulfamidates as electrophiles in an α -*N*-Boc alkylation reaction. The closest precedent was using an epoxide as the electrophile in the presence of a Lewis acid.²² Regardless, we wanted to examine if the bond could be forged using this route. Since sulfamidate **4-115** was not reported in the literature, we used a model sulfamidate (**4-116**) that was readily prepared from *N*-Boc-D-alinol in two steps (Scheme 4-26). Piperidine **4-72** was deprotonated using *sec*-BuLi in the presence TMEDA, followed by transmetalation to the cuprate and quenched with sulfamidate **4-116**, which formed intermediate **4-117** by ESI mass spectrometry. The intermediate was treated with HCl in order to afford fully elaborated piperidine **4-118** in 7% yield. Though a low yield was observed, this reaction proved to forge the desired bond. We were satisfied with this result because we believed we could further optimize this reaction to a higher yield on the real substrate.

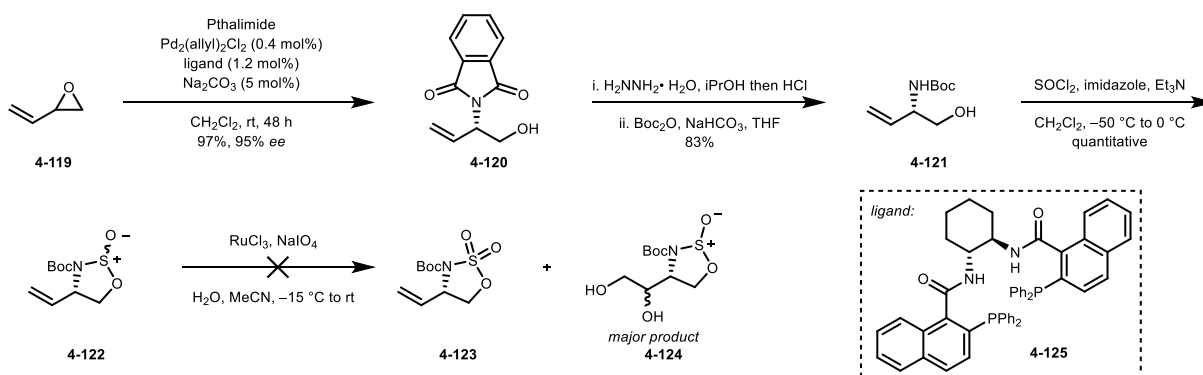
Scheme 4-26. Alkylation of piperidine **4-72** with a sulfamidate.



With this promising result, we turned efforts toward efficiently synthesizing vinyl sulfamidate **4-115**. Initially we examined using a literature known procedure to form amino

alcohol **4-121** (Scheme 4-27). In 2011, Trost reported a large-scale two-step enantioselective synthesis of amino alcohol **4-121** using palladium catalysis.²³ Using the same conditions, we were able to replicate the results to form phthalimide **4-120** in 95% *ee* using ligand **4-125**. Subsequent cleavage of the phthalimide using hydrazine hydrate followed by HCl proved effective in forming the free amine, which was directly converted to the carbamate (**4-121**) by neutralizing the mixture and adding Boc₂O. The corresponding carbamate was subjected to a cooled mixture of thionyl chloride, imidazole, and triethylamine to form sulfamidite **4-122** as a mixture of diastereomers and was used without further purification. The last step of the sequence was oxidation to the sulfamidate using RuCl₃ and NaIO₄.²⁴ Unfortunately, these oxidation conditions proceeded to dihydroxylate the olefin (**4-124**) instead of oxidizing to the sulfamidate.

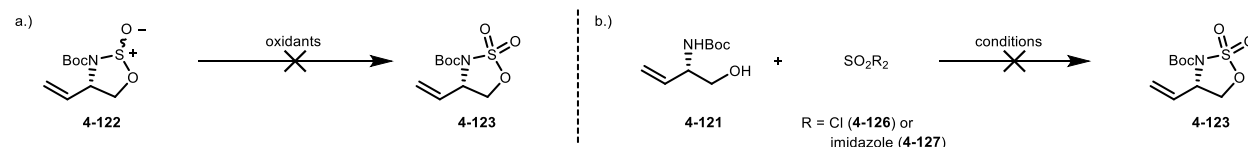
Scheme 4-27. Attempted formation of sulfamidate **4-123** using a key Tsuji-Trost amination.



With grams of sulfamidite **4-122** in hand, we tried to investigate different oxidants in hopes of chemoselective oxidation of the sulfamidite over the olefin (Scheme 4-28, a). Initial attempts with *m*CPBA and hydrogen peroxide at room temperature afforded only recovered starting material. In the case of *m*CPBA, some product, along with a mixture of epoxidation at the olefin, was formed upon heating to 60 °C. This presented some promise, but the danger of heating peroxides on scale deterred us from this approach. Other unsuccessful oxidation conditions examined were TPAP/NMO, Mn(OAc)₂/AcOOH, RuCl₃/NaOCl, and Br₂. In the case of Br₂, we

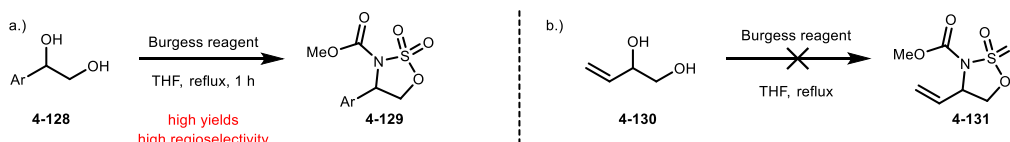
were hopeful of protecting the olefin as the dibromide and oxidizing the sulfamidite in one pot, which would be converted back to the olefin using Zn/AcOH. Unfortunately, we only recovered an insoluble polymer from this reaction.

Scheme 4-28. Attempts at oxidizing sulfamidite **4-122** to sulfamidate **4-123** (a) and attempts at directly transforming amino alcohol **4-121** into sulfamidate **4-123** using sulfuryl reagents (b).



Since direct oxidation of the sulfamidite (**4-122**) proved difficult, we thought we may be able to bypass oxidation by coming in with the right oxidation state (Scheme 4-28, b). We originally examined sulfuryl chloride (**4-126**) as our sulfur dioxide source. After many attempts with various bases, temperatures, and concentrations no product was ever formed. Instead, a variety of chlorinated products were observed. This was expected because SO_2Cl_2 is known to be an electrophilic source of chlorine. Switching to its less reactive counterpart, 1,1'-sulfonyldiimidazole, also proved unsuccessful. Many bases and temperatures were examined, but in most cases starting material was recovered. In the case of NaH, the major product observed was the vinyl aziridine.

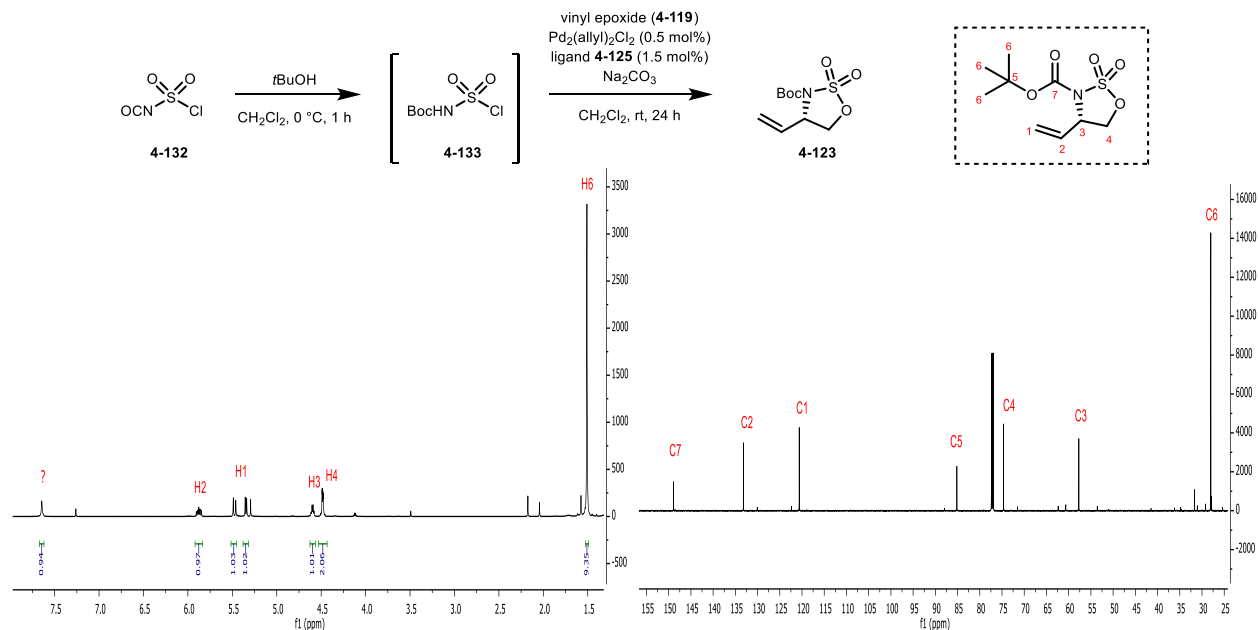
Scheme 4-29. Attempted one-step synthesis of sulfamidate **4-131**.



In 2004, Nicolaou reported a novel approach toward the synthesis of sulfamidates using diols and Burgess reagent (Scheme 4-29, a).²⁵ The precedent displayed that a variety of aryl diols could be used in this transformation, with net inversion of stereochemistry. They also demonstrated that Burgess reagent derivatives could be used to ultimately yield in Alloc, Cbz, and Troc protected

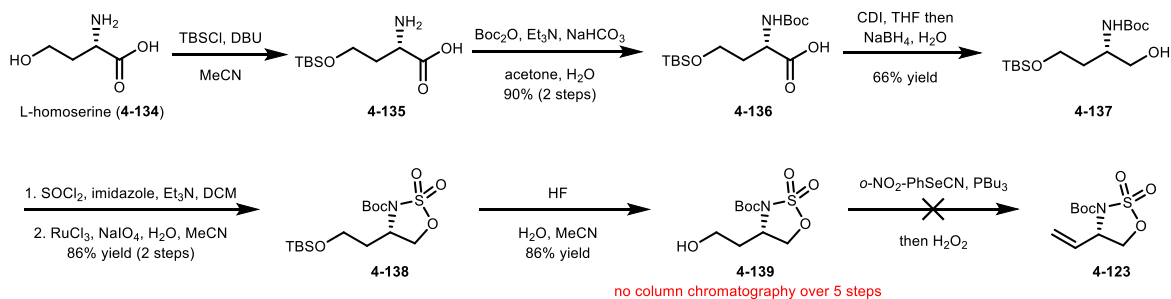
sulfamidates. Unfortunately, using vinyl diol **4-130** with Burgess reagent did not afford any desired sulfamidate (**4-131**).

Scheme 4-30. Novel approach toward the formation of sulfamidate **4-123**.



After months of no success, we devised a novel synthesis that, at first glance, seemed to afford the desired vinyl sulfamidate (**4-123**). We used the same Tsuji-Trost conditions as previous except the nucleophile was replaced with chlorosulfonamide **4-133**, which was pre-formed by the addition of dry *tert*-butanol to chlorosulfonyl isocyanate **4-132** (Scheme 4-30). Upon purification of the reaction mixture, a substance was isolated that seemed to be consistent with the expected proton and carbon NMR spectra. In the proton NMR, the *tert*-butyl group (H6) was apparent around 1.5 ppm. All three olefinic protons (H1 and H2) were at the expected ppm shift as were the protons at H3 and H4. The only discrepancy was the unexpected peak at about 7.6 ppm that integrated to 1H. We believed this proton might have been due to the alcohol not closing down to forge the S-O bond. The carbon NMR contained all 7 peaks that would be expected. Unfortunately, the singlet at 7.6 ppm caused concern about the structure of the isolated compound. Analysis by HRMS also did not show the correct *m/z*.

Scheme 4-31. Attempted synthesis of sulfamidate **4-123** from L-homoserine.



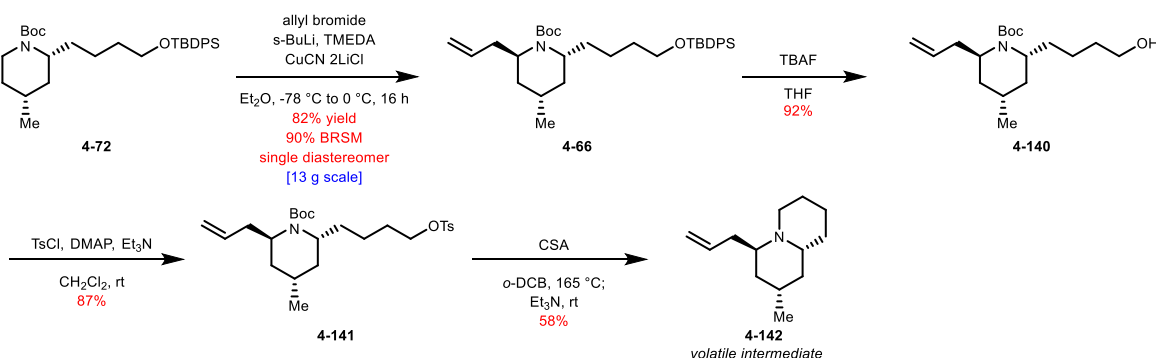
With no successful route to confidently access sulfamidate **4-123**, we attempted one last approach. The synthesis began with a TBS protection of the alcohol on L-homoserine followed by Boc protection of the free amine (Scheme 4-31). This was accomplished in 90% yield to afford carboxylic acid **4-136**. Reduction of the carboxylic acid using CDI with NaBH_4 provided primary alcohol **4-137**, which was directly subjected to the two-step sequence using thionyl chloride followed by RuCl_3 and NaIO_4 . The resulting TBS-sulfamidate **4-138** was deprotected using HF to afford alcohol **4-139**. The entire sequence was performed with no column chromatography. The final step was a Greico elimination, but unfortunately these conditions only resulted in decomposition. Yet again, the last step in the sequence proved unsuccessful.

4.4.8 Model System Used to Validate Late-Stage Quinolizidine Formation

After a long and unsuccessful venture towards synthesizing sulfamidate **4-123**, the overall disconnection was abandoned. Instead we turned back to the allylation chemistry. Treatment of N-Boc piperidine **4-72** with *sec*-BuLi and TMEDA followed by $\text{CuCN}\cdot 2\text{LiCl}$ and finally allyl bromide provided olefin **4-66** in 82% yield (90% BRSM) as a single diastereomer on a 13-gram scale (Scheme 4-32). With this material in hand, we wanted to validate the late-stage quinolizidine formation. TBAF deprotection of the TBDPS group yielded alcohol **4-140** which was treated with TsCl, DMAP, and Et_3N to furnish tosylate **4-141**. Finally, the tosylate was heated to 165 °C with CSA for 1 hour. By ESI-MS, some product was formed along with Boc deprotected amine.

Cooling to room temperature and allowing the crude mixture to stir with excess Et₃N funneled the remaining material to quinolizidine **4-142**. The low yield of this reaction was attributed to the volatility of this compound, since it evaporated after leaving on high vacuum overnight.

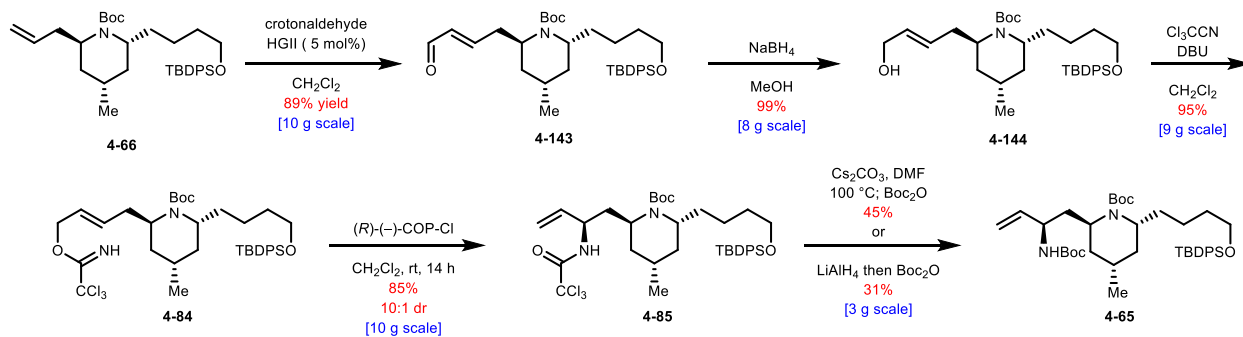
Scheme 4-32. Model system to examine the late stage quinolizidine formation.



4.4.9 Successful Route for the Synthesis of the Proposed Structure of (-)-Himeradine A

Encouraged by the promising end-game validation, we ventured towards completing the synthesis of the fully elaborated piperidine (**4-65**). Now that we were able to successfully synthesize alkene **4-66** in the enantiopure form, we did not have to worry about a late stage resolution that previously caused problems when trying to assign stereochemistry. We had to consider a way to install the last stereocenter at C17. Any of the three approaches discussed in section 4.3.4 would be viable for installation of the last stereocenter, but we believed that the Overman rearrangement would be the most reliable and robust.

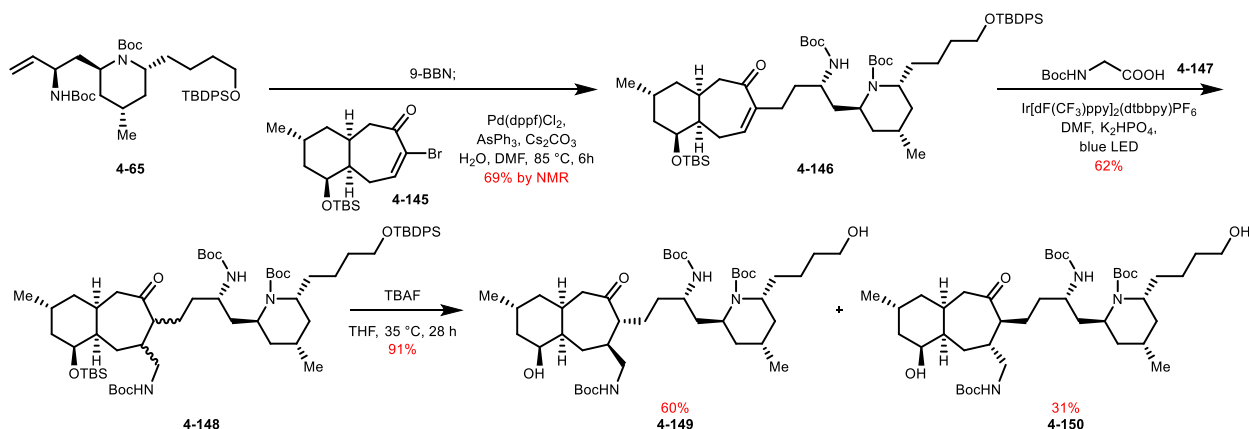
Scheme 4-33. Successful sequence for the synthesis of fully elaborated piperidine **4-65**.



Cross-metathesis of olefin **4-66** and crotonaldehyde mediated by Hoveyda-Grubbs II catalyst afforded enal **4-143** in high yield and solely as the *E*-isomer (Scheme 4-33). Substituting crotonaldehyde with acrolein stalled the reaction, with the best yield being 30% and 80% BRSM. Reduction of the aldehyde using NaBH₄ yielded allylic alcohol **4-144** in essentially quantitative yield with no 1,4-reduction observed. Formation of trichloroimidate **4-84** was accomplished by using trichloroacetonitrile in the presence of DBU in great yield. Subjecting the trichloroimidate (**4-84**) to (*R*)-(-)-COP-Cl affected the Overman rearrangement to provided trichloroamide **4-85** in 85% yield and a 10:1 dr.

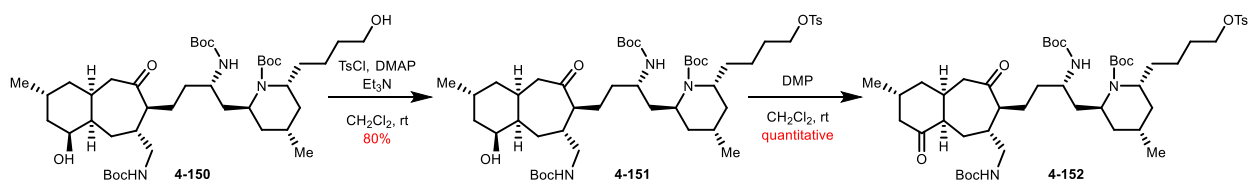
This last step in the sequence involved the deprotection of the trichloroacetamide and reprotection as the Boc carbamate. Unfortunately, this step proved to be the most difficult in the sequence. A variety of conditions were attempted including base hydrolysis using sodium hydroxide, reduction with sodium borohydride, and substitution with potassium *tert*-butoxide but none proved efficient in providing the desired product. Heating trichloroamide **4-85** in the presence of cesium carbonate followed by the addition of Boc₂O afforded Boc amine **4-65**, albeit in low yield. This was a result of isocyanate formation followed by trapping of free amine to form the symmetric urea. Unfortunately, the best yield observed for this reaction was 45%. The same transformation can be achieved using LiAlH₄ followed by Boc₂O, albeit in lower yield, but this method proved more efficient when running on larger scale.

Scheme 4-34. Suzuki cross-coupling, conjugate addition, and silyl deprotection.



With enantiopure allyl carbamate **4-65** in hand, the key hydroboration/B-alkyl Suzuki cross-coupling was examined (Scheme 4-34). To our delight, the reaction proceeded to afford enone **4-146** in 69% yield (by NMR). The product was difficult to separate from the remaining starting material (**4-65**), thus it was taken on to next step as a mixture. Conjugate addition using *N*-Boc glycine under photoredox conditions provided a complex mixture of inseparable diastereomers of **4-148** in 62% yield.²⁶ The mixture was treated with excess TBAF at a slightly elevated temperature to afford diastereomers **4-149** and **4-150** in a 91% combined yield, which were easily separable by column chromatography.

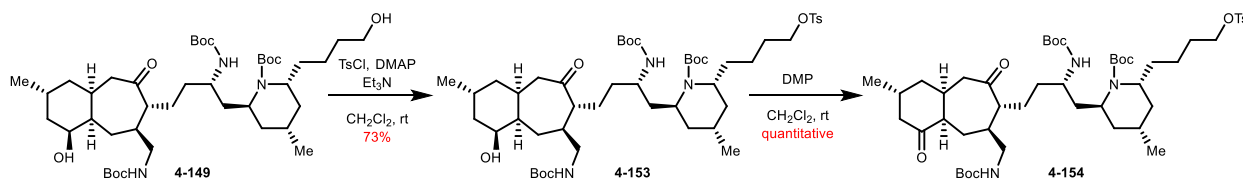
Scheme 4-35. Testing the tosylation and oxidation using the undesired diastereomer.



With both diastereomers **4-149** and **4-150** in hand, we decided to test the subsequent tosylation and oxidation on the undesired diastereomer (Scheme 4-35). Mono-tosylation of the primary alcohol over the secondary using TsCl with DMAP afforded tosylate **4-151** in 80% yield. Subsequent DMP oxidation provided diketone **4-152** in quantitative yield. With promising results

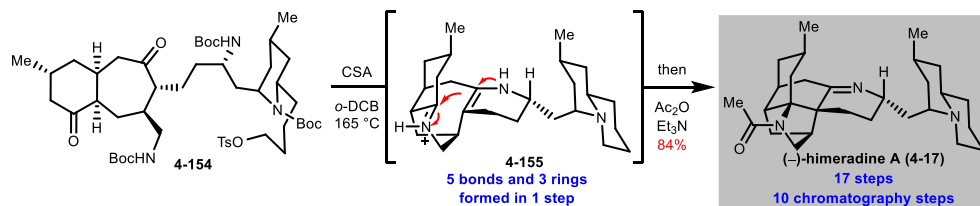
from the undesired diastereomer, we were able to carry the desired diastereomer (**4-149**) through the same sequence to successfully synthesize diketone **4-154** (Scheme 4-36).

Scheme 4-36. Tosylation and oxidation using the diastereomer.



The final step of the synthesis was performed by heating diketone **4-154** to 165 °C in *o*-DCB with camphorsulfonic acid for 1 hour followed by the addition of Ac₂O with Et₃N (Scheme 4-37). To our delight, this reaction provided (–)-himeradine A in 84% yield. This sequence proceeds through a trans-annular Mannich reaction via intermediate **4-155** to make 5 bonds and 3 rings in one step. The overall synthetic route requires 17 steps in the longest linear sequence with only 10 chromatography steps.

Scheme 4-37. Final trans-annular Mannich reaction to afford himeradine A.

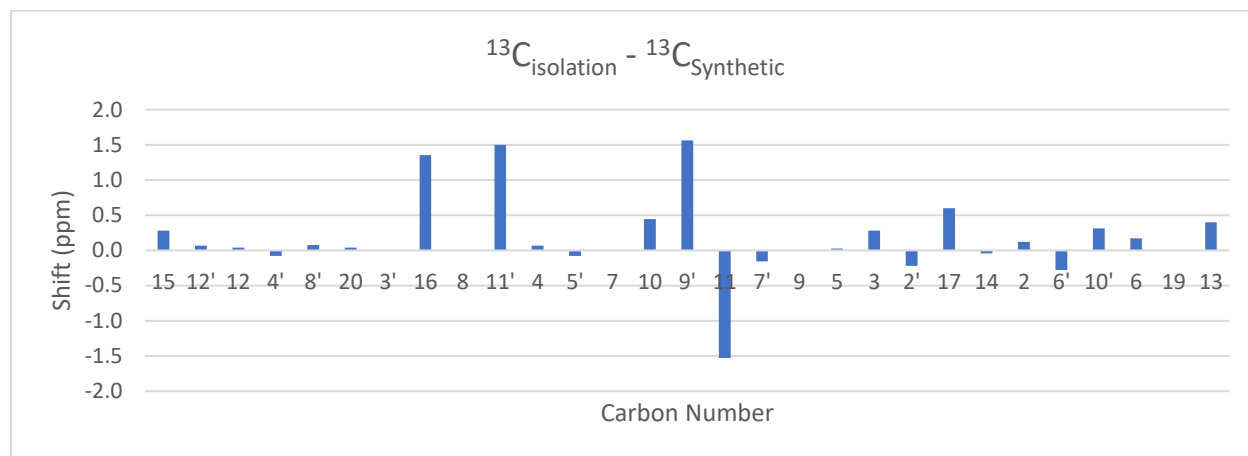


4.4.10 Comparison of (–)-Himeradine A Spectral Data

Our spectral data matched Shair's and was slightly inconsistent with that of the isolated natural product. The optical rotation for isolated (–)-himeradine A was $[\alpha]_{\text{D}}^{25} = -23$ ($c = 0.3$, MeOH), Shair's synthetic sample was $[\alpha]_{\text{D}}^{23} = -19$ ($c = 0.3$, MeOH), and Rychnovsky's synthetic sample was $[\alpha]_{\text{D}}^{22} = -16$ ($c = 0.3$, MeOH). Our proton NMR matched that of Shair's and contained the same H10' shift discrepancy with the natural product. The carbon NMR of the isolated natural product and that of our synthetic sample contained many discrepancies which are depicted in

Graph 4-1. As can be seen in Graph 4-1, there are four carbon shifts that are greater than 1 ppm in difference.

Graph 4-1. Carbon shift differences between the isolated natural product and the synthetic himeradine A.



A visual representation of the numbering of himeradine A and the carbon shift differences between the isolated natural product and Rychnovsky's synthetic sample is shown below (Figure 4-4). As can be seen, there are many carbons that are in good agreement with the natural product, but there are also 4 carbons that are 1.4 ppm or greater (highlighted in blue). Two of the most inconsistent carbons (C16 and C11') surround carbon 17, which would make one assume that the isolated natural product might be epimeric at that stereocenter. However, Shair synthesized the epimer at that position and the spectral data was still inconsistent with that of the isolated natural product.

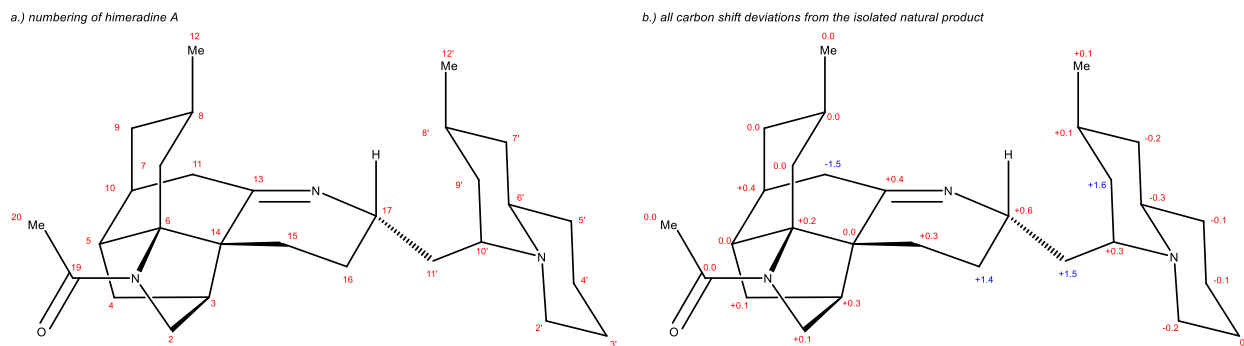
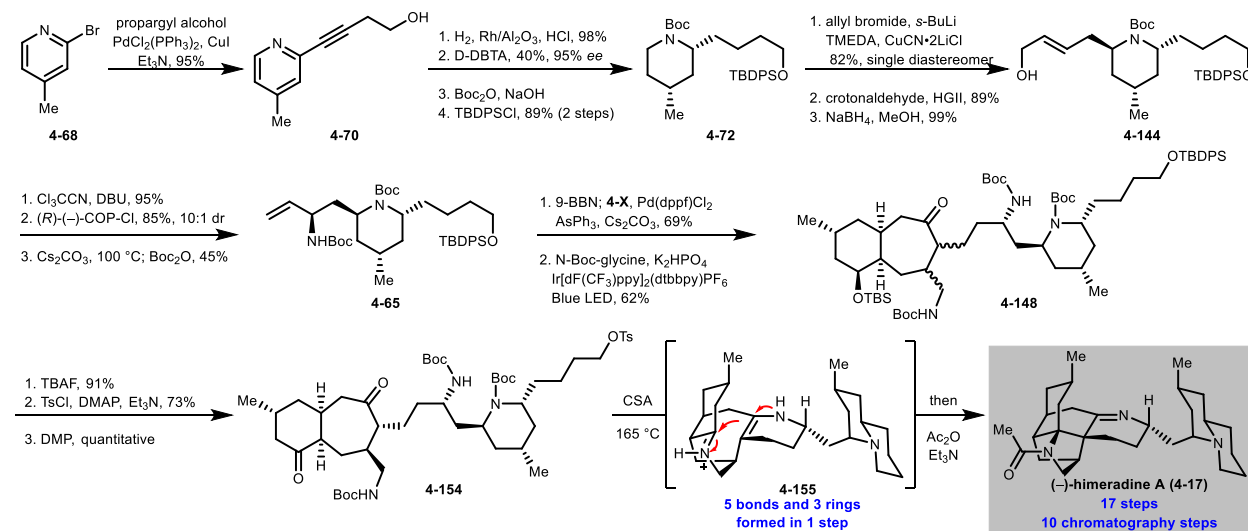


Figure 4-4. Carbon numbering of himeradine A (a) and carbon shift deviations from the isolated natural product (b).

4.4.11 Full Synthetic Route and Future Work

The total synthesis of the proposed structure of (–)-himeradine A was accomplished and the complete synthetic sequence is shown below (Scheme 4-38). The entire route contains only 17 steps, 10 of which require column chromatography. Though we were not able to completely match the spectral data with that of the isolated natural product, we were able to confirm that our structure matched Shair's. The actual structure of the natural product still remains ambiguous and future efforts can be placed in synthesizing epimers of the proposed structure. The route described herein can easily afford two diastereomers of the proposed structure. One can be synthesized by simply switching D-DBTA to L-DBTA in the resolution step and the other can be made by switching both the D-DBTA to L-DBTA in the resolution step and (*R*)-(–)-COP-Cl to (*S*)-(+)-COP-Cl in the Overman rearrangement. Synthesis of these diastereomers may reveal the actual structure of the isolated natural product. Our laboratory will report these findings in due course.

Scheme 4-38. Rychnovsky's complete synthetic sequence for the synthesis of the proposed structure of (–)-himeradine A.



4.5 Conclusions

In summary, a robust synthetic sequence for the synthesis of the proposed structure of (–)-himeradine A (**4-17**) was developed. The key features of this route include a dibenzoyl-tartaric acid resolution of a piperidine, diastereoselective N-Boc mediated piperidine allylation, B-alkyl Suzuki cross-coupling, photoredox mediated conjugate addition, and transannular Mannich cyclization. The sequence for the formation of elaborated piperidine **4-65** was performed on multi-gram scale to showcase the scalability of this route. The route described herein contains only 17 steps, which makes this the second and shortest synthesis to date.

Unfortunately, the synthetic sample prepared herein contained discrepancies in the spectral data when compared to the isolated natural product. However, our spectral data was consistent with that of Shair's. We believe that the structure of the isolated natural product may have been misassigned. With this robust sequence in hand, our laboratory is working towards the synthesis of diastereomers of the proposed structure of himeradine A. These syntheses will be reported in due time.

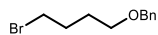
4.6 Experimental Section

4.6.1 General Experimental Details

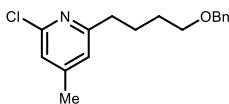
CDCl_3 was dried using Na_2SO_4 before use. ^1H NMR and ^{13}C NMR spectra were recorded at 500 MHz and 125 MHz at 298.0 K unless stated otherwise. Chemical shifts (δ) were referenced to either TMS or the residual solvent peak. The ^1H NMR spectra data are presented as follows: chemical shift, multiplicity (s = singlet, d = doublet, t = triplet, q = quartet, m = multiplet, dd = doublet of doublets, ddd = doublet of doublet of doublets, dddd = doublet of doublet of doublet of doublets, dt = doublet of triplets, dq = doublet of quartets, ddq = doublet of doublet of quartets, app. = apparent), coupling constant(s) in hertz (Hz), and integration. High-resolution mass spectrometry was performed using ESI-TOF.

Unless otherwise stated, synthetic reactions were carried out in flame- or oven-dried glassware under an atmosphere of argon. All commercially available reagents were used as received unless stated otherwise. Solvents were purchased as ACS grade or better and as HPLC-grade and passed through a solvent purification system equipped with activated alumina columns prior to use. Thin layer chromatography (TLC) was carried out using glass plates coated with a 250 μm layer of 60 \AA silica gel. TLC plates were visualized with a UV lamp at 254 nm, or by staining with *p*-anisaldehyde, potassium permanganate, phosphomolybdic acid, or vanillin. Liquid chromatography was performed using forced flow (flash chromatography) with an automated purification system on prepacked silica gel (SiO_2) columns unless otherwise stated. Infrared (IR) spectroscopy was performed on potassium bromide salt plates. Optical rotations were taken using a glass 50 mm cell with a sodium D-line at 589 nm. Electrospray ionization mass spectrometry (ESI-MS) was analyzed in positive mode with flow injection.

4.6.2 Compound Characterization:



((4-bromobutoxy)methyl)benzene (4-102): Sodium hydroxide pellets (18.5 g, 462 mmol) were added to a flask containing water (74.4 mL) in multiple portions and stirred until fully dissolved. The flask was then charged with benzyl alcohol (19.2 mL, 185 mmol), 1,4-dibromobutane (50.8 mL, 425 mmol) and tetrabutylammonium hydrogensulfate (1.57 g, 4.63 mmol) and the reaction mixture was stirred at 70°C for 4.5 h. Water (100 ml) was added and the product was extracted with hexane (2 x 200 ml). The organic layer was dried with sodium sulfate, filtered, and concentrated. The excess of dibromobutane was recovered by distillation (70 °C/0.35 torr). The resulting oil was purified by flash column chromatography (EtOAc/Hex) on silica to yield **4-102** as a clear oil (27.9 g, 62%). Spectral data were consistent with those previously reported for this compound.²⁷



2-(4-(benzyloxy)butyl)-6-chloro-4-methylpyridine (4-98): A flame-dried round bottom containing magnesium turnings (400 mg, 16.5 mmol), alkyl bromide **4-102** (2.00 g, 8.22 mmol), THF (29.6 mL), and a crystal of iodine was refluxed for 2 h before bringing the reaction mixture to room temperature. The solution of Grignard **4-97** was titrated with iodine to yield a titer of 0.0575 M. A separate flame-dried round bottom containing dichloropyridine **4-96** (212 mg, 1.31 mmol) dissolved in THF (6.66 mL) and NMP (1.14 mL) was charged with Fe(acac)₃ (23.1 mg, 0.0655 mmol) and cooled to 0 °C. The solution of Grignard **4-97** (25.0 mL, 1.44 mmol) was added dropwise over a period of 30 min. The reaction mixture was allowed to warm to room temperature before saturated aqueous NH₄Cl (40 mL) was added. The mixture was extracted with CH₂Cl₂ (3 x

50 mL), dried with sodium sulfate, filtered, concentrated, and purified by flash column chromatography (EtOAc/Hex) on silica to yield **4-98** as a clear oil (325 mg, 86%).

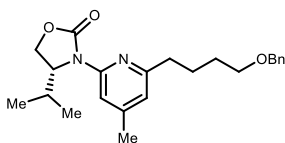
TLC R_f = 0.73 (silica gel, 20:80 EtOAc:Hex)

^1H NMR (500 MHz, CDCl_3) δ 7.35 – 7.30 (m, 5H), 7.29 – 7.24 (m, 1H), 6.95 (s, 1H), 6.86 (s, 1H), 4.49 (s, 2H), 3.49 (t, J = 6.6 Hz, 2H), 2.73 (t, J = 7.8 Hz, 2H), 2.28 (s, 3H), 1.83 – 1.74 (m, 2H), 1.67 (dt, J = 8.7, 6.4 Hz, 2H).

^{13}C NMR (125 MHz, CDCl_3) δ 162.8, 150.7, 150.5, 138.6, 128.4, 127.7, 127.6, 122.4, 122.0, 73.0, 70.2, 37.6, 29.4, 26.4, 20.8.

IR (FT-IR) 2934, 2858, 1599, 1552, 1454, 1104 cm^{-1} .

HRMS (ESI-TOF) m/z calcd for $\text{C}_{17}\text{H}_{21}\text{ClNO}$ ($\text{M} + \text{H}$) $^+$: 290.1312, found 329.1319.

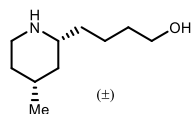


(R)-3-(6-(4-(benzyloxy)butyl)-4-methylpyridin-2-yl)-4-isopropylloxazolidin-2-one (4-100): A flame-dried Schlenk pressure tube was charged with chloropyridine **4-98** (390 mg, 1.35 mmol), (*R*)-(+)-4-Isopropyl-2-oxazolidinone **4-99** (209 mg, 1.62 mmol), DMEDA (58.0 μL , 0.540 mmol), CuI (51.4 mg, 0.270 mmol), K_2CO_3 (373 mg, 2.70 mmol), and toluene (1.60 mL). The vessel was sealed and heated to 140 $^\circ\text{C}$ for 7 days. The reaction mixture was then filtered through a pad of silica with EtOAc, concentrated, and purified by flash column chromatography (EtOAc/Hex) on silica to yield **4-100** as a clear oil (464 mg, 90%).

TLC R_f = 0.31 (silica gel, 10:90 EtOAc:Hex)

^1H NMR (500 MHz, CDCl_3) δ 7.77 (s, 1H), 7.36 – 7.31 (m, 4H), 7.31 – 7.24 (m, 1H), 6.69 (s, 1H), 4.89 (dt, J = 8.7, 3.7 Hz, 1H), 4.50 (s, 2H), 4.33 (t, J = 8.9 Hz, 1H), 4.24 (dd, J = 8.9, 3.7 Hz, 1H), 3.50 (t, J = 6.5 Hz, 2H), 2.67 (td, J = 7.3, 3.9 Hz, 2H), 2.45 (td, J = 7.0, 3.6 Hz, 1H), 2.32 (s,

3H), 1.83 – 1.75 (m, 2H), 1.70 – 1.62 (m, 2H), 0.90 (d, $J = 7.1$ Hz, 3H), 0.83 (d, $J = 7.0$ Hz, 3H).
 ^{13}C NMR (125 MHz, CDCl_3) δ 159.8, 155.6, 150.0, 149.6, 138.7, 128.5, 127.7, 127.6, 119.6, 112.1, 73.0, 70.3, 63.0, 59.1, 37.4, 29.4, 28.0, 25.9, 21.4, 18.1, 14.6.



(±)-4-(4-methylpiperidin-2-yl)butan-1-ol (4-71): Pyridine **4-70** (13.3 g, 82.6 mmol) was dissolved in EtOH (127 mL) in a beaker which was inserted in a steel bomb. To this solution was added 4 M HCl in dioxane (22.7 mL, 90.8 mmol) and allowed to stir for 10 min before 5% Rh/ Al_2O_3 (2.66 g, 20.0 wt%) was added. The steel bomb was sealed, purged with H_2 three times, pressurized to 60 atm with H_2 , and allowed to stir for 72 h. The bomb was then depressurized and the solution filtered through celite with MeOH (400 mL). The solution was concentrated before dissolving in aqueous 4 M NaOH (150 mL) and extracting with CH_2Cl_2 (3 x 150 mL). The solution was dried with Na_2SO_4 , filtered, and concentrated to afford **4-71** (13.8 g, 97%) as a white solid, which was spectroscopically pure and used without further purification.

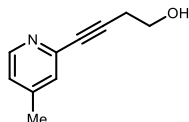
Melting Point 63 °C – 66 °C

^1H NMR (500 MHz, CDCl_3) δ 3.56 (t, $J = 6.5$ Hz, 2H), 3.04 (ddd, $J = 12.1, 4.3, 2.4$ Hz, 1H), 2.80 (s, 2H), 2.57 (td, $J = 12.3, 2.8$ Hz, 1H), 2.48 – 2.41 (m, 1H), 1.66 – 1.60 (m, 1H), 1.60 – 1.54 (m, 1H), 1.54 – 1.47 (m, 1H), 1.46 – 1.31 (m, 5H), 1.00 (qd, $J = 12.5, 4.2$ Hz, 1H), 0.87 (d, $J = 6.8$ Hz, 3H), 0.69 (q, $J = 11.8$ Hz, 1H).

^{13}C NMR (125 MHz, CDCl_3) δ 62.1, 56.6, 46.7, 41.6, 36.8, 35.0, 32.8, 31.3, 22.6, 22.1.

IR (FT-IR) 3366, 3290, 2923, 2864, 2622 cm^{-1} .

HRMS (ESI-TOF) m/z calcd for $\text{C}_{10}\text{H}_{21}\text{NONa}$ ($\text{M} + \text{Na}$) $^+$: 172.1701, found 172.1693.



4-(4-methylpyridin-2-yl)but-3-yn-1-ol (4-70): A flame-dried flask was charged with 2-bromo-4-methylpyridine **4-68** (50.0 g, 290.7 mmol), 3-butyn-1-ol (28.6 mL, 377.9 mmol), CuI (277 mg, 1.45 mmol), PdCl₂(PPh₃)₂ (1.02 g, 1.45 mmol), and 581 mL triethylamine and allowed to stir at room temperature for 24 h. The resulting heterogenous solution was filtered through a pad of silica using EtOAc (1 L) and concentrated to afford **4-70** (44.6 g, 95%) as a tan solid, which was spectroscopically pure and used without further purification.

TLC: R_f = 0.60 (silica gel, 10 : 90 MeOH:CH₂Cl₂)

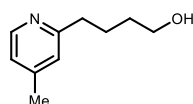
Melting Point 79 °C – 82 °C

¹H NMR (500 MHz, CDCl₃) δ 8.32 (d, *J* = 5.2 Hz, 1H), 7.17 (s, 1H), 6.98 (d, *J* = 5.1 Hz, 1H), 4.46 – 4.33 (m, 1H), 3.84 (q, *J* = 6.5 Hz, 2H), 2.68 (t, *J* = 6.6 Hz, 2H), 2.28 (s, 3H).

¹³C NMR (125 MHz, CDCl₃) δ 149.3, 147.7, 143.1, 127.7, 123.8, 87.9, 81.6, 60.7, 23.9, 20.9.

IR (FT-IR) 3336, 3231, 2942, 2237, 1603, 1057 cm⁻¹.

HRMS (ESI-TOF) *m/z* calcd for C₁₀H₁₀NONa (M + Na)⁺ : 184.0738, found 184.0737.



4-(4-methylpyridin-2-yl)butan-1-ol (4-67): Alkyne **4-70** (500 mg, 3.10 mmol) was dissolved in EtOAc (16 mL) before Pd/C (5% w/w) (330 mg, 0.155 mmol) was added. The flask was sealed and the atmosphere was purged with H₂ gas. After stirring for 24 h under an atmosphere of H₂, another portion of Pd/C (5% w/w) (330 mg, 0.155 mmol) was added and allowed to stir for another 24 h. The resulting reaction mixture was filtered through a pad of celite with EtOAc (30 mL) and

washed with CH₂Cl₂ (30 mL) before concentrating to yield alcohol **4-67** (514 mg, quantitative) as a spectroscopically pure white solid.

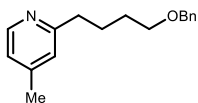
Melting Point 36 °C – 39 °C

¹H NMR (500 MHz, CDCl₃) δ 8.27 (d, *J* = 5.3 Hz, 1H), 6.92 (s, 1H), 6.87 (d, *J* = 4.8 Hz, 1H), 3.99 (s, 1H), 3.61 (t, *J* = 6.5 Hz, 2H), 2.76 – 2.67 (m, 2H), 2.25 (s, 3H), 1.75 (p, *J* = 8.0, 7.4 Hz, 2H), 1.58 (dt, *J* = 13.3, 6.6 Hz, 2H).

¹³C NMR (125 MHz, CDCl₃) δ 161.8, 148.6, 147.6, 123.8, 122.1, 61.9, 37.4, 32.2, 26.0, 21.0.

IR (FT-IR) 3286, 2927, 2859, 1607, 1561 cm⁻¹.

HRMS (ESI-TOF) *m/z* calcd for C₁₀H₁₆NO (M + H)⁺ : 166.1232, found 166.1230.

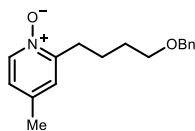


2-(4-(benzyloxy)butyl)-4-methylpyridine (4-67): A flame-dried round bottom containing NaH (60% in dispersion oil, 620 mg, 15.5 mmol) and THF (10.0 mL) was cooled to 0 °C before alcohol **4-67** (513 mg, 3.10 mmol) in THF (6.00 mL) was added dropwise. The resulting reaction mixture was allowed to stir for 30 min before benzyl bromide (0.480 mL, 4.03 mmol) and TBAI (344 mg, 0.930 mmol) were added. The reaction mixture was brought to room temperature and allowed to stir for 4 h. The solution was quenched by the addition of saturated aqueous NH₄Cl (25 mL), extracted with CH₂Cl₂ (3 x 30 mL), dried with sodium sulfate, filtered, concentrated, and purified by flash column chromatography (EtOAc/Hex) on silica to yield **4-67** as a clear oil (684 mg, 86%).

TLC R_f = 0.35 (silica gel, 30:70 EtOAc:Hex)

¹H NMR (500 MHz, CDCl₃) δ 8.39 – 8.33 (m, 1H), 7.32 (s, 4H), 7.30 – 7.24 (m, 1H), 6.95 (s, 1H), 6.90 (s, 1H), 4.48 (s, 2H), 3.50 (t, *J* = 5.5 Hz, 1H), 2.77 (t, *J* = 7.8 Hz, 1H), 2.29 (s, 2H), 1.87 – 1.77 (m, 2H), 1.73 – 1.64 (m, 2H).

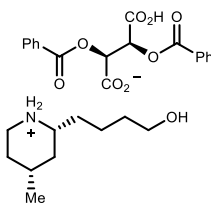
$^{13}\text{C NMR}$ (125 MHz, CDCl_3) δ 161.8, 148.9, 147.3, 138.7, 128.3, 127.6, 127.5, 123.7, 122.0, 72.9, 70.2, 37.9, 29.5, 26.5, 21.0.



2-(4-(benzyloxy)butyl)-4-methylpyridine 1-oxide (4-111): To a flask containing benzyl ether **4-67** (677 mg, 2.65 mmol) dissolved in CHCl_3 (5.30 mL) was added *m*CPBA (67%) (752 mg, 2.92 mmol) portion wise. The reaction mixture was allowed to stir at room temperature overnight before K_2CO_3 (1.46 g, 10.6 mmol) was added. After stirring for 15 min the reaction mixture was washed with water (3 x 10 mL). The organic layer was then dried with sodium sulfate, filtered, and concentrated to yield **4-111** as a clear oil (624 mg, 87%).

$^1\text{H NMR}$ (500 MHz, CDCl_3) δ 8.10 (d, $J = 6.6$ Hz, 1H), 7.31 (d, $J = 4.5$ Hz, 4H), 7.26 – 7.22 (m, 1H), 6.99 (d, $J = 2.7$ Hz, 1H), 6.89 (dd, $J = 6.6, 2.5$ Hz, 1H), 4.48 (s, 2H), 3.51 (t, $J = 6.3$ Hz, 2H), 2.94 – 2.81 (m, 2H), 2.27 (s, 3H), 1.80 (tt, $J = 8.7, 7.1$ Hz, 2H), 1.75 – 1.67 (m, 2H).

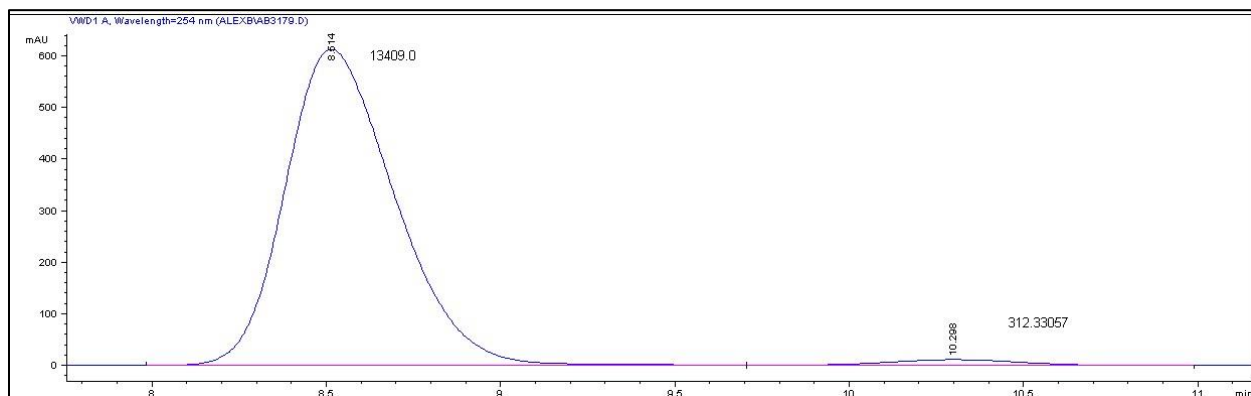
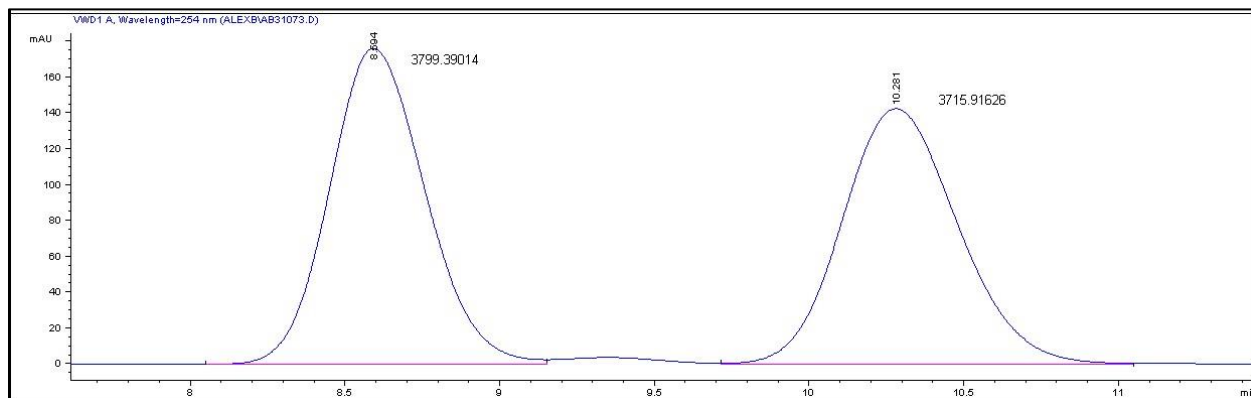
$^{13}\text{C NMR}$ (125 MHz, CDCl_3) δ 151.5, 139.0, 138.6, 137.1, 128.4, 127.7, 127.6, 126.1, 124.2, 73.0, 70.0, 30.2, 29.5, 22.9, 20.4.



(2R,4R)-2-(4-hydroxybutyl)-4-methylpiperidin-1-ium (2S,3S)-2,3-bis(benzoyloxy)-3-carboxy propanoate (4-113): Piperidine **4-71** (4.00 g, 23.4 mmol) was added to a pressure flask and dissolved in MeOH (160 mL) before charging with dibenzoyl-*D*-tartaric acid (8.37 g, 23.4 mmol). The resulting heterogeneous solution was sealed and placed in a pre-heated oil bath at 85 °C and allowed to stir for 1.5 h before cooling slowly to room temperature. The solution was filtered and

washed with CH₂Cl₂ (40 mL) to yield **4-113** (4.98 g, 40%) as a white crystalline solid. The enantiomeric excess was determined by converting to tosylate **4-156** and analyzing by HPLC using a Chiracel OD column (w/o guard) using 10% iPrOH/hexane at 1 mL/min.

Melting Point 187 °C – 188 °C



4.6.3 Data for 4-114 Crystal Structure

Table 1. Crystal data and structure refinement for sdr32.

Identification code	sdr32 (Alex Burtea)	
Empirical formula	C ₂₈ H ₃₅ N O ₉	
Formula weight	529.57	
Temperature	133(2) K	
Wavelength	0.71073 Å	
Crystal system	Orthorhombic	
Space group	P2 ₁ 2 ₁ 2 ₁	
Unit cell dimensions	a = 9.0943(5) Å	α = 90°.
	b = 13.3983(7) Å	β = 90°.

	$c = 22.3965(12) \text{ \AA}$	$\gamma = 90^\circ$.
Volume	$2729.0(3) \text{ \AA}^3$	
Z	4	
Density (calculated)	1.289 Mg/m^3	
Absorption coefficient	0.096 mm^{-1}	
F(000)	1128	
Crystal color	colorless	
Crystal size	$0.346 \times 0.247 \times 0.206 \text{ mm}^3$	
Theta range for data collection	1.771 to 28.885°	
Index ranges	$-11 \leq h \leq 11, -17 \leq k \leq 17, -28 \leq l \leq 29$	
Reflections collected	33067	
Independent reflections	6709 [R(int) = 0.0278]	
Completeness to theta = 25.500°	100.0 %	
Absorption correction	Semi-empirical from equivalents	
Max. and min. transmission	0.8621 and 0.8263	
Refinement method	Full-matrix least-squares on F^2	
Data / restraints / parameters	6709 / 0 / 479	
Goodness-of-fit on F^2	1.038	
Final R indices [$I > 2\sigma(I)$ = 6290 data]	R1 = 0.0321, wR2 = 0.0759	
R indices (all data, ? \AA)	R1 = 0.0356, wR2 = 0.0779	
Largest diff. peak and hole	0.316 and $-0.214 \text{ e.\AA}^{-3}$	

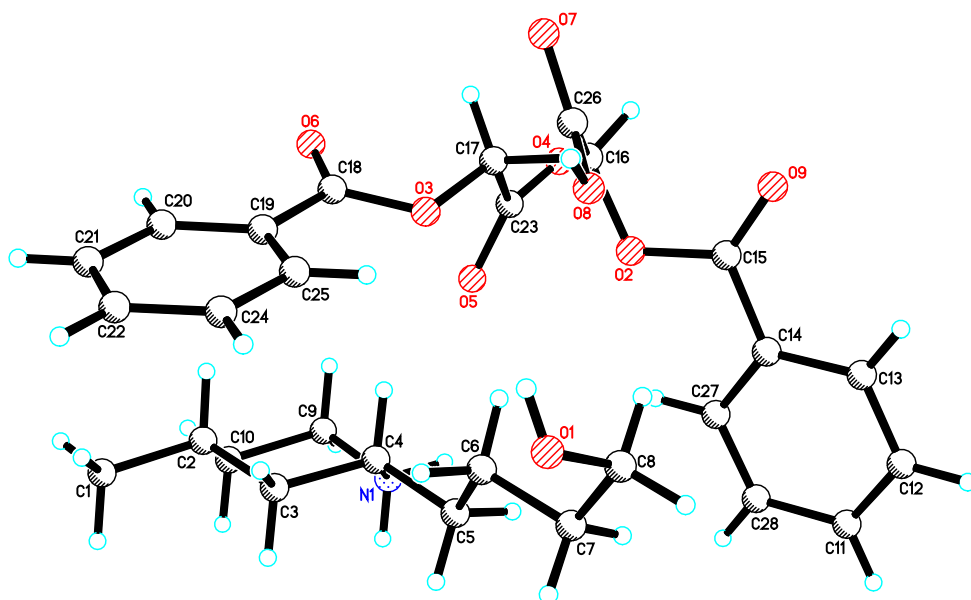


Table 2. Atomic coordinates ($\times 10^4$) and equivalent isotropic displacement parameters ($\text{\AA}^2 \times 10^3$) for sdr32. $U(\text{eq})$ is defined as one third of the trace of the orthogonalized U^{ij} tensor.

	x	y	z	$U(\text{eq})$
N(1)	6379(2)	3713(1)	3392(1)	18(1)
O(1)	6226(2)	-251(1)	1515(1)	30(1)
C(1)	6322(2)	2626(1)	3230(1)	16(1)
C(2)	5337(2)	2091(1)	3679(1)	20(1)
C(3)	5801(2)	2271(1)	4326(1)	24(1)
C(4)	5901(2)	3390(1)	4450(1)	22(1)
C(5)	6921(2)	3900(1)	4012(1)	23(1)
C(6)	5816(2)	2548(1)	2580(1)	18(1)
C(7)	6293(2)	1576(1)	2281(1)	20(1)
C(8)	5832(2)	1535(1)	1624(1)	19(1)
C(9)	6591(2)	708(1)	1282(1)	22(1)
C(10)	4754(3)	1763(2)	4761(1)	39(1)
O(2)	12185(1)	3412(1)	2906(1)	22(1)
O(3)	9835(1)	3310(1)	3195(1)	20(1)
O(4)	9850(1)	1277(1)	3116(1)	14(1)

O(5)	10584(2)	1400(1)	4070(1)	26(1)
O(6)	12260(1)	-57(1)	2415(1)	21(1)
O(7)	10196(1)	142(1)	1879(1)	20(1)
O(8)	10347(1)	2143(1)	1946(1)	15(1)
O(9)	11620(1)	1730(1)	1123(1)	22(1)
C(11)	11057(2)	2946(1)	3025(1)	15(1)
C(12)	11148(2)	1813(1)	2939(1)	14(1)
C(13)	11396(2)	1583(1)	2283(1)	15(1)
C(14)	11286(2)	454(1)	2183(1)	15(1)
C(15)	9773(2)	1047(1)	3705(1)	16(1)
C(16)	8585(2)	312(1)	3825(1)	16(1)
C(17)	7873(2)	-194(1)	3365(1)	18(1)
C(18)	6788(2)	-890(1)	3499(1)	22(1)
C(19)	6420(2)	-1081(1)	4088(1)	24(1)
C(20)	7139(2)	-587(2)	4546(1)	26(1)
C(21)	8222(2)	107(1)	4417(1)	21(1)
C(22)	10629(2)	2182(1)	1353(1)	16(1)
C(23)	9573(2)	2844(1)	1037(1)	17(1)
C(24)	8662(2)	3504(1)	1344(1)	19(1)
C(25)	7711(2)	4116(2)	1027(1)	26(1)
C(26)	7661(2)	4063(2)	410(1)	31(1)
C(27)	8572(3)	3410(2)	103(1)	32(1)
C(28)	9542(2)	2805(1)	415(1)	24(1)

Table 3. Bond lengths [\AA] and angles [$^\circ$] for sdr32.

N(1)-C(5)	1.495(2)
N(1)-C(1)	1.501(2)
O(1)-C(9)	1.425(2)
C(1)-C(2)	1.526(2)
C(1)-C(6)	1.531(2)
C(2)-C(3)	1.527(3)
C(3)-C(10)	1.522(3)
C(3)-C(4)	1.528(3)
C(4)-C(5)	1.513(3)
C(6)-C(7)	1.528(2)

C(7)-C(8)	1.532(2)
C(8)-C(9)	1.513(2)
O(2)-C(11)	1.230(2)
O(3)-C(11)	1.272(2)
O(4)-C(15)	1.3553(19)
O(4)-C(12)	1.437(2)
O(5)-C(15)	1.199(2)
O(6)-C(14)	1.234(2)
O(7)-C(14)	1.273(2)
O(8)-C(22)	1.3546(19)
O(8)-C(13)	1.4298(19)
O(9)-C(22)	1.201(2)
C(11)-C(12)	1.533(2)
C(12)-C(13)	1.518(2)
C(13)-C(14)	1.533(2)
C(15)-C(16)	1.486(2)
C(16)-C(17)	1.393(2)
C(16)-C(21)	1.395(2)
C(17)-C(18)	1.390(2)
C(18)-C(19)	1.384(3)
C(19)-C(20)	1.386(3)
C(20)-C(21)	1.384(3)
C(22)-C(23)	1.486(2)
C(23)-C(24)	1.393(2)
C(23)-C(28)	1.394(2)
C(24)-C(25)	1.388(3)
C(25)-C(26)	1.384(3)
C(26)-C(27)	1.387(3)
C(27)-C(28)	1.387(3)
C(5)-N(1)-C(1)	113.49(14)
N(1)-C(1)-C(2)	108.46(13)
N(1)-C(1)-C(6)	107.83(13)
C(2)-C(1)-C(6)	114.73(14)
C(1)-C(2)-C(3)	112.88(15)
C(10)-C(3)-C(2)	111.31(18)

C(10)-C(3)-C(4)	111.09(17)
C(2)-C(3)-C(4)	110.07(15)
C(5)-C(4)-C(3)	111.24(15)
N(1)-C(5)-C(4)	108.89(15)
C(7)-C(6)-C(1)	112.90(14)
C(6)-C(7)-C(8)	111.91(14)
C(9)-C(8)-C(7)	112.73(15)
O(1)-C(9)-C(8)	111.70(15)
C(15)-O(4)-C(12)	115.14(13)
C(22)-O(8)-C(13)	114.34(13)
O(2)-C(11)-O(3)	126.84(15)
O(2)-C(11)-C(12)	115.45(15)
O(3)-C(11)-C(12)	117.69(14)
O(4)-C(12)-C(13)	106.70(13)
O(4)-C(12)-C(11)	114.57(13)
C(13)-C(12)-C(11)	109.32(13)
O(8)-C(13)-C(12)	107.80(13)
O(8)-C(13)-C(14)	113.38(13)
C(12)-C(13)-C(14)	109.45(13)
O(6)-C(14)-O(7)	127.00(15)
O(6)-C(14)-C(13)	116.05(15)
O(7)-C(14)-C(13)	116.94(14)
O(5)-C(15)-O(4)	122.77(16)
O(5)-C(15)-C(16)	125.79(15)
O(4)-C(15)-C(16)	111.44(13)
C(17)-C(16)-C(21)	119.81(16)
C(17)-C(16)-C(15)	121.75(15)
C(21)-C(16)-C(15)	118.40(15)
C(18)-C(17)-C(16)	119.82(16)
C(19)-C(18)-C(17)	120.05(17)
C(18)-C(19)-C(20)	120.24(17)
C(21)-C(20)-C(19)	120.11(17)
C(20)-C(21)-C(16)	119.95(17)
O(9)-C(22)-O(8)	122.90(15)
O(9)-C(22)-C(23)	125.57(15)
O(8)-C(22)-C(23)	111.53(14)

C(24)-C(23)-C(28)	120.33(16)
C(24)-C(23)-C(22)	121.91(15)
C(28)-C(23)-C(22)	117.75(16)
C(25)-C(24)-C(23)	119.50(17)
C(26)-C(25)-C(24)	120.11(19)
C(25)-C(26)-C(27)	120.54(19)
C(26)-C(27)-C(28)	119.82(19)
C(27)-C(28)-C(23)	119.68(19)

Table 4. Anisotropic displacement parameters ($\text{\AA}^2 \times 10^3$) for sdr32. The anisotropic displacement factor exponent takes the form: $-2\pi^2[h^2 a^{*2}U^{11} + \dots + 2 h k a^* b^* U^{12}]$

	U^{11}	U^{22}	U^{33}	U^{23}	U^{13}	U^{12}
N(1)	21(1)	18(1)	16(1)	1(1)	2(1)	-3(1)
O(1)	26(1)	18(1)	45(1)	1(1)	-14(1)	1(1)
C(1)	15(1)	15(1)	17(1)	-1(1)	1(1)	0(1)
C(2)	20(1)	18(1)	22(1)	2(1)	4(1)	-1(1)
C(3)	25(1)	25(1)	20(1)	5(1)	5(1)	3(1)
C(4)	24(1)	27(1)	15(1)	-1(1)	3(1)	4(1)
C(5)	27(1)	24(1)	17(1)	-3(1)	0(1)	-3(1)
C(6)	17(1)	18(1)	18(1)	0(1)	-2(1)	0(1)
C(7)	22(1)	18(1)	19(1)	0(1)	-4(1)	2(1)
C(8)	21(1)	17(1)	19(1)	0(1)	-3(1)	0(1)
C(9)	23(1)	22(1)	22(1)	-3(1)	-1(1)	1(1)
C(10)	49(1)	37(1)	31(1)	9(1)	14(1)	-4(1)
O(2)	18(1)	16(1)	32(1)	-4(1)	2(1)	-3(1)
O(3)	19(1)	14(1)	26(1)	1(1)	5(1)	2(1)
O(4)	16(1)	14(1)	14(1)	1(1)	0(1)	-1(1)
O(5)	33(1)	29(1)	16(1)	-1(1)	-3(1)	-11(1)
O(6)	25(1)	16(1)	21(1)	-2(1)	-2(1)	7(1)
O(7)	22(1)	11(1)	26(1)	0(1)	-3(1)	-2(1)
O(8)	18(1)	13(1)	13(1)	2(1)	1(1)	1(1)
O(9)	24(1)	24(1)	18(1)	1(1)	4(1)	3(1)
C(11)	18(1)	15(1)	13(1)	0(1)	-1(1)	0(1)
C(12)	13(1)	14(1)	16(1)	0(1)	-1(1)	0(1)

C(13)	13(1)	15(1)	16(1)	0(1)	1(1)	1(1)
C(14)	18(1)	14(1)	14(1)	0(1)	5(1)	1(1)
C(15)	21(1)	13(1)	14(1)	0(1)	1(1)	3(1)
C(16)	17(1)	13(1)	17(1)	1(1)	0(1)	3(1)
C(17)	21(1)	17(1)	15(1)	1(1)	-1(1)	1(1)
C(18)	23(1)	21(1)	24(1)	-2(1)	-4(1)	-2(1)
C(19)	21(1)	21(1)	30(1)	5(1)	3(1)	-5(1)
C(20)	31(1)	29(1)	20(1)	6(1)	4(1)	-4(1)
C(21)	26(1)	21(1)	16(1)	1(1)	-1(1)	-2(1)
C(22)	19(1)	14(1)	15(1)	0(1)	0(1)	-4(1)
C(23)	18(1)	15(1)	18(1)	2(1)	-2(1)	-4(1)
C(24)	20(1)	18(1)	20(1)	2(1)	0(1)	-2(1)
C(25)	21(1)	22(1)	35(1)	4(1)	-2(1)	2(1)
C(26)	26(1)	31(1)	35(1)	11(1)	-12(1)	-1(1)
C(27)	37(1)	37(1)	21(1)	4(1)	-10(1)	-2(1)
C(28)	30(1)	25(1)	18(1)	-2(1)	-4(1)	-3(1)

Table 5. Hydrogen coordinates ($\times 10^4$) and isotropic displacement parameters ($\text{\AA}^2 \times 10^3$) for sdr32.

	x	y	z	U(eq)
H(1)	5410(30)	3973(16)	3362(9)	20(5)
H(2)	6930(30)	4000(18)	3134(11)	30(6)
H(1B)	6860(30)	-490(20)	1695(12)	38(7)
H(1A)	7350(20)	2393(14)	3273(8)	12(4)
H(2A)	5400(30)	1368(19)	3594(11)	31(6)
H(2B)	4350(30)	2317(16)	3624(9)	21(5)
H(3A)	6850(20)	2006(16)	4372(9)	21(5)
H(4A)	4900(30)	3688(17)	4414(10)	27(6)
H(4B)	6210(30)	3528(17)	4836(11)	27(6)
H(5A)	6930(30)	4635(18)	4056(10)	28(6)
H(5B)	7920(30)	3619(16)	4039(9)	20(5)
H(6A)	4740(30)	2638(17)	2573(10)	23(5)
H(6B)	6260(30)	3139(17)	2343(10)	25(5)
H(7A)	5880(20)	999(18)	2497(10)	25(6)

H(7B)	7380(30)	1530(18)	2308(11)	31(6)
H(8A)	4750(30)	1448(17)	1591(10)	27(6)
H(8B)	6040(20)	2169(16)	1425(9)	17(5)
H(9A)	6270(30)	737(17)	864(11)	28(6)
H(9B)	7690(30)	808(17)	1291(9)	24(5)
H(10A)	5070(40)	1900(20)	5188(15)	65(9)
H(10B)	4760(30)	1080(20)	4688(11)	31(6)
H(10C)	3760(30)	2050(19)	4694(11)	38(7)
H(7)	10175	-485	1887	24
H(12A)	11990(20)	1568(15)	3161(9)	14(5)
H(13A)	12360(20)	1784(15)	2177(9)	13(5)
H(17A)	8100(20)	-73(16)	2953(10)	24(6)
H(18A)	6260(30)	-1256(18)	3178(11)	33(6)
H(19A)	5720(30)	-1548(18)	4174(11)	28(6)
H(20A)	6880(30)	-733(19)	4947(12)	37(7)
H(21A)	8720(30)	448(17)	4727(11)	28(6)
H(24A)	8740(30)	3573(19)	1757(12)	35(6)
H(25A)	7150(30)	4542(19)	1234(11)	32(6)
H(26A)	7040(30)	4491(19)	201(11)	36(7)
H(27A)	8510(30)	3370(20)	-334(13)	44(7)
H(28A)	10200(30)	2340(18)	215(10)	31(6)

Table 6. Torsion angles [°] for sdr32.

C(5)-N(1)-C(1)-C(2)	57.59(19)
C(5)-N(1)-C(1)-C(6)	-177.61(14)
N(1)-C(1)-C(2)-C(3)	-53.95(19)
C(6)-C(1)-C(2)-C(3)	-174.55(15)
C(1)-C(2)-C(3)-C(10)	177.55(17)
C(1)-C(2)-C(3)-C(4)	53.9(2)
C(10)-C(3)-C(4)-C(5)	-179.09(18)
C(2)-C(3)-C(4)-C(5)	-55.3(2)
C(1)-N(1)-C(5)-C(4)	-60.1(2)
C(3)-C(4)-C(5)-N(1)	57.8(2)
N(1)-C(1)-C(6)-C(7)	156.44(15)
C(2)-C(1)-C(6)-C(7)	-82.61(19)
C(1)-C(6)-C(7)-C(8)	-177.53(14)

C(6)-C(7)-C(8)-C(9)	166.35(15)
C(7)-C(8)-C(9)-O(1)	62.3(2)
C(15)-O(4)-C(12)-C(13)	154.16(13)
C(15)-O(4)-C(12)-C(11)	-84.72(16)
O(2)-C(11)-C(12)-O(4)	176.25(14)
O(3)-C(11)-C(12)-O(4)	-5.4(2)
O(2)-C(11)-C(12)-C(13)	-64.08(19)
O(3)-C(11)-C(12)-C(13)	114.24(16)
C(22)-O(8)-C(13)-C(12)	166.60(13)
C(22)-O(8)-C(13)-C(14)	-72.09(17)
O(4)-C(12)-C(13)-O(8)	75.51(15)
C(11)-C(12)-C(13)-O(8)	-48.90(17)
O(4)-C(12)-C(13)-C(14)	-48.23(17)
C(11)-C(12)-C(13)-C(14)	-172.64(14)
O(8)-C(13)-C(14)-O(6)	172.86(13)
C(12)-C(13)-C(14)-O(6)	-66.75(19)
O(8)-C(13)-C(14)-O(7)	-8.2(2)
C(12)-C(13)-C(14)-O(7)	112.19(16)
C(12)-O(4)-C(15)-O(5)	12.1(2)
C(12)-O(4)-C(15)-C(16)	-167.46(13)
O(5)-C(15)-C(16)-C(17)	-168.17(17)
O(4)-C(15)-C(16)-C(17)	11.3(2)
O(5)-C(15)-C(16)-C(21)	9.6(3)
O(4)-C(15)-C(16)-C(21)	-170.89(14)
C(21)-C(16)-C(17)-C(18)	1.0(2)
C(15)-C(16)-C(17)-C(18)	178.72(16)
C(16)-C(17)-C(18)-C(19)	-0.2(3)
C(17)-C(18)-C(19)-C(20)	-0.5(3)
C(18)-C(19)-C(20)-C(21)	0.4(3)
C(19)-C(20)-C(21)-C(16)	0.4(3)
C(17)-C(16)-C(21)-C(20)	-1.1(3)
C(15)-C(16)-C(21)-C(20)	-178.89(17)
C(13)-O(8)-C(22)-O(9)	4.7(2)
C(13)-O(8)-C(22)-C(23)	-175.14(13)
O(9)-C(22)-C(23)-C(24)	-165.93(17)
O(8)-C(22)-C(23)-C(24)	13.9(2)

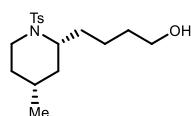
O(9)-C(22)-C(23)-C(28)	12.5(3)
O(8)-C(22)-C(23)-C(28)	-167.62(15)
C(28)-C(23)-C(24)-C(25)	0.6(3)
C(22)-C(23)-C(24)-C(25)	179.04(16)
C(23)-C(24)-C(25)-C(26)	0.6(3)
C(24)-C(25)-C(26)-C(27)	-0.9(3)
C(25)-C(26)-C(27)-C(28)	-0.1(3)
C(26)-C(27)-C(28)-C(23)	1.3(3)
C(24)-C(23)-C(28)-C(27)	-1.6(3)
C(22)-C(23)-C(28)-C(27)	179.94(17)

Table 7. Hydrogen bonds for sdr32 [\AA and $^\circ$].

D-H...A	d(D-H)	d(H...A)	d(D...A)	\angle (DHA)
N(1)-H(1)...O(1)#1	0.95(2)	1.84(2)	2.754(2)	161.6(19)
N(1)-H(2)...O(6)#2	0.86(3)	1.91(3)	2.7409(19)	163(2)
O(1)-H(1B)...O(2)#3	0.77(3)	1.93(3)	2.6416(19)	154(3)
O(7)-H(7)...O(2)#3	0.84	2.65	3.2085(17)	125.5
O(7)-H(7)...O(3)#3	0.84	1.62	2.4598(17)	172.1

Symmetry transformations used to generate equivalent atoms:

#1 $-x+1, y+1/2, -z+1/2$ #2 $-x+2, y+1/2, -z+1/2$ #3 $-x+2, y-1/2, -z+1/2$



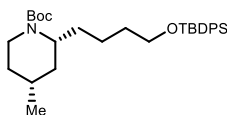
4-(4-methyl-1-tosylpiperidin-2-yl)butan-1-ol ((\pm)-4-156): To a flame-dried flask containing amine **4-71** (100 mg, 0.584 mmol) dissolved in CH_2Cl_2 (1.95 mL) was added TsCl (122 mg, 0.642 mmol) and Et_3N (98.0 μL , 0.701 mmol). The reaction mixture was stirred for 1 h before water (3 mL) was added and the mixture was extracted with CH_2Cl_2 (2 x 3 mL). The organic layer was

dried over sodium sulfate, filtered, concentrated, and purified by flash column chromatography (EtOAc/Hex) on silica to yield **4-156** as a white solid (91.0 mg, 48%).

TLC R_f = 0.14 (silica gel, 30:70 EtOAc:Hex)

^1H NMR (500 MHz, CDCl_3) δ 7.68 (d, J = 8.1 Hz, 2H), 7.25 (d, J = 8.0 Hz, 3H), 3.58 (t, J = 6.5 Hz, 3H), 3.52 – 3.45 (m, 2H), 3.40 (ddd, J = 14.0, 8.9, 5.1 Hz, 1H), 3.30 (dt, J = 14.1, 5.6 Hz, 2H), 2.39 (s, 3H), 1.82 (s, 2H), 1.76 – 1.67 (m, 1H), 1.67 – 1.56 (m, 3H), 1.51 (p, J = 6.9 Hz, 2H), 1.45 – 1.26 (m, 3H), 1.15 – 1.02 (m, 2H), 0.86 (d, J = 7.0 Hz, 3H).

^{13}C NMR (125 MHz, CDCl_3) δ 143.0, 138.1, 129.6, 127.2, 62.6, 56.2, 41.4, 36.0, 34.8, 32.6, 31.1, 26.8, 22.2, 21.6, 21.3.



tert-Butyl (2R,4R)-2-(4-((tert-butyldiphenylsilyl)oxy)butyl)-4-methylpiperidine-1-carboxylate (4-72): To an Erlenmeyer flask containing tartrate salt **4-113** was added aqueous 2 M NaOH (1 L), CH_2Cl_2 (1 L), Et_3N (7.94 mL, 57.0 mmol), and Boc_2O (6.21 g, 28.5 mmol). The biphasic mixture was allowed to stir overnight. The phases were partitioned and the aqueous phase extracted with CH_2Cl_2 (3 x 300 mL), dried over Na_2SO_4 , filtered and concentrated. The crude mixture was taken up in dry CH_2Cl_2 (142 mL) and charged with imidazole (2.71 g, 39.9 mmol), DMAP (35.0 mg, 0.285 mmol), and TBDPSCl (8.15 mL, 31.3 mmol) before stirring at room temperature for 16 h. The reaction was quenched with water (200 mL), extracted with CH_2Cl_2 (3 x 200 mL), dried over Na_2SO_4 , filtered, and concentrated. The crude residue was purified by flash column chromatography (EtOAc/Hex) on silica to yield **4-72** as a clear oil (12.9 g, 89% over 2 steps).

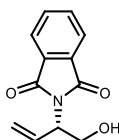
TLC R_f = 0.42 (silica gel, 10:90 EtOAc:Hex)

Optical Rotation $[\alpha]_D^{22} = -29.8$ ($c = 1.98$, CHCl_3)

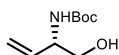
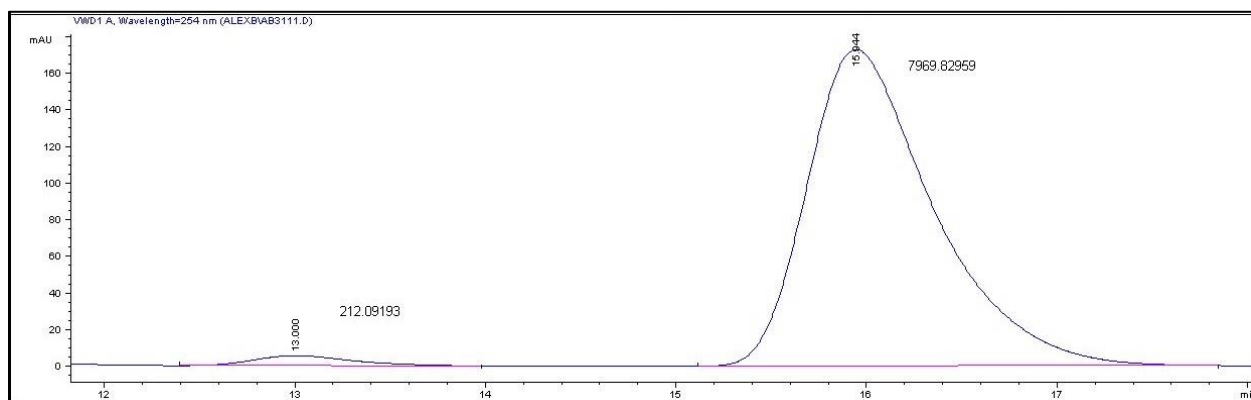
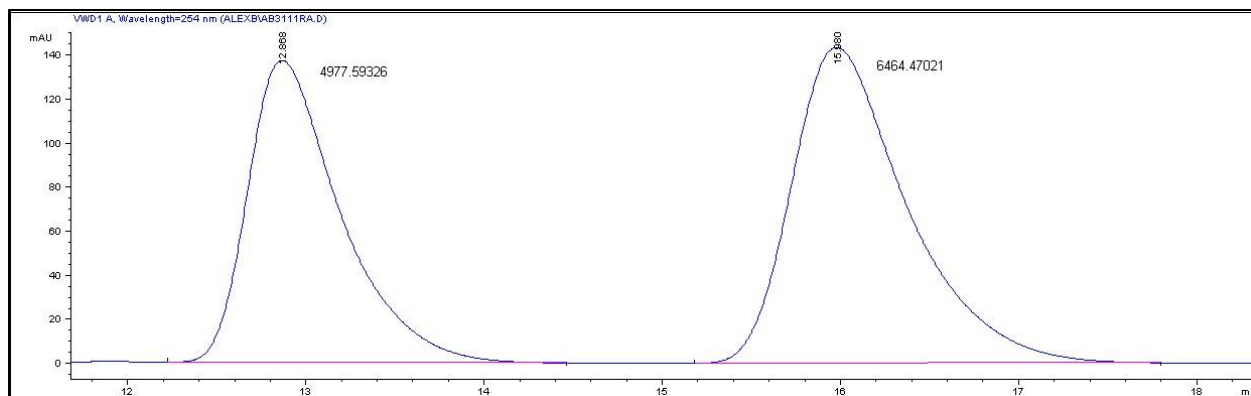
^1H NMR (600 MHz, CDCl_3) δ 7.69 – 7.64 (m, 4H), 7.44 – 7.35 (m, 6H), 3.81 (p, $J = 7.1$ Hz, 1H), 3.70 (ddd, $J = 13.5, 7.1, 3.1$ Hz, 1H), 3.65 (tt, $J = 5.7, 2.8$ Hz, 2H), 2.98 (ddd, $J = 13.8, 10.2, 6.0$ Hz, 1H), 1.87 (ddt, $J = 13.6, 10.0, 7.0$ Hz, 1H), 1.72 (ddd, $J = 13.4, 6.8, 4.0$ Hz, 1H), 1.67 – 1.50 (m, 5H), 1.44 (s, 9H), 1.40 – 1.24 (m, 3H), 1.12 – 1.07 (m, 1H), 1.05 (s, 9H), 0.97 (d, $J = 6.7$ Hz, 3H).

^{13}C NMR (150 MHz, CDCl_3) δ 155.7, 135.7, 134.3, 129.6, 127.7, 79.0, 64.0, 53.4, 37.4, 35.8, 34.5, 32.7, 31.5, 28.7, 27.0, 26.4, 22.7, 21.7, 19.4.

HRMS (ESI-TOF) m/z calcd for $\text{C}_{31}\text{H}_{47}\text{NO}_3\text{SiNa}$ ($\text{M} + \text{Na}$) $^+$: 532.3223, found 532.3201.

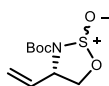


(S)-2-(1-hydroxybut-3-en-2-yl)isoindoline-1,3-dione (4-120): A flame-dried flask was charged with phthalimide (2.94 g, 20.0 mmol), Na_2CO_3 (106 mg, 1.00 mmol), $\text{Pd}_2(\text{allyl})_2\text{Cl}_2$ (29.2 mg, 0.0800 mmol), (*S,S*)-DACH-naphthyl Trost Ligand (190 mg, 0.240 mmol) and CH_2Cl_2 (160 mL). The reaction mixture was purged with argon for 15 min before butadiene monoxide **4-119** (1.62 mL, 20.0 mmol) was added. The mixture was allowed to stir for 72 h before concentrating, filtering through a plug of silica with EtOAc (200 mL), and concentrating again to afford **4-120** (4.22 g, 97%, 95% *ee*) as a white solid. Spectral data were consistent with those previously reported for this compound.²³

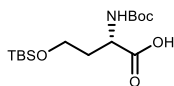


***tert*-butyl (S)-(1-hydroxybut-3-en-2-yl)carbamate (4-121):** A flame-dried flask containing phthalimide **4-120** (3.98 g, 18.3 mmol) dissolved in *i*PrOH (42.0 mL) at 0 °C was charged with hydrazine hydrate (1.07 mL, 22.0 mmol). The reaction mixture immediately turned into a white gel. After 10 min of stirring, 6 M HCl (80.0 mL) was added and the mixture dissolved to a clear solution. The flask was heated to 80 °C for 1 h and then cooled to 0 °C for 10 min before filtering off the white solid that formed. The reaction mixture was neutralized by the addition of solid NaHCO₃. Once neutral by pH paper, THF (64.0 mL) and Boc₂O (8.00 g, 36.6 mmol) were added and the mixture was stirred for 48 h. Water (100 mL) was added, extracted with EtOAc (3 x 100 mL), dried with sodium sulfate, filtered, concentrated, and purified by flash column

chromatography (EtOAc/Hex) on silica to yield **4-121** as a clear oil (2.85 g, 83%). Spectral data were consistent with those previously reported for this compound.²⁸

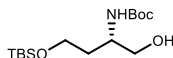


***tert*-Butyl (4*S*)-4-vinyl-1,2,3-oxathiazolidine-3-carboxylate 2-oxide (4-122):** A flame-dried flask was charged with imidazole (233 mg, 3.42 mmol), Et₃N (0.260 mL, 1.84 mmol), CH₂Cl₂ (7.60 mL) and cooled to -50 °C. Thionyl chloride (70.0 μL, 0.957 mmol) was added dropwise followed by the dropwise addition of alcohol **4-121** (160 mg, 0.855 mmol) in CH₂Cl₂ (1.00 mL) over 20 min. The reaction mixture was allowed to stir from -50 °C to 0 °C overnight. Water (20 mL) was added, the layers separated, the organic layer was washed with brine (20 mL), dried over sodium sulfate, filtered, and concentrated. The crude mixture was used without further purification.

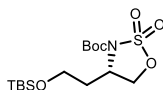


***N*-(*tert*-Butoxycarbonyl)-*O*-(*tert*-butyldimethylsilyl)-*L*-homoserine (4-136):** A flame-dried flask was charged with *L*-homoserine (4.96 g, 41.6 mmol), DBU (6.54 mL, 43.7 mmol), and MeCN (99.0 mL) and cooled to 0 °C. TBSCl (6.59 g, 43.7 mmol) was added and the mixture was allowed to stir for 16 h. The resulting white solid was filtered, washed with cold MeCN (250 mL) then cold Et₂O (200 mL), and dried by high vacuum. The crude residue was dissolved in water (100 mL) and acetone (100 mL) and Boc₂O (10.9 g, 50.0 mmol) and Et₃N (8.71 mL, 62.5 mmol) were added. The reaction mixture was allowed to stir for 18 h before it was acidified to pH 2 with an aqueous 10% citric acid solution. The mixture was extracted with EtOAc (3 x 200 mL), dried over sodium sulfate, filtered, and concentrated to afford **4-136** (12.5 g, 90%) as a clear oil. The crude mixture

was used without further purification. Spectral data were consistent with those previously reported for this compound.²⁹



tert-Butyl (S)-4-((tert-butyldimethylsilyloxy)-1-hydroxybutan-2-yl)carbamate (4-137): A flask containing carboxylic acid **4-136** (13.1 g, 39.3 mmol) dissolved in THF (131 mL) was charged with CDI (8.47 g, 52.2 mmol) and allowed to stir for 10 min. The resulting yellow solution was cooled to 0 °C before NaBH₄ (2.97 g, 78.6 mmol) in H₂O (98.0 mL) was added. After stirring for 30 min. saturated aqueous NaHCO₃ (25 mL) was added, the mixture extracted with EtOAc (3 x 200 mL), dried over sodium sulfate, and concentrated to afford **4-137** (8.24 g, 66%) as a yellow oil. The crude mixture was used without further purification. Spectral data were consistent with those previously reported for this compound.³⁰



tert-Butyl (S)-4-(2-((tert-butyldimethylsilyloxy)ethyl)-1,2,3-oxathiazolidine-3-carboxylate 2,2-dioxide (4-138): *Note: the amount of RuCl₃ used was 20x more than what should be used.* A flame-dried flask was charged with imidazole (4.26 g, 62.6 mmol), Et₃N (4.69 mL, 33.6 mmol), CH₂Cl₂ (150 mL) and cooled to -50 °C. Thionyl chloride (1.28 mL, 17.5 mmol) was added dropwise followed by the dropwise addition of alcohol **4-137** (5.00 g, 15.6 mmol) in CH₂Cl₂ (6.00 mL) over 20 min. The reaction mixture was allowed to stir from -50 °C to 0 °C overnight. Water (20 mL) was added, the layers separated, the organic layer was washed with brine (20 mL), dried over sodium sulfate, filtered, and concentrated. The crude mixture was dissolved in MeCN (126 mL) and cooled to 0 °C. Sodium periodate (3.58 g, 16.7 mmol), RuCl₃ (65.0 mg, 0.313 mmol), and water (98.0 mL) were added and the reaction mixture was allowed to stir for 2 h before additional

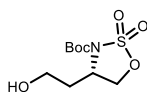
water (150 mL) was added. The mixture was extracted with Et₂O (3 x 100 mL), dried over magnesium sulfate, filtered, and concentrated. The resulting oil was filtered through a pad of silica with Et₂O (400 mL) and concentrated to afford sulfamidate **4-138** (5.16 g, 86%) as a yellow oil. The crude mixture was used without further purification.

TLC R_f = 0.52 (silica gel, 25:75 EtOAc:Hex)

¹H NMR (500 MHz, CDCl₃) δ 4.69 – 4.61 (m, 2H), 4.42 – 4.34 (m, 1H), 3.83 – 3.77 (m, 1H), 3.72 (ddd, *J* = 10.8, 8.5, 3.8 Hz, 1H), 2.18 – 2.09 (m, 1H), 2.06 – 1.98 (m, 1H), 1.54 (s, 9H), 0.88 (s, 9H), 0.07 – 0.02 (m, 6H).

¹³C NMR (125 MHz, CDCl₃) δ 148.8, 85.5, 70.6, 60.1, 57.4, 34.4, 28.1, 26.0, 18.3, -5.4.

HRMS (ESI-TOF) *m/z* calcd for C₁₅H₃₁NO₆SSiNa (M + Na)⁺ : 404.1539, found 404.1535.



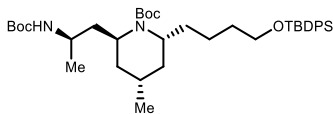
tert-Butyl (S)-4-(2-hydroxyethyl)-1,2,3-oxathiazolidine-3-carboxylate 2,2-dioxide (4-139):

Silyl ether **4-138** (70.0 mg, 0.184 mmol) was dissolved in MeCN (1.00 mL) before a 95:5:5 MeCN:HF:H₂O solution (0.60 mL) was added. After 20 min, saturated aqueous NaHCO₃ (4 mL) was added, the mixture was extracted with EtOAc (3 x 4 mL), dried with magnesium sulfate, filtered, and concentrated to afford alcohol **4-139** (42.0 mg, 86%) as a clear oil. The crude mixture was used without further purification.

TLC R_f = 0.33 (silica gel, 60:40 EtOAc:Hex)

¹H NMR (500 MHz, CDCl₃) δ 4.72 (dd, *J* = 9.2, 5.8 Hz, 1H), 4.51 (qd, *J* = 6.7, 1.8 Hz, 1H), 4.47 (dd, *J* = 9.2, 1.9 Hz, 1H), 3.78 (dt, *J* = 11.8, 4.8 Hz, 1H), 3.69 (ddd, *J* = 12.0, 9.2, 3.5 Hz, 1H), 2.74 (s, 1H), 2.09 (dddd, *J* = 14.2, 7.0, 4.9, 3.6 Hz, 1H), 2.02 – 1.96 (m, 1H), 1.54 (s, 9H).

¹³C NMR (125 MHz, CDCl₃) δ 149.6, 86.1, 70.9, 58.5, 55.7, 35.3, 27.9.



***tert*-Butyl (2*S*,4*S*,6*R*)-2-((*R*)-2-((*tert*-butoxycarbonyl)amino)propyl)-6-(4-((*tert*-butyldiphenylsilyl)oxy)butyl)-4-methylpiperidine-1-carboxylate (4-118):**

The CuCN·2LiCl solution was prepared as follows: CuCN (37.9 mg, 0.418 mmol) and LiCl (35.5 mg, 0.837 mmol) were flame-dried under vacuum, then dissolved using THF (0.840 mL), and stirred vigorously at room temperature until homogenous.

Piperidine **4-72** (248 mg, 0.487 mmol) was dissolved in dry Et₂O (2.00 mL), to which freshly distilled TMEDA (0.100 mL, 0.633 mmol) was added in one portion at room temperature. The Schlenk flask was submerged up to the neck in a vacuum-Dewar, and cooled to -78°C , at which point *sec*-BuLi (1.20 M, 0.530 mL, 0.633 mmol) was added dropwise, and the reaction was allowed to stir at -78°C for 7 h, during which time the solution turned a pale-yellow color. After 7 h, the room-temperature solution of CuCN·2LiCl (0.5 M in THF, 0.580 mL, 0.290 mmol) was added via syringe (equipped with a 12-gauge needle) as rapidly as possible in one portion, and allowed to stir for 1 h, at which point sulfamidate **4-116** (173 mg, 0.730 mmol) in THF (4.42 mL) was added dropwise. The dry ice bath was filled as full as possible with dry ice and acetone, covered with aluminum foil, and then allowed to stir overnight. The next morning (10-12 hours), the temperature of the acetone bath was typically observed to be between -20°C and 0°C . The reaction was quenched by the addition of 6 M HCl (0.243 mL, 1.46 mmol). The reaction mixture was allowed to stir for 2 h before it was basified with 3 M NaOH (1 mL). The solution was then diluted with H₂O (5 mL), the layers separated, and the aqueous layer was extracted with Et₂O (3 x 200 mL). The combined organic layers were dried with MgSO₄, filtered, concentrated, and purified

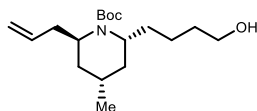
by flash column chromatography (EtOAc/Hex) on silica to yield a single diastereomer of **4-118** (21.0 mg, 7%) as a clear oil.

TLC R_f = 0.31 (silica gel, 10:90 EtOAc:Hex)

^1H NMR (600 MHz, CDCl_3) δ 7.66 (d, J = 7.1 Hz, 4H), 7.44 – 7.32 (m, 6H), 4.69 (s, 1H), 3.99 (s, 1H), 3.66 (t, J = 6.5 Hz, 2H), 3.62 (s, 1H), 3.46 (s, 1H), 1.86 – 1.69 (m, 5H), 1.64 – 1.50 (m, 4H), 1.45 (s, 9H), 1.43 (s, 9H), 1.38 – 1.31 (m, 2H), 1.29 – 1.21 (m, 2H), 1.14 (d, J = 6.4 Hz, 3H), 1.04 (s, 9H), 0.95 (d, J = 6.6 Hz, 3H).

^{13}C NMR (150 MHz, CDCl_3) δ 155.7, 155.6, 135.7, 134.3, 129.6, 127.7, 79.4, 78.9, 64.1, 53.1, 49.9, 44.5, 39.4, 35.6, 34.2, 32.8, 28.7, 28.6, 27.0, 24.0, 23.5, 23.4, 23.3, 22.0, 19.4.

HRMS (ESI-TOF) m/z calcd for $\text{C}_{39}\text{H}_{62}\text{N}_2\text{O}_5\text{SiNa}$ ($\text{M} + \text{Na}$) $^+$: 689.4326, found 689.4327.



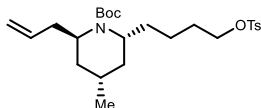
(±)-*tert*-Butyl (2*R*,4*S*,6*R*)-2-allyl-6-(4-hydroxybutyl)-4-methylpiperidine-1-carboxylate (**4-140**): Piperidine **4-66** (205 mg, 0.820 mmol) was dissolved in a 1 M TBAF solution (1.23 mL, 1.23 mmol) and allowed to stir at room temperature for 48 h. Water (5 mL) was added and the mixture was extracted with EtOAc (3 x 6 mL), dried with sodium sulfate, filtered, and concentrated to afford **4-140** (107 mg, 92%) as a yellow oil, which was used without further purification.

TLC R_f = 0.29 (silica gel, 25:75 EtOAc:Hex)

^1H NMR (500 MHz, CDCl_3) δ 5.70 (ddt, J = 17.1, 10.2, 7.0 Hz, 1H), 5.05 – 4.94 (m, 2H), 3.95 (dtd, J = 9.1, 5.7, 3.3 Hz, 1H), 3.59 (tt, J = 6.8, 3.6 Hz, 2H), 3.42 (qd, J = 7.3, 4.1 Hz, 1H), 2.45 (dt, J = 13.6, 6.6 Hz, 1H), 2.34 (s, 1H), 2.16 (dt, J = 15.1, 8.2 Hz, 1H), 1.92 – 1.76 (m, 2H), 1.76 – 1.64 (m, 2H), 1.59 – 1.47 (m, 3H), 1.41 (s, 9H), 1.38 – 1.31 (m, 2H), 1.30 – 1.17 (m, 2H), 0.91 (d, J = 7.0 Hz, 3H).

^{13}C NMR (125 MHz, CDCl_3) δ 155.8, 136.0, 116.4, 79.3, 62.4, 52.9, 52.7, 37.0, 35.1, 34.9, 34.2, 32.4, 28.6, 24.1, 23.2, 23.0.

HRMS (ESI-TOF) m/z calcd for $\text{C}_{18}\text{H}_{33}\text{NO}_3\text{Na}$ ($\text{M} + \text{Na}$) $^+$: 334.2358, found 334.2355.



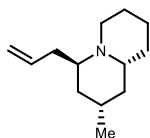
(±)-*tert*-Butyl (2*R*,4*S*,6*R*)-2-allyl-4-methyl-6-(4-(tosyloxy)butyl)piperidine-1-carboxylate (**4-141**): Alcohol **4-140** (100 mg, 0.321 mmol) was dissolved in CH_2Cl_2 (3.20 mL) before Et_3N (45.0 μL , 0.642 mmol), DMAP (4.00 mg, 0.0321 mmol), and TsCl (80.0 mg, 0.417 mmol) were added. After stirring for 12 h, another portion of DMAP (40.0 mg, 0.321 mmol) and TsCl (80.0 mg, 0.417 mmol) were added. After stirring for 15 min, the reaction was washed with an aqueous 10% citric acid solution (3 x 5 mL), dried with sodium sulfate, filtered, concentrated, and purified by flash column chromatography (EtOAc/Hex) on silica to yield **4-141** (130 mg, 87%) as a clear oil.

TLC R_f = 0.54 (silica gel, 25:75 $\text{EtOAc}:\text{Hex}$)

^1H NMR (600 MHz, CDCl_3) δ 7.76 (d, J = 8.3 Hz, 2H), 7.32 (d, J = 8.0 Hz, 2H), 5.71 (ddt, J = 17.1, 10.1, 7.0 Hz, 1H), 5.06 – 4.95 (m, 2H), 4.00 (t, J = 6.6 Hz, 2H), 3.97 – 3.90 (m, 1H), 3.37 (qd, J = 7.3, 4.2 Hz, 1H), 2.48 – 2.43 (m, 1H), 2.43 (s, 3H), 2.17 (dt, J = 13.7, 8.4 Hz, 1H), 1.86 – 1.74 (m, 2H), 1.73 – 1.66 (m, 2H), 1.66 – 1.60 (m, 2H), 1.47 – 1.43 (m, 1H), 1.41 (s, 9H), 1.34 – 1.21 (m, 3H), 1.17 (dt, J = 14.3, 7.3 Hz, 1H), 0.92 (d, J = 6.8 Hz, 3H).

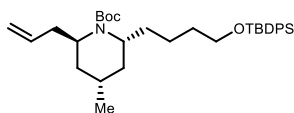
^{13}C NMR (150 MHz, CDCl_3) δ 155.8, 144.7, 136.0, 133.3, 129.9, 128.0, 116.5, 79.3, 70.7, 52.7, 52.6, 37.0, 34.9, 34.9, 34.1, 28.9, 28.6, 24.1, 23.2, 22.9, 21.7.

HRMS (ESI-TOF) m/z calcd for $\text{C}_{25}\text{H}_{39}\text{NO}_5\text{SNa}$ ($\text{M} + \text{Na}$) $^+$: 488.2447, found 488.2434.



(±)-(2*S*,4*R*,9*aR*)-4-Allyl-2-methyloctahydro-2*H*-quinolizine (**4-142**): A flask was charged with tosylate **4-141** (30.0 mg, 0.0644 mmol), CSA (224 mg, 0.966 mmol), and *o*-DCB (3.00 mL). The reaction mixture was heated to 165 °C while stirring before cooling to room temperature and adding Et₃N (90.0 μL, 0.644 mmol). The reaction mixture was stirred for 48 h before acidifying with 2 M HCl (2 mL) and extracting with Et₂O (3 x 4 mL). The aqueous phase was basified with 3 M NaOH (3 mL) and extracted with Et₂O (3 x 4 mL). The resulting organic phase was dried with magnesium sulfate, filtered, and concentrated to provide quinolizidine **4-142** (7.00 mg, 58%) as a volatile yellow oil.

¹H NMR (500 MHz, CDCl₃) δ 5.72 (dddd, *J* = 16.3, 9.9, 8.3, 6.1 Hz, 1H), 5.05 – 4.95 (m, 2H), 2.91 – 2.83 (m, 1H), 2.65 (d, *J* = 11.3 Hz, 1H), 2.51 (td, *J* = 11.5, 3.1 Hz, 1H), 2.48 – 2.39 (m, 1H), 2.34 – 2.26 (m, 1H), 2.16 (dt, *J* = 13.4, 9.3 Hz, 1H), 1.74 – 1.53 (m, 8H), 1.34 – 1.11 (m, 3H), 0.86 (d, *J* = 6.4 Hz, 3H).



tert-Butyl (2*R*,4*S*,6*R*)-2-allyl-6-(4-((*tert*-butyl)diphenylsilyl)oxy)butyl)-4-methylpiperidine-1-carboxylate (**4-66**): The CuCN·2LiCl solution was prepared as follows: CuCN (1.93 g, 21.5 mmol) and LiCl (1.82 g, 43.1 mmol) were flame-dried under vacuum, then dissolved using THF (44 mL), and stirred vigorously at room temperature until homogenous.

Piperidine **4-72** (12.8 g, 25.0 mmol) was dissolved in dry Et₂O (126 mL), to which freshly distilled TMEDA (4.84 mL, 32.5 mmol) was added in one portion at room temperature. The Schlenk flask was submerged up to the neck in a vacuum-Dewar, and cooled to –78°C, at which point *sec*-BuLi (1.4 M, 23.2 mL, 32.5 mmol) was added dropwise, and the reaction was allowed to stir at –78°C for 7 h, during which time the solution turned a pale-yellow color. After 7 h, the room-temperature

solution of CuCN·2LiCl (0.5 M in THF, 30.0 mL, 15.0 mmol) was added via syringe (equipped with a 12-gauge needle) as rapidly as possible in one portion, and allowed to stir for 1 h, at which point distilled neat allyl bromide (3.25 mL, 37.5 mmol) was added dropwise. The reaction immediately turned a bright yellow/orange after the first drop of allyl bromide was added, and then the color gradually faded away. The dry ice bath was filled as full as possible with dry ice and acetone, covered with aluminum foil, and then allowed to stir overnight. The next morning (-10-12 h), the temperature of the acetone bath was typically observed to be between -20 °C and 0 °C. The reaction vessel was transferred to a 0°C ice bath, where it was quenched by the addition of 50 mL aqueous NH₄OH (diluted 6:4 H₂O:NH₄OH), then warmed to room temperature and stirred for 1 h until the mixture turned a royal blue color. The solution was then diluted with H₂O (125 mL), the layers separated, and the aqueous layer was extracted with Et₂O (3 x 200 mL). The combined organic layers were dried with MgSO₄, filtered, concentrated, and purified by flash column chromatography (EtOAc/Hex) on silica to yield a single diastereomer of **4-66** (11.3 g, 82%) as a clear oil.

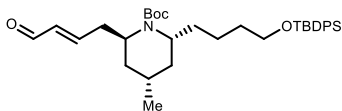
TLC R_f = 0.55 (silica gel, 10:90 EtOAc:Hex)

Optical Rotation [α]²²_D = -1.41 (c = 1.00, CHCl₃)

¹H NMR (600 MHz, CDCl₃) δ 7.70 – 7.66 (m, 4H), 7.44 – 7.35 (m, 6H), 5.77 (dddd, *J* = 16.6, 10.1, 7.7, 6.3 Hz, 1H), 5.06 (dd, *J* = 17.1, 1.8 Hz, 1H), 5.01 (dd, *J* = 10.2, 2.2 Hz, 1H), 4.02 – 3.95 (m, 1H), 3.67 (t, *J* = 6.4 Hz, 2H), 3.51 – 3.44 (m, 1H), 2.55 – 2.48 (m, 1H), 2.21 (dt, *J* = 13.8, 8.4 Hz, 1H), 1.90 – 1.70 (m, 4H), 1.58 (ddt, *J* = 22.2, 9.4, 6.6 Hz, 2H), 1.54 – 1.48 (m, 1H), 1.45 (s, 9H), 1.43 – 1.30 (m, 3H), 1.29 – 1.23 (m, 1H), 1.06 (s, 9H), 0.97 (d, *J* = 6.7 Hz, 3H).

¹³C NMR (150 MHz, CDCl₃) δ 155.8, 136.2, 135.7, 134.3, 129.6, 127.7, 116.4, 79.2, 64.1, 53.0, 52.5, 37.3, 35.5, 34.4, 33.9, 32.8, 28.7, 27.0, 23.9, 23.4, 23.4, 19.3.

HRMS (ESI-TOF) m/z calcd for $C_{34}H_{51}NO_3Na$ ($M + Na$)⁺ : 572.3536, found 572.3517.



tert-Butyl (2*R*,4*S*,6*S*)-2-(4-((*tert*-butyldiphenylsilyl)oxy)butyl)-4-methyl-6-((*E*)-4-oxobut-2-en-1-yl)piperidine-1-carboxylate (4-143): A flask containing alkene **4-66** (10.4 g, 18.9 mmol) dissolved in CH_2Cl_2 (62 mL) was charged with crotonaldehyde (15.6 mL, 189 mmol) and HGII (591 mg, 0.943 mmol). The resulting solution was stirred at room temperature for 18 h before being concentrated and purified by flash column chromatography (EtOAc/Hex) on silica to yield **4-143** (9.02 g, 83%) as a clear oil.

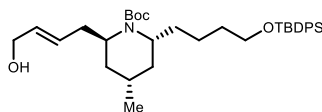
TLC R_f = 0.29 (silica gel, 15:85 EtOAc:Hex)

Optical Rotation $[\alpha]_D^{21} = -3.17$ ($c = 2.00$, $CHCl_3$)

¹H NMR (600 MHz, $CDCl_3$) δ 9.49 (d, $J = 7.8$ Hz, 1H), 7.67 (d, $J = 6.2$ Hz, 4H), 7.43 – 7.34 (m, 6H), 6.80 (dt, $J = 15.0, 7.2$ Hz, 1H), 6.14 (dd, $J = 15.6, 7.9$ Hz, 1H), 4.11 (tt, $J = 8.0, 4.2$ Hz, 1H), 3.67 (t, $J = 6.4$ Hz, 2H), 3.58 – 3.45 (m, 1H), 2.83 (dt, $J = 13.4, 6.8$ Hz, 1H), 2.49 (dt, $J = 14.8, 8.0$ Hz, 1H), 1.89 – 1.74 (m, 3H), 1.71 (ddd, $J = 13.9, 6.2, 3.7$ Hz, 1H), 1.65 – 1.47 (m, 4H), 1.44 (s, 9H), 1.41 – 1.33 (m, 2H), 1.29 (dt, $J = 13.4, 6.1$ Hz, 1H), 1.05 (s, 9H), 0.98 (d, $J = 6.5$ Hz, 3H).

¹³C NMR (150 MHz, $CDCl_3$) δ 193.9, 155.6, 135.6, 134.2, 134.2, 134.1, 129.6, 127.7, 79.7, 64.0, 53.1, 51.6, 36.5, 35.5, 34.4, 33.8, 32.6, 28.6, 27.0, 23.7, 23.3, 23.3, 19.3.

HRMS (ESI-TOF) m/z calcd for $C_{35}H_{51}NO_4SiNa$ ($M + Na$)⁺ : 600.3485, found 600.3485.



tert-Butyl (2*R*,4*S*,6*S*)-2-(4-((*tert*-butyldiphenylsilyl)oxy)butyl)-6-((*E*)-4-hydroxybut-2-en-1-yl)-4-methylpiperidine-1-carboxylate (4-144):

To a flask containing aldehyde **4-143** (8.41 g, 14.6 mmol) dissolved in MeOH (56 mL) was added NaBH₄ (1.09 g, 29.1 mmol) in one portion. After stirring for 30 min, the reaction was quenched by the addition of saturated aqueous NH₄Cl (150 mL) and the reaction mixture was allowed to stir for 1.5 h. The solution was then extracted with CH₂Cl₂ (3 x 100 mL). The combined organic layers were dried with Na₂SO₄, filtered, concentrated, and purified by flash column chromatography (EtOAc/Hex) on silica to yield **4-144** (8.35 g, 99%) as a clear oil.

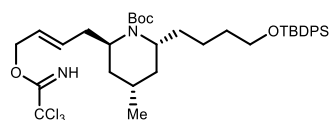
TLC R_f = 0.10 (silica gel, 15:85 EtOAc:Hex)

Optical Rotation [α]²³_D = -0.60 (c = 2.00, CHCl₃)

¹H NMR (600 MHz, CDCl₃) δ 7.69 – 7.64 (m, 4H), 7.44 – 7.35 (m, 6H), 5.66 (qt, *J* = 15.4, 6.0 Hz, 2H), 4.07 (d, *J* = 5.3 Hz, 2H), 4.00 – 3.91 (m, 1H), 3.66 (t, *J* = 6.4 Hz, 2H), 3.55 – 3.39 (m, 1H), 2.48 (dt, *J* = 12.9, 6.2 Hz, 1H), 2.25 – 2.17 (m, 1H), 1.89 – 1.75 (m, 3H), 1.72 (ddd, *J* = 13.8, 6.1, 3.3 Hz, 1H), 1.64 – 1.53 (m, 3H), 1.52 – 1.48 (m, 1H), 1.44 (s, 9H), 1.40 – 1.30 (m, 3H), 1.29 – 1.21 (m, 1H), 1.05 (s, 9H), 0.96 (d, *J* = 6.7 Hz, 3H).

¹³C NMR (150 MHz, CDCl₃) δ 155.8, 135.7, 134.2, 134.2, 131.1, 130.2, 129.6, 127.7, 79.3, 64.1, 63.7, 52.9, 52.6, 35.7, 35.5, 34.2, 33.9, 32.7, 28.7, 27.0, 23.8, 23.4, 19.3.

HRMS (ESI-TOF) *m/z* calcd for C₃₅H₅₃NO₄SiNa (M + Na)⁺ : 602.3641, found 602.3615.



***tert*-Butyl (2*R*,4*S*,6*S*)-2-(4-((*tert*-butyldiphenylsilyl)oxy)butyl)-4-methyl-6-((*E*)-4-(2,2,2-trichloro-1-iminoethoxy)but-2-en-1-yl)piperidine-1-carboxylate (**4-84**):**

Allylic alcohol **4-144** (9.15 g, 15.8 mmol) was dissolved in CH₂Cl₂ (96 mL) before DBU (0.47 mL, 3.16 mmol) was added and the solution cooled to 0 °C. Trichloroacetonitrile (2.37 mL, 23.7 mmol) was added dropwise before the solution was warmed to room temperature and stirred for 2

h. The solution was concentrated and purified by flash column chromatography (EtOAc/Hex) on silica to yield **4-84** (10.8 g, 95%) as a clear oil.

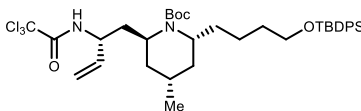
TLC R_f = 0.44 (silica gel, 15:85 EtOAc:Hex)

Optical Rotation $[\alpha]_D^{21} = -0.44$ ($c = 1.00$, CDCl_3)

$^1\text{H NMR}$ (600 MHz, CDCl_3) δ 8.27 (s, 1H), 7.69 – 7.64 (m, 4H), 7.44 – 7.34 (m, 6H), 5.77 (ddt, $J = 52.8, 15.3, 6.5$ Hz, 2H), 4.78 – 4.70 (m, 2H), 3.96 (d, $J = 5.1$ Hz, 1H), 3.66 (t, $J = 6.3$ Hz, 2H), 3.50 – 3.44 (m, 1H), 2.53 (dt, $J = 13.3, 6.2$ Hz, 1H), 2.24 (dt, $J = 15.2, 8.4$ Hz, 1H), 1.88 – 1.75 (m, 3H), 1.74 – 1.69 (m, 1H), 1.62 – 1.47 (m, 3H), 1.44 (s, 9H), 1.40 – 1.30 (m, 3H), 1.25 (dt, $J = 13.6, 6.6$ Hz, 1H), 1.05 (s, 9H), 0.96 (d, $J = 6.6$ Hz, 3H).

$^{13}\text{C NMR}$ (150 MHz, CDCl_3) δ 162.7, 155.7, 135.7, 134.3, 134.0, 129.6, 127.7, 125.1, 91.6, 79.3, 69.8, 64.1, 53.0, 52.4, 35.8, 35.6, 34.1, 33.8, 32.7, 28.7, 28.7, 27.0, 23.7, 23.4, 23.4, 19.4.

HRMS (ESI-TOF) m/z calcd for $\text{C}_{37}\text{H}_{53}\text{Cl}_3\text{N}_2\text{O}_4\text{SiNa}$ ($\text{M} + \text{Na}$) $^+$: 745.2738, found 745.2755.



tert-Butyl (2R,4S,6S)-2-(4-((tert-butylidiphenylsilyl)oxy)butyl)-4-methyl-6-((R)-2-(2,2,2-trichloroacetamido)but-3-en-1-yl)piperidine-1-carboxylate (4-85):

A flask was charged with trichloroimidate **4-84** (10.6 g, 14.6 mmol), (*R*)-(-)-COP-Cl (1.07 g, 0.732 mmol), and CH_2Cl_2 (29 mL) and stirred for 18 h at room temperature. The solution was concentrated and purified by flash column chromatography (EtOAc/Hex) on silica to yield **4-85** (8.97 g, 85%) as a clear oil in a 10:1 dr.

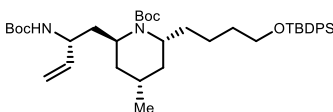
TLC R_f = 0.38 (silica gel, 15:85 EtOAc:Hex)

Optical Rotation $[\alpha]_D^{22} = -3.3$ ($c = 1.00$, CDCl_3)

¹H NMR (600 MHz, CDCl₃) δ 7.92 (d, *J* = 7.3 Hz, 1H), 7.67 (d, *J* = 6.1 Hz, 4H), 7.45 – 7.36 (m, 6H), 5.84 (ddd, *J* = 16.5, 10.4, 5.6 Hz, 1H), 5.29 (d, *J* = 17.1 Hz, 1H), 5.23 (d, *J* = 10.6 Hz, 1H), 4.43 (p, *J* = 6.0 Hz, 1H), 4.02 – 3.97 (m, 1H), 3.67 (t, *J* = 6.5 Hz, 2H), 3.53 – 3.45 (m, 1H), 2.04 (dt, *J* = 14.3, 5.8 Hz, 1H), 1.97 – 1.84 (m, 1H), 1.80 – 1.68 (m, 3H), 1.64 – 1.51 (m, 4H), 1.44 (s, 9H), 1.36 – 1.25 (m, 3H), 1.05 (s, 9H), 0.99 (d, *J* = 6.8 Hz, 3H).

¹³C NMR (150 MHz, CDCl₃) δ 161.6, 156.0, 135.7, 135.7, 134.2, 134.2, 129.6, 127.7, 116.5, 93.0, 80.0, 64.0, 53.4, 52.6, 49.1, 36.8, 35.6, 35.6, 33.7, 32.7, 28.6, 27.0, 23.7, 23.5, 23.2, 19.3.

HRMS (ESI-TOF) *m/z* calcd for C₃₇H₅₃Cl₃N₂O₄SiNa (M + Na)⁺ : 745.2738, found 745.2753.



tert-Butyl (2*S*,4*S*,6*R*)-2-((*R*)-2-((*tert*-butoxycarbonyl)amino)but-3-en-1-yl)-6-(4-((*tert*-butyl)di-phenylsilyl)oxy)butyl)-4-methylpiperidine-1-carboxylate (4-65): *LiAlH₄* procedure:

Trichloroacetamide **4-85** (3.31 g, 4.57 mmol) was dissolved in Et₂O (45 mL) and cooled to 0 °C. To this solution was added 4 M LiAlH₄ in Et₂O (3.40 mL, 13.7 mmol) and allowed to stir for 15 min before quenching with water (0.3 mL). After 5 min of stirring, 15% NaOH (0.3 mL) was added followed by more water (0.3 mL) and this mixture was allowed to stir for 15 min. Magnesium sulfate was then added and the mixture was allowed to stir for 15 min before it was filtered and concentrated. The resulting oil was dissolved in CH₂Cl₂ (26 mL) and Et₃N (1.27 mL, 9.14 mmol) and Boc₂O (1.20 g, 5.48 mmol) were added. After stirring for 18 h, the reaction was concentrated and purified by flash column chromatography (EtOAc/Hex) on silica to yield **4-65** (970 mg, 31%) as a clear oil.

Cs₂CO₃ procedure: A flask containing trichloroamide **4-85** (86.0 mg, 0.119 mmol), DMF (5.00 mL), and Cs₂CO₃ (155 mg, 0.475 mmol) was heated to 95 °C for 25 min. The mixture was cooled

to room temperature before Boc₂O (31.0 mg, 0.142 mmol) was added. After stirring for 2 h, EtOAc (5 mL) was added and the mixture was washed with water (4 x 5 mL). The organic layer was dried with sodium sulfate, filtered, concentrated, and purified by flash column chromatography (EtOAc/Hex) on silica to yield **4-65** (36.0 mg, 45%) as a clear oil.

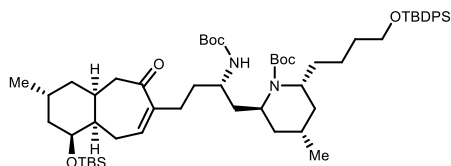
TLC R_f = 0.32 (silica gel, 15:85 EtOAc:Hex)

Optical Rotation [α]²²_D = -8.79 (c = 4.07, CHCl₃)

¹H NMR (500 MHz, CDCl₃) δ 7.73 (d, *J* = 7.3 Hz, 4H), 7.50 – 7.40 (m, 6H), 5.86 (ddd, *J* = 16.9, 10.5, 6.1 Hz, 1H), 5.25 (d, *J* = 17.2 Hz, 1H), 5.17 (d, *J* = 10.4 Hz, 1H), 4.97 (s, 1H), 4.14 (s, 1H), 4.11 – 4.01 (m, 1H), 3.73 (t, *J* = 6.5 Hz, 2H), 3.53 – 3.43 (m, 1H), 2.04 (dt, *J* = 13.8, 6.8 Hz, 1H), 1.93 – 1.83 (m, 2H), 1.82 – 1.72 (m, 3H), 1.71 – 1.59 (m, 4H), 1.51 (s, 9H), 1.49 (s, 9H), 1.39 – 1.31 (m, 2H), 1.25 (dt, *J* = 13.6, 8.0 Hz, 1H), 1.12 (s, 9H), 1.01 (d, *J* = 6.7 Hz, 3H).

¹³C NMR (125 MHz, CDCl₃) δ 155.8, 138.5, 135.6, 134.2, 129.5, 127.6, 115.0, 79.4, 64.0, 53.6, 51.4, 49.8, 37.1, 35.6, 35.1, 35.0, 32.7, 28.6, 28.5, 26.9, 24.9, 23.4, 22.9, 19.3.

HRMS (ESI-TOF) *m/z* calcd for C₄₀H₆₃N₂O₅Si (M + H)⁺ : 679.4506, found 679.4534.



tert-Butyl (2*S*,4*S*,6*R*)-2-((*S*)-2-((tert-butoxycarbonyl)amino)-4-((1*S*,3*R*,4*aS*,9*aR*)-1-((tert-butyl)dimethylsilyl)oxy)-3-methyl-6-oxo-2,3,4,4*a*,5,6,9,9*a*-octahydro-1*H*-benzo[7]annulen-7-yl)butyl)-6-(4-((tert-butyl)diphenylsilyl)oxy)butyl)-4-methylpiperidine-1-carboxylate (**4-146**):

Note: all solvents were freeze, pump, thawed for 5 cycles. To a solution of allylcarbamate **4-65** (210 mg, 0.309 mmol) in THF (0.40 mL) was added a solution of 9-BBN (0.50 M in THF, 0.88 mL, 0.440 mmol) at room temperature. After stirring for 4 h, the solution was treated with water (40.0 μL, 2.22 mmol) and stirred for 20 min. In a separate Schlenk flask was added bromoenone

4-145 (67.0 mg, 0.173 mmol), Cs₂CO₃ (124 mg, 0.380 mmol), AsPh₃ (26.0 mg, 0.0865 mmol), and Pd(dppf)Cl₂ (71.0 mg, 0.0865 mmol), and the atmosphere purged via high-vacuum/argon cycles (4x) before the addition of DMF (1.10 mL). The resulting mixture was then stirred for 15 min before the borane solution was added in one portion. The reaction was heat to 80 °C, at which point the mixture turned black. After heating for 6 h, the mixture was cooled to room temperature, diluted with Et₂O (5 mL), and filtered through a plug of Celite. Concentration *in vacuo* followed by purification via flash column chromatography (EtOAc/hexanes) on silica to afford enone **4-146** (220 mg, 69% (by NMR with internal standard)) as an inseparable mixture of product and allylcarbamate **4-65**. An analytically pure sample was obtained by concentrating a single fraction from flash column chromatography for characterization.

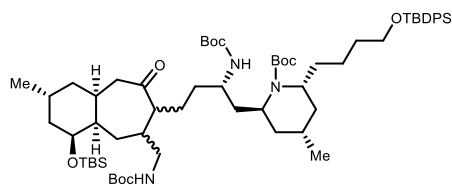
TLC R_f = 0.32 (silica gel, 15:85 EtOAc:Hex)

Optical Rotation [α]_D²¹ = +5.6 (c = 3.0, CHCl₃)

¹H NMR (600 MHz, CDCl₃) δ 7.69 – 7.63 (m, 4H), 7.43 – 7.35 (m, 6H), 6.43 (dd, *J* = 9.2, 4.6 Hz, 1H), 4.67 (s, 1H), 3.99 (s, 1H), 3.87 (dt, *J* = 6.7, 3.3 Hz, 1H), 3.66 (t, *J* = 6.4 Hz, 2H), 3.49 (s, 1H), 3.37 (s, 1H), 2.93 (dd, *J* = 15.8, 11.3 Hz, 1H), 2.54 – 2.44 (m, 1H), 2.38 – 2.31 (m, 1H), 2.31 – 2.21 (m, 2H), 2.18 – 2.10 (m, 2H), 1.96 – 1.89 (m, 1H), 1.88 – 1.82 (m, 1H), 1.82 – 1.75 (m, 2H), 1.73 – 1.64 (m, 5H), 1.62 – 1.58 (m, 2H), 1.58 – 1.51 (m, 3H), 1.42 (s, 9H), 1.42 (s, 9H), 1.33 – 1.24 (m, 5H), 1.17 (tdd, *J* = 14.0, 9.5, 5.7 Hz, 2H), 1.04 (s, 9H), 0.92 (dd, *J* = 6.8, 5.1 Hz, 6H), 0.86 (s, 9H), 0.02 (s, 3H), 0.00 (s, 3H).

¹³C NMR (150 MHz, CDCl₃) δ 206.6, 155.9, 142.7, 139.6, 135.7, 134.3, 129.6, 127.7, 79.3, 70.2, 64.1, 53.6, 50.2, 48.4, 41.1, 40.5, 38.7, 37.4, 35.8, 35.2, 35.0, 33.9, 32.8, 31.1, 29.8, 29.5, 28.7, 28.6, 27.0, 26.2, 26.0, 24.9, 23.6, 23.5, 23.1, 21.1, 19.4, 18.2, -4.4, -4.8.

HRMS (ESI-TOF) *m/z* calcd for C₅₈H₉₄N₂O₇Si₂Na (M + Na)⁺ : 1009.6497, found 1009.6507.

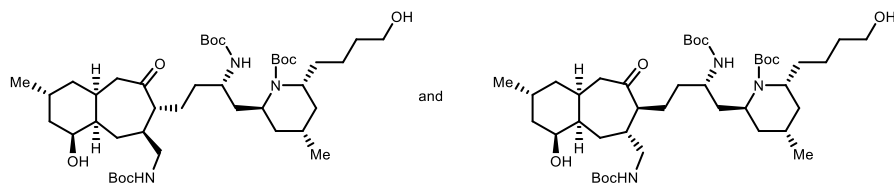


tert-Butyl (2S,4S,6R)-2-((2S)-2-((tert-butoxycarbonyl)amino)-4-((1S,3R,4aS,9aR)-8-(((tert-butoxycarbonyl)amino)methyl)-1-((tert-butylidimethylsilyl)oxy)-3-methyl-6-oxodecahydro-1H-benzo[7]annulen-7-yl)butyl)-6-(4-((tert-butylidiphenylsilyl)oxy)butyl)-4-methyl

piperidine-1-carboxylate (4-148): A flame-dried half dram vial was charged with enone **4-146** (118 mg, 0.119 mmol), carboxylic acid **4-147** (63.0 mg, 0.358 mmol), K₂HPO₄ (68.0 mg, 0.394 mmol), DMF (0.30 mL), and finally Ir[dF(CF₃)ppy]₂(dtbbpy)PF₆ (2.70 mg, 0.00239 mmol). The reaction mixture was purged with argon for 15 min before allowing to stir under blue LED light for 20 h. EtOAc (3 mL) was added and the mixture was washed with water (3 x 5 mL). The organic layer was dried with magnesium sulfate, filtered, concentrated, and purified by flash column chromatography (EtOAc/hexanes) on silica to afford tricarbamate **4-148** (82.0 mg, 62%) as a white foam and as an inseparable mixture of diastereomers in *ca.* 2:1 mixture.

TLC R_f = 0.24 (silica gel, 15:85 EtOAc:Hex)

HRMS (ESI-TOF) *m/z* calcd for C₆₄H₁₀₇N₃O₉Si₂Na (M + Na)⁺: 1140.7444, found 1140.7432.



tert-Butyl (2S,4S,6R)-2-((S)-2-((tert-butoxycarbonyl)amino)-4-((1S,3R,4aS,7R,8S,9aR)-8-(((tert-butoxycarbonyl)amino)methyl)-1-hydroxy-3-methyl-6-oxodecahydro-1H-benzo[7]annulen-7-yl)butyl)-6-(4-hydroxybutyl)-4-methylpiperidine-1-carboxylate (4-149) and tert-Butyl (2S,4S,6R)-2-((S)-2-((tert-butoxycarbonyl)amino)-4-((1S,3R,4aS,7S,8R,9aR)-8-(((tert-butoxycarbonyl)amino)methyl)-1-hydroxy-3-methyl-6-oxodecahydro-1H-benzo[7]annulen-

7-yl)butyl)-6-(4-hydroxybutyl)-4-methylpiperidine-1-carboxylate (4-150): To a flask containing silyl alcohol **4-148** (80.0 mg, 0.0715 mmol) was added 1 M TBAF in THF (0.80 mL, 0.800 mmol) and the reaction mixture was allowed to stir at 35 °C for 28 h. After cooling to room temperature, water (6 mL) was added and the reaction mixture was extracted with EtOAc (4 x 6 mL), dried over magnesium sulfate, filtered, concentrated, and purified by flash column chromatography (EtOAc/hexanes) on silica to afford diol **4-149** (33.0 mg, 60%) as a white foam and diol **4-150** (17.0 mg, 31%) as a white foam.

Major Diastereomer (4-149):

TLC R_f = 0.64 (silica gel, 80:20 EtOAc:Hex)

¹H NMR (600 MHz, CDCl₃) δ 5.02 (s, 1H), 4.68 (s, 1H), 4.03 (s, 1H), 3.91 (dt, J = 9.3, 4.0 Hz, 1H), 3.63 (dtd, J = 22.7, 11.1, 6.1 Hz, 2H), 3.42 (s, 1H), 3.28 (s, 1H), 3.17 (d, J = 10.1 Hz, 1H), 3.01 (s, 1H), 2.65 (d, J = 8.1 Hz, 1H), 2.50 – 2.29 (m, 3H), 2.25 (s, 1H), 2.01 – 1.92 (m, 4H), 1.87 – 1.80 (m, 1H), 1.80 – 1.68 (m, 3H), 1.63 – 1.47 (m, 10H), 1.42 (s, 18H), 1.41 (s, 9H), 1.37 – 1.30 (m, 3H), 1.23 – 1.16 (m, 3H), 1.11 (dt, J = 13.1, 9.8 Hz, 1H), 0.95 (d, J = 7.1 Hz, 3H), 0.88 (d, J = 6.6 Hz, 3H).

¹³C NMR (150 MHz, CDCl₃) δ 214.0, 156.5, 156.2, 155.7, 79.5, 79.4, 79.1, 68.5, 62.4, 58.1, 53.9, 50.6, 49.2, 46.4, 45.5, 45.4, 41.7, 37.1, 37.0, 36.5, 34.3, 33.3, 32.5, 31.1, 30.8, 29.8, 28.7, 28.6, 28.5, 28.5, 26.2, 25.5, 23.3, 22.6, 19.9, 17.5.

HRMS (ESI-TOF) m/z calcd for C₄₂H₇₅N₃O₉Na (M + Na)⁺ : 788.5401, found 788.5415.

Minor Diastereomer (4-150):

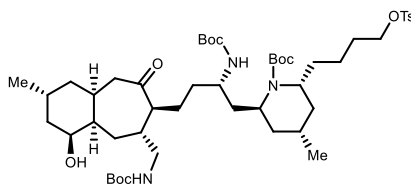
TLC R_f = 0.39 (silica gel, 80:20 EtOAc:Hex)

¹H NMR (600 MHz, CDCl₃) δ 5.25 (s, 1H), 4.63 (s, 1H), 4.06 (s, 1H), 3.88 (s, 1H), 3.64 (qt, J = 11.0, 6.0 Hz, 2H), 3.51 (s, 1H), 3.28 (s, 1H), 3.23 (s, 2H), 2.67 (s, 1H), 2.59 – 2.47 (m, 1H), 2.42

– 2.23 (m, 4H), 2.01 – 1.89 (m, 4H), 1.88 – 1.80 (m, 1H), 1.80 – 1.73 (m, 2H), 1.68 – 1.51 (m, 10H), 1.50 – 1.36 (m, 27H), 1.34 – 1.27 (m, 3H), 1.24 – 1.18 (m, 3H), 1.17 – 1.07 (m, 1H), 0.93 (d, $J = 6.9$ Hz, 3H), 0.90 (d, $J = 6.6$ Hz, 3H).

^{13}C NMR (150 MHz, CDCl_3) δ 213.5, 156.9, 156.3, 155.9, 79.6, 79.2, 79.1, 69.3, 62.5, 53.8, 52.2, 50.6, 49.0, 48.2, 43.1, 39.9, 38.5, 37.1, 37.0, 36.8, 34.4, 33.4, 32.5, 31.2, 29.8, 28.7, 28.6, 28.6, 27.3, 26.1, 24.0, 23.5, 23.4, 22.6, 21.0, 19.5.

HRMS (ESI-TOF) m/z calcd for $\text{C}_{42}\text{H}_{75}\text{N}_3\text{O}_9\text{Na}$ ($\text{M} + \text{Na}$) $^+$: 788.5401, found 788.5389.



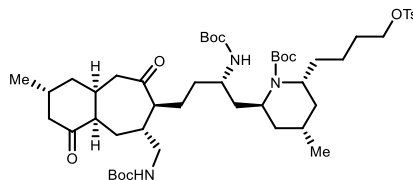
tert-Butyl (2S,4S,6R)-2-((S)-2-((tert-butoxycarbonyl)amino)-4-((1S,3R,4aS,7S,8R,9aR)-8-(((tert-butoxycarbonyl)amino)methyl)-1-hydroxy-3-methyl-6-oxodecahydro-1H-benzo[7]annulen-7-yl)butyl)-4-methyl-6-(4-(tosyloxy)butyl)piperidine-1-carboxylate (4-151): A flame-dried flask was charged with diol **4-150** (17 mg, 0.022 mmol), CH_2Cl_2 (0.40 mL), DMAP (3.0 mg, 0.024 mmol), Et_3N (16 μL , 0.11 mmol), and TsCl (5.0 mg, 0.024 mmol). After stirring for 1 h, MeOH (100 μL) was added, the reaction mixture was concentrated, and purified by flash column chromatography (EtOAc /hexanes) on silica to afford tosylate **4-151** (16 mg, 80%) as a clear oil. **TLC** $R_f = 0.27$ (silica gel, 40:60 EtOAc :Hex)

^1H NMR (600 MHz, CDCl_3) δ 7.78 (d, $J = 7.9$ Hz, 2H), 7.34 (d, $J = 7.9$ Hz, 2H), 5.21 (s, 1H), 4.65 – 4.57 (m, 1H), 4.01 (t, $J = 6.6$ Hz, 2H), 3.96 (s, 1H), 3.91 – 3.84 (m, 1H), 3.50 (s, 1H), 3.34 – 3.17 (m, 3H), 2.65 (s, 1H), 2.57 – 2.49 (m, 1H), 2.44 (s, 3H), 2.30 (s, 1H), 2.04 (s, 1H), 1.99 – 1.91 (m, 1H), 1.89 – 1.81 (m, 2H), 1.80 – 1.73 (m, 3H), 1.71 – 1.51 (m, 11H), 1.43 (s, 9H), 1.41 (s, 18H), 1.35 – 1.18 (m, 9H), 1.11 (dt, $J = 13.7, 8.6$ Hz, 1H), 0.94 (d, $J = 6.9$ Hz, 3H), 0.91 (d, J

= 6.6 Hz, 3H).

^{13}C NMR (150 MHz, CDCl_3) δ 213.2, 157.0, 156.0, 155.8, 144.8, 133.3, 130.0, 128.0, 79.6, 79.1, 70.7, 69.3, 53.4, 52.2, 50.4, 49.3, 48.4, 43.1, 40.0, 38.6, 37.8, 36.1, 35.6, 34.6, 33.1, 31.1, 29.8, 29.0, 28.7, 28.6, 28.6, 27.3, 25.2, 23.2, 22.9, 21.8, 20.9.

HRMS (ESI-TOF) m/z calcd for $\text{C}_{49}\text{H}_{81}\text{N}_3\text{O}_{11}\text{SNa}$ ($\text{M} + \text{Na}$) $^+$: 942.5490, found 942.5481.



***tert*-Butyl (2*S*,4*S*,6*R*)-2-((*S*)-2-((*tert*-butoxycarbonyl)amino)-4-((3*R*,4*aS*,7*S*,8*R*,9*aR*)-8-(((*tert*-butoxycarbonyl)amino)methyl)-3-methyl-1,6-dioxodecahydro-1*H*-benzo[7]annulen-7-yl)butyl)-4-methyl-6-(4-(tosyloxy)butyl)piperidine-1-carboxylate (4-152):** To a flask containing alcohol **4-151** (16 mg, 0.017 mmol) dissolved in CH_2Cl_2 (0.30 mL) was added DMP (10 mg, 0.023 mmol). After 24 h another portion of DMP (20 mg, 0.046 mmol) was added and the mixture was allowed to stir overnight before the addition of saturated aqueous NaHCO_3 (0.5 mL) and saturated aqueous $\text{Na}_2\text{S}_2\text{O}_3$ (0.5 mL). After stirring for 2 h, the mixture was extracted with CH_2Cl_2 (4 x 2 mL), dried over magnesium sulfate, filtered, concentrated, and purified by flash column chromatography (EtOAc/hexanes) on silica to afford diketone **4-152** (16 mg, quantitative) as a yellow oil.

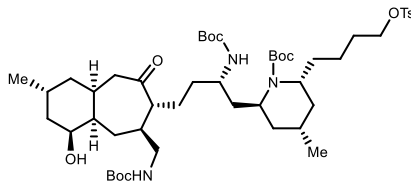
TLC R_f = 0.27 (silica gel, 40:60 EtOAc:Hex)

^1H NMR (600 MHz, CDCl_3) δ 7.78 (d, J = 8.3 Hz, 2H), 7.34 (d, J = 8.0 Hz, 2H), 5.52 (s, 1H), 4.57 (s, 1H), 4.02 (t, J = 6.6 Hz, 2H), 3.96 (s, 1H), 3.52 (s, 1H), 3.39 (d, J = 12.7 Hz, 1H), 3.31 – 3.23 (m, 1H), 2.94 (ddd, J = 13.4, 8.3, 5.3 Hz, 1H), 2.66 (t, J = 11.7 Hz, 1H), 2.60 (s, 2H), 2.44 (s, 3H), 2.18 (dd, J = 14.9, 4.8 Hz, 1H), 1.97 – 1.89 (m, 3H), 1.86 – 1.73 (m, 5H), 1.72 – 1.59 (m, 6H), 1.58 – 1.50 (m, 2H), 1.44 (s, 9H), 1.41 (s, 9H), 1.40 (s, 9H), 1.36 – 1.29 (m, 4H), 1.28 – 1.22

(m, 3H), 1.18 – 1.07 (m, 3H), 1.00 (d, $J = 5.6$ Hz, 3H), 0.91 (d, $J = 6.6$ Hz, 3H).

^{13}C NMR (150 MHz, CDCl_3) δ 213.6, 211.6, 156.7, 155.9, 155.7, 144.7, 133.4, 130.0, 128.0, 79.5, 79.2, 79.0, 70.7, 54.9, 53.3, 50.3, 50.3, 47.7, 43.9, 43.7, 41.0, 40.4, 37.5, 36.2, 35.8, 35.5, 34.7, 32.3, 30.1, 29.8, 29.0, 28.9, 28.7, 28.6, 28.6, 26.8, 25.1, 23.1, 23.0, 22.4, 21.8.

HRMS (ESI-TOF) m/z calcd for $\text{C}_{49}\text{H}_{79}\text{N}_3\text{O}_{11}\text{SNa}$ ($\text{M} + \text{Na}$) $^+$: 940.5333, found 940.5321.



***tert*-Butyl (2*S*,4*S*,6*R*)-2-((*S*)-2-((*tert*-butoxycarbonyl)amino)-4-((1*S*,3*R*,4*aS*,7*R*,8*S*,9*aR*)-8-(((*tert*-butoxycarbonyl)amino)methyl)-1-hydroxy-3-methyl-6-oxodecahydro-1*H*-benzo[7]**

annulen-7-yl)butyl)-4-methyl-6-(4-(tosyloxy)butyl)piperidine-1-carboxylate (4-153): A

flame-dried flask was charged with diol **4-149** (33 mg, 0.043 mmol), CH_2Cl_2 (0.60 mL), DMAP (3.0 mg, 0.024 mmol), Et_3N (16 μL , 0.11 mmol), and TsCl (8.2 mg, 0.043 mmol). After stirring for 1 h, another portion of TsCl (8.2 mg, 0.043 mmol) was added and the mixture was allowed to stir for another 30 min before MeOH (100 μL) was added. The reaction mixture was concentrated and purified by flash column chromatography (EtOAc /hexanes) on silica to afford tosylate **4-153** (29 mg, 73%) as a clear oil.

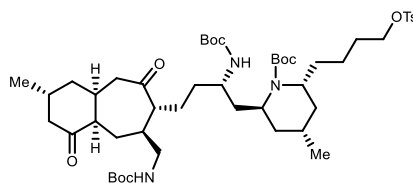
TLC $R_f = 0.38$ (silica gel, 60:40 EtOAc :Hex)

^1H NMR (600 MHz, CDCl_3) δ 7.77 (d, $J = 8.0$ Hz, 2H), 7.33 (d, $J = 7.9$ Hz, 2H), 4.90 (s, 1H), 4.63 (s, 1H), 4.01 (t, $J = 6.6$ Hz, 2H), 3.97 – 3.88 (m, 2H), 3.42 (s, 1H), 3.29 (s, 1H), 3.16 (d, $J = 13.5$ Hz, 1H), 3.06 (s, 1H), 2.64 (d, $J = 12.5$ Hz, 1H), 2.44 (s, 3H), 2.34 (d, $J = 12.1$ Hz, 1H), 2.27 (s, 1H), 2.07 – 1.99 (m, 2H), 1.93 – 1.86 (m, 1H), 1.84 (d, $J = 9.7$ Hz, 1H), 1.80 – 1.70 (m, 4H), 1.69 – 1.60 (m, 5H), 1.55 (d, $J = 9.9$ Hz, 2H), 1.42 (s, 9H), 1.41 (s, 18H), 1.35 – 1.28 (m, 6H),

1.26 – 1.17 (m, 5H), 1.09 (dt, $J = 13.5, 8.8$ Hz, 2H), 0.95 (d, $J = 7.1$ Hz, 3H), 0.90 (d, $J = 6.6$ Hz, 3H).

^{13}C NMR (150 MHz, CDCl_3) δ 213.7, 156.4, 156.0, 155.6, 144.7, 133.3, 130.0, 128.0, 79.5, 79.3, 79.0, 70.8, 68.6, 58.1, 53.5, 50.3, 49.2, 46.4, 45.5, 45.4, 41.7, 37.2, 36.2, 35.8, 34.5, 33.1, 32.0, 30.8, 29.8, 29.5, 28.9, 28.7, 28.6, 28.5, 28.4, 25.4, 23.1, 22.8, 21.8, 19.9, 17.6.

HRMS (ESI-TOF) m/z calcd for $\text{C}_{49}\text{H}_{81}\text{N}_3\text{O}_{11}\text{SNa}$ ($M + \text{Na}$) $^+$: 942.5490, found 942.5496.



***tert*-Butyl (2S,4S,6R)-2-((S)-2-((tert-butoxycarbonyl)amino)-4-((3R,4aS,7R,8S,9aR)-8-(((tert-butoxycarbonyl)amino)methyl)-3-methyl-1,6-dioxodecahydro-1H-benzo[7]annulen-7-yl)butyl)-4-methyl-6-(4-(tosyloxy)butyl)piperidine-1-carboxylate (4-154):** To a flask containing alcohol **4-153** (27 mg, 0.029 mmol) dissolved in CH_2Cl_2 (0.40 mL) was added DMP (25 mg, 0.059 mmol) and the mixture was allowed to stir for 9 h before saturated aqueous NaHCO_3 (1 mL) and saturated aqueous $\text{Na}_2\text{S}_2\text{O}_3$ (1 mL) were added. After stirring for 2 h, the mixture was extracted with CH_2Cl_2 (3 x 2 mL), dried over magnesium sulfate, filtered, concentrated, and purified by flash column chromatography (EtOAc/hexanes) on silica to afford diketone **4-154** (27 mg, quantitative) as a yellow oil.

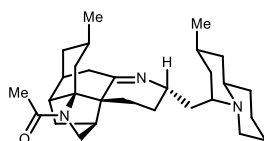
TLC $R_f = 0.61$ (silica gel, 60:40 EtOAc:Hex)

^1H NMR (500 MHz, CDCl_3) δ 7.77 (d, $J = 8.0$ Hz, 2H), 7.33 (d, $J = 8.1$ Hz, 2H), 4.93 (s, 1H), 4.61 (s, 1H), 4.01 (t, $J = 6.5$ Hz, 2H), 3.92 (s, 1H), 3.43 (s, 1H), 3.34 – 3.27 (m, 1H), 3.21 – 3.08 (m, 1H), 3.01 – 2.92 (m, 1H), 2.88 – 2.76 (m, 1H), 2.58 – 2.49 (m, 2H), 2.44 (s, 3H), 2.42 – 2.38 (m, 1H), 2.23 (dd, $J = 14.9, 10.6$ Hz, 1H), 2.18 – 2.07 (m, 2H), 1.98 (dd, $J = 13.5, 8.5$ Hz, 1H),

1.91 (ddd, $J = 13.7, 8.1, 5.1$ Hz, 1H), 1.83 – 1.72 (m, 3H), 1.69 – 1.56 (m, 8H), 1.41 (s, 27H), 1.34 – 1.21 (m, 8H), 1.14 – 1.05 (m, 2H), 0.97 (d, $J = 6.8$ Hz, 3H), 0.90 (d, $J = 6.6$ Hz, 3H).

$^{13}\text{C NMR}$ (125 MHz, CDCl_3) δ 212.0, 211.9, 156.3, 156.0, 155.6, 144.7, 133.4, 129.9, 128.0, 79.5, 79.5, 79.1, 70.7, 58.2, 53.6, 50.2, 49.1, 47.7, 45.5, 44.1, 39.6, 37.1, 36.2, 35.9, 35.7, 34.5, 33.1, 33.1, 29.8, 29.4, 29.0, 28.7, 28.7, 28.6, 28.5, 28.3, 25.4, 23.1, 22.8, 21.7, 21.0.

HRMS (ESI-TOF) m/z calcd for $\text{C}_{49}\text{H}_{79}\text{N}_3\text{O}_{11}\text{SNa}$ ($\text{M} + \text{Na}$) $^+$: 940.5333, found 940.5338.



(–)-Himeradine A (4-17): A flame-dried flask was charged with diketone **4-154** (14.0 mg, 0.0153 mmol), CSA (35.0 mg, 0.153 mmol), and *o*-DCB (1 mL) before it was heated to 165 °C for 1 h. The reaction mixture was cooled to room temperature and Et_3N (106 μL , 0.763 mmol) was added. After stirring for 30 min, Ac_2O (1.40 μL , 0.0153 mmol) was added and the mixture was stirred for an additional 30 min. The reaction was quenched with saturated aqueous NaHCO_3 (2 mL) and extracted with EtOAc (3 x 1 mL). The organic layer was dried with magnesium sulfate, filtered, concentrated, and purified by flash column chromatography ($\text{CHCl}_3/\text{MeOH}/\text{NH}_4\text{OH}$) on silica to yield (–)-himeradine A **4-17** (5.90 mg, 84%) as a clear oil which was treated with a 1:1 $\text{TFA}:\text{CH}_2\text{Cl}_2$ mixture (1 mL) for 15 min before concentrating to afford the double TFA salt as a white solid.

All characterization is based on the double TFA salt.

TLC $R_f = 0.65$ (silica gel, 80:18:2 $\text{CHCl}_3:\text{MeOH}:\text{NH}_4\text{OH}$)

Optical Rotation $[\alpha]_{\text{D}}^{22} = -16$ ($c = 0.3$, MeOH)

$^1\text{H NMR}$ (500 MHz, CD_3OD) δ 4.07 (s, 1H), 3.80 (d, $J = 9.6$ Hz, 1H), 3.63 (d, $J = 10.8$ Hz, 1H), 3.37 (d, $J = 9.5$ Hz, 2H), 3.26 – 3.13 (m, 2H), 3.04 (t, $J = 13.3$ Hz, 1H), 2.71 – 2.64 (m, 1H), 2.63

– 2.56 (m, 1H), 2.51 – 2.43 (m, 1H), 2.39 (d, $J = 4.9$ Hz, 1H), 2.32 – 2.22 (m, 1H), 2.12 (t, $J = 12.8$ Hz, 1H), 2.03 (s, 3H), 2.01 – 1.94 (m, 7H), 1.87 – 1.74 (m, 5H), 1.72 – 1.64 (m, 3H), 1.63 – 1.58 (m, 1H), 1.55 (t, $J = 10.3$ Hz, 2H), 1.35 – 1.30 (m, 3H), 1.25 – 1.17 (m, 1H), 1.01 (d, $J = 5.9$ Hz, 3H), 0.99 (d, $J = 6.0$ Hz, 3H).

$^{13}\text{C NMR}$ (125 MHz, CDCl_3) δ 196.3, 174.3, 75.9, 59.7, 58.7, 57.4, 57.1, 56.0, 53.1, 45.1, 43.0, 40.7, 40.7, 40.5, 35.4, 35.1, 35.0, 32.6, 31.5, 29.6, 27.7, 24.6, 24.6, 24.4, 24.1, 23.0, 22.8, 21.4, 20.3.

HRMS (ESI-TOF) m/z calcd for $\text{C}_{29}\text{H}_{46}\text{N}_3\text{O}$ ($\text{M} + \text{H}$) $^+$: 452.3641, found 452.3641.

Table 4-3. Comparison how the ^{13}C ppm shifts at each carbon of (-)-himeradine A (4-17).

carbon number	^{13}C shift (ppm)		
	Isolation	Shair	Rychnovsky
15	20.6	20.3	20.3
12'	21.5	21.4	21.4
12	22.8	22.8	22.8
4'	22.9	23.0	23.0
8'	24.2	24.1	24.1
20	24.4	24.4	24.4
3'	24.6	24.6	24.6
16	26.0	24.6	24.6
8	27.7	27.7	27.7
11'	31.1	29.6	29.6
4	31.6	31.5	31.5
5'	32.5	32.6	32.6
7	35.0	35.0	35.0
10	35.5	35.3	35.1
9'	37.0	35.4	35.4
11	39.0	40.5	40.5
7'	40.5	40.6	40.7
9	40.7	40.7	40.7
5	43.0	43.0	43.0
3	45.4	45.1	45.1
2'	52.9	53.1	53.1
17	56.6	55.9	56.0
14	57.1	57.1	57.1
2	57.5	57.4	57.4
6'	58.4	58.7	58.7
10'	60.0	59.7	59.7
6	76.1	75.9	75.9
19	174.3	174.3	174.3
13	196.7	196.5	196.3

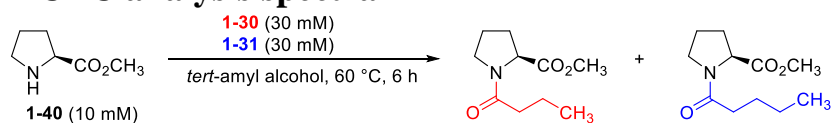
4.7 References

1. Bödeker, K., Lycopodin, Das Erste Alkaloïd Der Gefässkryptogamen. *Justus Liebigs Ann. Chem.* **1881**, 208, 363–367.
2. Ma, X.; Gang, D. R., The Lycopodium Alkaloids. *Nat. Prod. Rep.* **2004**, 21, 752–772.
3. Conroy, H., Biogenesis of Lycopodium Alkaloids. *Tetrahedron Lett.* **1960**, 1, 34–37.
4. (a) Hemscheidt, T.; Spenser, I. D., A Classical Paradigm of Alkaloid Biogenesis Revisited: Acetonedicarboxylic Acid as a Biosynthetic Precursor of Lycopodine. *J. Am. Chem. Soc.* **1996**, 118, 1799–1800; (b) Hemscheidt, T.; Spenser, I. D., Biosynthesis of Lycopodine: Incorporation of Acetate Via an Intermediate with C_{2v} Symmetry. *J. Am. Chem. Soc.* **1993**, 115, 3020–3021.

5. Morita, H.; Hirasawa, Y.; Kobayashi, J. I., Himeradine a, a Novel C₂₇N₃-Type Alkaloid from *Lycopodium Chinense*. *J. Org. Chem.* **2003**, *68*, 4563–4566.
6. (a) Gerard, R. V.; MacLean, D. B., GC/MS Examination of Four *Lycopodium* Species for Alkaloid Content. *Phytochemistry* **1986**, *25*, 1143–1150; (b) Gerard, R. V.; MacLean, D. B.; Fagianni, R.; Lock, C. J., Fastigiatine, a *Lycopodium* Alkaloid with a New Ring System. *Can. J. Chem.* **1986**, *64*, 943–949.
7. Ishiuchi, K. i.; Kubota, T.; Ishiyama, H.; Hayashi, S.; Shibata, T.; Mori, K.; Obara, Y.; Nakahata, N.; Kobayashi, J. i., Lyconadins D and E, and Complandine E, New *Lycopodium* Alkaloids from *Lycopodium Complandatum*. *Bioorg. Med. Chem.* **2011**, *19*, 749–753.
8. Collett, N. D.; Carter, R. G., Stereoselective Synthesis of the Eastern Quinolizidine Portion of Himeradine A. *Org. Lett.* **2011**, *13*, 4144–4147.
9. Lee, A. S.; Liao, B. B.; Shair, M. D., A Unified Strategy for the Synthesis of 7-Membered-Ring-Containing *Lycopodium* Alkaloids. *J. Am. Chem. Soc.* **2014**, *136*, 13442–13452.
10. Samame, R. A.; Owens, C. M.; Rychnovsky, S. D., Concise Synthesis of (+)-Fastigiatine. *Chem. Sci.* **2015**, *7*, 188–190.
11. DeForest, J. C.; Samame, R. A.; Suryan, G.; Burtea, A.; Rychnovsky, S. D., Second-Generation Synthesis of (+)-Fastigiatine Inspired by Conformational Studies. *J. Org. Chem.* **2018**, *83*, 8914–8925.
12. DeForest, J. C. Progress Towards the Total Synthesis of (–)-Batrachotoxin a, Computationally Inspired Second-Generation Synthesis of (+)-Fastigiatine, Progress Towards the Total Synthesis of (–)-Himeradine a and Strategies Towards the 4,5-Spirocyclic Fragment of Phainanoid F. Ph. D. Dissertation, University of California, Irvine, Irvine, CA, 2017.
13. (a) Beak, P.; Lee, W.-K., α -Lithioamine Synthetic Equivalents from Dipole-Stabilized Carbanions: The T-Boc Group as an Activator for α' -Lithiation of Carbamates. *Tetrahedron Lett.* **1989**, *30*, 1197–1200; (b) Beak, P.; Lee, W. K., α -Lithioamine Synthetic Equivalents: Syntheses of Diastereoisomers from Boc Derivatives of Cyclic Amines. *J. Org. Chem.* **1993**, *58*, 1109–1117; (c) Beak, P.; Lee, W. K., α -Lithioamine Synthetic Equivalents: Syntheses of Diastereoisomers from the Boc-Piperidines. *J. Org. Chem.* **1990**, *55*, 2578–2580.
14. Liu, G.; Cogan, D. A.; Ellman, J. A., Catalytic Asymmetric Synthesis of Tert-Butanesulfinamide. Application to the Asymmetric Synthesis of Amines. *J. Am. Chem. Soc.* **1997**, *119*, 9913–9914.
15. (a) Leitner, A.; Shekhar, S.; Pouy, M. J.; Hartwig, J. F., A Simple Iridium Catalyst with a Single Resolved Stereocenter for Enantioselective Allylic Amination. Catalyst Selection from Mechanistic Analysis. *J. Am. Chem. Soc.* **2005**, *127*, 15506–15514; (b) Cannon, J. S.; Overman, L. E., Palladium(II)-Catalyzed Enantioselective Reactions Using COP Catalysts. *Acc. Chem. Res.* **2016**, *49*, 2220–2231.
16. (a) Glorius, F., Asymmetric Hydrogenation of Aromatic Compounds. *Org. Biomol. Chem.* **2005**, *3*, 4171–4175; (b) Glorius, F.; Spielkamp, N.; Holle, S.; Goddard, R.; Lehmann, C. W., Efficient Asymmetric Hydrogenation of Pyridines. *Angew. Chem. Int. Ed.* **2004**, *43*, 2850–2852.
17. Everson, D. A.; Buonomo, J. A.; Weix, D. J., Nickel-Catalyzed Cross-Electrophile Coupling of 2-Chloropyridines With. *Synlett* **2014**, *25*, 233–238.
18. Jin, J.; MacMillan, D. W. C., Alcohols as Alkylating Agents in Heteroarene C–H Functionalization. *Nature* **2015**, *525*, 87.
19. Minisci, F.; Bernardi, R.; Bertini, F.; Galli, R.; Perchinummo, M., Nucleophilic Character of Alkyl Radicals—VI: A New Convenient Selective Alkylation of Heteroaromatic Bases. *Tetrahedron* **1971**, *27*, 3575–3579.

20. Gros, P.; Choppin, S.; Julien Mathieu, A.; Fort, Y., Lithiation of 2-Heterosubstituted Pyridines with BuLi–LiDMAE: Evidence for Regiospecificity at C-6. *J. Org. Chem.* **2002**, *67*, 234–237.
21. (a) Londregan, A. T.; Jennings, S.; Wei, L., Mild Addition of Nucleophiles to Pyridine-N-Oxides. *Org. Lett.* **2011**, *13*, 1840–1843; (b) Cunha, R. L. O. R.; Diego, D. G.; Simonelli, F.; Comasseto, J. V., Selectivity Aspects of the Ring Opening Reaction of 2-Alkenyl Aziridines by Carbon Nucleophiles. *Tetrahedron Lett.* **2005**, *46*, 2539–2542.
22. Liniger, M.; Estermann, K.; Altmann, K.-H., Total Synthesis of Hygrolines and Pseudohygrolines. *J. Org. Chem.* **2013**, *78*, 11066–11070.
23. Trost, B. M.; O'Boyle, B. M.; Torres, W.; Ameriks, M. K., Development of a Flexible Strategy Towards FR900482 and the Mitomycins. *Chem. Eur. J.* **2011**, *17*, 7890–7903.
24. Rousseau, J.-F.; Chekroun, I.; Ferey, V.; Labrosse, J. R., Concise Preparation of a Stable Cyclic Sulfamidate Intermediate in the Synthesis of a Enantiopure Chiral Active Diamine Derivative. *Org. Process Res. Dev.* **2015**, *19*, 506–513.
25. Nicolaou, K. C.; Snyder, S. A.; Longbottom, D. A.; Nalbandian, A. Z.; Huang, X., New Uses for the Burgess Reagent in Chemical Synthesis: Methods for the Facile and Stereoselective Formation of Sulfamidates, Glycosylamines, and Sulfamides. *Chem. Eur. J.* **2004**, *10*, 5581–5606.
26. Chu, L.; Ohta, C.; Zuo, Z.; MacMillan, D. W. C., Carboxylic Acids as a Traceless Activation Group for Conjugate Additions: A Three-Step Synthesis of (±)-Pregabalin. *J. Am. Chem. Soc.* **2014**, *136*, 10886–10889.
27. Versteegen, R. M.; van Beek, D. J. M.; Sijbesma, R. P.; Vlassopoulos, D.; Fytas, G.; Meijer, E. W., Dendrimer-Based Transient Supramolecular Networks. *J. Am. Chem. Soc.* **2005**, *127*, 13862–13868.
28. Gahalawat, S.; Pandey, S. K., Enantioselective Total Synthesis of (+)-Serinolamide A. *RSC Adv.* **2015**, *5*, 41013–41016.
29. Tejada, E. J. C.; Bello, A. M.; Wasilewski, E.; Koebel, A.; Dunn, S.; Kotra, L. P., Noncovalent Protein Arginine Deiminase (PAD) Inhibitors Are Efficacious in Animal Models of Multiple Sclerosis. *J. Med. Chem.* **2017**, *60*, 8876–8887.
30. Pan, X.; Li, X.; Lu, Q.; Yu, W.; Li, W.; Zhang, Q.; Deng, F.; Liu, F., Efficient Synthesis of Sitagliptin Phosphate, a Novel DPP-IV Inhibitor, Via a Chiral Aziridine Intermediate. *Tetrahedron Lett.* **2013**, *54*, 6807–6809.

Appendix A CEC analysis spectra

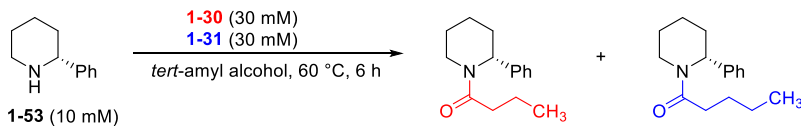
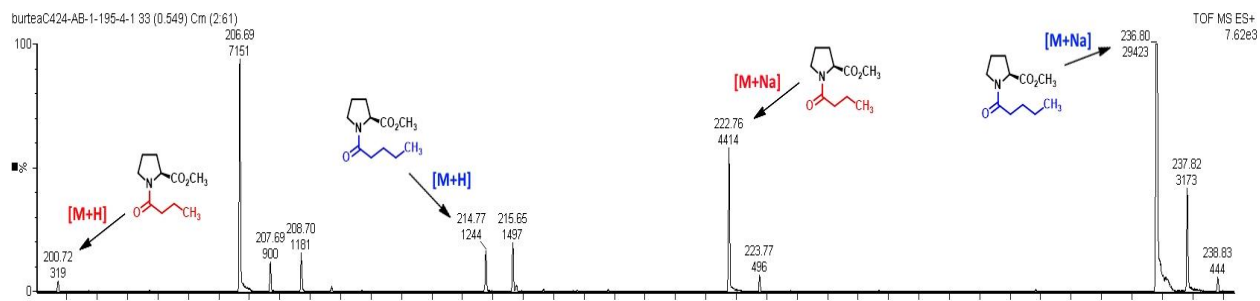


$$[M+H] + [M+Na] = 319 + 4414 = 4733$$

$$4733 / (4733 + 30667) (100) = 13\%$$

$$[M+H] + [M+Na] = 1244 + 29423 = 30667$$

$$30667 / (4733 + 30667) (100) = 87\%$$

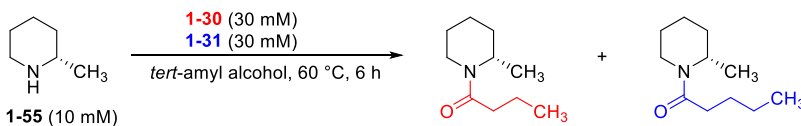
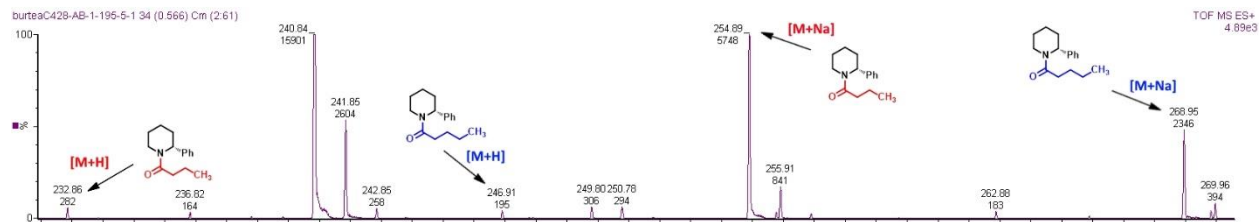


$$[M+H] + [M+Na] = 282 + 5748 = 6030$$

$$6030 / (6030 + 2541) (100) = 70\%$$

$$[M+H] + [M+Na] = 195 + 2346 = 2541$$

$$2541 / (6030 + 2541) (100) = 30\%$$

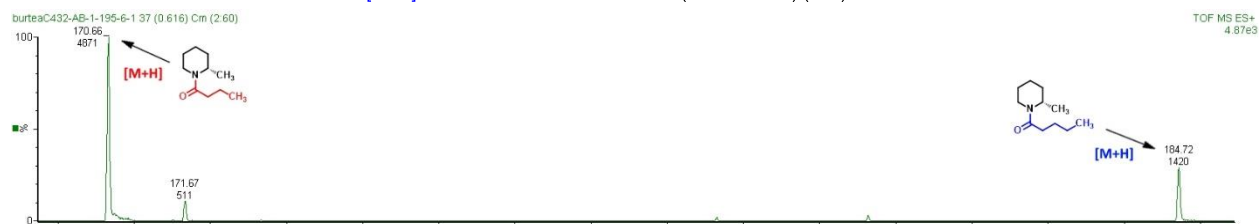


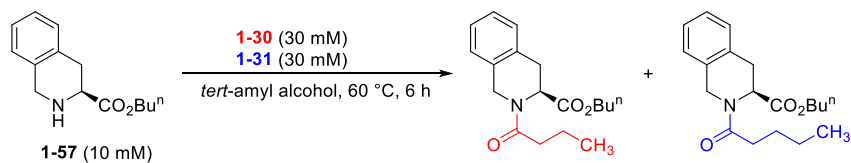
$$[M+H] = 4871$$

$$4871 / (4871 + 1420) (100) = 77\%$$

$$[M+H] = 1420$$

$$1420 / (4871 + 1420) (100) = 23\%$$



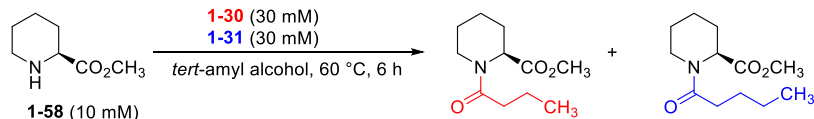
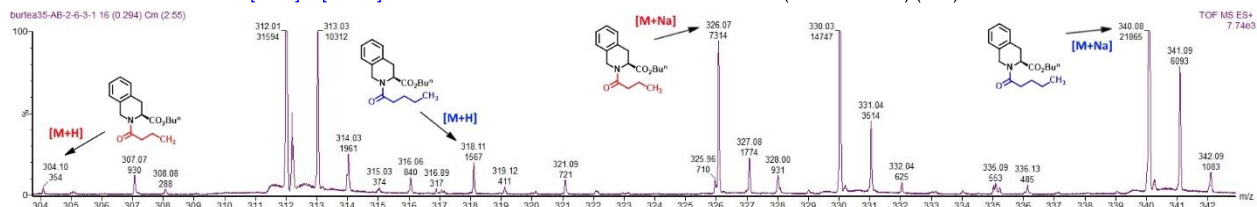


$$[M+H] + [M+Na] = 354 + 7314 = 7668$$

$$7668 / (7668 + 23432) (100) = 25\%$$

$$[M+H] + [M+Na] = 1567 + 21865 = 23432$$

$$23432 / (7668 + 23432) (100) = 75\%$$

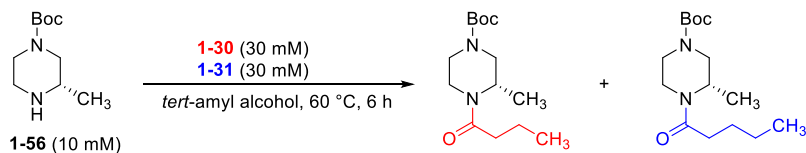
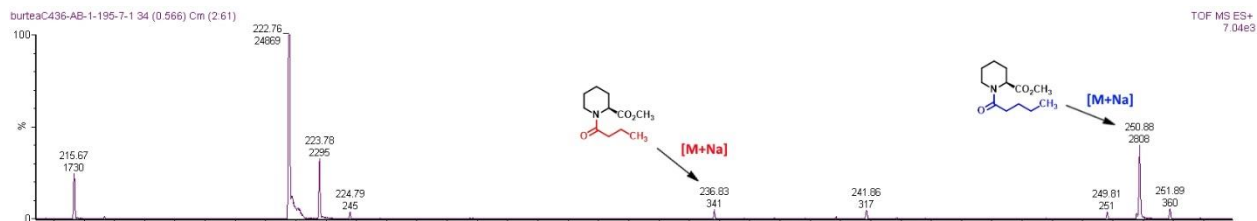


$$[M+H] + [M+Na] = 0 + 341 = 341$$

$$341 / (341 + 2808) (100) = 11\%$$

$$[M+H] + [M+Na] = 0 + 2808 = 2808$$

$$2808 / (341 + 2808) (100) = 89\%$$

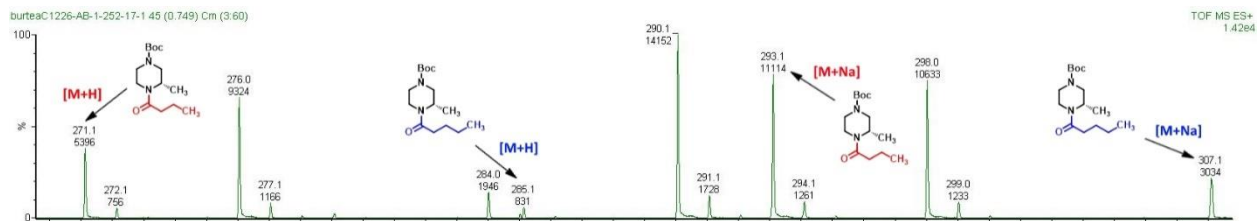


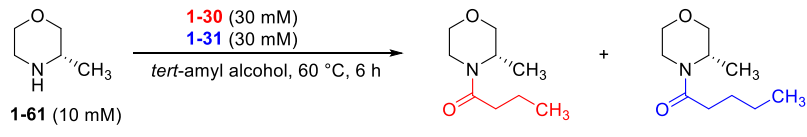
$$[M+H] + [M+Na] = 5396 + 11114 = 16510$$

$$16510 / (16510 + 3865) (100) = 81\%$$

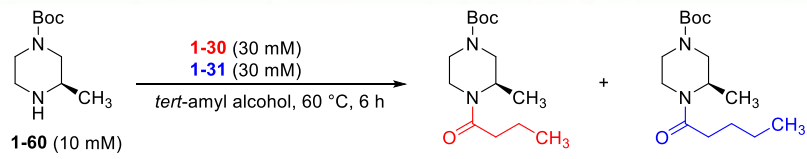
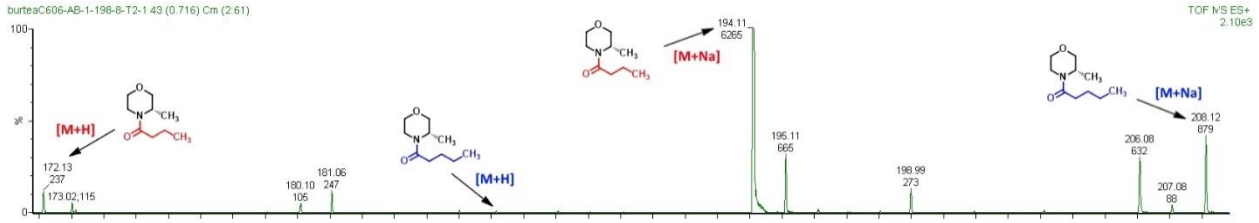
$$[M+H] + [M+Na] = 831 + 3034 = 3865$$

$$3865 / (16510 + 3865) (100) = 19\%$$

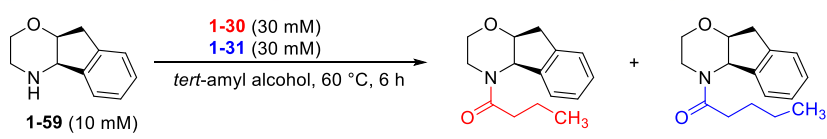
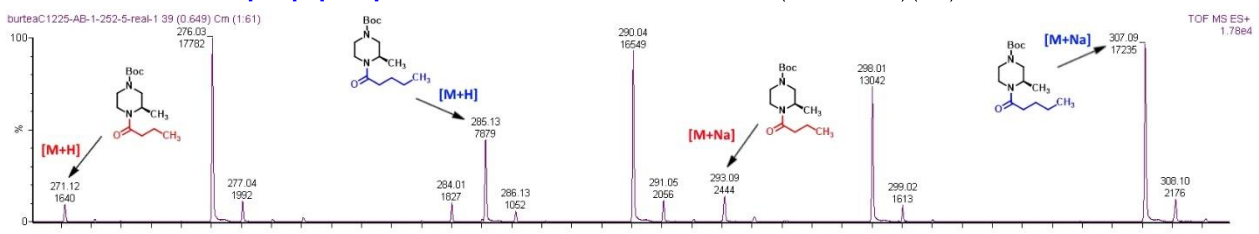




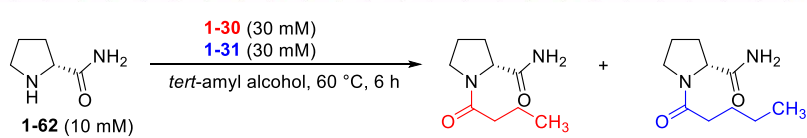
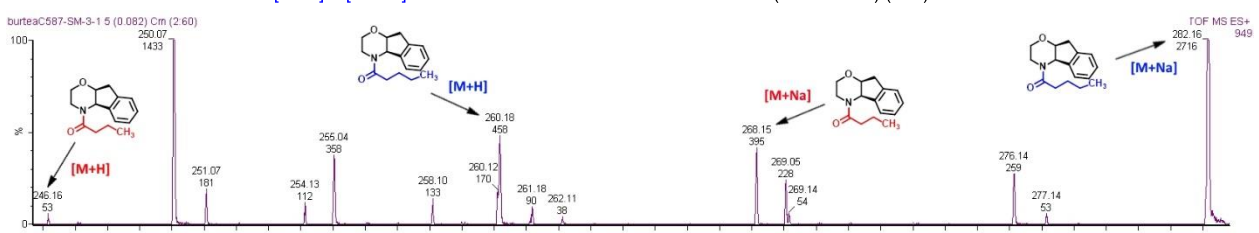
$[M+H] + [M+Na] = 237 + 6265 = 6502$ \rightarrow $6502 / (6502 + 879) (100) = 88\%$
 $[M+H] + [M+Na] = 0 + 879 = 879$ \rightarrow $879 / (6502 + 879) (100) = 12\%$



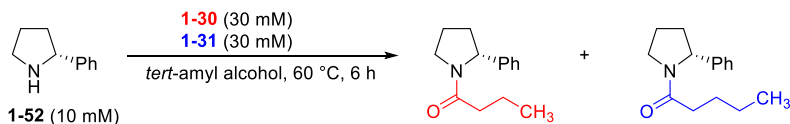
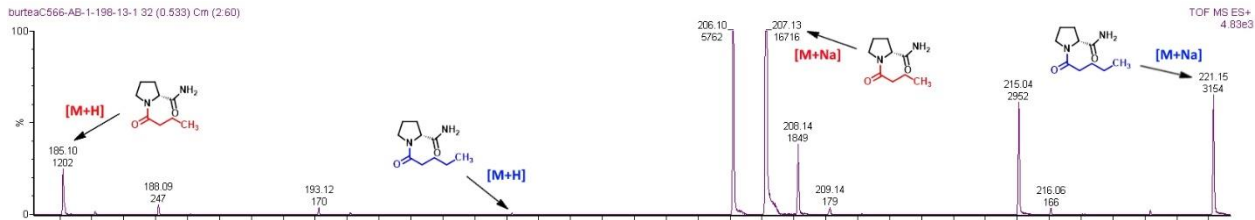
$[M+H] + [M+Na] = 1640 + 2444 = 4084$ \rightarrow $4084 / (4084 + 25114) (100) = 14\%$
 $[M+H] + [M+Na] = 7879 + 17235 = 25114$ \rightarrow $25114 / (4084 + 25114) (100) = 86\%$



$[M+H] + [M+Na] = 53 + 395 = 448$ \rightarrow $448 / (448 + 3174) (100) = 12\%$
 $[M+H] + [M+Na] = 458 + 2716 = 3174$ \rightarrow $3174 / (448 + 3174) (100) = 88\%$

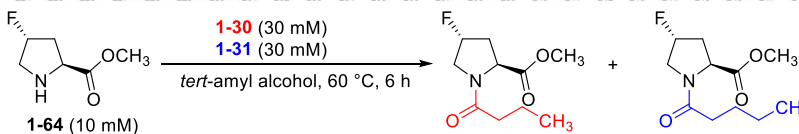
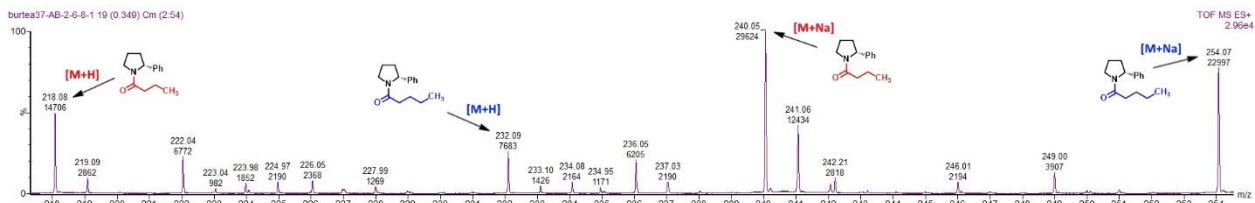


$[M+H] + [M+Na] = 1202 + 16716 = 17918$ \rightarrow $17918 / (17918 + 3154) (100) = 85\%$
 $[M+H] + [M+Na] = 0 + 3154 = 3154$ \rightarrow $3154 / (17918 + 3154) (100) = 15\%$



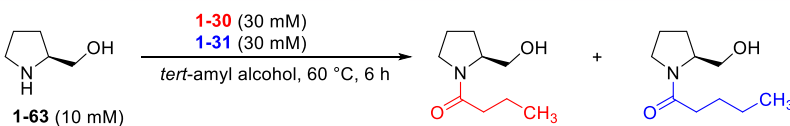
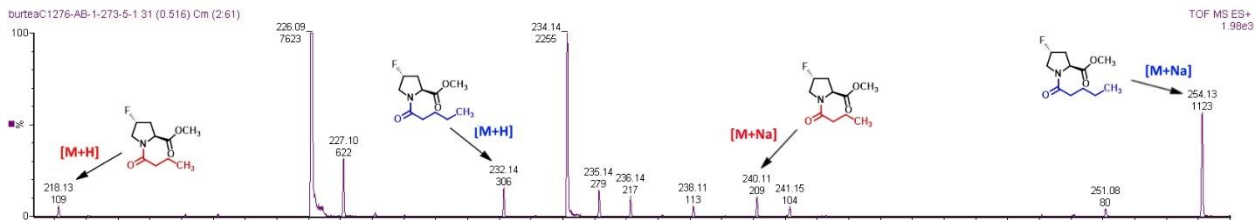
$[M+H] + [M+Na] = 14706 + 29624 = 44330$ \rightarrow $44330 / (44330 + 30680) (100) = 59\%$

$[M+H] + [M+Na] = 7683 + 22997 = 30680$ \rightarrow $30680 / (44330 + 30680) (100) = 41\%$



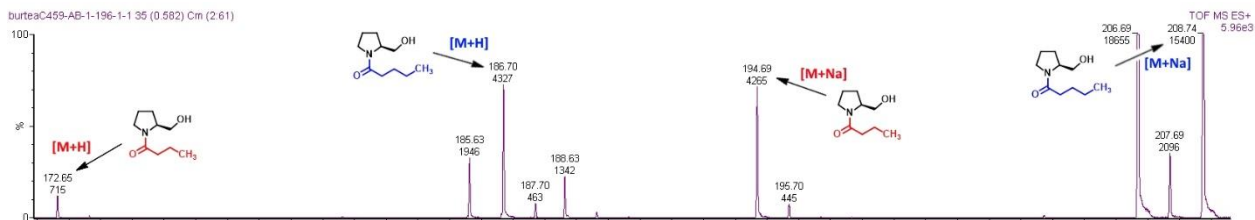
$[M+H] + [M+Na] = 109 + 209 = 318$ \rightarrow $318 / (318 + 1429) (100) = 18\%$

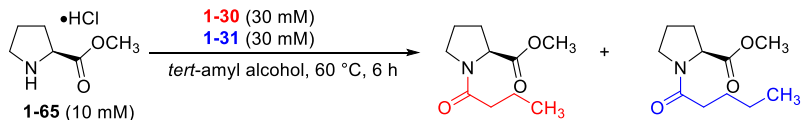
$[M+H] + [M+Na] = 306 + 1123 = 1429$ \rightarrow $1429 / (318 + 1429) (100) = 82\%$



$[M+H] + [M+Na] = 715 + 4265 = 4980$ \rightarrow $4980 / (4980 + 19727) (100) = 20\%$

$[M+H] + [M+Na] = 4327 + 15400 = 19727$ \rightarrow $19727 / (4980 + 19727) (100) = 80\%$



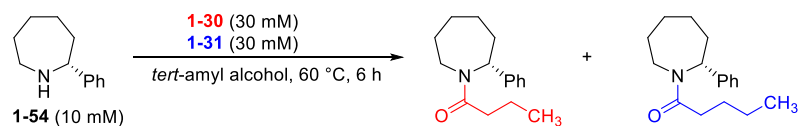
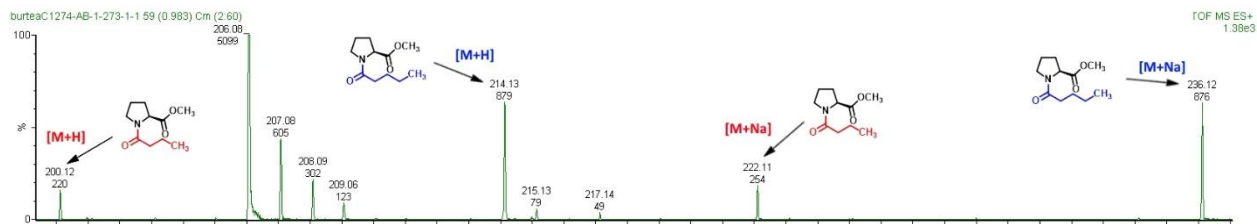


$$[M+H] + [M+Na] = 220 + 254 = 474$$

$$[M+H] + [M+Na] = 879 + 876 = 1755$$

$$474 / (474 + 1755) (100) = 21\%$$

$$1755 / (474 + 1755) (100) = 79\%$$

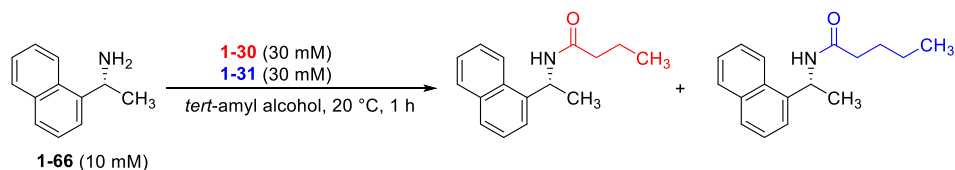
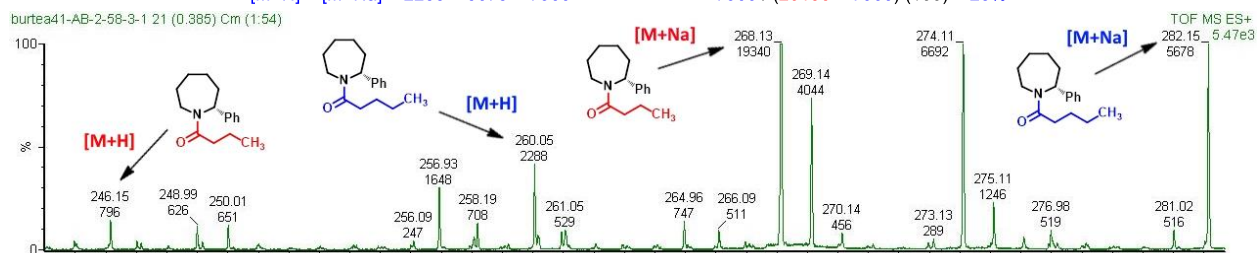


$$[M+H] + [M+Na] = 796 + 19340 = 20136$$

$$[M+H] + [M+Na] = 2288 + 5678 = 7966$$

$$20136 / (20136 + 7966) (100) = 72\%$$

$$7966 / (20136 + 7966) (100) = 28\%$$

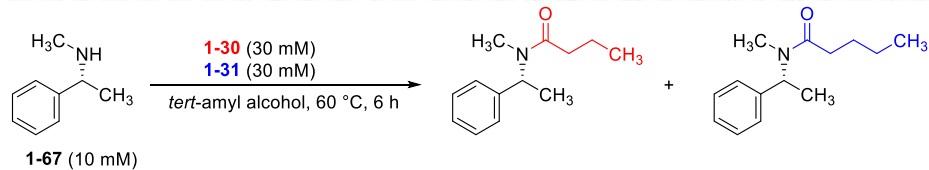
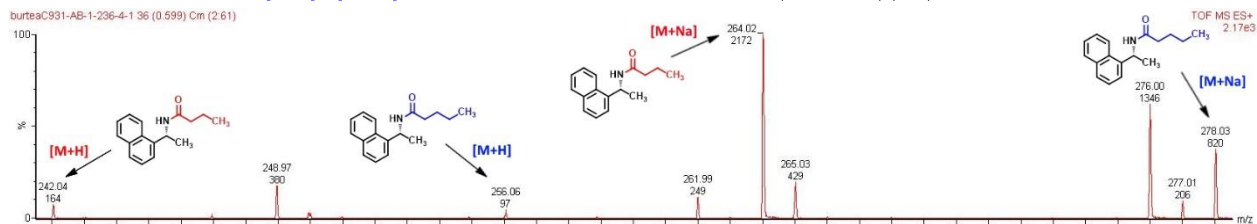


$$[M+H] + [M+Na] = 164 + 2172 = 2336$$

$$[M+H] + [M+Na] = 97 + 820 = 917$$

$$2336 / (2336 + 917) (100) = 72\%$$

$$917 / (2336 + 917) (100) = 28\%$$

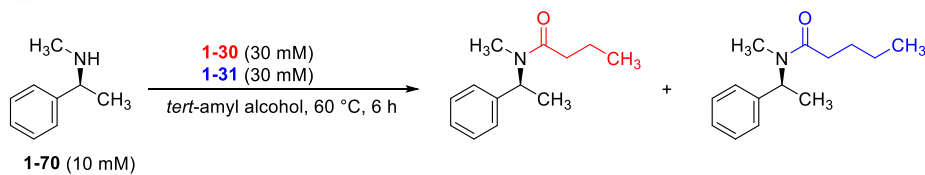
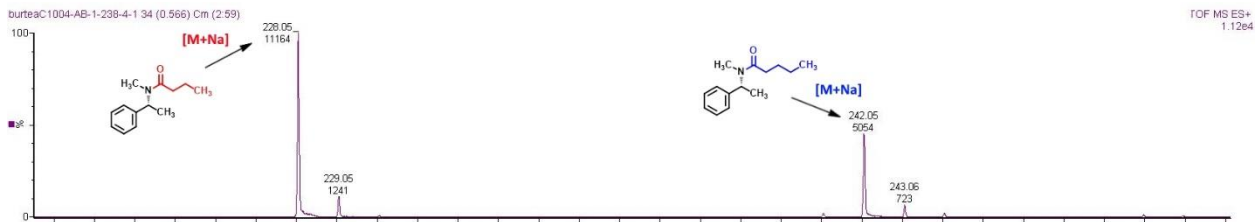


$$[M+Na] = 11164$$

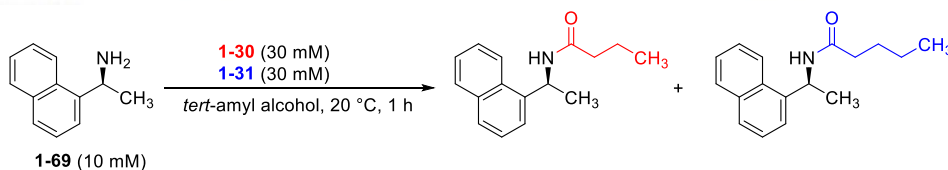
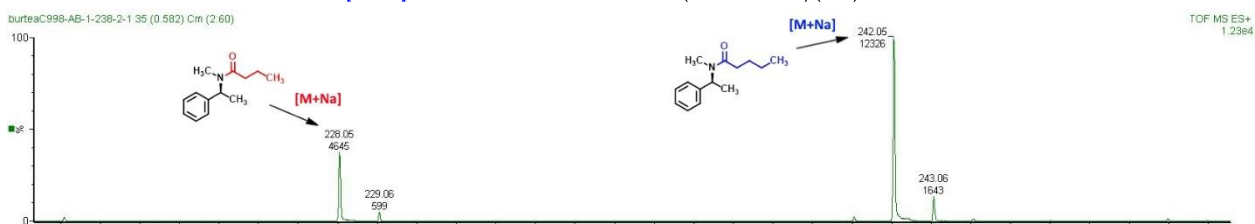
$$[M+Na] = 5054$$

$$11164 / (11164 + 5054) (100) = 69\%$$

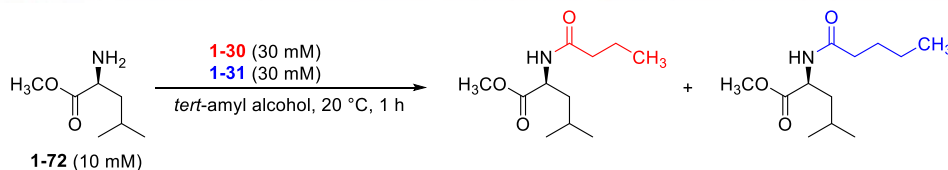
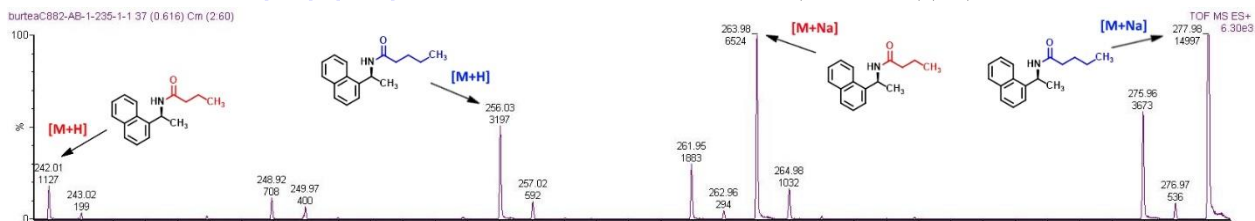
$$5054 / (11164 + 5054) (100) = 31\%$$



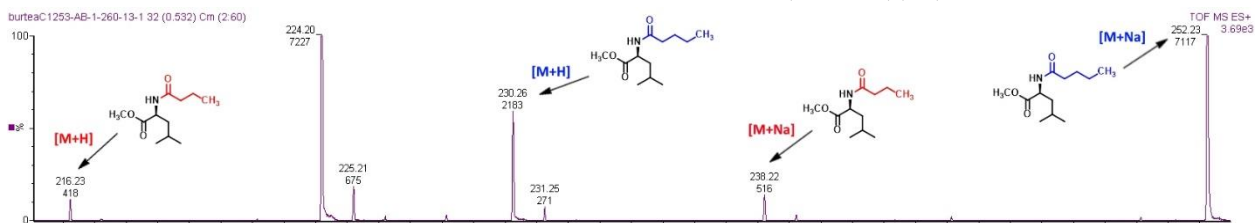
$$\begin{aligned}
 &[\text{M}+\text{Na}] = 4645 \quad \rightarrow \quad 4645 / (4645 + 12326) (100) = 27\% \\
 &[\text{M}+\text{Na}] = 12326 \quad \rightarrow \quad 12326 / (4645 + 12326) (100) = 73\%
 \end{aligned}$$

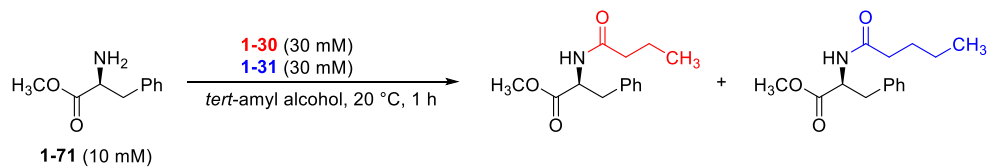


$$\begin{aligned}
 &[\text{M}+\text{H}] + [\text{M}+\text{Na}] = 1127 + 6524 = 7651 \quad \rightarrow \quad 7651 / (7651 + 18194) (100) = 30\% \\
 &[\text{M}+\text{H}] + [\text{M}+\text{Na}] = 3197 + 14997 = 18194 \quad \rightarrow \quad 18194 / (7651 + 18194) (100) = 70\%
 \end{aligned}$$



$$\begin{aligned}
 &[\text{M}+\text{H}] + [\text{M}+\text{Na}] = 418 + 516 = 934 \quad \rightarrow \quad 934 / (934 + 9300) (100) = 9\% \\
 &[\text{M}+\text{H}] + [\text{M}+\text{Na}] = 2183 + 7117 = 9300 \quad \rightarrow \quad 9300 / (934 + 9300) (100) = 91\%
 \end{aligned}$$



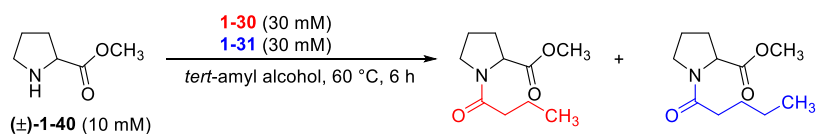
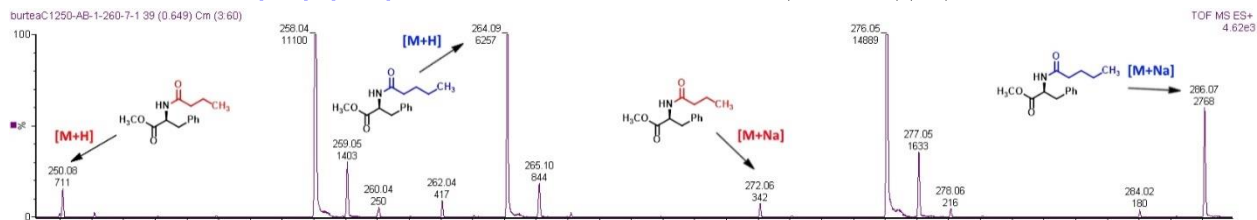


$$[M+H] + [M+Na] = 711 + 342 = 1053$$

$$1053 / (1053 + 9025) (100) = 10\%$$

$$[M+H] + [M+Na] = 6257 + 2768 = 9025$$

$$9025 / (1053 + 9025) (100) = 90\%$$

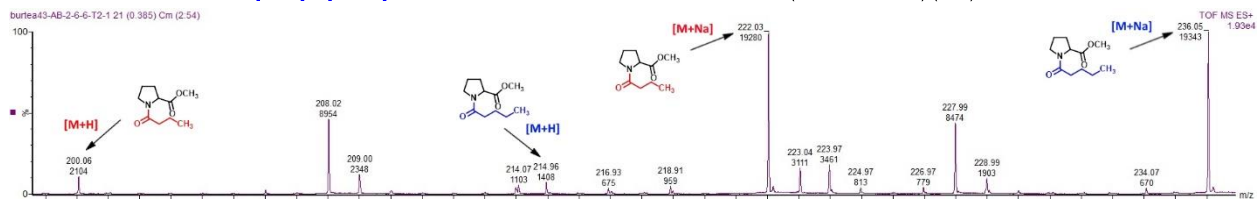


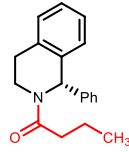
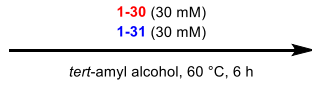
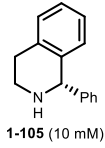
$$[M+H] + [M+Na] = 2104 + 19280 = 21384$$

$$21384 / (21384 + 20751) (100) = 51\%$$

$$[M+H] + [M+Na] = 1408 + 19343 = 20751$$

$$20751 / (21384 + 20751) (100) = 49\%$$

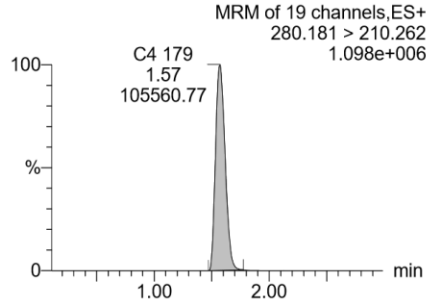




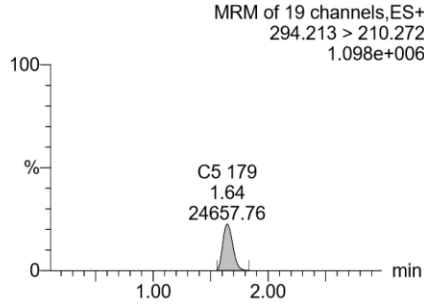
+



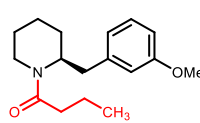
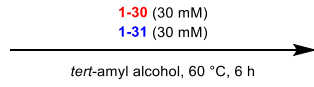
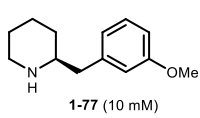
C4 Amide:



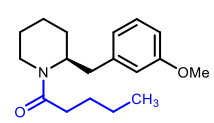
C5 Amide:



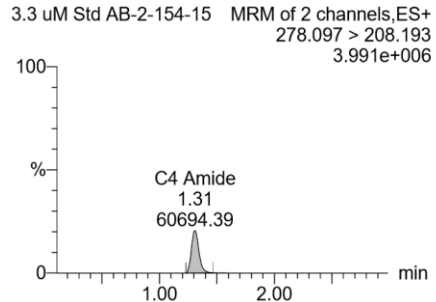
C4	:	C5
105560.77	:	24657.76
81	:	19



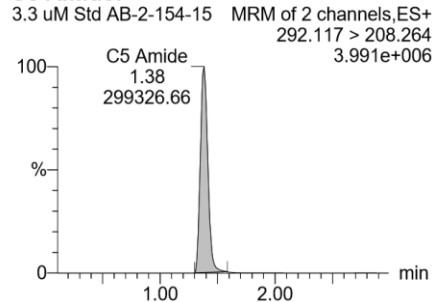
+



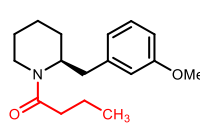
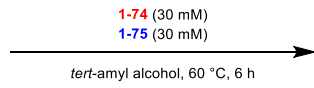
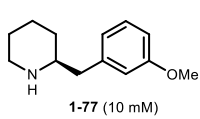
C4 Amide:



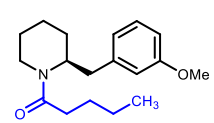
C5 Amide:



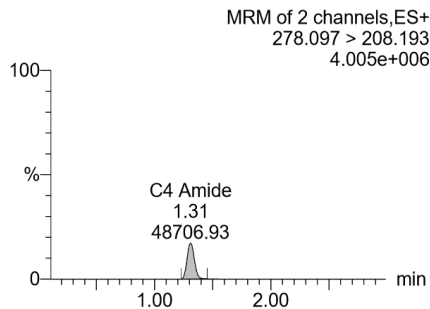
C4	:	C5
60694.39	:	299326.66
17	:	83



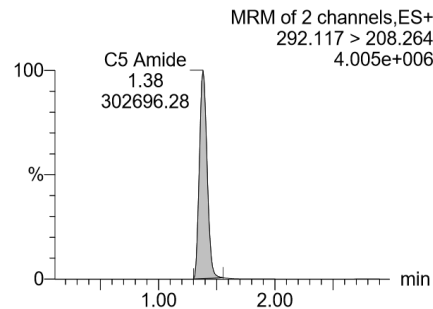
+



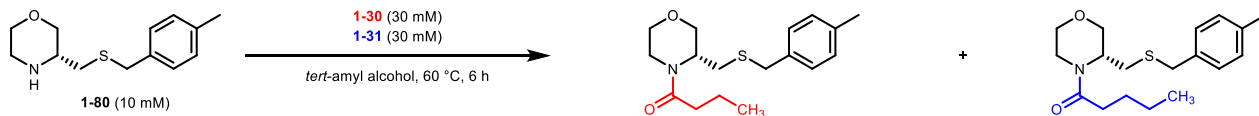
C4 Amide:



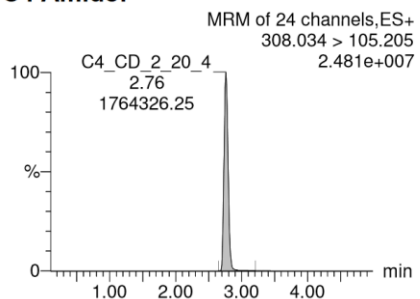
C5 Amide:



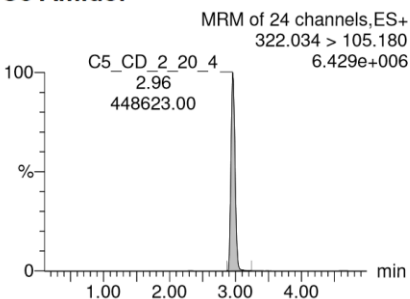
C4	:	C5
48706.93	:	302696.28
14	:	86



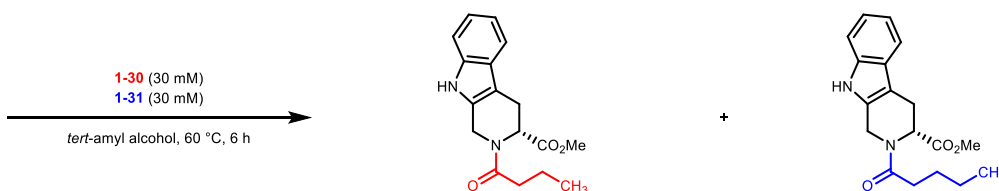
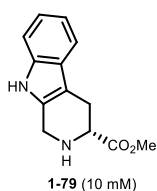
C4 Amide:



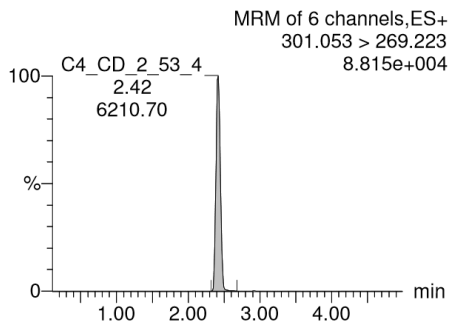
C5 Amide:



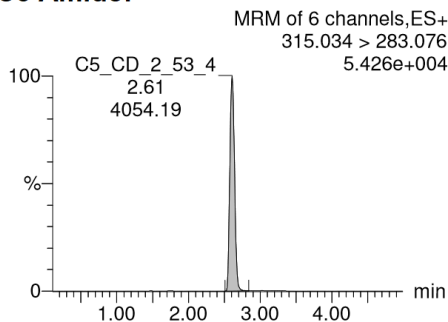
C4	:	C5
1764326.25	:	448623.00
80	:	20



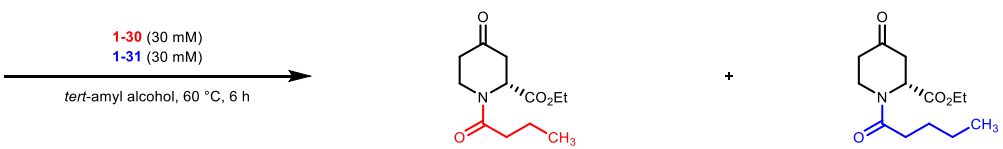
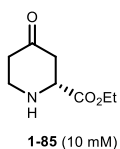
C4 Amide:



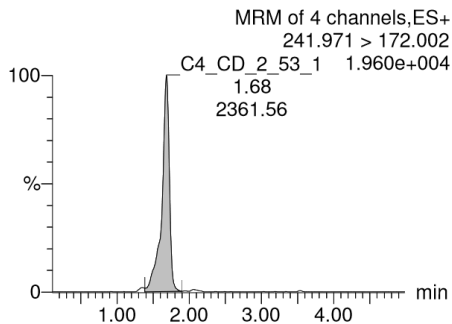
C5 Amide:



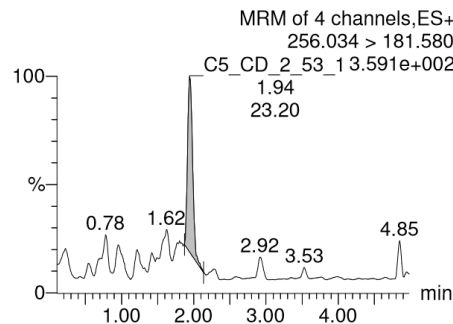
C4	:	C5
6210.7	:	4054.19
61	:	39



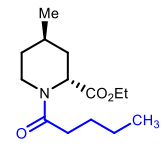
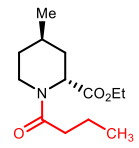
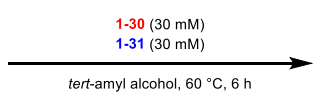
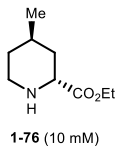
C4 Amide:



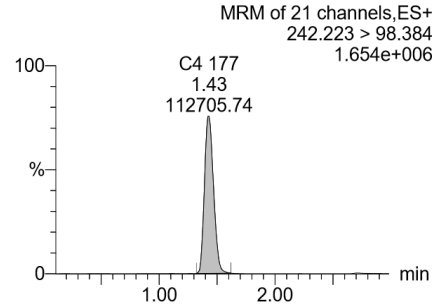
C5 Amide:



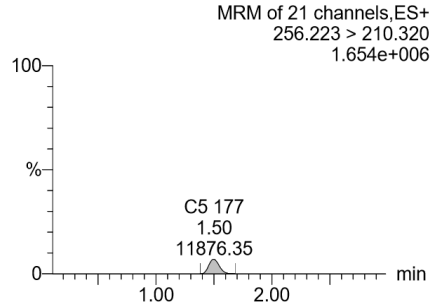
C4	:	C5
2361.56	:	23.20
99	:	1



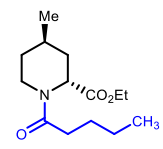
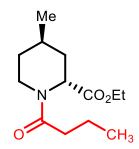
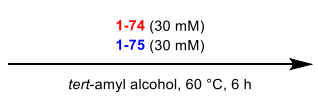
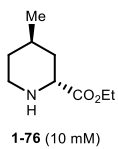
C4 Amide:



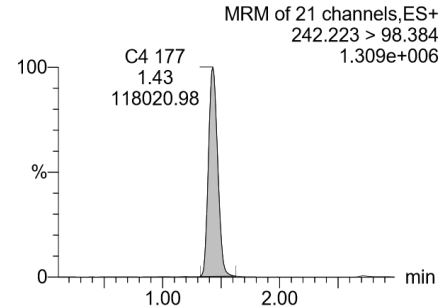
C5 Amide:



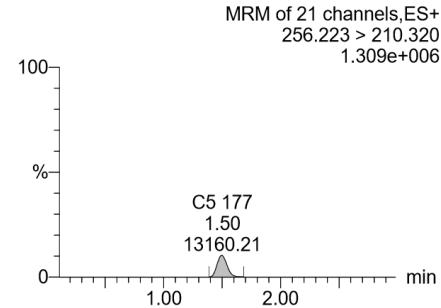
C4	:	C5
112705.74	:	11876.35
90	:	10



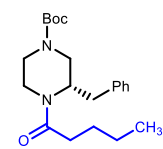
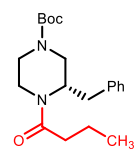
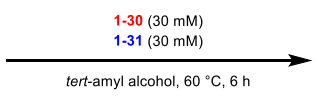
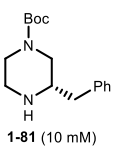
C4 Amide:



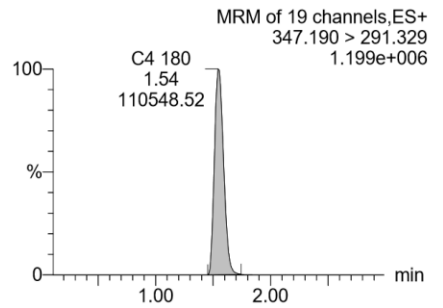
C5 Amide:



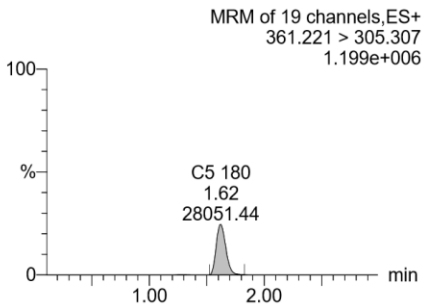
C4	:	C5
118020.98	:	13160.21
90	:	10



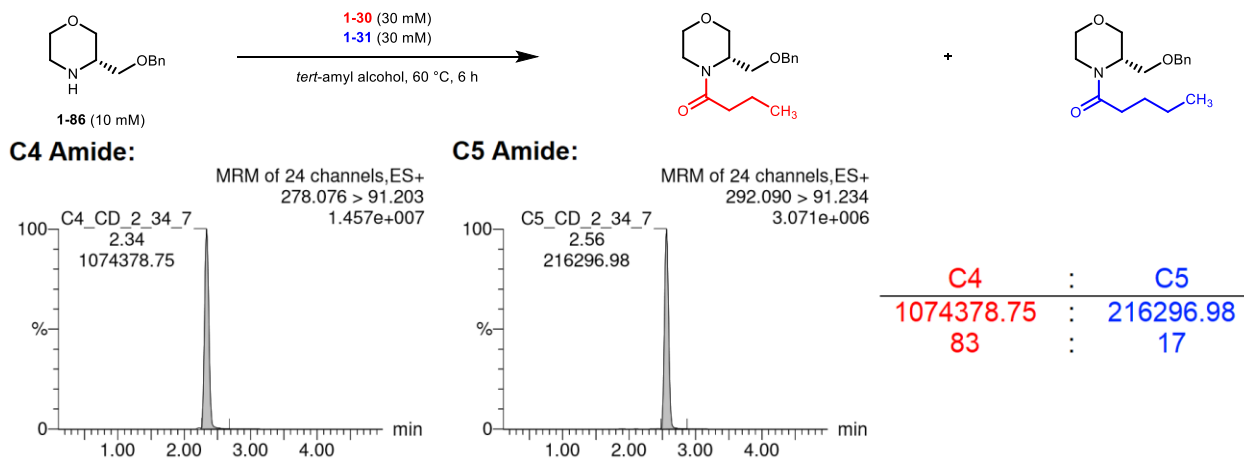
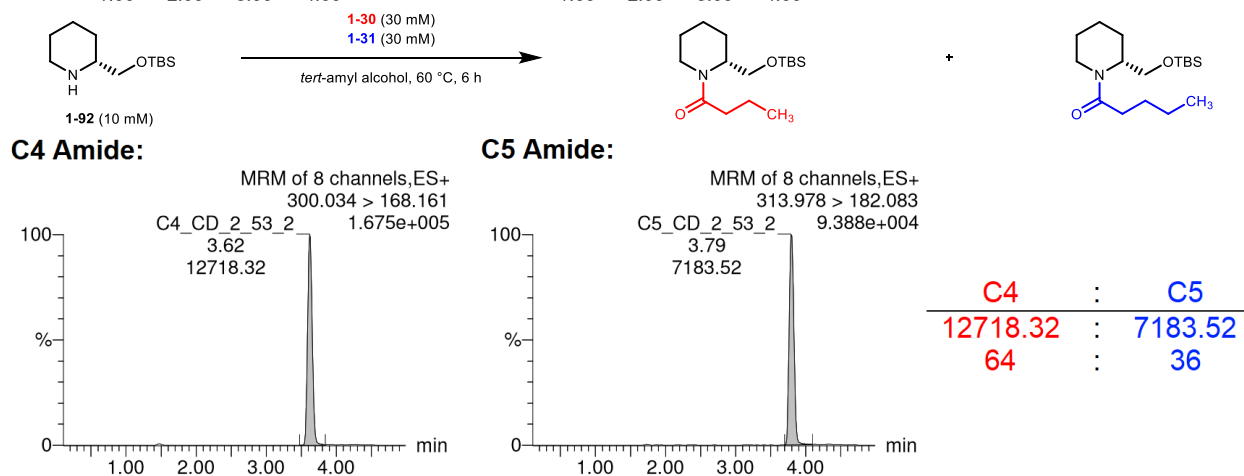
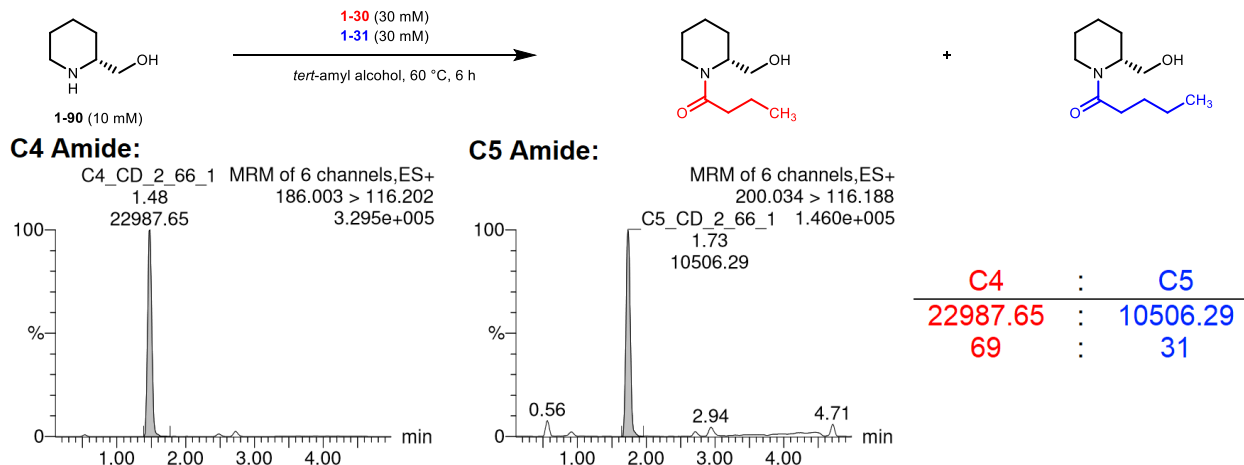
C4 Amide:



C5 Amide:

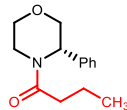
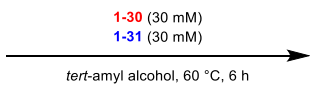


C4	:	C5
110548.52	:	28051.44
80	:	20

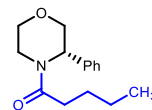




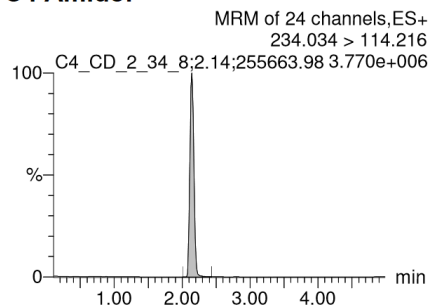
1-87 (10 mM)



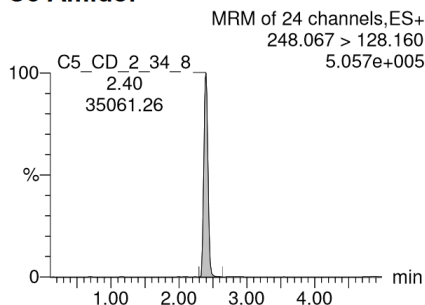
+



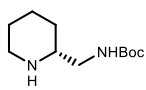
C4 Amide:



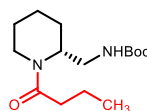
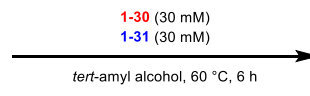
C5 Amide:



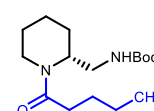
C4	:	C5
255663.98	:	35061.26
88	:	12



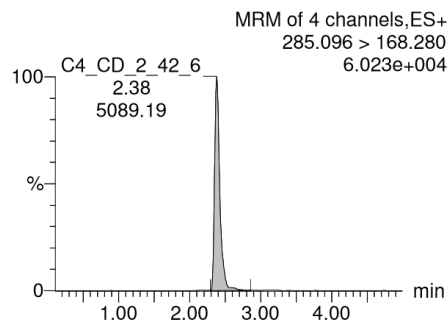
1-91 (10 mM)



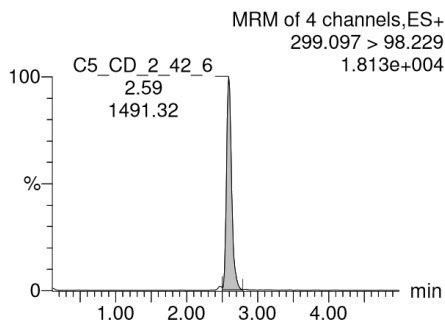
+



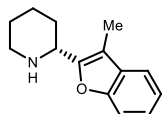
C4 Amide:



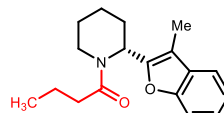
C5 Amide:



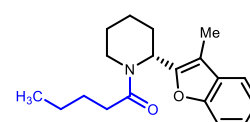
C4	:	C5
5089.19	:	1491.32
77	:	23



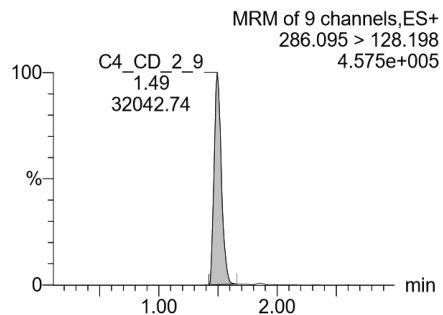
1-96 (10 mM)



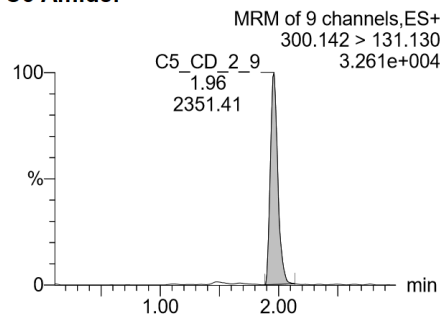
+



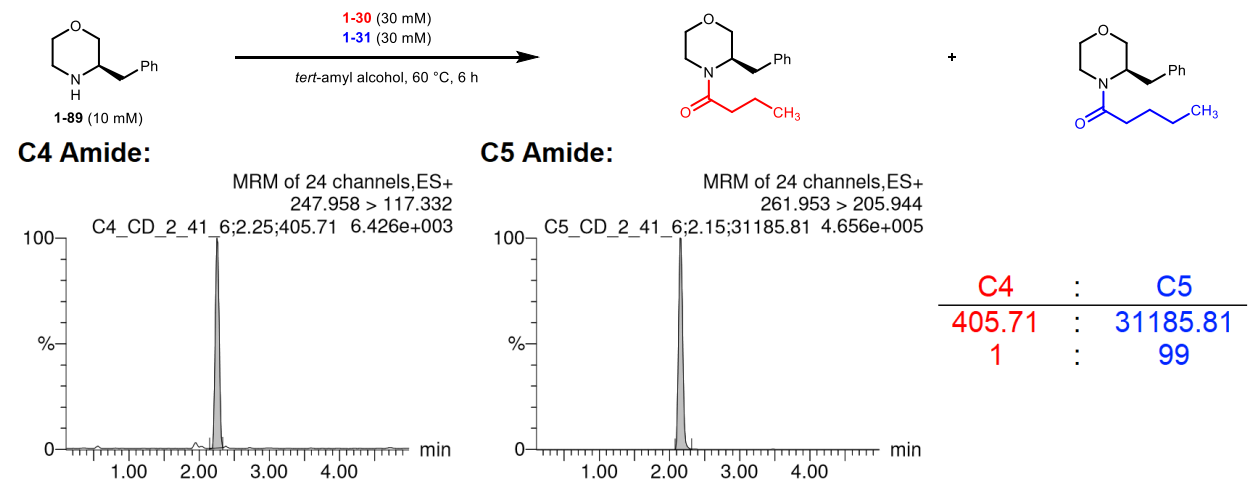
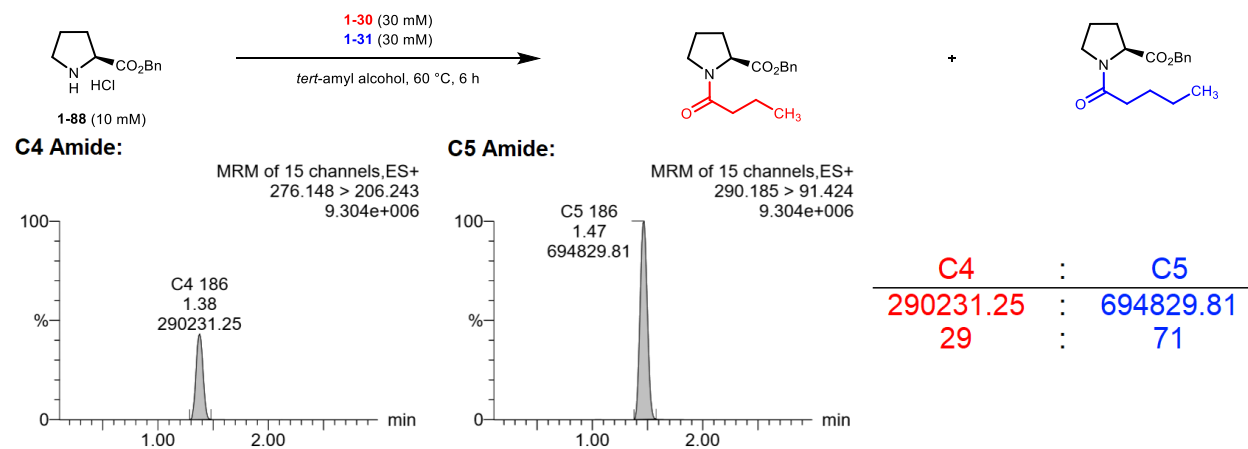
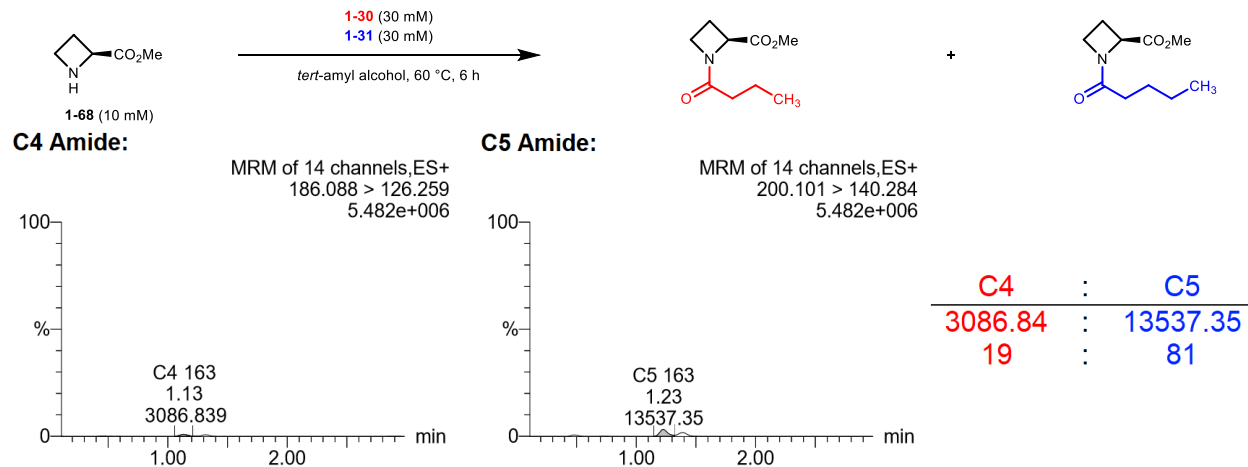
C4 Amide:

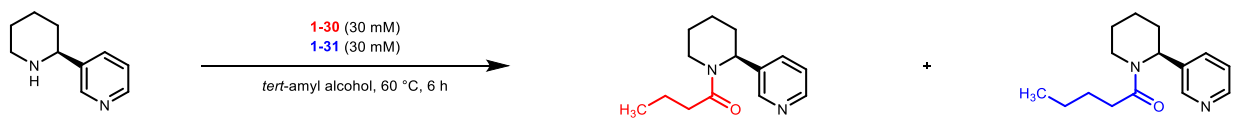


C5 Amide:

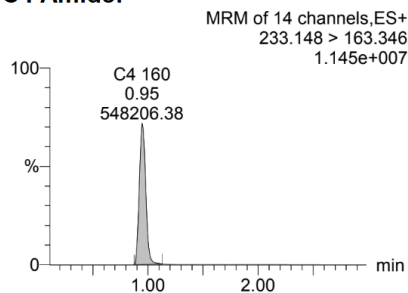


C4	:	C5
32042.74	:	2351.41
93	:	7

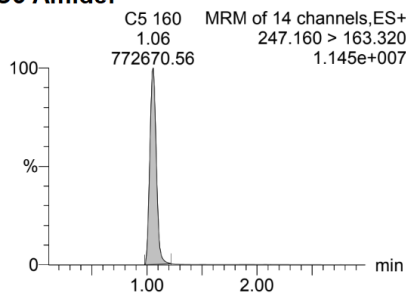




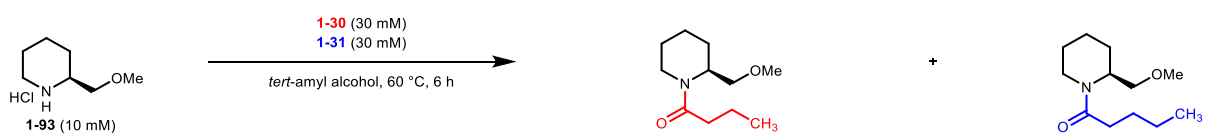
C4 Amide:



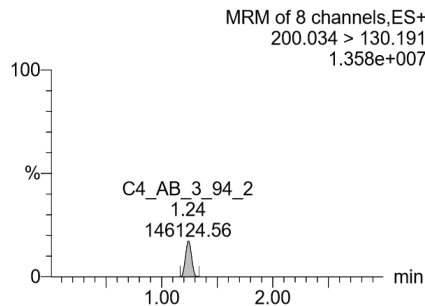
C5 Amide:



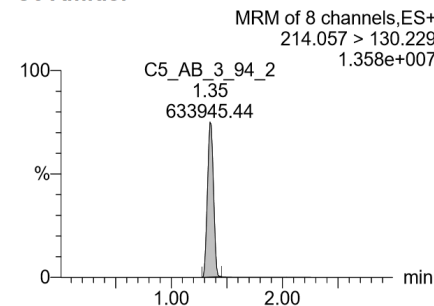
C4	:	C5
548206.38	:	772670.56
42	:	58



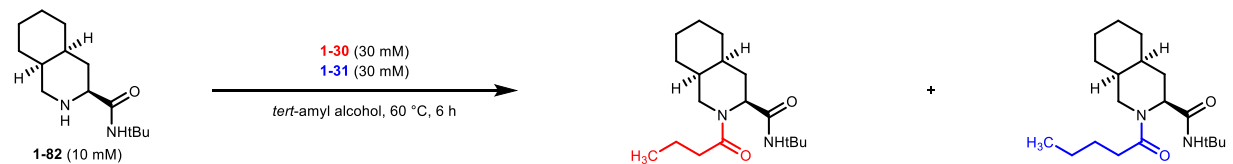
C4 Amide:



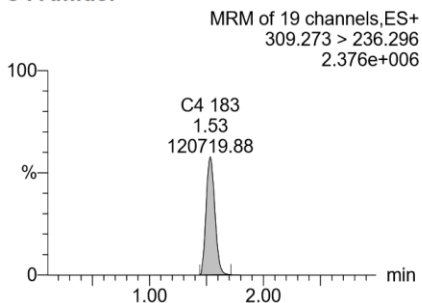
C5 Amide:



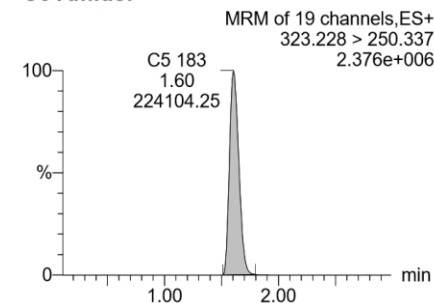
C4	:	C5
146124.56	:	633945.44
19	:	81



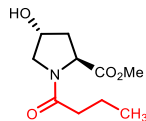
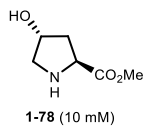
C4 Amide:



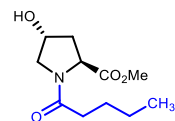
C5 Amide:



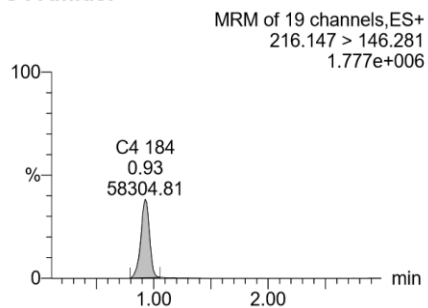
C4	:	C5
120719.88	:	224104.25
35	:	65



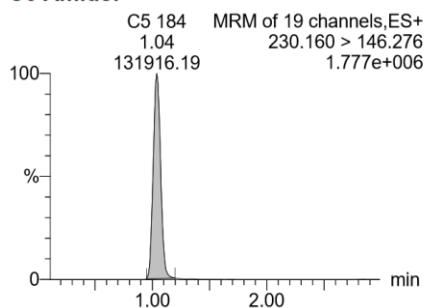
+



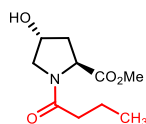
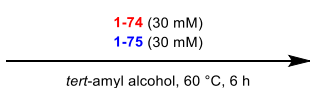
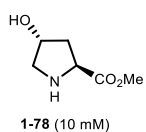
C4 Amide:



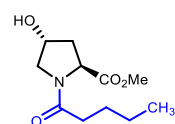
C5 Amide:



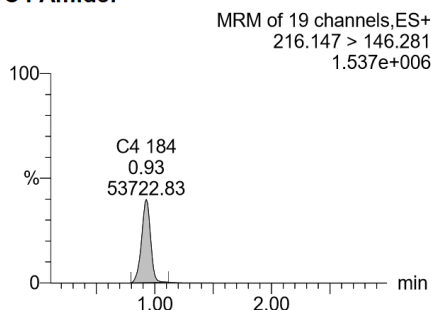
C4	:	C5
58304.81	:	131916.19
31	:	69



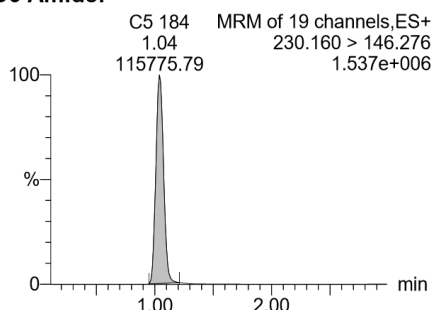
+



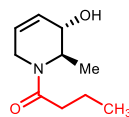
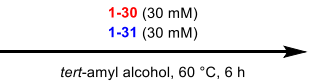
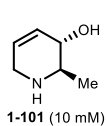
C4 Amide:



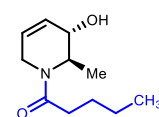
C5 Amide:



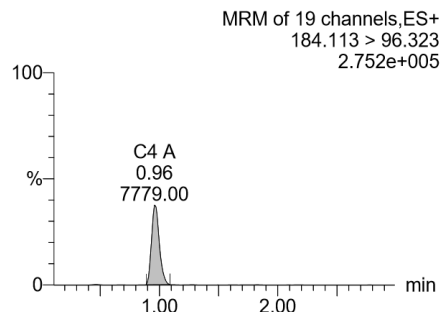
C4	:	C5
53722.83	:	115775.79
32	:	68



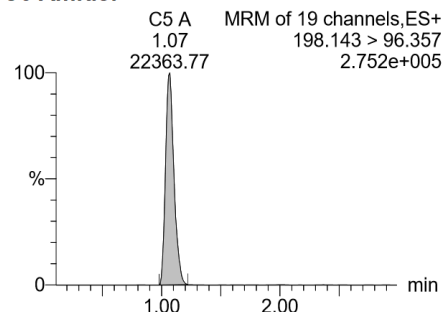
+



C4 Amide:



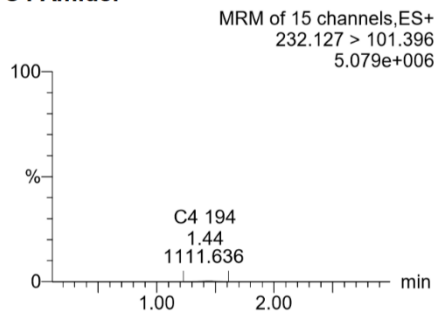
C5 Amide:



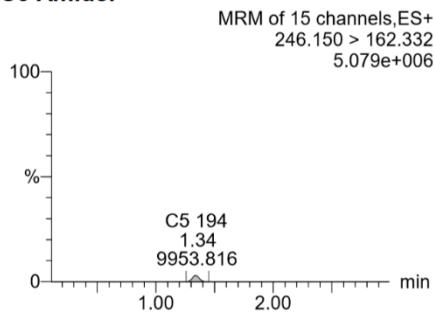
C4	:	C5
7779.00	:	22363.77
26	:	74



C4 Amide:



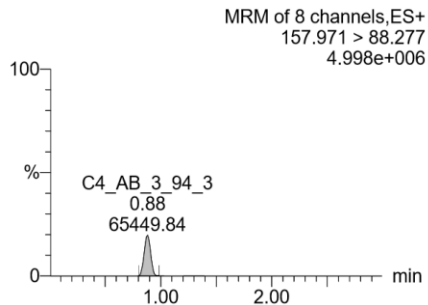
C5 Amide:



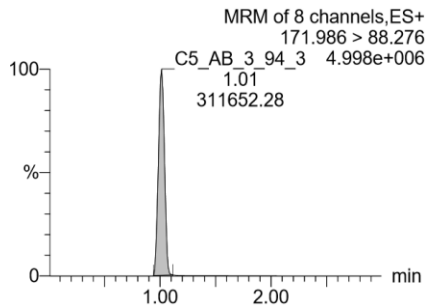
C4	:	C5
1111.636	:	9953.816
10	:	90



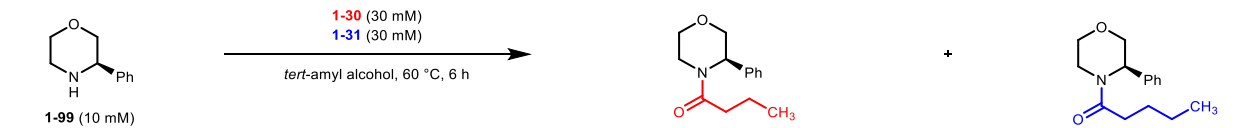
C4 Amide:



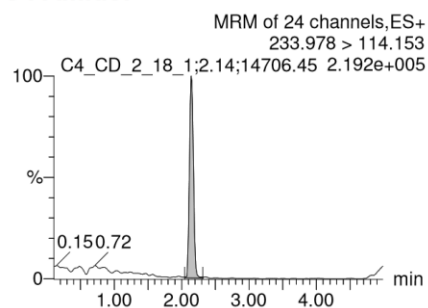
C5 Amide:



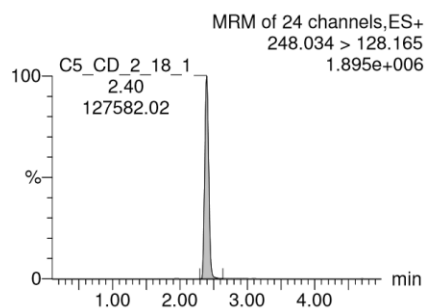
C4	:	C5
65449.84	:	311652.28
17	:	83



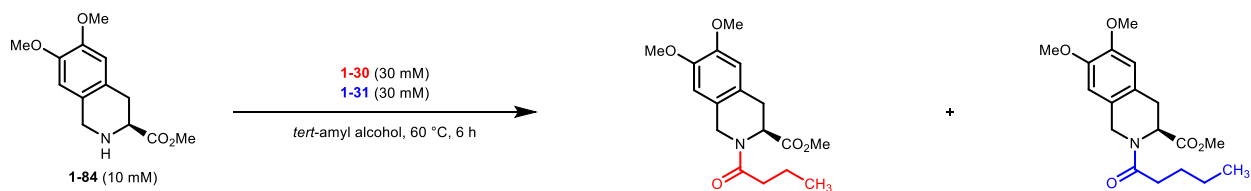
C4 Amide:



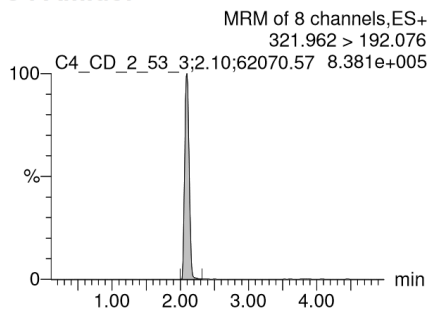
C5 Amide:



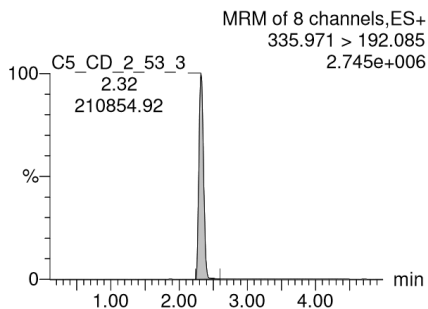
C4	:	C5
14706.45	:	127582.02
10	:	90



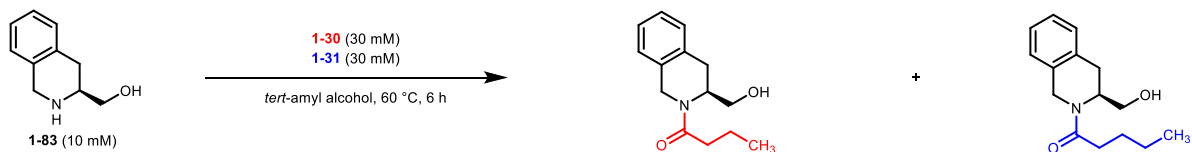
C4 Amide:



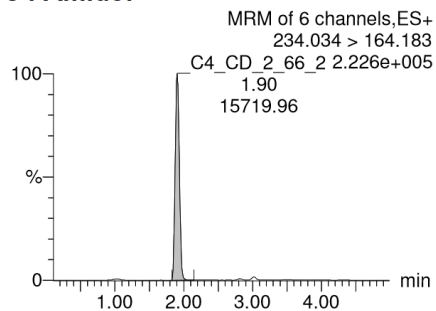
C5 Amide:



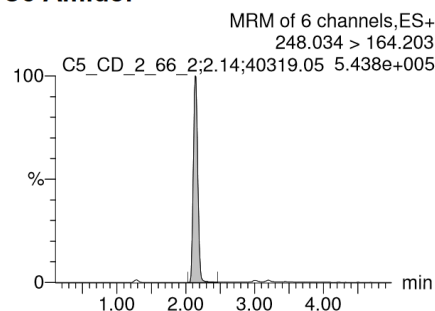
C4	:	C5
62070.57	:	210854.92
23	:	77



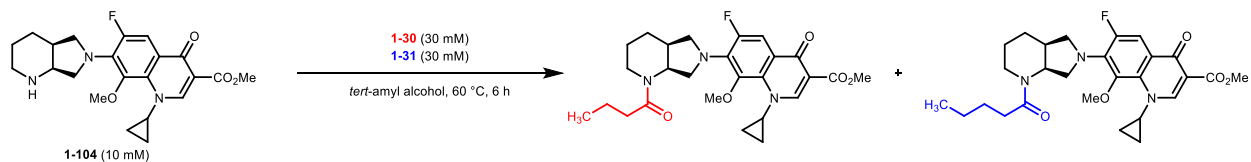
C4 Amide:



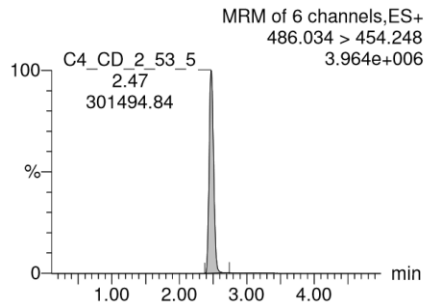
C5 Amide:



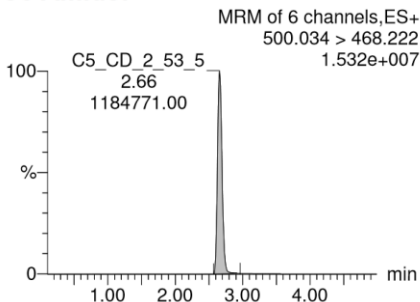
C4	:	C5
15719.96	:	40319.05
28	:	72



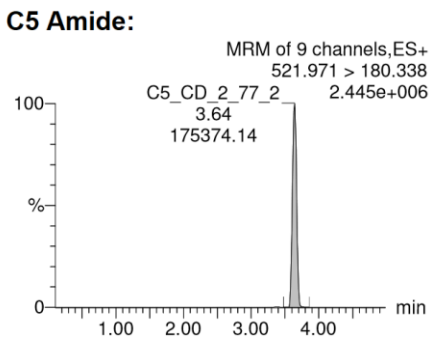
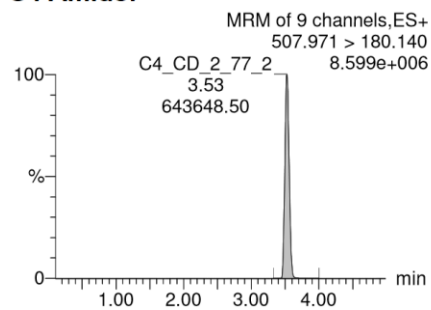
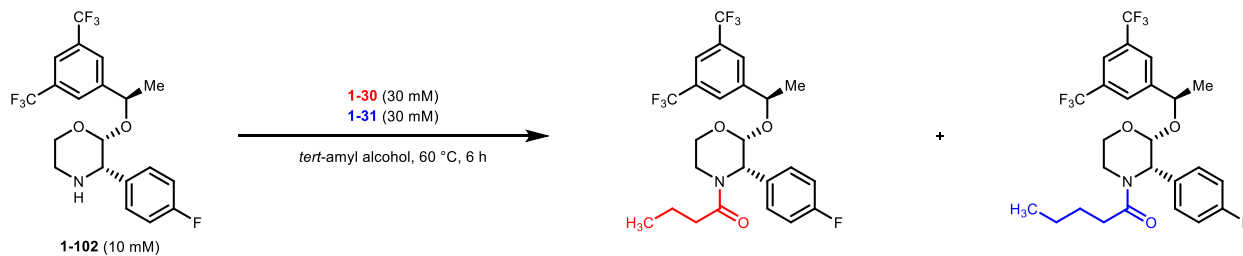
C4 Amide:



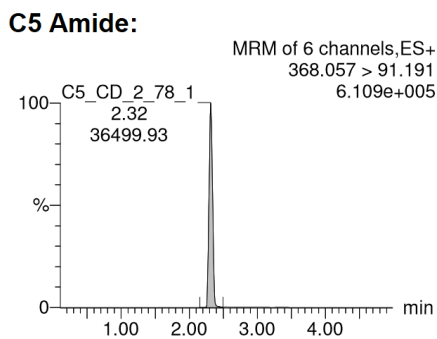
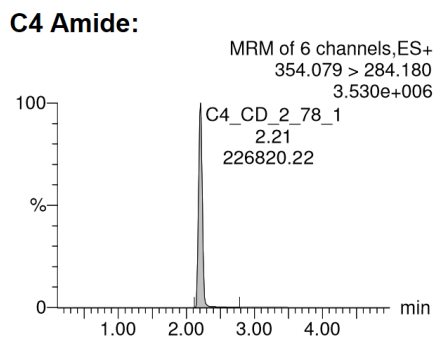
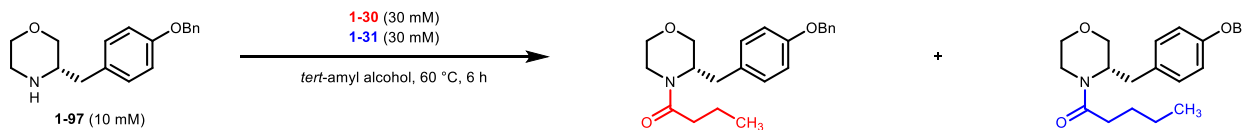
C5 Amide:



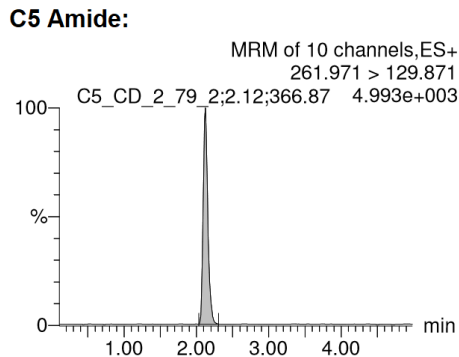
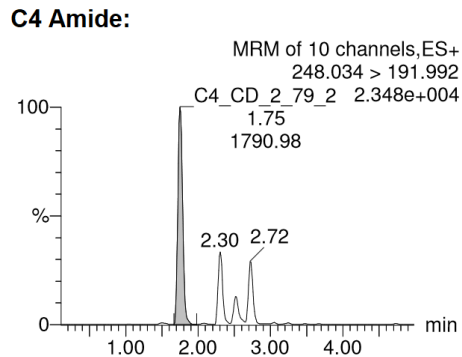
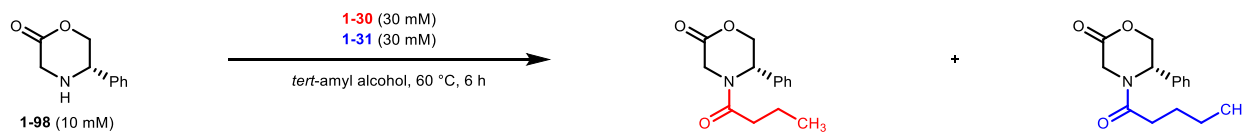
C4	:	C5
301494.84	:	1184771.00
20	:	80



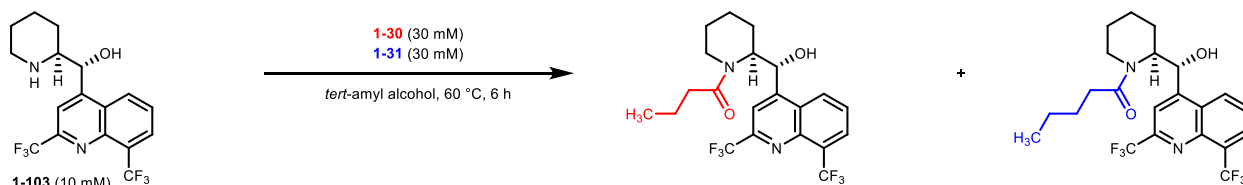
C4	:	C5
643648.50	:	175374.14
79	:	21



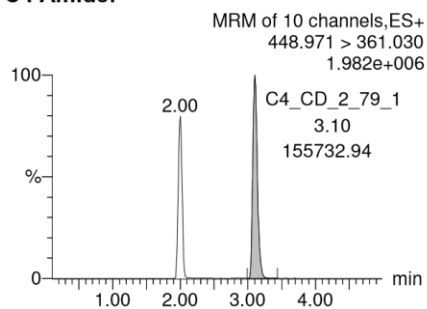
C4	:	C5
226820.22	:	36499.93
86	:	14



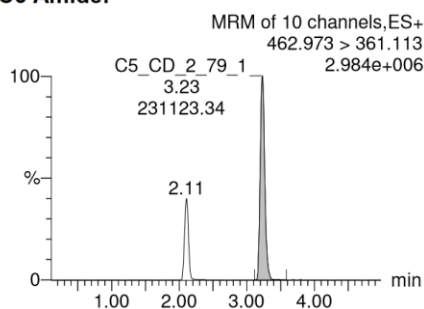
C4	:	C5
1790.98	:	366.87
83	:	17



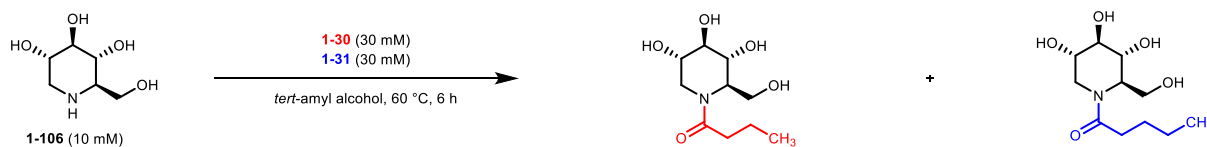
C4 Amide:



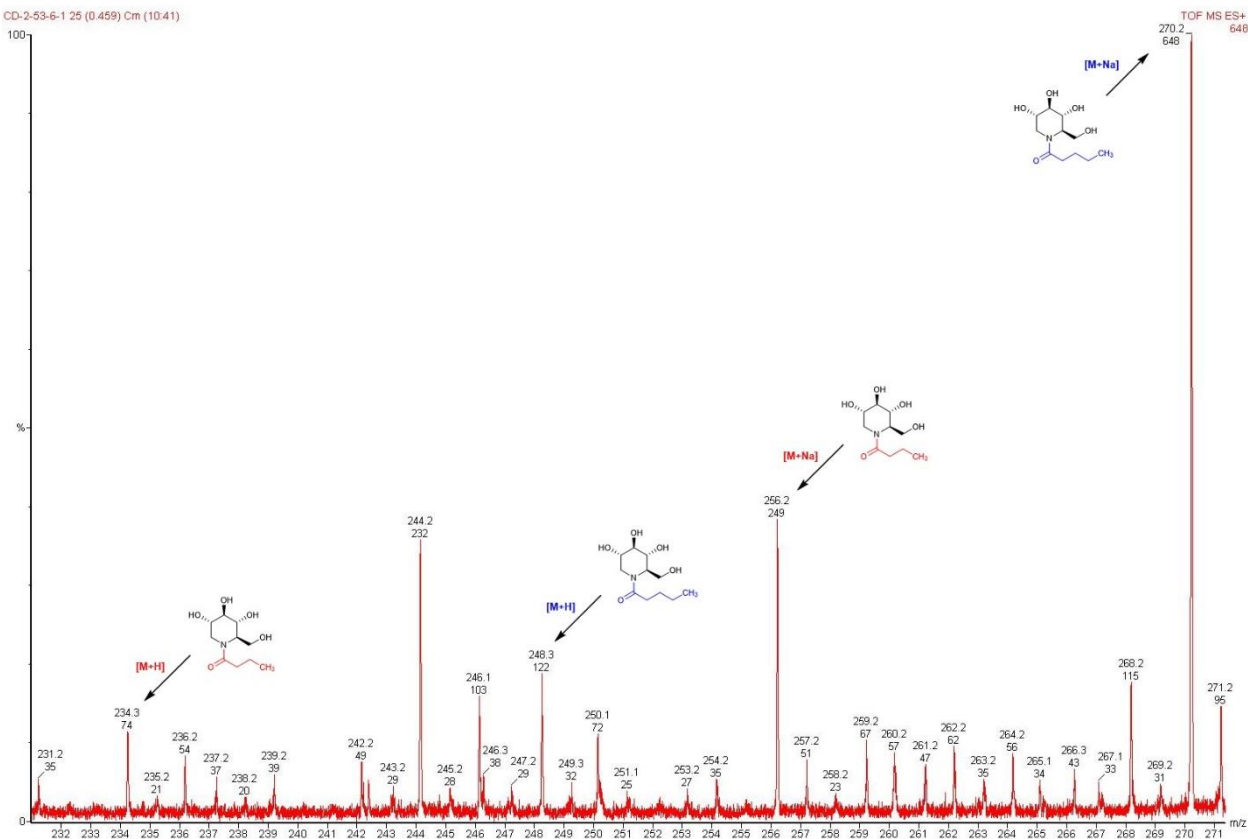
C5 Amide:



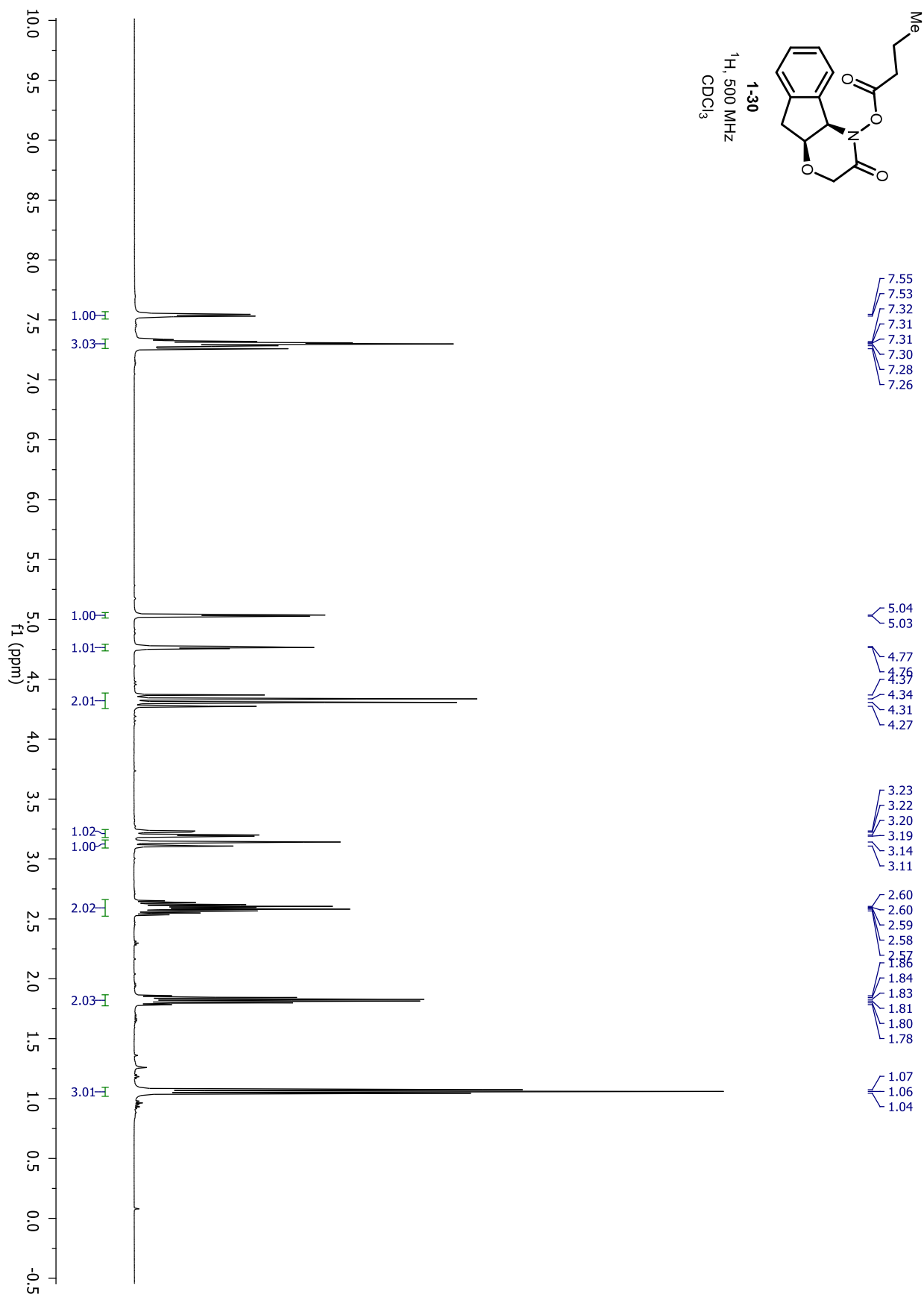
C4	:	C5
155732.94	:	231123.34
40	:	60

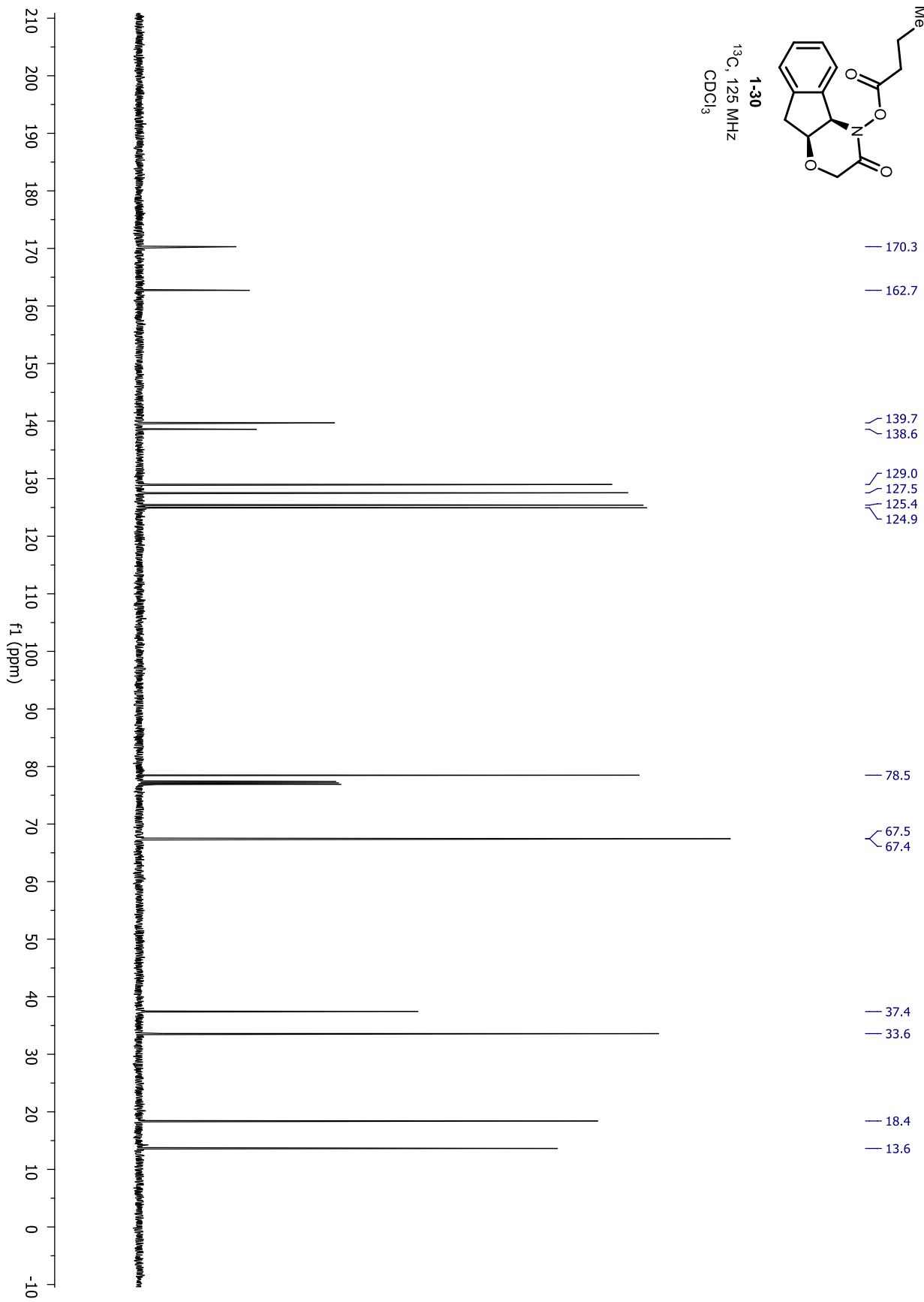
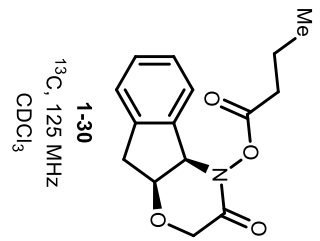


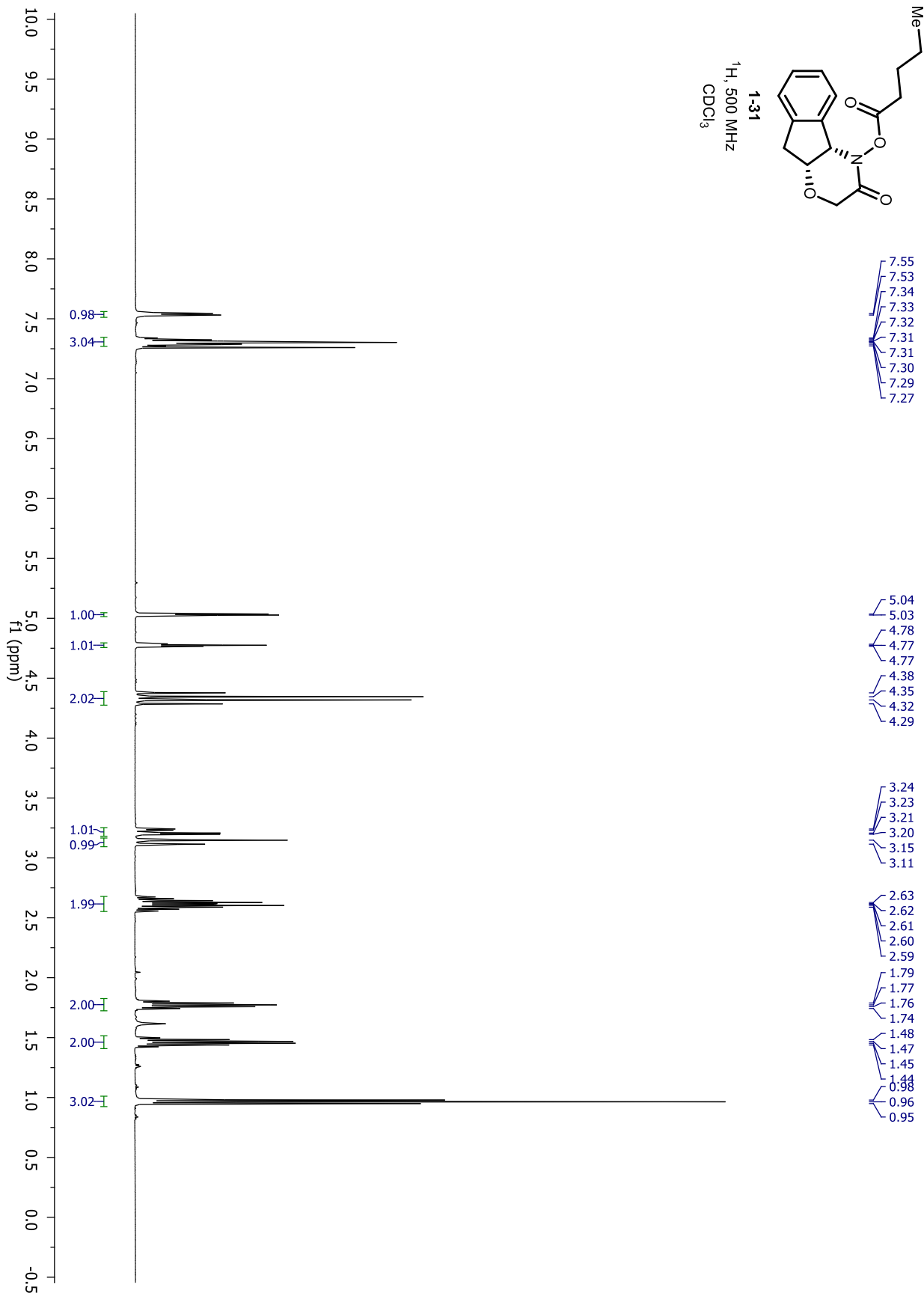
CD-2-53-6-1 25 (0.459) Cm (10.41)

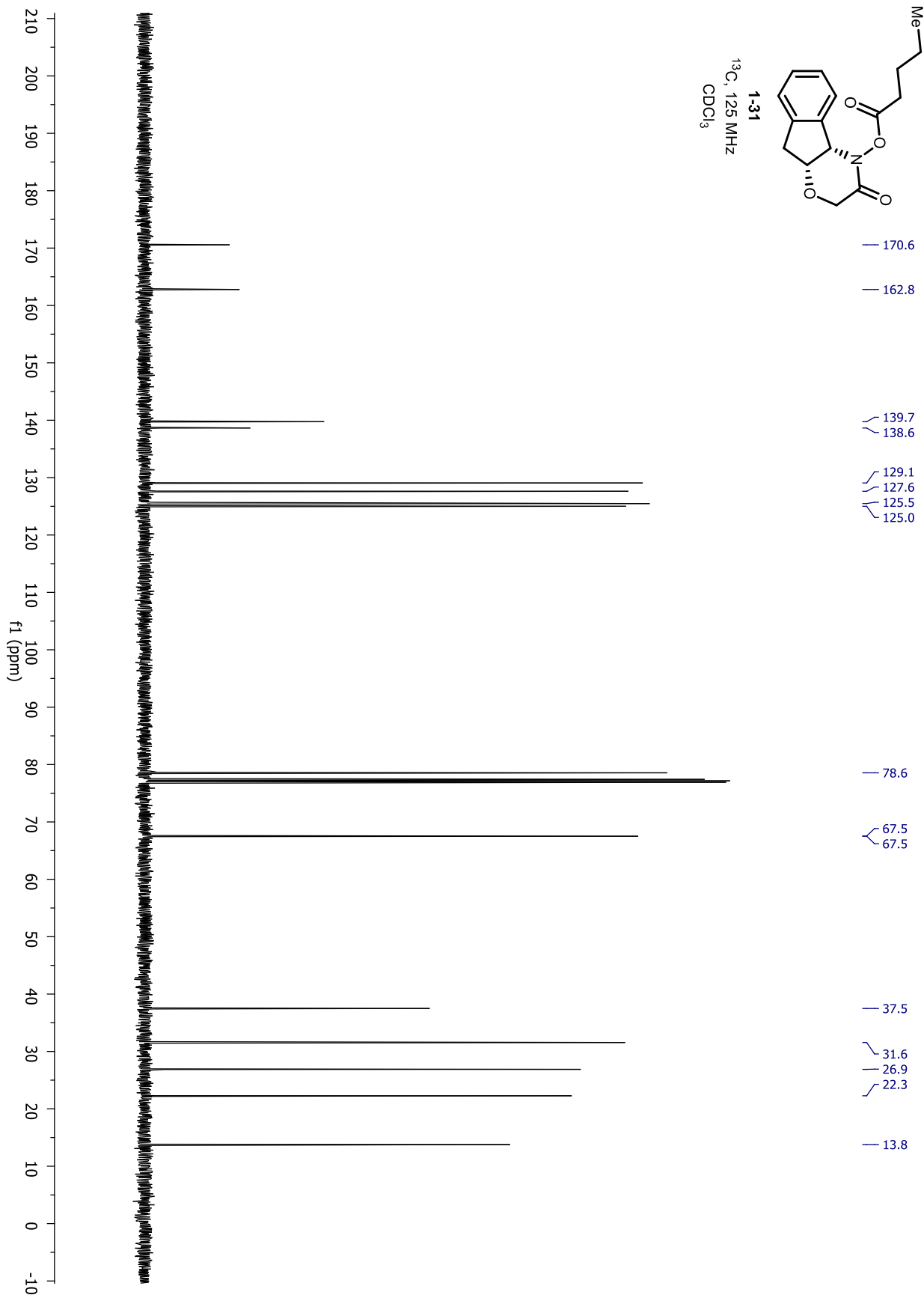


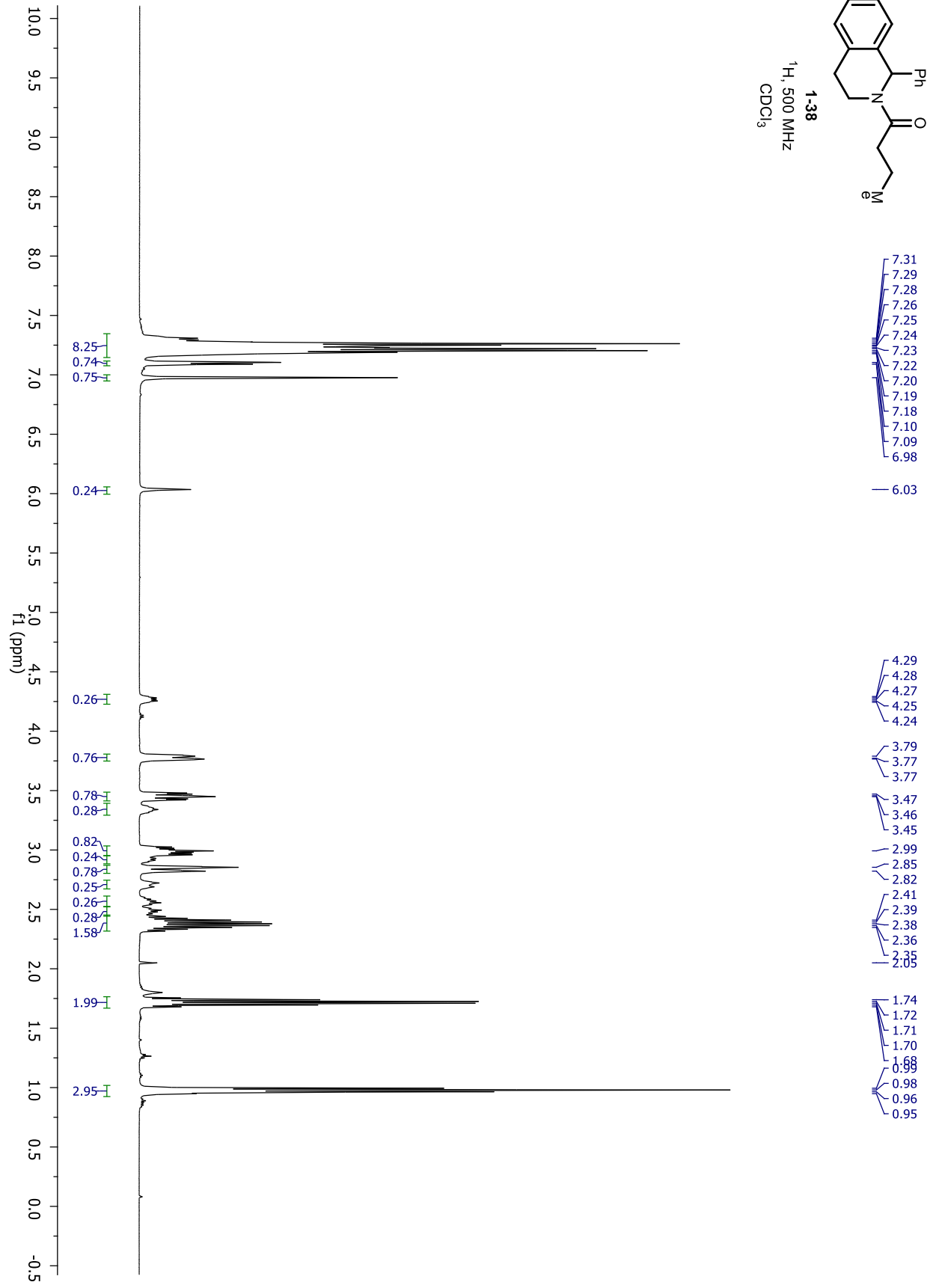
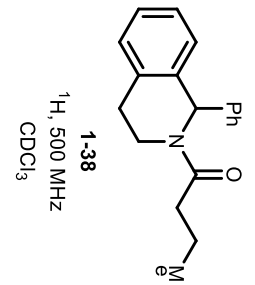
Appendix B NMR Spectra

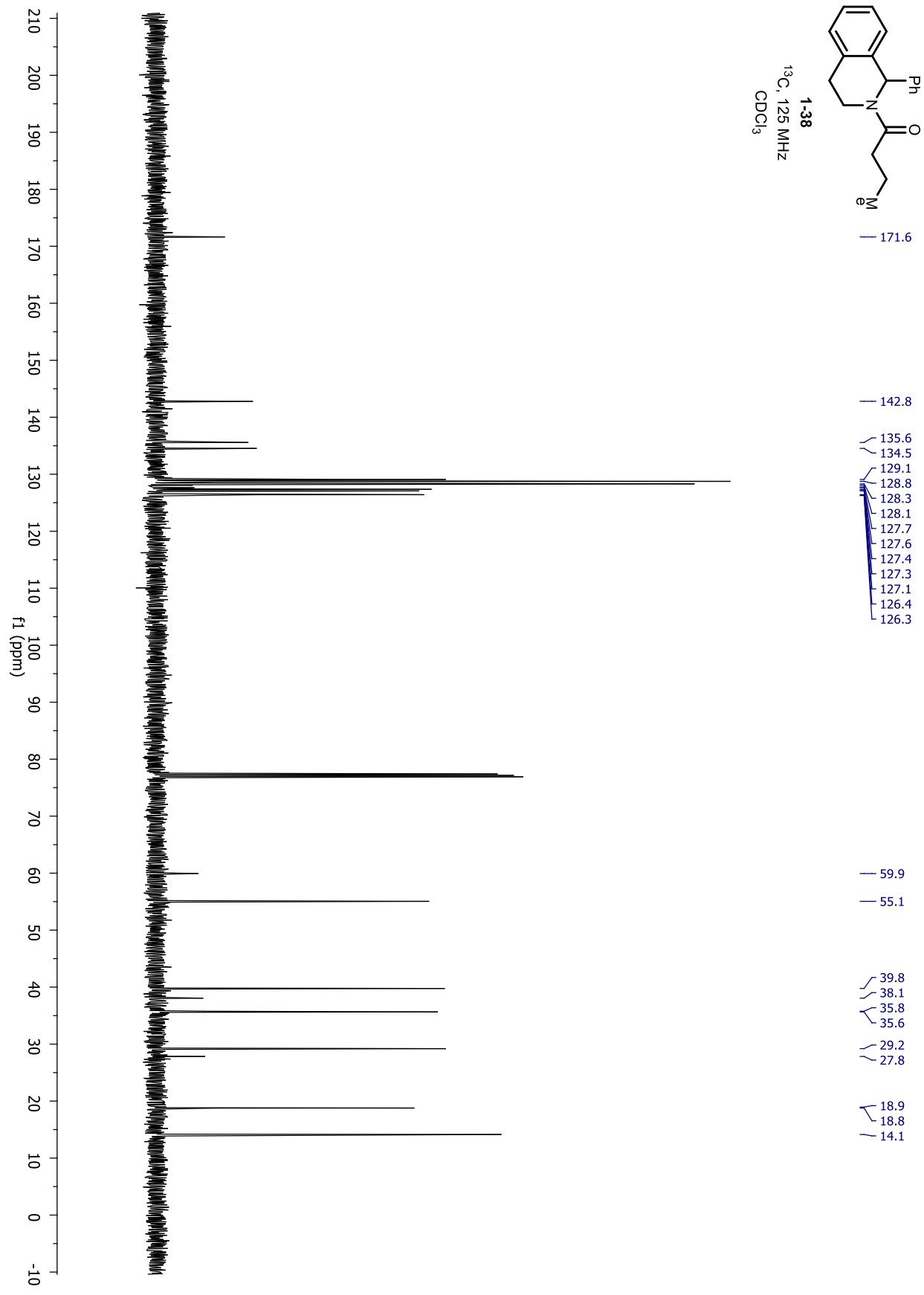
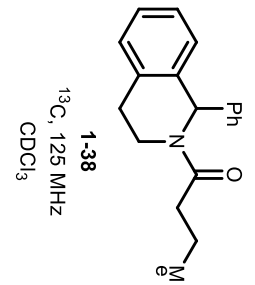


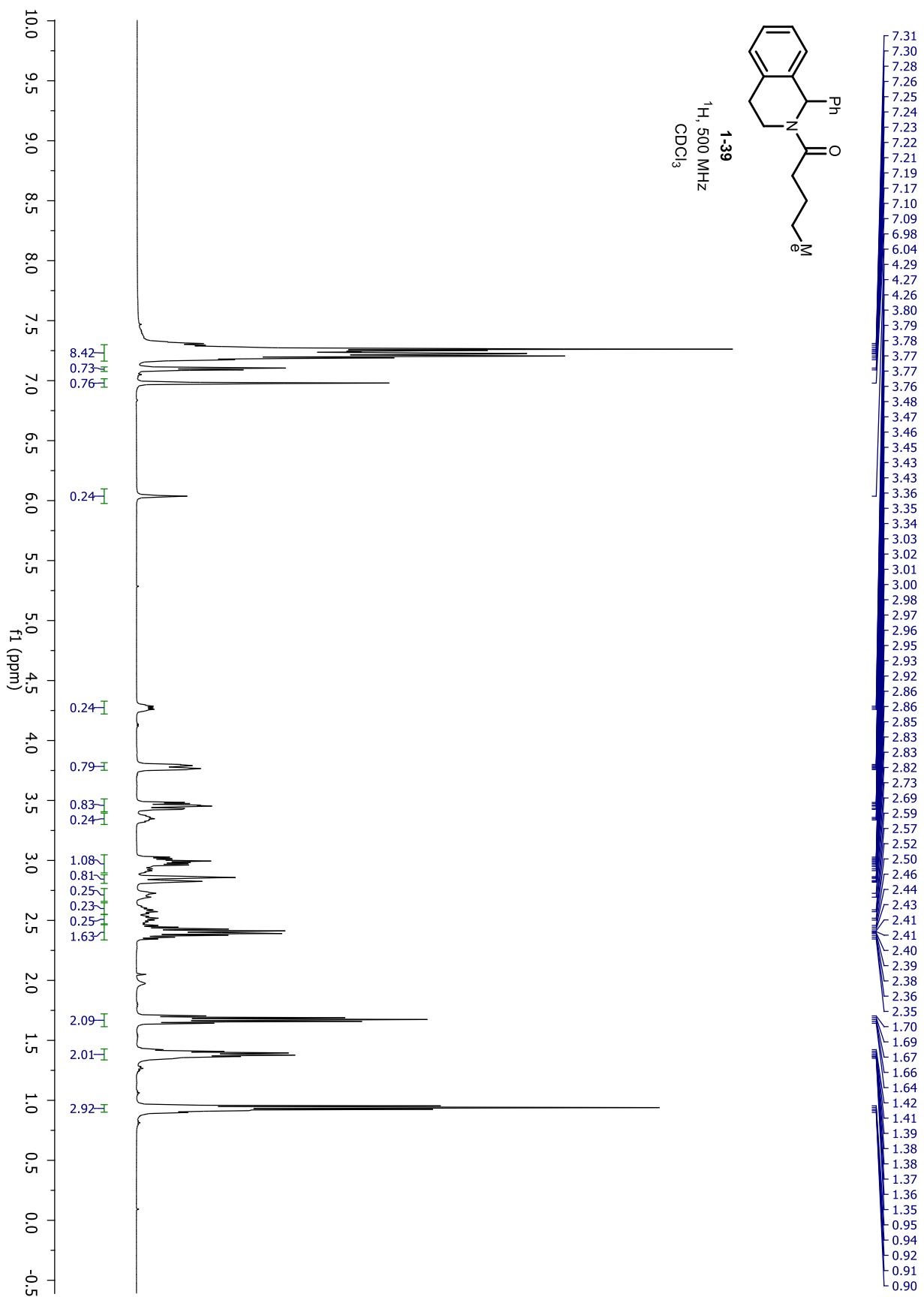


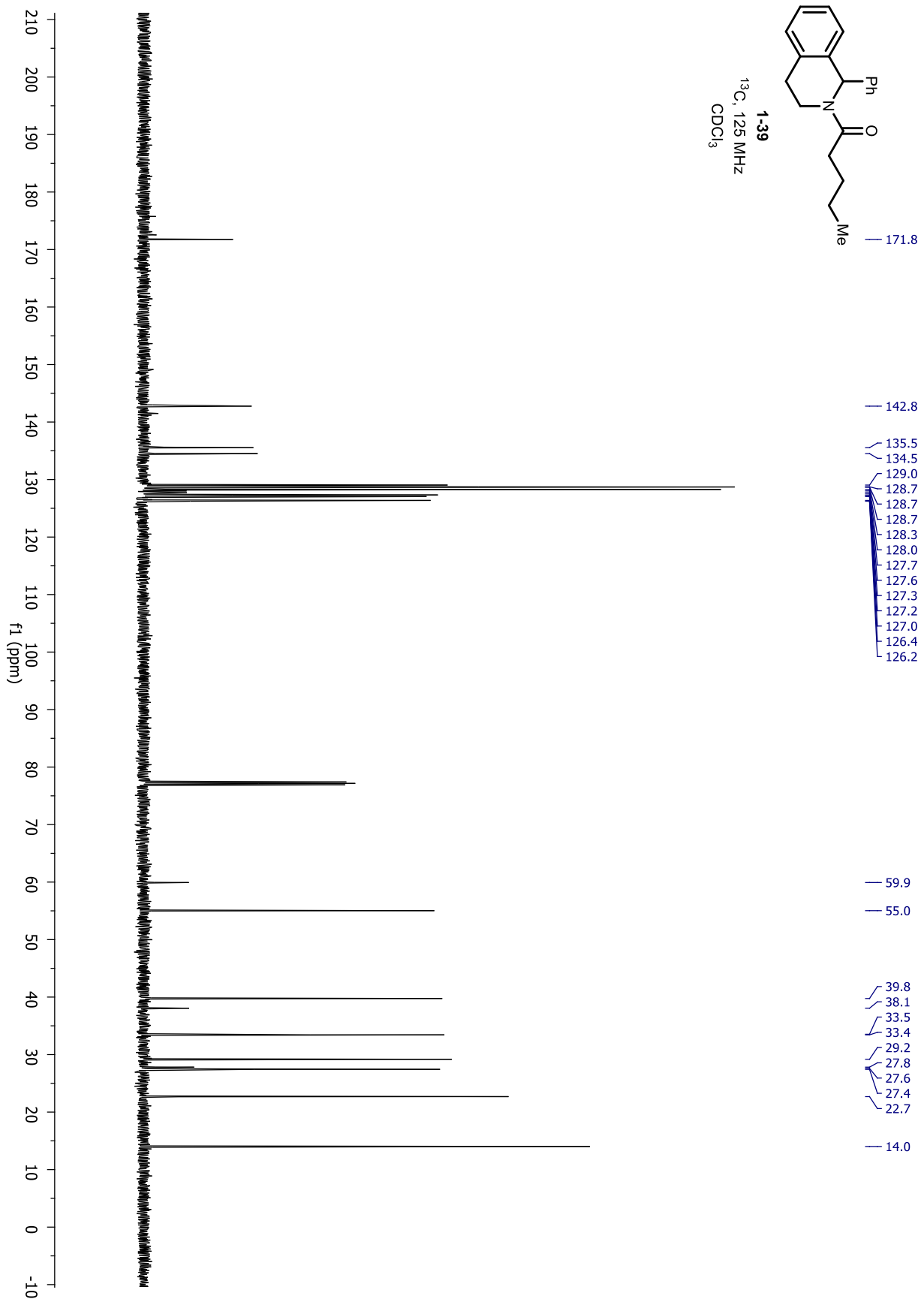


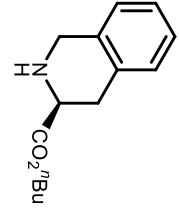




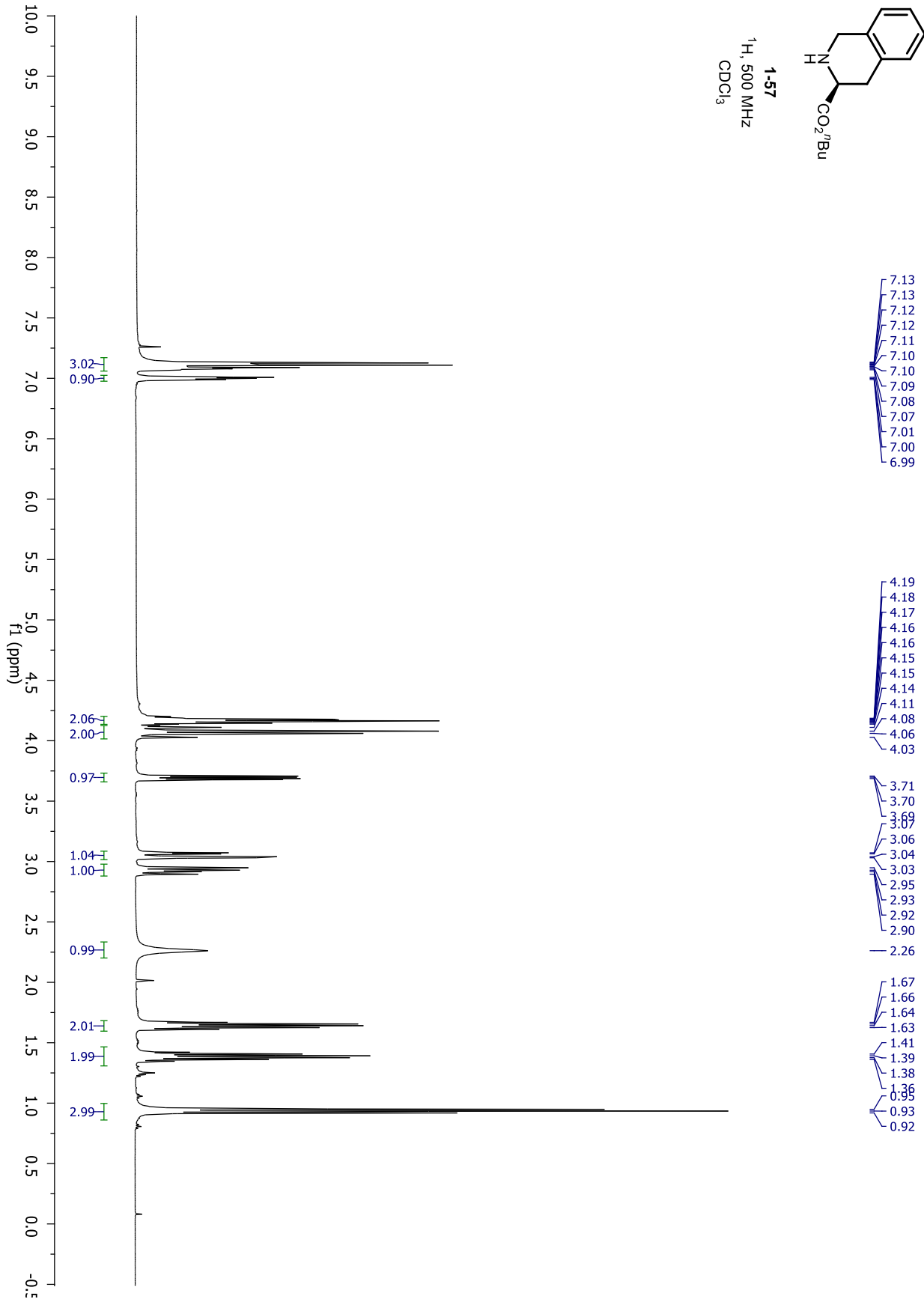


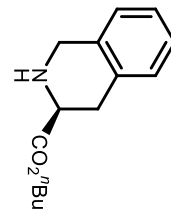






1-57
 ^1H , 500 MHz
 CDCl_3

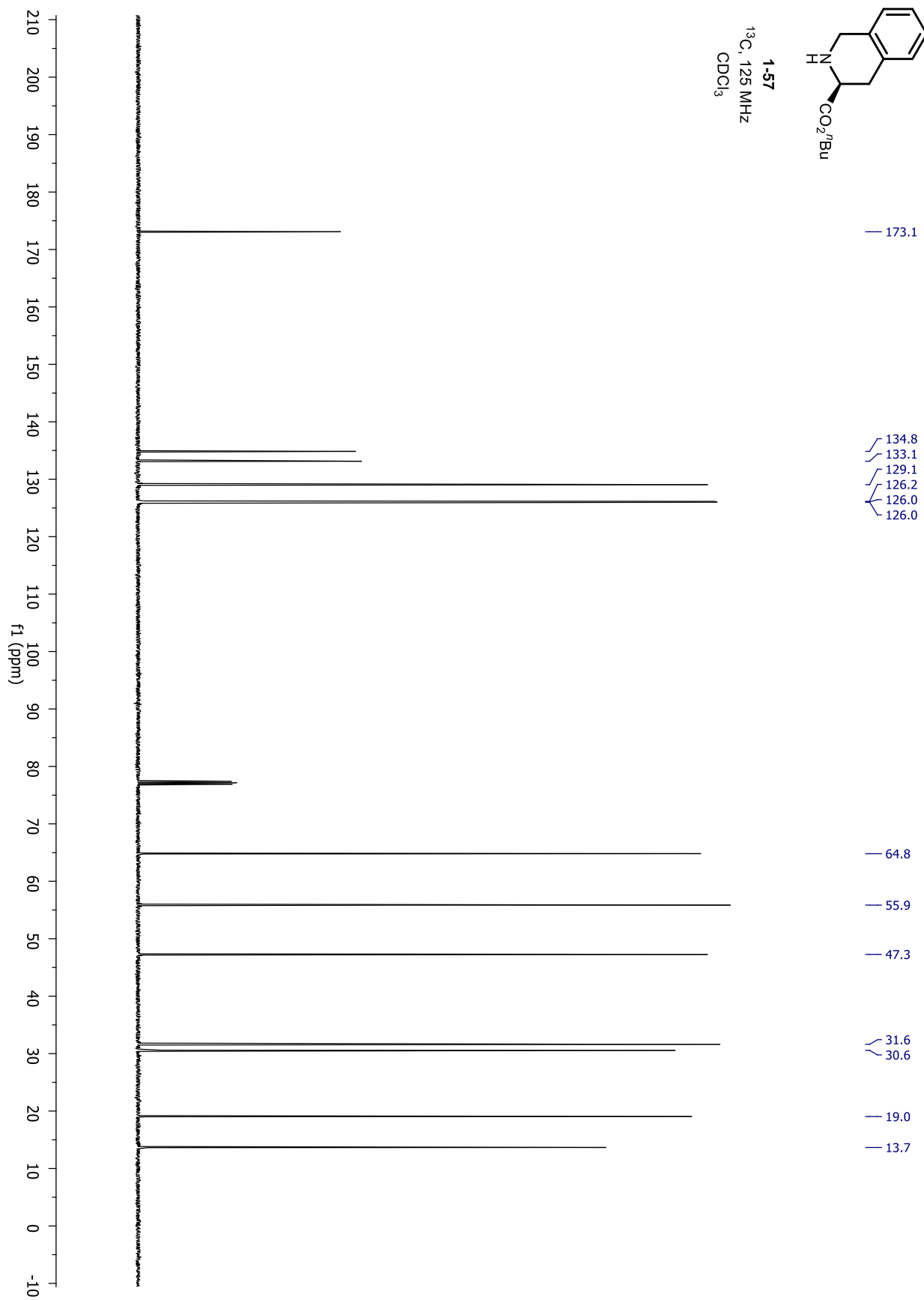


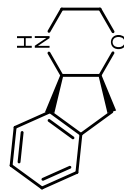


1-57

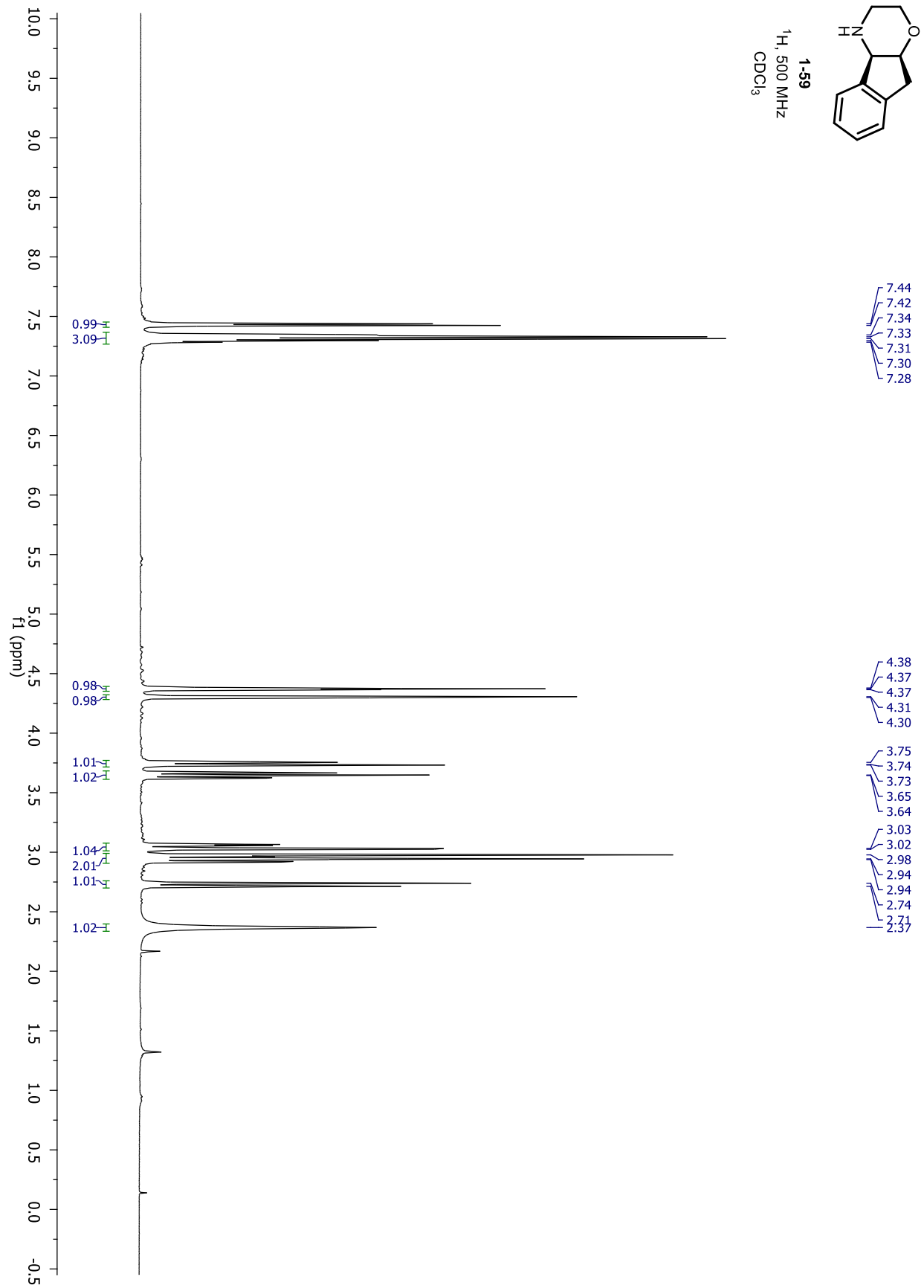
^{13}C , 125 MHz

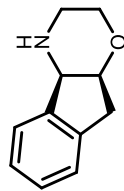
CDCl_3



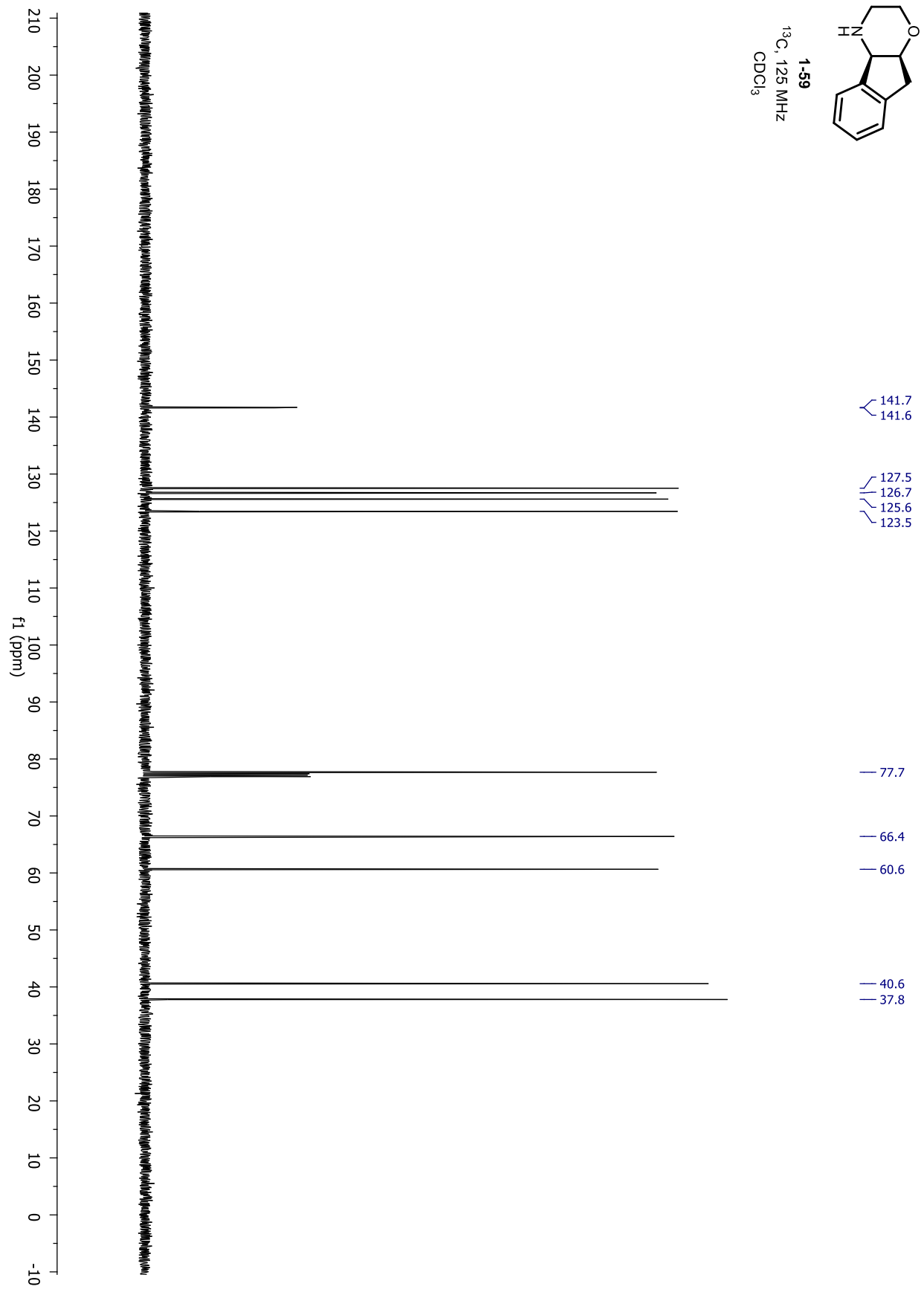


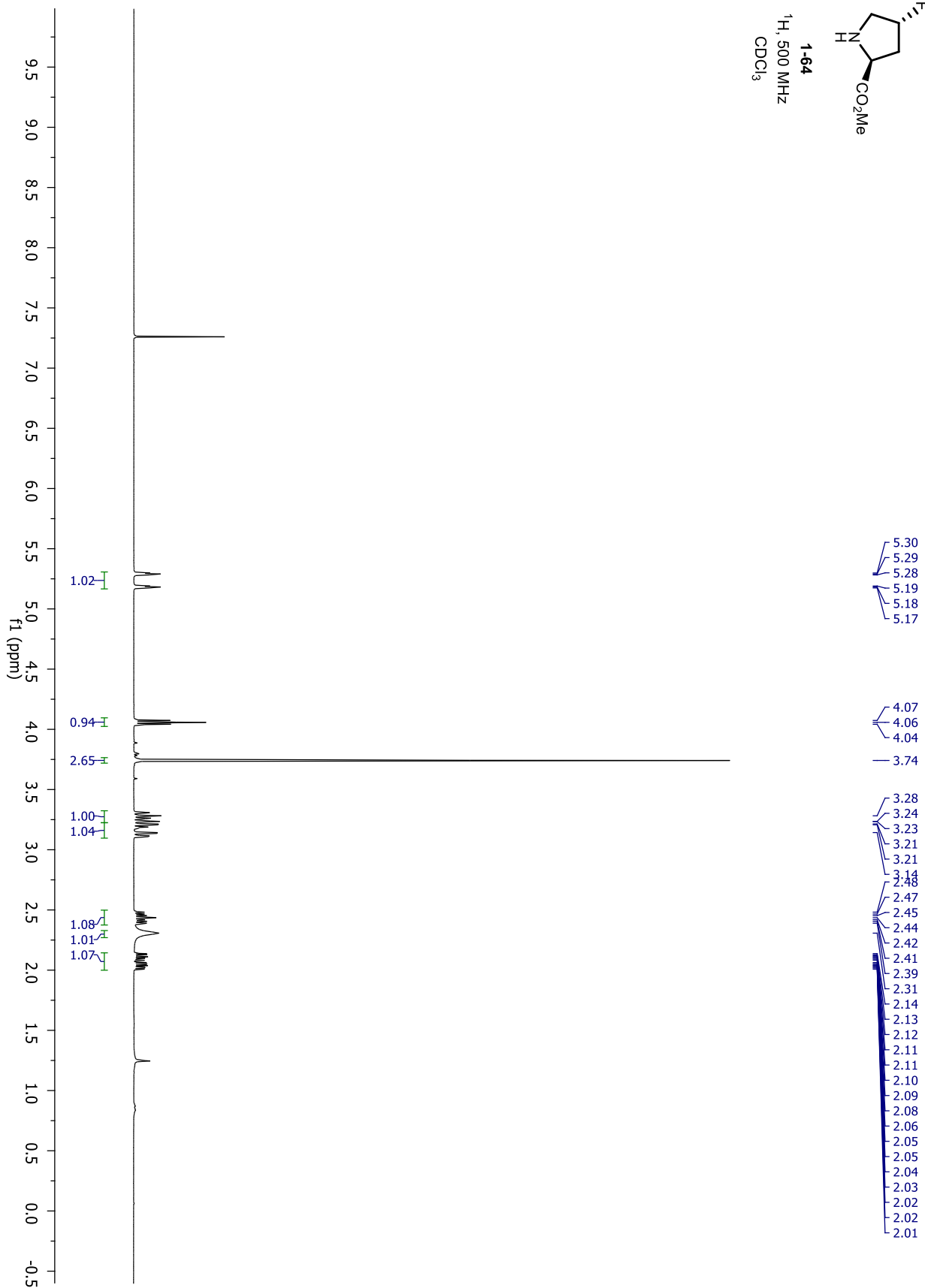
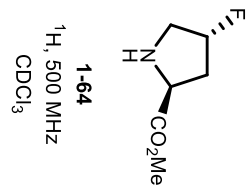
1-59
¹H, 500 MHz
CDCl₃

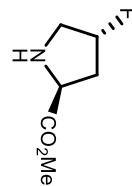




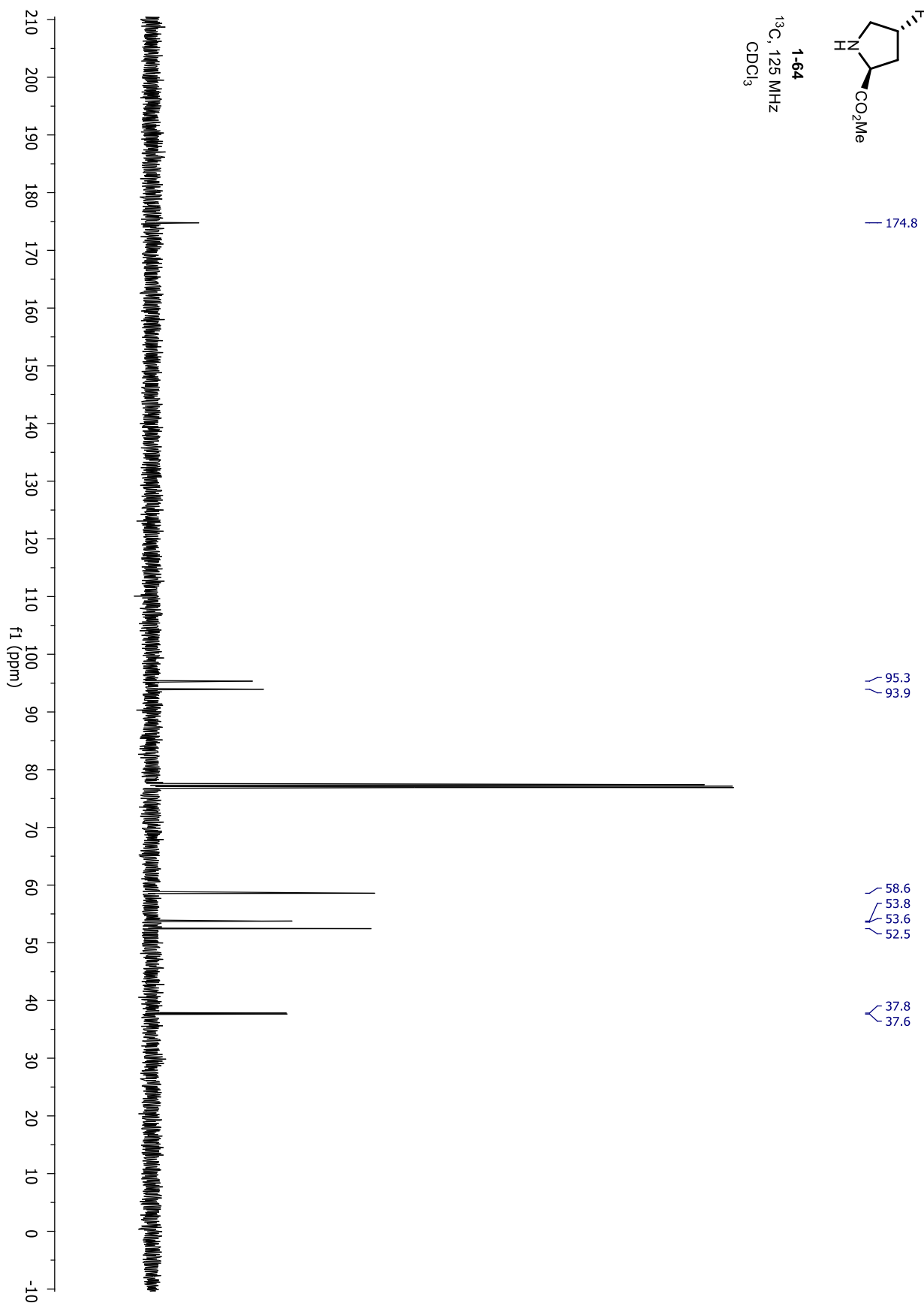
1-59
 ^{13}C , 125 MHz
 CDCl_3

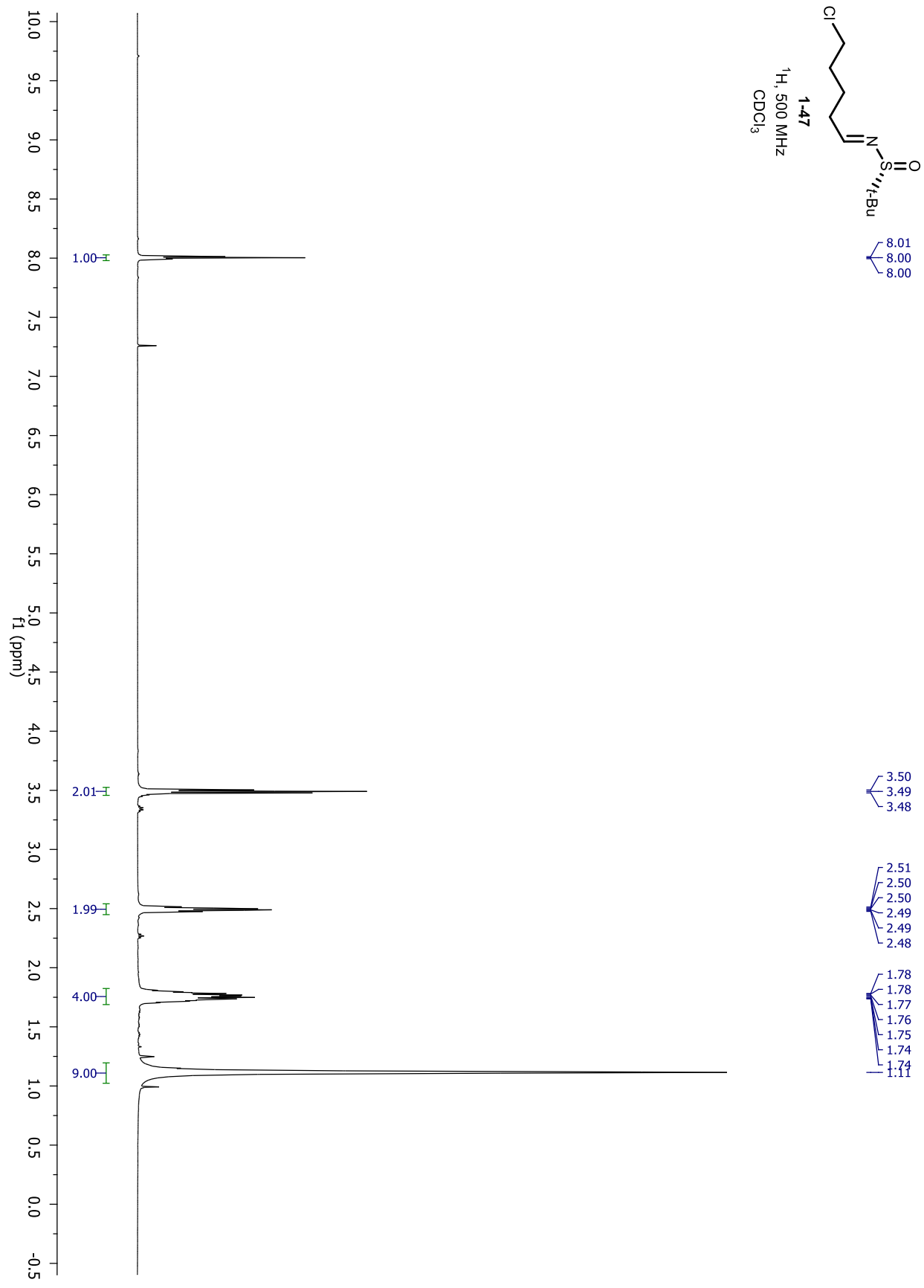
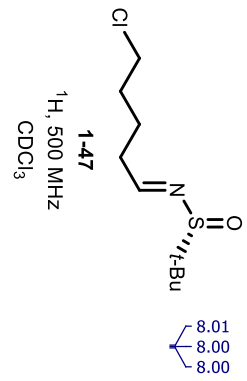


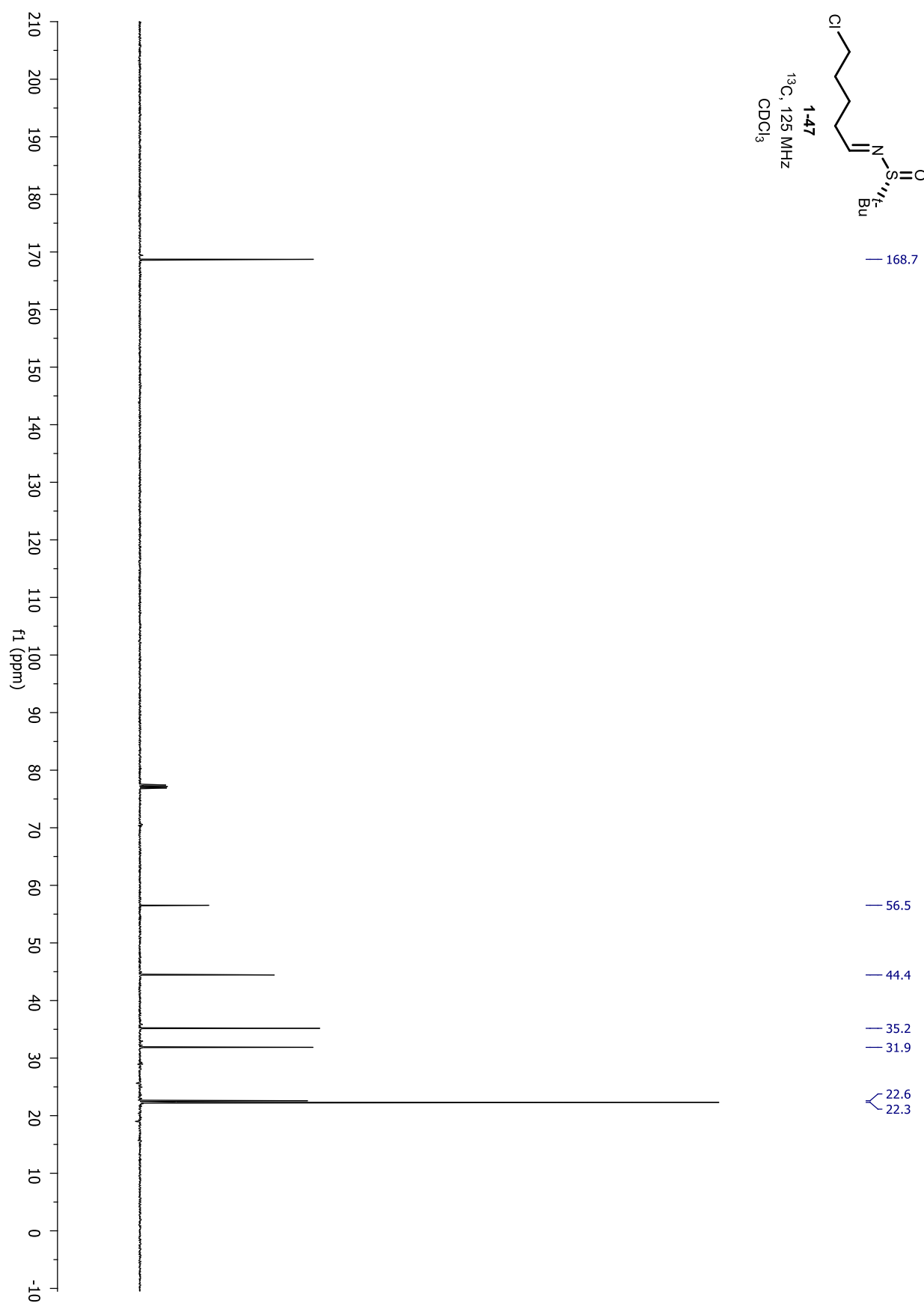
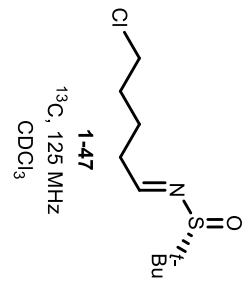


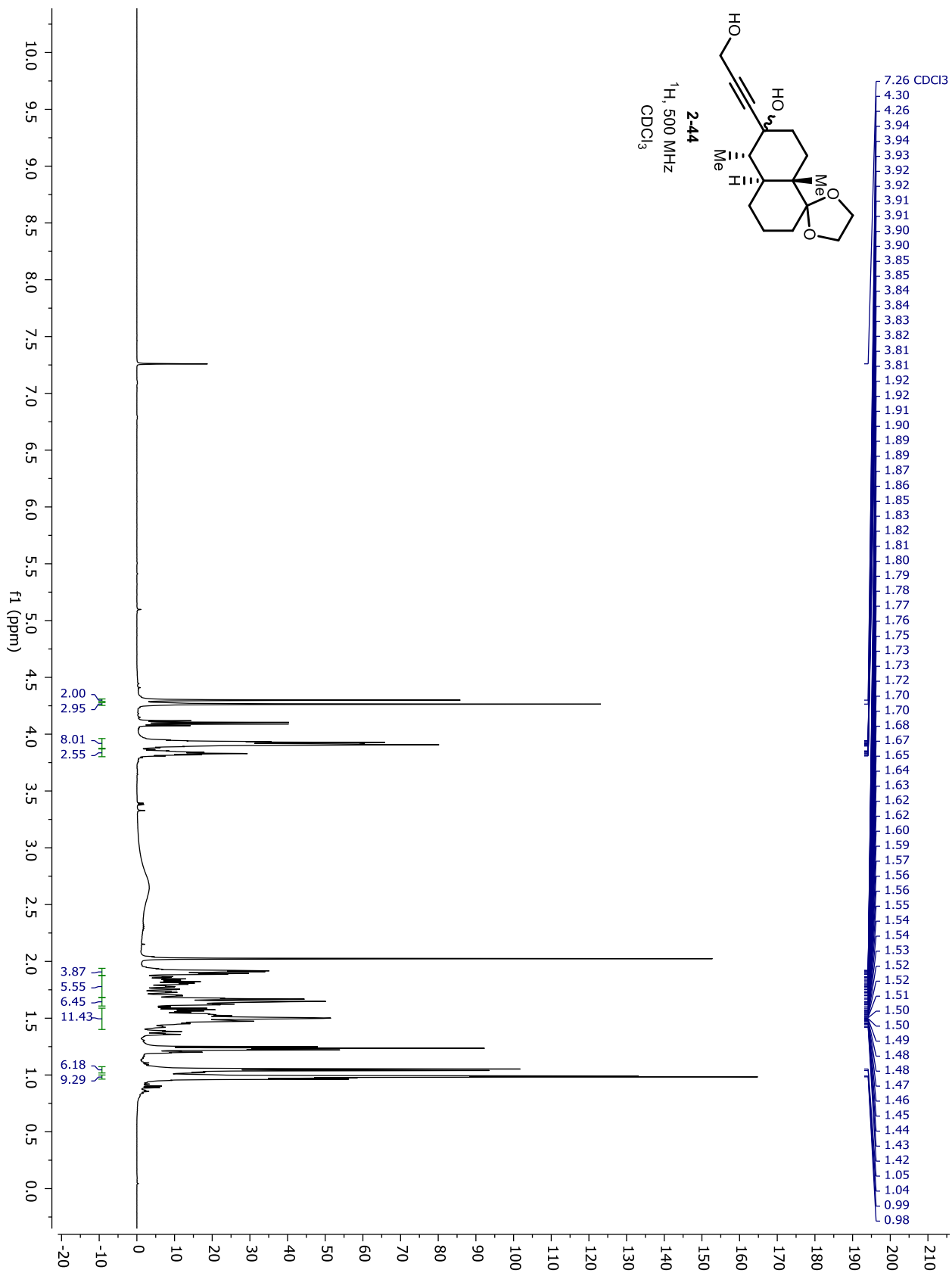


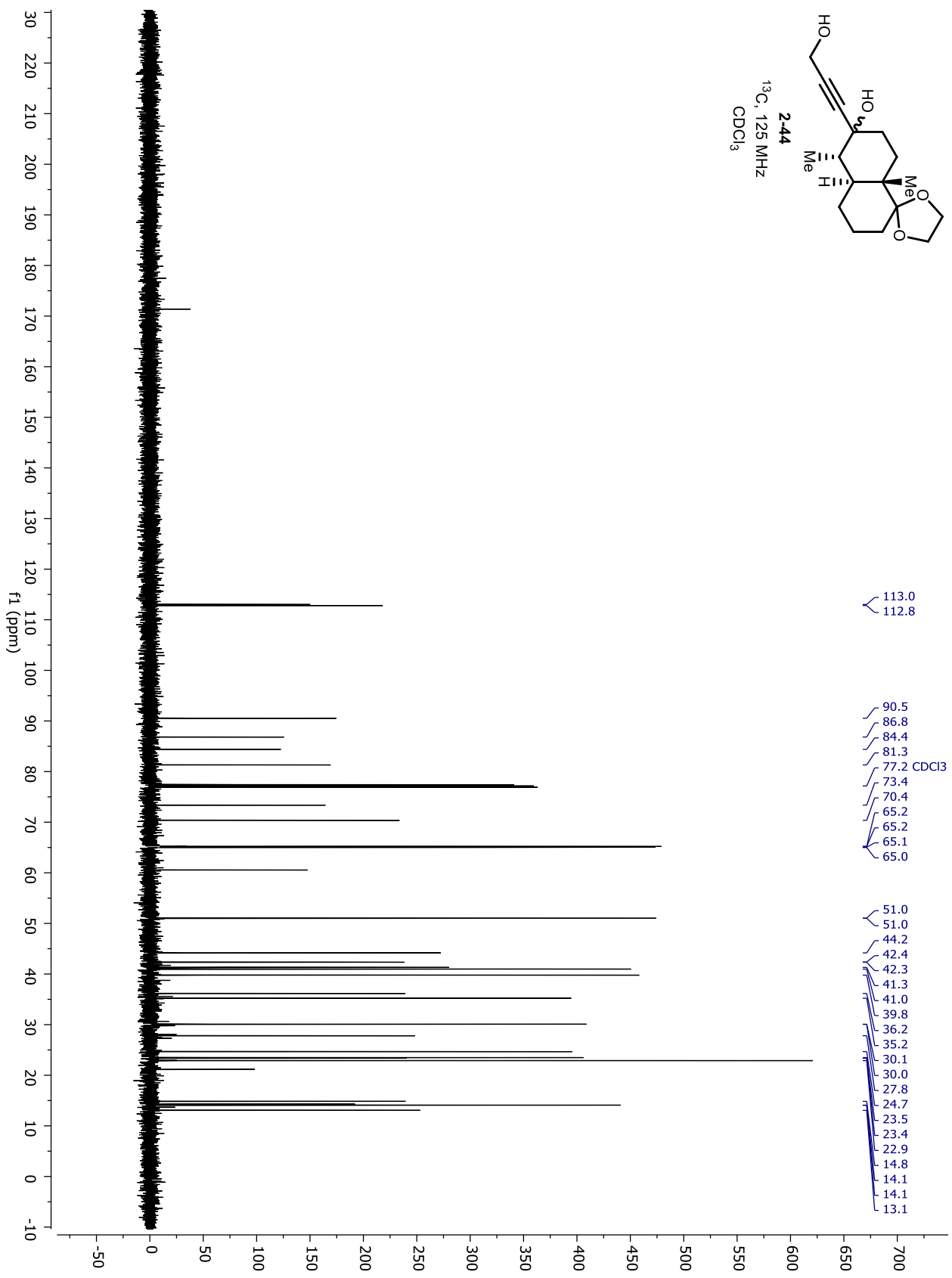
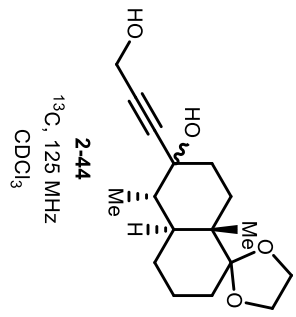
1-64
¹³C, 125 MHz
CDCl₃

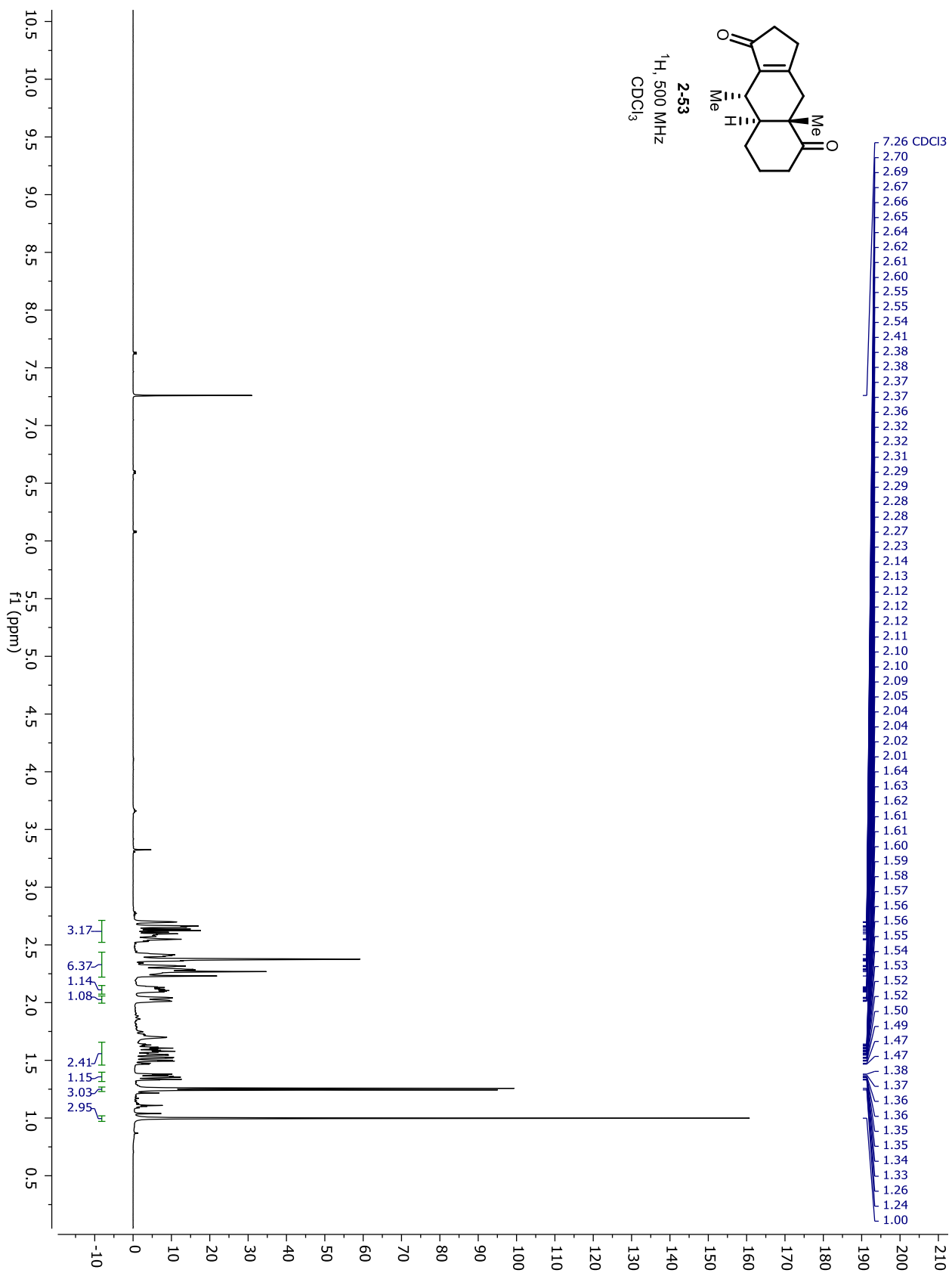
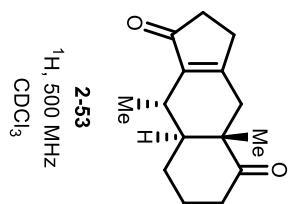


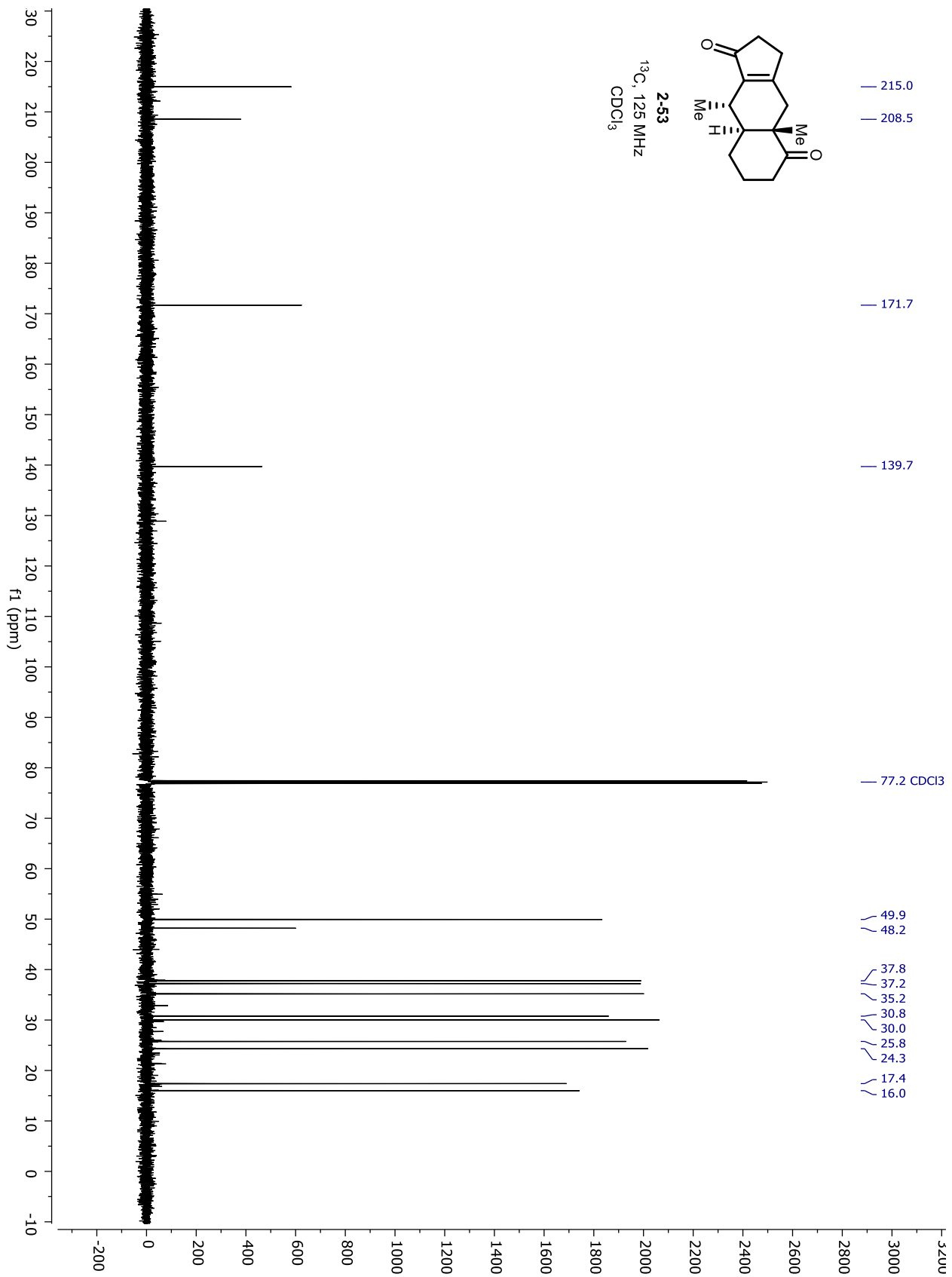


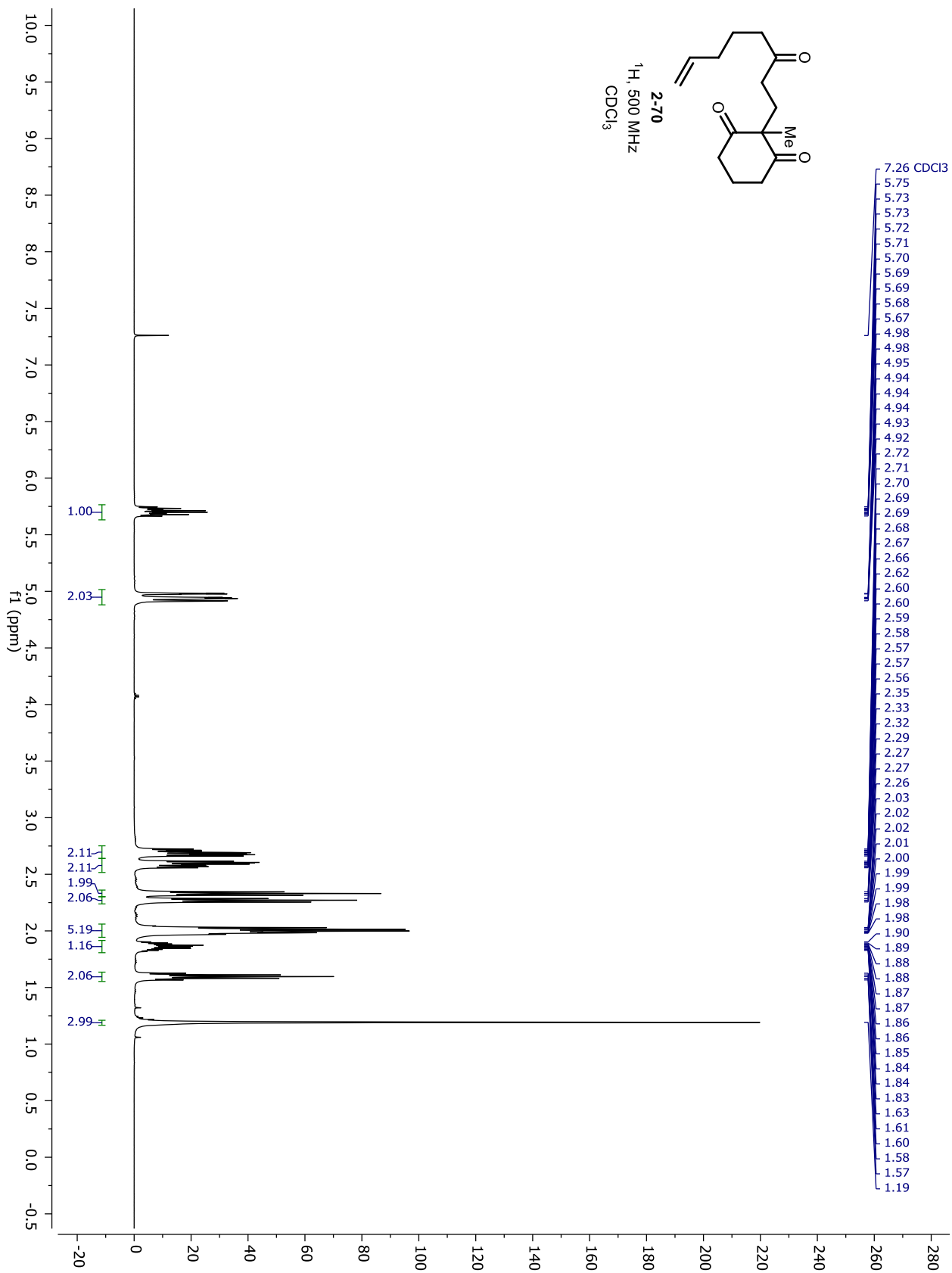


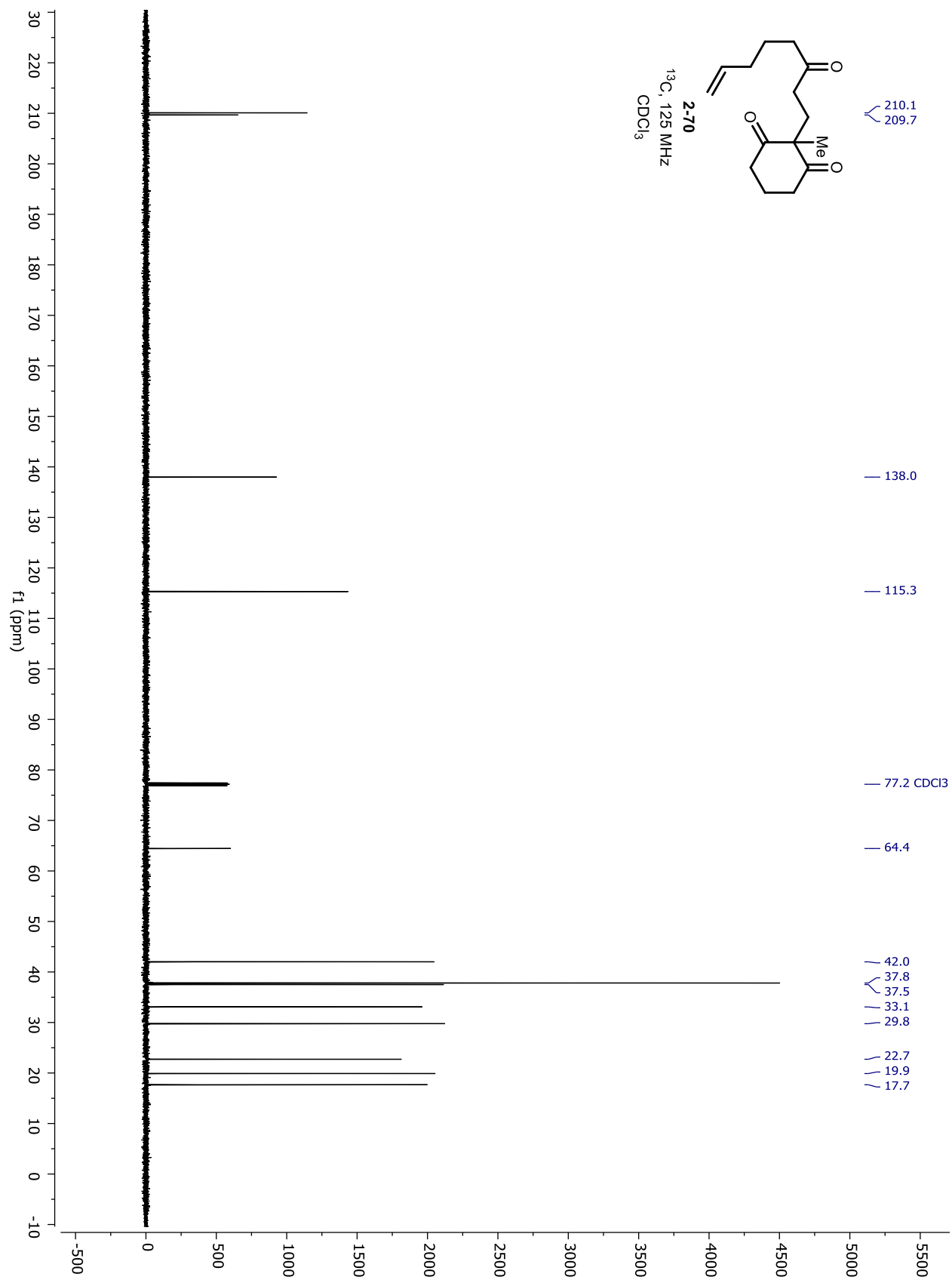


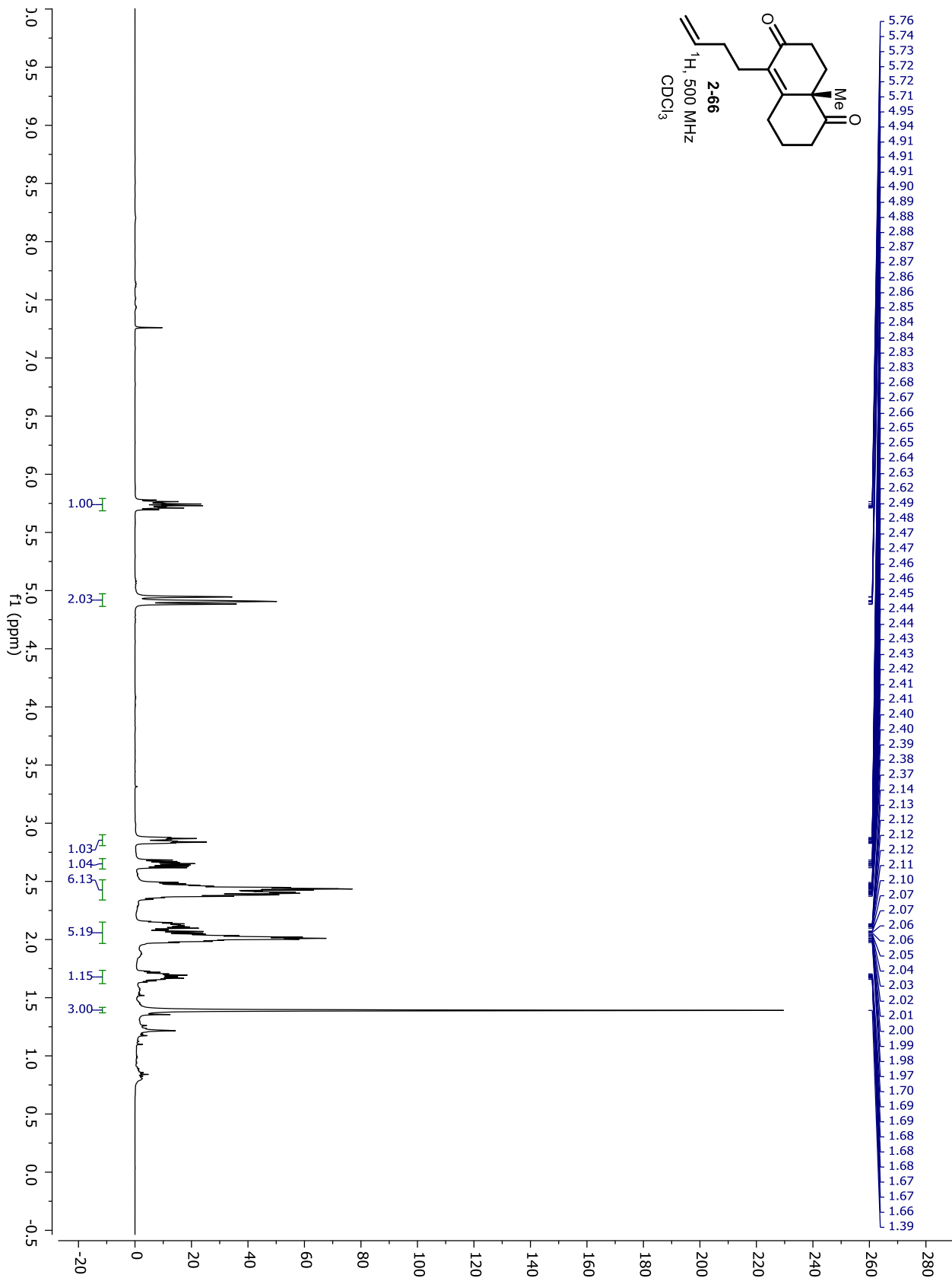


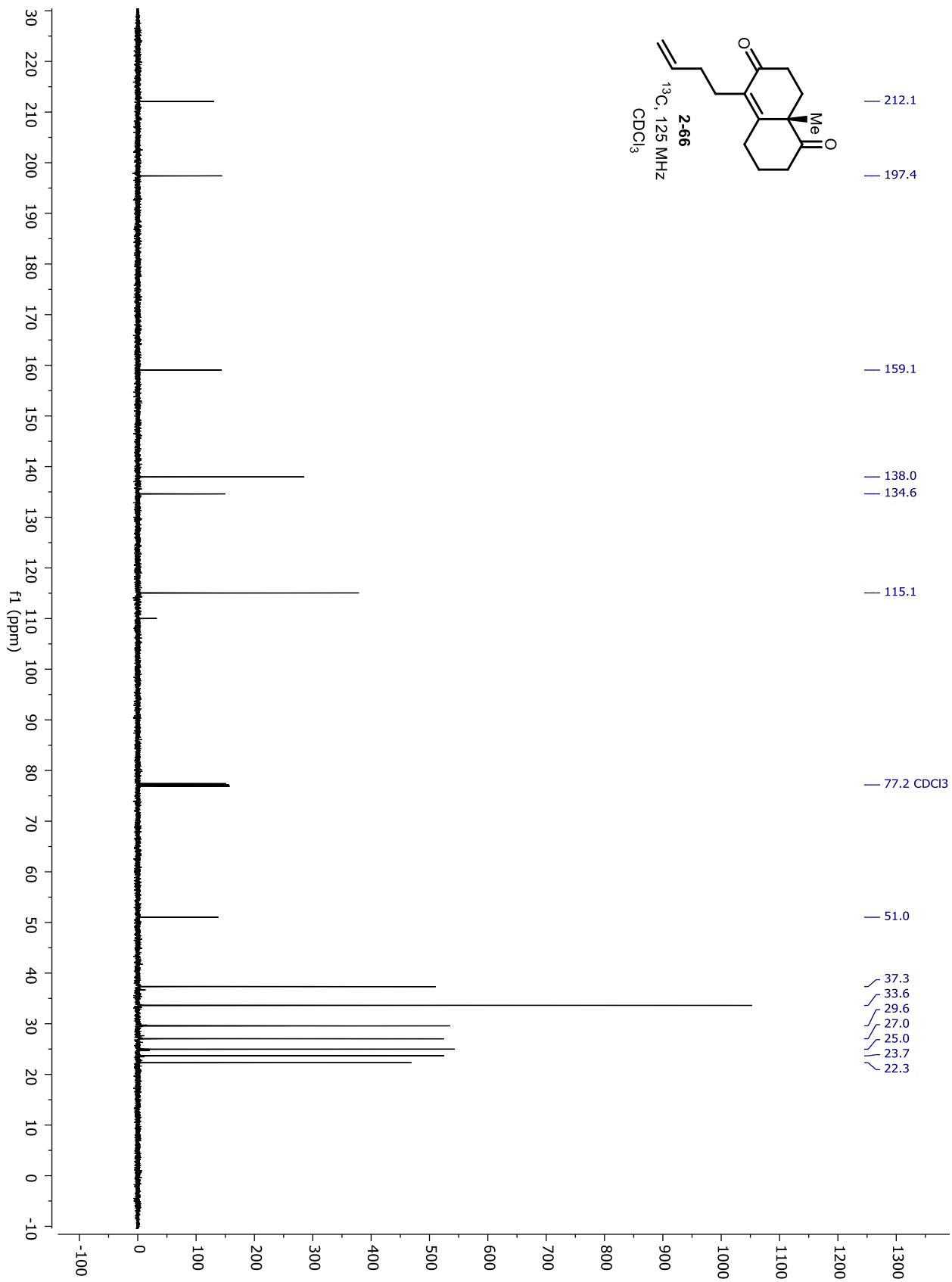


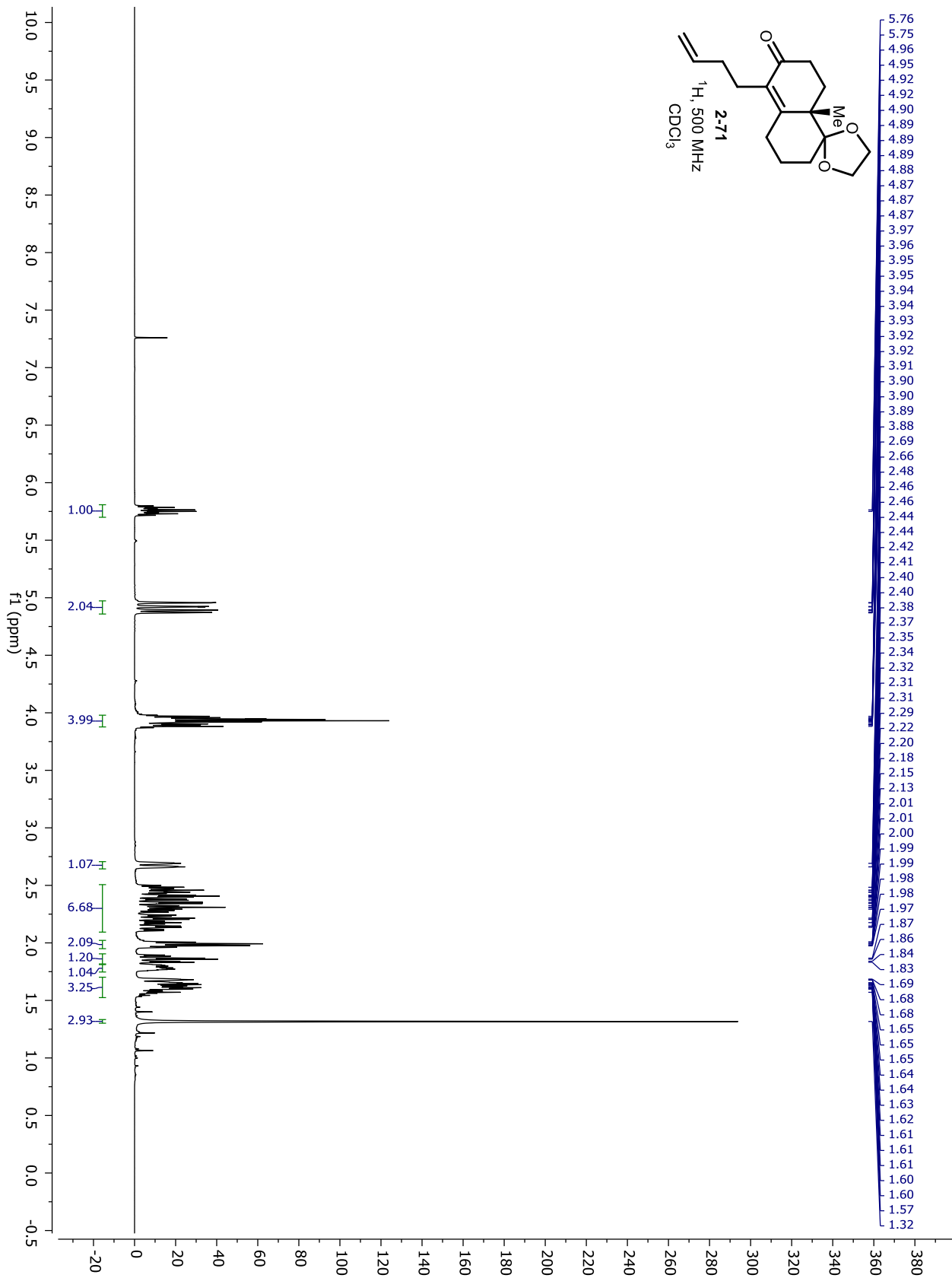


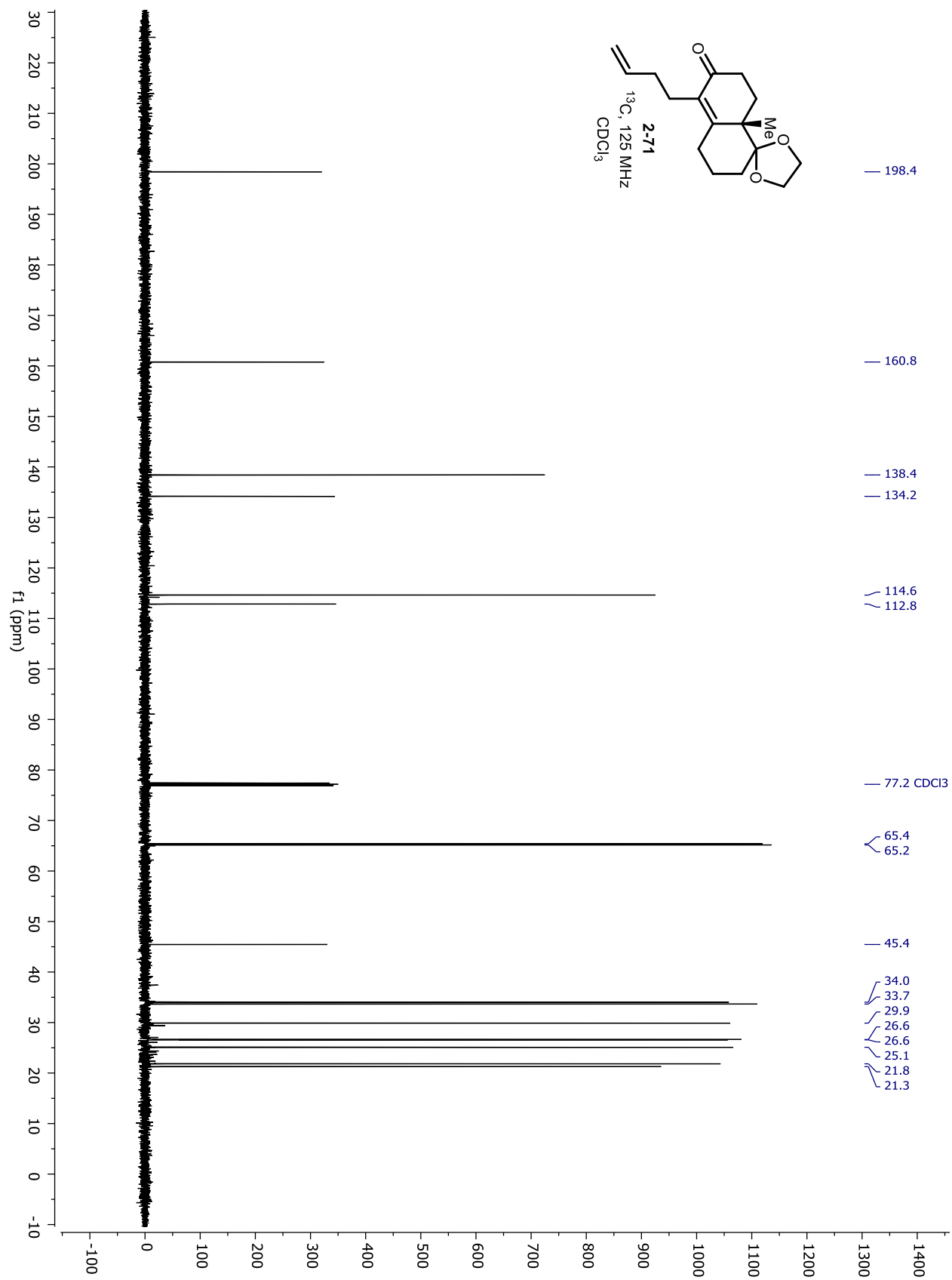


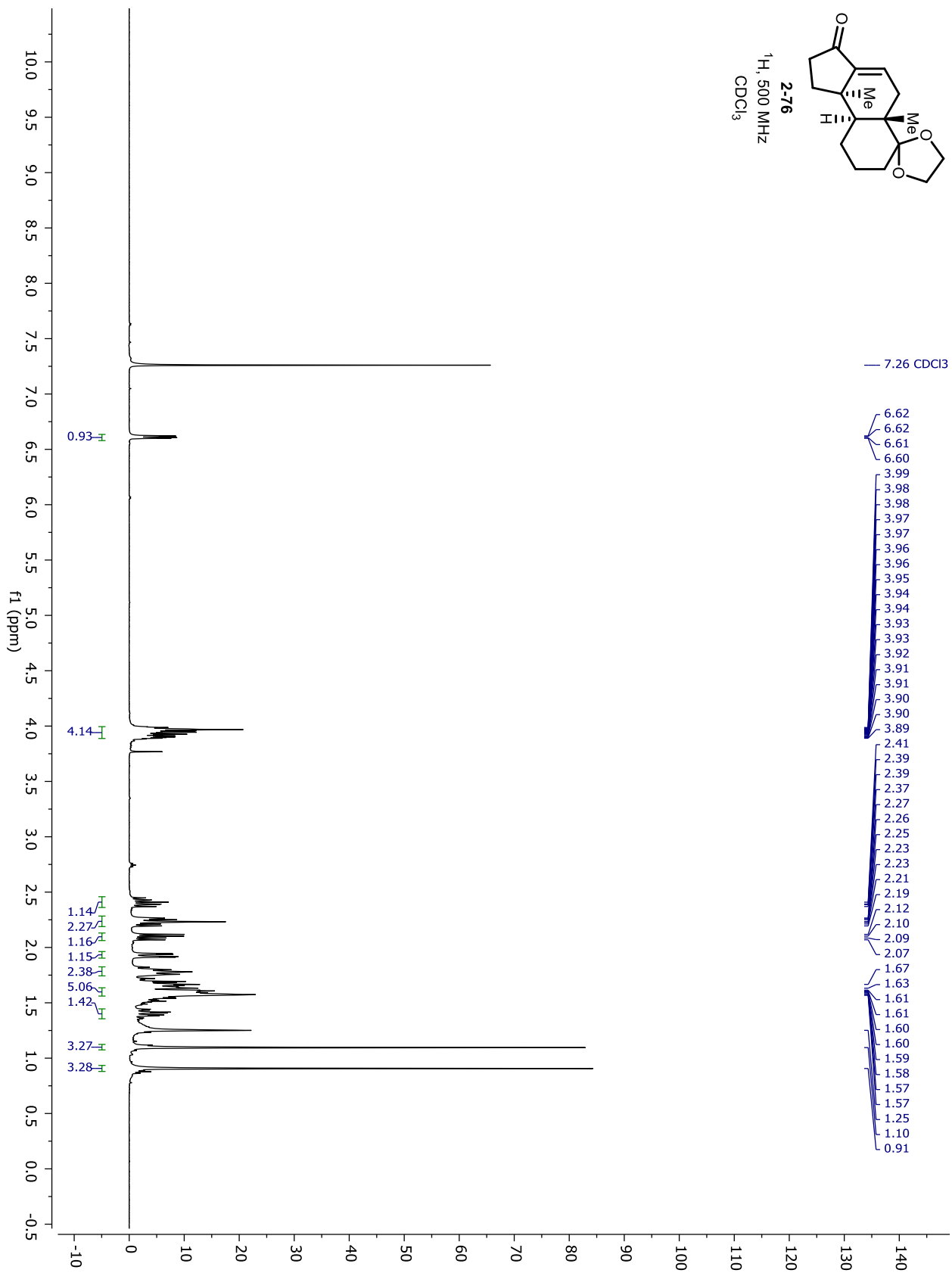
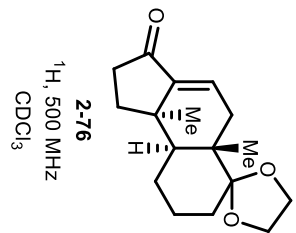


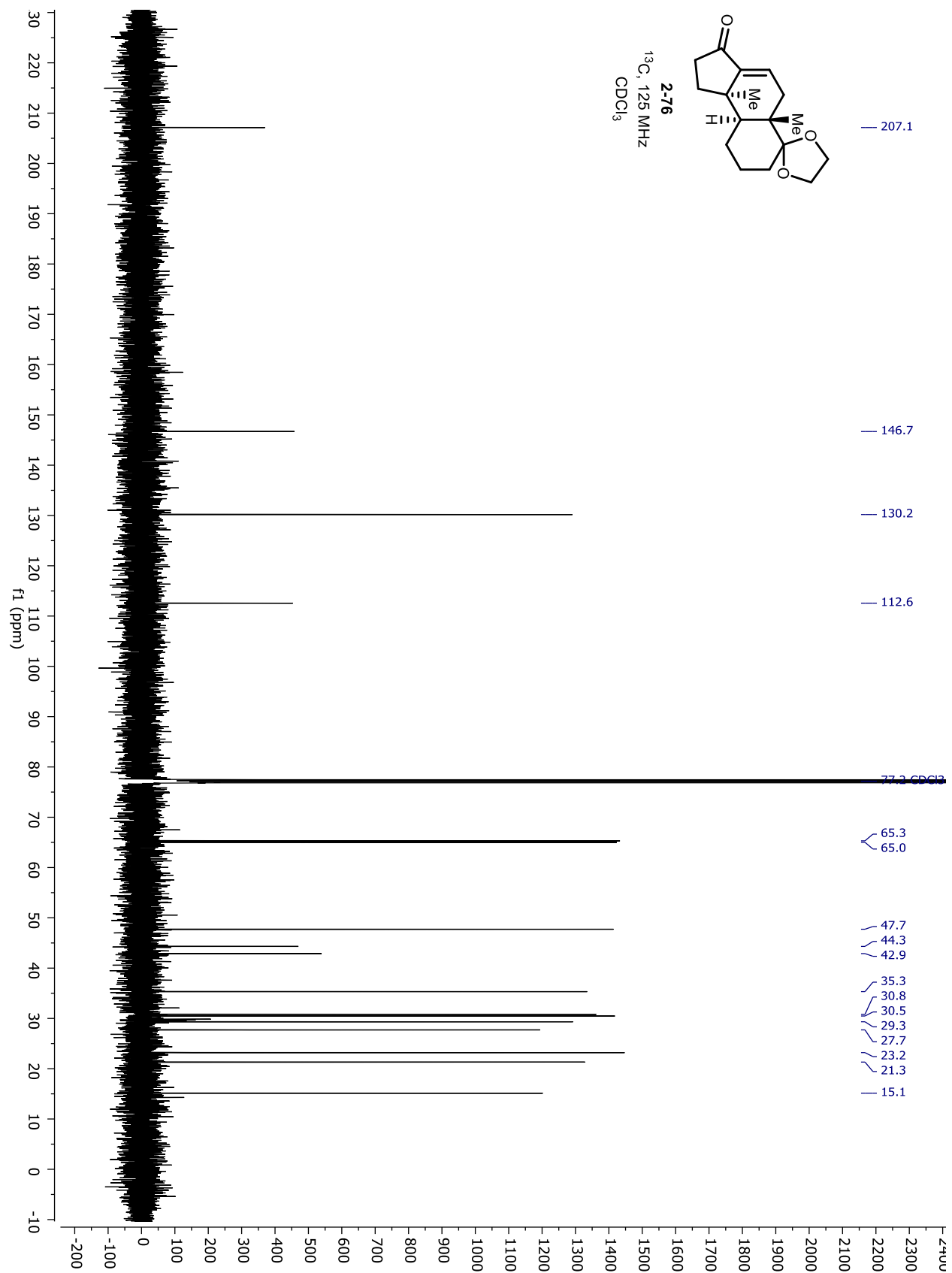


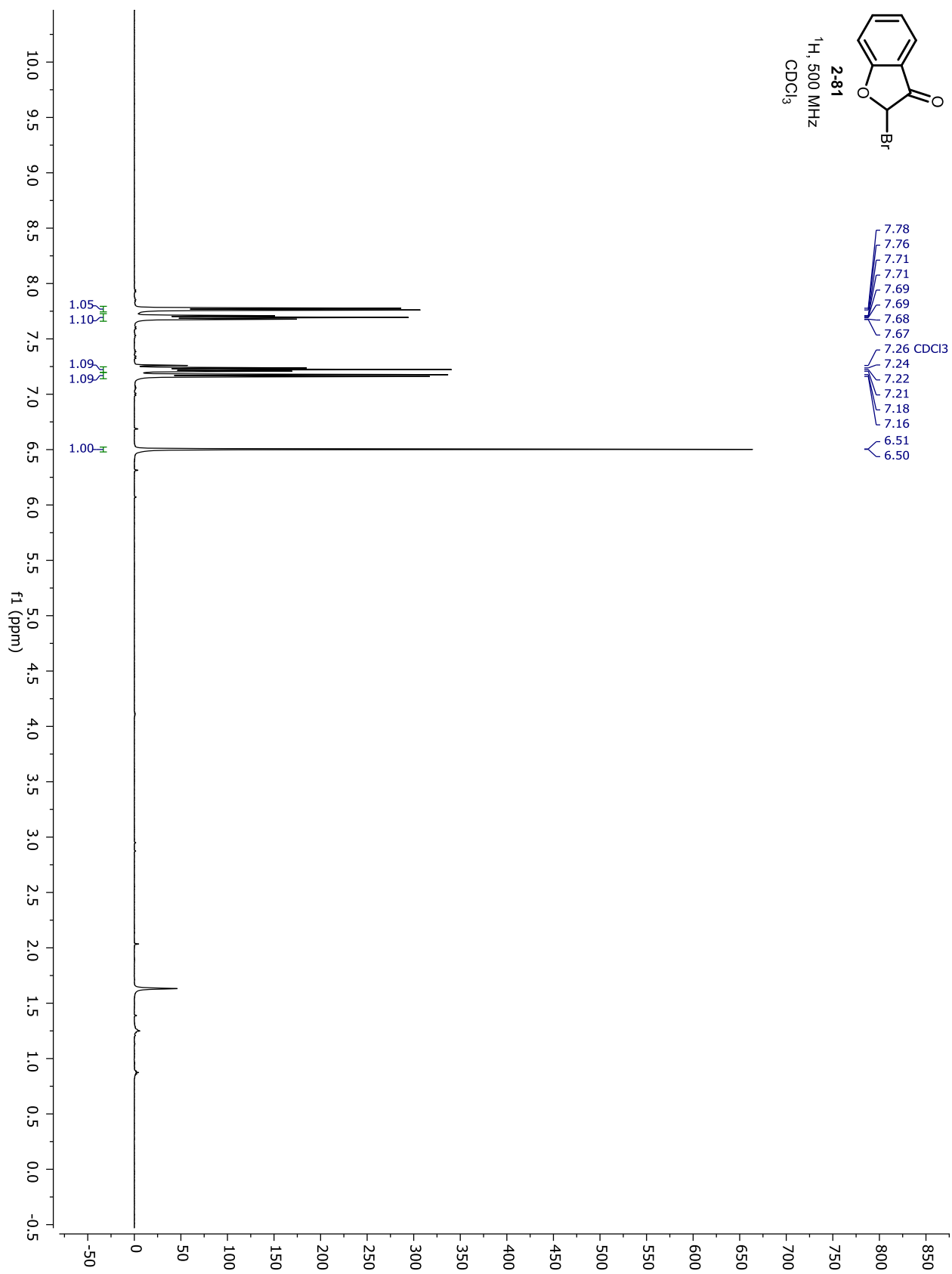
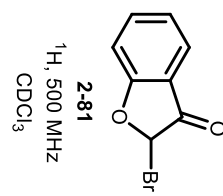


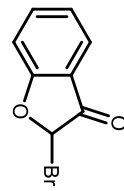




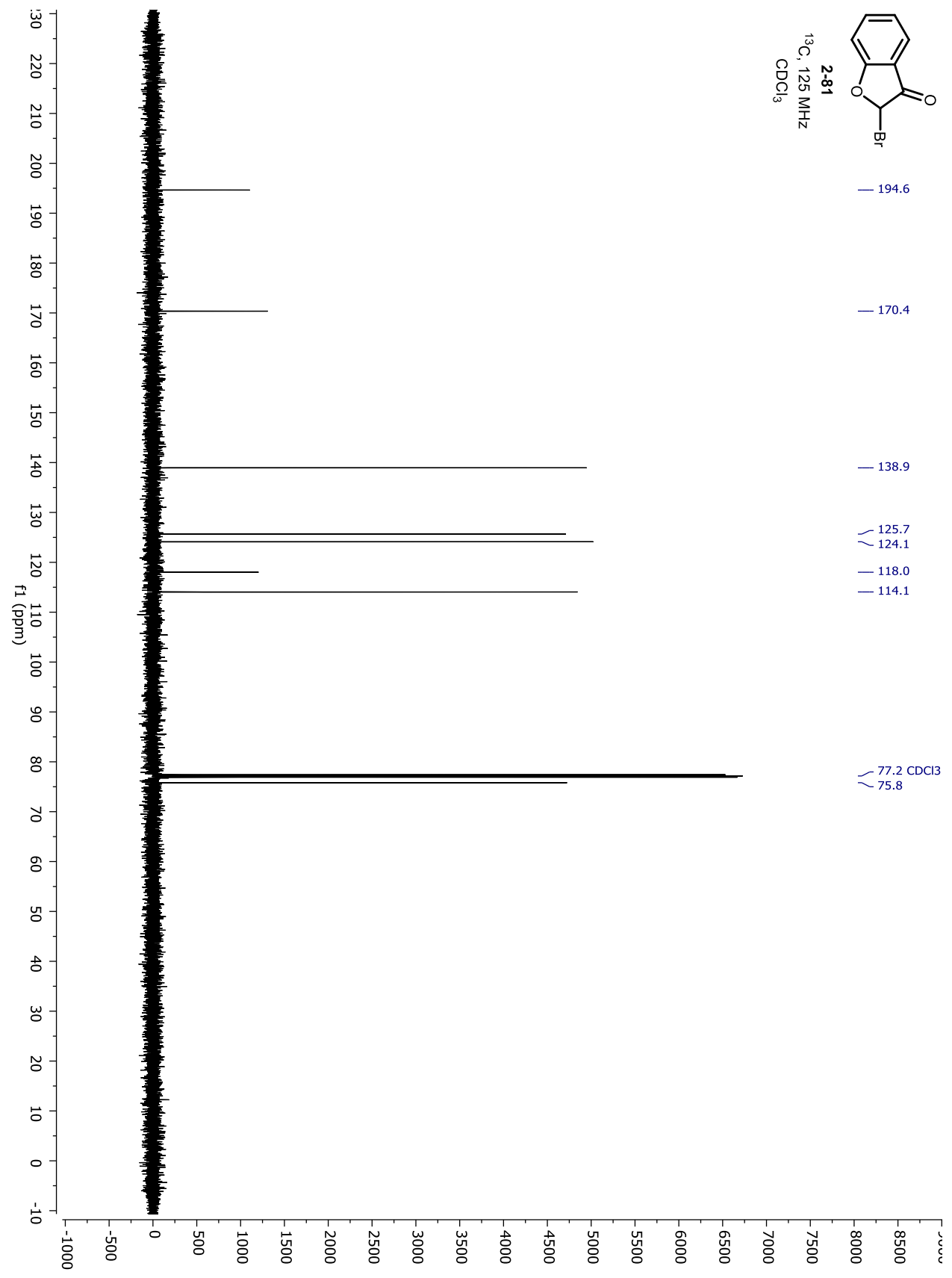


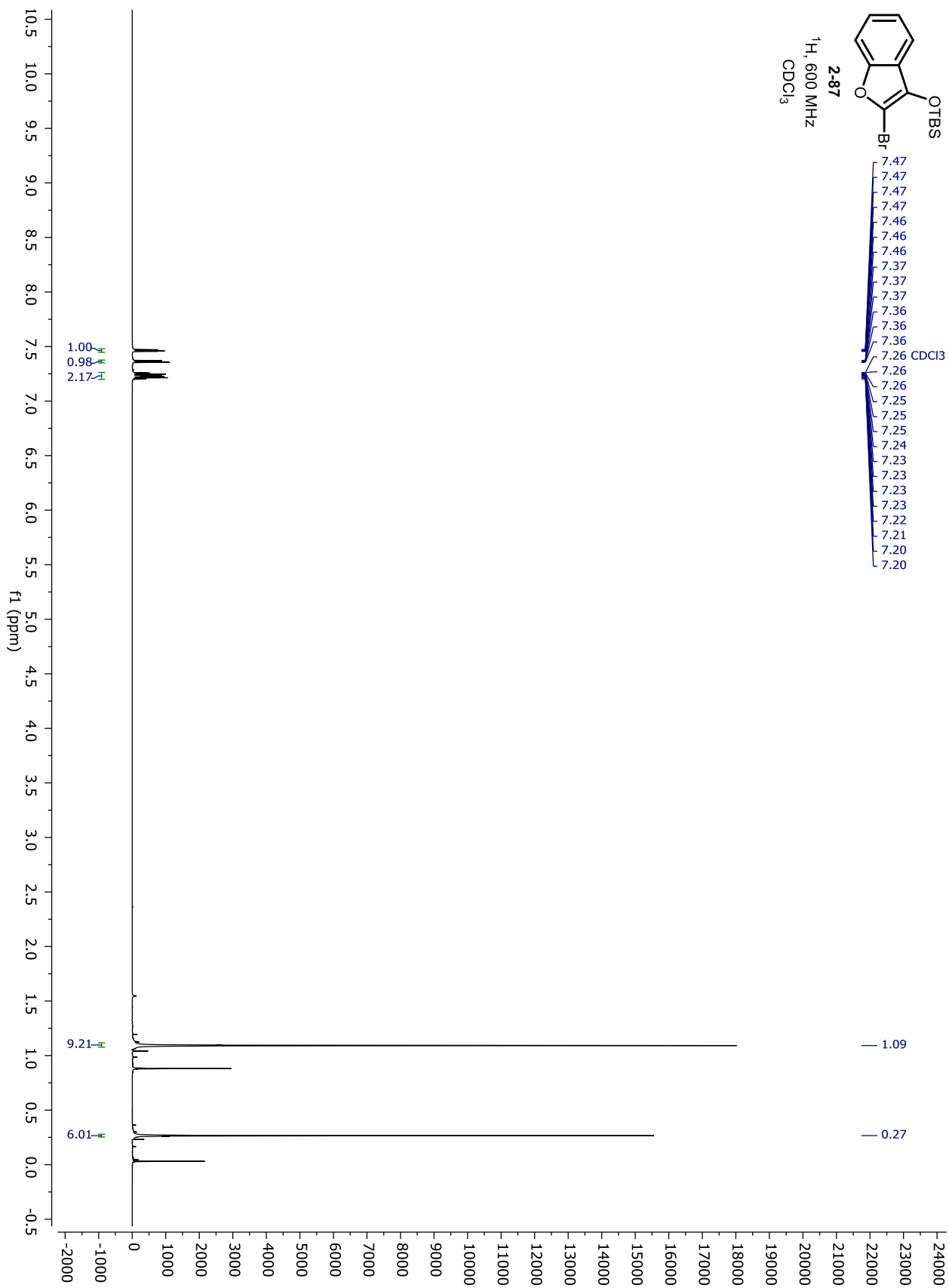
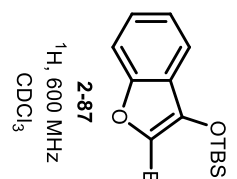


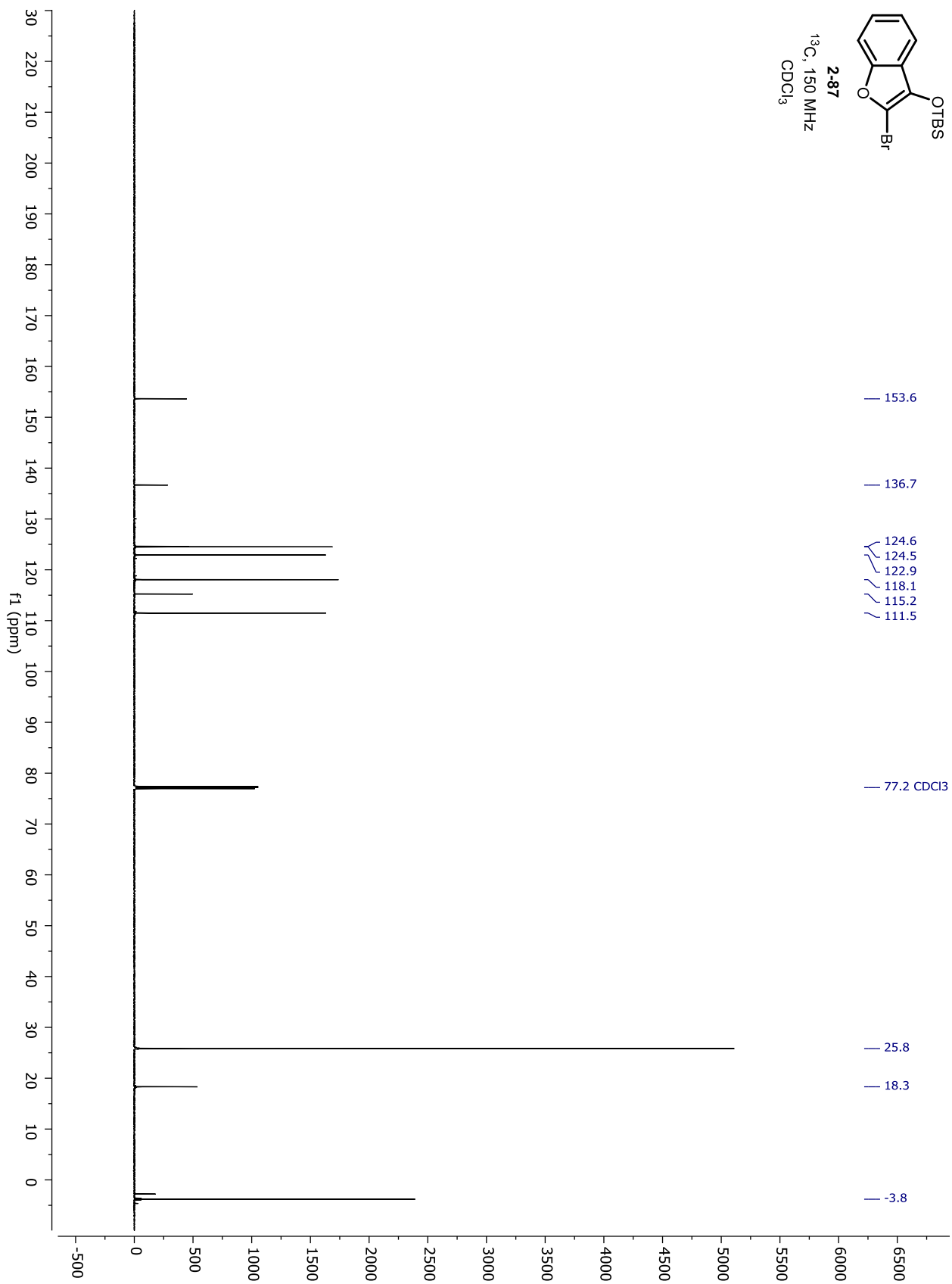
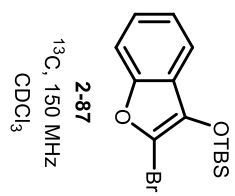


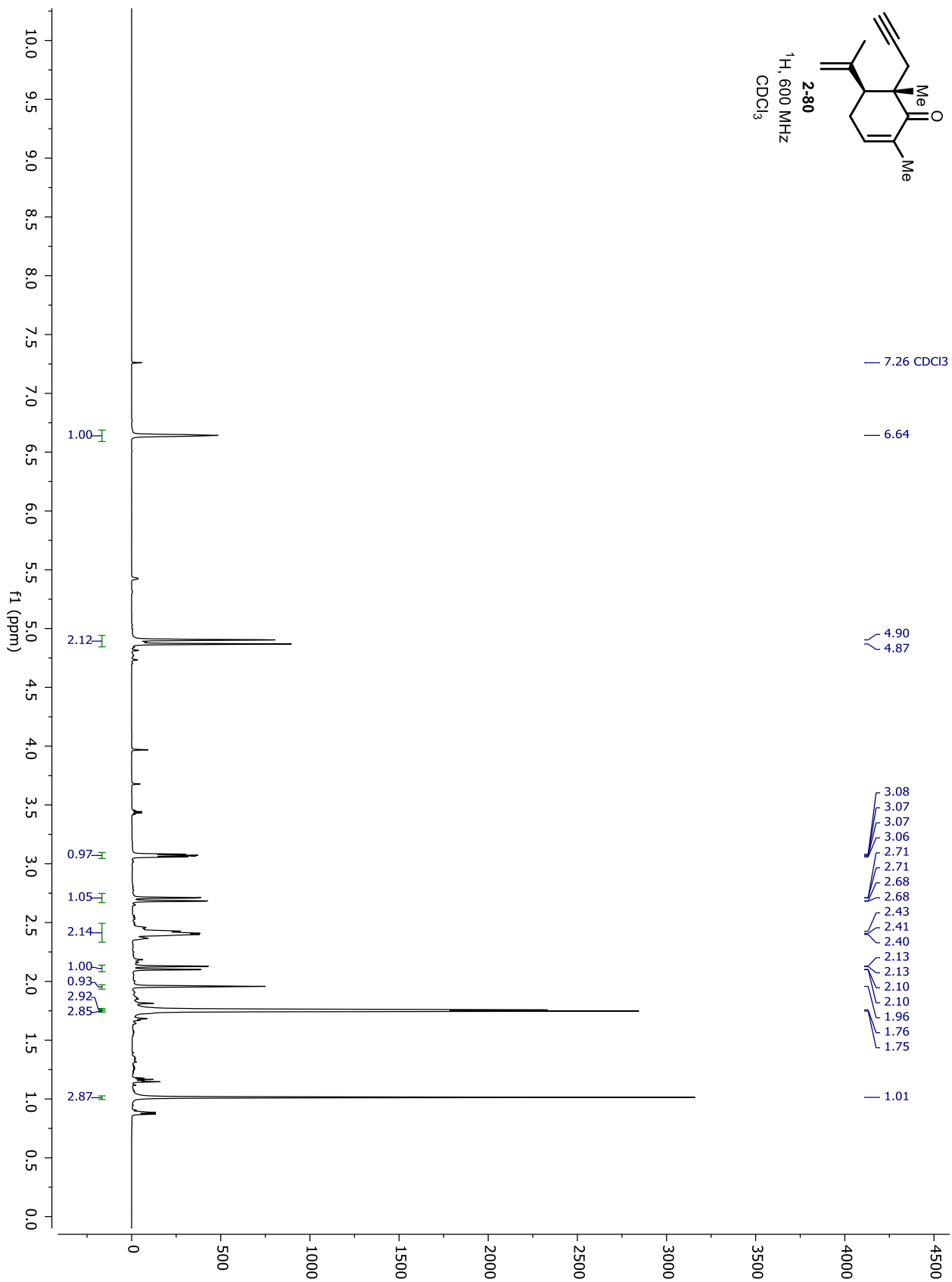
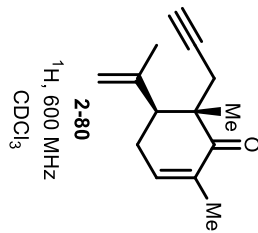


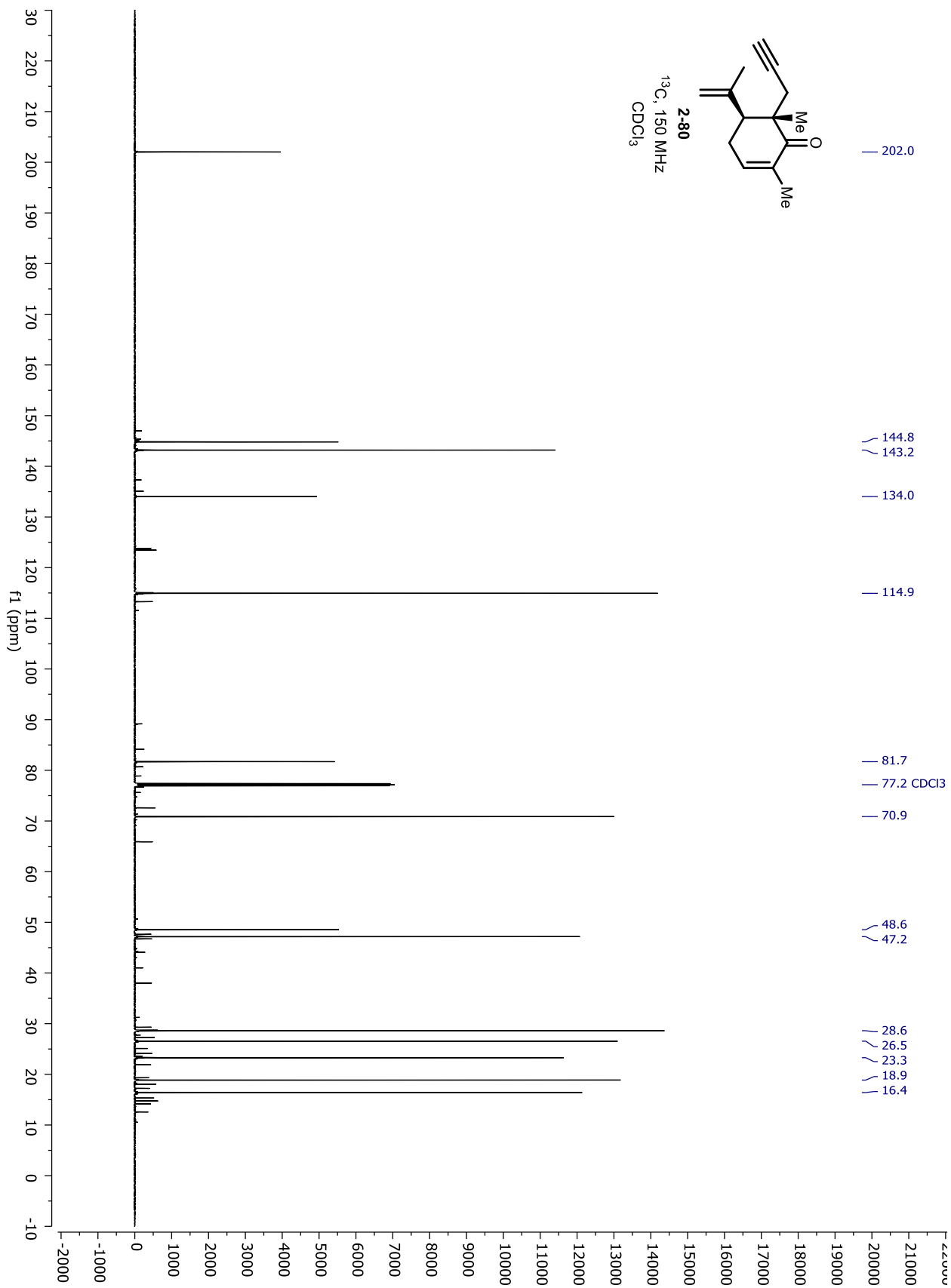
¹³C, 125 MHz
CDCl₃

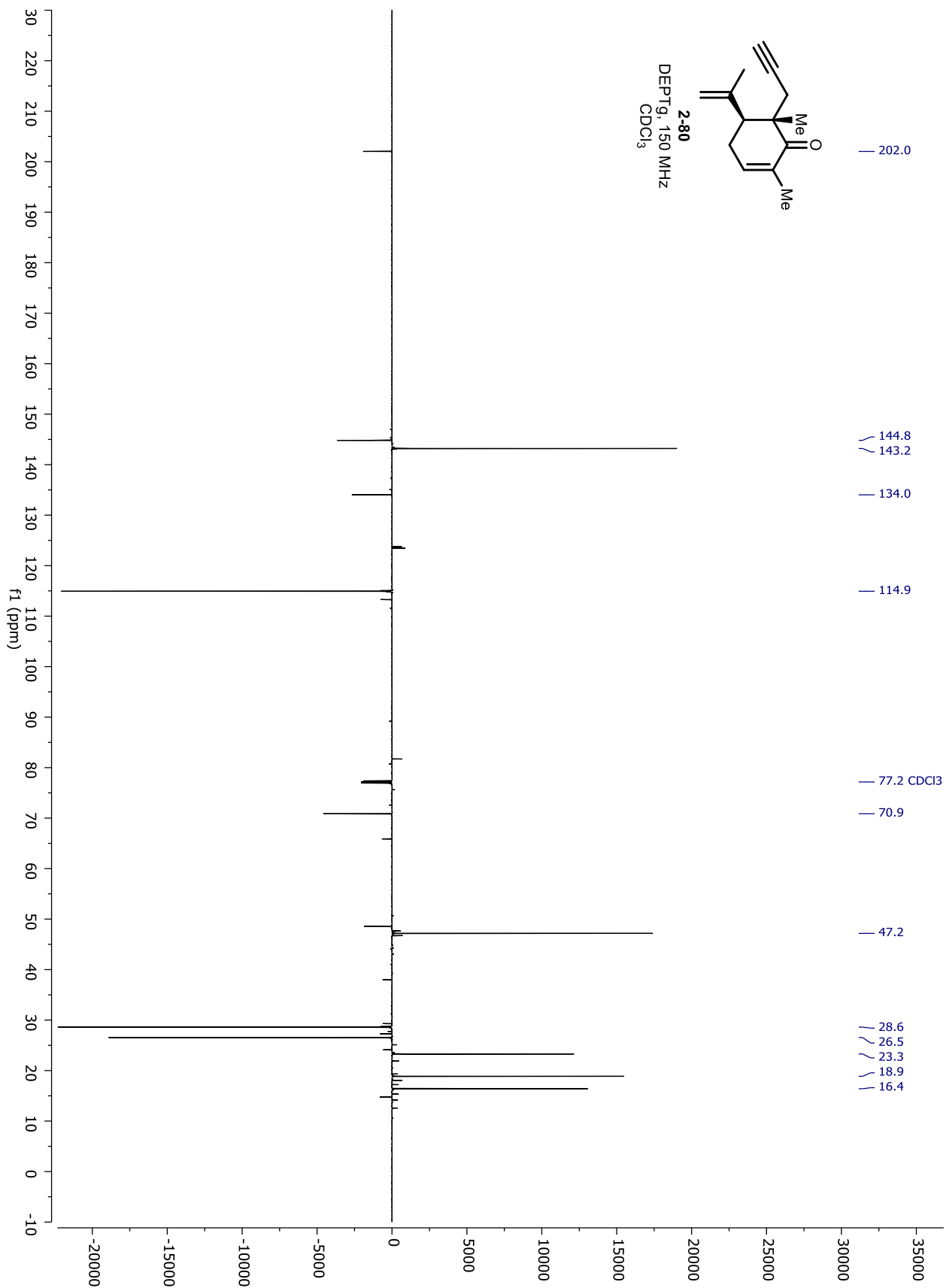


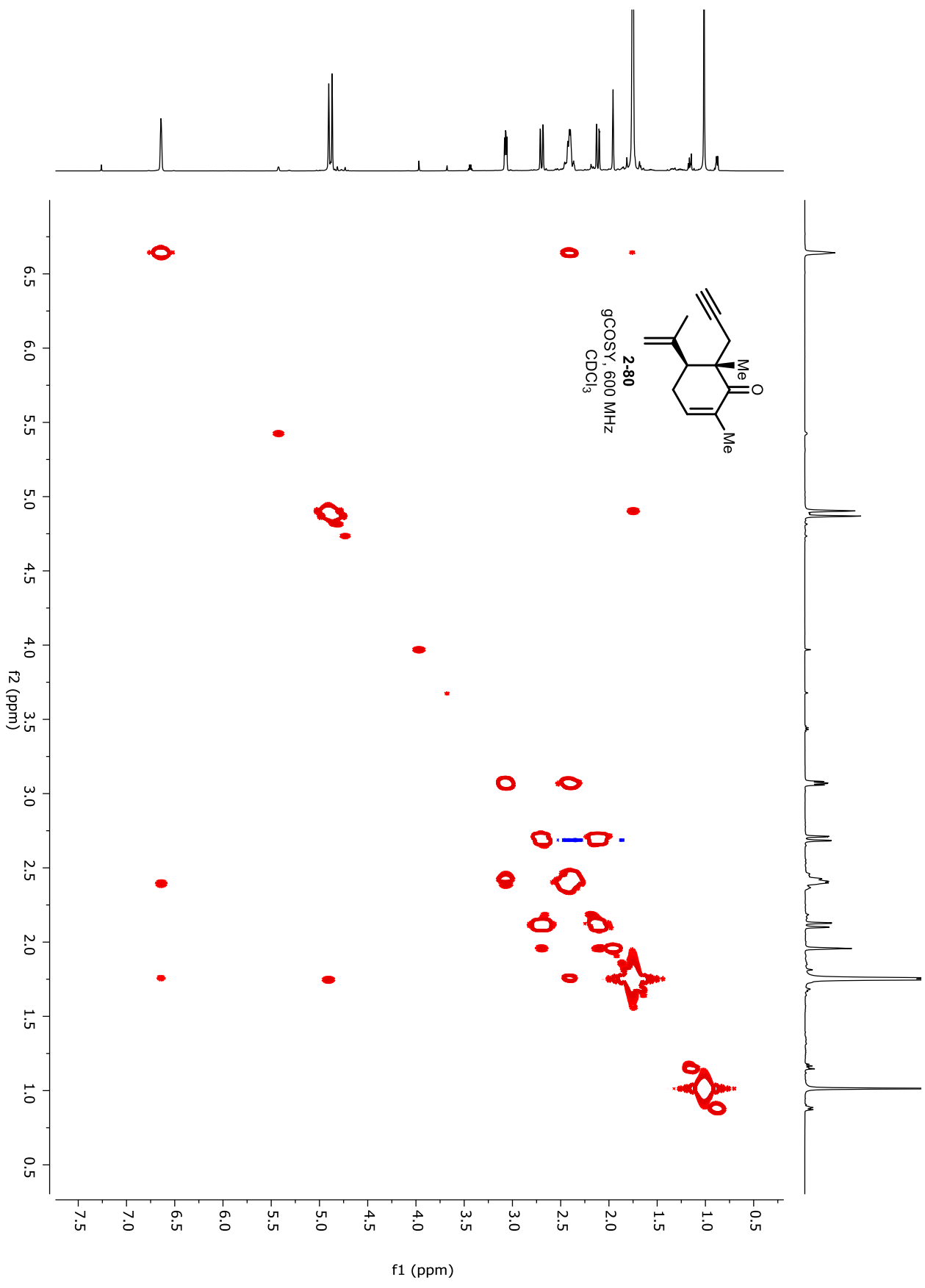


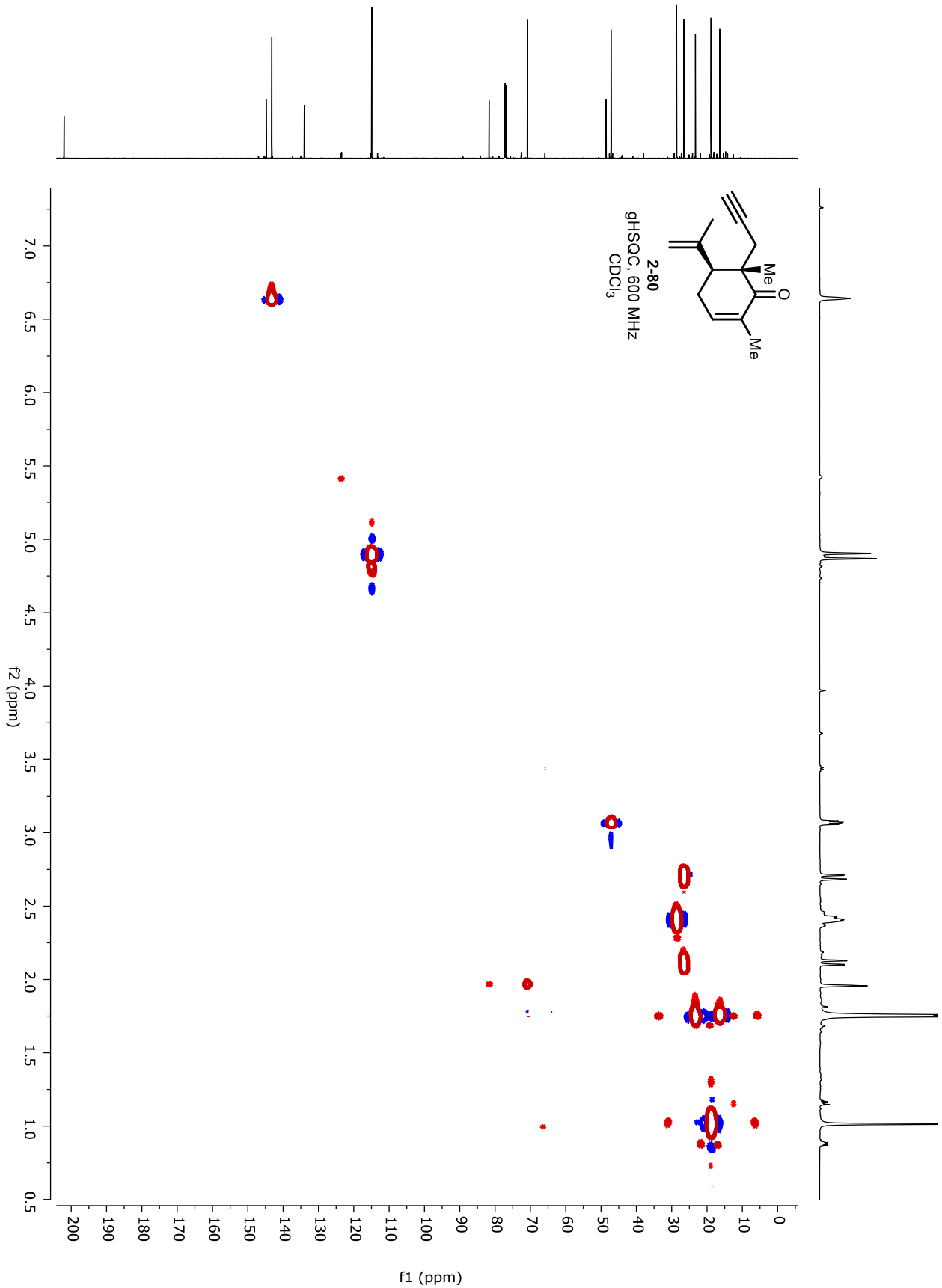


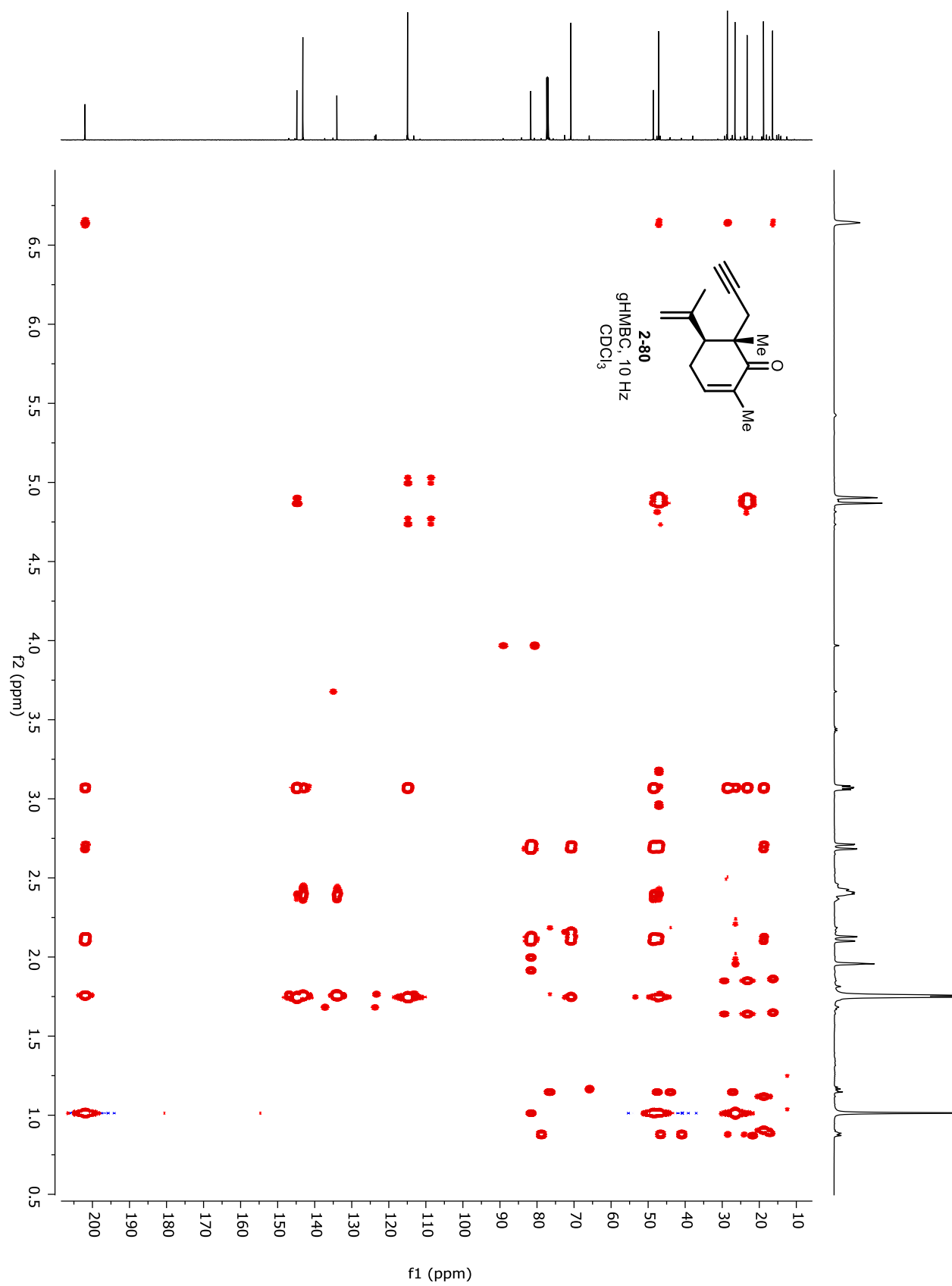


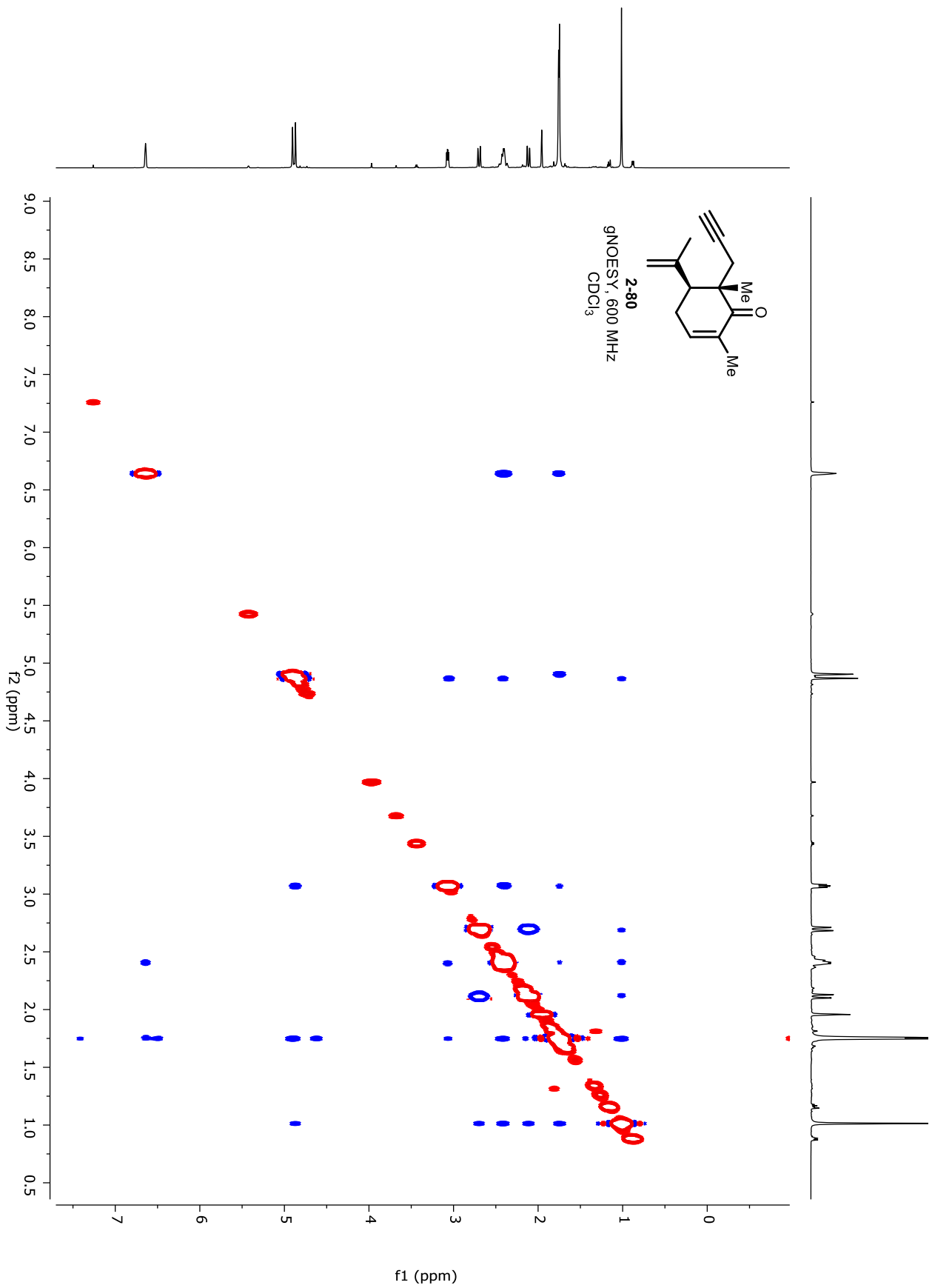


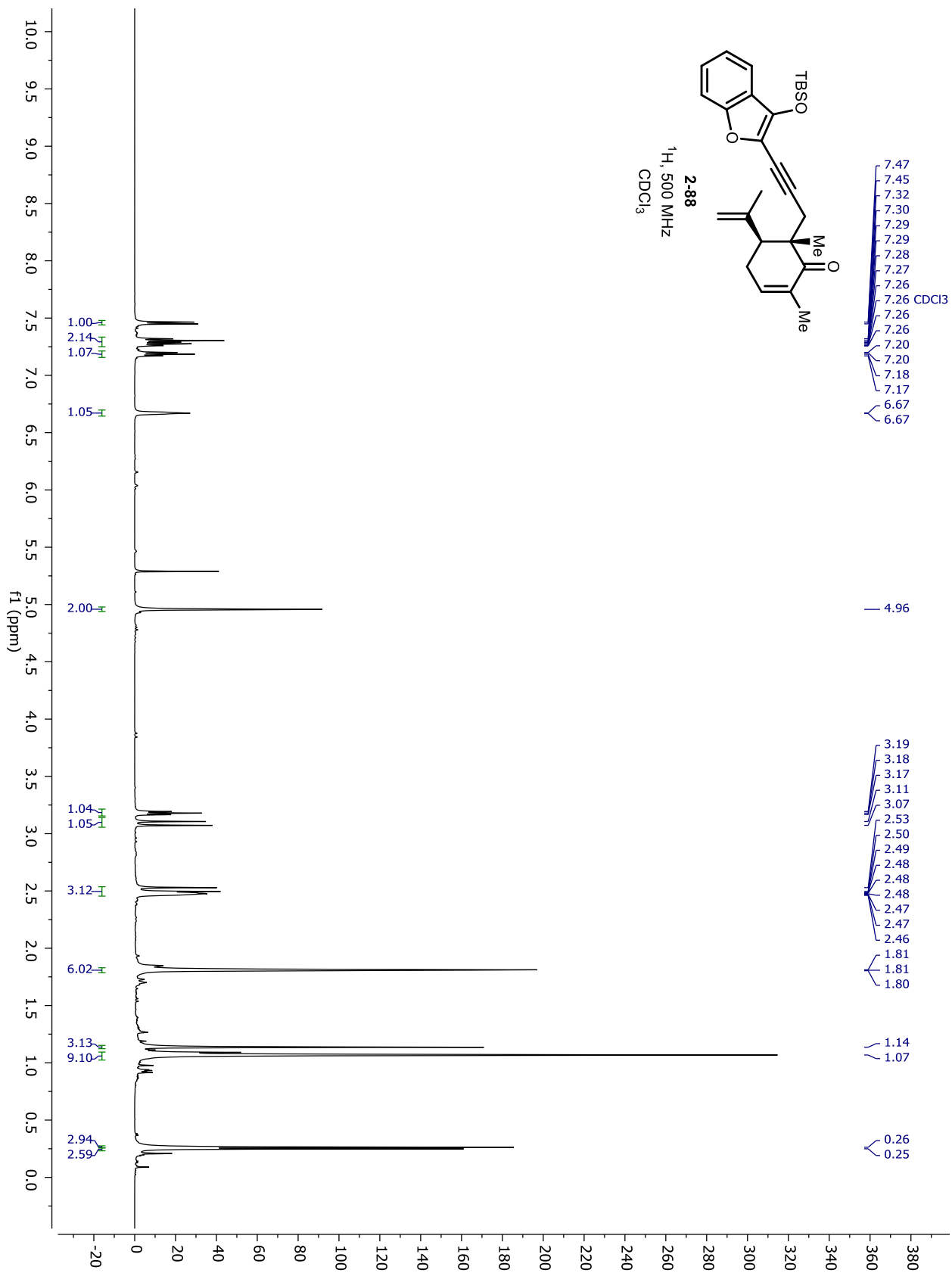


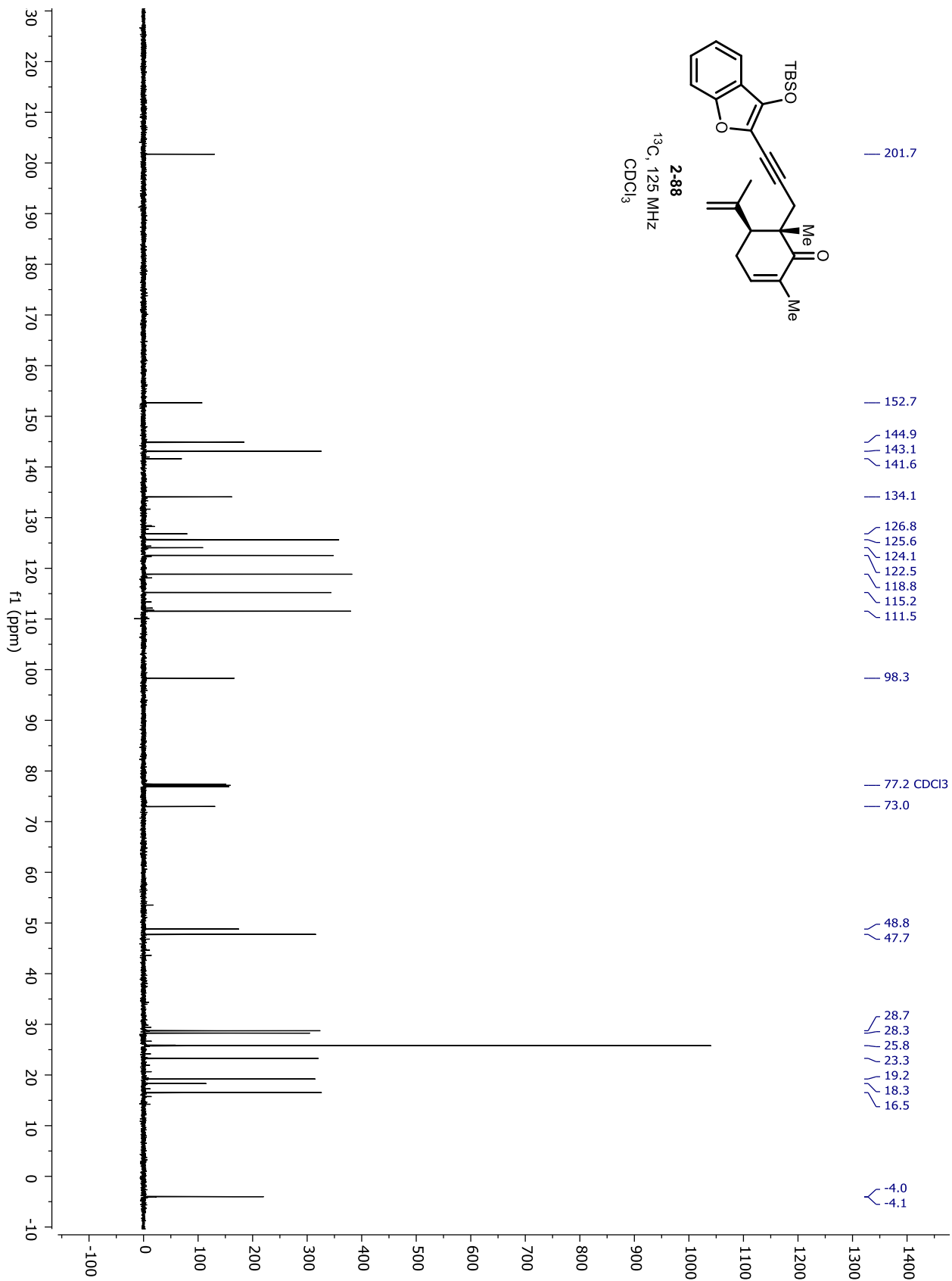


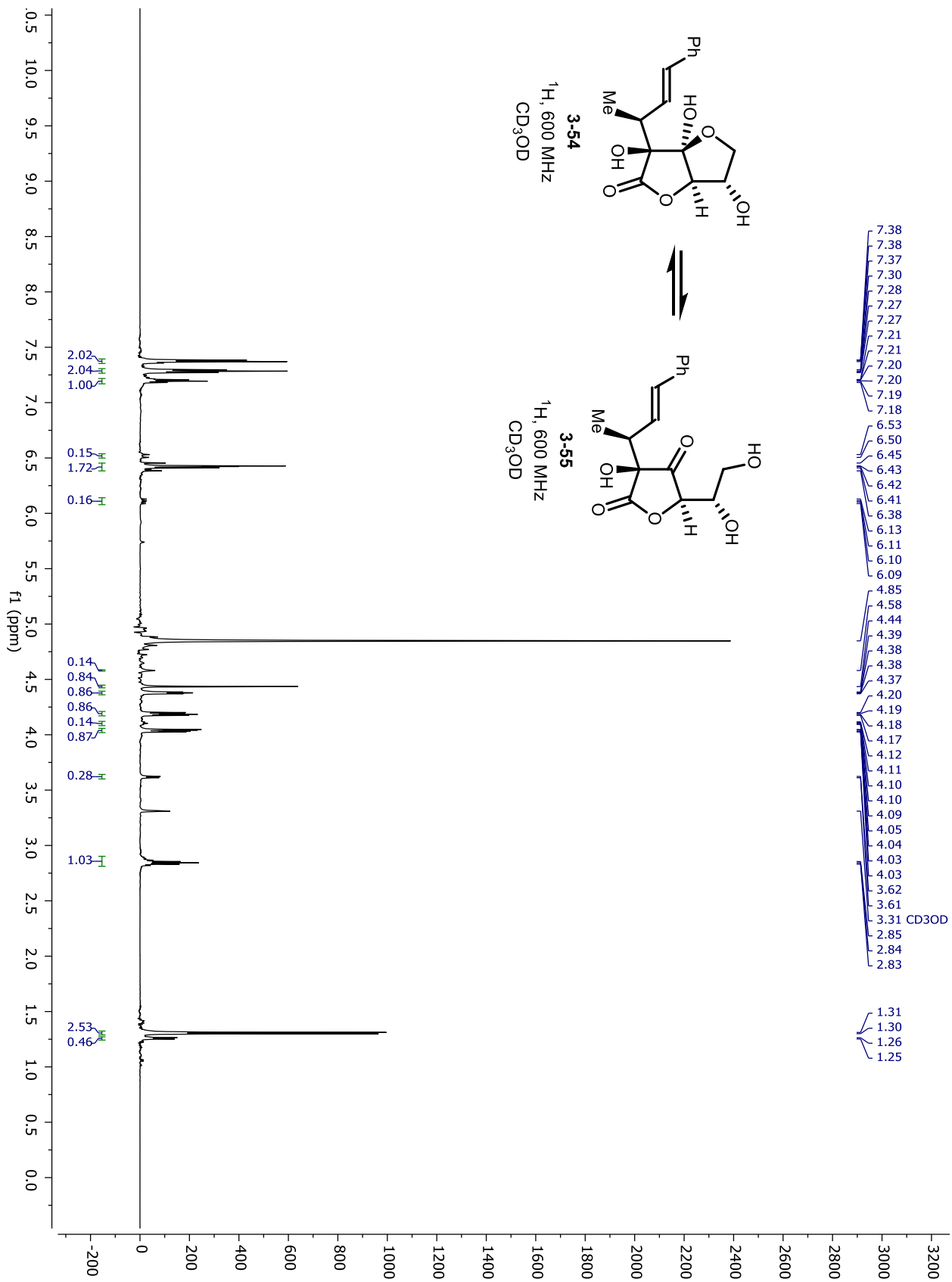


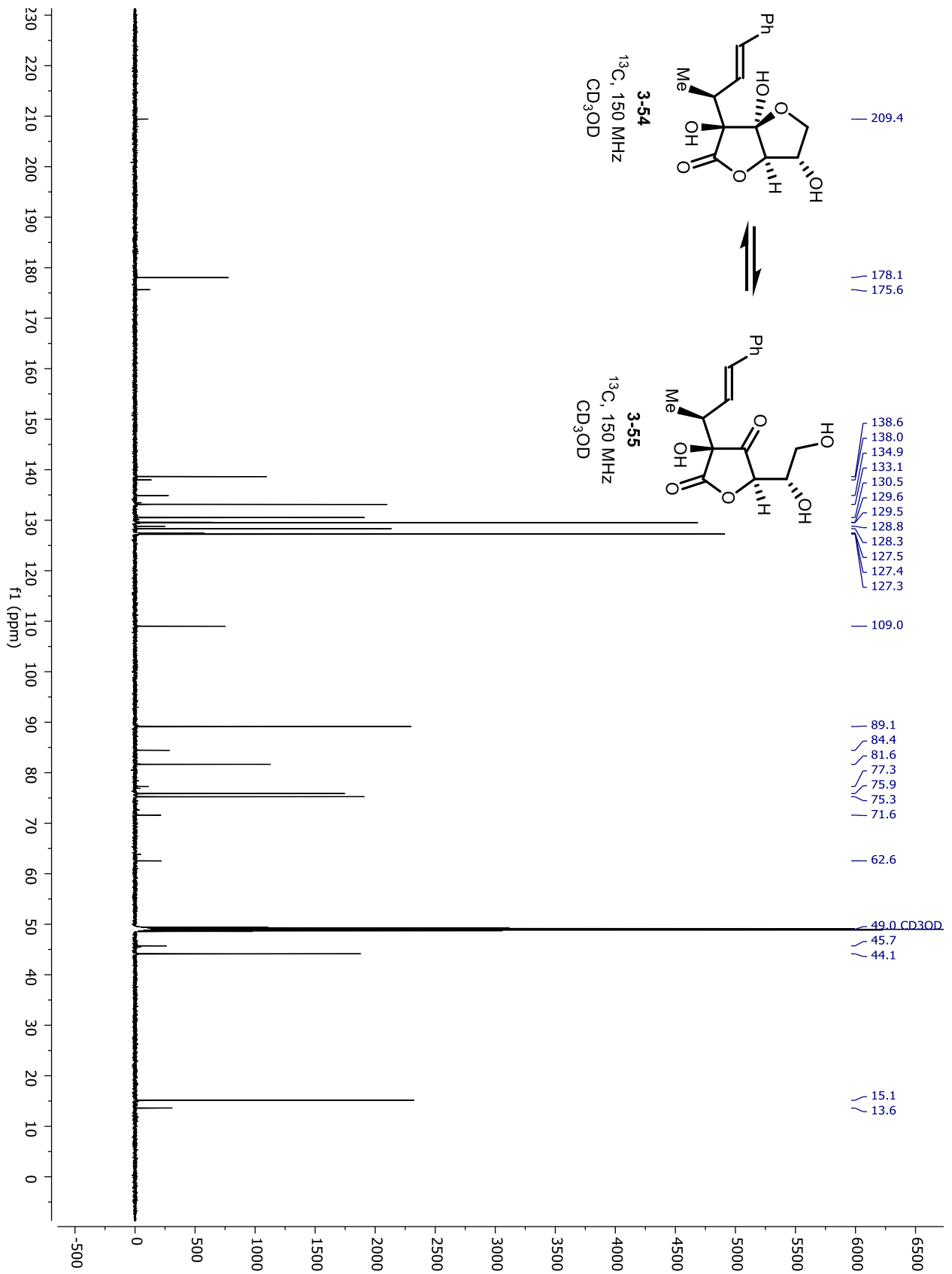


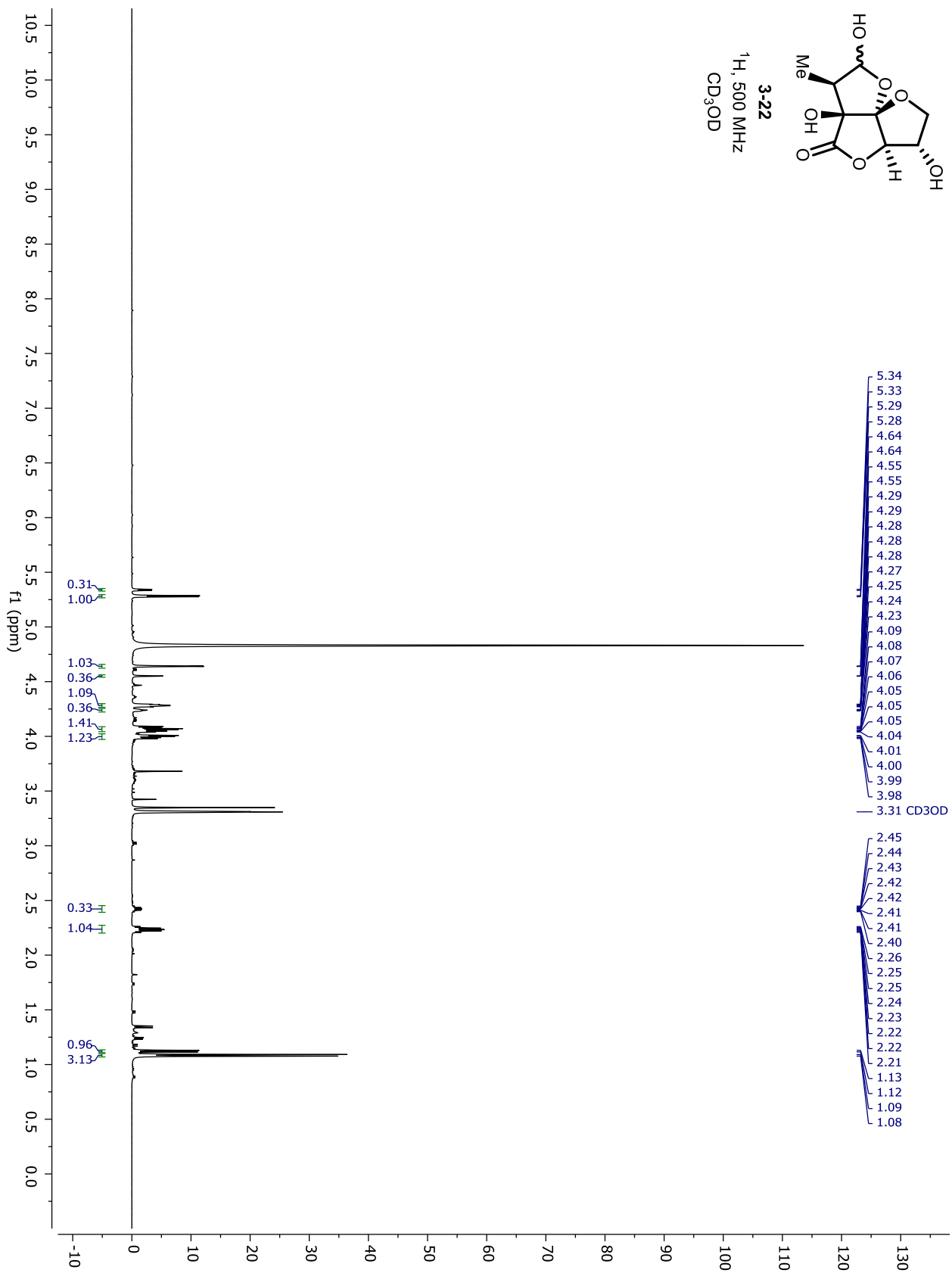
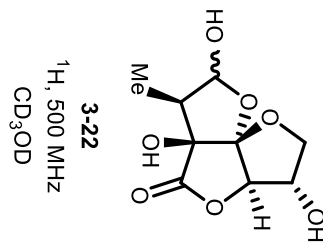


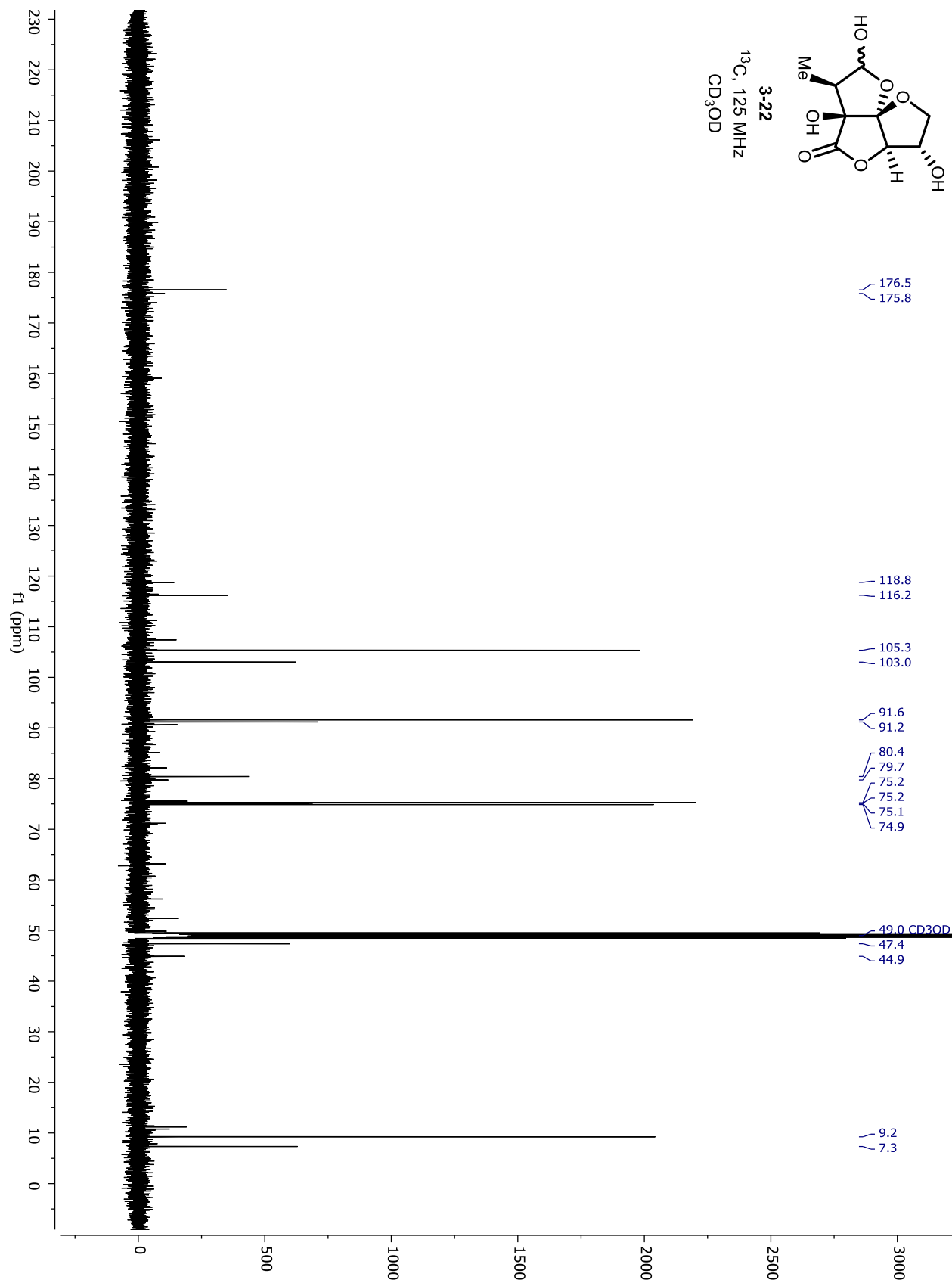


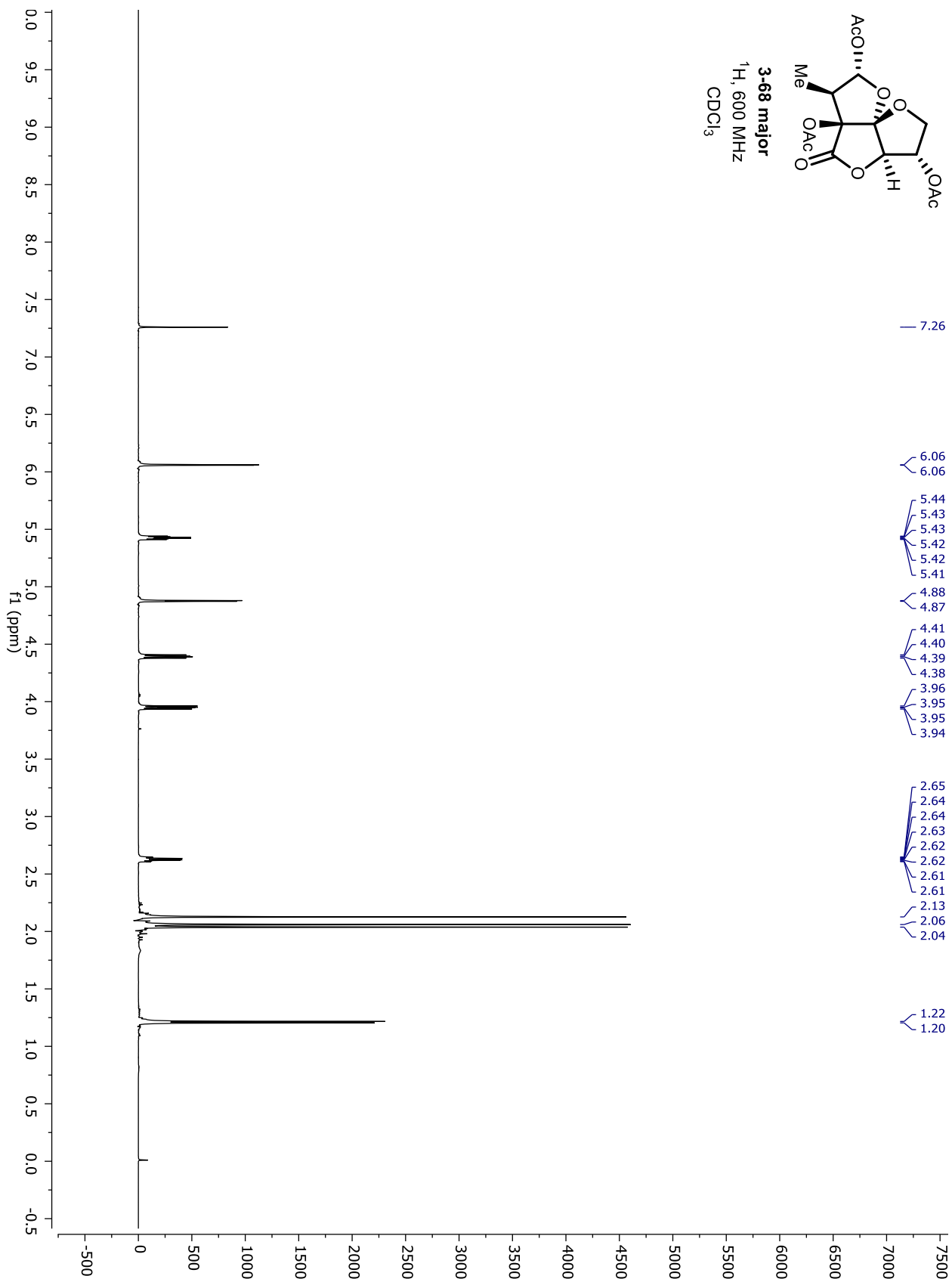
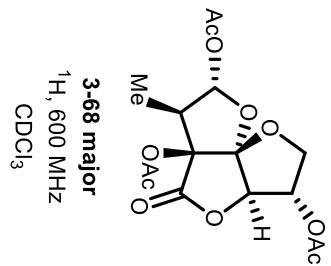


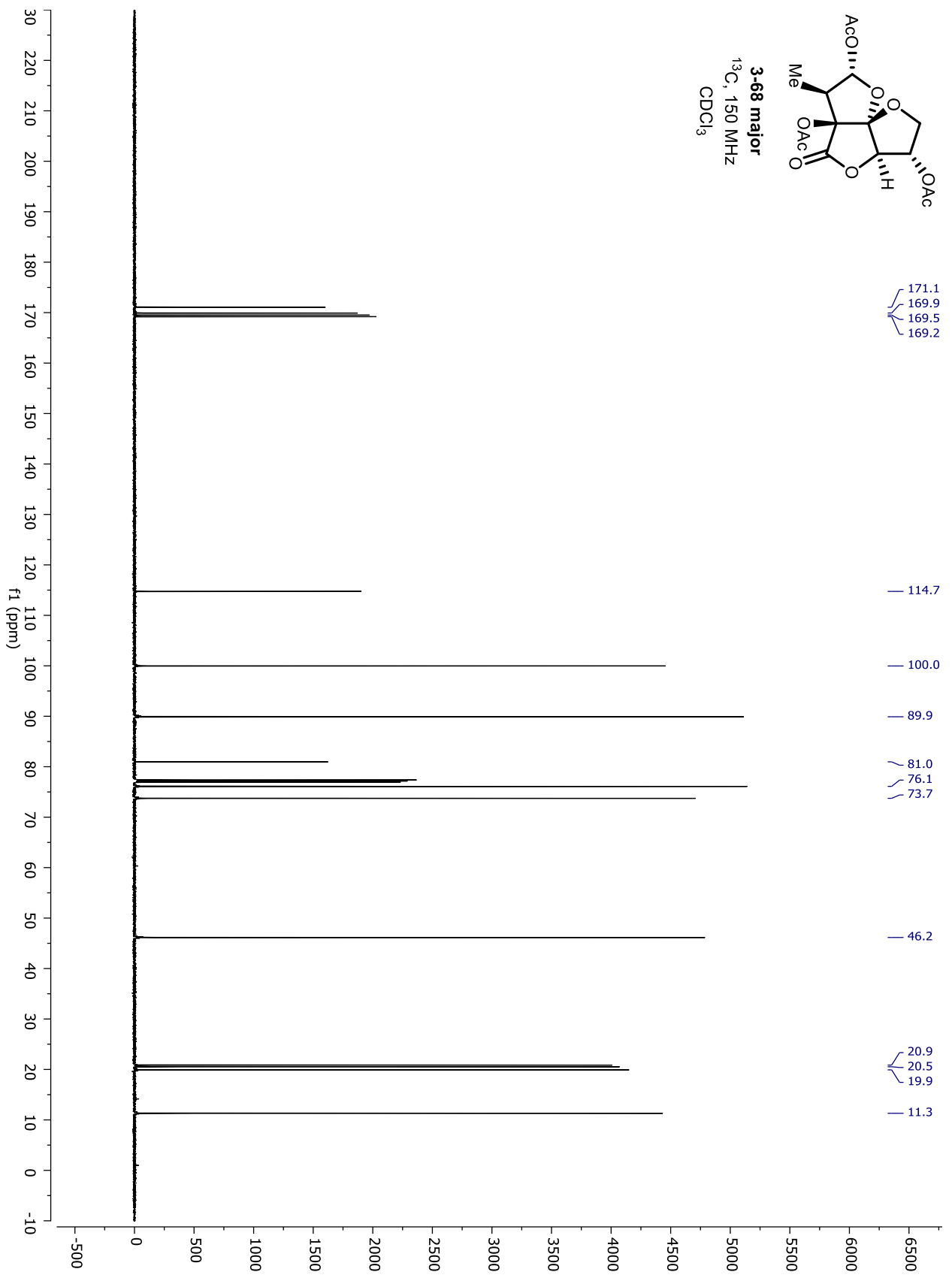
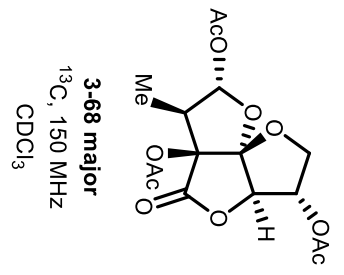


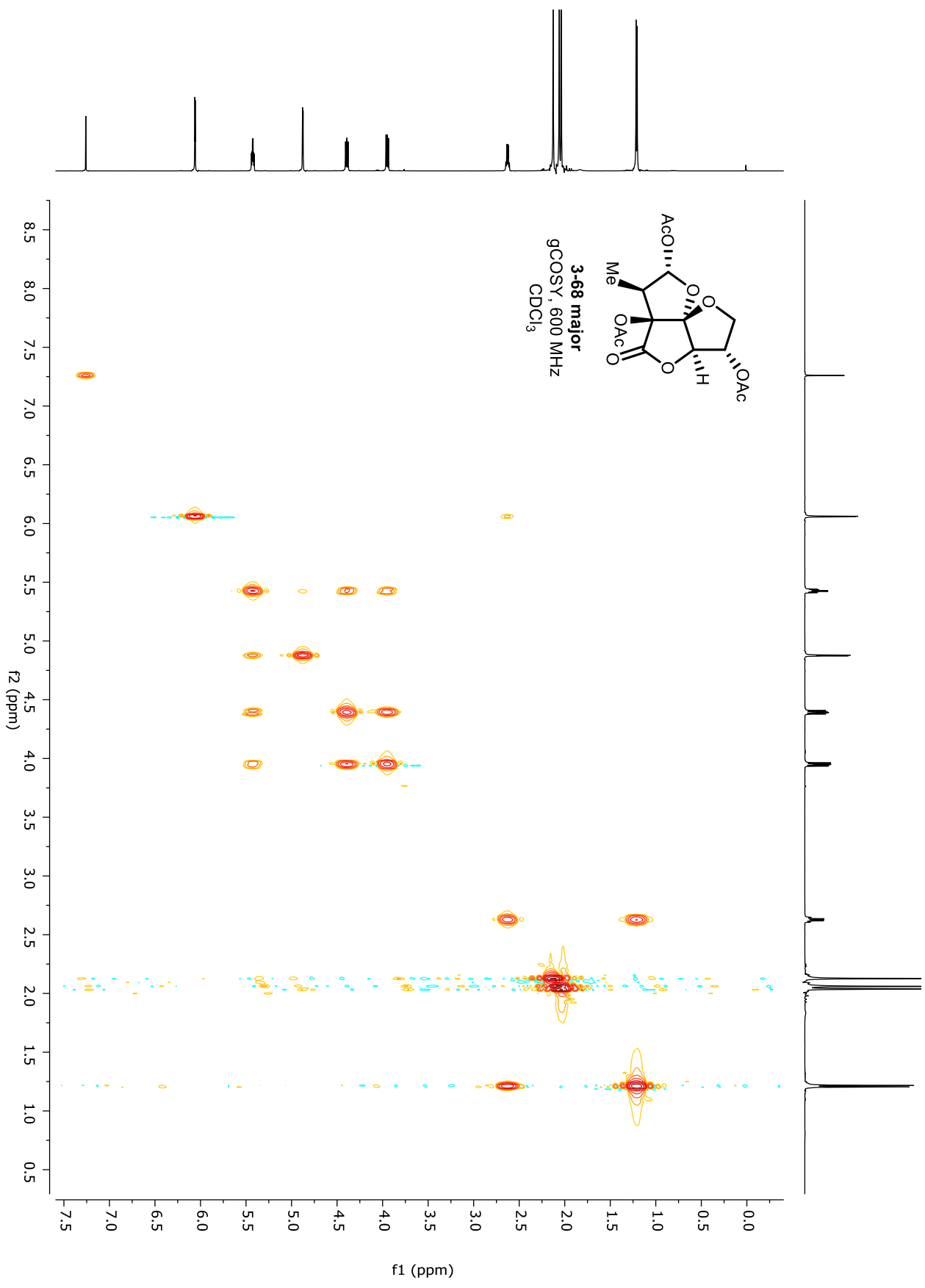


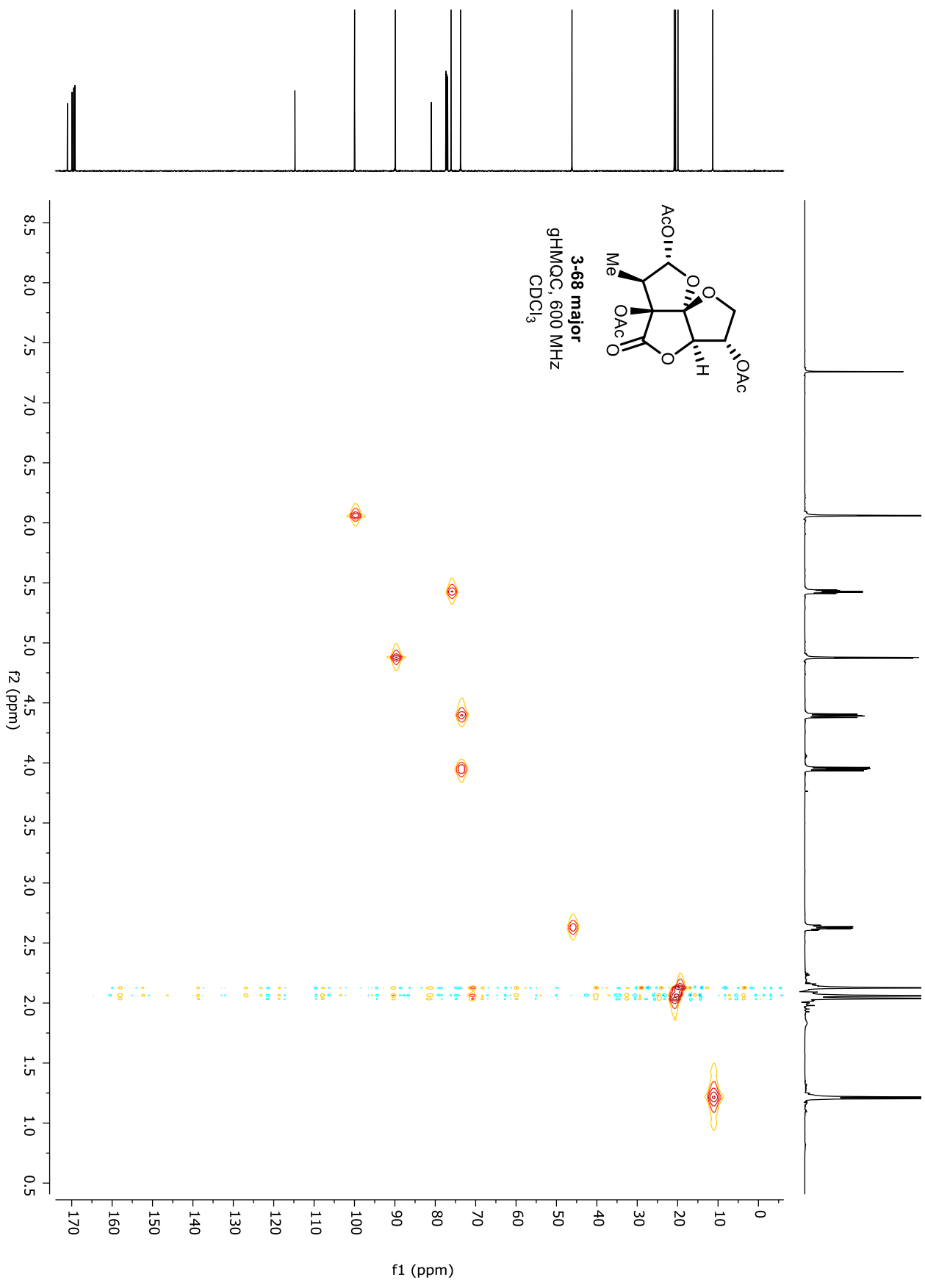


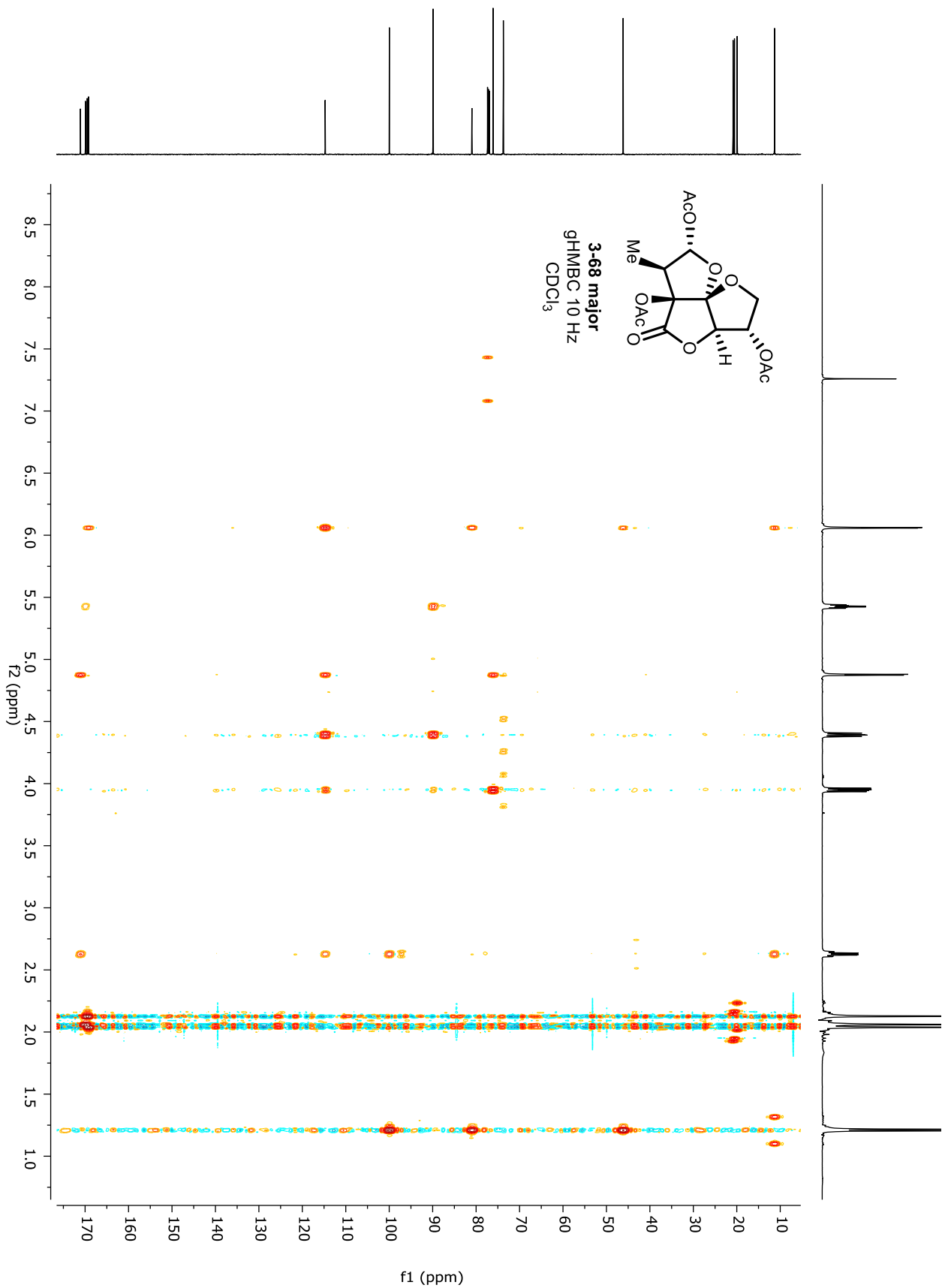


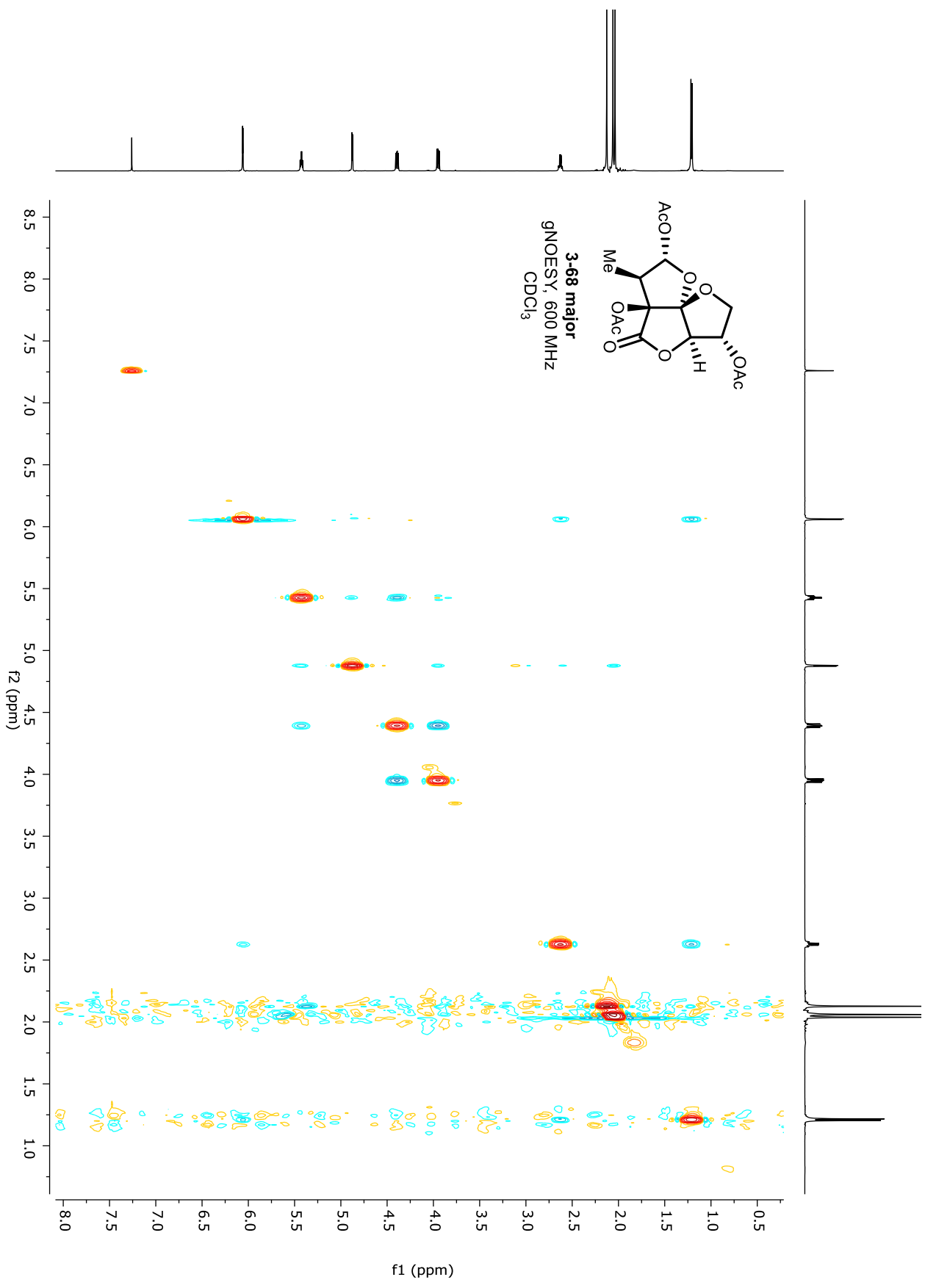


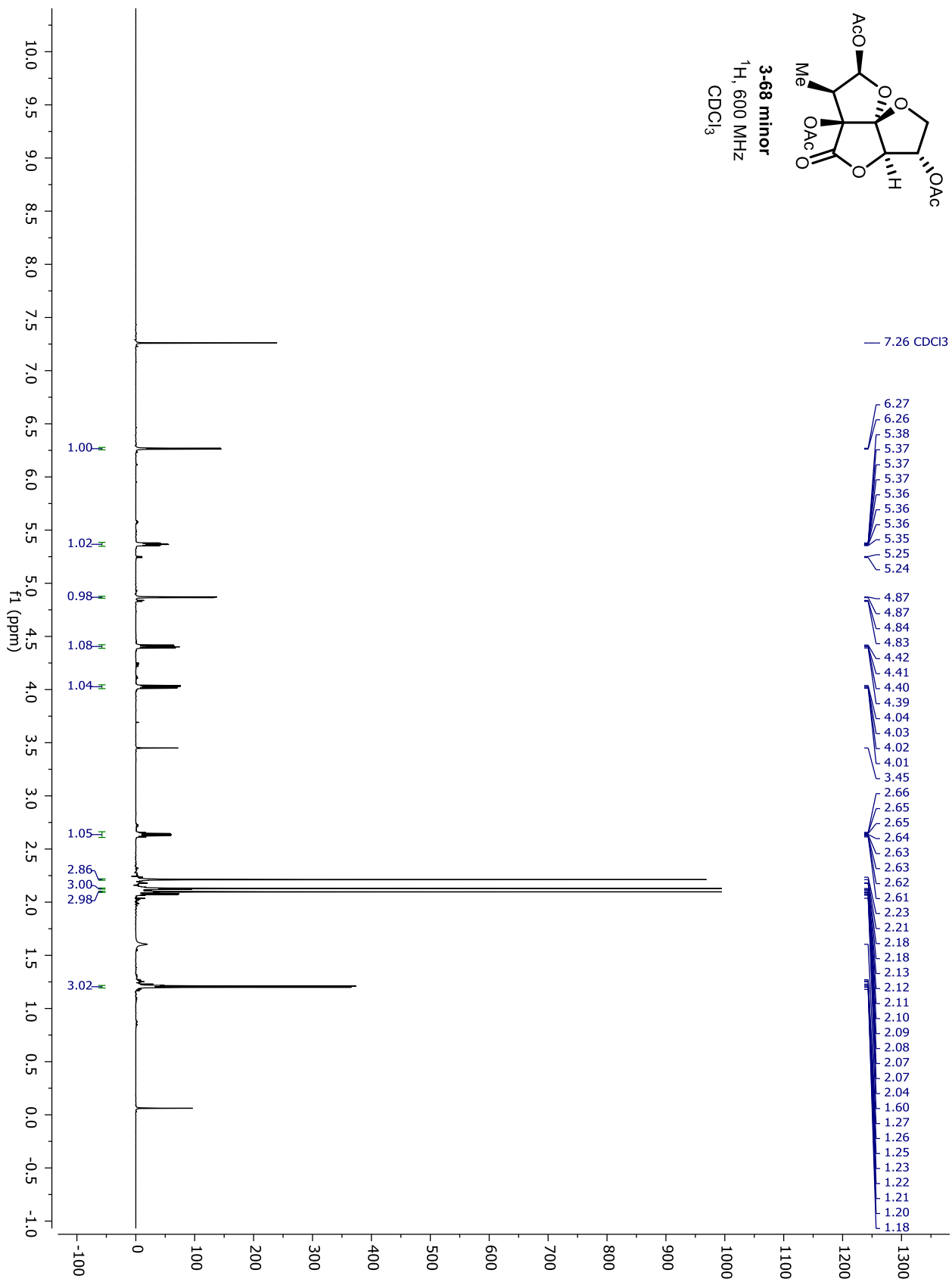
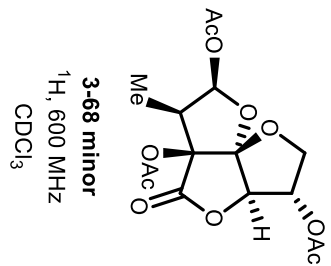


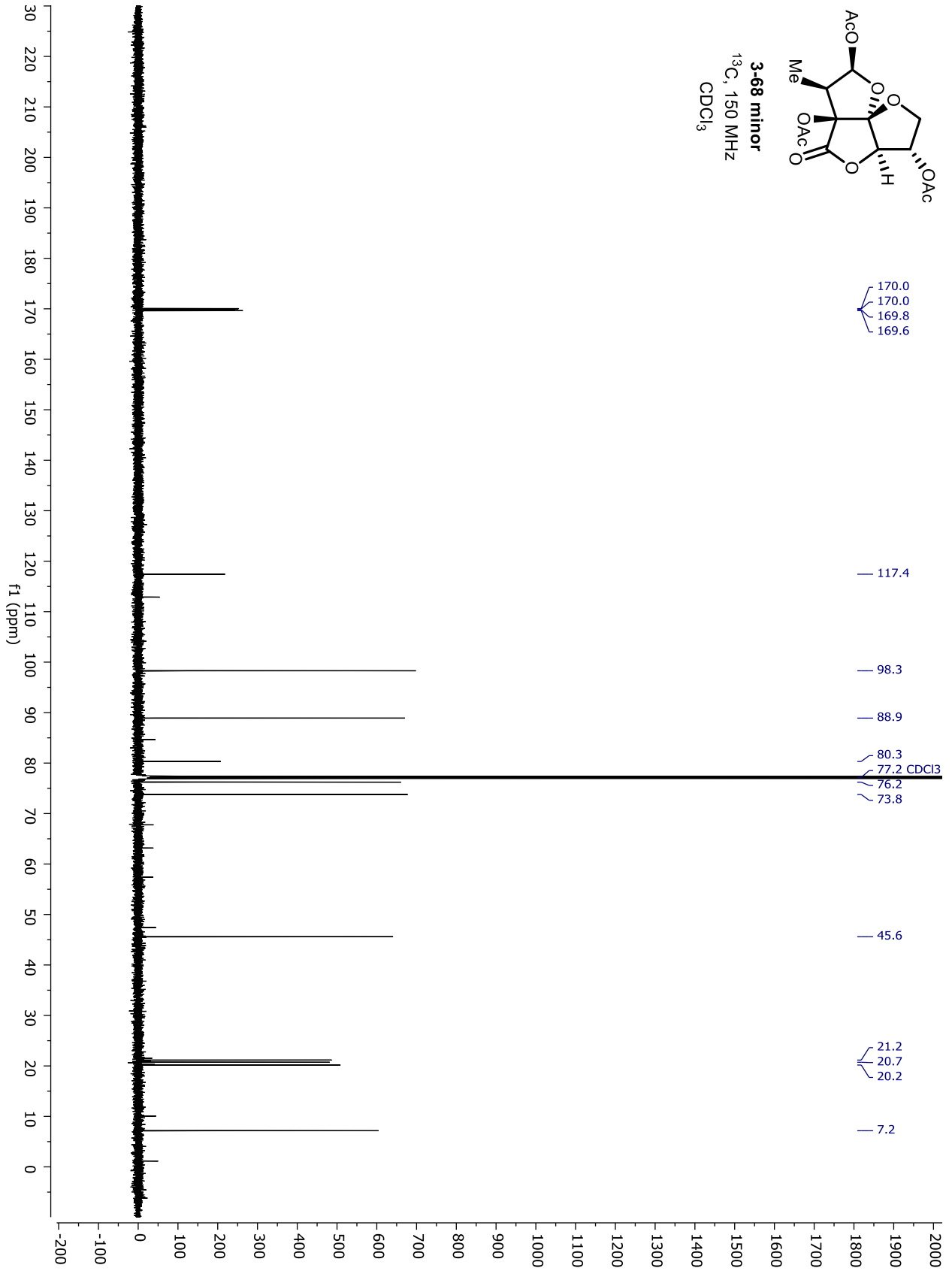
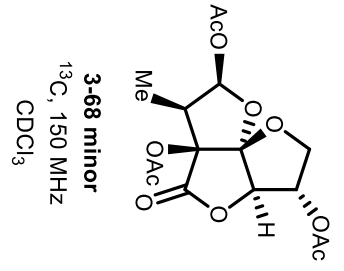


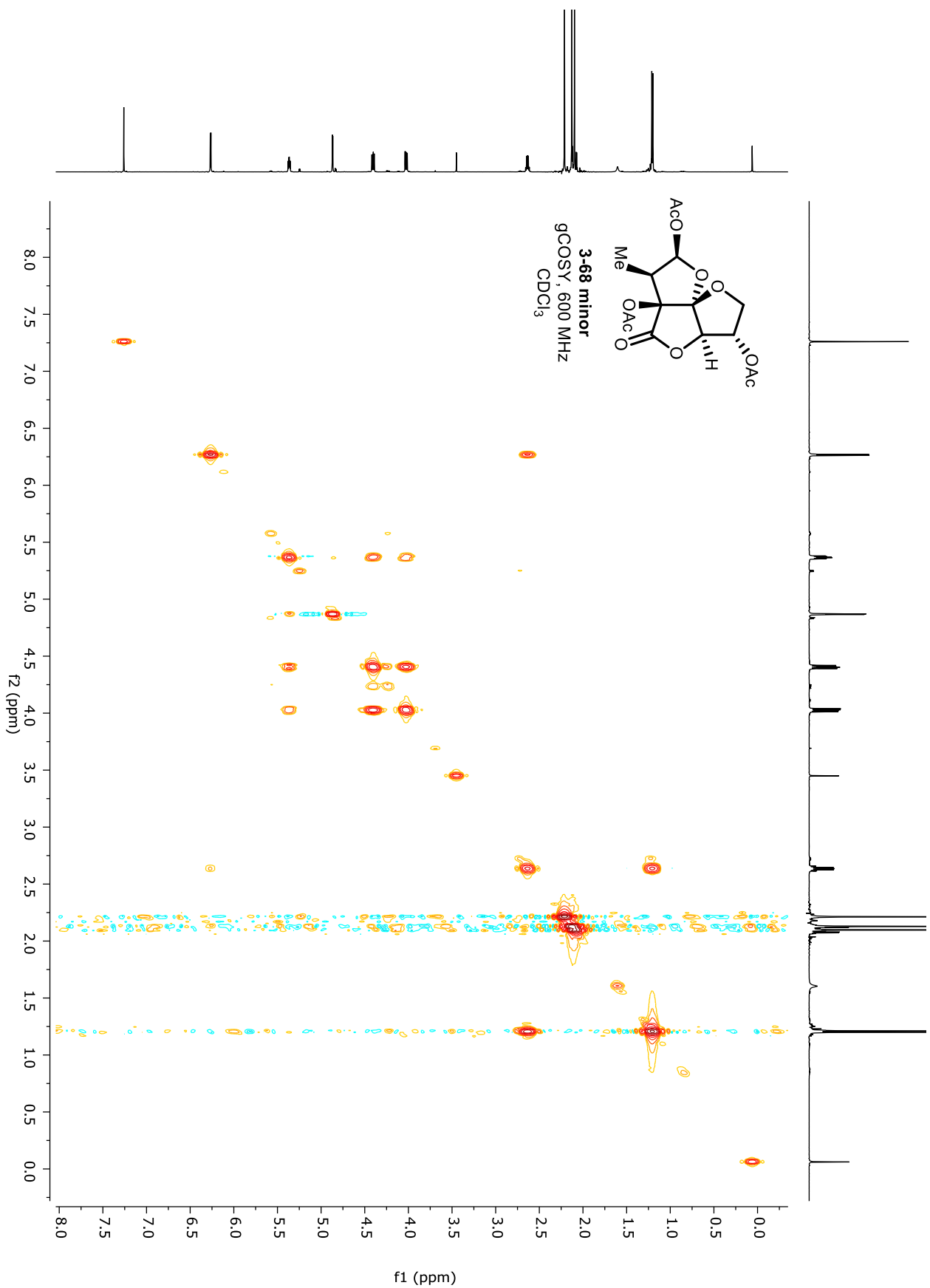


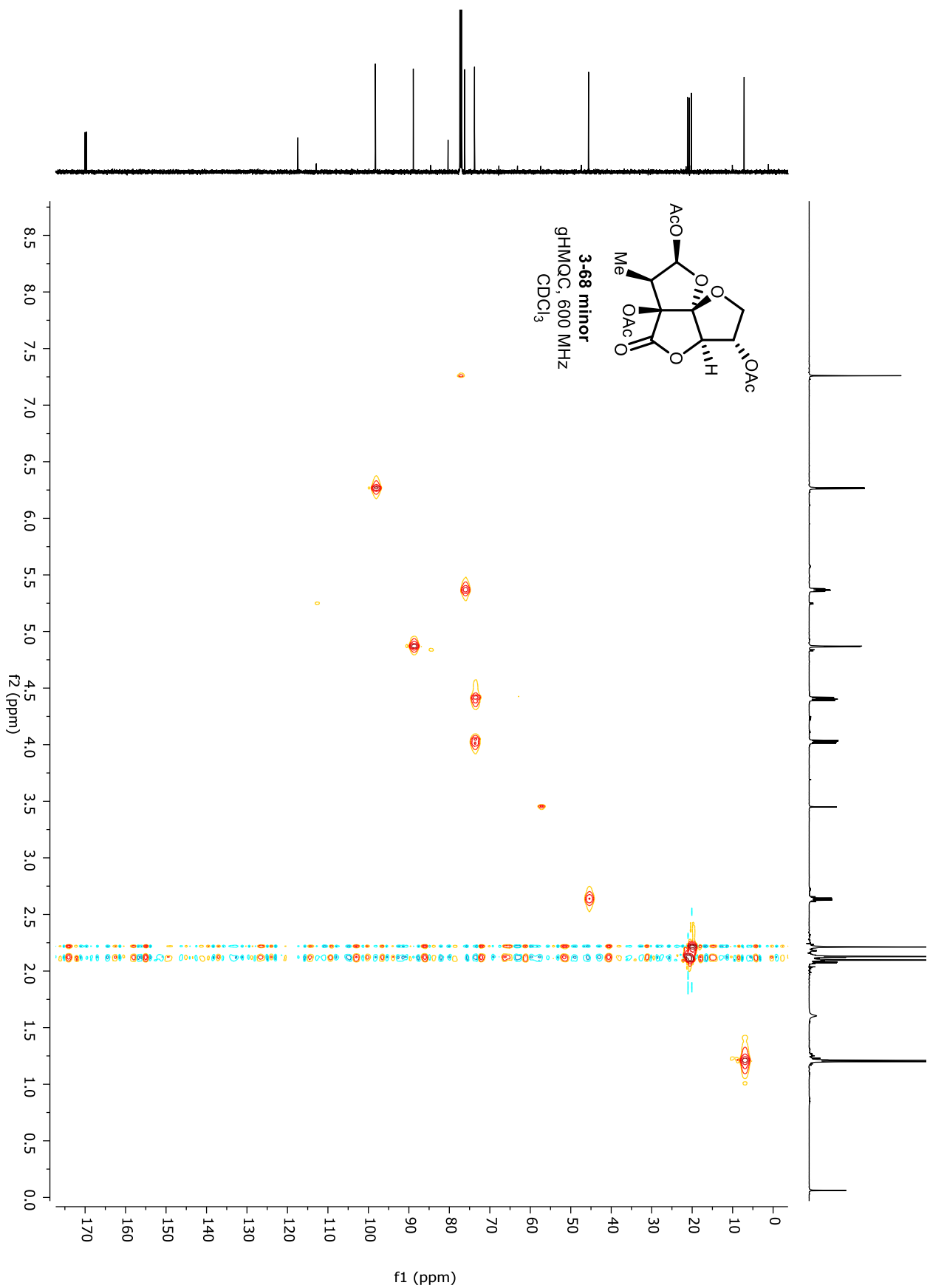


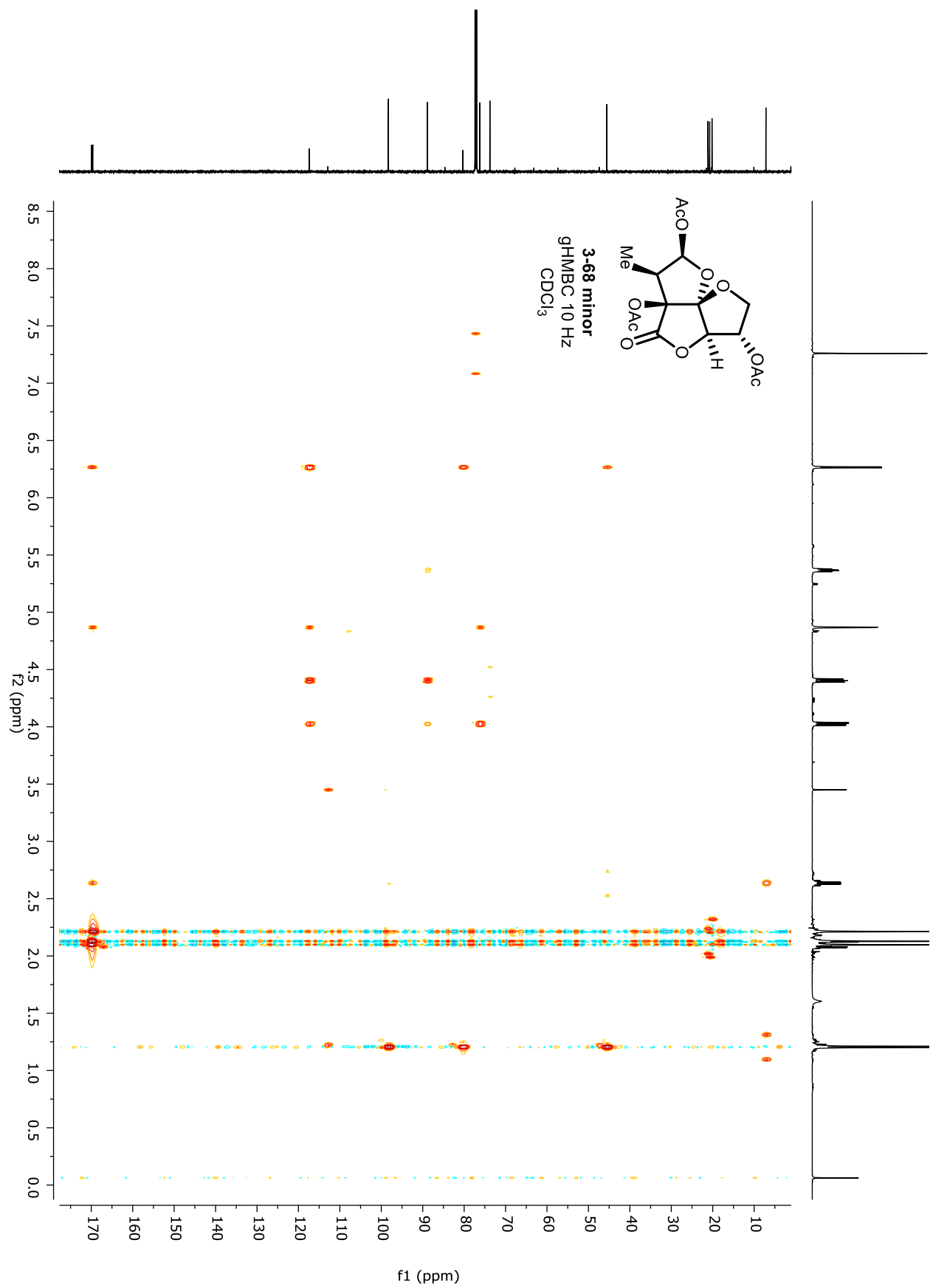


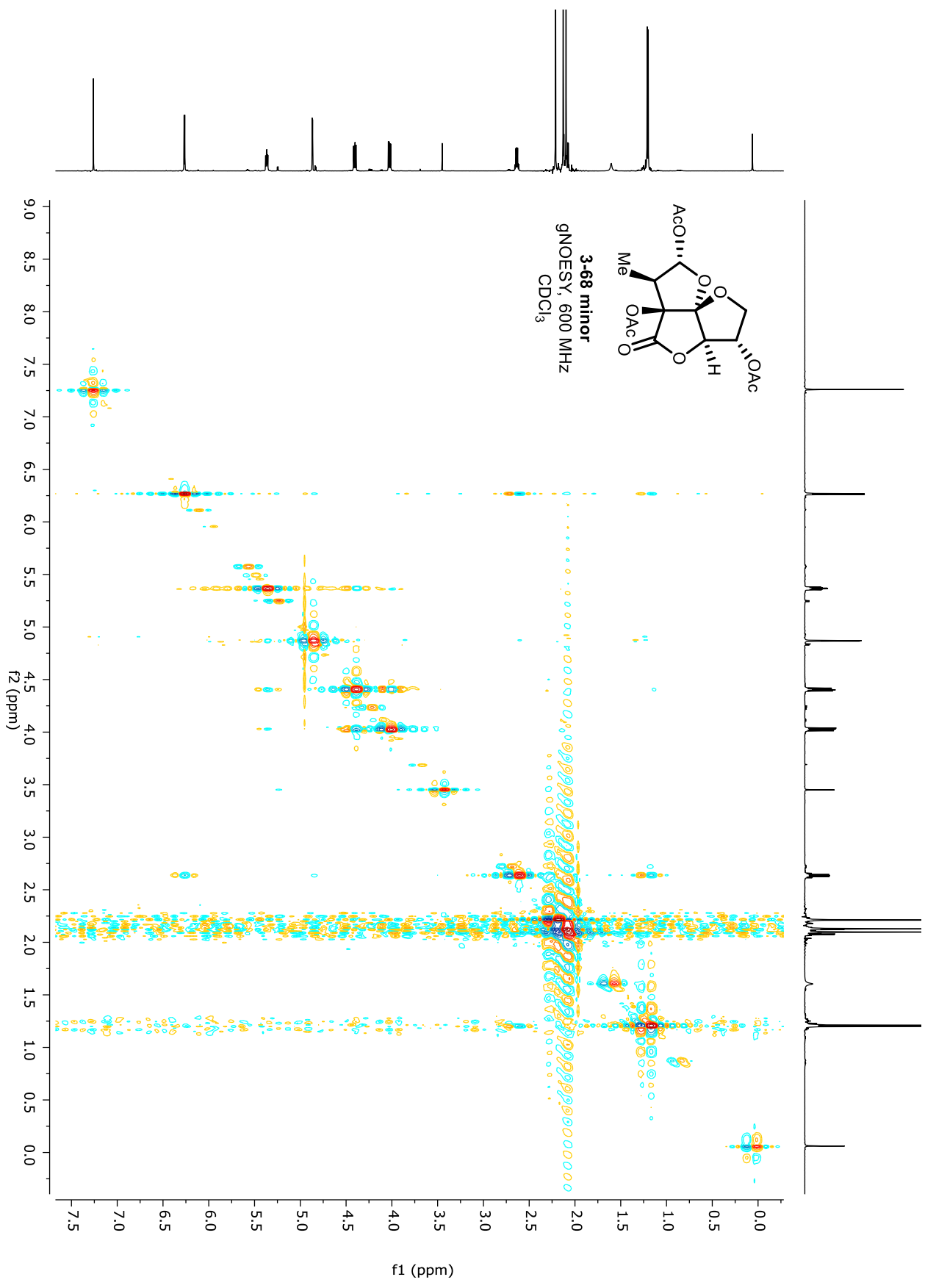


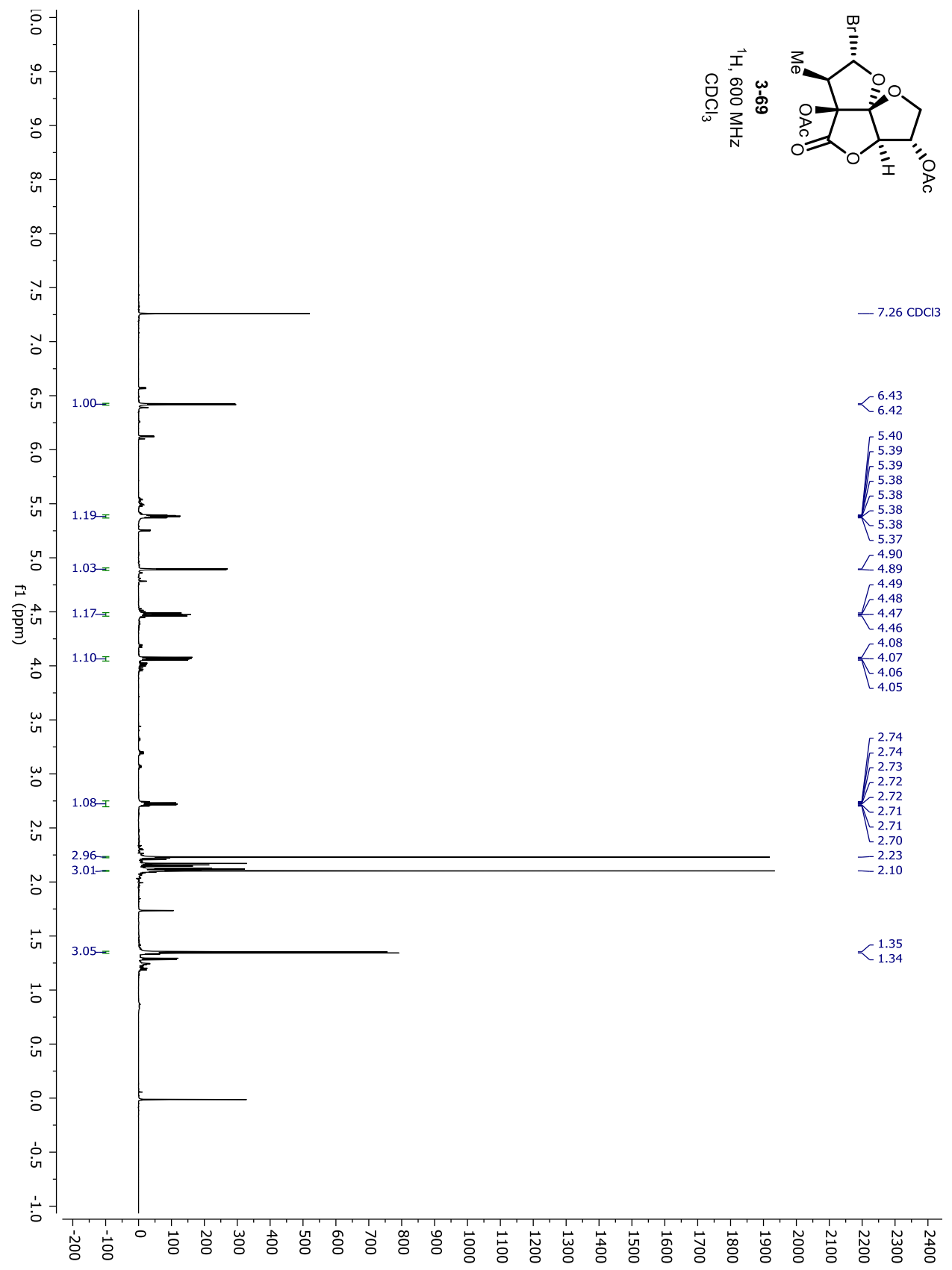
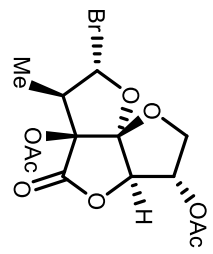


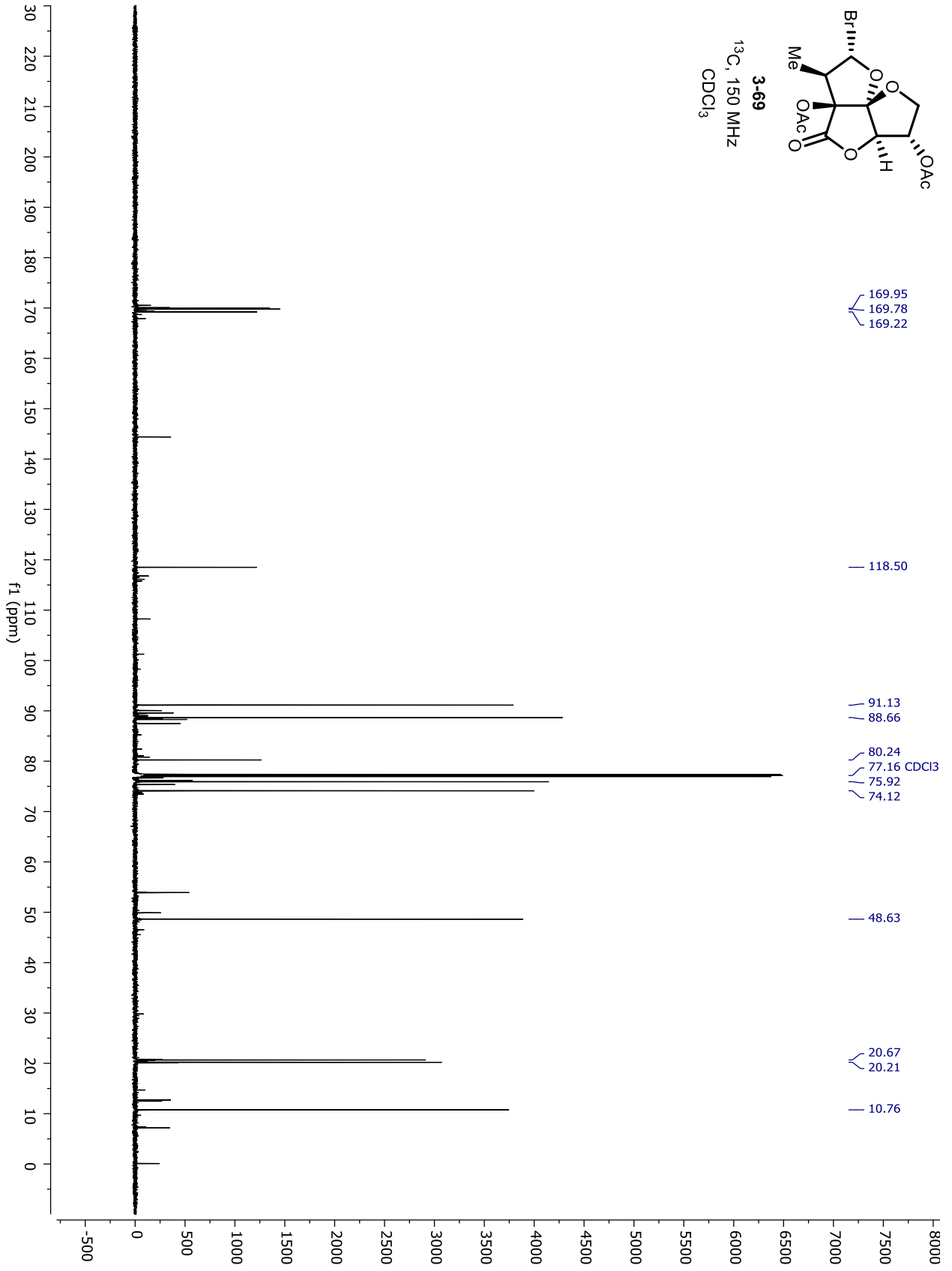
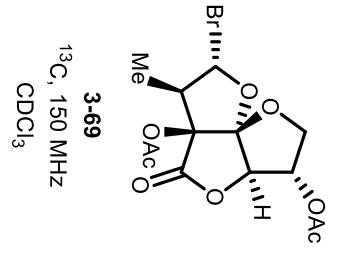


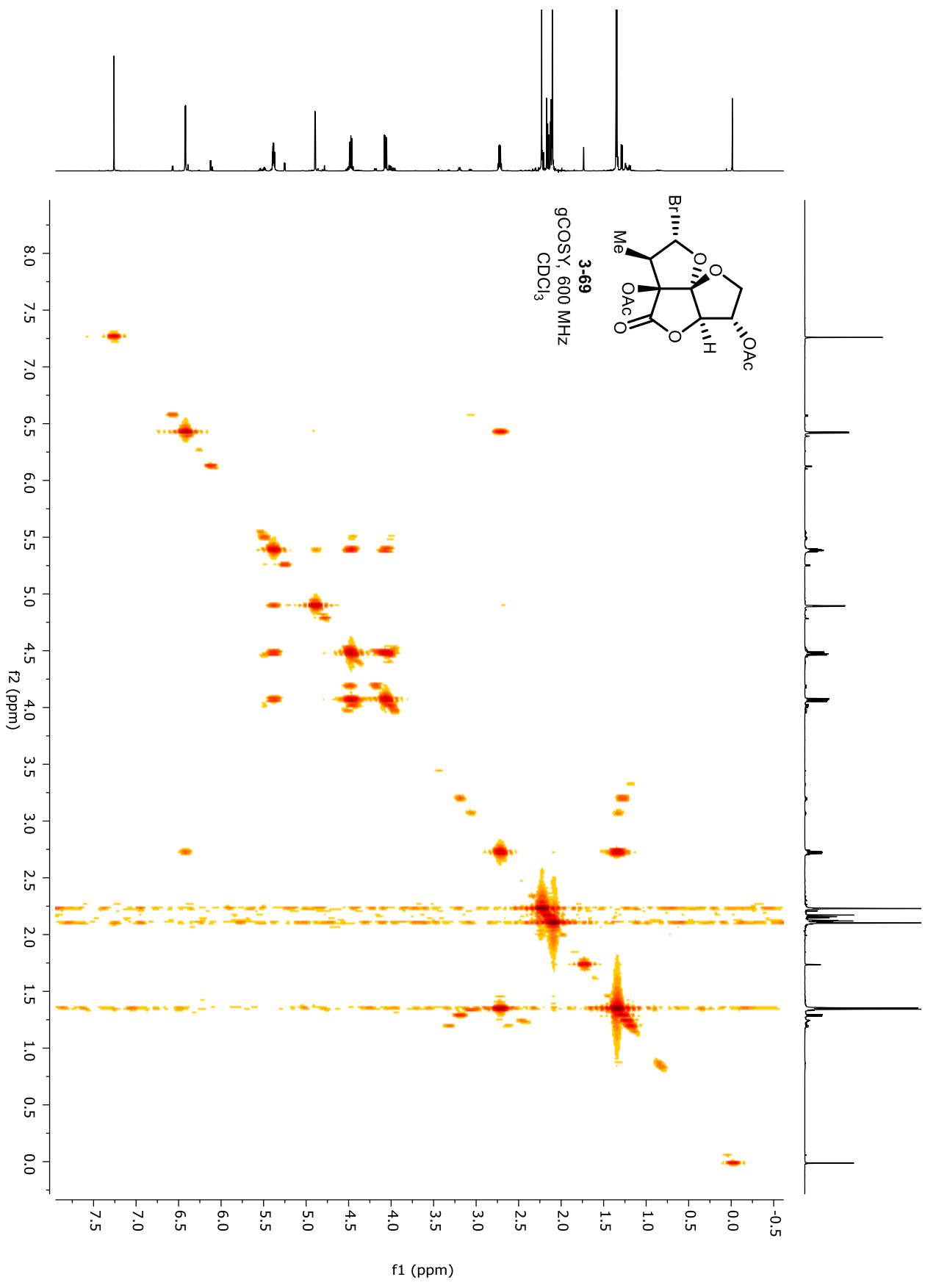


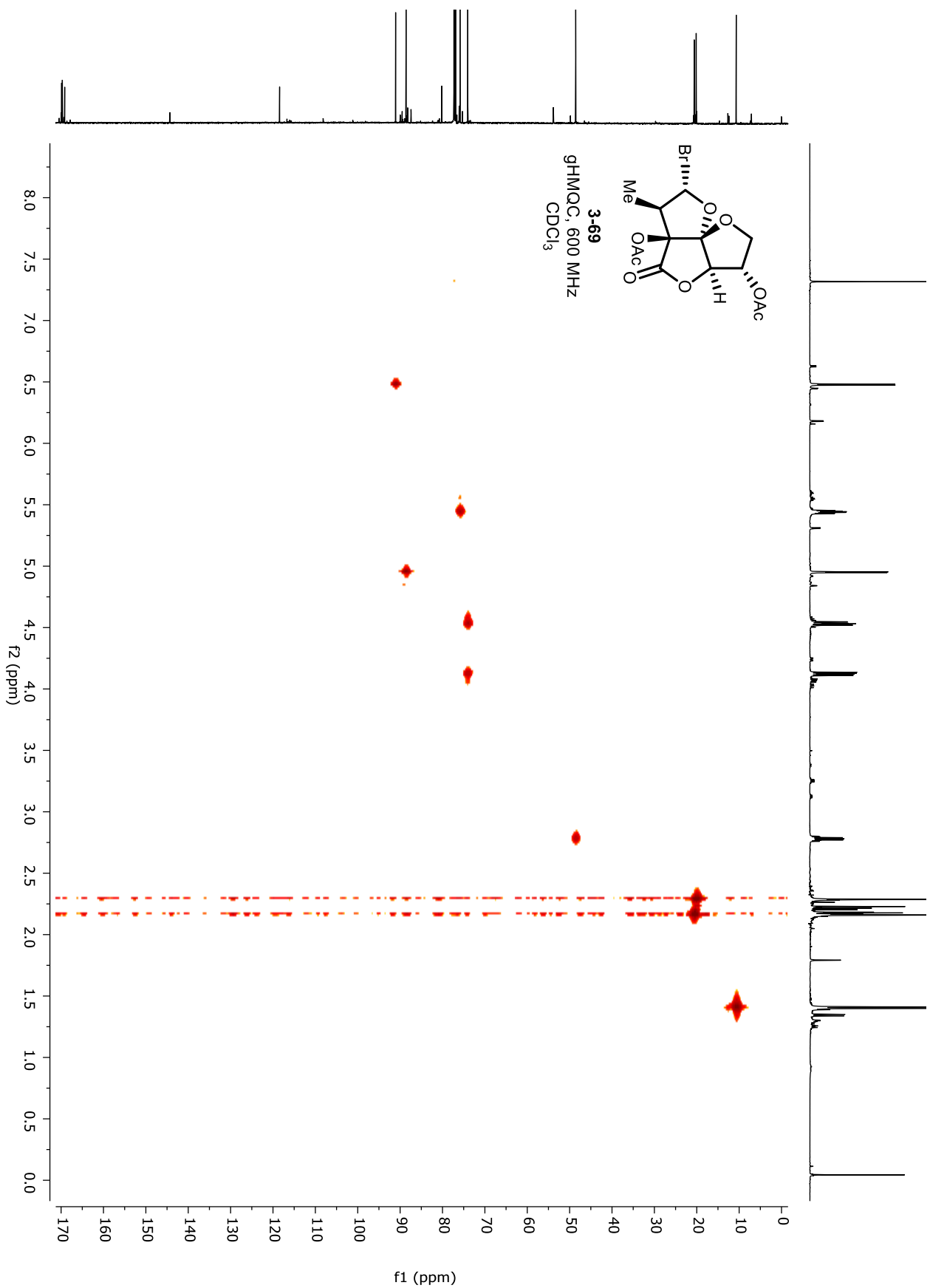


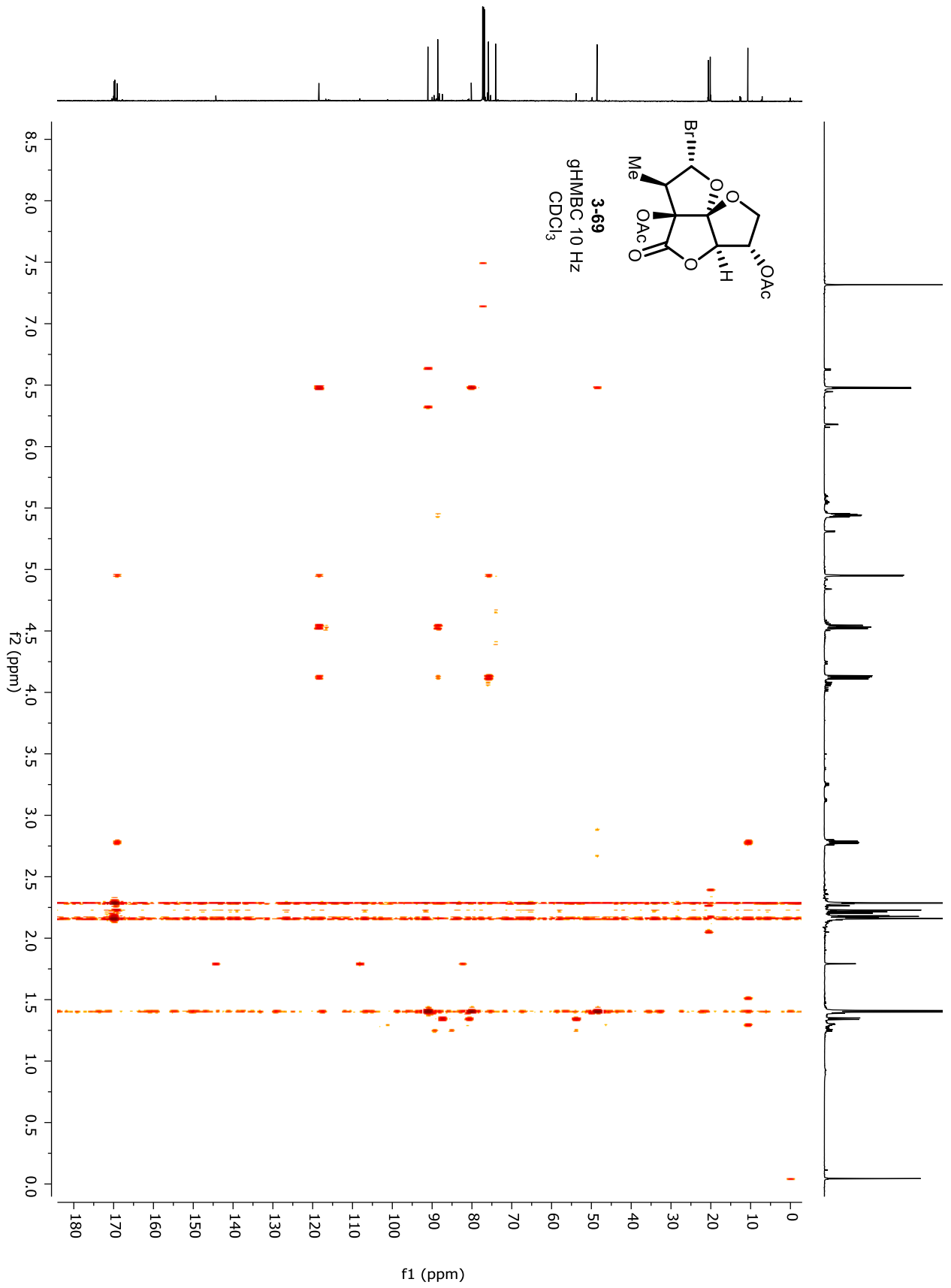


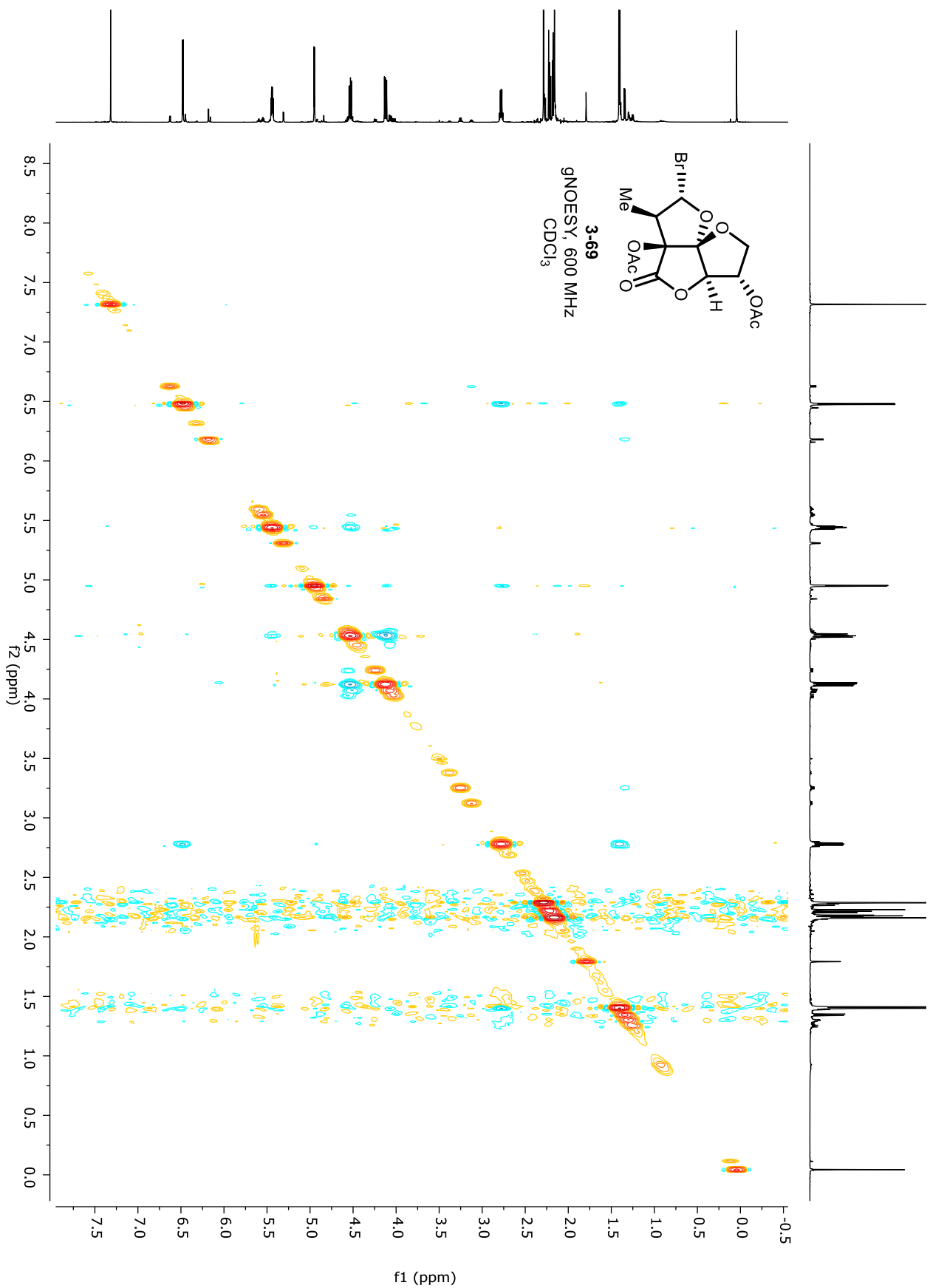


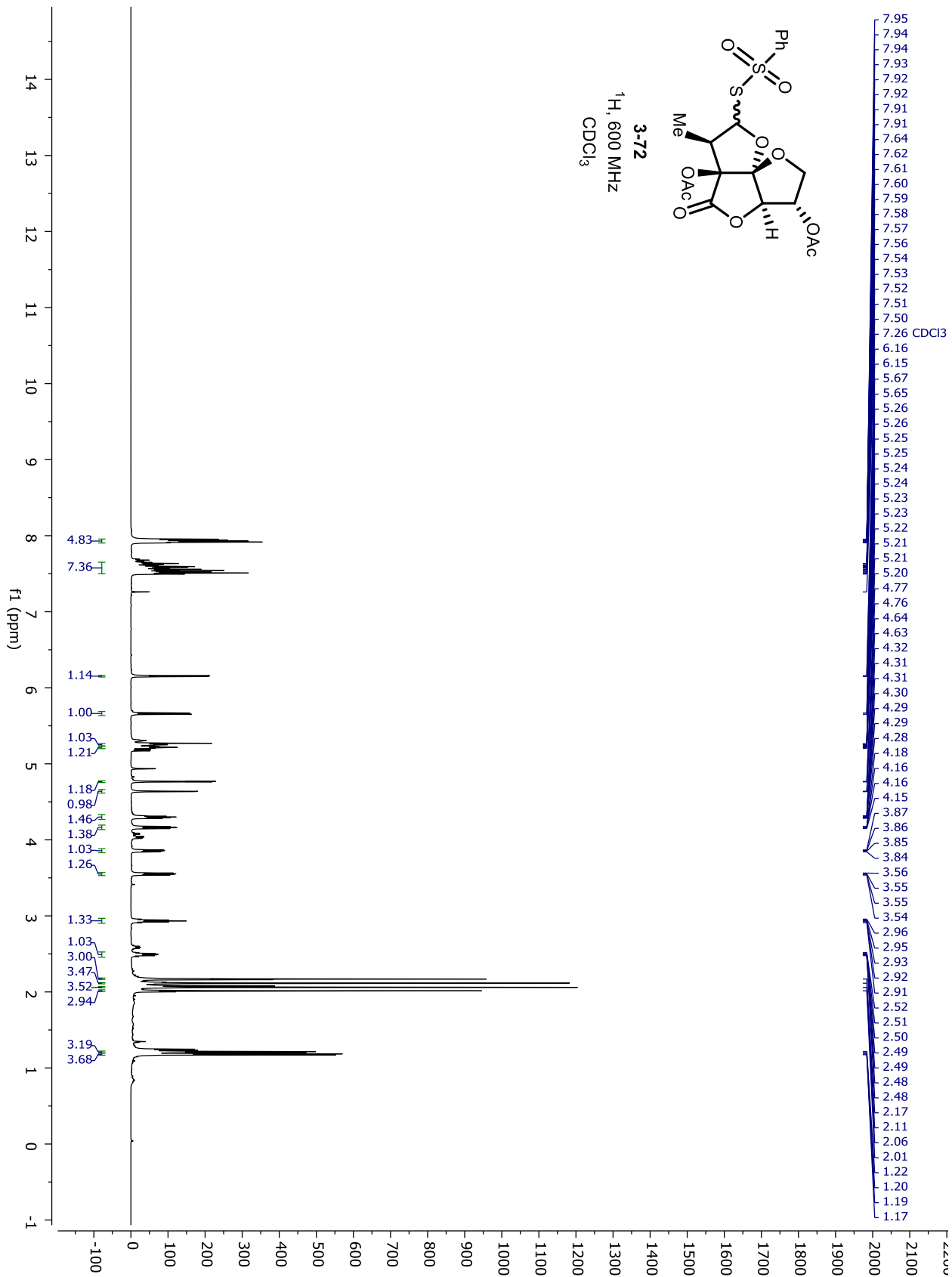


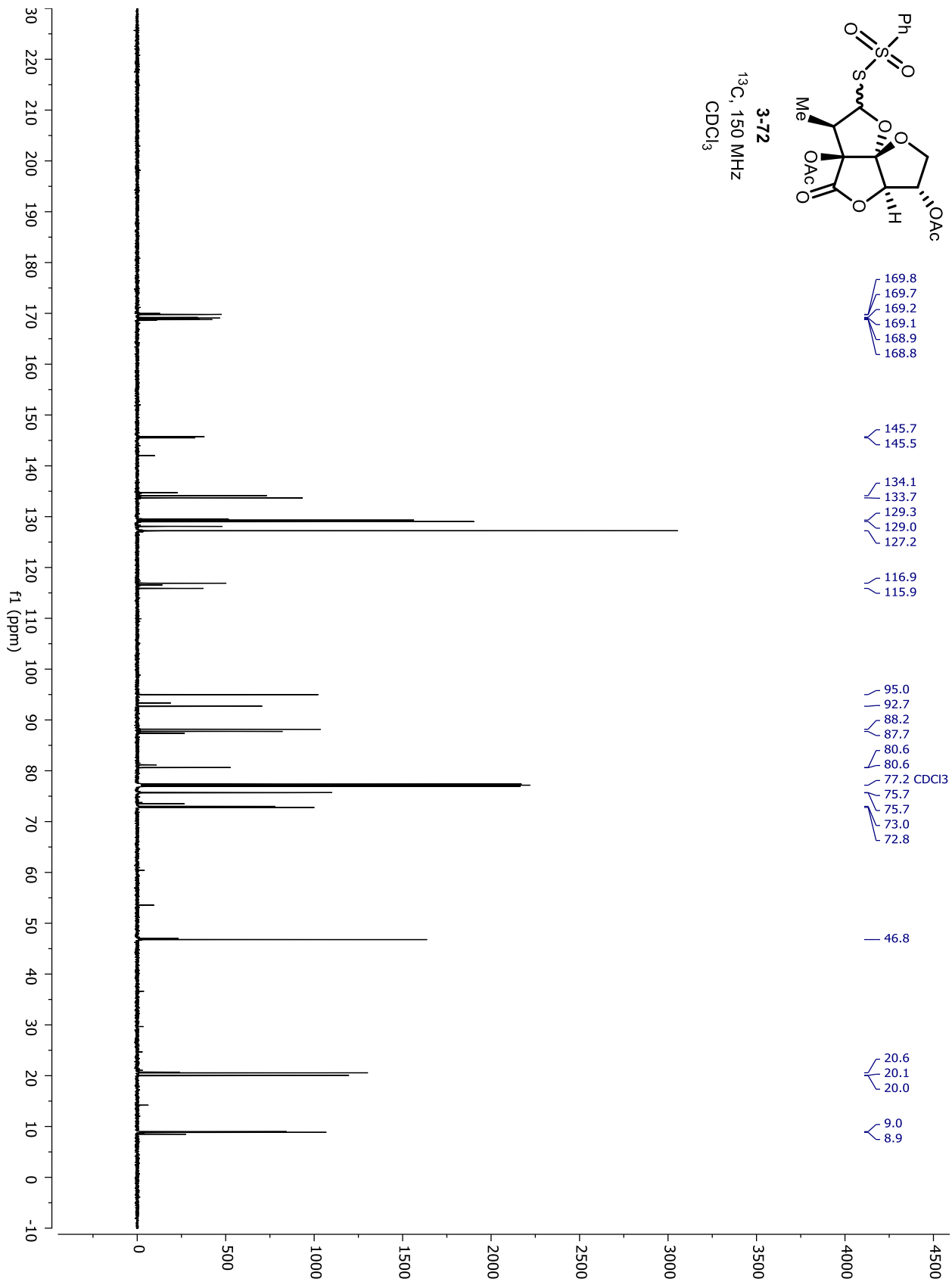


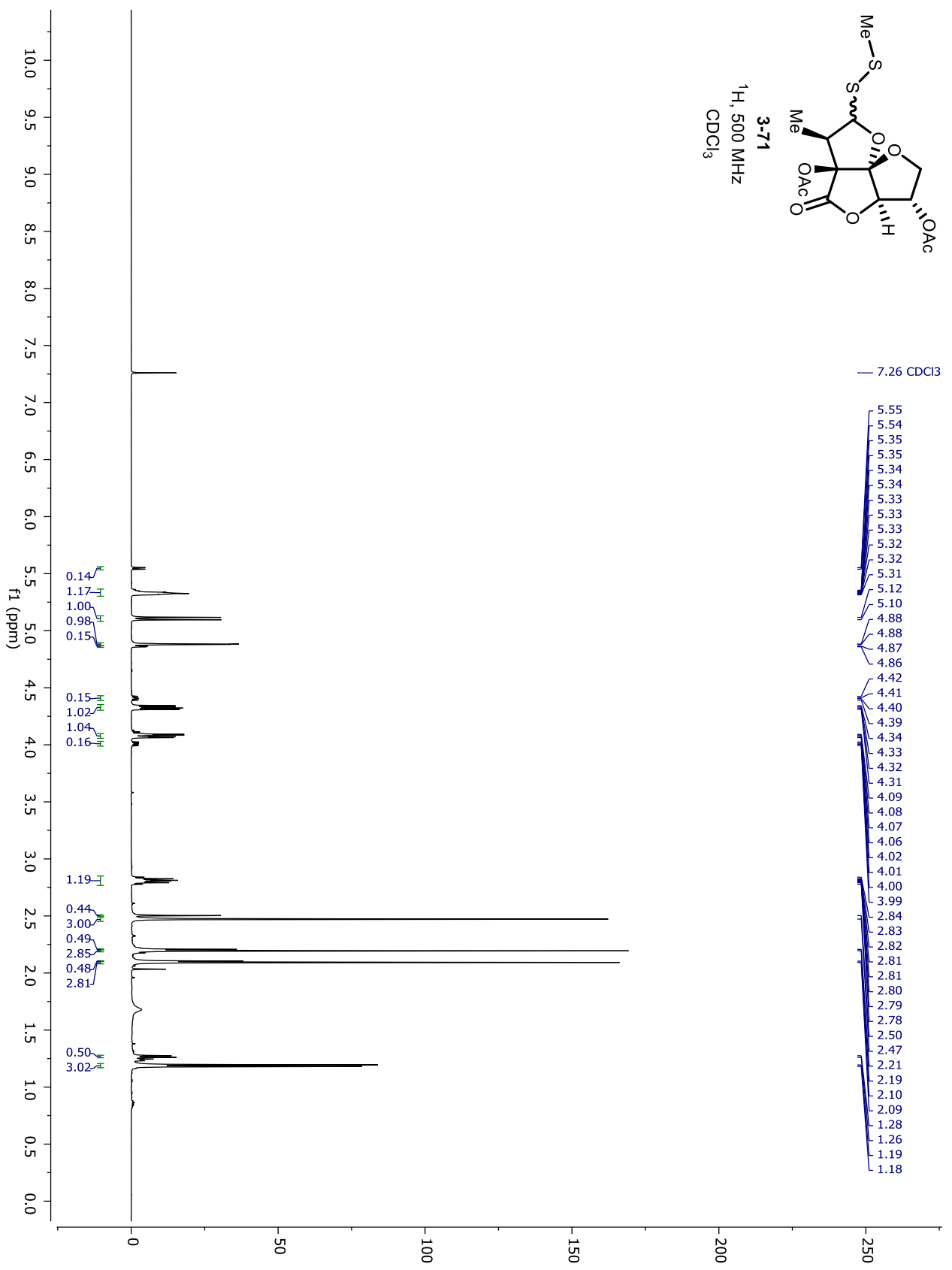
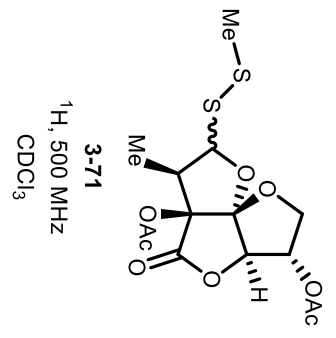


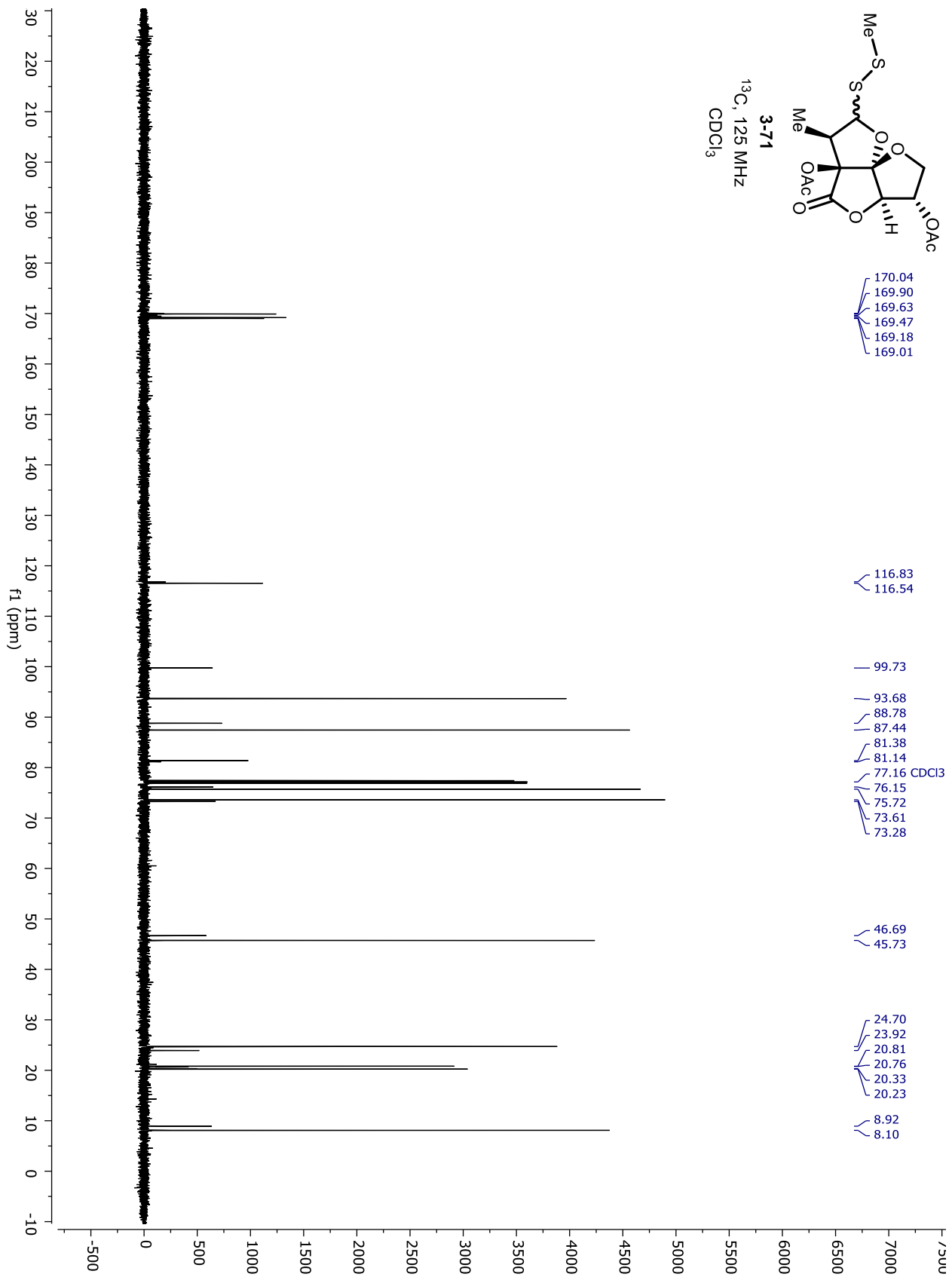


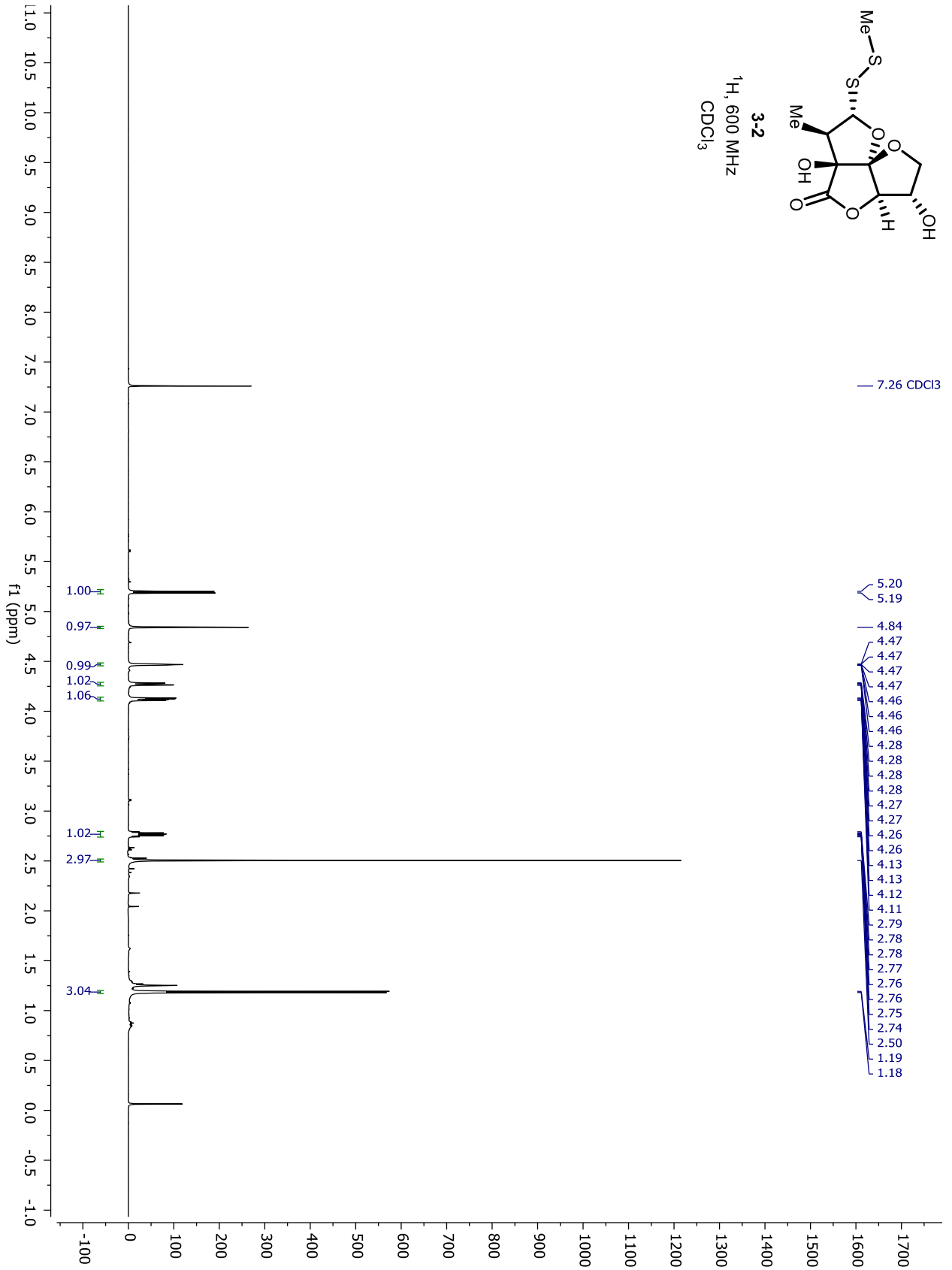
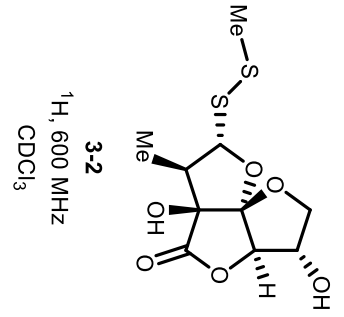


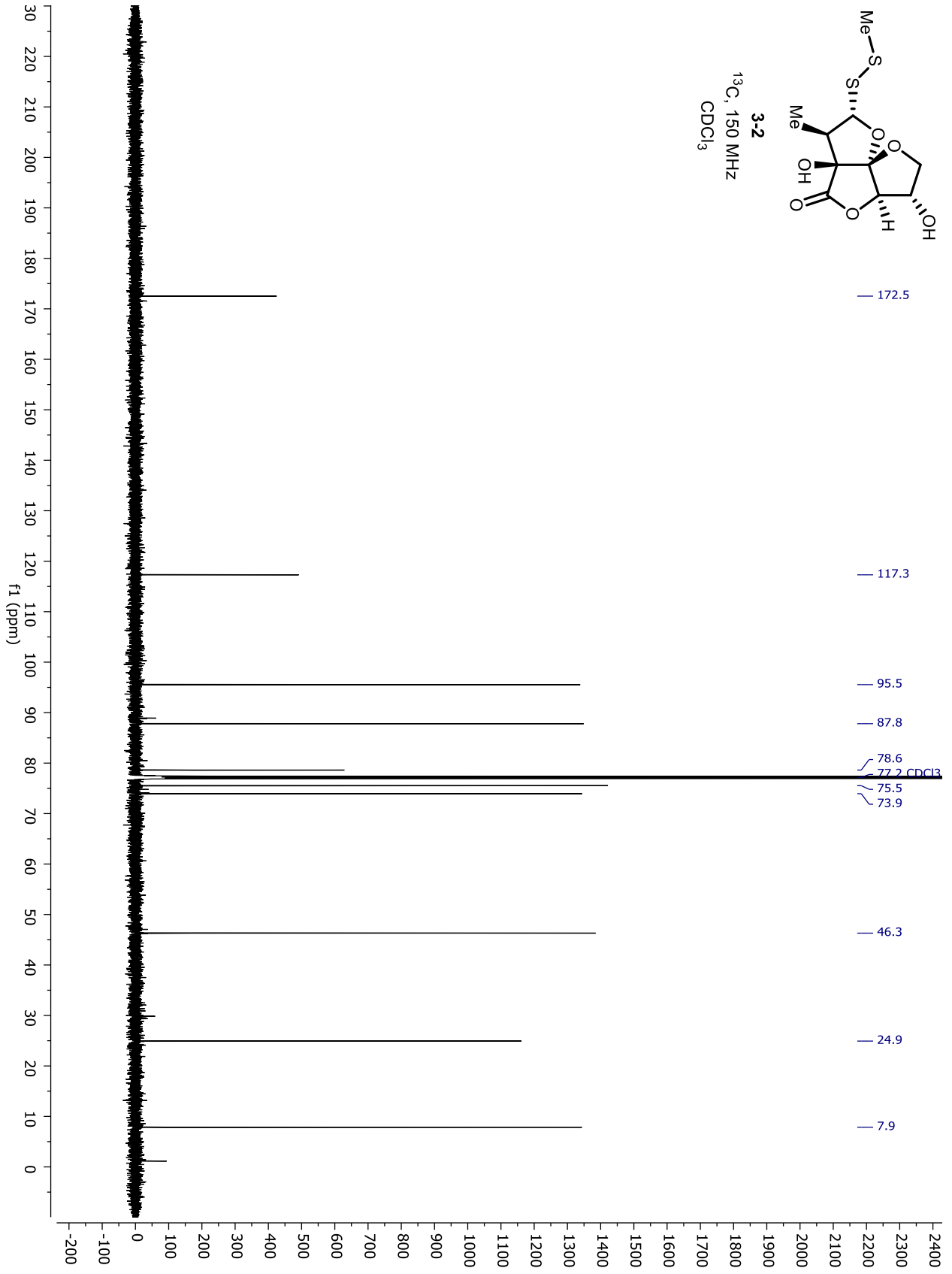
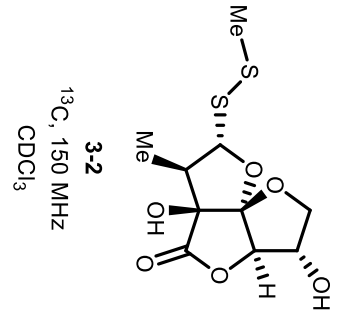


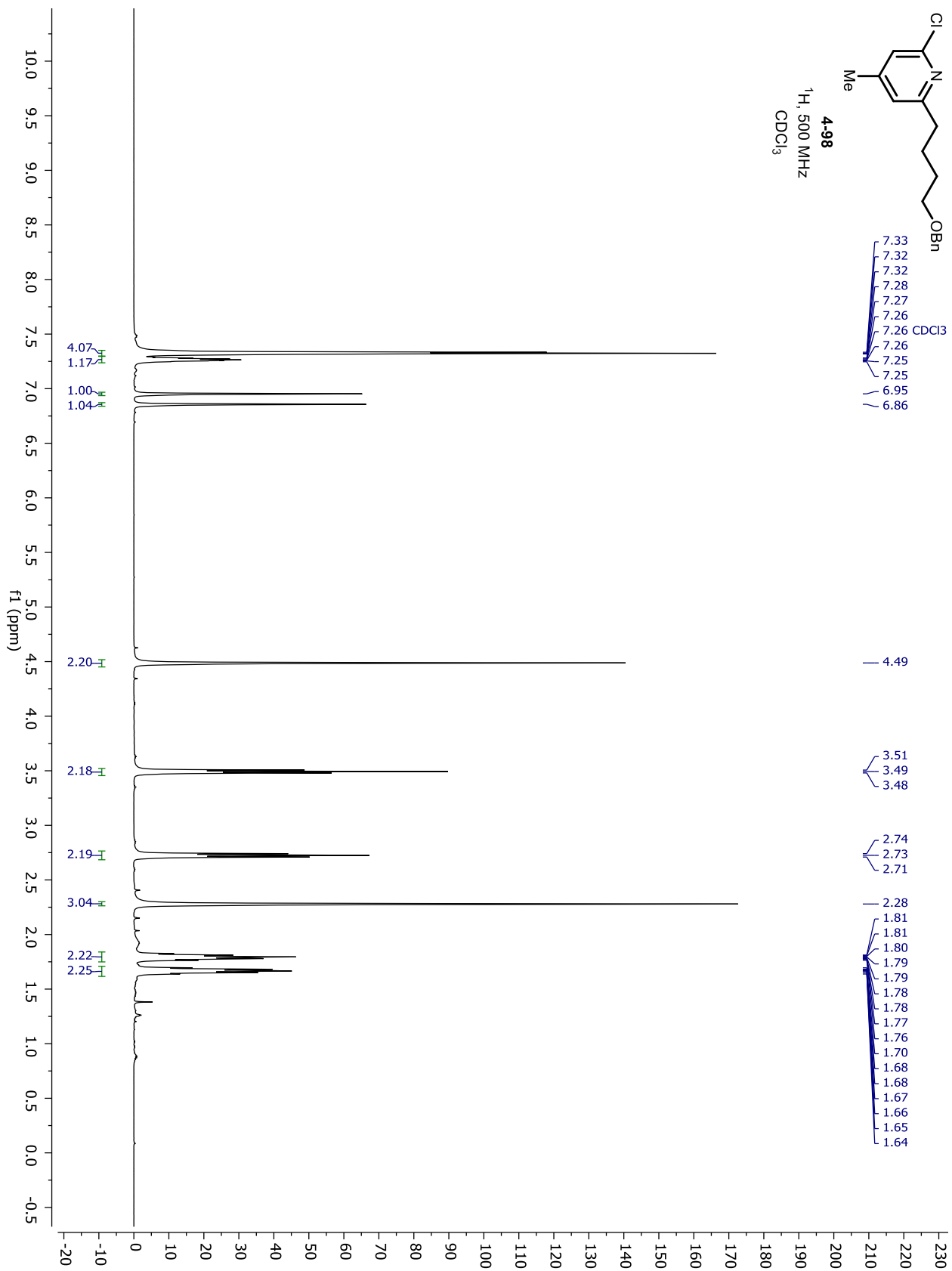


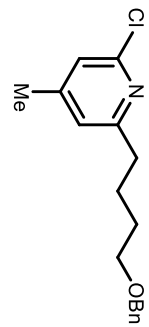












¹³C, 125 MHz
CDCl₃

